22nd Annual Event

Proceedings

Uranium-REE Conference

Including

Lithium Processing Forum

13th Annual Uranium Event

ALTA Metallurgical Services, Melbourne, Australia
www.altamet.com.au

PROCEEDINGS OF

ALTA 2017 URANIUM-REE SESSIONS

Including

Lithium Processing Forum

25-26 May 2017

Perth, Australia

ISBN: 978-0-9925094-9-1

Celebrating 32 years of service to the global mining and metallurgical industry.

ALTA Metallurgical Services was established by metallurgical consultant **Alan Taylor** in 1985, to serve the worldwide mining, minerals and metallurgical industries.

Consulting: High level metallurgical and project development consulting.

Conferences: ALTA conferences are established major events on the international metallurgical industry calendar. The event is held annually in Perth, Australia. The event comprises three conferences over five days: Nickel-Cobalt-Copper, Uranium-REE and Gold-Precious Metals.

Short Courses: Technical Short Courses are presented by Alan Taylor, Managing Director.

Publications: Sales of proceedings from ALTA Conferences, Seminars and Short Courses.

MetBytes: Free technical articles offering metallurgical commentary and insights.

Free Library: Conference proceedings and technical papers. The library will be expanded each year, providing a major ongoing resource to the industry.

ALTA Metallurgical Services PO Box 1211, Blackburn North, Vic, 3130, Australia
T: +613 9894 7420 | www.altamet.com.au

ALTA Metallurgical Services

Celebrating 32 Years of Service

ALTA Metallurgical Services (**ALTA**) was established by metallurgical consultant **Alan Taylor** in 1985, to serve the worldwide mining, minerals and metallurgical industries. **ALTA** offers a wide range of services and resources to the metallurgical industry.

Consulting

High-level metallurgical and project development consulting.

Short Courses

Practically-oriented short courses presented by Alan Taylor. Topics include treatment of nickel laterites, copper ore leaching, uranium ore processing, copper SX-EW, heap leaching and solvent extraction.

Conferences

ALTA conferences are one of the world's premier annual metallurgical events. **ALTA 2018** is the 23rd annual conference and will be held 19-26 May in Perth, Australia. The event comprises three technical conferences, three short courses and an international trade exhibition. It features a highly-focused program, topical forums and presentations from key international speakers.

Publications

Proceedings and manuals from ALTA conferences, seminars and short courses.

MetBytes

Free technical articles offering metallurgical commentary and insights.

Free Library

Includes proceedings from 1995-2015 Nickel-Cobalt-Copper, Uranium-REE and Gold-PM conferences for free download (1260+ papers). The library will be expanded regularly, providing a major ongoing resource to the industry. A selection of papers from recent conferences are also available.

Alan has over 40 years' experience in the metallurgical, mineral and chemical processing industries in Australasia, New Zealand, North and South America, Africa, Asia and Europe. He has worked in metallurgical consulting, project development, engineering/construction, plant operations, plant start-up and technology development. Projects and studies have involved copper, gold/silver, nickel/cobalt, uranium and base metals.

Since 1985, as an independent metallurgical consultant, Alan has as undertaken feasibility studies, project assessment, project development, supervision of testwork, flowsheet development, basic engineering, supervision of detailed engineering, plant commissioning and peer reviews and audits. Clients have included a variety of major and junior mining, exploration and engineering companies throughout Australia and overseas.

Extensive experience in:	...including
• Gold/Silver • Copper • Nickel/Cobalt • Uranium • Base Metals	• Leaching: atmospheric, heap, in-place, bio. and pressure • Cyanidation and CIP/CIL • Solid/liquid separation • Flotation • Electrowinning and electrorefining • Solvent extraction/ion exchange

Enquiries: allisontaylor@altamet.com.au www.altamet.com.au

ALTA 2017

Nickel-Cobalt-Copper, Uranium-REE and Gold-PM

Conference Report

22nd Annual Event

Thank you to our Sponsors Co-Sponsors, Partners and Exhibitors

Sponsors

EKATO
STEULER KCH
SOLVAY
BEAVER PROCESS EQUIPMENT
NobelClad
MOGAS SEVERE SERVICE BALL VALVES
pexgol X-LINKED PIPING SOLUTIONS
BASF We create chemistry
Purolite
FLSmidth
ExxonMobil
ORICA
DOW

Co-Sponsors and Partners

TMS The Minerals, Metals & Materials Society
SAIMM The Southern African Institute of Mining and Metallurgy
IAEA International Atomic Energy Agency
COM 2017 Conference of Metallurgists Met Soc hosting World Gold & Nickel-Cobalt
The Power is U 2017 Global Uranium Symposium
MEI
International Mining
Perth Convention Bureau
Tourism Western Australia

Exhibitors

EKATO
TURTLE TOUGH SENSORS
STEULER KCH
SGS
ISHIGAKI Oceania Experts in Filtration & Separation
pexgol X-LINKED PIPING SOLUTIONS
MEXTRAL
SPXFLOW
BEAVER PROCESS EQUIPMENT
KOCH KNIGHT
MINTEK
CGIS The World's Best Valves
REMA TIP TOP
Nm Neometals
MOGAS SEVERE SERVICE BALL VALVES
Teck
Diemme Filtration A brand of Aqseptence Group
CORE
filtaquip (pty) ltd Leaders in Filtration Technology
ORICA

Uranium-REE Contents

CLICK TO NAVIGATE TO PAPERS	Page
OPENING ADDRESS	**1**
RED BOOK 2016; INSIGHTS INTO URANIUM SUPPLY AND DEMAND Dr Peter Woods, Team Leader, Uranium Resources and Production Subprogramme, International Atomic Energy Agency (IAEA) (Austria); Authored by Dr Adrienne Hanly, Dr Peter Woods, IAEA (Austria)	2
KEYNOTE ADDRESS	**11**
PLANNING FOR A SUCCESSFUL URANIUM PILOT PLANT PROGRAM Grenvil Dunn, Principal Process Engineer, Orway Mineral Consultants, (Australia)	12
PROJECT DEVELOPMENT	**38**
AN UPDATE ON A-CAP RESOURCES' LETLHAKANE URANIUM PROJECT IN BOTSWANA Paul Woolrich, A-Cap Resources Limited (Australia); Alan Taylor, ALTA Metallurgical Services (Australia); Grenvil Dunn, Orway Mineral Consultants (Australia); Randall Pyper, Kappes Cassidy & Associates (Australia)	39
PILOT TESTWORK FOR THE PROCESS DEVELOPMENT OF THE MULGA ROCK PROJECT Chad Czerny, Andrew Wydler, Tony Chamberlain, Vimy Resources Limited (Australia)	56
METALLURGY OF THE NGUALLA RARE EARTH PROJECT - CHALLENGES, CHOICES AND INNOVATIONS Gavin Beer, Consulting Metallurgist (Australia), Roy Gordon, Peak Resources (Australia)	72
PROCESS TECHNOLOGY	**82**
IAEA'S OVERVIEW OF WORLDWIDE IN SITU LEACH URANIUM MINING Peter Woods, International Atomic Energy Agency (IAEA) (Austria)	83
METALLURGICAL TEST WORK AND MODELLING TOWARDS UNDERSTANDING THE SUITABILITY OF A URANIUM DEPOSIT FOR IN-SITU PROCESSING Laura Kuhar, Karl Bunney, Michael Jackson, Peter Austin, Jian Li, Dave Robinson, Henning Prommer, CSIRO Mineral Resources (Australia); Henning Prommer, Jing Sun, University of Western Australia; Jess Oram, Asha Rao, Cauldron Energy (Australia)	92
R&D PROGRESS OF URANIUM MINING AND METALLURGICAL INDUSTRY IN CHINA Yahui Tan, Wensheng Liao, Yijun Zeng, Beijing Research Institute of Chemical Engineering and Metallurgy (BRICEM) (China)	107
PILOT STUDY ON URANIUM RECOVERY FROM VIETNAM URANIUM SANDSTONE LOW GRADE ORES BY HEAP LEACHING Than Van Lien, Tran The Dinh, Nguyen Dinh Van, Nguyen Ba Tien, Nguyen Thi Kim Dung, Institute for Technology of Radioactive and Rare Elements (ITREE) (Vietnam)	115
ANION EXCHANGE OF URANIUM FROM SULFURIC ACID SOLUTION: ADSORPTION AND KINETICS CHARACTERISTICS Yasser Khawassek, Nuclear Materials Authority (Egypt)	126
RECOVERY OF RARE EARTH, URANIUM AND THORIUM FROM INDUSTRY RESIDUE LEACHING EXPERIMENTS Janúbia C.B.S. Amaral, Carlos A. Morais, Pedro H. M. Andrade, Monique R. Salum, Centro de Desenvolvimento da Tecnologia Nuclear (CDTN) (Brasil)	141
JAROGAIN PROCESS FOR RECOVERING VALUE-ADDED METALS FROM RLE ZINC RESIDUE Pertti Koukkari, Petteri Kangas, Max Nyström VTT, Technical Research Centre of Finland (Finland); Mari Lundström, Benjamin Wilson, Aalto University (Finland); Jussi Rastas, Pekka Saikkonen, Promeca Consulting (Finland)	151
SEPARATION OF THORIUM, URANIUM AND RARE EARTH ELEMENTS FROM SULFURIC LIQUOR Carlos A. Morais and Janúbia C. B. S. Amaral, Centro de Desenvolvimento da Tecnologia Nuclear (CDTN) (Brasil)	162
LITHIUM PROCESSING FORUM	**170**
APPLICATIONS OF ADVANCED ANALYTICAL AND MASS SPECTROMETRY TECHNIQUES TO THE CHARACTERIZATION OF LITHIUM BEARING ORES Mark G. Aylmore, Kelly Merigot, William D.A. Rickard, David W. Saxey, Denis Fougerouse, Steven M. Reddy, Zakaria Quadir, Noreen Evans, Bradley McDonald, Brent I.A. McInnes, Curtin University; Enej Catovic, Peter Spitalny, Lithium Australia (Australia)	171
ONLINE LITHIUM ANALYSIS IN SPODUMENE CONCENTRATION Lauri Koresaar, Juha Timperi, Outotec (Finland)	181

Uranium-REE Contents

CLICK TO NAVIGATE TO PAPERS	Page
LITHIUM PROCESSING FORUM (continued)	
SPECIALIZED IMPELLERS FOR HYDROMETALLURGICAL PROCESSING APPLICATIONS WITH FOCUS ON LITHIUM Wolfgang Keller, Jochen Jung, EKATO RMT (Germany)	189
REVIEW OF LITHIUM PRE-CONCENTRATION, EXTRACTION, SEPARATION AND OR PURIFICATION USING DOW WATER AND PROCESS SOLUTIONS TECHNOLOGIES Jaco Bester, Daryl Gisch and Valeria Burlakova, Dow Water & Process Solutions (Netherlands)	199
THE CASE FOR SECONDARY LITHIUM RESOURCES Grant Harman, Lithium Consultants Australasia (Australia)	210
A BROAD LOOK AT LITHIUM EXTRACTION Mike Dry, Arithmetek Inc. (Canada)	225
LITHIUM EXTRACTION FROM COMPLEX SILICATES Damian Connelly, Mineral Engineering Technical Services Pty Ltd (METS) (Australia)	240
LITHIUM PROCESS FLOWSHEETS - CHALLENGES AND OPPORTUNITIES Chris Griffith, ANSTO Minerals (Australia)	262
HYDROMETALLURGICAL PROCESSES FOR THE RECOVERY OF LITHIUM Adrian Griffin, Lithium Australia (Australia)	279
NOT PRESENTED	288
QUANTITATIVE ANALYSIS OF URANIUM AND THORIUM CONTAINING MATERIALS USING INDUSTRIAL ON-LINE XRF ANALYZER Elena Hasikova, Alexander Sokolov, Vitaly Titov, Baltic Scientific Instruments (Latvia)	289
ALUMINUM OXIDE GRAFTED KAOLINITE FOR EFFICIENT URANIUM REMOVAL FROM AQUEOUS SOLUTION Hussein A. E. M., Nuclear Materials Authority (Egypt)	300
STUDY ON REES LEACHED IN PHOSPHATE CONCENTRATE WITH PHOSPHORIC ACID Xunxiong Jiang, Shengdong Wang, LinYong Feng, Yanqing Fan, Wei Jiang, Beijing General Research Institute of Mining & Metallurgy (BGRIMM) (China)	315

Uranium-REE Proceedings

Opening Address

Uranium-REE Opening

RED BOOK 2016: INSIGHTS INTO URANIUM SUPPLY AND DEMAND

By

Adrienne Hanly and Peter Woods

Presenter and Corresponding Author

Dr Peter Woods
Team Leader, Uranium Resources and Production Subprogramme
International Atomic Energy Agency (IAEA), Austria

p.woods@iaea.org

ABSTRACT

The 26th edition of “Uranium 2016: Resources, Production and Demand”, the “Red Book”, was released in November 2016. This well-recognised world reference on uranium was jointly prepared by the Nuclear Energy Agency of the Organization for Economic Co-operation and Development (OECD-NEA) and the International Atomic Energy Agency (IAEA). The report provides analyses and information from 49 countries. The new edition provides a thorough review of world uranium market fundamentals and presents data on global uranium exploration, resources, production and reactor-related requirements. It offers information on established uranium production centres and mine development plans, as well as projections of nuclear generating capacity and reactor related requirements through 2035.

Among the key findings in the latest report is that the total identified uranium resources as of 1 January 2015 increased by only 0.1 percent since 2013, with the resource base changing very little due to lower levels of investment and associated exploration efforts reflecting the currently depressed conditions of the global uranium market.

More than 20 countries around the globe produce uranium, with the largest producers Kazakhstan, Canada and Australia accounting for approximately two-thirds of world output. Global uranium mine production, meanwhile, had decreased by 4 percent between 2013 and 2015, though it remains above 2011 levels. The drop is due mainly to decreased production in Australia and lower output in Brazil, the Czech Republic, Malawi, Namibia and Niger. Kazakhstan, the world’s largest producer, continued to increase output, although at a slower pace.

Regarding future demand for nuclear power, the Red Book’s projections vary from region to region. While the Fukushima Daiichi accident led to a change of policies in some countries, nuclear power looks set to keep expanding globally both in low and high case scenarios, particularly in Asia.

While current uranium resources are more than adequate to meet the high growth scenario, doing so would “depend upon timely investments to turn resources into refined uranium ready for nuclear fuel production,” according to the report, adding that “significant investment and technical expertise” would be needed “to bring those resources to market”.

Keywords: Uranium Resources, Uranium Demand, OECD-NEA, IAEA, Red Book

"Red Book"

Recognized source for Global Resource information

Longstanding OECD/NEA and IAEA cooperation - published every 2 years

Relies principally on input from country representatives nominated by governments to the Uranium Group

Summary chapters on Supply and Demand

2016 Edition: 49 Country reports (12 are Secretariat estimates)

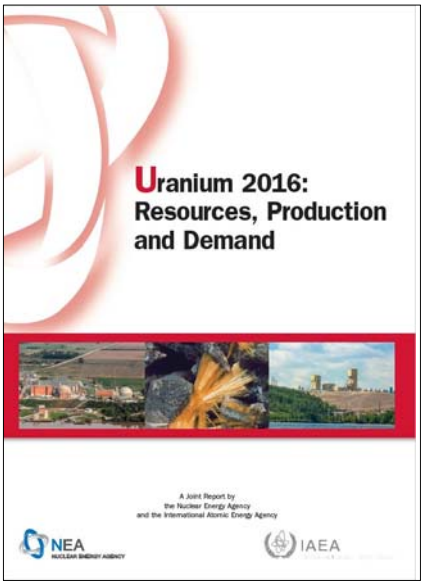

Uranium Resources Production and Demand-Red Book

Key messages in recent editions:

Resources more than adequate to meet high case demand scenarios

Investment and expertise required to bring resources into production*

Production costs increasing*

Long lead times owing to regulatory requirements and public resistance*

*Contributing to potential supply challenges over next 5-10 years

Red Book 2016

Time slice of a dynamic system – reference date 1Jan 2015 – Red Book outlines situation based on available information on that date

Red Book released by OECD publications as PDF free of charge

http://www.oecd-nea.org/ndd/pubs/2016/7301-uranium-2016.pdf

Red Book 2016 – Distribution of Resources*

15 countries represent approx. 95% of total world U resources

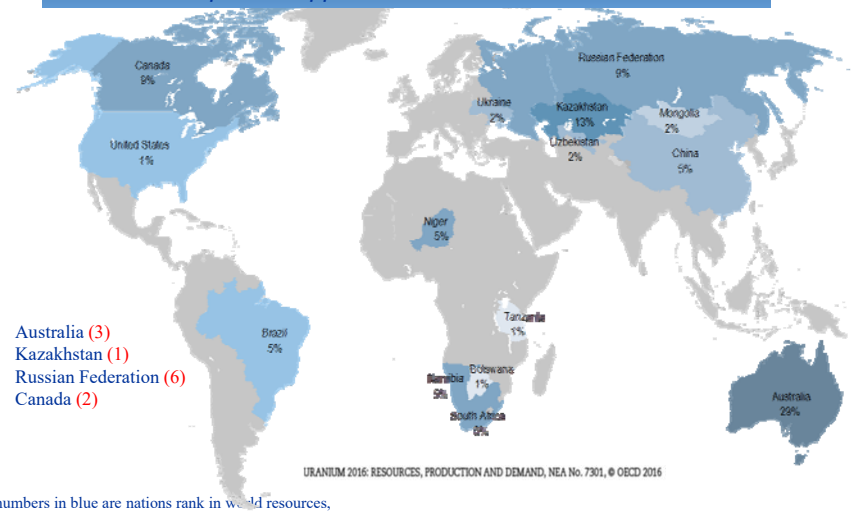

1. Australia (3)
2. Kazakhstan (1)
3. Russian Federation (6)
4. Canada (2)

Note: numbers in blue are nations rank in world resources, those in red are the nations rank in world production.

*Identified Resources at <USD130 kg/U as of January 1, 2015

Red Book 2016– Resource Trends

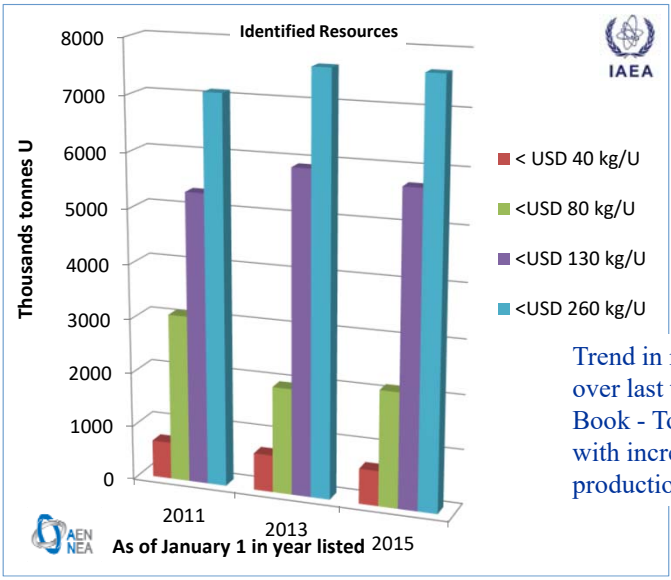

Trend in resource inventory over last three editions of Red Book - Total increasing along with increasing costs of production.

Red Book 2016 – Expenditures

- Exploration and mine development expenditures continued to increase, driven mainly by Husab (Namibia) mine development and Cigar Lake (Canada)
- Total exploration expenditures alone decreased

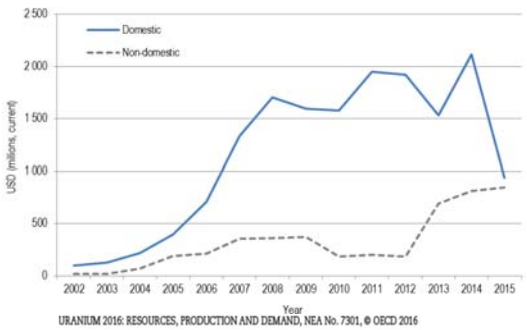

Notes:
*2015 values are estimates
* Domestic exploration and development expenditures represent the total expenditure from domestic and foreign sources within each country.

Red Book 2016 – Summary of Exploration and Resources

- Total exploration and mine development expenditures have increased since the last reporting period. However, no significant resources have been added and the expenditure increase reflects investments in the Cigar Lake mine in Canada and the Husab mine in Namibia.
- Total identified resources (RAR + Inferred) have increased by only 0.1% since 2013 (reflecting lack of investment in exploration)
- Overall reductions in <USD40 kg/U and <USD130kg/U categories.
- Decreases in RAR were offset by increases in the Inferred Resources category.
- Notably 208 400 tU from China and Kazakhstan was added to Inferred Resources category.

World Uranium Production

Uranium production has decreased by 4% since 2013

2014 production ~56 000 tU

Kazakhstan responsible for 41% of production in 2014 (production rate continued to increase but not as rapidly as in previous years)

Canada (16%) and Australia (9%) remain significant producers and production expected to increase in coming years

Largest production decrease was from Australia-dropped to 9% from 12% of world total in 2012

Also lower output from Brazil, the Czech Republic, Malawi, Namibia and Niger

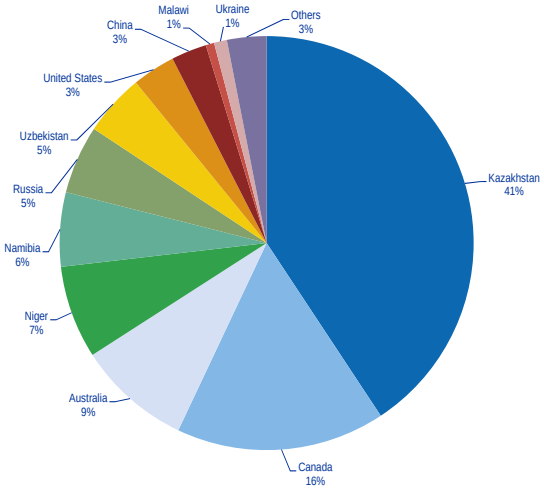

URANIUM 2016: RESOURCES, PRODUCTION AND DEMAND, NEA No. 7301, © OECD 2016

Total Uranium Production for 2014 and 2015 (expected) by Method

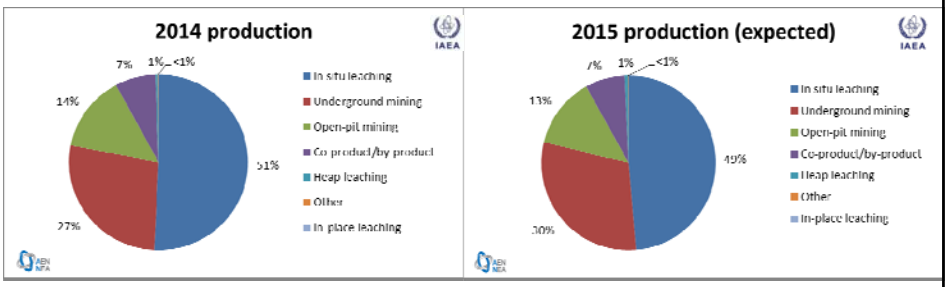

Since 2009, In situ leach (also known as in situ recovery) method is the dominant uranium production method in the world making up over 50% of 2014 production with similar forecasts for 2015.

A large part of this is due to production in Kazakhstan, the world's largest uranium producer.

Underground mining is second, with a large portion coming from the world's second largest producer, Canada.

World Nuclear Capacity and U Requirements (as of January 1, 2015)

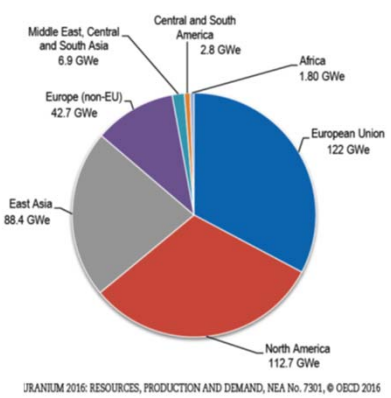

World installed nuclear capacity: 377.4 Gwe net

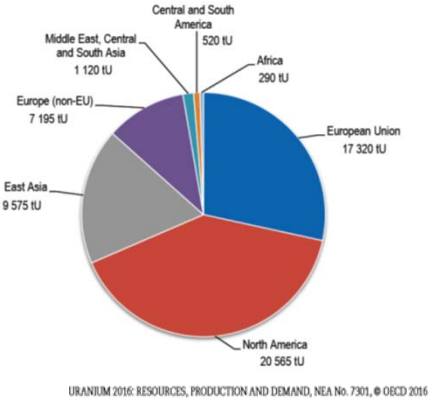

World uranium requirements: 56 585 tU (excluding MOX)

Uranium was produced in 21 countries in 2014, with total global production amounting to 55 975 tU which was about 99% of world reactor requirements for that year

Projected Nuclear Capacity to 2035 (as of January 1, 2015)

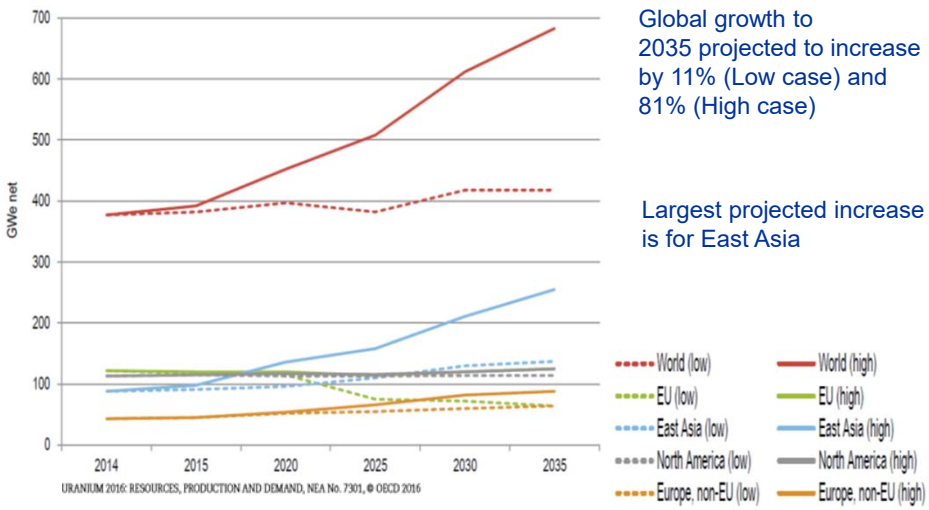

Global growth to 2035 projected to increase by 11% (Low case) and 81% (High case)

Largest projected increase is for East Asia

Uranium Requirements to 2035

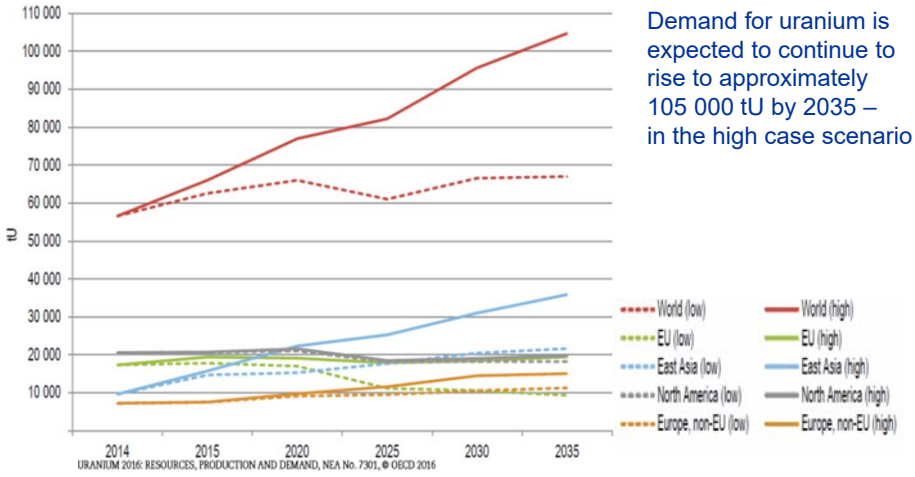

Demand for uranium is expected to continue to rise to approximately 105 000 tU by 2035 – in the high case scenario

Uranium Production Capability vs Demand

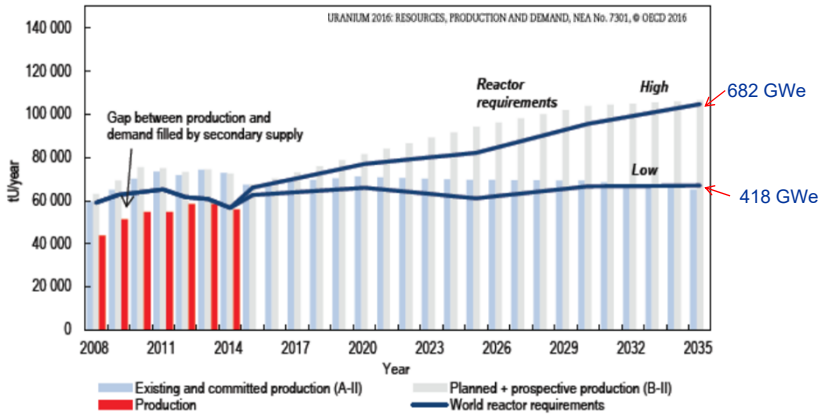

* Includes all existing, committed, planned and prospective production centres supported by reasonably assured resources and inferred resources recoverable at a cost of <USD 130/kgU. Does not include the secondary supply forecast.

Summary and Conclusions

- Growth continues in the nuclear industry-commitment remains in many countries; pace has slowed down in some
- Demand for uranium will continue to rise for the foreseeable future
- Identified Resources are more than adequate to meet high case demand projections to 2035

Summary and Conclusions

- Mine developments delayed; strong market conditions required to bring resources to market
- Increased production capability (i.e. expansions and new mines) will be required for projected growth in nuclear demand (high case scenario)
- To meet demand in the long term uranium production is projected to expand and with this a strong safety and environmental record must be maintained, communicated and continuously re-evaluated

Acknowledgements

- The compilers of this joint publication are Drs Adrienne Hanly of the IAEA and Luminita Grancea of the OECD-NEA, to whom inquiries should be made
  - A.Hanly (at) iaea.org
  - Luminita.GRANCEA (at) oecd.org
- Permission to reproduce tables or figures from the Red Book should be requested of the OECD-NEA
- If you downloaded the Red Book 2016 prior to April 2016, please revisit the site and download again for the revised official version
- http://www.oecd-nea.org/ndd/pubs/2016/7301-uranium-2016.pdf

Uranium-REE Proceedings

Keynote Address

PLANNING FOR A SUCCESSFUL URANIUM PILOT PLANT PROGRAM

By

Grenvil Dunn
Principal Process Engineer
Orway Mineral Consultants (WA) Pty Ltd, Australia

Grenvil.Dunn@orway.com.au

ABSTRACT

Many there are in Project Development and Engineering that consider Pilot Plant work before understanding all they should about their uranium containing feed ore(s). Premature commitment to piloting can, inter alia, result in the adoption of an inappropriate flowsheet in piloting. The consequence of this outcome can be far reaching; from project closure on the one hand because of cost and or schedule blow out, through to adopting a flowsheet yielding a sub-optimal return on the other.

This paper addresses the key aspects in the preparation and planning a pilot plant for a uranium project.

Keywords: Pilot Plant, Uranium, Sample Selection, Batch Testing, Variability Testing, Data Interpretation

INTRODUCTION

Many there are in Project Development and Engineering that consider Pilot Plant work before understanding all they need to about their uranium containing feed ore(s). Premature commitment to piloting can, inter alia, result in the adoption of an inappropriate flowsheet. The consequence of this outcome can be far reaching; from project closure on the one hand through to adopting a flowsheet yielding a sub-optimal return on the other.

The procedure advocated for planning for a uranium pilot plant is no different to that employed for most metals apart from some of the unique features associated with radiation.

Pre-pilot preparatory work can take from several months to several years and its duration is normally related to the complexity and variability of the ores to be processed.

This paper will address the importance of:

- Sample selection, representivity and mineralogy,
- Understanding project and process constraints, for example, environmental factors, impurity deportment, gangue reagent consumers, water quality etc.,
- Upgrade opportunities,
- Batch and batch variability testing,
- Early mass balances,
- Flowsheeting and interim project costing,
- Scoping and managing the pilot plant campaign.

SAMPLE SELECTION AND REPRESENTIVITY

Sample selection and representivity are important to ensure that the ore submitted to testwork is relevant to the mine plan and the resource. Selecting unsuitable samples or non-representative samples may result in an:

- incorrect or a sub-optimal process flowsheet being selected,
- incorrect economic analysis on the viability of the project as testwork may show lower or higher than expected recovery and reagent consumption.

The importance of understanding the orebody cannot be understated. A recent uranium acid leach project in South Africa is an example where there was insufficient knowledge of the orebody. This resulted in a lower than expected uranium head grade to the plant and with that the plant has been shut down.

There have been similar cases in Africa where alkaline leach processes have failed because of inter alia insufficient knowledge of the orebody before committing to the project.

Ore sampling and committing the samples to a rigorous testing regiment has no substitute in the development of uranium projects.

Sampling can be undertaken using several different methods depending on the type and location of the deposits. Methods such as trench sampling shown in Figure 1 and Figure 2 may be suitable for surficial deposits whereas diamond drill core sampling (shown in Figure 3) may be more suitable for deeper deposits.

Figure 1: Radiometry mapping of trench wall
(Courtesy of JUMCO)

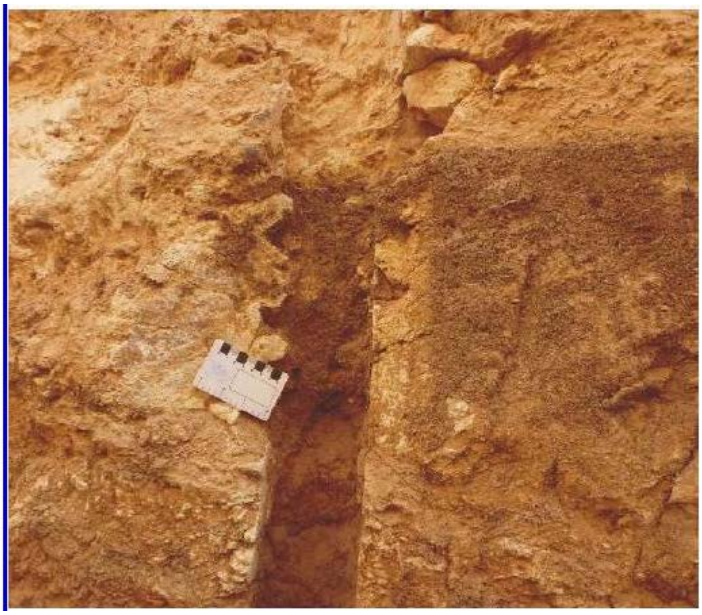

Figure 2: Channel sample cut in the trench wall by a diamond saw
(Courtesy of JUMCO)

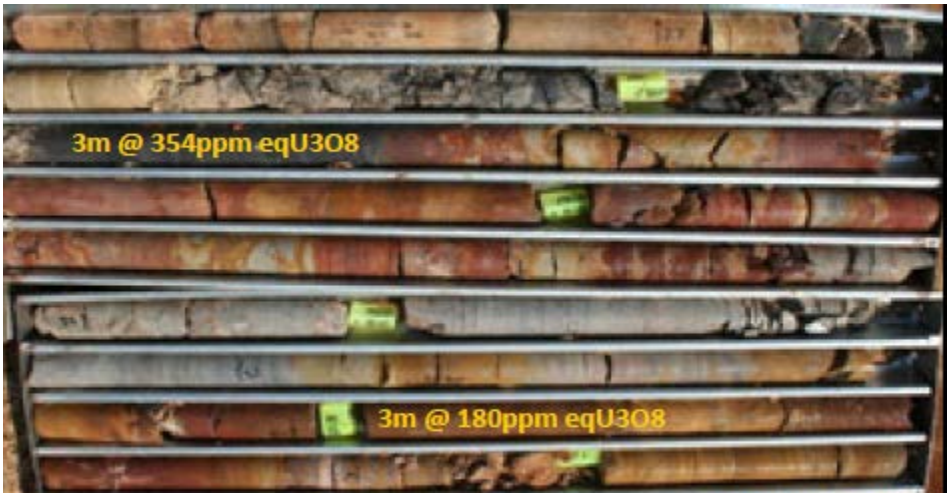

Figure 3: Diamond drill core sample[1] (Courtesy of A-Cap Resources)

Metallurgical samples should be split from material that represents the orebody:

- Spatially,
- At depth,
- By lithology, and
- In its variability.

PROJECT AND PROCESS CONSTRAINTS

Two key project constraints will be discussed, namely;

- effluent, and
- water.

Environmental and Effluent

The selection of a process flowsheet will need to take into consideration environmental constraints and effluent management. Tailings disposal in open dams which have been common practice to current time is unlikely to be condoned in the future as issues such as tailings dam failures, seepage and acid mine drainage become apparent after mine closure.

An example of a uranium legacy mine site is Rum Jungle which was closed in 1971 and subsequently there was significant environmental damage from acid and metalliferous drainage polluting the Finniss River[2]. Remediation work on the Rum Jungle site was first undertaken in the 1980s and is still ongoing today to improve water quality, vegetation and aesthetics.

Figure 4: Rum Jungle Legacy Mine Remediation Site[2]

The best practices today as recommended by the Nuclear Regulatory Commission for the management of uranium tailings is to store dry tailings in below grade disposal sites[3]. This will require the tailings to be filtered rather than disposed of into a tailings dam as slurry. An example of a site which has adopted below grade dry tailings disposal is the Moab Tailings Relocation project. The task at hand involves excavating 14.5 million tonnes of inactive tailings and relocating it to a below-grade disposal site approximately 50km away at Crescent Junction in Colorado[4]. At the disposal site, the tailings are stacked to a depth of 7.5m below grade and 7.5m above grade and capped with 2.5m thick multi-layer cover as shown in Figure 7. The ground water at the MOAB tailings site is also being remediated to remove ^{226}Ra from seepage fluids.

Figure 5: Moab Tailings Site[4] (Courtesy of US DOE)

Figure 6: Below Grade Tailings Disposal Site at Crescent Junction[4] (Courtesy of US DOE)

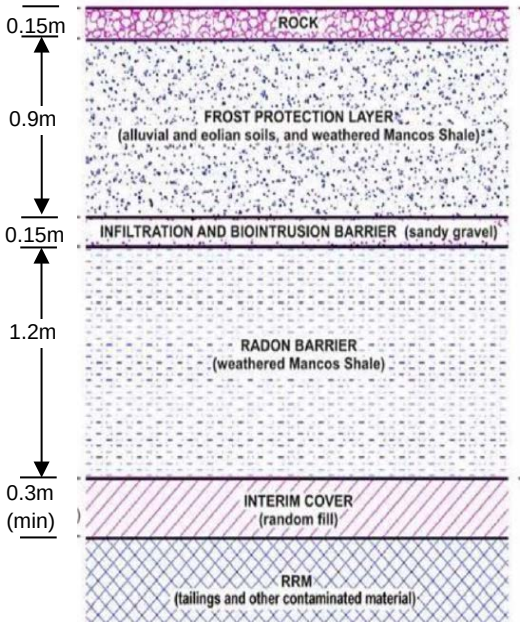

Figure 7: Disposal Cell Cover[4]

The upliftment of uranium tailings and relocation to another site followed by remediation of the first and capping at the second site is costly and would unlikely have been envisaged in the initial project economics.

Hitherto, governments and tax payers have often been called on to fund these remediation activities, a practice that is unlikely to be acceptable going forward.

Operators should therefore only consider a flowsheet that embraces a residue or tailings concept that adequately contains the waste components and in the case of uranium, its daughters as well.

Flowsheets that are tested at bench and pilot scale should therefore give consideration to incorporate a final residue form that meets these requirements. This will invariably include receiving return fluids

and leachates into the process from the tailings facility, which in turn may result in elevated concentrations of conservative elements within the circulating process liquors.

Water

Water and water quality are critical to the hydrometallurgical recovery of uranium from ores and concentrates.

Some factors that need to be considered in the metallurgical testing are:

- regional water salinity and the expected water quality available to the leach process,
- regional water availability and possible restrictions on use,
- if water de-ionisation is required for the process, and the constraints that will likely be placed on the disposal of the concentrate (brine).

There are limits on the concentration of chlorides in water, not only from materials of construction perspective but primarily because chloride is a competing ion in the transfer processes of solvent extraction and ion exchange.

MINERALOGY

Gangue Reagent Consumers

The method for processing an ore for the recovery of uranium is determined by the ore's mineralogy. The mineralogy of the gangue minerals rather than that of the uranium minerals often determine the leach regime employed.

In leach processes employing sulfuric acid, only a relatively small quantity of acid is gainfully employed in extracting uranium from the host ore. The remainder of the acid is consumed by the gangue constituent minerals. There are new projects that are being considered today have a gangue acid consumption in excess of 95% of the total applied fresh acid.

Many of the gangue elements that are solubilised by sulfuric acid report to the leachate where they build up in concentration within a closed flowsheet. In some cases, the impact of this may be deleterious to the extraction of uranium, whilst in others there have been some benefits identified when leaching in high solute concentration solutions.

Similarly, in alkaline leaching, where the unit reagent cost is approximately 3 times that of sulfuric acid, the ore that is leached must also have economically low levels of reagent consumption.

In the Namibia, West Africa, Jordan and other desert locations where the uranium is carbonate hosted for example, the upper ores are often not treated because they contain elevated levels of labile sulfate e.g. strontium and calcium sulfate which increase the reagent consumption.

Quantitative Mineralogy

It is important to quantify the reagent consuming gangue minerals both in the leach feed and the leach residue in order to construct the mass balance.

Biotite, for example, is common in many ores and reacts with sulfuric acid.

Figure 8: Biotite Minerals[5] ($KMg_{1.5}Fe_{1.5}(AlSi_3O_{10})(OH)_2$)

$2KMg_{1.5}Fe_{1.5}(AlSi_3O_{10})(OH)_2(s) + 6H_2SO_4(aq) \rightarrow 2KAlSi_3O_8(s) + 3MgSO_4(aq)+3FeSO_4(aq) +8H_2O\ (l)$

Carbonates of the type ankerite, dolomite etc, consumes acid in a n acid heap leach operation. Invariably at the toe, gypsum crystallization is evident as the leach front moves through heap.

Figure 9: Gypsum precipitate at the toe of an Acid Leach Pad

$Ca(Fe,Mg)(CO_3)_2(s) + 2H_2SO_4(aq) \rightarrow CaSO_4(aq) + 0.5\ MgSO_4(aq) + 0.5\ FeSO_4(aq) + 2H_2CO_3(aq)$

$CaSO_4\ (aq) \xrightarrow{H_2O} CaSO_4{\bullet}2H_2O\ (s)$

Simple elemental chemistry is both insufficient and inadequate to model the uranium and related gangue minerals in the leaching process. Quantitative mineralogy will provide a clear indication of the mineral alterations in the leach and a basis and foundation for the mass balance.

Uranium Minerals Particle Size and Liberation

The required ore particle size can impact the flowsheet selection as it can impact the comminution step required to liberate the uranium minerals.

Figure 10 shows some QEMSCAN particle images in which the uranium is either locked or liberated in copper-iron-sulfides and oxides. Accessing the uranium that is locked may be facilitated by further particle size reduction or similar means.

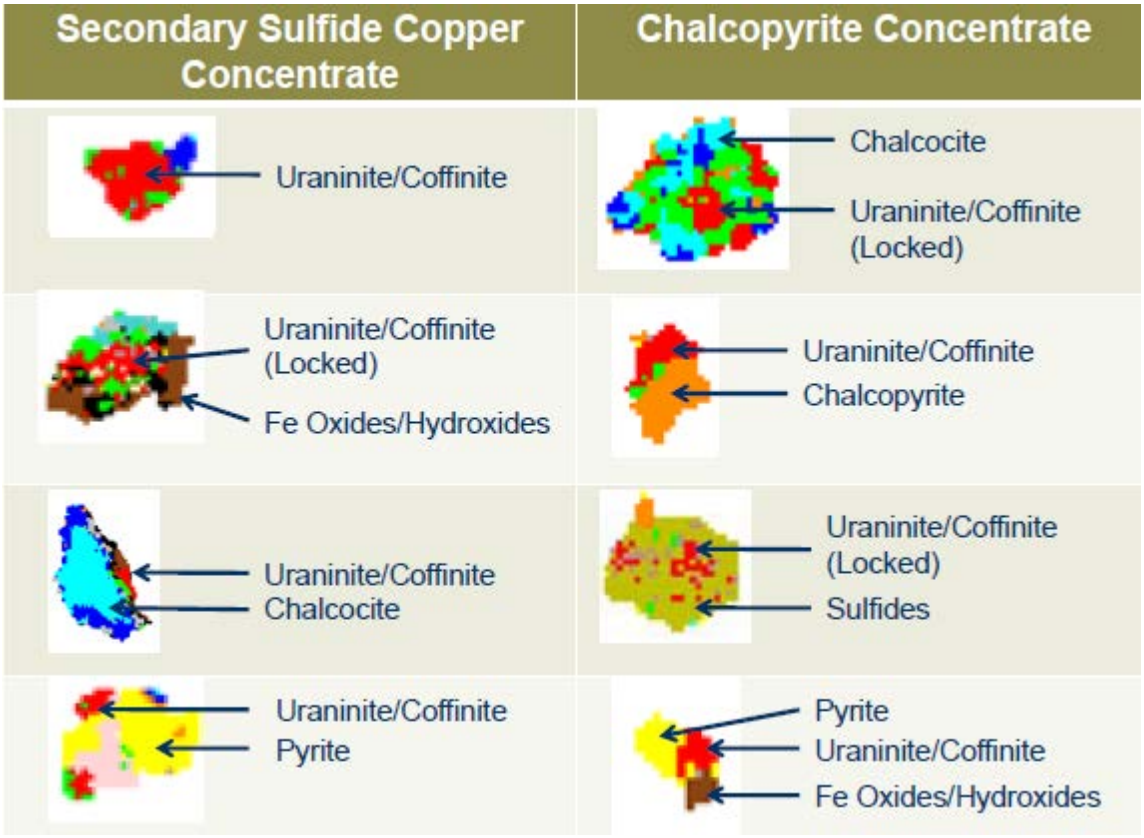

Figure 10: QEMSCAN Particle Image of Uranium Bearing Minerals in Copper Concentrate

UPGRADE PROCESSES

Some uranium ores are amenable to upgrade processes. Upgrading has several benefits:

- Converting lower grade ores into an economic feed grade,
- Reducing the size of processing plant – lower capital cost,
- Reducing reagent consumption as less reagent will be wasted in gangue ore leaching – lower operating cost,
- Reducing the amount of processed tailings and hence the environmental footprint of a project.

The following processes have been examined for upgrading uranium ores:

Radiometric Ore Sorting (ROS) - the uranium distribution in the ore must be heterogeneous (e.g. Vein) and uranium and radium must be in equilibrium[6] for it to be a possible candidate for ROS.

Flotation – flotation has been used to float sulfides to reject gangue minerals or to recover secondary product. Olympic Dam employs this process[6].

Scrub and Screen – Scrubbing and screening upgrading has been employed on surficial ore to recover a uranium concentrate. Langer Heinrich currently employs this process[8].

U-PGrade™ Process – This has been patented by Marenica Energy and employs scrubbing, size separation by screening elutriation and cyclone and standard carbonate removal. The first commercial application is reported likely to be the Reptile Uranium Namibia Tumas Project[9].

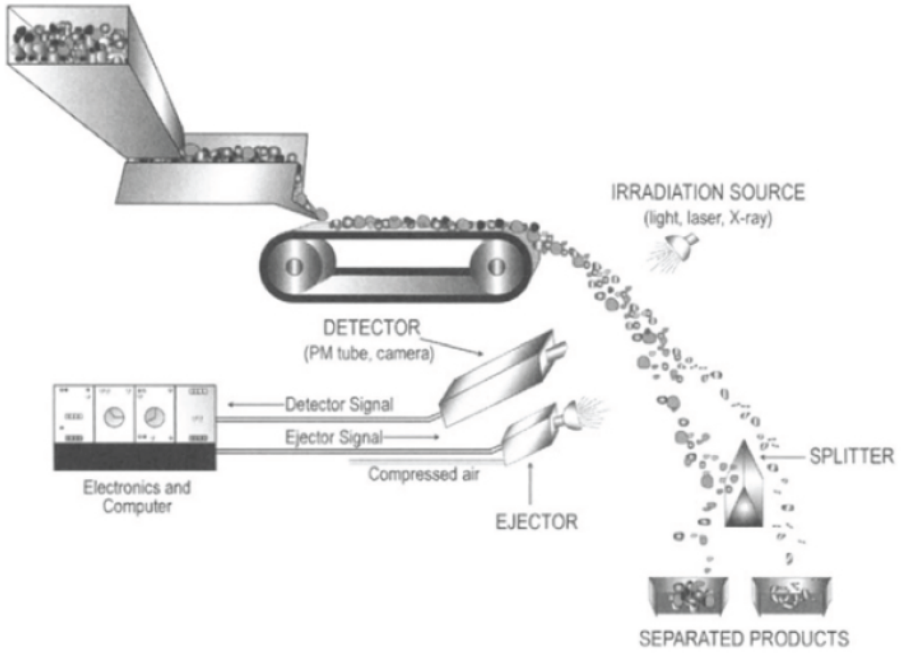

Figure 11: Schematic of Radiometric Ore Sorter[7]

PLANNING BATCH TESTWORK

Testwork Quality

The quality of testwork has been found to have a direct impact on plant start-up and more importantly on ramp-up and hence project economics.

The duration of a plant's ramp up period and whether at the end of ramp-up the plant achieves name plate capacity can invariably be linked to the diligence of the project team to include appropriate and sufficient test work.

Delays in plant startup can be costly and in some cases, it can result in the plant's premature shutdown. Based on the startup pattern of 41 greenfields projects, McNulty[10] found that there was a link between the extent of testing conducted during the process development and the plant ramp up time. This effect is shown in Figure 12. The characteristics for each series can be summarised as follows with respect to the testwork component:

- Series 1 – the plant flowsheet was based on mature technology. Thorough pilot plant testing was conducted on potentially risky unit operations,
- Series 2 – the plant flowsheet was based on a new process with incomplete pilot plant testing or pilot testing that was conducted on non-representative samples,
- Series 3 – Very limited pilot plant testing conducted on the plant flowsheet with some important process steps ignored. Feed characteristics were poorly understood,
- Series 4 – No pilot plant testing conducted on the plant flowsheet or process chemistry was poorly understood.

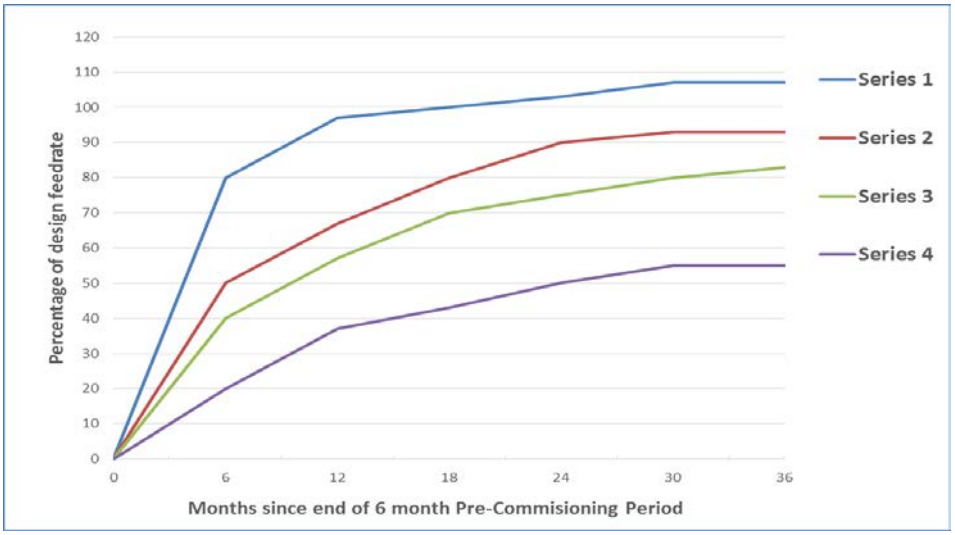

Figure 12: Design Feed Rate Achieved and Ramp- Up Time (McNulty Series 1 - 4[10])

Batch Testwork

When planning a batch test work program, there are some well tested guiding principles:

- Batch tests for uranium recovery can be conducted either in stirred tank or percolation columns.
- Batch tests are employed to optimize the process conditions of;
    - Temperature,
    - Reagent concentration,
    - Grind size,
    - Eh,
    - SG (Percent solids in case of tank leach or application rate for columns).
- Batch tests (and not pilot) are employed to establish the kinetics in dynamic leach processes. Pilot continuous with tracer testing is employed to corroborate the batch test outcomes.
- Batch tests initially focus on the Leach Step but are often extended to other building blocks such as thickening, filtration, solvent extraction, ion exchange etc.
- The common lixiviants in the case of uranium ores and concentrates are sulfuric acid and a sodium carbonate / sodium bicarbonate blend.
- Acid lixiviants are employed for both primary and secondary uranium ores where gangue acid consumption is acceptable.
- Alkaline lixiviants are employed on secondary ores and then only when gangue reagent consumers are at acceptably low levels.
- In some cases and where uranium mineral liberation permits a coarse grind in the leach step can be economically attractive particularly where gangue reagent consumption may be prohibitive at normal leach grind size.

Figure 13: Leach Tank for Coarse Grind Ore P80 = 1.5mm at 68% solids SG [(11)]

Critical to all batch leach testwork are the following objectives:

- maximise economic overall uranium recovery,
- minimise reagent input,
- consider only a sustainable process flowsheet and employ a process that delivers minimal harm to the environment (consider dry solid waste disposal).

Give consideration that the above objectives may only be achievable by processing an “accept” fraction from an upgrade process in order to minimize harm to the environment.

Open and Closed Circuit Testing

Batch leach testwork normally begins in open circuit with local fresh water employed in the make-up fluid.

Uranium recovery flowsheets are rarely one-pass open circuit and at some stage, it will be prudent to migrate to closed circuit testing.

In column leaches, it is customary after the basic leach parameters have been determined, to re-confirm the process conditions in a closed circuit with solvent extraction or ion exchange being employed to “close” the flowsheet. Refer to Figure 14.

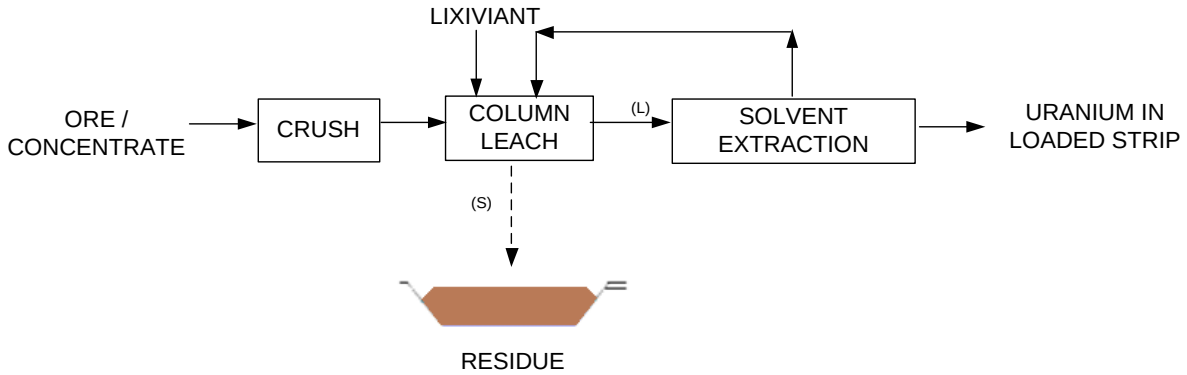

Figure 14: Example of a Closed Circuit Column Leach Flowsheet with Solvent Extraction

As the solute levels in the lixiviant build up in a closed circuit, recoveries may decline.

In the Lethlakane project, A-Cap Resources Limited discovered that high solute levels of 350 g/L did not materially impact the recovery of uranium in column leaches (refer to Figure 15).

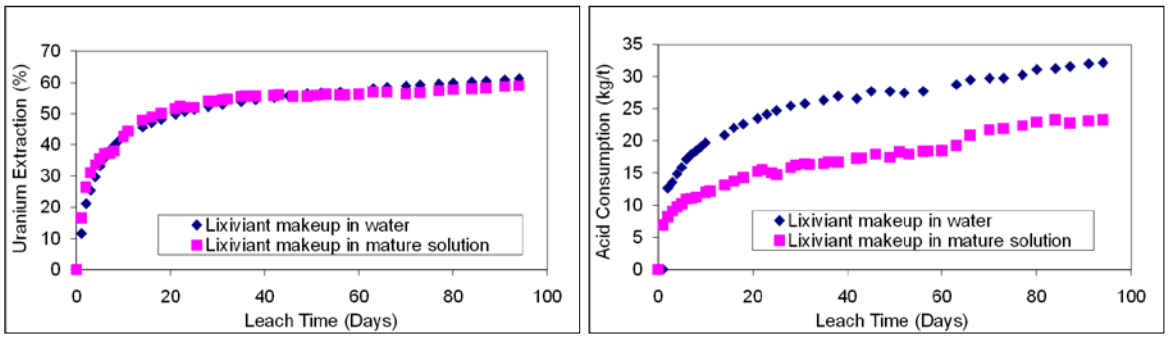

Figure 15: Column Leach Uranium Extraction and Acid Consumption Comparisons Between Lixiviant Makeup in Water and Mature Solution (Courtesy of A-Cap Resources Limited) [11]

Standard Batch Leach Tests

A Standard Batch Leach Procedure (SBLP) coupled to an economic model is invaluable for ranking competing ores.

The SBLP is normally developed from extensive leach trials and the geomet model.

Additionally, the SBLP would normally employs a synthetic lixiviant the composition of which is determined by the closed circuit mass balance.

Batch Lock - Cycle Testing

Batch lock-cycle leaches are sometimes employed in the form of intermittent bottle rolls and batch leach tests to establish the impact of recycles.

PLANNING BATCH VARIABILITY TESTWORK

Bulk ores are normally subjected to the standard batch leach procedures and the outcomes of that work applied to the geomet model.

However, where variability is significant and where the mine plan suggests that the variability cannot be “blended out”, it may then be prudent to consider these variability ores not only in batch leach testing but also for inclusion into a pilot plant campaign.

Table 1 shows that the Letlhakane project has at least two significant ores in addition to the dominant primary ores. The variability ores have varying levels of organic carbon compared to the primary ores. These two variability ore types, namely mixed oxide and mudstone, have been tested on a batch basis in open and closed circuit columns.

Table 1 : Letlhakane Uranium Project Primary and Variability Ores[12]
(Courtesy of A-Cap Resources)

Analysis	Unit	Kraken Primary	Gorgon Primary	Mixed Oxide	Shallow Mudstone
Al	%	9.22	10.01	8.38	13.3
Fe	%	0.68	1.15	2.72	0.99
K	%	0.50	0.41	0.00	0.54
Mg	%	0.11	0.12	0.10	0.42
S	%	0.13	0.68	0.2	0.05
Si	%	25.8	23.3	-	25.4
U	ppm	202	198	182	136
V	ppm	329	522	234	138
Total C	%	5.48	11.0	2.54	0.77
C Org	%	4.34	9.59	2.43	0.38
CO_3_C	%	1.14	1.41	0.11	0.39
Acid Neut. Capacity	kg H_2SO_4/t	17	7	NA	NA

The uranium in, for example, copper iron sulfide as derived from the Gawler Craton region in South Australia, reports to both the primary and secondary sulfides.

As can be seen from Figure 10, for the secondary sulfide, the uranium is locked in the iron oxides hosting the ore whilst some is surficial on the copper-iron-sulfide.

For the primary chalcopyrite rich concentrates, the uranium mineralization is both surficial and locked in the sulfides.

Because the uranium deportment was so different in the primary and secondary concentrates, batch testing was not considered to be adequate for the secondary concentrates and so piloting was embarked on to confirm sustainable removal of uranium[13].

The process employed a blend of metathesis and hydrothermal mechanisms in which the concentrate was subjected to a pressure leach in the presence of low concentrations of aqueous copper.

The reason for employing a copper leach was to alter the copper-iron-sulfides concentrate sufficiently to release uranium (and its associated daughters) whilst producing a super-concentrate with low levels (< 0.2 Bq/g) of uranium and enriched levels of copper.

Figure 16 shows the fractured mineral structure of the dominant concentrate created when iron from chalcopyrite ($CuFeS_2$) leaves the mineral particles.

It is this fracturing that is thought to create pathways for uranium to escape and allow the upgrade process to take place.

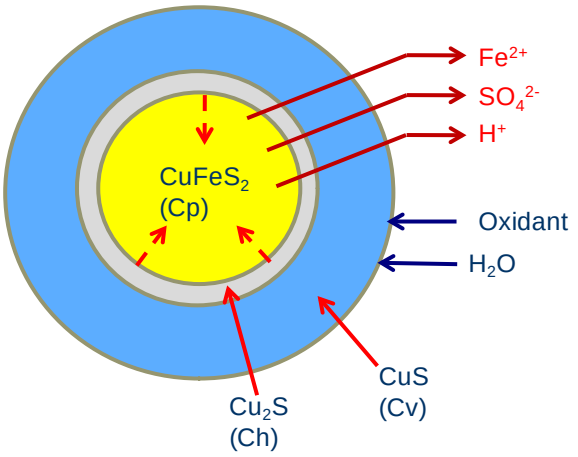

$$1.8CuFeS_2 + 0.8H_2O + 4.8O_2 \rightarrow Cu_{1.8}S + 1.8FeSO_4 + 0.8H_2SO$$

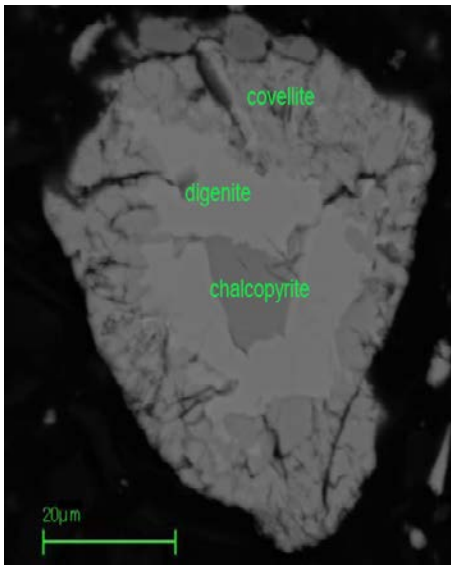

Figure 16: Chalcopyrite Alteration under Metathetic and Hydrothermal Conditions at > 200˚C

The kinetic relation for this process is given in Figure 17.

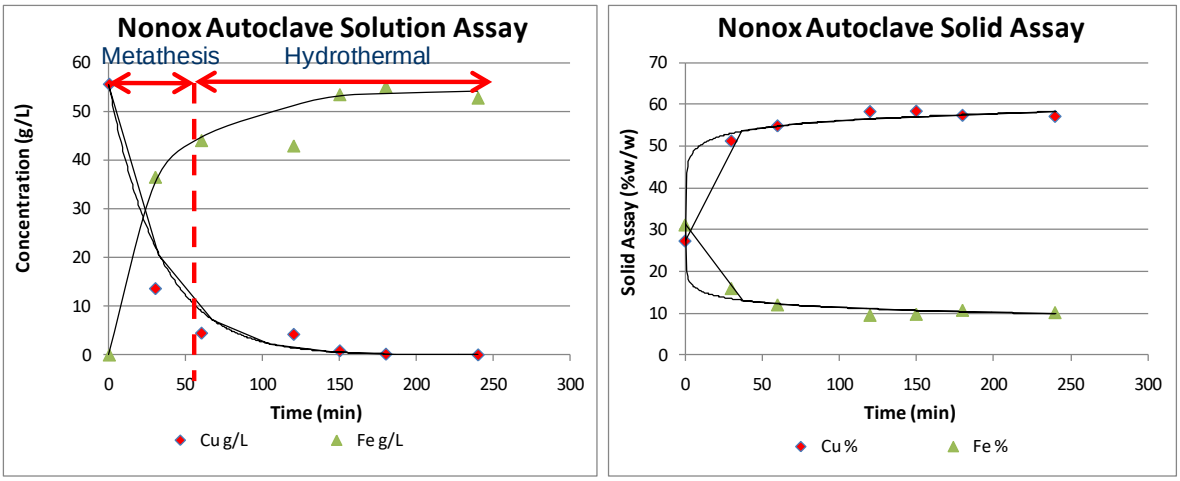

Figure 17: Concentrate Leach Kinetics

The mineral alteration is shown in Figure 18.

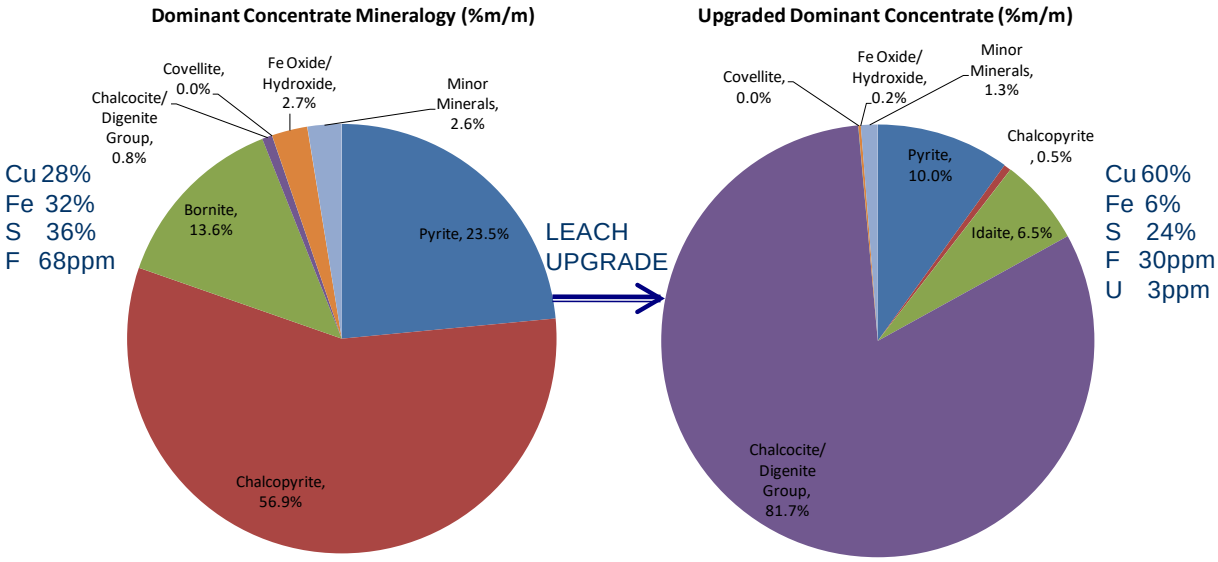

Figure 18: Dominant Concentrate Leach Feed and Product[13]

In the case of the Secondary Concentrate, the removal of uranium was less complete and kinetically impaired probably an account of the slow transformation of the iron oxides under weak acid conditions in the autoclave (see Figure 19).

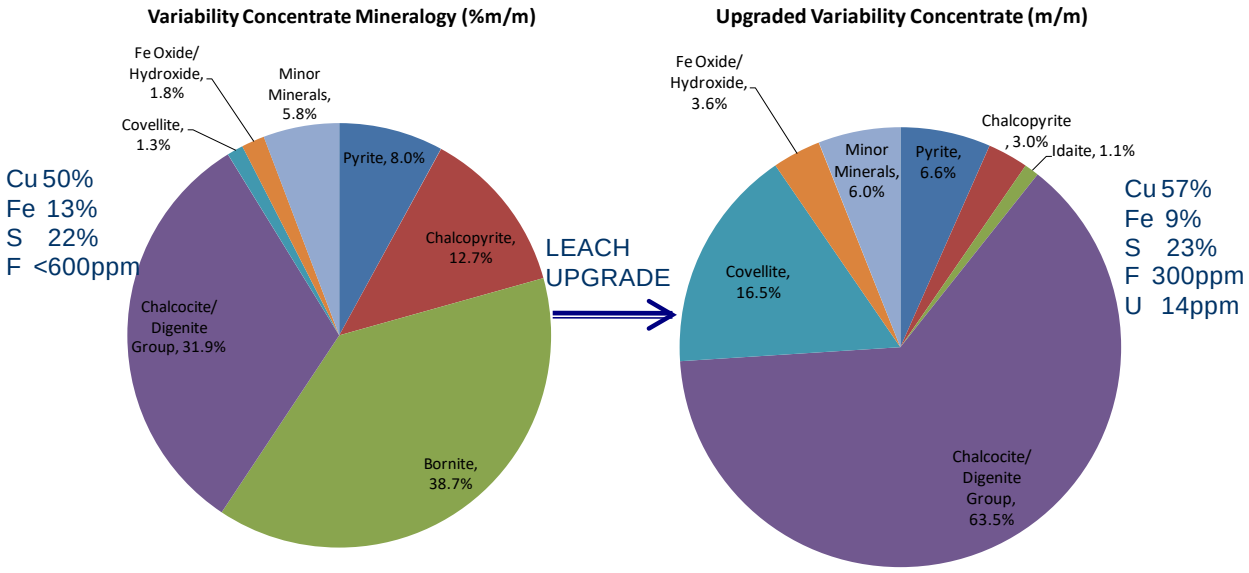

Figure 19: Variability Concentrate Leach Feed and Product[13]

PRE-PILOT INTERIM PROJECT COSTING

Well scoped closed circuit batch testwork generally provides sufficient data from which to develop interim project economics for the process plant. Interim Project Costing (IPC) is extremely valuable for guiding process flowsheet finalisation and is recommended as a pre-pilot decision making tool.

IPC is possibly best undertaken at a Scoping Study Level when the batch testwork has achieved an acceptable degree of completion.

The refinery circuit of a uranium flowsheet is reasonably well understood as far as risks and uncertainties are concerned. The important process costs are in:

- ore preparation,
- leaching,
- the leach “closing step” of solvent extraction and ion exchange, and most importantly,
- the tailings facility.

The outcomes of the study, both Capex and Opex, as well as projected revenue flows, can identify whether the project is ready to commit to a pilot campaign.

STUDY COMPONENTS AND SKILLS

Mass and Energy Balance

The important inputs to the mass balance are:

- Mine plan – the dominant and variability ore types,
- Quantitative mineralogy of these ore types,
- Quantitative mineralogy of the leach residues,
- Solid-liquid separation data relevant to the residues derived from the ore types,
- Inputs to the important process areas of ore preparation, leaching, leach closure and tailings disposal.

Preliminary Engineering

Preliminary engineering normally comprises:

- Process Flow Diagrams (these are also imported into the model),
- Process Design Basis,
- Mechanical Equipment listing with electrical power determined, and
- Simple plot plan of the plant.

Capital and Operating Cost Estimate

The study will provide an estimate of the process plant capital and operating costs to a level of accuracy as determined by the engineers.

Excluded from the estimate will ordinarily be:

- Pre-project expenses,
- Infrastructure,
- Mining,
- Closure.

The operating costs draw on the usual inputs of:

- Labour,
- Energy,
- Maintenance spares,
- Reagents and consumables,
- Residue disposal,
- Cost of sales.

Third Party Review

A third party review of the batch testwork and process economics is recommended prior to committing to a pilot campaign.

All the key building blocks of the flowsheet should be scrutinised using the IPC outcomes and opportunities to minimise costs should be interrogated. This may lead to a further iteration in the Batch Testwork program before the project is ready for continuous pilot plant testing.

SCOPING THE PILOT PLANT

The purpose of a pilot plant is to deliver data required for engineering the project's next phase. The production of uranium oxide concentrates (UOC) maybe a secondary objective.

Pilot Plant Service Provider (Laboratory)

It is important for the Client's team/ Consulting Engineer to provide a scope of work for the pilot plant. The scope of work is then issued to competent Laboratories to tender for the work.

In most cases, the Pilot Plant Laboratories do not know the test flowsheet as well as the Client's team does. As a result, the Laboratory needs to be provided with a scope of work that adequately address the pilot flowsheet so that it can assemble the pilot plant and also understand clearly what data is required. Laboratories are unable to guess the unwritten needs that the Client's team requires in an under-scoped program of work. This could lead to conflict and cost overruns at the expense of good data delivery.

Laboratories will also need to assemble a team of process, analytical and mineralogy specialist to deliver the pilot plant.

Process Engineering has moved on from the days when Laboratories were asked to provide a proposal without a written comprehensive work scope.

Scope of Work - General

The scope of work should address at least the following:

- Flowsheet to be tested
    - Process flow diagrams for all building blocks,
    - Process conditions for each building block,
    - De-scoped mass balance to pilot plant nominated flows to allow for equipment sizing and costing of equipment set up.

Figure 20 provides a sample flowsheet for a column leach campaign as part of an integrated pilot campaign.

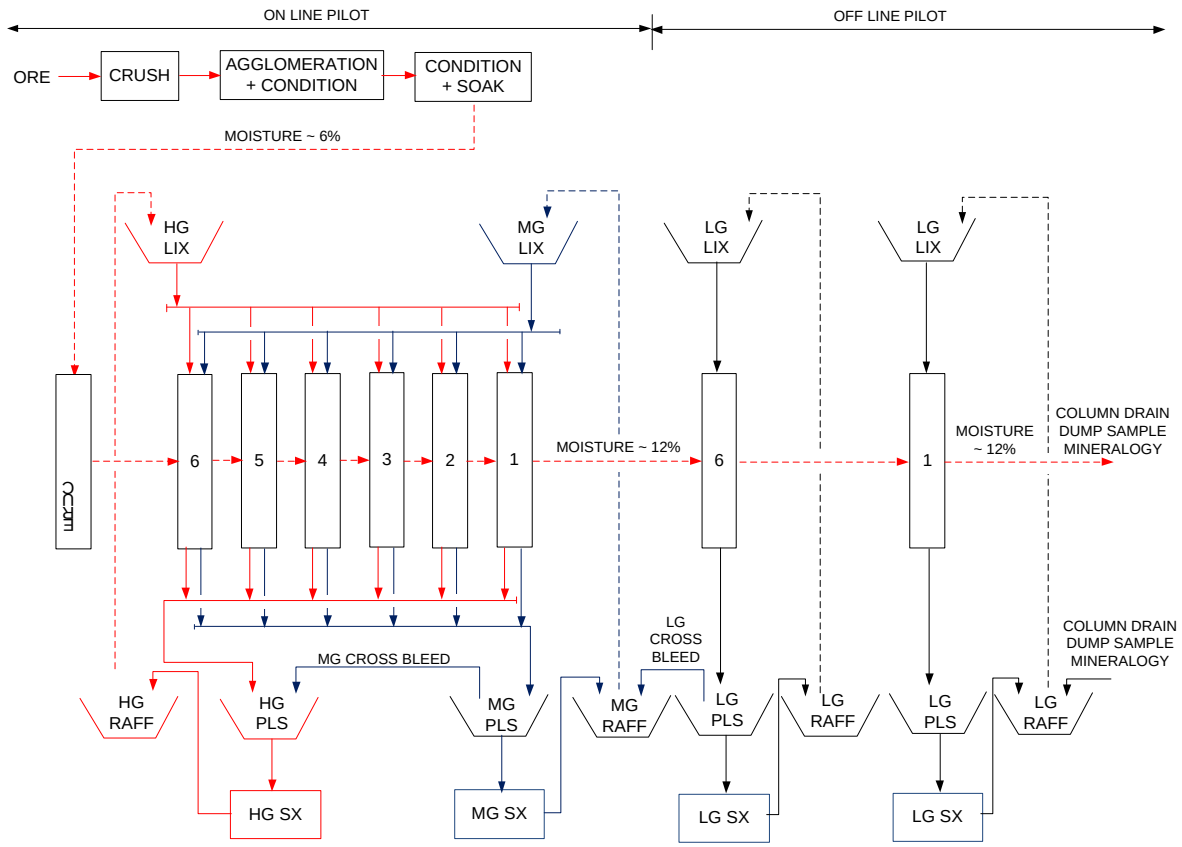

Figure 20: Example of Testwork Flowsheet

- Environmental Health and Safety

  Uranium is invariably accompanied by some of its daughters (refer to Figure 21 for the ^{238}U decay chain).

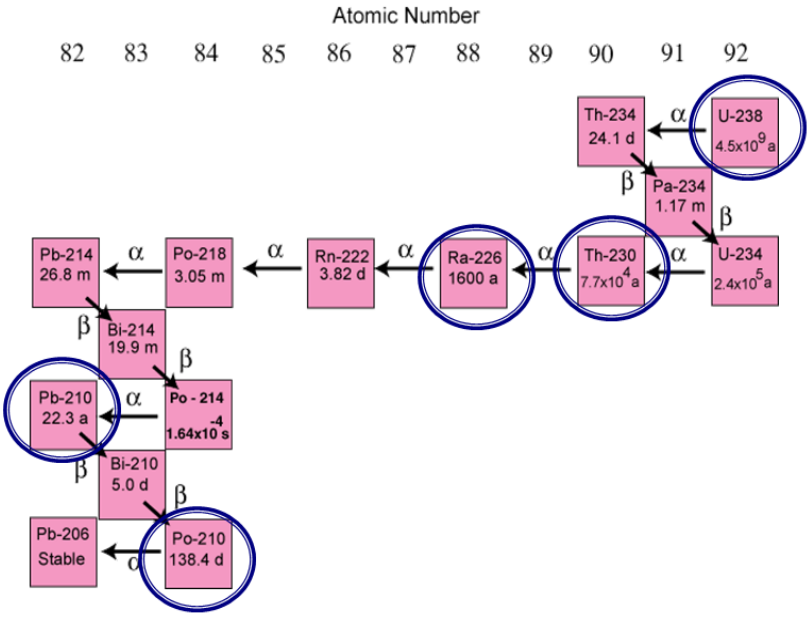

Figure 21: Uranium 238 Decay Chain[14]

In the case of primary uranium, there is normally a secular equilibrium between ^{238}U and its daughters. This equilibrium can be disturbed in the case of flotation concentrates where the activities of ^{210}Pb and ^{210}Po can often exceed that of the parent (refer to Table 2)

Table 2 : Radionuclide Assay of a High Uranium Copper Concentrate[15]

	DNA		Gamma			Radiochemistry
	U-238		Th-230	Ra-226	Pb-210	Po-210
	ppm	Bq/g	Bq/g	Bq/g	Bq/g	Bq/g
Drum 5 Composite	1179	14.6	14.8	14.1	17.9	18.6

Secondary uranium ores are generally derived from uranium that has leached from exposed granites for example and has moved as an aqueous front until it was attenuated in a location remote from its source. Consequently the equilibrium has been disturbed and the long lived daughter products are sometimes not present to any significant extent.

Laboratories need to be made aware of these alterations so that they can establish their Environmental Health and Safety plan for operating the pilot plant.

- Feed to Pilot Plant

  The Client is responsible for providing the dominant (and any variability) ores to the pilot plant. These are delivered to the Laboratory under a chain-of-custody. The ores tested normally represent the first 5 to 8 years of the project life.

- Pilot Periods to be Negotiated

  The pilot plant periods need to be agreed with the Laboratory. Included in this are:

  - Commissioning and ramp up – a reliability determining period,
  - Operating Periods – these could span one or more weeks. The duration will be dependent on the time to establish steady state. Any testing of variability ores could extend the operating period,
  - Breaks – for rest and relaxation.

- Pilot Plant exclusions

  The Laboratory should be requested to provide any exclusions whether called up or otherwise in the Scope of Work.

This assists the Client's team to understand what contingency may be needed in the budget. Exclusion could include:

- Return of ripios and waste to country of origin,
- Radio-assay etc.

Pilot Plant Deliverables

These include:

- Batch confirmatory testwork – (small column or batch tank leach tests) may be required to confirm the leach parameters. This is particularly the case if the pilot feed materials do not derive from an early batch testwork campaign,
- Synthetic lixiviants and water (site and process). Water may need to be calcium saturated to simulate plant process water,
- Vendor Tests:
  - Comminution testing,
  - In-line assay amenability,
  - Thickening,
  - Rheology,
  - Filtration,
  - Geochemistry tests,
  - Geotechnical tests.
- Analytical:
  - Sample preparation methods,
  - Analytical precision and tolerances,
  - Matrix matched standards and frequency of standards testing,
  - External laboratory cross checks.
- Nominated deliverables:
  - Control assay – including priority control assays,
  - Profiles and how they are to be presented,
  - Mass balance,
  - Daily metallurgical report,
  - Particle size determination,
  - Absolute density of solids,
  - Bulk density,
  - Transportable moisture levels,
  - Corrosion coupon tests for (see example in Table 3 below):
    - Alloys,
    - Coatings,
    - Glass (in cases where fluorides are present).
  - Scale mapping,
  - Mineralogy,
  - Retention time testing,
  - Gas analysis,
  - Radio assays,
  - Geochemical tests (e.g. Toxicity characteristic leaching procedure (TCLP) tests),
  - Geotechnical test,
  - ICP multi-element scans.
- Daily meeting and reports,
- Decommissioning and waste disposal for the laboratory to include in their pricing,
- Pilot Plant Testwork Report – normally, with an agreed table of contents,

Table 3 : List of Corrosion Coupon Specified for Testing in a Pilot Campaign

Location	Position	Materials of Construction												
		Ti Gr 2	Ti Gr 17	SAF 2507	SAF 2205	D411-350	D470-300	D441- 400	VE-8300	VE-8730	VE-8360	UHMWPE	HDPE	GLASS
No. 1 Leach Feed	Vapour			X										
	Slurry	X				X	X	X	X	X	X	X	X	
No. 2 Leach Feed	Slurry					X	X	X	X	X	X	X	X	
Reagent Trim Tank	Aqueous					X	X	X	X	X	X	X	X	
Leach Tank 2	Vapour	X	X											
	Slurry	X	X											
Leach Tank 5	Vapour													X
No. 2 Barren Liquor Neutralisation Tank	Slurry			X	X	X	X	X	X	X	X	X	X	

Adjudication of Proposals

Proposals are often requested from multiple Laboratories.

Alignment meetings with the Laboratories are recommended to ensure expectations on both sides are understood.

Consider adjudicating conforming proposals and then examine non-conforming bids on their merits.

The team selected for the adjudication process could comprise Consultants, Clients and Engineers. Generally allow 2 to 4 weeks for the proposal and alignment period.

As the scope of pilot plant may change during the testing period, a contingency commensurate with any envisaged scope growth is recommended.

MANAGING THE PILOT PLANT

The Pilot Plant activities need to be carefully managed to ensure:

- the objectives are achieved, and
- quality data produced is suitable for the next level of engineering.

Client Project Manager

The Client's Project Manager provides:

- technical oversight,
- reviews data and reports to the Laboratory Project Manager in a timely fashion,
- requests trouble shooting and reviews outcomes of investigations,
- ensures that data stipulated in the Scope of Work is being attended to.

Laboratory Project Manager

The Laboratory Project manager:

- provides operational management,
- manages the data flow according to Figure 22,
- leads the daily meetings at which the following data is presented and reviewed;
    - Daily Metallurgical Report and Mass Balance,
    - Control Assays,
    - Profile Assays,
    - Water Balance,
    - Trouble Shooting Outcomes,
    - Go-Forward Plans,
    - Any Vendor Activities and Special Samples.

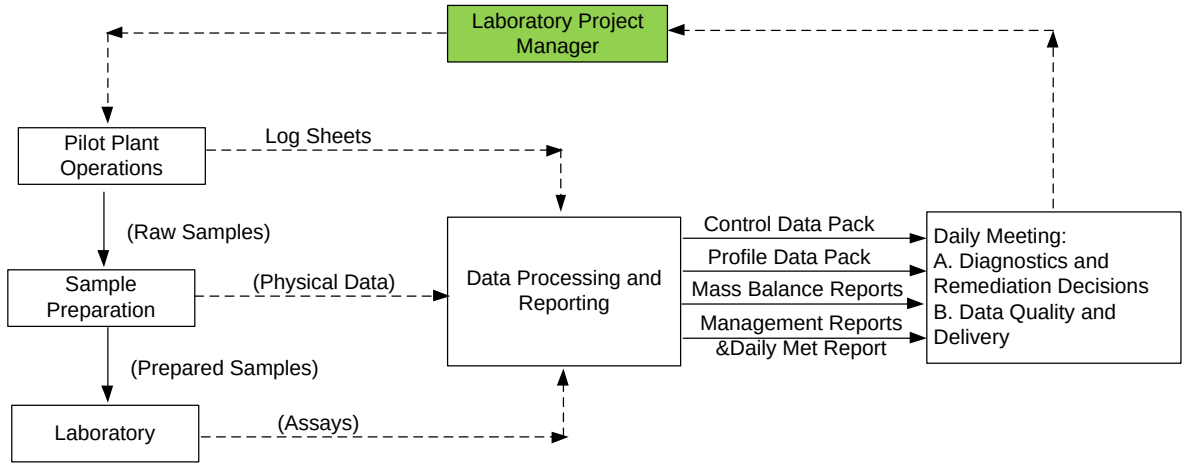

Figure 22: Data Delivery Structure

Water Balance

The water balance of a Pilot Plant can be delicate and is influenced by:

- Evaporation losses from elevated temperature steps,
- Sample abstraction,
- Sample return net of that required by sample preparation,
- Vendor samples,
- Spills and losses.

The expected sample load can be factored into the starting aqueous inventory so that only water top-up for evaporation is considered during the pilot campaign. The downside of this is the higher overall circuit retention time and the longer time to achieve steady state. See

Table 4 as a simple example of how a Pilot Plant retention time is determined.

Table 4 : Example of Pilot Plant Retention Time (refer Figure 23)

Equipment	No. of Tanks	Retention time per Tank (h)	Total Retention Time (h)
Leach Feed Makeup Tanks	2 (alternates)	3	3
Leach Tanks	5	3	15
Filter Feed Tank	1	2	4
PLS Tanks	1	4	4
Ion Exchange Circuits			4
Loaded Eluate Tank	1	2	2
Solvent Extraction Feed Tank	1	2	2
Solvent Extraction Mixer -Settlers	4E + 1 A/S, 3 Sc, 3S, 1W	0.5	6
Solvent Extraction Loaded Strip Tank	1	2	2
Sodium Diuranate Precipitation Tanks	4	1.25	15*
Sodium Diuranate Precipitation Thickener	1	5	5
SUBTOTAL (Leach, IX, SX, SDU)			62
SDU Resolution Tanks	2	2	4
Uranium Oxide Precipitation Tanks	4	1	12*
Uranium Oxide Precipitation Thickener	1	5	5
TOTAL			83

* Seed Recycle allowed for

Alternatively, a lower solution starting inventory could be considered; however, in this option, a solute and solvent (water) makeup will be required during the pilot campaign.

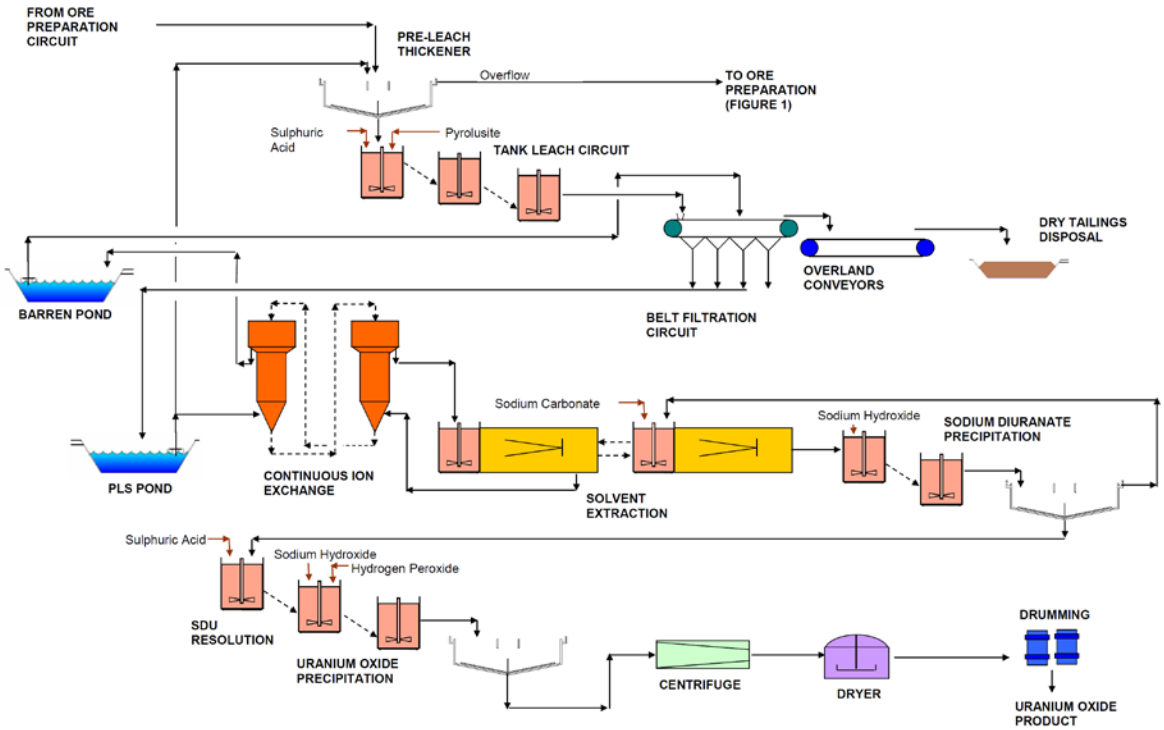

Figure 23: Example of Acid Tank Leach Flowsheet

Metal Accounting

Metal accounting across a pilot plant is vital to demonstrate the expected value metal recoveries. Generally, any uranium unaccounted cannot be assessed to be recoverable.

A typical metal accounting log across the flowsheet in Figure 23 is highlighted in Table 5.

Table 5 : Typical Met Accounting Proforma

Parameters	Wet Mass (kg)	Dry Mass (kg)	Volume (L)	U Assay (ppm)	U Mass (g)
INPUTS Ore / Concentrate First Fill					
TOTAL INPUT					
OUTPUTS MEASURED: UOC / SDU Samples - Assay - Vendor - Stored Off Tails - Residue Spills					
Measured Out					
CALCULATED: Open Stock (Tanks, Ponds, IX, SX) Closing Stock (Tanks, Ponds, IX, SX)					
Calculated Change					
GRAND TOTAL OUTPUT					
UNACCOUNTED					

WHEN TO CONSIDER DEMONSTRATION SCALE

Pilot plant data generated in a steady state conditions should provide;

- confirmation of the metallurgy and mineralogy of the process,
- the solid-liquid separation fluxes and related rheology,
- an early understanding of the deportment of scale, and
- the adequacy of any materials of construction that may have been tested.

For novel processes without an adequate operating reference plant or where there is uncertainty in the long term suitability of materials and/or equipment selection, there could be merit to consider an extended Demonstration Plant campaign.

Table 6 provides a high level comparison between Pilot and Demonstration Plants.

Table 6 : Comparison between Pilot and Demonstration Plants

Pilot Plant	Demonstration Plant
• Small equipment – laboratory bench top, • Provides retention time data, • Provides steady state assay data, • Provides steady state solid-liquid separation information, • Preliminary data on materials suitability, • Short running time (2 – 6 weeks), • Limited or no data on adequacy of mechanical equipment, • Cost range A$1 - 6 M (rental basis).	• Longer running time (4 to 5 months minimum), • Requires larger quantities of feed, • Permits longer term testing of materials of construction, • Employs real mechanical equipment, • Long term understanding on build-up of minor elements in closed circuit flowsheet, • Generally considered for novel or established processes with one or more novel steps, • Costs can be A$20-50 M or more (rental basis).

Risk Mitigation

Pilot and demonstration plant testing provides and additional level of risk mitigation over batch testing that will guide flowsheet development. Some are however prepared to design the commercial plant from Batch testwork. However, as shown by McNulty, inadequate testing may lead to long ramp uptime and the risk of not achieving the design throughput.

Demonstration scale testing provides additional risk reduction over what can be expected in a well scoped and managed pilot plant. Figure 24 and Figure 25 show typical pilot and demonstration plant filters. The filter presses employed in a uranium removal demonstration campaign (Figure 25) involved the use of inflatable membrane chambers. This filter press was fitted with commercial cloths and the cakes were washed with process fluids and finally squeezed and air blown.

Figure 24: Pilot Plant Pot Filters

Figure 25: Demonstration Plant Filter

In the extended running time of the demonstration plant, the long term adequacy of filter fabrics and the need for a cloth wash program was identified – thus extending the expected filter cycle time.

The longer running time of a demonstration plant permits additional data gathering. Figure 26 shows a Class 600 Titanium Grade 2 ball valve that failed two months into a demonstration plant campaign. A Scanning Electron Microscopy (SEM) study on the corroded ball confirmed crevice corrosion as responsible for the loss of metal.

Ball Valve Body Leakage

Valve Ball displaying Crevice Corrosion

Figure 26: Ball Valve Leakage and Ball Valve Crevice Corrosion

Figure 27 shows scale development on a Demonstration Plant leach reactor shaft. Mapping the scale growth rate assists in identifying the duration of an operating cycle in the commercial plant.

Figure 27: Metallurgical Scale on a Leach Vessel Agitator Shaft and Impeller

CONCLUSIONS

Pre-Pilot:

- Relevant ores / concentrates to be tested.
- Comprehensive Batch Dominant ore and Variability ore tests to be conducted.
- Testwork to actively embrace the final residue disposal method and any recycles therewith.
- Mineralogy of Feeds and Residues are critical to modelling the flowsheet.
- Consider upgrade and therewith minimise environmental footprint (be good stewards of what has been entrusted to us).
- Use Interim Project Costing as a tool to optimise the flowsheet.

Pilot Plant:

- Comprehensive pilot plant scope of work document aligns the Laboratory with Client's expectations and requirements.
- Pre-pilot batch and Pilot plant testwork thoroughness has been shown to impact the Commercial plant ramp-up and NPV.
- Pilot plants have a limited suite of deliverable restricted by short running times and frequent use of non-mechanical equipment.
- Pilot plant may not offer sufficient risk mitigation. A demonstration plant may be appropriate where the process is novel.
- A demonstration plant could cost at least 10 times more than a pilot plant and run for several months.

REFERENCES

1. Woolrich, P. and Large, P., Mineralogical Variation in the Letlhakane Uranium Project, Botswana and Implications on Process Options, ALTA 2010 Uranium Conference.
2. Northern Territory Government, Plans to Continue Clean-Up of Rum Jungle Legacy Mine, October 2016
3. Robinson, P., Best Practices for Uranium Mines and Mills: Where are they needed?, World Uranium Symposium, April 2015.
4. Metzler D, Moab Uranium Mill Tailings Remedial Action (UMTRA) Project Overview, IAEA Site Tour, 27 September 2016
5. http://geology.com/minerals/biotite.shtml
6. Taylor, A., Uranium Ore Processing Short Course, Alta Metallurgical Services, May 2010
7. Kumar, A., Ore sorting, TechnoMine, February 2014
8. Marsh, D., Development and Expansion of the Langer Heinrich Operation in Namibia, IAEA Tecdoc Series, June 2009
9. Tumas Project: Marenica Technology Licence Agreement Executed, Deep Yellow Limited ASX Announcement, September 2016
10. McNulty, TP., Minimization of Delays in Plant Startups, Society for Mining, Metallurgy and Exploration, 1 Jan 2004.
11. Dunn, G., and Teo, Y.Y., The Critical Role of Gangue Element Chemistry in Heap and Agitated Tank Leaching of Uranium Ores, ALTA 2012 Uranium Conference.
12. Cairns D., et. al., Letlhakane Uranium Project Alta Conference Presentation, Alta Conference, May 2013.
13. Weidenbach, M., Dunn, G. and Teo, Y.Y., Removal of Impurities from Copper Sulfide Mineral Concentrates, Alta 2016 Conference, May 2016
14. https://pubs.usgs.gov/of/2004/1050/uranium.htm
15. Urch, H., The Unique Properties of Methane Sulfonic Acid for the Mining Industry, Alta 2013 Conference, May 2013

Uranium-REE Proceedings

Project Development

AN UPDATE ON A-CAP RESOURCES' LETLHAKANE URANIUM PROJECT IN BOTSWANA

By

[1]Paul Woolrich, [2]Alan Taylor, [3]Grenvil Dunn and [4]Randall Pyper

[1]A-Cap Resources Limited, Australia
[2]ALTA Metallurgical Services, Australia
[3]Orway Mineral Consultants, Australia
[4]Kappes Cassidy & Associates, Australia

Corresponding Author

Paul Woolrich
pawoolrich@bigpond.com

Presenter

Alan Taylor
alantaylor@altamet.com.au

ABSTRACT

A-Cap Resources' Letlhakane Uranium Project in Botswana is globally one of the largest undeveloped uranium resources of 366 Mlbs U3O8. Extensive metallurgical testwork has been completed at SGS Perth and ANSTO over the last 8 years using a high acid heap leach process with an innovative SX/IX recovery process to achieve good recoveries. An extensive technical study completed in 2015 was used to support a Mining Licence application which was granted by the Botswana Government in September 2016 following EIA approval in May 2016.

Project economics, focusing on a higher grade resource consisting of 103.8Mt @ 450ppm U3O8 and targeting production of 9Mt ROM/annum averaging 3Mlbs/annum, is encouraging with operating costs of US$35/lb U3O8 for the first five years.

Future work will include optimising project economics by completing further feasibility studies including trial mining and grade control in selected areas to obtain better lithological controls on the mineralisation to refine the JORC compliant reserves and to confirm mining costs utilising surface miners. A-Cap also plans to carry out a Pilot Plant test programme using bulk drill samples to confirm process recoveries, operating and capital costs. These studies will be used to finalise mining and process design work.

Keywords: A-Cap, Letlhakane, Botswana, Uranium, Heap Leach, SX/IX, project economics, pilot plant

A-Cap Overview

CORPORATE

WELL FUNDED - with strong shareholder support

BASED IN BOTSWANA - safe and stable jurisdiction

EXPERIENCED MANAGEMENT- and technical team

Letlhakane Uranium Project Overview

- **Advanced Uranium Project** – Mining licence granted Sep-16
- **Environmental Impact Statement** – approved May-16
- **Surface Rights** – provisionally granted, Jun-16
- **Low cost mining and processing operation**
- **Low CAPEX** – all infrastructure available
- **Initial production (3Mlbs pa U_3O_8) - 18 year Mine Life***

  Project planned for early development and production - capitalising on recovery of uranium market
- **A-Cap production timeline -** in line with uranium market demand and price increases

Botswana

- Botswana ranks FIRST in Africa for political stability, democracy and rule of law
- Stable, multi-party democracy since 1966
  - Skilled mining work force
  - English speaking
  - Highest GDP per capita in Africa
- Mining accounts for 40% of current GDP and is critical for continued economic growth
- Botswana a safe and secure place to invest with an easy to understand mineral law and security of tenure

Letlhakane Uranium Project

- First uranium project in Botswana to secure a Mining Licence
- Environmental Impact Statement approved
- Provisional surface rights granted
- Shallow open pit mining operation with low cost acid heap leach to produce 3Million pounds U_3O_8 per annum
- Initial construction CAPEX of US$351 million*
- 3Mlbs p.a. U_3O_8 life of mine*

	DCR	Pre-tax	Post-tax
Project NPV*	8%	383M	240M
Project IRR*		29%	24%

- Operating costs of US$35/lb U_3O_8 over first 5 years and approximately $41/lb U_3O_8 over 18 year process life

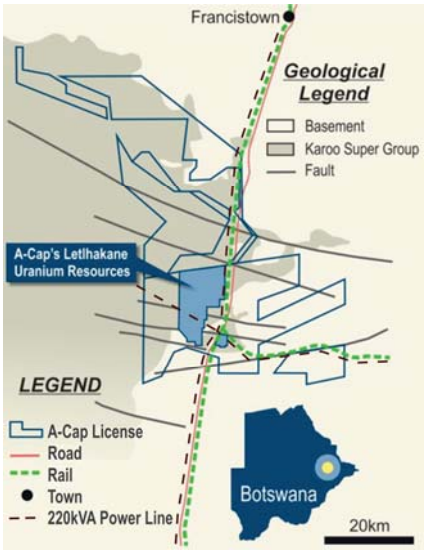

Letlhakane - Resource

- Global top ten undeveloped uranium resource of 365.7Mlbs
- Re-assessment of Total Resource was completed in September 2015 using Localised Uniform Conditioning (LUC)
- LUC method of resource calculation better reflects the mining method selectivity using continuous miners.

Cut-off (U_3O_8 ppm)	Total Indicated			Total Inferred			Global Total		
	Mt	U_3O_8 (ppm)	Contained U_3O_8 (Mlbs)	Mt	U_3O_8 (ppm)	Contained U_3O_8 (Mlbs)	Mt	U_3O_8 (ppm)	Contained U_3O_8 (Mlbs)
100	197.1	197	85.5	625	203	280.1	822.1	202	365.7
200	59.2	323	42.2	209.7	321	148.2	268.9	321	190.4
300	22.2	463	22.7	81.6	446	80.3	103.8	450	102.9

The above global mineral resource, completed by an independent expert and reported in compliance with the JORC 2012 code, was announced to the market on the 5th October 2015 ("release"). A-Cap confirms that it is not aware of any new information or data that materially affects the information included in the release and, in the case of estimates of mineral resources, that all material assumptions and technical parameters underpinning the estimates in the release continue to apply and have not materially changed.

Resource Growth

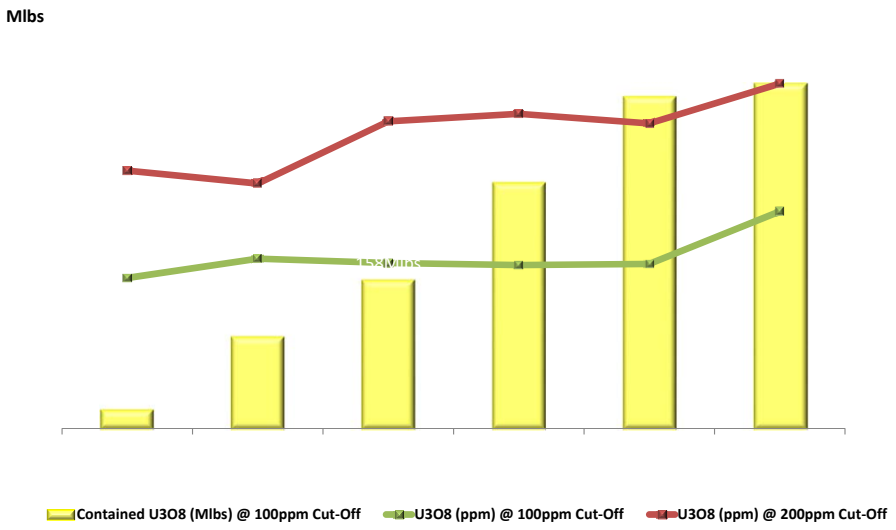

Major Infrastructure in Place

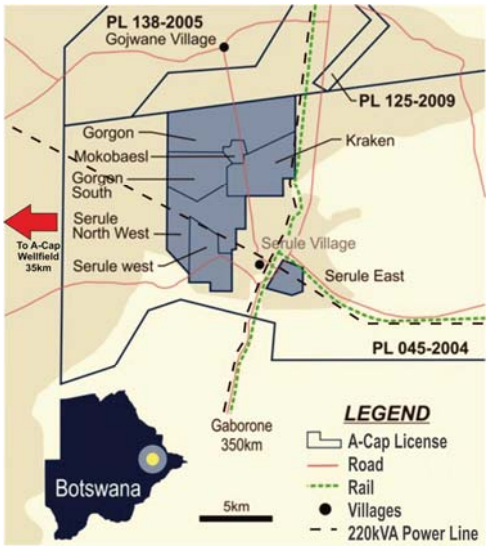

Rail
Road
Power
Water

Available

Experienced Management & Technical Team

- Highly experienced technical and operational team
- World best expertise in geology, mining, metallurgy, process design and development engaged
- Team with project development, infrastructure & construction expertise
- Board and management with strong track record of taking projects from exploration to production
- Demonstrated ongoing continuous improvement in project economics

Ore Body – flat, shallow, easy to mine

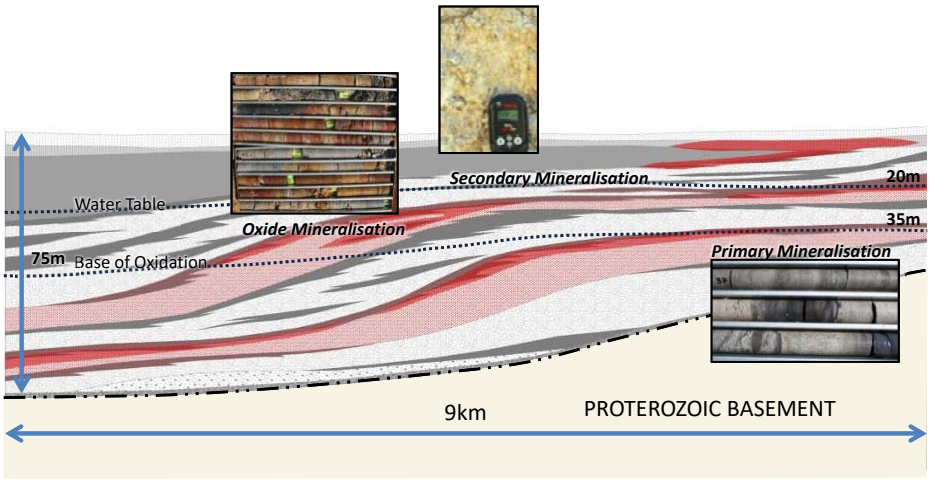

- Shallow, flat, simple, easy to mine, dips W at 1˚
- Layer cake type deposit with series of upward fining sequences

Ore Types

The boundaries of the three ore types are determined in the field by their relationship with respect to the base of oxidation and the “wet” season water table high mark:

- **Primary mineralisation is defined as that below the base of oxidation – 83% Resource**
- **Oxide occurs between the base of oxidation and water table – 16% Resource**
- **Secondary occurs between the surface and the water table – 1% Resource**

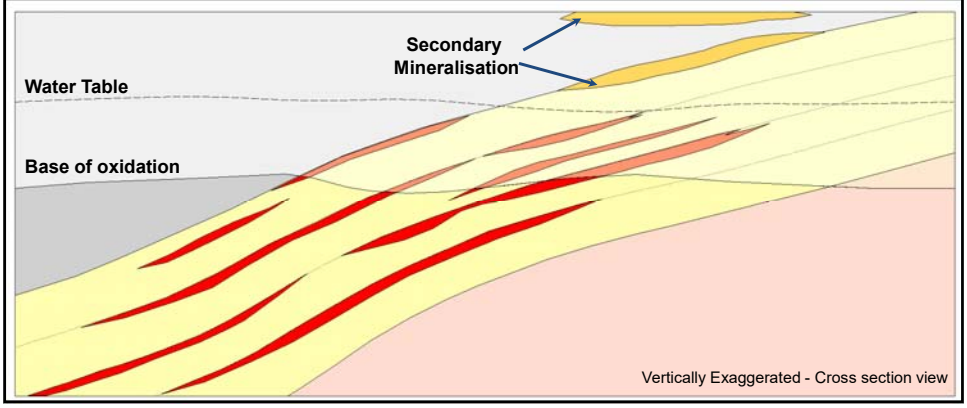

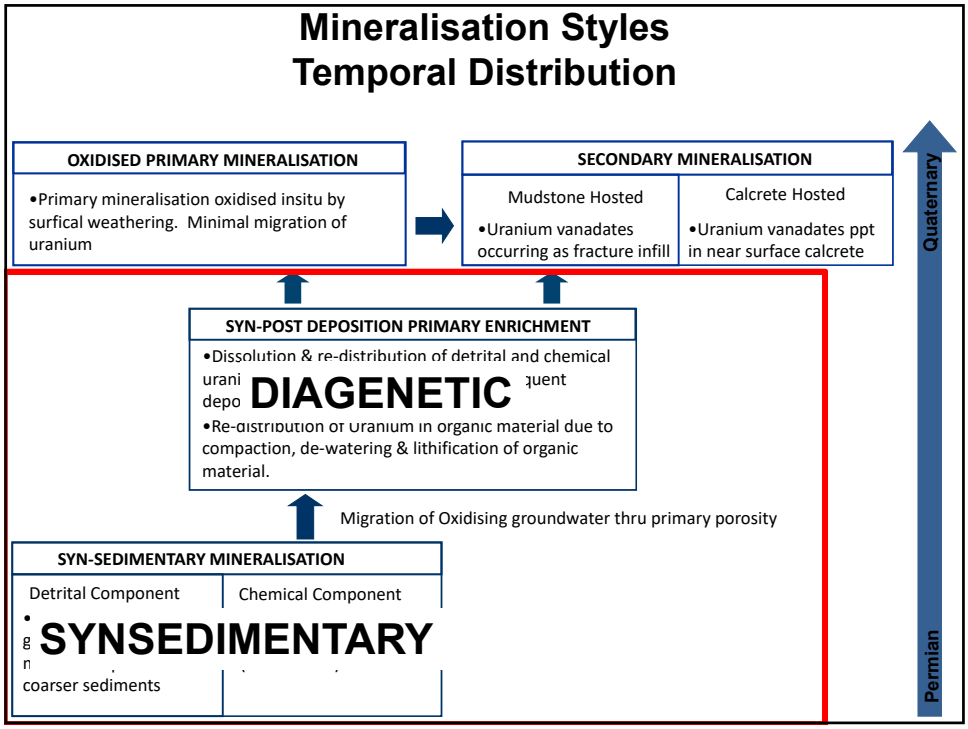

Mineralisation Styles

1. Primary Mineralisation

Syn-sedimentary uranium

- Detrital heavy mineral accumulations containing orthobrannerite, uraninite, uraniferous zircon, monazite
- Uranium ionically bonded to long chain organic molecules in carbonaceous mudstone (humate ore)

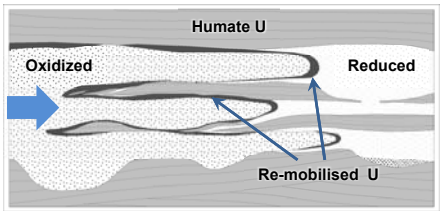

Diagenetic re-mobilised uranium

- Oxidized groundwater migrating through the sediments, liberated syn-sedimentary uranium and re-precipitated it in reductive portions of the stratigraphy
- Mineralogy: uraninite, pitchblende and humate ore

Mineralisation Styles

Oxide Mineralisation

2. Oxide Mineralisation

- Variable weathering of primary mineralisation to depths of up to 40 m.
- Distribution, grade & continuity of mineralisation mirrors primary occurrences
- Uranium remains largely in-situ
- Dominant species include coffinite and uranophane occurring as replacement of primary mineralogy

3. Secondary Mineralisation

- Hosted by pedogenic calcrete, calcareous mudstones and fractured, non-calcareous oxidised mudstone
- Developed above the watertable (15 m) via remobilisation of uranium from the oxide facies into the evaporative environment
- Dominance of hexavalent uranium minerals, e.g., carnotite, francevillite

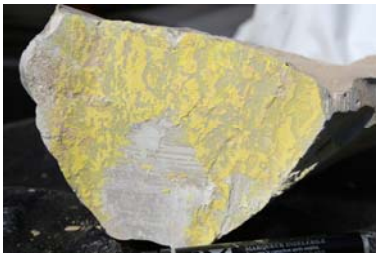

Summary of Ore Types – grain size

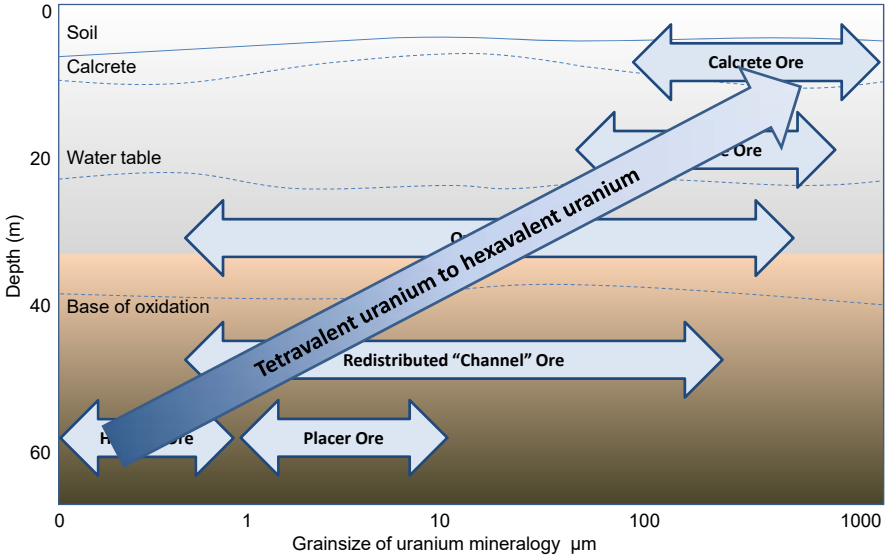

Metallurgy

Metallurgical Testwork

- Commenced at Mintek in 2008 but majority carried out at SGS Perth from 2009 and ANSTO from 2014
- Due to the overall low head grades of mineralisation a heap leach process is the preferred route
- Acid heap leaching of the Oxide and Primary ore indicates better recovery and leach kinetics compared to alkali leaching
- Alkali leaching of the Secondary ores is the preferred process route however this only accounts for 1% of the total resource
- Majority of initial acid heap leach column testwork carried out using minus 8mm crushed material

Metallurgy – Column Results

Acid leaching of primary & oxide ore

- Large number of mini, 1m & 2m columns completed using all ore types and mainly 2 acid regimes:-10kg/t acid at agglom/50g/L acid in leach & 25kg/t acid at agglom/100g/L acid in leach
- Data generated includes residue profile samples, sand traps at base of columns and mineralogical studies of feed and residue samples
- Results indicate that at lower acid strengths there is significant preg robbing – confirmed by comparison of 1m & 2m column results & profile residue samples
- Optimum leach conditions confirmed to be 25kg/t acid at agglom/100g/L acid in leach
- Using this acid regime on Gorgon primary ore gave similar recoveries for 1m, 2m & 4m columns – therefore leach extraction not affected by bed height
- Leaching using -19mm crushed material indicate similar recoveries to -8mm samples

Metallurgy – 2m Optimisation Columns

Total 17 x 2m column carried out at SGS

- 4 ores tested:- MO-Mixed Oxide, SWP-Serule Primary, GSP-Gorgon Primary, KRP-Kraken Primary
- Evaluated 3 crushed sizes (-8mm, -19mm & -30mm) & 3 acid regimes
- Acid regimes include 2 stage leach (25kg/t acid at agglom/300g/L acid leach stage 1 & 50g/L acid stage 2), single stage leach 25kg/t acid at agglom/100g/L acid in leach and single stage leach using 10kg/t/50g/L acid
- Results indicate that a 2 stage leach using 200-400 g/L acid in stage 1 improves recoveries and leach kinetics
- A top size of 19mm crushed material is optimum for the Primary and Oxide heap leach circuit
- This was followed up with 3X4m columns at ANSTO where the PLS was processed through a SX/IX recovery circuit

Metallurgy – 2m Optimisation Columns

Column	Ore Type	Crush Size, mm	Acid Regime	Calc Head ppm U	Recovery %
OT-1	SWP	19	2 Stage	335	76.5
OT- 4	SWP	19	25/100	313	76.5
OT- 5	SWP	19	10/50	321	73.3
OT-10	SWP	8	25/100	291	72.9
OT-14	SWP	30	25/100	284	75.1
OT-3	GSP+KRP	19	2 Stage	330	74.9
OT-9	GSP+KRP	19	25/100	313	72.4
OT-7	GSP	19	25/100	284	70.3
OT-12	GSP	8	25/100	288	70.0
OT-16	GSP	30	25/100	305	68.5
OT-8	KRP	19	25/100	271	67.3
OT-13	KRP	8	25/100	281	70.4
OT-17	KRP	30	25/100	274	70.4
OT-2	MO	19	2 Stage	218	68.0
OT-6	MO	19	25/100	208	64.6
OT-11	MO	8	25/100	212	65.2
OT-15	MO	30	25/100	207	67.8

Metallurgy and Process Design

- 4m column leach tests completed at ANSTO & confirm good recoveries
- The PLS from these columns were closed with the SX/IX circuit & achieved excellent recoveries
- Uranium Oxide Concentrate product from the refinery circuit contained low contaminants & no penalty expected
- Low cost and innovative process route
- Acid approx. 50% of total processing costs
- Investigating various options for local feed for our acid plant

Heap Leach Process Plan

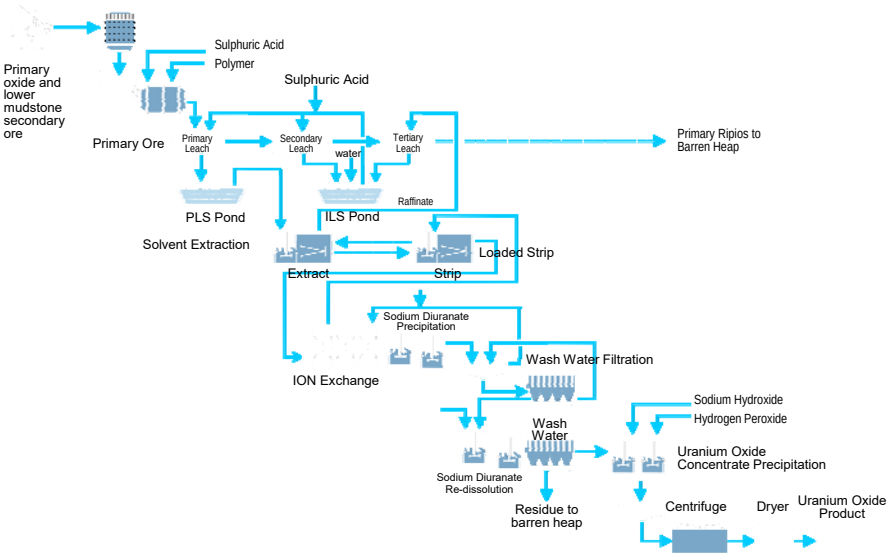

Mining

- Innovative mining using state of the art surface miners (below) in open pit operation
- Surface miners allow very selective mining, less expensive than conventional mining
- Optimal particle size of 19mm eliminating first stage crushing
- Falling contractors rates for contract mining

Wirtgen 4200 Direct Loading

Vermeer T1255DD

Uranium Market

Peer Group U_3O_8 Deposits: Grade U_3O_8 vs Contained lbs

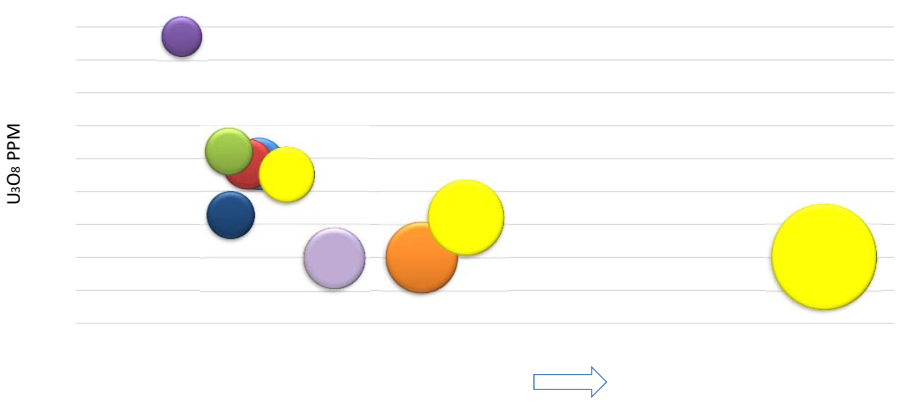

Uranium Market

Enterprise Value / lb U_3O_8 Mineral Resource

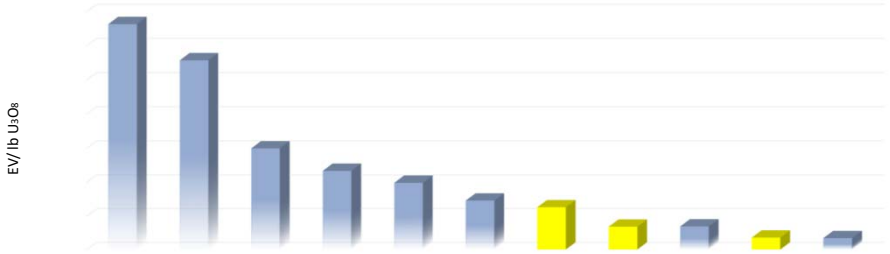

Uranium Market

447 reactors Operational*

59 under construction*

513 planned and proposed*

* Source: World Nuclear Association, Sep-16

Uranium Market

NUCLEAR ENERGY is the fastest growing ENERGY source globally

Forecast Uranium Prices

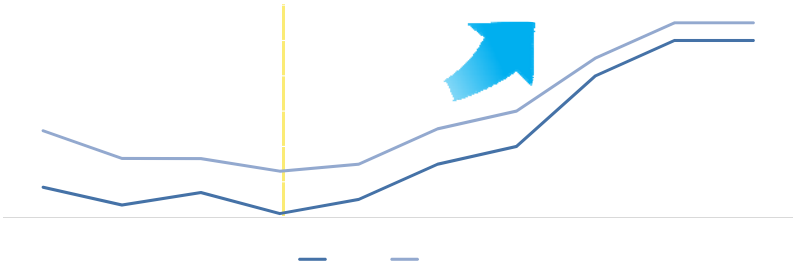

Uranium price source: Ux Consulting, WNA, RBC Capital Market Estimates Q2, 2016

Uranium Market

Prices must more than double to incentivise production and head off projected global uranium deficit

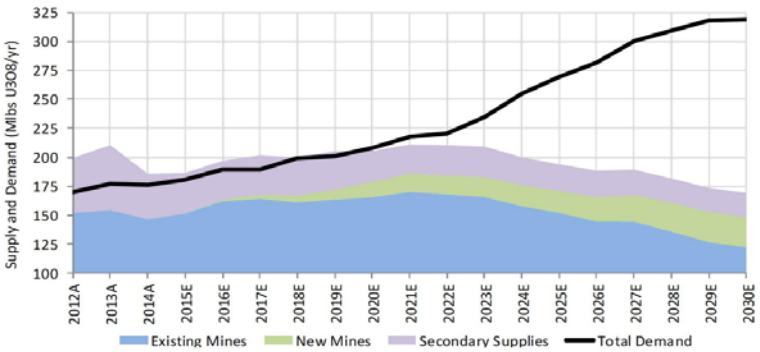

Above graph source: WNA, Raymond James, 2016

Road to Production

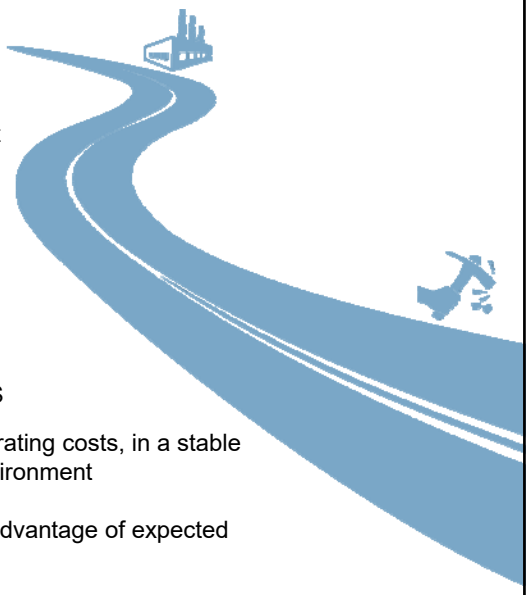

- Letlhakane has all of the key ingredients for a successful project and is one of the largest undeveloped uranium deposits in the world
- The mining licence was granted in September 2016
- Ongoing work will be directed at completing a JORC-compliant PFS
- Low capital costs, competitive operating costs, in a stable political and permitting friendly environment
- Project development will take full advantage of expected uranium price recovery

Planned Work

- Finalise PFS
- Pilot plant metallurgical work on bulk samples obtained from drilling will be undertaken
- Trial mining in selected areas will be done to assess surface miners as well as obtain better lithological controls on the mineralisation and grade control drilling
- In order for JORC reserves to be refined, further infill drilling is required
- Complete mining studies and pit optimisation and finalise metallurgical and process design work
- Board decision point to list on HK Stock Exchange

Summary

- **CREATE** – Serious value for shareholders
- **STRATEGY –** Prepare project for early production to capture upswing in the uranium market
- **SCALE -** Very large uranium deposit with significant high grade resource 103.8Mt at 450ppm U_3O_8
- **LOW CAPEX**– Low capital heap leach processing with all infrastructure in place
- **COMPARATIVE ADVANTAGE** - One of the few new sources of production with low Capex, competitive operating costs and low sovereign risk
- **STRATEGIC** - Discussions with strategic partners
- **BOTSWANA** - A safe and stable investment destination
- **STRONG REGISTER** – Strong on-going support from major shareholders

Uranium Investment Proposition

- **URANIUM** – Current price all-time low offering considerable upside
- **LONG LIFE –** The deposit style is perfectly suited to expansion with increasing uranium price. Perfectly suited to end user seeking a reliable long term U_3O_8 supply for nuclear builds.
- **WORLD CLASS –** Letlhakane ranks in the top ten undeveloped deposits in the world
- **SECURE JURISDICTION**– Botswana is a stable country with excellent infrastructure
- **CONTINUAL DE-RISKING**- Recent mining lease submission adds to the continual derisking of this project. Securing off-take and supply arrangements for heap leach processing
- **STRONG SHAREHOLDER BASE** – Well supported by major shareholders Jiangu Shengan Resources, Ansheng Investments & China Growth Minerals

Disclaimer

This presentation has been prepared by A-Cap Resources Limited ("A-Cap"). The information contained in this presentation is for informational purposes only and does not constitute an offer to issue, or arrange to issue, securities or other financial products. The information contained in this presentation is not investment or financial product advice and is not intended to be used as the basis for making an investment decision. The presentation has been prepared without taking into account the investment objectives, financial situation or particular needs of any particular person. No representation or warranty, express or implied, is made as to the fairness, accuracy, completeness or correctness of the information, opinions and conclusions contained in this presentation. To the maximum extent permitted by law, none of A-Cap, its directors, employees or agents, nor any other person accepts any liability, including, without limitation, any liability arising out of fault of negligence, for any loss arising from the use of the information contained in this presentation. In particular, no representation or warranty, express or implied is given as to the accuracy, completeness or correctness, likelihood of achievement or reasonableness or any forecasts, prospects or returns contained in this presentation nor is any obligation assumed to update such information. Such forecasts, prospects or returns are by their nature subject to significant uncertainties and contingencies. No representation is made that, in relation to the tenements the subject of this presentation, A-Cap has now or will at any time in the future develop further resources or reserves within the meaning of the Australian Code for Reporting of Exploration Results, Mineral Resources and Ore Reserves (The JORC Code).

Before making an investment decision, you should consider, with or without the assistance of a financial adviser, whether an investment is appropriate in light of your particular investment needs, objectives and financial circumstances.

By accepting this presentation, the recipient represents and warrants that it is a person to whom this presentation may be delivered or distributed without a violation of the laws of any relevant jurisdiction. This presentation is not to be disclosed to any other person or used for any other purpose and any other person who receives this presentation should not rely or act upon it. Information contained in this presentation is confidential information and the property of A-Cap. It is made available strictly for the purposes referred to above. The presentation and any further confidential information made available to any recipient must be held in complete confidence and documents containing such information may not be reproduced, used or disclosed without the prior written consent of A-Cap. This presentation must not be disclosed, copied, published, reproduced or distributed in whole or in part at any time without the prior written consent of A-Cap and by accepting the delivery or making to it of this presentation, the recipient agrees not to do so and to return any written copy of this presentation to A-Cap at the request of A-Cap.

The information relating to forecast production and project economics set out on slides 4 and 12 are based on the outcomes of a Technical Study which was previously released to the ASX on 11 September 2015 *"Mining Licence Application Submitted & Technical Study Outcomes"*. All material assumptions underpinning production targets or forecast financial information derived from production targets in the aforementioned initial announcement continue to apply and have not materially changed. The Technical Study outcomes and production targets reflected in this presentation are preliminary in nature as conclusions are drawn partly from indicated mineral resources and partly from inferred mineral resources. The Technical Study is based on lower level technical and economic assessments and is insufficient to support estimation of ore reserves or to provide assurance of an economic development case at this stage, or to provide certainty that the conclusions of the Technical Study will be realised. There is a low level of geological confidence associated with inferred mineral resources and there is no certainty that further exploration work will result in the determination of indicated mineral resources or that the production target itself will be realised.

PILOT TESTWORK FOR THE PROCESS DEVELOPMENT OF THE MULGA ROCK PROJECT

By

Chad Czerny, Andrew Wydler and Tony Chamberlain

Vimy Resources Limited, Australia

Presenter and Corresponding Author

Chad Czerny
CCzerny@vimyresources.com.au

ABSTRACT

The pilot-scale testwork programs conducted Vimy Resources Limited (Vimy) in support of the Definitive Feasibility Study (DFS) for the Mulga Rock Project are presented, and discussed with focus on the process development.

The Mulga Rock Project is located approximately 240 km ENE of Kalgoorlie in the Great Victoria Desert of Western Australia. The Project will have the capacity to produce around 1,360 tpa of U_3O_8 (~3Mlb U_3O_8), contained in a uranyl peroxide product, for a Life-of-Mine of up to 17 years. The Pre-feasibility Study for the project was completed in Q4 of 2015, with the DFS being finalised in Q3 of 2017.

Extensive continuous piloting programs to demonstrate the proposed project flowsheets were conducted during 2016. Approximately 34 tonnes of blended ROM ores obtained from two open-pit trial mines excavated at the Ambassador East deposit were processed in these programs.

The piloting testwork undertaken to develop the DFS process flowsheet is summarised and the implications of the results for the process selection for beneficiation (by gravity separation) and for downstream hydrometallurgical recovery of uranium are discussed.

The beneficiation plant proposed for ore processing comprises of: a ROM ore mineral sizer, logwasher for ore slurrying and attritioning, fines removal using hydrocyclones, and upgrading of a middlings fraction by mass rejection of between 45 and 50% of a siliceous fraction using two stages of Upcurrent Classification (UCC), to produce a uranium-enriched concentrate, and barren rejects (sands). The rejects are returned to the pit voids. Upgraded ore is ground and thickened to produce a leach feed slurry which is forwarded to the Uranium Hydrometallurgical Plant.

Uranium is extracted from the leach feed by agitated tank sulphuric acid leaching followed by recovery of the dissolved uranium in a Resin-in-Pulp (RIP) circuit. The eluate obtained by resin elution is upgraded by Nano-filtration, followed by direct precipitation using hydrogen peroxide to produce a uranyl peroxide hydrate ($UO_4.xH_2O$) product.

Keywords: "Mulga Rock", Uranium, Beneficiation, Resin-In-Pulp, Uranyl Peroxide

Mulga Rock Project

- Target production of 3Mlbs U_3O_8 pa for Life of Mine ~17 years
- 76.8 Mlb U_3O_8 Indicated & Inferred Mineral Resource
- 31.2 Mlb U_3O_8 Probable Ore Reserve
- 240 km east of Kalgoorlie mining centre
- Deposits covered by granted Mining Leases on unallocated Crown land

Project Location

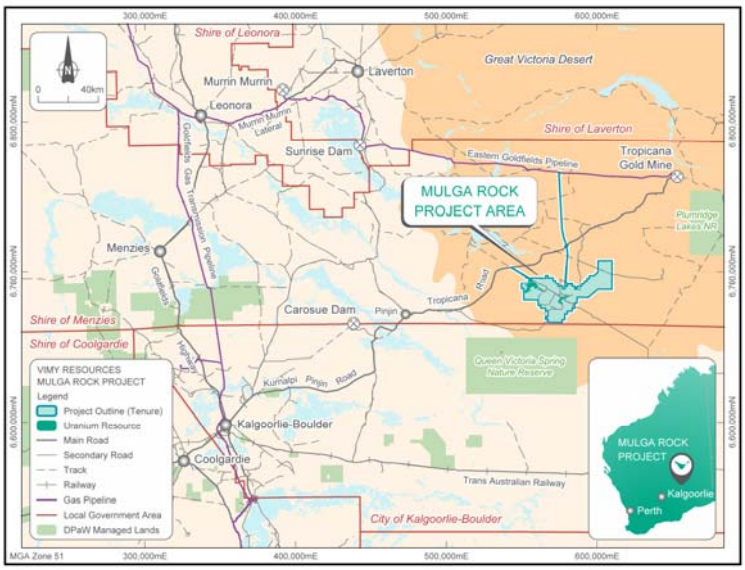

Mulga Rock Mineral Resource

Resource Estimates as of 7 November 2016

Deposit	Resource Estimate Classification	Cut-off grade (ppm U_3O_8)	Tonnes (Mt)	U_3O_8 (ppm)	Total metal U_3O_8 (Mlb)
Mulga Rock East	Indicated	150	21.1	720	33.4
	Inferred	150	13.0	340	9.8
Sub-total			**34.1**	**580**	**43.2**
Mulga Rock West	Indicated	150	1.9	680	2.9
	Inferred	150	31.8	440	30.7
Sub-total			**33.8**	**450**	**33.6**
Total Resource			**67.8**	**510**	**76.8**

This Resource estimate was released to the ASX on 7 November 2016. http://www.asx.com.au/asx/statistics/displayAnnouncement.do?display=pdf&idsId=01799630

Mulga Rock Deposits - Generalised Geology

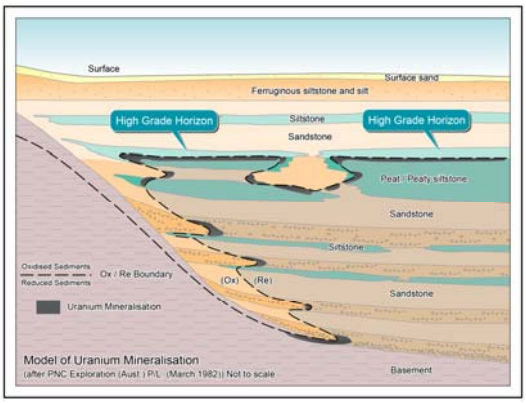

- Uranium hosted within weathered sediments: carbonaceous sandstones, shales and silts; sandy lignites and lignitic clays
- Significant supergene weathering -> oxidation of lignites -> metals dissolved and mobilised in oxygenated groundwater
- Enrichment of solubilised metals at Redox boundary; non-oxidised lignitic sediments below
- Most uranium as: finely disseminated **Uraninite (UO_2),** surface bound U(VI) ions on carbonaceous and clay minerals; minor refractory minerals (coffinite and brannerite)
- Polymetallic deposit - Base Metals (Co, Cu, Fe, Ni and Zn) as disseminated sulphides or nodules

Mulga Rock Ore Mineralogy - Process Implications

- Oxidising conditions required for dissolution of uranium minerals
- Lignite has a low SG ~1.2 – 1.4; focus on settling/thickening performance
- Adsorption of uranium onto carbonaceous minerals and clays
- Saline process feed water (~4 g/L Cl^-)

The MRP process flowsheet has been designed accordingly:

- Salinity assists settling of beneficiated concentrate
- Ferric ion used as chemical oxidant in Leach: U^{4+} -> UO_2^{2+} (*UO_2 readily soluble in slightly acidic oxidising conditions when liberated).*
- Resin-In-Pulp (RIP) process; affinity of selected IX resin for uranyl sulfate complex anion $UO_2(SO_4)_3^{4-}$ >> Lignite and clays

Process Development – DFS Continuous Pilot Testwork

- Vimy sought to demonstrate the process flowsheet as proposed in the PFS was commercially feasible and robust
- Enabled confirmation and validation of final process design criteria & engineering for the full-scale plant
- Provided an opportunity to “fine tune” the flowsheet
- Allowed vendor testwork on representative samples to confirm reagents, and equipment selection and sizings,
- Corrosion coupon testing (materials of construction)
- Generated final products for evaluation by refiners and potential off-takers

MRP Process Block Flow Diagram

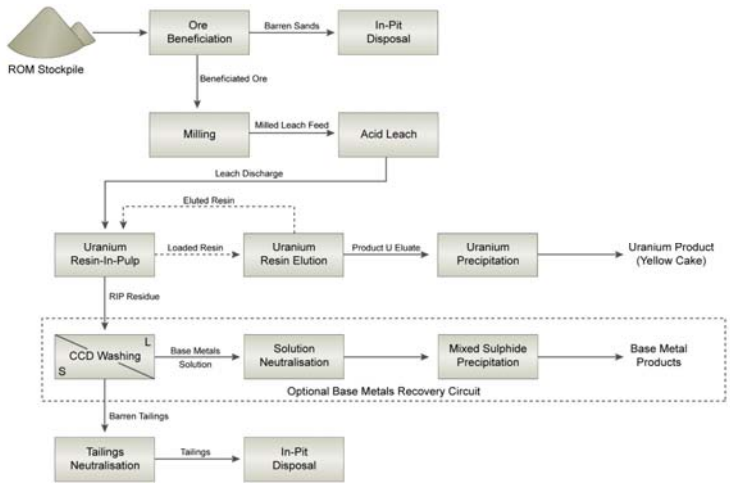

Each processing step was evaluated by piloting, with initial target operating conditions established from the PFS based on results of pre-piloting laboratory batch testwork.

Bulk ROM Ore Samples for Piloting (Trial Pits)

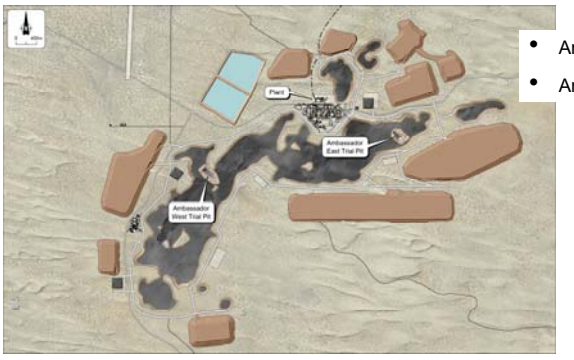

- Ambassador East – Mining Years 2-6
- Ambassador West – Mining Years 7-10

Bulk ROM Ore Samples /Blending

- Ambassador East pit: ~50t wet excavated, ~17t blended to generate bulk sample for beneficiation (target mine grade 1160 ppm U_3O_8); ~16t concentrate slurry (~ 28% w/w) produced
- Ambassador West pit: – ~50t wet excavated, ~ 17t blended to generate bulk sample for beneficiation (target mine grade ~660 ppm U_3O_8); ~22 t concentrate slurry (~29% w/w) produced

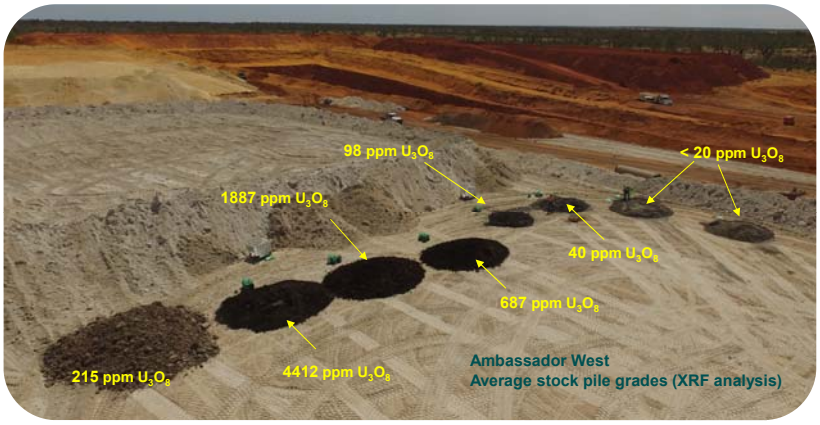

Ore Beneficiation Plant Schematic Flowsheet

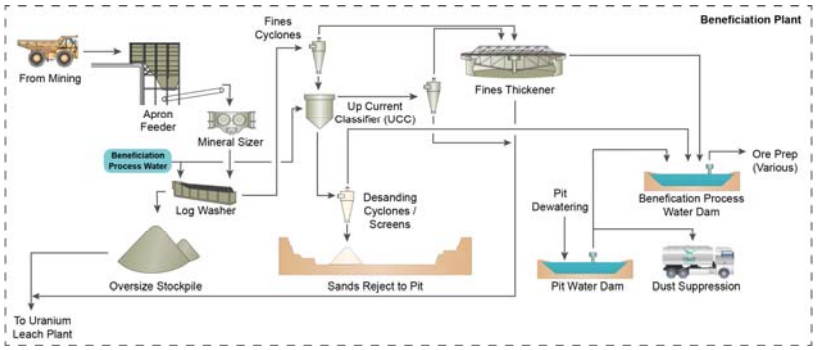

- Logwasher – ore attritioning and slurrying
- Coarse Screen – Logwasher discharges screened at 1.7mm
- Fines Removal – Fines removed by hydrocyclones at 150 μm
- Middlings fraction – two-stage UCC (Rougher / Scav. and Rougher / Cleaner piloted);
- UCC Underflow – “barren” sands dewatering (cyclones) / in-pit disposal

Ore Beneficiation Piloting – Logwasher Products

Stream	Size Fraction (mm)	Mass (% of ROM)	Uranium (ppm U_3O_8)	Uranium (% of total ROM)	
Feed	- 63	100.0	764	100.0	
Coarse	+1.7	13.3	2215	38.8	→ Screens
Mids	-1.7 + 0.15	58.5	187	10.8	→ UCCs
Fines	-0.15	28.2	1802	50.4	→ Cyclones

Ore Beneficiation – Pilot Testwork Key Results

Performance Indicator	Units	Ambassador East	Ambassador West
Uranium Recovery (to Leach Feed)	%	95.3	98.6
Mass Rejection (to Barren Sands)	%	52.2	47.3
Uranium Upgrade	ratio	2.1	1.9
ROM Head Grade	ppm U_3O_8	1,073	764
Beneficiated Concentrate (Leach Feed)	ppm U_3O_8	2,205	1,489
Barren Sands Uranium Grade	ppm U_3O_8	< 100	< 15

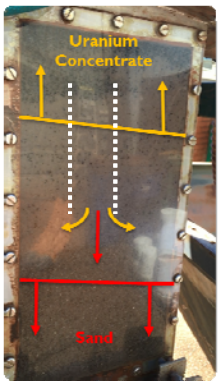

- Low (~15%) recovery of Uranium from Ro UCC tails with Scavenger UCC (-150 μm fines recovered but coarser lignite reporting to tails)
- UCC circuit reconfigured as Rougher /Cleaner with significant performance improvement
- Able to use higher upward water velocities in Rougher UCC -> increased recovery of U-rich coarse lignite as well -150 μm fines (plus silica gangue) – silica mostly removed by Cleaner UCC).

Batch /Pilot Ore Beneficiation – Comparison

- Mass rejection (lower than PFS) but higher U recoveries achieved than PFS
- Higher U recoveries can be targeted but at trade-off with lower mass rejection
- UCC Configuration: Rougher /Cleaner gave better U recovery than Rougher/Scavenger
- Based on results from both campaigns:
  - 45- 50% mass rejection (vs 55 – 65% from batch tests)
  - Uranium recoveries > 97.5% (vs 96 – 97% from batch tests)
- 2x Upgrade factor (ratio of uranium grade in beneficiated ore to the original grade)

Modified Ore Beneficiation Flowsheet (Piloting outcome)

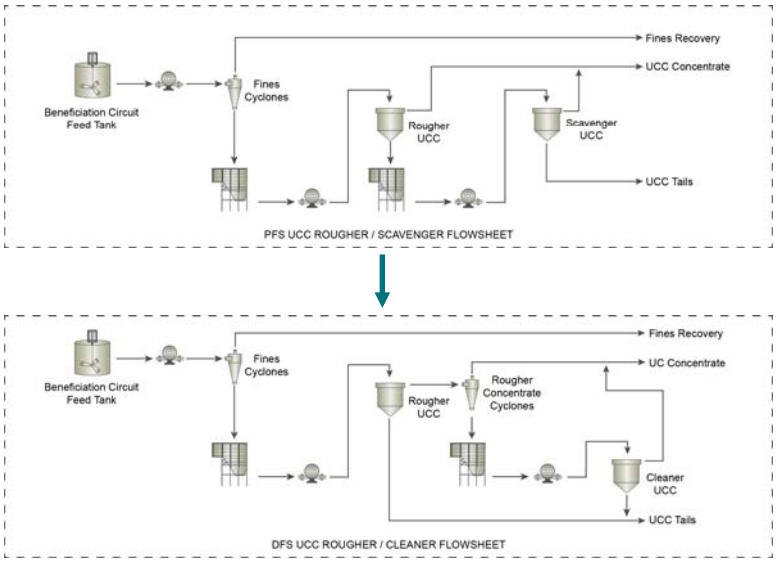

Modified Concentrate Thickening Flowsheet (Piloting outcome)

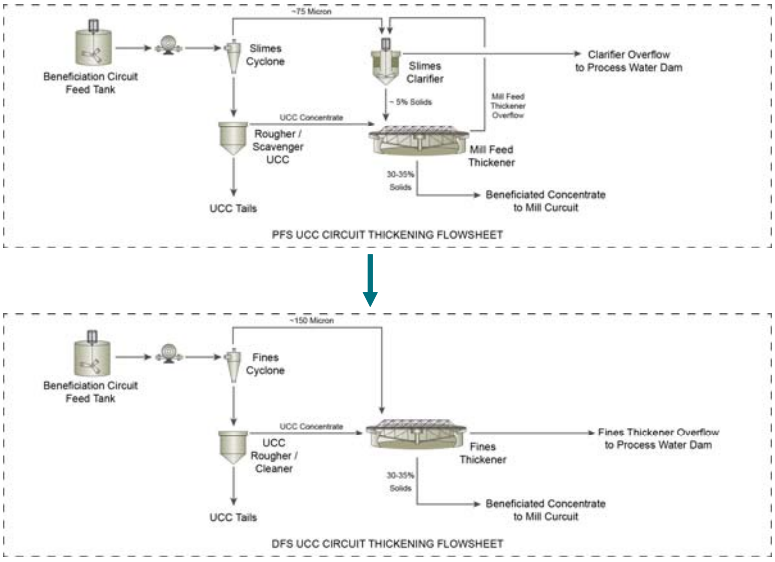

Uranium Hydrometallurgical Plant Flowsheet

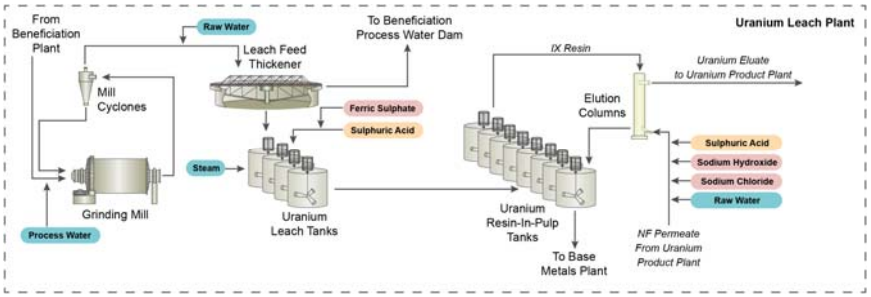

- Atmospheric agitated acid leach circuit
- Uranium recovered via continuous RIP; very few impurities are adsorbed (Fe, Zn)
- Loaded resin recovered by Primary and Secondary Screens
- Elution circuit - Scrub and Elution:
  - Loaded resin scrubbed with pH adjusted water (effectively desorbs most impurities)
  - NaCl solution used as eluent
  - Eluate (~ 2 g/L U_3O_8) treated via UF/NF -> U-enriched Concentrate (~ 20 g/L U_3O_8)

Continuous Pilot Plant: Integrated Leach – RIP – Elution Circuits

Leach Circuit Operation (~52 L/h)

Run 1 (AE) ~ 190 hrs; ~12 t slurry (~28% w/w)
Run 2 (AW) ~ 238 hrs; ~15t slurry (~30% w/w)
Run 3 (AE) ~ 79 hrs; ~0.8 t slurry (~28% w/w)

RIP Circuit Operation (~ 52 L/h)

Run 1 ~ 190 hrs; ~12 t slurry
Run 2 ~ 228 hrs; ~15 t slurry
Run 3 ~ 79 hrs

U-Leach Pilot Circuit – General Conditions

Parameter	Units	Ambassador East (Run 1)	Ambassador West (Run 2)
U in Leach Feed	ppm U_3O_8	~2230	~1480
C(T) in Leach Feed	%	~16	~25
Leach Residence Time (Design) *	h	3	3
Temperature	°C	60	60
Sulfuric Acid Addition	kg /t leach feed	~32	~33
Ferric Ion Addition	g/L feed solution	~2.2	~3.7
Leach Discharge Liquor - ORP	mV	~370	~376

*** > 93% of recoverable uranium is extracted within first 1-1.5 hrs**

U-RIP Pilot Circuit – Average Conditions

Parameter	Units	Ambassador East (Run 1)	Ambassador West (Run 2)
Contact Stages	No	8	8
Temperature (average)	°C	~50	~55
Slurry Residence Time	h	4.5	4.7
Resin Residence Time	h	~16	~16
Resin Concentration	% v/v	~9	~6
U in RIP Feed Solution	mg/L U_3O_8	~515	~536
U in RIP Discharge Liquor	mg/L U_3O_8	~17	~18
U Loading on Resin - range	g U_3O_8/L wsr	~25	~25
Residual U on Eluted Resin	g U_3O_8/L wsr	~3	< 0.2
OVERALL U Extraction (Leach & RIP) *	**%**	**~90**	**~92**

Batch/ Pilot Leach - Results Comparison

- **Batch Resin-in-Leach/RIP tests (using pilot plant Leach Feed):**

Ore	Acid (kg/t)	Fe^{3+} (g/L)	Feed U_3O_8 (ppm)	Leach U Extn. (%)	Final U Extn. Following U-RIP (%)
Amb. East	30	2.0	2 240	71	90
Amb. West	30	2.0	1 533	71	92

- **Overall Uranium Extractions (piloting):**
  > Ambassador East: 90% (at 35 kg acid/t dry leach feed; 3.0 g Fe^{3+}/L)

  > Ambassador West: 92% (at 30 kg acid/t dry leach feed; 3.5 g Fe^{3+}/L)

Leach/RIP Pilot Testwork - Important Findings

- Overall U-Leach/U-RIP Recoveries of Uranium of 90-93% from solids
- Increased leaching of BMs observed with the extended slurry residence time
- Extraction of Zn was largely unaffected by changes in leach conditions
- Extractions of Co, Ni and Cu increased with ferric addition
- Uranium concentration in leach/RIP residue decreased across RIP train as adsorbed uranium was recovered by the resin
- Kinetics of uranium loading onto resin was dependent on RIP tank temperatures
- Optimum RIP performance obtained with a resin residence time of 2h/stage
- Minimal resin degradation and bead breakage (< 1%) observed during piloting

Pilot Plant – Resin Screening/Wash - Elution Circuits

- Total (22 days) ~500L (wsr) resin eluted; ~6 m^3 eluate produced
- Primary and Secondary Resin Wash Screens
- Moving packed bed elution column
- Scrub Column effective in removal of impurities (Zn and Fe)
- Elution uses pH controlled NaCl solution
- Elution efficiencies for uranium: > 99.3% *(optimised operation)*
- Average eluate concentrations: 2.0 – 2.4 g/L U_3O_8 *(optimised operation)*

Resin Screening (500 μm)/ Washing

Column Elution Circuit

Uranyl Peroxide Precipitation (UPP) Schematic Flowsheet

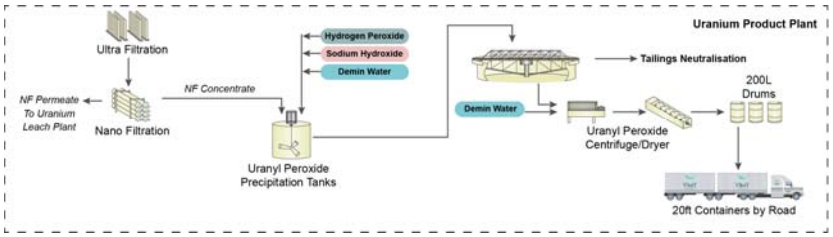

Uranyl Peroxide Precipitation (UPP) Pilot Testwork

- Conventional circuit (3 reactor tanks in series) using generally industry standard conditions; 120h operation
- pH maintained at ~3.5 in first tank via caustic solution addition
- 50% w/w H_2O_2 addition (stoichiometric excess to attain ORP ~500 – 540mV)
- Rapid precipitation kinetics: 99.2% in first stage (20 g/L reduced to ~80-200 mg/L U_3O_8)
- Uranium % precipitation target 99.9% (achieved)
- Terminal uranium concentration in discharge liquor: < 10 mg/L U_3O_8
- Thickener underflow recycled as “seed”
- Product thickening; washing and filtration (cf. centrifuge/dryer for commercial plant)

Uranyl Peroxide Product (Pilot Plant)

- Approx. 8.5 kg (dry basis) uranyl peroxide product obtained
- Uranium grade (> 82.5% U_3O_8) meets Standard Specification for Uranium Ore Concentrate (ASTM C967-13) *
- Product quality meets standard specifications with metallic impurity levels below “without penalty” limit
- Potential impurities originating from entrained process liquor such as Cl^- and SO_4^{2-} effectively removed by washing of precipitate filter cake
- Low S (0.07%); Low Cl (< 0.01%); Low Na (< 0.01%)
- Cu < 0.005%; Fe < 0.1%, Zn < 0.001%,
- SiO_2 < 0.03%; Zr < 0.02%; Mg < 0.09%
- K < 0.01%; Ti < 0.01%; P < 0.01%

Mulga Rock Project – Overall Process Schematic (and Stages Piloted and Successfully Demonstrated < 10 months)

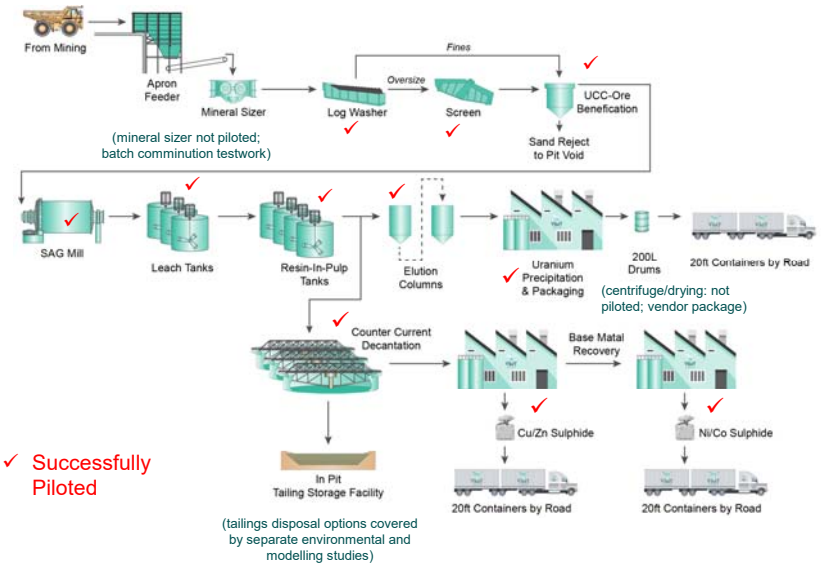

Conclusions

- Key Objectives of the DFS pilot testwork program fulfilled:
  - > Demonstrated that proposed MRP process plant can be successfully operated on a continuous basis
  - > Confirmed metallurgical performance and robustness of the plant flowsheet using two bulk composite samples from known periods of the project mining schedule
  - > Confirmed data input into DFS design criteria for the process plant
  - > Created representative process samples for vendor testing
  - > Generated final products: UPP and MSP for evaluation and analysis by downstream refiners
- DFS piloting identified areas of the PFS process plant flowsheet that could be optimised to improve both plant operability and plant performance; Identified flowsheet improvements have been incorporated into the DFS process plant flowsheet.

Acknowledgements

The provision of testwork and/or consulting services by the following parties is gratefully acknowledged:

- Allied Mineral Laboratories (Osborne Park, WA) – Gravity separation / UCC piloting (with ALS)
- Alfa Laval (Canning Vale, WA) – Tailings pilot centrifuge trial
- ALS Metallurgy (Balcatta, WA) – Mineral Processing Piloting Team / Batch Hydrometallurgy
- Ansto Minerals (Lucas Heights, NSW) – Hydrometallurgy, RN deportment studies and Consulting Services *(M.Maley, J.Quinn, K.Soldenhoff & the ageless guru Bob Ring)*
- BASF (Henderson, WA) – Flocculants
- Extrin Consultants (Canning Vale, WA) – Corrosion Coupon Analysis
- FLSmidth (Welshpool, WA) – Thickening testwork
- GR Engineering Services (GRES) (Belmont, WA) – DFS Manager and Study Engineer
- Outotec (West Perth, WA) – Filtration and Thickening testwork
- SGS Minerals Metallurgy (Malaga, WA) – Hydrometallurgical Piloting Group/ Batch Hydrometallurgy
- Bureau Veritas Minerals (Canning Vale, WA) – XRF/LA analysis; Tailings testwork
- Process Technical Review – R. Bradford, and S. LaBrooy *(consultants)*
- Veolia Australia and New Zealand (Bibra Lake, WA) - UF/NF testwork
- Dangerous Goods International (DGI) - UOC shipments

The authors also wish to thank the Management of Vimy Resources Limited for the permission to present at this conference, and acknowledge the technical input and support of fellow Vimians and the entire DFS team based both in West Perth and at the Mulga Rock site.

General Disclaimer

The purpose of this presentation is to provide general information about Vimy Resource Limited (**Vimy**); it constitutes a professional opinion only and is given in good faith. It is not recommended that any person makes any investment decision in relation to Vimy based on this presentation. To the extent that this presentation contains "forward-looking statements" they are only subjective predictions and are subject to inherent risks and uncertainties which could cause outcomes to differ materially from those expressed, implied or projected in such forward-looking statements. No representation or warranty, express or implied, is made by Vimy that the material contained in this presentation is accurate, reliable, relevant or complete, or will be achieved or prove to be correct.

To the extent permitted by law, Vimy and its officers, employees, related bodies corporate, agents and advisers, disclaim any responsibility for the accuracy or completeness of the material contained in this presentation and excludes all liability whatsoever (including in negligence) for any loss or damage which may be suffered by any person as a consequence of any information in this presentation or any error or omission therefrom. Vimy accepts no responsibility to update any person regarding any inaccuracy, omission or change in information in this presentation or any other information made available to a person nor any obligation to furnish the person with any further information. All amounts expressed are in $A unless stated otherwise.

METALLURGY OF THE NGUALLA RARE EARTH PROJECT – CHALLENGES, CHOICES AND INNOVATIONS

By

[1]Gavin Beer and [2]Roy Gordon

[1]Consulting Metallurgist, Australia
[2]Peak Resources, Australia

Presenter and Corresponding Author

Gavin Beer
gavin@metchemconsult.com.au

ABSTRACT

ASX listed Peak Resources Limited ("Peak") is developing the Ngualla Rare Earth Project in Tanzania. The project holds a JORC 2012 compliant Mineral Resource of 214.4 million tonnes at 2.15% rare earth oxides (REO) at +1% REO cut-off including a high grade weathered Bastnaesite Zone of 21.3 million tonnes of 4.75% at +1% REO cut-off. A Bankable Feasibility Study was recently completed based on a novel flowsheet which includes multiple stages beneficiation at Ngualla in Tanzania and calcination, selective leaching and separation into rare earth oxide products at Tees Valley in England.

This paper discusses how the metallurgical processes have been selected and developed to deal with the challenges of project logistics, processing technical risks and low rare earth prices which are faced by all existing and emerging rare earth producers.

Keywords: Process Development, Rare Earths, Bastnaesite, Alkali Roasting, Selective Leaching, Solvent Extraction

INTRODUCTION

Outside of China, both emerging and existing rare earth producers face many hurdles to ensure a profitable and sustainable business model is achieved. While each rare earth deposit has its own unique challenges, there is an underlying complexity within the sector of the combination of project location, processing technical risks and the present low rare earth pricing.

Project location is often understated as many gold and base metal operations have (and continue to be) successfully constructed and commissioned in remote locations. Rare earth processing, however, is significantly more complex and poses unique challenges. Molycorp's Mt Pass operation in California, USA was the largest integrated operation outside of China. This integrated mine, beneficiation, extraction and separation operation ceased operations in 2015, despite having excellent logistical infrastructure and access to cheap gas for power and steam production. Falling rare earth prices combined with a focus on cerium production and tight environmental operating constraints ultimately resulted in the economic unsustainability of the project.

Lynas Corporations' rare earth operations are reporting positive cash flows in 2017[(1)] by producing a rare earth mineral concentrate from the Mt Weld operation in Western Australia and exporting to their extraction and separation plant at Kuantan in Malaysia. The commissioning process was not without issues, however, with significant delays reported in the "cracking" (sulphuric acid baking) process in Malaysia[(2)].

Peak is especially cognisant of the challenges faced by previous and existing rare earth produces and has incorporated these learnings into their recently completed Bankable Feasibility Study[(3)].

NGUALLA RARE EARTH PROJECT

The Ngualla Rare Earth Project is centred on the Ngualla Carbonatite in southern Tanzania, 147 kilometres from the city of Mbeya on the edge of the East African Rift Valley as shown in Figure 1.

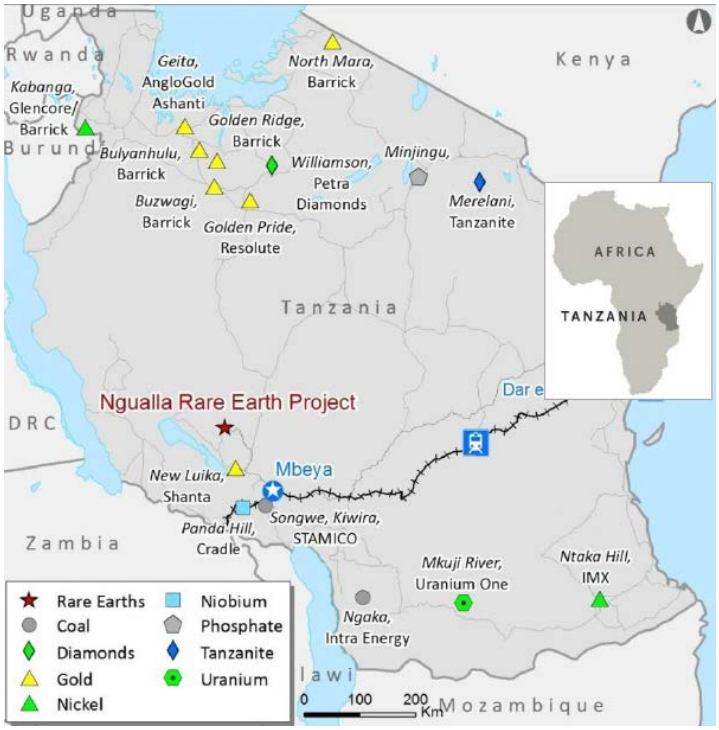

Figure 1: Location of the Ngualla Rare Earth Deposit

The Total Ngualla Mineral Resource estimate above a 1% rare earth oxide (REO) cut-off is 214.4 million tonnes at 2.15% REO. Included in the Total Mineral Resource is the Weathered Bastnaesite Zone Mineral Resource (Bastnaesite Zone) which consists of 21.3 million tonnes at 4.75% REO[(4)]. The relationship between the two Resources is shown in Figure 2.

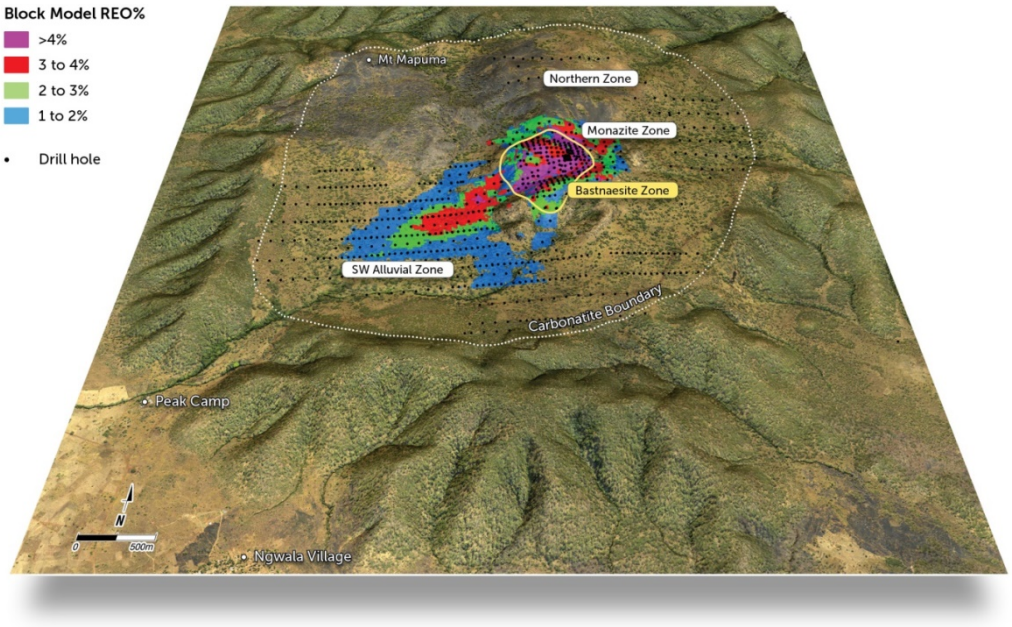

Figure 2: Oblique view of the Ngualla Mineral Resource Block Model

The Bastnaesite Zone, shown in the yellow ring in Figure 2, occurs as a thick blanket of high grade rare earth mineralisation from surface. The mining operation for this ore will be straight forward via low strip ratio open pit techniques.

MINERALOGY

The Ngualla deposit is extensive and contains a number of differing styles of mineralisation within the carbonatite complex. This presented an opportunity to examine if any mineralisation styles may be amenable to metallurgical upgrade and/or extraction.

The Bastnaesite Zone was selected as the initial target for development over the neighbouring Monazite and Alluvial Zones. In addition to being high grade and outcropping to surface, it also presents a metallurgically favourable mineralogy.

The rare earths are contained solely within the mineral bastnaesite, a mineral that doesn't require extreme chemical processing to "crack" the mineral matrix. The bastnaesite has some association with iron oxide gangue minerals, but can be almost completely liberated from the main gangue mineral of barite via grinding. This weathered ore also has the advantage of containing very low levels of phosphate, carbonate, uranium and thorium compared to other rare earth deposits. The mineral and gangue associations are shown visually in Figure 4 along with their relative proportions within the ore.

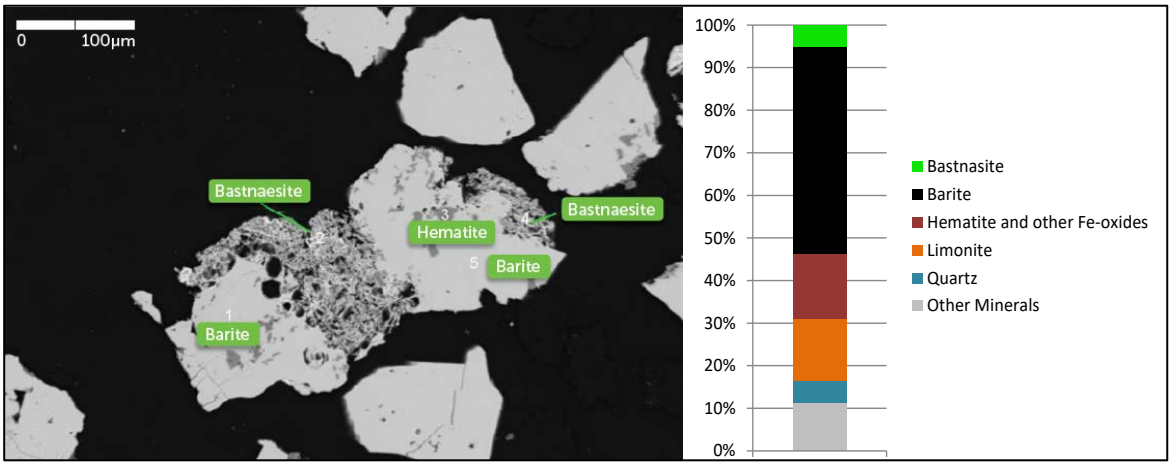

Figure 4: SEM Image of Bastnaesite Zone Ore and the Relative Proportions of Constituent Minerals

PROJECT LOGISTICS

Given the location of Ngualla, logic dictates that transporting large volumes of either ore (for the comminution stage) or reagents (for the extraction or separation stages) should be avoided where possible.

Rare earth processing is generally a long process, which can be grouped in to four basic stages: mining, beneficiation, chemical extraction and separation. Since this is a relatively long processing chain, there are opportunities to separate the processes in order to minimise high costs of operating in a remote location. As a generalisation, the cost, complexity and technical risk also increases at each stage of processing as shown in Figure 3.

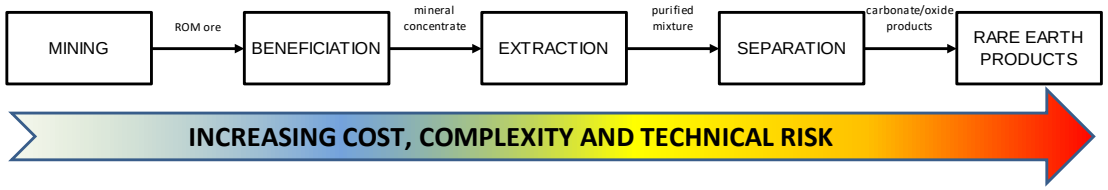

Figure 3: Generalised Stages of Rare Earth Processing

With regards to processing at Ngualla, there is a choice as to what stages are required (or are sensible to undertake) on site versus at what is appropriate at a secondary, more suitable location. Transporting of whole ore is clearly undesirable due to the large volumes and transport challenges. Likewise, extracting rare earths into a purified intermediate requires transport of large volumes of chemical reagents to site. It was therefore decided to focus on the production of a low mass, high grade rare earth mineral concentrate for transport to a second site. This was achieved through development of a robust beneficiation flowsheet, which is described in the following section.

BENEFICIATION FLOWSHEET

On the basis of mineralogical investigations, a beneficiation flowsheet was developed incorporating grinding, barite flotation, regrinding and finally rare earth flotation. A block diagram is shown in Figure 5 summarising the beneficiation flowsheet.

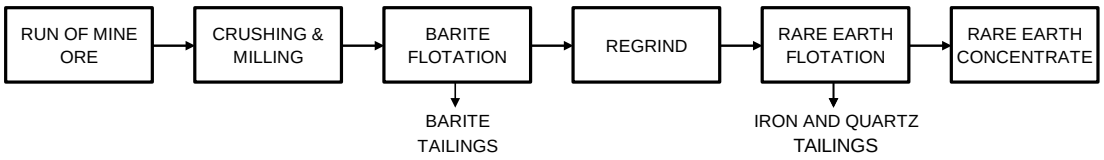

Figure 5: Beneficiation Flowsheet Developed for the Weathered Bastnaesite Mineralisation

As discussed previously, the barite is easily liberated from the bastnaesite through grinding, while the iron oxides are more intimately associated. This enables early separation of the barite which would otherwise float during rare earth flotation stage and dilute the final concentrate grade. Since barite makes up approximately 40% of the mass, a significant mass rejection is achieved during the barite flotation stage. The barite flotation tailings (rare earth containing stream) are reground to further liberate the rare earth from the iron oxides in addition to polishing surfaces prior to rare earth flotation. This stage concentrates the REO into approximately 5% of the overall mass at a grade of 45% REO.

This flowsheet was demonstrated at pilot plant scale on 56 tonnes of typical weathered bastnaesite mineralisation in December 2015 at ALS in Perth[5]. From an average feed grade of 5.9% REO, concentrate grades of up to 52% REO were achieved with an average grade of 40% for the entire program.

By selecting the Bastnaesite Zone as the initial target and designing the process around its favourable mineralogy, production of a low mass high grade concentrate is attained utilising conventional flotation technology. A small influx of non-hazardous freight and reagents (diesel, flotation reagents, mill balls, etc) is required and to produce a modest export quantity of 28,300 t/a of rare earth mineral concentrate. As an added advantage, the ability to produce a high grade/ low mass rare earth mineral concentrate opens up a wealth of choices with regards to downstream processing.

REDUCTION OF DOWNSTREAM PROCESSING TECHNICAL RISKS

Typically, rare earth processing flowsheets are complex and may include chemical cracking, multiple stages of leaching and purification prior to separation into products via solvent extraction (SX). From here, multiple SX circuits are required, with the total number mixer settlers often numbering into the hundreds depending on the number and purity required for the final products.

As the lead time from commissioning to full production depends on the technical risk of the process it is imperative to keep the process as simple as possible. Similarly, as downstream technical expertise is scarce outside of China, there is further risk utilising inexperienced operators. Therefore, in order to minimise commissioning and subsequent down time due to technical issues, it is important to keep the process as simple as possible and use conventional equipment where appropriate.

EXTRACTION FLOWSHEET

In addition to producing a high grade low mass concentrate, an advantage of selecting bastnaesite as the primary rare earth host mineral over others, such as monazite which is present within the Alluvial Zone, enables a choice of viable downstream processing options. Bastnaesite does not require energy and reagent intensive cracking processes to enable extraction of the rare earths, as the refractory phosphate minerals of monazite and xenotime do. It is amenable to simple acid leaching at low temperatures and also caustic conversion (reaction with sodium hydroxide solutions) at modest temperatures (up to 80°C).

Flowsheet Options

As there were multiple process options that were feasible for Ngualla's concentrate, a selection process was undertaken which consisted of a literature survey and diagnostic testwork in order to narrow down the most promising flowsheets for subsequent evaluation and optimisation via further metallurgical testwork. The two most promising flowsheets selected were the Alkali Roast and the Caustic Conversion processes. These two processes are shown in Figure 6.

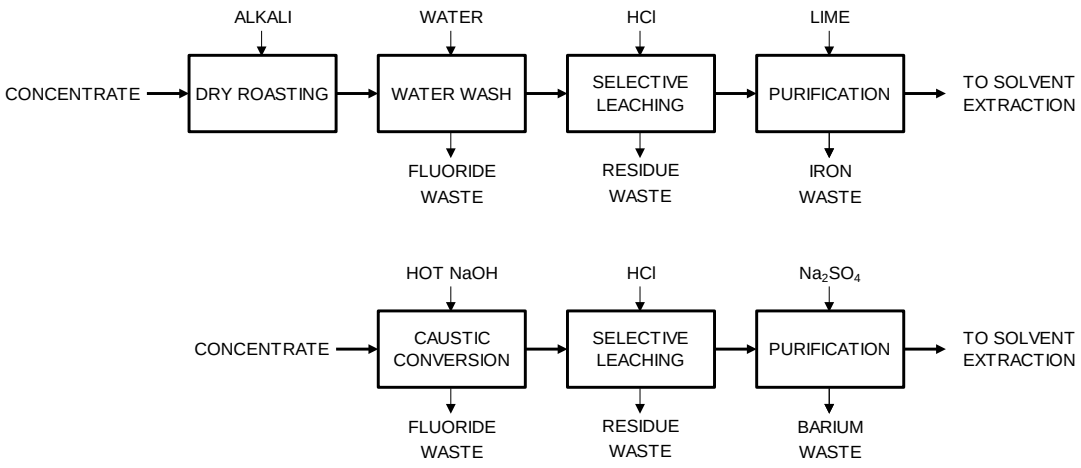

Figure 6: Alkali Roast (top) and Caustic Conversion (bottom) Extraction Flowsheets

Alkali Roast Process

The Alkali Roast process consists of dry roasting the bastnaesite with an alkali at elevated temperatures. During the roast process the following notable reactions occur:

- The trivalent rare earths in the bastnaesite (rare earth fluoro carbonate) are converted to weak acid soluble oxides.
- The trivalent rare earth, cerium, is converted to a +4 oxidation state, which is insoluble in weak acid.
- The iron oxides and hydroxides are converted to largely weak acid insoluble haematite.
- Any thorium present is also oxidised and rendered weak acid insoluble.
- The problematic (for down-stream processing) fluorine is converted to water soluble sodium fluoride.

Post roasting, a water wash first removes the soluble fluorides from the roasted solids. After this a selective leach is undertaken in weak hydrochloric acid (less than 1% w/w) targeting the trivalent (i.e. non-cerium) rare earths. The desired extraction of cerium can be controlled via adjustment to the roasting and acid leaching conditions. A small amount of iron is also dissolved and this is removed by simple pH adjustment with lime to precipitate the iron as a waste solid.

Caustic Conversion Process

The Caustic Conversion process, utilises a hot concentrated sodium hydroxide solution to breakdown the bastnaesite mineral matrix and solubilise the fluoride component, leaving rare earth hydroxides in the solid residue. A drying/oxidising stage can be implemented on the solids residue, if desired, in order to oxidise (and therefore reject) the cerium in a similar manner to the Alkali Roast. The residual solids containing rare earth hydroxides are dissolved in dilute hydrochloric acid along with some barium which is precipitated during purification via sodium sulphate addition.

Selection of the Alkali Roast Process

Metallurgical testwork was undertaken at bench scale on both processes and the results then modelled using SysCAD® in order to derive mass and energy balances and to estimate comparative capital and operating costs for a commercial operation.

While both flowsheets offered comparable metallurgical performance with respect to rare earth extraction, the ability to control cerium recovery and the SX feed solution purity; the Alkali Roast process was selected as it offered simplicity in operation through the use of conventional processing equipment operating at modest temperature and pH regimes. Ultimately this translated to a significantly lower capital and operating cost estimate compared to the Caustic Conversion flowsheet.

The Alkali Roast flowsheet was optimised at bench scale prior to comprehensively demonstrating the process at pilot plant scale at ANSTO Minerals (ANSTO) in Sydney during 2016 on the concentrate generated from the beneficiation pilot plant[6].

SEPARATION AND PRODUCT SELECTION

The selection of final products also has significant impact on the back end of the circuit; with the number of products and the purity of each product influencing the number of separation stages required along with reagent and power costs.

Peak successfully developed and demonstrated rare earth separation on the Ngualla mineralisation in 2013[7] at ANSTO's dedicated solvent extraction (SX) piloting facility producing samples of the following high purity products:

1. A middle and heavy (samarium to lutetium plus yttrium) rare earth oxide
2. A neodymium and praseodymium oxide

3. A cerium oxide

4. A lanthanum oxide

As a result of marketing research, off-take discussions and cost/benefit analyses, only the second product (neodymium and praseodymium or Nd/Pr) will be produced as a very high purity oxide as it accounts for 90% of the product revenue stream[3]. The other products will be sold as high purity carbonates. The resulting separation flowsheet that will be commercialised is shown in Figure 7 and represents the simplest arrangement to produce the required high value products specifications while minimising excessive costs, complexity and the associated technical risks.

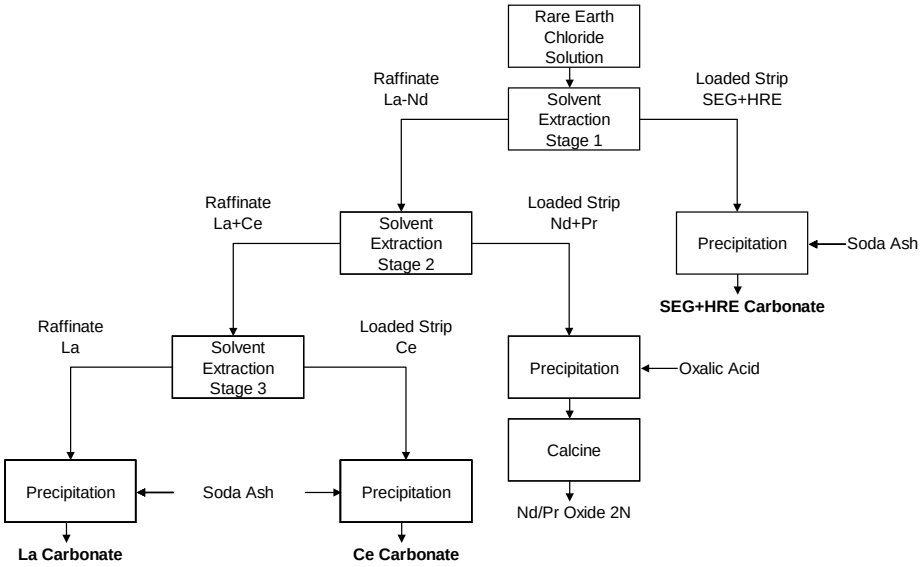

Figure 7: Separation Flowsheet

Of note was the decision to site the SX separation facility adjacent to the extraction facility, allowing for the purified rare earth solution to be sent directly to separation rather than going through a mixed rare earth intermediate product (e.g. carbonate, chloride etc.). This results in significant cost savings by eliminating the following:

- Additional reagents such as soda ash to precipitate an intermediate product and then acid to redissolve the intermediate.

- Additional equipment such as thickener, filter, drier and bagging plant.

- The need for packaging and transportation between the extraction and separation plants.

Additional cost reduction strategies, which are vital in the present climate of low rare prices, are discussed in the following sections.

LOW RARE EARTH PRICES

Rare earth prices recently hit a six year low after the boom experienced in 2011 as illustrated in Figure 8. It is now widely believed that prices have bottomed with recent price increases for Nd/Pr increasing 10% over the six months to April 2017[8].

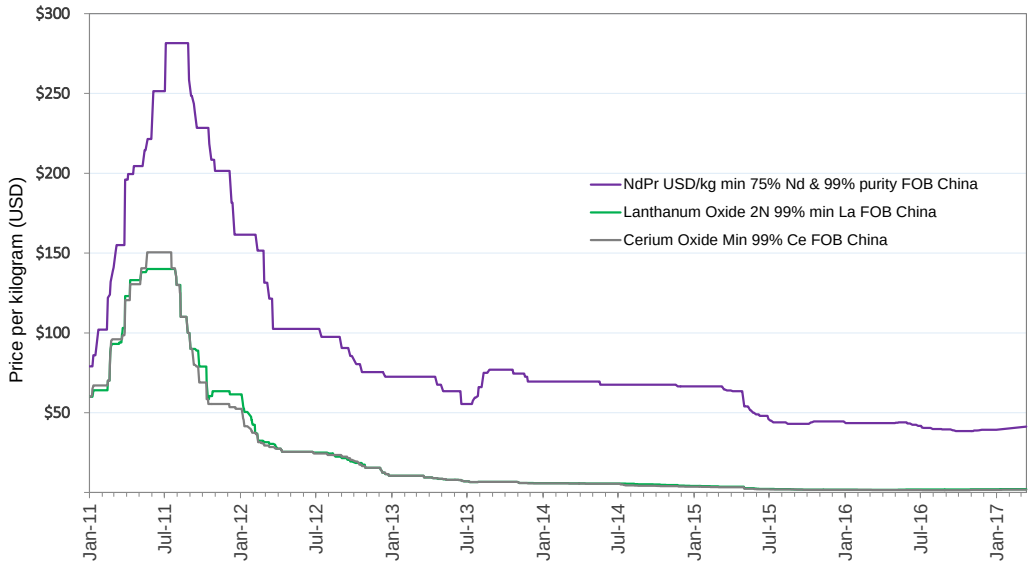

Figure 8: Historic Rare Earth Price Trends[8]

The recent increases notwithstanding, it is essential for emerging rare earth producers to focus on the high value contributors of Nd/Pr and to ensure the lowest production costs for these rare earth products through optimal flowsheet design, engineering and location of the refinery.

REDUCING OPERATIONAL EXPENDITURE

In order to be competitive in a low rare earth price environment, the Operational Expenditure (OPEX) needs to be a foremost consideration when developing the overall metallurgical flowsheet. Peak aggressively adopted this strategy during the resource definition, mine design, metallurgical flowsheet development and finally product selection. Specifically this has been achieved throughout the development of the project via:

- Selection of the Bastnaesite Zone mineralisation which is of high grade, highly weathered and outcrops to surface.
- Adoption of an open pit mine plan with a very low mining ore to waste strip ratio.
- Development of a beneficiation flowsheet to ensure a low mass high grade concentrate can be produced; reducing transport and downstream costs.
- Selection of a simple extraction flowsheet that minimises gangue dissolution and offers the ability to control the extraction of the low value rare earth cerium, thereby minimising reagent consumption during the leaching and separation stages.
- Appropriate selection of the SX separation flowsheet to deliver the required purity and form of the products whilst balancing complexity and technical risk.
- A coupled extraction-separation plant to eliminate the requirement for an additional intermediate precipitation stage as well as transportation and re-dissolution of the intermediate.
- The extensive piloting of the beneficiation, extraction and separation stages provides design data and further de-risks the project.

The majority of these cost savings come from the reduction of reagent consumption, either directly (e.g. reducing acid consumption during leaching) or indirectly (via the early rejection of cerium). As reagents typically account for more than half of the OPEX of an integrated (beneficiation, extraction and separation) rare earth plant, reagent prices can make or break a project depending on the project location. By producing a high grade low mass concentrate, the modest transport costs are easily outweighed by the cost savings that can be realised by selection of a favourable processing site.

THE TEES VALLEY REFINERY

Following an extensive global search and site evaluation process, Peak selected the location of its proposed Rare Earth Refinery, incorporating the extraction and separation circuits, to be at the Tees Valley on the north-east coast of the United Kingdom[9] (see Figure 9). This location offered the following advantages:

- Close proximity to ports, bulk low cost reagent supplies and a highly skilled workforce.
- Access to an existing industrial park with “plug and play” utilities including low cost power.
- Environmentally sustainable options for tailings and effluent disposal.
- Strong UK Government and Local Authority support for the project.
- Close to UK and European rare earth markets.

Figure 9: Location of the Tees Valley Rare Earth Refinery

Through the selection of the Tees Valley location, significant cost savings have been achieved through the accessibility of bulk low cost reagents and low cost grid power. Furthermore, the availability of local skilled workforce reduces technical risk as the labour force will contain the required expertise.

CONCLUSION

Each rare earth deposit is unique with regards to its mineralogy and location, and it is ultimately these two factors that must measure up to the prevailing rare earth prices.

Peak is in an enviable position with its Ngualla Rare Earth Project in that it has in excess of 20 million tonnes of high grade mineralisation that is both low cost to mine and amenable to physical concentration. The resulting rare earth mineral concentrate can be simply and economically treated to produce four products, the most important of which is the high purity Nd/Pr oxide which is seeing strong growth in demand and pricing.

Through an innovative “blank sheet” approach to exploration, mining, processing and marketing coupled with an aggressive focus on reducing OPEX, Peak will emerge as one of the lowest cost rare earth product producers amongst its peers.

REFERENCES

1. Lynas Quarterly Report Period Ending 31 March 2017, available from www.lynascorp.com

2. Lynas 2015 Annual Report, available from www.lynascorp.com

3. Peak Resources ASX announcement 12 April 2017, *“BFS positions Ngualla one of world’s lowest cost RE projects”* available from www.peakresources.com.au

4. Peak Resources ASX announcement 22 February 2016, *“Higher grade Resource for Ngualla nearly 1M tonnes REO”* available from www.peakresources.com.au

5. Peak Resources ASX announcement 30 December 2015, *“Concentrate grades exceed expectations in pilot testwork”* available from www.peakresources.com.au

6. Peak Resources ASX announcement 27 October 2016, *“Third and final stage of Ngualla Processing Flowsheet confirmed”* available from www.peakresources.com.au

7. Peak Resources ASX announcement 16 October 2013, *“Successful Completion of Solvent Extraction Pilot Plant”* available from www.peakresources.com.au

8. Metals Pages: www.metal-pages.com/metalprices/rareearths/

9. Peak Resources ASX announcement 6 December 2016, *“Rare Earth Refinery site selected in United Kingdom”* available from www.peakresources.com.au

Uranium-REE Proceedings

Process Technology

IAEA'S OVERVIEW OF WORLDWIDE IN SITU LEACH URANIUM MINING

By

Peter Woods

International Atomic Energy Agency, Austria

Presenter and Corresponding Author

Peter Woods
p.woods@iaea.org

ABSTRACT

In situ leach or leaching (ISL), also called in situ recovery (ISR) uranium mining, has become one of the standard production methods for this energy metal. ISL's application to amenable uranium deposits, in certain sedimentary formations, has grown over the last two decades in consequence of its competitive production costs and low surface impacts. A recent IAEA publication (In Situ Leach Uranium Mining: An Overview of Operations, IAEA Nuclear Energy Series No. NF-T-1.4 (2016)), provides an historical overview and shows how ISL experience around the world can be used to direct the development of technical activities, taking into account environmental considerations and emphasizing the economics of the process, from exploration, development and operations to responsible mine closure. The publication provides information on how to design, operate and regulate current and future projects safely and efficiently, with a view to maximizing performance and minimizing negative environmental impact.

Keywords: In Situ Leach, In Situ Leaching, In Situ Recovery, Uranium Mining, IAEA.

INTRODUCTION

In situ leach (ISL), also called in situ leaching or in situ recovery (ISR) mining, has become one of the standard uranium production methods, following early experimentation and production in the 1960s. Its application to amenable uranium deposits (in certain sedimentary formations) has been growing in consequence of its competitive production costs and low surface impacts. In 1997, the ISL share in total uranium production was 13%; by 2009 it had grown to over 30%, reaching 46% in 2011 and 51% in 2014. In the past, ISL technology was applied mainly in Bulgaria, the Czech Republic/Czechoslovakia, Kazakhstan, Ukraine, the United States of America and Uzbekistan. Recently, it has been used in Australia, China, Kazakhstan, the Russian Federation, the USA and Uzbekistan, with minor operations or experiments conducted elsewhere.

The IAEA released an overview publication in 2016 to illustrate how ISL experience gained around the world can be used to direct the development of technical activities, taking into account environmental considerations and with an emphasis on the economics of the process, including responsible mine closure[(1)]. With this publication, the IAEA's Member States and interested parties have more information with which to take informed decisions regarding the design and the efficient and safe regulation of current and future projects, with a view to maximizing economic performance and minimizing negative environmental impact. Highlights of the publication's findings are provided in this paper along with a summary of the IAEA's involvement in ISL over recent decades. Text has been abbreviated from the report[(1)] and includes some updates. Many reference links are provided in the full report, but of necessity only a selection are included in this paper, together with some other significant recent publications on the subject.

FUNDAMENTALS

Brief Definition

The uranium ISL method is defined in the IAEA report[(1)] as the extraction of uranium from the host (in general, sedimentary formations dominated by highly permeable sandstone) by chemical solutions (lixiviants) and the recovery of uranium at the surface. ISL extraction is conducted by: (i) injecting a suitable leach solution into the ore zone below the water table, (ii) oxidizing, complexing, and mobilizing the uranium, (iii) recovering the pregnant (loaded) solutions through production wells (extraction wells or recovery wells) and (iv) pumping the uranium-bearing solution to the surface for further processing. Several useful general descriptions are available in the literature [(2-6)].

Conditions of Application

The IAEA report[(1)] considers that the

"following major conditions are necessary in order to apply the ISL method of mining uranium[1]:

1. Water-saturated aquifer host formation with a water head high enough for a stable hydraulic pumping regime;
2. Sufficient permeability of the host formation to circulate mining fluids (usually dominated by sand or sandstone);
3. The ability for multiple recycling of the leaching solution through the ore formation;
4. Confinement of the host formation (aquifer);
5. Leachability of the mineral matrix containing uranium, in particular low abundance of interfering minerals or other constituents;
6. Disposal system for waste water and other residues.

"ISL for uranium recovery is usually applied to ores confined to water-saturated sandstone aquifers of variable consolidation… The (sedimentary) host formation of the uranium ore needs to be permeable enough to provide a quantitative flow rate from injection to extraction well within the wellfield pattern. Since the flow rate is dependent on several additional factors (hydraulic head, thickness of ore zone, well construction details), there is no definite

[1] Some experiments or operations only partly satisfy conditions 1 and 4, requiring special considerations and adaptations to the common ISL technologies described in the report and briefly in this paper.

permeability limit… ISL mining involves the extensive recycling of lixiviant as only a limited proportion of the uranium is mobilized with each 'pass' of mining solution (determined by the 'leachability' of the ore, i.e. the kinetic rate of uranium mineral dissolution). Mining solution may be pumped through a particular portion of ore 50 to 100 times or sometimes more to achieve the targeted recovery, over a period ranging from a few months to two or more years.

"An orebody normally occupies only part of its hosting aquifer, which by its nature is typically in semi-confined to confined aquifer conditions. Mining solution control and environmental protection are easier to achieve where the hydrogeology of the deposit and the surrounding geological formations allow effective confinement of mining solutions, commonly between impermeable clay rich strata (aquitards). Alternatively, the anisotropy of permeability in larger aquifer formations may be sufficient to control the mining fluid within the mining zone."

Importance of Environmental Aspects

Good design and construction of extraction and injection wells is required to avoid the contamination of non-target aquifers with mining or disposal liquids, as well as to minimize the risk of surface spills or environmental hazards caused by other infrastructure, including the processing plant and any associated ponds. Good environmental practices are described in documents such as the U.S. Nuclear Regulatory Commission's Generic Environmental Impact Assessment for In-situ Leach Uranium Milling[7] and the Australian Federal Government's In situ Recovery Uranium Mining Best Practice Guide[8], as well as a number of older IAEA reports referred to in the recent IAEA report[1].

Radiation Protection

Although uranium ore is not exposed at the surface, nor are radioactive tailings produced, the management of radiation risk remains important at ISL uranium mines, albeit that the risks are in general lower than those at a conventional uranium mine with a similar production capacity. Precautions are particularly important at the final purification and packing stages of the uranium ore concentrate product. The need for a radiation management plan and radioactive waste management plan, with their appropriate and demonstrable implementation, is asserted here, but no specific discussion or advice is within the remit of the IAEA report[1] or this paper. Guidance for these aspects must be found elsewhere.

Recovery Technologies: Leaching

Internationally, sulfuric acid is the dominant leaching medium (Australia, Kazakhstan and Uzbekistan), whereas currently in the USA only alkaline leaching is used. Just as important is the highly oxidizing nature of the lixiviants, which is maintained by the addition of oxidizing agents ranging from, but not restricted to, air or oxygen through to hydrogen peroxide and ferric iron.

The IAEA report[1] summaries the main criteria used in choosing between acid or alkaline leaching reagents as follows:

- "Composition of the host rock and the ore;
- Reagent cost and consumption;
- Uranium recovery and leaching intensity (residence time, uranium concentration in recovered solution);
- Environmental considerations (e.g. aquifer quality, connectedness to other aquifers) and regulatory requirements."

Typically, it is the abundance of carbonate in the ore that drives the decision. One frequently quoted 'rule of thumb' is that for the economic leaching of uranium ore using the acid route, the carbonate content of the ore should be less than 2%, otherwise the alkaline leaching route is preferred. However, like all rules of thumb, this figure should be treated with caution and used as an initial guide only, as other factors may drive a decision regarding the most appropriate method.

Recovery Technologies: Extraction

On the basis of broad industry experience, as summarized by the IAEA report[1], there are "two main pathways for the further recovery and processing of uranium extracted in mining solution; ion

exchange (IX) and solvent extraction (SX), or potentially a combination of the two." Historically and currently, ion exchange is the dominant method for both acid and alkaline leaching. Solvent extraction has sometimes been preferred for ISL amendable uranium deposits where the salinity, and particularly the chlorinity, of the groundwater present (and therefore the lixiviant, which is fortified groundwater) is high. Over the last two to three decades, IX resins have been developed to be effective up to about 5 mg/L or reportedly higher[9,10]. The best known recent ISL uranium projects to use SX are Honeymoon in Australia[11,12] and Uzbekistan operations[1]; others use IX.

Satellite Mining

This term refers to uranium extraction at a location away from a main processing plant. In the case of ISL, uranium is extracted and partially processed at a satellite mine, typically to the stage of uranium loaded resin. The resin is then trucked to a main processing plant for further treatment and purification to a saleable product. It has been used in both the USA and Kazakhstan for a number of years and was introduced in Australia (Beverley North) in 2010–2011[13] and since then to the Four Mile[14] operation. Resin is regenerated at the central plant and returned to the satellite plant for reuse. In Uzbekistan, a later stage intermediate product is produced which is transported elsewhere for final processing[1].

Groundwater Remediation and Closure

According to the IAEA report[1]

"remediation[2] of residual mining (and in some cases disposal) solution that remains in the mined aquifer at the completion of mining may or may not be required, depending on the prevailing regulatory environment, the original pre-mining quality of groundwater in the aquifer intended for mining, the known or expected end-use of the aquifer, the connectedness of the mined aquifer to other groundwater resources, users or the environment, and the likelihood of migration of residual mining or disposal water."

This issue, which can be contentious, is discussed further in References (1) and (15).

In brief, groundwater remediation of uranium ISL mines under closure is being undertaken in the Czech Republic[16] on acid ISL mines and in the USA on alkaline leach ISL mines[17]. Examples of projects where monitored natural attenuation is practiced or proposed include Australia and Kazakhstan.

Regardless of the closure method used, all groundwater wells not required for ongoing monitoring should be appropriately decommissioned at the end of mining — or preferably, progressively — to avoid the possibility of cross-aquifer contamination. Similarly, at the end of mining, all surface facilities not handed over for subsequent use should be appropriately decommissioned and the land surface returned to an agreed post-mining land use.

INTERNATIONAL OVERVIEW

The IAEA report[1] recalls that the ISL of uranium commenced in the 1960s in both the former Soviet Union and Eastern Block and the USA. There was modest application of the technology in both areas by the late 1970s. Development then stagnated for several decades, largely due to low uranium prices. The dissolution of the former Soviet Union in the early 1990s opened the door to western investment in central Asia, with price increases in the early 2000s spurring a rapid increase in investment and subsequent increased production.

A discussion on the ISL uranium mining experience in different countries is provided in the IAEA report, as summarized in Table 1.

[2] As defined in the IAEA safety glossary and relevant articles in Section 5 of General Safety Requirements Part 3, with regard to radiological protection, some old ISL sites can be treated as an existing exposure situation, for which the term remediation can be used. However, some new or younger ISL sites should be considered as planned exposure situations. For the later cases, restoration may be a better term, although this may have different connotations with regard to non-radiological contaminants and so is not used here.

Table 1: International Overview of Uranium ISL Mining

Country	Active years	Notes
Australia	Tests from 1977, mining 2000–present	Four deposits in South Australia have been mined. Other deposits have been investigated to various degrees
Bulgaria	Production 1967–1992	Some production during environmental cleanup since 1992
China	Tests from 1970, production since 1991	Ongoing interest and development
Czech Republic/ former Czechoslovakia	Tests from 1967, production 1971–1995	Small production during environmental cleanup since 1995
Hungary	Tests 1988	Tests showed Dinnyerberki deposit was not amenable to ISL mining
Kazakhstan	Tests from 1970, production since late 1970s–present	Since 2000, rapidly expansion saw Kazakhstan become the world's leading uranium producer in 2009, a position maintained until the present day
Mongolia	Tests since 1994	Significant potential to enter commercial production
Niger	Tests in early 2000s (hydraulic only, no leaching)	Tests showed Imouraran deposit was not amenable to ISL mining
Pakistan	Tests from 1990, intermittent production since 1995	Small scale by world standards
Russian Federation	Tests from 1984, production since mid-2000s	Production was increased slowly at the Dalur and Khiagda deposits
Tanzania[3]	Tests 2012	Deposit development on hold, method or method combination still under consideration
Ukraine	Intermittent production 1966–1993	Three deposits mined by ISL, possibilities for future ISL production
USA	1961–present	One early acid project, all others alkaline leaching
Uzbekistan	1961–present	Second highest cumulative ISL production after Kazakhstan

OUTLOOK

The Expected Future of ISL Uranium Mining

ISL uranium mining recently passed the 50% mark of world mine production and seems likely to remain the dominant mining method for uranium for the next few years at least. In the longer term, this percentage may decrease as additional underground high grade production in Canada is likely as uranium prices recover, and as additional low grade heap leach (perhaps with upgrading) deposits in Africa are potentially brought into production. Nevertheless, ISL has the ability to exploit deeper and lower grade deposits. Its relative position as a method of uranium mining compared with other means will depend on its ability to remain competitive through efficiencies and technological advances. The mining technology's low surface 'footprint' can also be an advantage in reducing environmental impact, where groundwater aspects are adequately addressed.

[3] Not included in the IAEA report[(1)] (see Reference (18)).

Key Factors

Uranium production in general is strongly influenced by political and social forces as well as by the prevailing regulatory regimes. Social, political and regulatory aspects will continue to strongly influence all forms of uranium mining, with ISL being no exception. As well as environmental protection, appropriate community and stakeholder consultation is recommended by the IAEA[19] and others (see References (20) and (21)). The models developing in some 'western' countries may not necessarily translate directly into best practice in new areas of ISL uranium mining. Hence, it is important to remember that what is considered and accepted as appropriate can be expected to develop in each country or region, taking into account local circumstances and culture and *informed* by what happens elsewhere through inputs from government, industry and non-governmental organizations.

Economics

A uranium deposit that is amenable to ISL mining has meant that this mode of production is nearly always the most cost effective. Capital costs are relatively low, as no mining excavations or crushing/grinding circuits are required, and operating costs are also often relatively low. However, the method is not without economic risk. Uranium recovery from the mined formation can be difficult to predict, particularly if the characteristics of a deposit show variations in lithology, geochemistry, permeability and the like. This risk can be offset, to a degree, by a field leach trial (pilot testing)[22]. The likelihood of success, or at least the time frame and cost of success of groundwater restoration, where required, can also be difficult to predict.

Despite its reputation in some circles as a method for mining low grade uranium deposits, which is indeed demonstrated at some sites, the ore grades of some deposits such as Beverley and Four Mile in Australia are over 0.1% U and comparable to many conventional mines. Economies of scale and output are important in all commercial or industrial-scale uranium production, although ISL may be more economic for smaller deposits and production rates than is conventional mining.

Technology

The basic technology of alkaline and acid ISL uranium mining has not changed greatly after the first decade or two, where various alkalis and acids were trialled until the industry settled on carbonate–bicarbonate and sulfuric acid, respectively (although there are exceptions). The improvement in control systems and automation has been marked and, as already mentioned, the development of IX resins that operate effectively at high chlorinity has also been important. Advances in drilling methods include well designs that allow rescreening. Numerical modelling has also advanced, especially with regard to geophysical data and linked groundwater flow and geochemical interactions (and hence uranium recovery rates and, where required, aquifer restoration rates). The IAEA report[1] notes:

> "Further developments in mining solution additives, to reduce costs, environmental impact or speed groundwater remediation (where active intervention is required) will be considered... All will require field demonstration before they would be seriously considered by producers or accepted by regulators."

Environmental Management

Good environmental management is, and will remain, an important aspect of ISL uranium mining and indeed of all mining, both because of the generally heightened attention given to uranium mines in general by the public and governments[20, 21, 23] and in particular because of the perceived and real impacts to groundwater. Historical groundwater contamination at the former ISL uranium mines in the Czech Republic are well known[16] and actual or perceived difficulties elsewhere have also been publicized. This combination of historical fact and ongoing concerns continues to influence some aspects of public opinion and the government approach to ISL uranium mining.

The IAEA[10,19] recommends a risk assessment approach to environmental management. The 2016 IAEA report[1] suggests that by

"identifying, understanding, managing and minimizing potential adverse impacts, good environmental management contributes to:

- Improved environmental outcomes;
- Demonstrated good corporate governance and accountability;
- Improved socioeconomic outcomes;
- Improved liability management;
- Reduced closure and rehabilitation costs."

Further guidance is given in Section 7.5 of the report, and in many references cited throughout the report, a selection of which has been cited here.

CONCLUSIONS

ISL mining of uranium is nowadays the dominant production method employed due, primarily, to its application in Kazakhstan and Uzbekistan, together with significant contributions from Australia, China and the USA and minor contributions elsewhere. This dominance is likely to continue over the next few years at least. Although the basic technology has been established for decades, significant improvements in many areas are apparent and ongoing improvements to the technique will be required to enable it to maintain its place as a major uranium production method. This situation is likely to prevail as long as additional ISL amenable deposits continue to be discovered and their viability for mining demonstrated.

Further to these technological aspects, the IAEA report[(1)] concludes:

> "In summary, safety, societal aspects, environmental and radiation protection and successful progressive and final rehabilitation will continue to be vital to ongoing uranium mining globally, to ISL as much as more 'conventional' mining."

ACKNOWLEDGMENTS

The author would like to thank the following experts who also contributed to the IAEA report[(1)], listed here alphabetically:

- Vladimir Beneš (DIAMO/private consultant, Czech Republic);
- Olga Gorbatenko (Kazatomprom/JV Inkai, Kazakhstan);
- Bryn Jones (Uranium Equities, Australia);
- Horst Märten (UIT GmbH Dresden, Germany/Heathgate Resources, Australia);
- Tom Pool (International Nuclear Inc., USA);
- Jan Slezak (IAEA);
- Igor Solodov (ARMZ Uranium Holding Co., Russian Federation).

Although this summary paper is based closely on the official IAEA report, the choice of themes to emphasize, the summarizing of the salient text and which references to retain remain the responsibility of the author, as is the choice of updated information and references. John Benbow (IAEA) is thanked for his careful review and improvement of this manuscript before submission. The permission of IAEA management to publish this summary paper is appreciated.

REFERENCES

1. IAEA, 2016. In Situ Leach Uranium Mining: An Overview of Operations. IAEA Nuclear Energy Series No. NF-T-1.4, pp 60 + annexes. http://www-pub.iaea.org/books/iaeabooks/10974/In-Situ-Leach-Uranium-Mining-An-Overview-of-Operations

2. IAEA, 2001. Manual of Acid In Situ Leach Uranium Mining Technology, IAEA-TECDOC-1239.

3. Abzalov, M. Z., 2016, Uranium Deposits (In-Situ Leach Projects), *in* Abzalov, M., Applied Mining Geology, chapter 32, pp 391-404, Modern Approaches in Solid Earth Sciences 12 (Springer International Publishing Switzerland).

4. Pelizza, M.S., Bartels, C.S., 2016. Introduction to uranium in situ recovery technology, in Uranium for Nuclear Power: Resources, Mining and Transformation to Fuel, chapter 7 (ed: Hore-Lacy, I.), 157-213 (Woodhead Publishing: Cambridge).

5. Seredkin, M., Zabolotsky, A., Jeffress, G., 2016. In situ recovery, an alternative to conventional methods of mining: Exploration, resource estimation, environmental issues, project evaluation and economics. Ore Geology Reviews 79, 500-514.

6. Boytsov, A.V., *in press*. Worldwide ISL uranium mining outlook. Proc. Int. Symp. on Uranium Raw Material for the Nuclear Fuel Cycle: Exploration, Mining, Production, Supply and Demand, Economics and Environmental Issues (URAM-2014), 23–27 June 2014 IAEA, Vienna, Austria. (Abstract published 2014).

7. US Nuclear Regulatory Commission, 2009, Generic Environmental Impact Statement for In-situ Leach Uranium Milling, NUREG-1910.

8. Commonwealth of Australia, 2010, Australia's in situ recovery uranium mining best practice guide, Canberra, Australia.

9. Hall, S., 2012, Metallurgical development of the Samphire uranium project. Proc. uranium sessions at ALTA 2012, 31 May – 1 June 2012, Perth, Western Australia, 151-166.

10. Fainerman-Melnikova, M., Soldenhoff, K., 2012, Uranium Extraction from Saline Solutions Using Weak Base Anionic Resins, CIM J. (Canadian Institute of Mining) 3 (2) 117-124.

11. Anonymous, 2013, Fact Sheet Uranium One Honeymoon Mine, Australasian Mining and Metallurgical Operating Practices 2, 1819-1822, AusIMM, Melbourne.

12. Ballestrin, S., Low, R., Reynaud, G., Crane, P., 2014. Honeymoon Mine Australia: Commissioning and operation of the process plant using novel solvent extraction reagent mixture in a high chloride environment. Proc. ALTA 2014 Uranium-REE sessions, 29-30 May 2014, Perth, Western Australia, 291-307.

13. Märten, H., Phillips, R., Woods, P., 2012, New Uranium ISR Satellites at Beverley North, South Australia, The New Uranium Mining Boom, (Proc. Int. Conf. Uranium Mining and Hydrogeology VI, Freiberg, Germany, 2011) (Eds Merkel, B., Schipek, M.) Springer Berlin, Heidelberg, 23-30.

14. Taylor, G., 2014, Four Mile uranium mine opening, MESA J. 73 (2), 5-7.

15. Woods, P., *in press,* An overview of in-situ leach uranium mining and associated remediation issues, Selected Uranium Production Cycle Papers 2012-2015, Proceedings of Technical Meetings Organized by the IAEA and held in Vienna, Austria, in 2012, 2013 and 2015, in Dolni Rozinka, Czech Republic, in 2013 in Freiberg, Germany, in 2014 and in Bad Schlema, Germany, in 2015, IAEA-TECDOC, (number and pages to be assigned).

16. Mužák, J., 2008, Remediation of Consequences of Chemical Leaching of Uranium in Stráž pod Ralskem, Proc. 10th Int. Mine Water Assoc. Cong., 2008, Karlsbad, Czech Republic (Eds Hrkal, Z., Rapantova, N.) 217-220.

17. Davis, J.A., Curtis G.P., 2007, Consideration of Geochemical Issues in Groundwater Restoration at Uranium In-Situ Leach Mining Facilities, USGS, Washington, NUREG/CR-C870.

18. Boytsov, A., Stander, S., Martynenko, V., *in press*, The outlook on potential uranium ISL mining at Nyota Deposit (Tanzania), Proc. Int. Symp. on Uranium Raw Material for the Nuclear Fuel Cycle: Exploration, Mining, Production, Supply and Demand, Economics and Environmental Issues (URAM-2014), 23–27 June 2014 IAEA, Vienna, Austria. (Abstract published 2014).

19. IAEA, 2010 Best Practice in Environmental Management of Uranium Mining, IAEA Nuclear Energy Series NF-T-1.2.

20. Woods, P., 2015, Environmental and social aspects of feasibility studies, mining operations and closure; balancing realities and expectations from different angles, Proc. ALTA 2015 Uranium-REE sessions, 28-29 May 2015, Perth, Western Australia, 2-16.

21. Woods, P., *in press*, The uranium mine life cycle. From Start to Finish – A Life-of-Mine Perspective, AusIMM Spectrum Series, (AusIMM, Melbourne).

22. Woods, P., Jeuken, B., 2015, Hydrogeological testing for ISL uranium mining: some Australian experience. International Conference 2014: Uranium Mining and Hydrogeology VII, Freiberg, Saxony, Germany, 21-25 September 2014, *in* Uranium - Past and Future Challenges, (Eds Merkel, B., Arab, A.), 211-220.

23. Harris, F., 2016. Management for health, safety, environment, and community in uranium mining and processing, *in* Uranium for Nuclear Power: Resources, Mining and Transformation to Fuel, chapter 14 (Ed. Hore-Lacy, I), pp 385-404 (Woodhead Publishing: Cambridge).

METALLURGICAL TEST WORK AND MODELLING TOWARDS UNDERSTANDING THE SUITABILITY OF A URANIUM DEPOSIT FOR IN-SITU PROCESSING

By

Laura Kuhar[1], Karl Bunney[1], Michael Jackson[1], Peter Austin[1], Jian Li[1], Dave Robinson[1], Henning Prommer[1,2], Jing Sun[2], Jess Oram[3] and Asha Rao[3]

[1]CSIRO Mineral Resources, Australia
[2]University of Western Australia, Australia
[3]Cauldron Energy, Australia

Presenter and Corresponding Author

Laura Kuhar
Laura.Kuhar@csiro.au

ABSTRACT

In-situ recovery (ISR) refers to the injection of lixiviant into an ore body, lixiviant contact and dissolution of metals from value and gangue minerals, and the recovery of the metals of interest at the surface through further processing. Despite the use of an ISR approach to the recovery of approximately half of globally produced uranium, the application of ISR to new regions of mineralisation is not without significant challenges. Knowledge of ore body deposit properties at a centimetre to metre scale would be ideal for the initial planning and the eventual recovery of metals in an ISR process. However, many of the tools required for the in-situ determination of these properties throughout the ore body and at depth do not exist. As the next-best alternative, downhole logs and laboratory tests and analysis of drilled (core) samples are the main sources of information for modelling and insight into the expected behaviour of the deposit during leaching, and provide a means of reducing the potential risks that could be faced during operation.

Test work was conducted on samples from a deposit with well-defined horizontal uranium mineralisation that exists in shallow unconsolidated sandstone, with a view to understanding the suitability of such a deposit for processing by ISR. Critical parameters included an understanding of the uranium and gangue deposit mineralogy and leach chemistry; the selection of an optimum lixiviant/oxidant system and a route for uranium recovery; an understanding of the hydrogeology of the deposit; and the development of a preliminary predictive reactive transport model. This paper will discuss the approach taken and describe some of the outcomes from this work.

Keywords: In-Situ Recovery, Characterisation, Leaching Tests, Hydrogeological modelling, Reactive transport modelling

Uranium opportunities in Australia

Current uranium mining in Australia

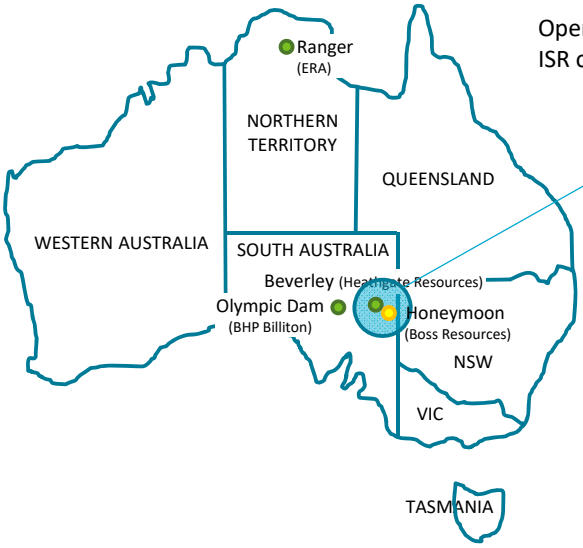

Operating mines
ISR operations: care and maintenance

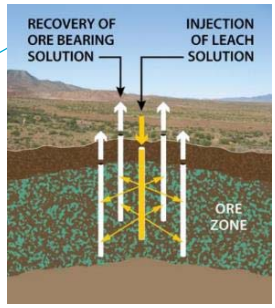

In-situ recovery (ISR)
- Economically attractive because of U commodity price

Economics of uranium mining – the case for ISR

- Uranium commodity price decrease to ~$25/lb (2017)
- Exploitation of Australian (and WA) uranium deposits uneconomic
- ISR economically attractive compared with other conventional mining/processing options
- However, in WA, despite

only one ISR trial has been conducted (Manyingee, 1986) but not commercialised

Uranium mining in Western Australia

Yanrey deposit

- Indicated plus Inferred Mineral Resource: 38.9 million tonnes at 360 ppm U_3O_8
- Favourable for ISR recovery

Aerially extensive deposit with horizontal well-defined uranium mineralisation in shallow unconsolidated sandstone host

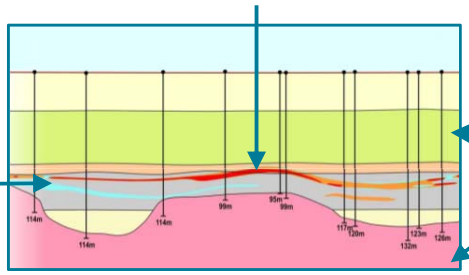

Permeability >1000 mDa in mineralised zones

Mineralised zones confined by mostly impermeable aquiclude and basement

Saturated deposit, all mineralisation beneath water table

Project objectives

Research to reduce potential risks during the field trials

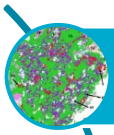

To characterise deposit mineralogy

To understand leaching behaviour

To establish downstream processing option for uranium recovery

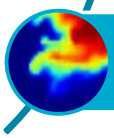

To support optimal design of field trials

Characterisation

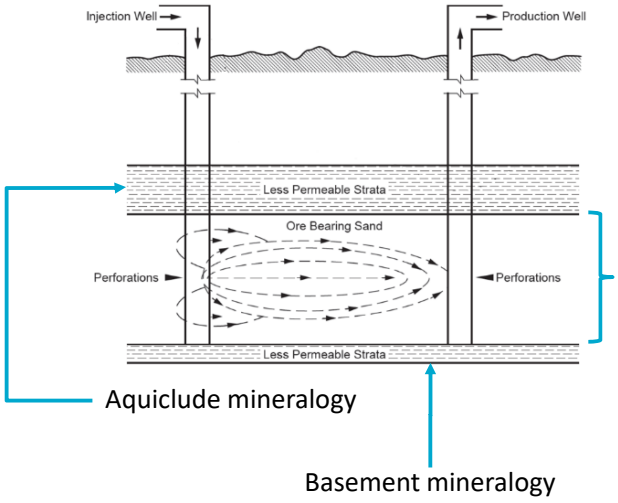

Characterisation: XRD analysis

- Quartz – main gangue mineral
- Trace to moderate amounts of other minerals that can act as:
  - Adsorbents, e.g., kaolinite
  - Permeability modifiers, e.g., smectite
  - Reagent consumers, e.g., carbonate

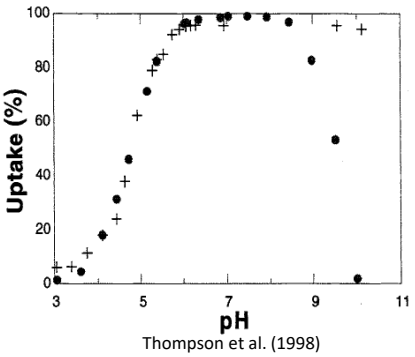

Thompson et al. (1998)

Characterisation: uranium mineralogy

- Uranium in zircon

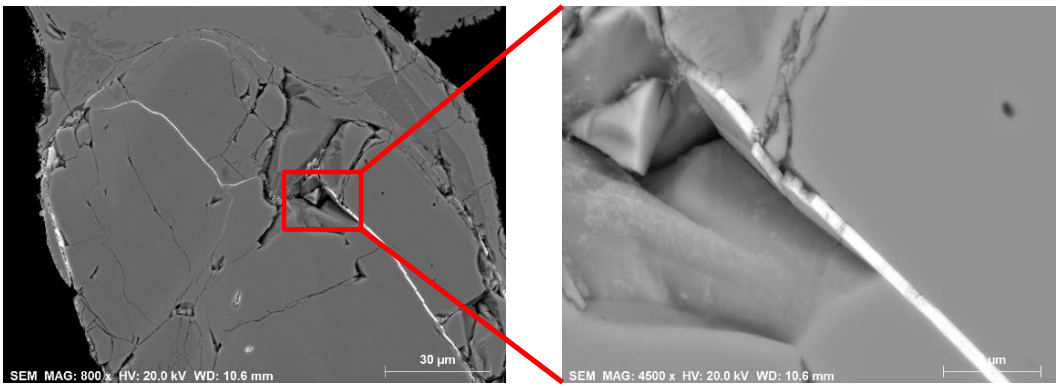

Characterisation: uranium mineralogy

- Possibly autunite (calcium uranyl phosphate)

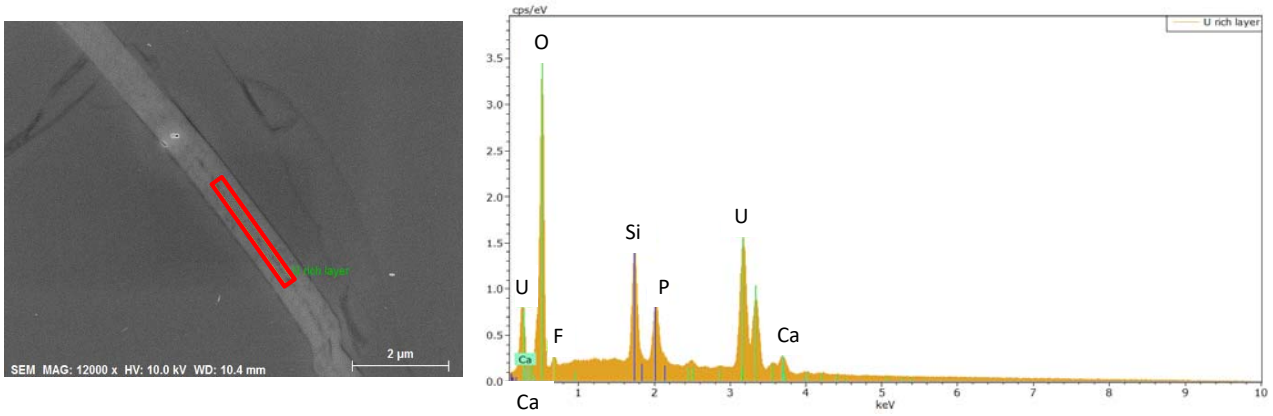

Characterisation: uranium mineralogy

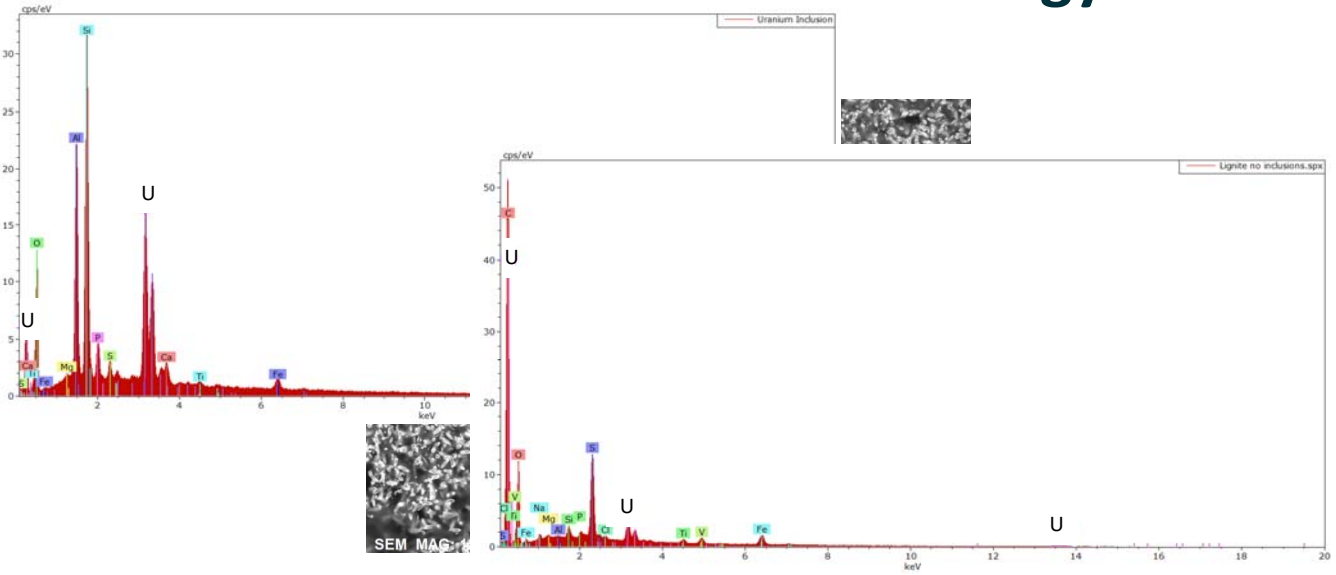

Characterisation: uranium mineralogy

- X-ray microdiffraction (coffinite in ellipsoids) and XRD in upgraded sample (coffinite)

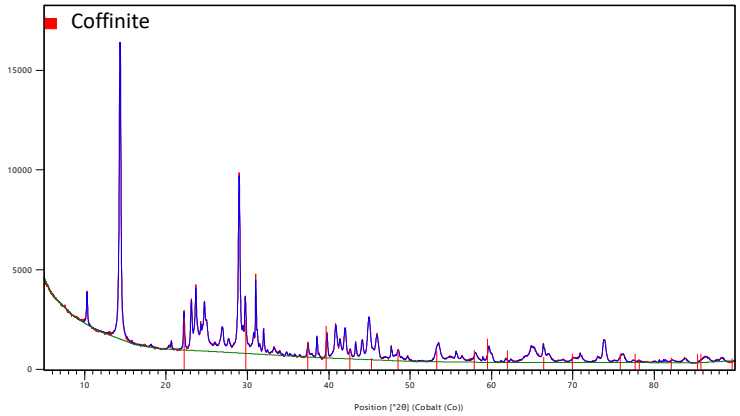

Characterisation: uranium mineralogy

- Grain-mount SEM imagery

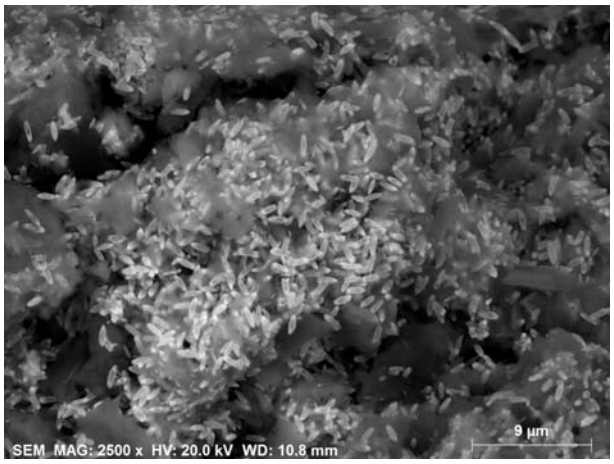

Characterisation: uranium mineralogy

- Uraniferous rutile

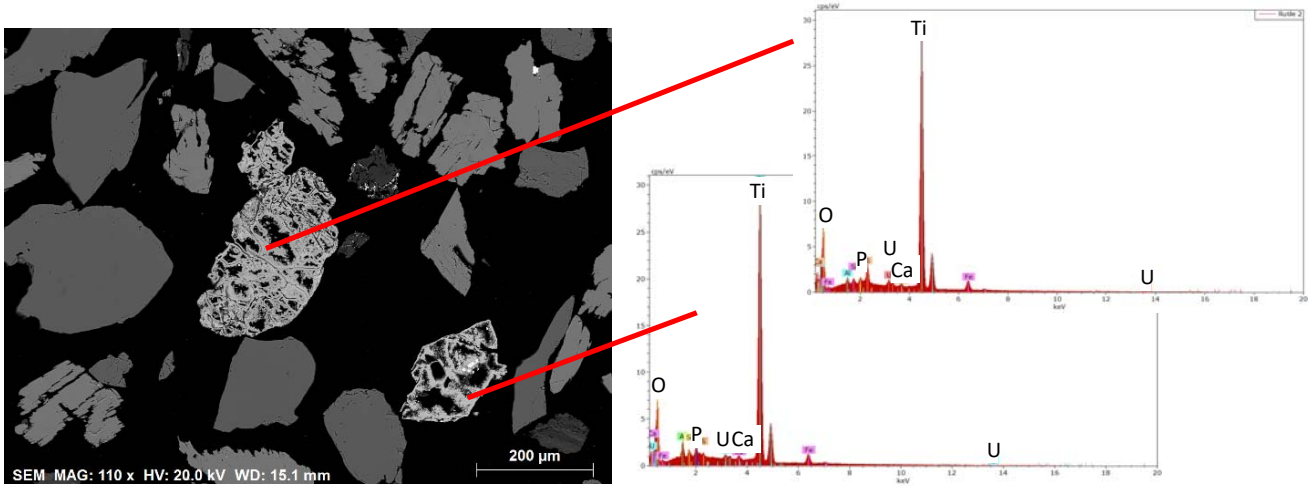

Leaching: bottle roll results

- Extensive bottle roll leaches
  - To select between acid or carbonate system
  - Oxidant requirements
  - Ambient temperature
  - Milled material
  - Site water
  - Low-level radiation laboratory

Leaching: bottle roll results

- Confirmed prior bottle roll leach results by ANSTO
- Both acid and carbonate leaching options work
- Oxidant addition increases uranium extraction

Acid leach

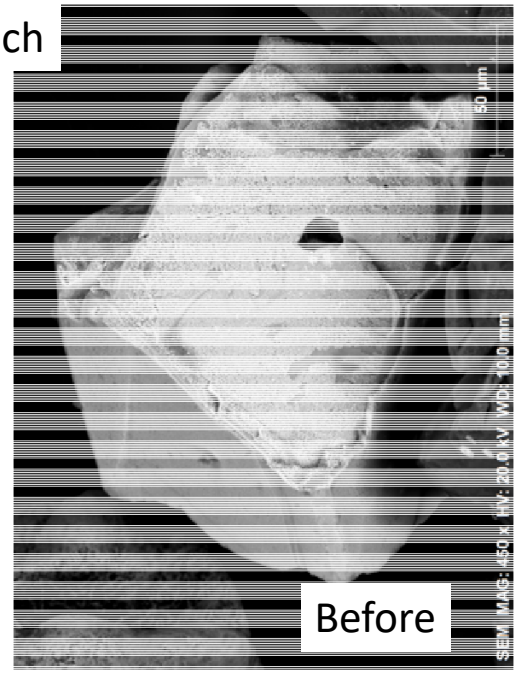

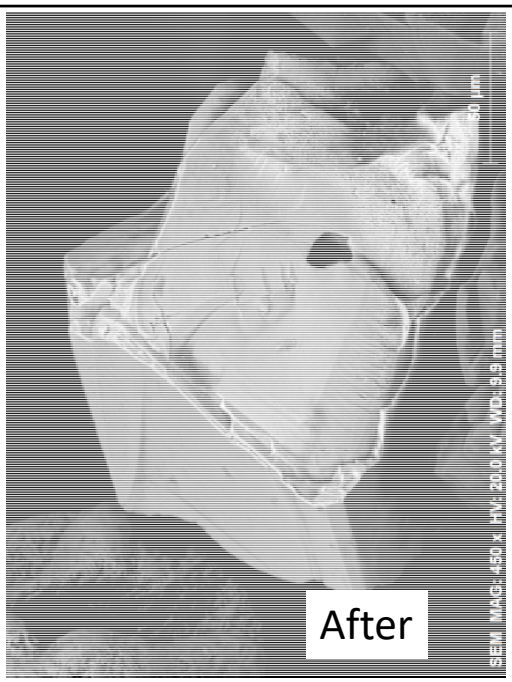

Carbonate leach

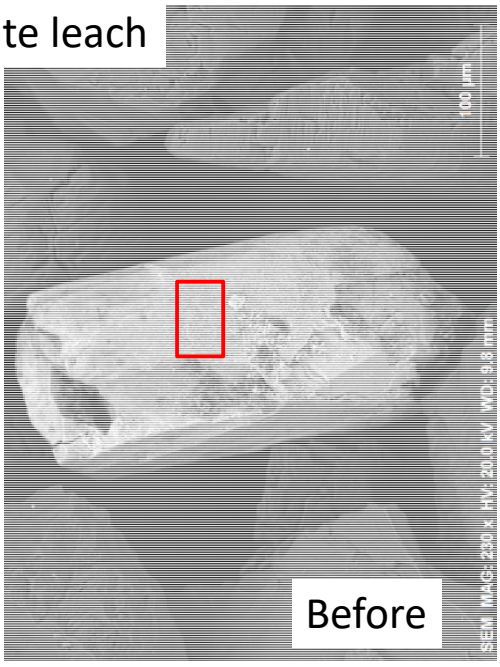

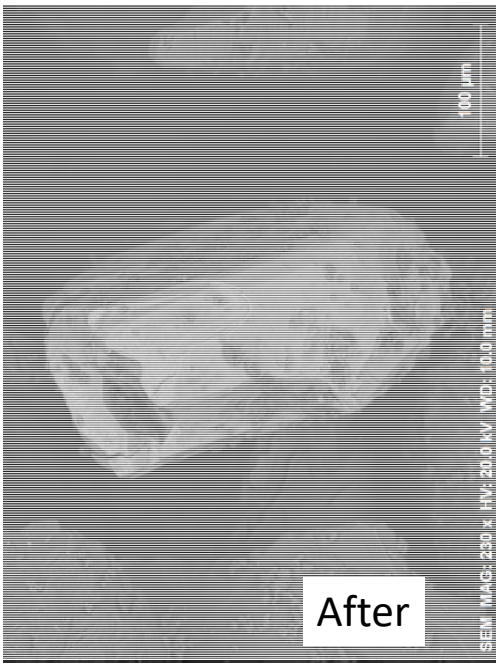

Carbonate leach

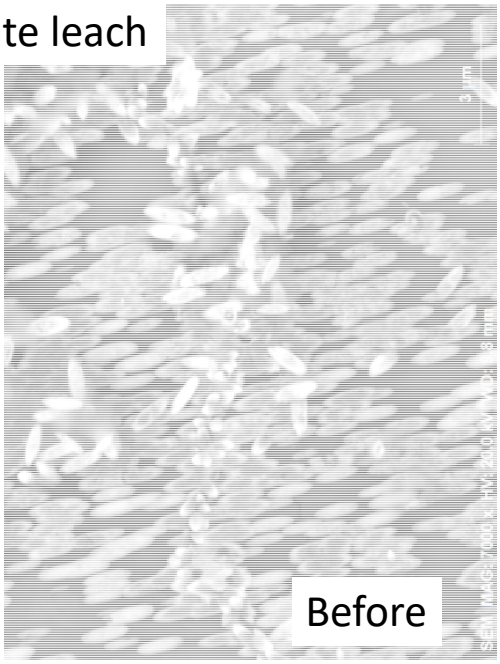

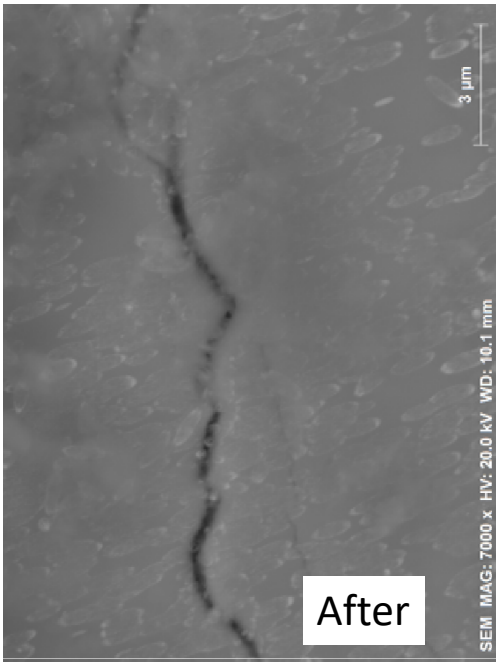

Leaching: column tests

1. Flush with site water
2. Tracer tests
3. Acid and carbonate leach tests
   a) without oxidant
   b) with oxidant
4. Flush with site water

Leaching: column tests

- Bromide tracer test

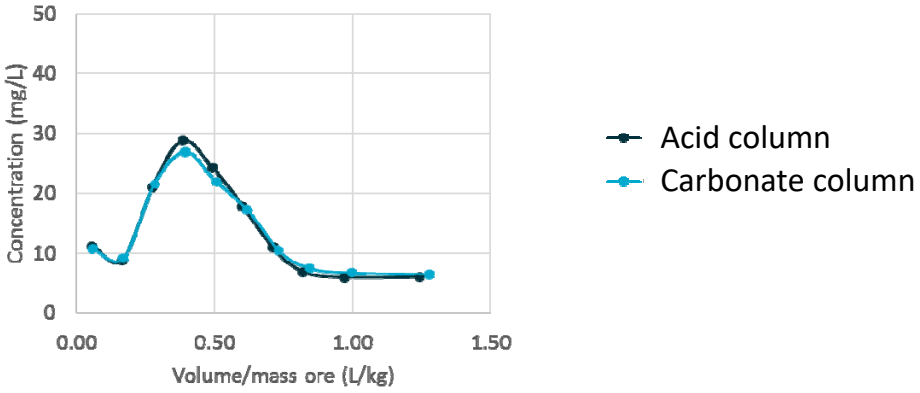

Leaching: column tests

- Uranium extractions in line with bottle roll leach results

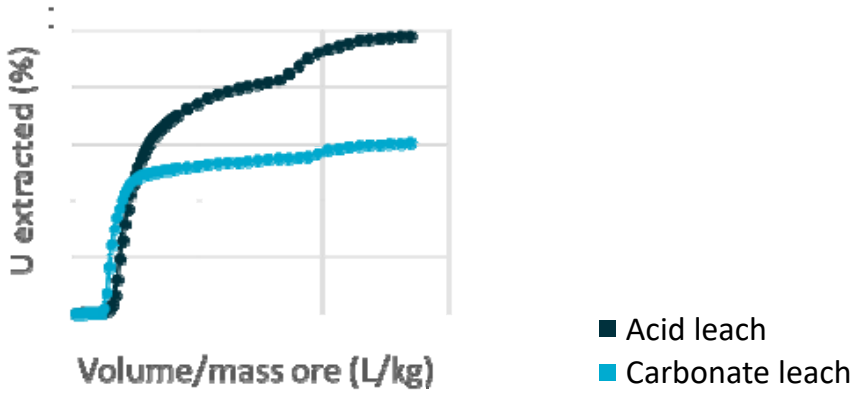

Ion exchange

- Screening tests on 9 resins
  - Range of pH and oxidant conditions
- Options for acidic and carbonate systems
- Excess oxidant hinders loading
  - Competition from iron in acid
  - Stable uranium complexes that resist adsorption in carbonate
- 100% elution

Reactive transport modelling

- Model expected chemical reactions for use in the field
- Tracer tests to identify flow/solute transport behaviour
- Dual-domain approach to account for preferential flow through columns

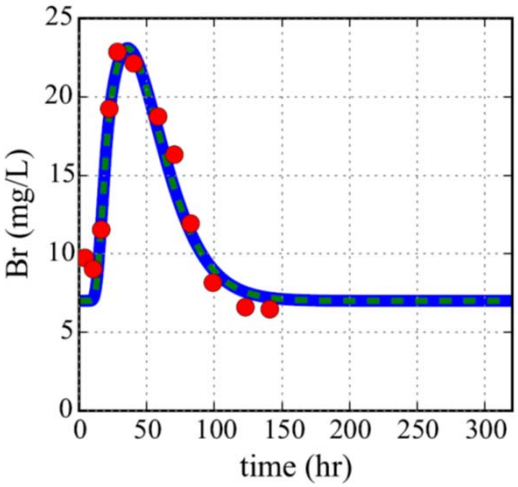

Reactive transport modelling

- First peak: autunite
- Second peak: coffinite oxidative dissolution

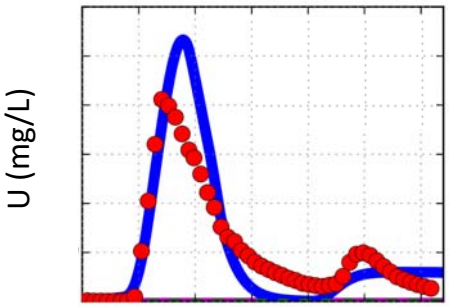

Reactive transport modelling

- Implement reactive transport models based on column data in the field

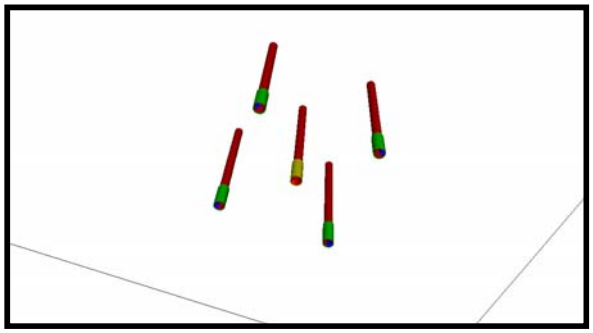

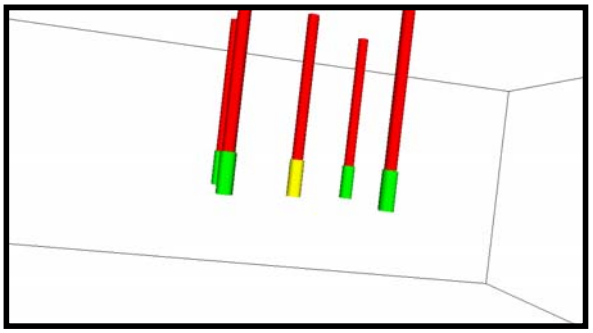

Summary

- Uranium mineralogy: suspected autunite, definitely coffinite, uraniferous rutile
- Gangue mineralogy: mostly quartz, moderate to trace levels of other impurities
- Acid and carbonate leaching systems promising
- Oxidant yields additional uranium recovery
- Suitable ion-exchange resin available for acid or carbonate leach
- Extension of reactive transport modelling can be used for the experimental design of the field trial to maximise value of data

Acknowledgements

- MRIWA
- Innovation Connections
- Co-authors and Cauldron Energy
- CSIRO characterisation program

R&D PROGRESS OF URANIUM MINING AND METALLURGICAL INDUSTRY IN CHINA

By

Yahui Tan, Wensheng Liao and Yijun Zeng

Beijing Research Institute of Chemical Engineering and Metallurgy Beijing (BRICEM), China

Presenter and Corresponding Author

Wensheng Liao
Liao_ws@139.com

ABSTRACT

After 60 years of development, China has established its integrated technical system of uranium mining and metallurgical industry which is suitable for the characteristics of Chinese uranium resources. In recent years, the rapid development of Chinese nuclear power has given rise to an urgent demand for natural uranium products which enhances the innovation and development of Chinese uranium mining and metallurgy.

This paper introduces the latest research and development progress of uranium conventional mining and metallurgy, heap leaching, in-situ leaching, in-place leaching, safety and environmental protection, and comprehensive recovery of polymetals associated with uranium in China. And the R&D direction of Chinese uranium mining and metallurgy is proposed.

Keywords: uranium mining and metallurgy, research and development progress, China

INTRODUCTION

After 60 years of development, China has established its integrated technical system of uranium mining and metallurgical industry which meets the demand of natural uranium for the development of nuclear industry. In accordance with its industrial development, Chinese uranium mining and metallurgical technology system was also formed to be suitable for the characteristics of Chinese uranium resources, which consists of conventional mining and metallurgy, heap leaching, in-situ leaching as well as in-place leaching, etc. In recent years, with rapid development of Chinese nuclear power, the innovative development of Chinese uranium ore mining and metallurgical technology has been promoted. The conventional mining and metallurgical techniques of intensified agitation leaching with high free acid as well as pressure leaching with acid are innovated. The comprehensive recovery of polymetallic uranium ore had a breakthrough. The new heap leaching techniques of strong acid pugging and curring-high iron leaching[1], heap leaching with acid granulation[2], percolation leaching[3] as well as intensified leaching with the tailings by heap leaching[4] are commercially applied. The auto-control of complete process flow in the field of in-situ leaching[5] is realized, and the technique of in-situ leaching with CO_2 and O_2 is applied extensively[6]. The heap construction technique of straticulate sector deep hole extrusion in the field of in-place leaching process[7] has greatly increased the efficiency of heap construction with blasting. The technical level of Chinese uranium ore mining and metallurgy is further promoted, the utilization rate of uranium resources is increased as well as the scope of development and utilization of uranium resources is extended by these technical achievements.

RESEARCH AND DEVELOPMENT PROGRESS

Conventional Hydrometallurgy

The leading process of Chinese uranium hydrometallurgy was conventional agitation leaching. According to characteristics of variety of Chinese uranium deposits and complexity of ore mineralogy, techniques such as the solvent extraction process of clarified solution for granitic ore, acidic Eluex process for volcanic ore, ion exchange process of acid leaching liquor for carbonaceous-silicious-argillaceous ore, hot-pressure and alkaline leaching process for carbonated ore, combination process of electricity generation in low temperature with uranium-containing coal and solvent extraction from acidic coal ash had been developed.

In recent years, to reduce the processing cost of conventional agitation leaching and improve the uranium recovery rate, a series of innovative researches have been launched, and good results are obtained. The new agitation leaching processes including alkaline leaching of carbonaceous-silicious-argillaceous ore after grading and tailing-discarding, intensified agitation leaching with superfluous acid, and acidic pressured leaching of titanium-bearing uranium ore were studied to treat ore with complex mineralogy and refractory ores[8,9]. The results showed that through acid pressure leaching, compared to conventional leaching, the acid consumption was reduced by 25%, the uranium leaching rate was increased by 2% with the leached pulp filtration rate doubled. To solve the solid/liquid separation problem, resin in pulp process was improved by innovated pulp and sand separation technology. The application of pulp adsorption process is expanded by coarse sand washing technology and fluidized classification washing technology. The ion exchange technology of fluidized-bed with continuous countercurrent flow was developed to deal with high density pulp, and the problem of high resin wear rate is solved. The two-step precipitation process with uranium direct precipitation in the pregnant leaching solution and the circulation precipitation process of uranium slurry in the qualified stripped solution are employed to significantly reduce the moisture content and increase the quality of product. A new type of ion exchange resin was developed to solve the technical problem of recovery uranium in the acid leaching solution with high concentration of chlorine, and the uranium adsorption capacity is improved. Some processing equipment was invented such as fluidized settler, multi-functional precipitation tank and new mix-settler tank.

Extraction of Uranium-containing Polymetallic Ore

With the rapid development of Chinese nuclear power industry, the demand of natural uranium products has been increased. More and more low grade of uranium-containing polymetallic ore are gradually developed. Recently, to obtain an economic and technical development of such resources, China contributed a great effort on the R&D of the comprehensive recovery of polymetallic ore and has achieved positive results.

1) Fengcheng uranium-containing paigeite deposit (average grade of uranium 0.0048%)[10]. The joint process including magnetic separation, gravity concentration and uranium ore agitation leaching was employed to acquire 61% grade of iron concentrate (Fe_2O_3), >0.13% grade of uranium concentrate and 13% grade of boron concentrate, then the uranium concentrate was processed into biuranate by hydrometallurgical processing.

2) Guyuan uranium-molybdenum symbiotic deposit[11]. According to the different characteristics of high grade uranium-molybdenum ore and low grade uranium-molybdenum ore, individual agitation leaching processes were developed and two-step solvent extraction was developed to separate uranium and molybdenum, then ammonium tetramolybdate and sodium diuranate (SDU) were prepared.

3) Ruoergai polymetallic uranium deposit with carbonaceous-silicious limestone. Flotation was employed to grouping. The organic matters and sulfide concentrates were treated by conventional acid leaching and hot-pressure with oxygen leaching process. Recoveries of uranium, molybdenum, nickel and zinc were 98%, 88%, 98% and 88%, separately. The carbonate minerals (tailings) were treated by alkaline leaching with recovery of uranium and molybdenum 85% and 80% respectively.

4) Huayangchuan polymetallic deposit with low grade uranium. Gravity concentration was employed to enrich uranium-containing niobium, titanium and other main associated metals. Magnetic separation was employed to enrich magnetite and flotation to separate and enrich galena and niobium-titanium uranium ore, 0.3% grade of uranium-containing niobium concentrate, 40% grade of lead concentrate and 60% grade of the iron concentrate were obtained.

Heap Leach

Heap leach is widely used in the Chinese uranium mining and metallurgical industry, generally with the uranium recovery more than 90% and the leaching period of 60 to 150 days. Compared to conventional leaching, agent consumption of heap leaching is lowered by 30% to 40%, the average mining and metallurgical costs were reduced by about 30%.

In recent years, to solve the relatively low recovery of uranium, the scaling of ore heap compaction, uranium level fluctuation in solution, longer leaching period and other issues occurring in the heap leaching process, new techniques, new equipment and new processes have been explored and developed, including the mixed acid curing-high iron percolation leaching technology[1], low-permeability ore pelletized acid leaching technology[2], multi-pile heap leaching with fine-grained ore technology, series column-operating adsorption- stripping process, packed moving bed saturation-re-adsorption technology, new Eluex process and large flow fixed bed ion exchange equipment.

Concentrated acid pugging and curing - high iron leaching technology was employed, the leaching period of high grade uranium ore could be shortened to 60~100 days, with uranium concentration 7g/L~9g/L and tailing grade <0.03%. Bacterial oxidation in heap leaching could reduce sulfuric acid consumption by 12.5%, shorten leaching period by 25%~45%, double uranium concentration of the leaching solution, and decrease solid/liquid ratio of leaching solution from 4~5:1 to 2~3:1. Percolation leaching, which could avoid the heap compaction, reduced the leaching period from 300 days to less than 60 days, with uranium recovery increased from about 60% to more than 90%, thus the ore processing cost is reduced by 40% in comparison with the conventional hydrometallurgical process. By using the intensified leaching method of mixing tailings with acid, tailings grade could be reduced to below 0.01%. Fine-grained ore heap leaching solved the problem of low recovery and long leaching period. Multi-pile heap leaching improved the uranium concentration 2~3 times, the consumption of acid, oxidant and other material were reduced by about 20%~30%. Acid granulation leaching with clay and powder obtained metal recovery over 95%. Compared with direct heap leaching, the leaching period of acid granulation leaching was shortened by 70%, uranium concentration was increased by more than 50%. Fixed bed ion exchange equipment and multi-columns adsorption in series and stripping technology could be adapted to large fluctuation of uranium in solution. Combined with the merits of fixed bed and fluidized bed, the saturation-readsorption technology of moving bed column has achieved the resin transformation and circulation of eluent. The new Eluex process was employed to treat low grade ore, the recycling of process water was realized.

ISL (In-Situ Leaching) Uranium Recovery

In-situ leach was successfully tested in 1985 in China. Then the first commercial uranium mine with ISL was constructed in 2000. After 30 years of development, in-situ leach has become the main method of uranium mining in China, with an integrated technical system including in-situ leachable uranium resource evaluation, well structure and completion technology, well push-pull system and its optimization, formula and application of leaching agents, numerical simulation and control of leaching scope, uranium pregnant solution processing and automation control, etc.

In recent years, more than 20 sandstone type uranium deposits have been explored. Under the support of IAEA, the systems, Expert System of In-situ Leaching Uranium (ESILU) and Economical Evaluation System of In-situ Leaching Uranium (EESILU), had been developed, which could rapidly evaluate the leachable sandstone type uranium resources. A sandstone type uranium deposit database has also been established through carrying out the study of classification and technical-economic evaluation. Those works preliminarily set up the evaluation standard of in-situ leachable sandstone type uranium deposit.

Regarding to the drilling and completion of wells, vegetable gelatin drilling, negative pressure drilling with foaming and water, which significantly reduce the pollution of drilling fluid on the ore horizon and effectively protect the permeability of formation([12]), were developed. The local expansion at the ore horizon could increase the production capacity by 10% - 20%([13]). Deep well drilling was investigated, which lays a solid foundation for the deep sandstone type uranium ore mining (>600m). The technologies of reverse cementing, layered gravelling, casing cutting and two-times drilling were also studied([14]), which improve the efficiency and quality of drilling and provide a technical support for mining multi-layer ore body within one wellbore.

Acid leaching technology has been continuously developed with positive results that the leaching efficiency was further improved, and that the technology of acid-oxygen leaching was investigated to solve the problem of high consumption of acid for some refractory deposits([15]). The breakthrough of using CO_2+O_2 as leaching agents in in-situ leaching solved the blockage problems when using acid leaching in high carbonate uranium deposits and has already been commercially applied on a large scale([16]).

Numerical simulation and control of leaching scope could reduce the dilution and “dead area” of leaching agents, with the coverage ratio increasing to more than 90% and the concentration and recovery of uranium increased as well. Uranium leaching solution control in thick sandbody, thin orebody broke the limit of uranium ore/sand ratio of no more than 1:10 in in-situ leaching, resulting in the ore/sand ratio of 1:33 mine to be cost-effective developed. The technology of forming water curtain by injecting water into drilling wells and lifting underground water table solved the difficulty of mining the weak confined aquifer sandstone-type uranium deposit([16]), leading to the further expansion of the application of in-situ leaching of uranium.

The saturation-readsorption process of moving packed bed and the Eluex (Elution extraction process) in acid in-situ leaching process reduces the cost of processing low concentration uranium solution([17]). The processes of fixed bed adsorption-moving elution as well as the saturation-readsorption of moving packed bed and fixed bed elution applied in recovery of pregnant solution in CO_2+O_2 leaching improved the adsorption efficiency, and the compaction problem in the resin bed was solved. The process of in-situ dispersed adsorption and concentrated elution which improved the utilization of stripping, precipitation, filter press equipment in the processing plant was used, and it is of great significance to the development of small orebodies in China. The whole process automatic control improved the automation level of in-situ leach, and a solid foundation of digital mines was established for in-situ leach mines.

In-place Leaching

Chinese in-place leaching uranium is developed based on heap leach of underground mining ore after shallow hole stope([18]). In-place leaching could decrease the transportation volume of low grade ore by about 75%, thus the processes of management of mining field, ore crushing and grinding, solid-liquid separation as well as slag discharge were saved, with the cost of comprehensive mining reduced by about 30% and the level of radioactive pollution in ground decreased. The new technologies of "upward sublevel millisecond compression blasting deep hole sector ore heap" and “underground non electric millisecond delay control blasting" made blasted heap rock particle effectively controlled, ore micro-fissures developed. Spray irrigation, drop irrigation and drilling injection eliminated the "dead zone" of ore heap leaching, and the effect of

heap leaching was improved, with recovery increased to over 65%. Leakage loss was effectively prevented by the engineering optimization of tunnels and drilling holes solution collection.

Safety and Environmental Protection

Since the establishment of the Chinese uranium mining and metallurgical industry, safety, environmental protection and radiation protection have been paid high attention. A series of work has been constructed such as the law of migration and diffusion of radon in uranium mining and metallurgy, radon and radon progeny measurement, radon reduction by mine ventilation, radiation dose measurement and evaluation of occupation staff, drainage and waste disposal, safety and environmental protection in the decommissioning of uranium mining and metallurgy facilities. Many important results have been achieved, and a series of standards have been set up, for example, “Regulations for radiation and environmental protection in uranium mining and milling”[19], “Regulation for radiation environmental impact assessment in uranium mine and mill”[20], “Technical regulations for radon exhaustion and ventilation in underground uranium mine”[21] and “Code for safety design of uranium mills tailings pond in nuclear industry”[22].

In recent years, according to the different developing and mining methods of uranium deposit, projects such as “study of ventilation and reducing radon in shrinkage mining”, “comparison study of uranium mine ventilation and radon reduction”, “study of the relationship between shaft ore lifting capacity and the ventilation system” and “radon transfusion and control technology" were carried out to provide technical support in improving the radiation status of uranium mine ventilation systems, increasing the uranium mine safety level of radiation. The development of KF608 intelligent instrument for measuring radon and radon progeny has been applied into uranium mining and metallurgy enterprises. The KF606 type personal dose meter for miners has become a routine monitoring instrument for radiation dose of uranium mining staff. The ratio of underground workers wearing personal dosimeters reaches 100%, ground staff >30%. The personal radiation dose witnessed a continuous decline. In 2013, radiation dose of mine employees was of 8.47mSv/a, individual effective dose of 4.27mSv/a. All these statistics suggested that the safety and health of uranium mining and metallurgy workers are effectively protected[19].

Wastewater treatment processes of lime - neutralization treating tailings and waste water, pyrolusite or barium chloride removing radium, barium chloride multi-step neutralization treating acid mine water, pyrolusite adsorption removing radium - flocculation removing radium to clean up alkaline wastewater, acidification with sulfuric acid to treat alkaline wastewater, flocculation and precipitation - freezing and crystallization process with alkaline precipitated mother liquor, reverse osmosis treatment with the high concentration transformation wastewater in CO_2+O_2 in-situ leach, natural evaporation with processing wastewater of in-situ leach, gravity separation and coalescence method in recycling waste organic phase solution and process, effectively ensured management of the wastewater in the process of uranium mining and metallurgy, ensured the radionuclide emission meeting the discharge standard requirements. The ratio of wastewater recycling of in-situ leach and heap leach has reached more than 70%, while part of mine water realized reusing.

Some techniques like “study of precipitation of radon in uranium tailings and waste rock pile”, “farmland pollution treatment”, “sealing of uranium mines”, “tailings reservoir safety and stability” and “dam water seepage treatment” provided technical support for decommissioning of uranium mining and metallurgical facilities in China. By the end of 2014, decommissioning of 37 uranium mining and processing facilities had been completed, with radioactive waste effectively isolated, ecological environment restored and the regional environmental quality improved. The public maximum individual effective dose has decreased by 70%~95% and the collective effective dose by 50%~90%, which met the public requirements of limit value.

R&D DIRECTIONS OF CHINESE URANIUM MINING AND METALLURGY

The rapidly-increasing demand for natural uranium product enables low grade uranium resources proven and uranium-bearing polymetallic resources, which is in poor mining conditions, complex mineralogy and intractable, to become the principal part of the development and utilization. As a consequence, the mining and metallurgy is in urgent need of breakthrough innovations. Therefore, the research and development direction of China’s Uranium mining and metallurgy will be the high efficient drilling and well completion for in-situ leaching, the leaching mechanisms of intractable uranium resources and the heap leaching-processing combined process, the safety and environmental protection in Uranium mining, the digital mine, and so on.

Breakthrough of In-Situ Leaching for the Complicated Sandstone Uranium Deposits

In recent years, complicated sandstone type uranium deposits, such as those with high-salinity formation water, thick sandbody and thin orebody, ore deep buried and low-permeability, multi-orebody overlapping, and refractory to alkaline-leaching and acid-leaching, have been found in China. Various techniques, therefore, should be carried out for diffident deposits, including effective leaching processes, highly efficient drilling and complete technique, mining technology for multi-orebody deposits, stimulation for low-permeability deposits, and artificially confined layer building for thick sandbody and thin orebody deposits. And researches should be focused on solving the following key technique problems: the efficient drilling and completion of wells for deep buried deposits, permeability enhancing for low-permeability deposits, and artificial water resisting layers building, and flow control of leaching solution for thick sandbody deposits.

Strengthening Combination Process of Heap Leaching and Equipment

After decades of exploration, the high grade and leachable uranium resources were exhausted, leaving a large amount of low grade, intractable uranium resources to be urgently exploited and utilized. In order to solve the problems of long processing time, high reagent consumption, and high production costs for conventional hydrometallurgical processes, such R&D should be carried out emphatically, as heap leaching-metallurgy combined processes for the low grade, high acid dosage, intractable uranium ore, selective breeding for high-efficient bioleaching, and process optimization of bioleaching, and technologies and equipment for high-efficient leaching and solid-liquid separation for the intractable ores. As for the intractable uranium ore with complex mineralogy, the R&D will be focused on key techniques and equipment, such as crushing and grinding, pressure leaching, and solid-liquid separation. Due to low recovery, poor filtering capability of pulp, and difficult solid-liquid separation for alkaline ores, such as the carbonate-siliceous-mud rock type uranium deposit, and carbonate uranium deposit, R&D will be conducted on the key techniques and key equipment in conventional alkaline leaching processes.

Promoting Safety and Environmental Protection

The problems of underground mining environment and the treatment of groundwater for in-situ leach uranium mining, have increasingly attracted social concern and attention. Therefore, the research and development of safety and environmental protection in uranium mining and metallurgy process should be focused on such techniques as the waste minimization, treatment of waste residue and piled slope by dry slag, high-efficiency ventilation reducing radon, recycling of process water, uranium removal by microbes-plants, artificial wetland, pollution control and restoration techniques for groundwater in in-situ leaching, and the remediation of soil contaminated in mine.

Intensifying Beneficiation and Metallurgical process of Uranium-containing Polymetallic Ore

The large amount of low grade uranium polymetallic resources in China will increasingly become the principal part of the development and utilization. Because of the complex composition and abundant usable elements of low grade uranium-bearing polymetallic resources, recovering uranium only, i.e. single extraction uranium process will waste resources and have poor economic benefit. Therefore, one of the important directions of dealing with uranium-bearing polymetallic ore resources is to develop a new type of comprehensive recovery process. It will not only improve the ratio of comprehensive utilization of uranium and polymetallic resources, but also increase the economic efficiency of uranium mines.

Focusing on Unconventional Uranium Resources

At present, with the increasing production costs and difficulty of the development, the amount of Chinese identified uranium resources is limited. Research and development of unconventional uranium resources, especially the high-salt low-uranium water system, such as salt lakes, ocean, will be conducted. Strengthening the research of uranium extraction technology for the high-salt low-uranium water system will be emphatically focused on highly effective adsorption materials and corresponding extraction equipment.

CONCLUSIONS

The research and development of Chinese Uranium mining and metallurgy adapts itself to the characteristics of Chinese uranium resources, and meets the requirements of safety production, environmental protection and radiation protection regulations. The difficult problems which includes the complicated hydrogeological condition, paragenetic and associated multi-compositions, complex mineralogy, low recovery as well as low comprehensive utilization, will be placed in front of us in the coming decades. According to the characteristics and developing conditions of Chinese uranium resources, therefore, in compliance with the requirements of rational exploitation, effective use, low consumption and high efficiency, safety and environmental protection, the R&D directions in the future are as follows: strengthening the innovation of Chinese uranium mining and metallurgy, striving to make breakthroughs to improve resource utilization, developing advanced and applicable uranium mining and metallurgical processes, and expanding the application range of uranium resources, to meet the demand of natural uranium product suitable for the rapid development of Chinese nuclear power.

ACKNOWLEDGMENTS

The authors would like to thank Mr. Huidong Deng for his provision of materials and some professional translation to finish this paper. The authors also acknowledge the management of BRICEM for permission to submit this paper.

REFERENCES

1. Jin, S.-Q., Xiang, Q.-F., Guo, J.Z., etc., 1998. Acid-curing and ferric-trickle leaching effluent used in closed circuit uranium extractive process. Uranium mining and metallurgy. 17(2), 111-120. In Chinese.

2. Zeng, Y.J., 2004. Acid agglomeration heap leaching: Present status, principle and applications. Uranium mining and metallurgy. 23(4),175-181. In Chinese.

3. Jiang, L., Wang, H.-T., He, J.-M., 2006. Application of percolation leaching in Fuzhou uranium mine. Uranium mining and metallurgy. 25(4),182-185. In Chinese.

4. Liu, J., Fan, B.-T., Meng, Y.S., etc., 2009. Ways and measures for reducing tailings grade of heap leaching. Uranium mining and metallurgy. 28(4),176-180. In Chinese.

5. Wu, X.-Y., Zhang, C.-P., Shi, J.-M., etc., 2010. Application of automatic detection and control system in in-situ leaching system of a uranium mine in Xinjiang. Uranium mining and metallurgy. 29(3),138-144. In Chinese.

6. Du, Z.-M., Niu, X.-J., Su, X.-B., CO_2+O_2 in-situ leaching test of one uranium deposit in Inner Mongolia. Uranium mining and metallurgy. 32(1),1-4. In Chinese.

7. Li, Q., 2009. The uranium mining up fan type deep-holes and milli-second squeezed blasting for heap-making and safety. Metal mine. 11(Suppl):419-424. In Chinese.

8. Chang, X.-X., Zhong, P.-R., Li, T.-Q., 2015. Pressure acid leaching of a refractory uranium ore. Hydrometallurgy of China. 3, 204-207. In Chinese.

9. Niu, X.-J., Tan, Y.-H., Su, Y.-R., Su, X.-B., Chen, H., 2013. Development direction and key task of uranium mining and metallurgy techniques in China. Uranium mining and metallurgy. 32(1), 22-26. In Chinese.

10. Zhang, T., Liang, H.-J., Xue, X.-X., 2009. Elementary researches on Liaoning Fengcheng uranium-bearing B-Fe complex ore separation. Journal of Materials and Metallurgy. 8(4), 242-245. In Chinese.

11. Meng, J., Wang, H.-M., Chen, R.-Q., etc., 2008. Study of comprehensive utilization and separation of U-Mo by ion exchange from lixivium of a uranmolybdatite ore. Uranium mining and metallurgy. 24(4), 173-176. In Chinese.

12. Liao, W.-S., Wang, L.-M., Jiang, G.-P., etc. 2011. Study of Formation Protection Technics of a Low-permeable Sandstone Uranium Deposit. Progress report on China nuclear science & technology, Vol.2. In Chinese.

13. Li, X.-J., Jiang, Y., Yao, Y.-X., etc., 2010. Technical measures of reinforcing the discharge of in-situ leaching drillholes and applications. Uranium mining and metallurgy, 29(2), 57-61, 69. In Chinese.

14. Jiang, Y., Hu, B.-S., Tan, Y.-H., etc., 2014. Filter construction technology in mining drilling hole for in-situ leaching of multilayer deposit. Uranium mining and metallurgy. 33(4), 185-191. In Chinese.

15. Liao, W.-S., Tan, Y.-H., Wang, L.-M., Li, J.H., 2016. Oxygen used as an oxidizer in acid in-situ leach uranium-from theory to practice. Proceeding of the 24th International Conference on Nuclear Engineer(ICONE 24)/ Charlotte, USA/Jun 26-30 2016, Paper No. ICONE24-60126.

16. Xie, T.-T., Wang, X.-D., Tan, Y.-H., etc., 2015. Three-dimensional numerical modeling of aquifer for in-situ leaching uranium with water injection curtain, Uranium mining and metallurgy, 34(2): 91-96. In Chinese.

17. Yang, Y.-H., Long, H.-F., 2007. Application of loaded resin readsorption process in Yining uranium mine. Uranium mining and metallurgy. 26(2), 105-109. In Chinese.

18. Quan, A.-G., 1998. Technical research and application prospect on uranium extraction by stope leaching. Uranium mining and metallurgy. 17(1), 1-6. In Chinese.

19. CNNC, 2009. GB 23727-2009 Regulations for radiation and environmental protection in uranium mining and milling. In Chinese.

20. CNNC, 2009. GB 23728-2009 Regulation for radiation environmental impact assessment in uranium mine and mill. In Chinese.

21. CNNC, 2006. EJ/T 359-2006 Technical regulations for radon exhaustion and ventilation in underground uranium mine. In Chinese.

22. CNNC, 2009. GB 50520-2009 Code for safety design of uranium mills tailings pond in nuclear industry. In Chinese.

PILOT STUDY ON URANIUM RECOVERY FROM VIETNAM URANIUM SANDSTONE LOW GRADE ORES BY THE HEAP LEACHING METHOD

By

Than Van Lien, Tran The Dinh, Nguyen Dinh Van, Nguyen Ba Tien and Nguyen Thi Kim Dung

Institute for Technology of Radioactive and Rare Elements (ITREE), Vietnam

Presenter and Corresponding Author

Than Van Lien
tvlien59@yahoo.com.vn

ABSTRACT

Heap leaching has been a well-known technique which is used in mining industry to recover valuable metals such as copper, nickel, gold and uranium from their low grade ores. Vietnam has uranium deposits located in the Nong Son Basin belonging Quang-Nam province in the middle area of the country, but the uranium content in these ores is relatively low (average from 0.01 % - 0.06%U) and the content of Fe in some deposits is high (nearly 2%). In this paper, several fundamental and applied studies on the column and box leaching behaviour of the Nong Son Basin uranium low grade are reported.

The heap leaching of low-grade uranium sandstone ores on a pilot scale, with capacities of 500 kg/batch and 3 000 kg/box of ore was carried out and the selective recovery of uranium from leach liquor was investigated. The optimum parameters for heap leaching were as follows: ores particle size 1 cm; acid H_2SO_4 concentration of the irrigation solution 50 – 75 g/L and irrigation flow rate was 10-30 $l/m^2.h$; oxidant MnO_2 powder 4 kg/t ore; necessary leaching duration for a batch was 15 days, and that for a box was 25 days with acid consumption of around 40 kg/ore tone. The leaching efficiency of uranium recovery was 75%.

The uranium concentration of leach liquor (in the case of box leaching) after 25 days was 1.25 gU/L, and the concentration of iron was 10 – 12 gFe/L. Treatment of leaching solution by ion-exchange using GS300 anion resin was conducted and was followed by precipitation to obtain yellowcake product with high quality of over 80% U_3O_8.

Key words: Uranium, low grade ores, heap-leaching, column and box tests, uranium recovery

INTRODUCTION

Uranium deposits in Vietnam are rather low grade and relatively small in extent as compared to present worldwide commercial practice. The results of uranium exploration showed that the uranium deposits were concentrated in Nong Son Basin areas of Quang Nam Province in the middle part of Vietnam, in which the Palua - Parong uranium deposit is located.

The geological investigations show that in the Pa Lua - Parong deposit there are two rock formations with three rock layers containing uranium ore ranging from 0.04% to 0.06% and average content of 0.05% U_3O_8. The main impurity of Pa Lua - Parong deposit is iron. It was confirmed that Palua - Parong was the most prospective mine in Vietnam at present.

The research on uranium ore processing of Pa Lua - Parong deposit was carried out by Institute of Radioactive and Rare Elements.

Leaching is known as an important step in the processing of a uranium ore. Some techniques for leaching include agitation leaching, pressure leaching, strong acid pugging and curing, heap leaching and in situ leaching. The choice between these leaching techniques is mainly determined by the uranium content in the ore, uranium mineralogy and the gangue. Heap leaching is one of the oldest hydrometallurgical techniques, which can offer a relatively low-capital cost method for recovering uranium from low grade ores but it can also suffer from poor recovery, without offering the cost savings associated with in situ leaching. The ores have to be mined, transported and sometimes crushed before being leached. The preparation of an impervious base is usually required. Improvements in extraction efficiency require innovations such as pelletizing (agglomeration) and the provision of leach vats. Finally, the dump has to be removed, or otherwise processed to meet environmental requirements[1,2,3,4].

In the studied case, the selection of suitable leaching methods for Palua – Parong uranium ore treatment was carried out by different techniques such as agitation leaching and heap leaching. The recovery of uranium showed that heap leaching was the most suitable technique for processing this uranium sandstone ore. Tests for heap leaching procedure were done in different stages, such as laboratorial tests to optimize the technical parameters, semi-pilot tests to define significant parameters for pilot tests, and pilot studies in boxes to validate the operating conditions for a future industrial process.

Palua – Parong uranium sandstone ores were treated by sulphuric acid, followed by a purification stage using the resin ion exchange method and staged precipitation using MgO reagent. The chemical reactions are the following[5]:

Acid (H_2SO_4) leaching

$$UO_2 + MnO_2 + H_2SO_4 \rightarrow UO_3 + MnSO_4 + H_2O$$
$$UO^{2+}{}_2 + 3SO_4^{2-} \rightarrow [UO_2(SO_4)_3]^{4-}$$

Solution purification using ion exchange resin

$$4[R_4N]^+Cl^- + [UO_2(SO_4)_3]^{4-} \rightarrow [R_4N]_4[UO_2(SO_4)_3] + 4Cl^-$$

Precipitation

$$UO_2SO_4 + Mg(OH)_2 \rightarrow MgU_2O_7 + MgSO_4 + H_2O$$

Leaching of impurities should also be taken into account

$$Al_2O_3 + 3H_2SO_4 \rightarrow Al_2(SO_4)_3 + 3H_2O$$
$$Fe_2O_3 + 3H_2SO_4 \rightarrow Fe_2(SO_4)_3 + 3H_2O$$
$$CaCO_3 + H_2SO_4 \rightarrow CaSO_4 + H_2O + CO_2$$

In the present work, the results of heap leaching of Palua - Parong low-grade uranium sandstone ores on a laboratory scale with capacity of 10 kg ore/column and on semi-pilot scale with capacity of 500kg ore/column and then a pilot scale of 3000 kg ore/box are presented. Selective recovery of uranium from the leach liquor by ion exchange resin (GS300, Indian made) followed by precipitation with MgO agent to get yellowcake product was used.

EXPERIMENTAL

Tests at Laboratory Scale

Heap leaching tests were carried out in columns. The height of the columns was 1.1 m with an internal diameter of 0.1 m. A tank with 0.1 m^3 capacity was laid below the leaching column for the collection of solution draining from the column.

A tank containing H_2SO_4 acid for ore leaching was placed above that column and acid solution was irrigated on the top to percolate to the bottom of ore column. The size of the uranium ore used in this test, after crushing, was below 10 mm. The loading capacity of each column was 10 kg with that size ore. MnO_2 oxidant was used at the ratio of 4 kg MnO_2/t ore. Uranium ore after crushing was agglomerated in a rolling drum by spraying water while mixing. Leaching agent was H_2SO_4 acid. At the laboratory scale, the test was carried out for the study of experimental parameters of uranium leaching efficiency such as ore particle size, acid consumption, acid concentration, irrigation rate of leaching solution, the depth of ore bed in the column, and leaching time. Results obtained from these tests would be contributed to the selection of suitable parameters for the heap leaching process.

Tests at Semi-Pilot Scale

These heap leaching tests were carried out in a large volume column with a height of 5.5 m, and internal diameter of 0.3 m. The capacity of the drained-solution collection tank was of 0.2 m^3. Each test column in the semi-pilot scale phase was loaded with 500 kg of sandstone ore. The original concentration of H_2SO_4 was 50 g/L. The leaching process was applied similarly to that at the laboratory scale, otherwise noted in the experimental details. The leach liquor passed through the ore sample by gravity and re-circulated through a side loop with a peristaltic pump without the addition of further acid. Leach liquor was sampled from this tank to determine the concentration of all components in solution, uranium dissolution and acid balance.

Pilot Scale with Box Tests

The leaching boxes were constructed with acid resistant brick with a capacity of 3 to 3.3 t of ore as shown in Fig. 1. The size of each box was 1.15 x 1.15 x 3.0 m (denoted as LxWxH). A window of 0.8 m width was designed for loading and unloading the uranium ore. The walls and bottom of the boxes were coated with bitumen layers in order to resist the acidity.

Each leaching box was lined with a 20 cm pebble layer of about 5-25mm particle size at the bottom, followed by a 5 cm thick layer of -5mm pebbles. A plastic net was placed on top of that pebble layer to prevent the ore particles mixing with the pebble liner.

An irrigation frame made of plastic tubes Ø20 mm was used as illustrated in Fig. 1; the distance between tubes was arranged as 10 cm and each tube had a row of 2 mm diameter holes for directing down to the surface of leaching box. A tank of 50 litre volume was placed on a stand above that irrigation frame.

The scheme of leaching box and accompanied devices was given in Fig.1.

Methods of Analysis

Mineralogical characterization of uranium sandstone ore was done by using X-ray diffraction analysis. The chemical composition of the uranium ore was determined by inductively coupled plasma mass spectrometry (ICP-MS) (Agilent 7500a, USA). Uranium and other major elements in the ore, in leaching solutions and in leach liquor were determined using volumetric titration and/or spectrophotometry (SPECTRONIC 20D, USA).

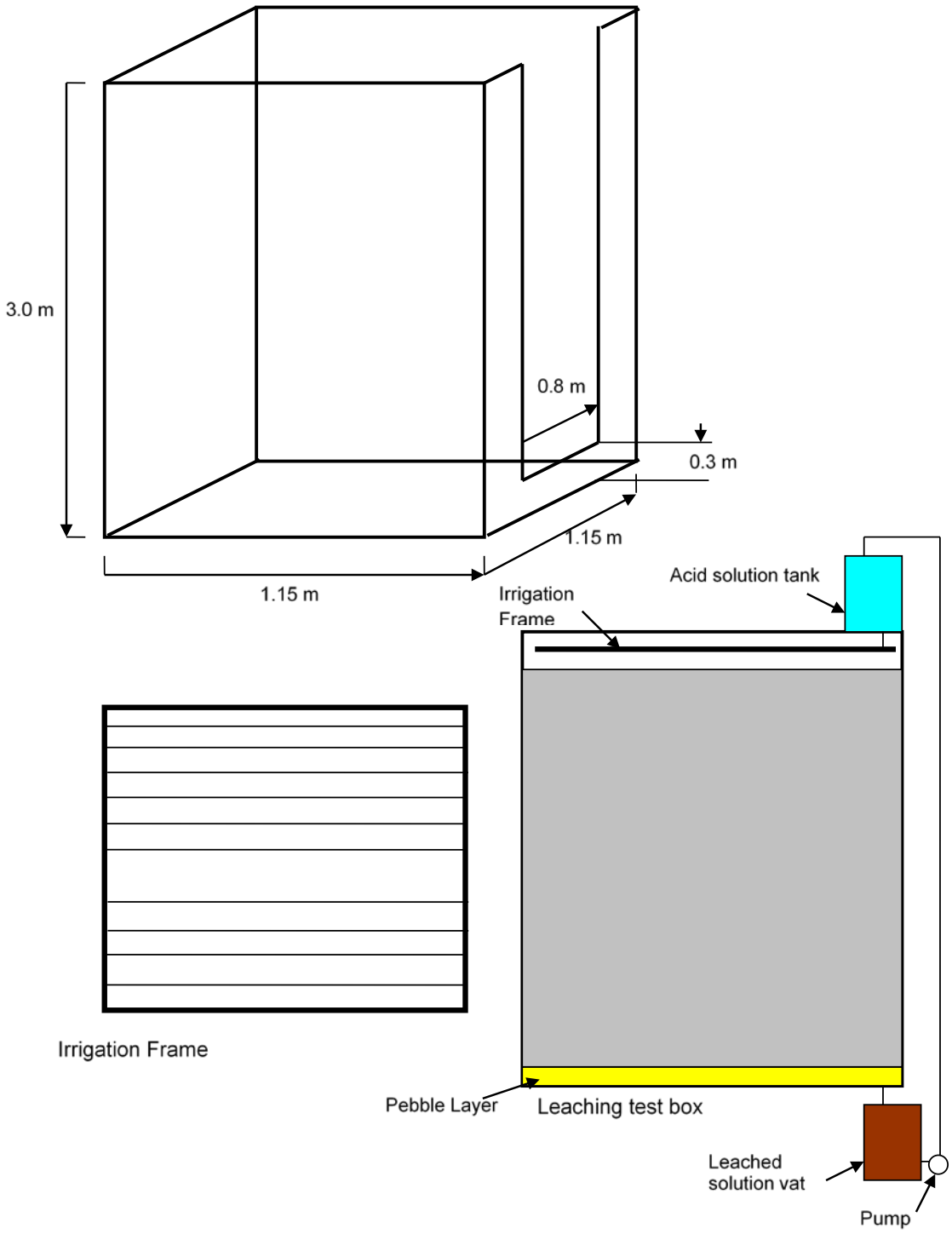

Fig. 1 Leaching box for testing low-grade uranium sandstone ore

RESULTS AND DISCUSSION

Mineralogical and Chemical Compositions of Palua - Parong Low Grade Uranium Sandstone Ore

The X-ray analysis of this sandstone ore showed that the main minerals included quartz (SiO_2), albite ($NaAlSi_3O_8$), glauconite ($(K,Na)(Fe^{+3},Al,Mg)_2(Si,Al)_4O_{10}(OH)_2$), calcite ($CaCO_3$), kaolinite ($Al_2Si_2O_5(OH)_4$), sericite ($K_2O.3Al_2O_3.6SiO_2.2H_2O$), illite ($(KH_3O)Al_2Si_3AlO_{10}(OH)_2$), siderite ($FeCO_3$), sphene($CaO.SiO_2.TiO_2$). The mineral containing uranium was mainly Nasturan ($(U,Th)O_2.(O_{0,5\text{-}3})$ UO_3. xPbO). The results of mineralogical identification confirmed that the content of carbonate and clay minerals, especially montmorrillonite clays in this sandstone ore were very low, meaning that the uranium minerals could be leached using sulfuric acid.

The chemical composition of this sandstone ore was determined using ICP – MS and is given in Table 1. The uranium content in the ore was 0.053% U_3O_8. The most abundant impurities were silica (average 64.90%), aluminum (14.32% as Al_2O_3), iron (2.15%), potassium, sodium and alkaline earth metals together with other impurities. The distribution of uranium based on particle size seemed relatively uniform.

Table 1: Chemical composition of uranium sandstone ore

No.	Component	Content, %	No.	Component	Content, %
1	SiO_2	64.90	7	CaO	3.54
2	Fe_2O_3	2.15	8	Al_2O_3	14.32
3	MgO	5.59	9	V_2O_5	0.14
4	TiO_2	0.40	10	Th	0.0011
5	P_2O_5	0.011	11	U_3O_8	0.053
6	K_2O	2.71	12	MnO_2	0.13

Treatment of Uranium Ore by Heap Leaching in Laboratorial Scale

Effect of Sulphuric Acid Concentration on the Leaching Efficiency

The efficiency of uranium ore leaching seemed dependent on the H_2SO_4 acid concentration. The leaching tests were implemented with various H_2SO_4 acid concentrations from 30 g/L up to 100 g/L. The experimental data was shown in Fig. 2. It can be seen that the leaching efficiency was enhanced with the increase of H_2SO_4 acid concentration. At 30 g/L H_2SO_4 acid concentration, the yield of uranium leaching was the lowest while the highest value was reached at leaching solution containing 100 g/L H_2SO_4 acid. However, under this high acidity leaching condition iron and other impurities were also released into the solution together with an excess of free acid, which could cause difficulties in later neutralization of leach liquor and in the uranium purification stage. Hence, a sulfuric acid concentration was selected between 50 g/L and 75 g/L for the optimum leaching process.

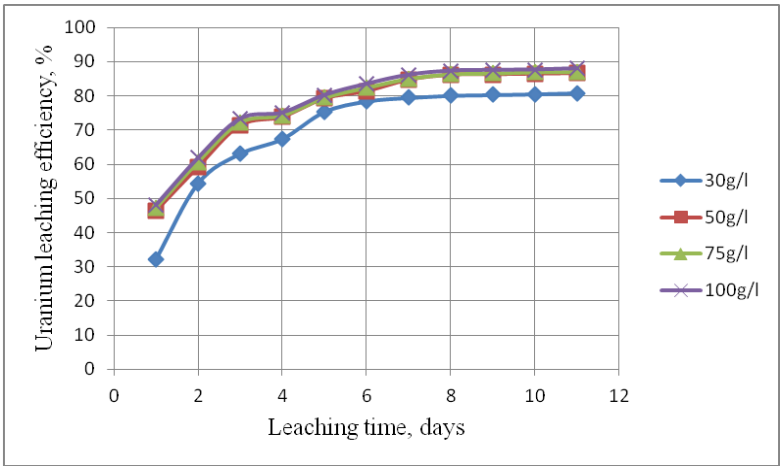

Fig. 2 Effect of sulfuric acid concentration on uranium leaching efficiency

Effect of Sulphuric Acid Consumption

The leaching tests were taken part with different amounts of H_2SO_4 acid consumption. Fig. 3 illustrates the uranium yields obtained in columns as a function of sulphuric acid consumption. The experimental results showed that, the uranium yield increased with increasing quantity of H_2SO_4 acid consumption. Thus this was a key parameter that defined the uranium recovery. The optimum amount of acid was therefore dependent on an economic function between uranium recovery and acid cost. It was also necessary to note the Palua-Parong sandstone ore containing relatively significant impurity of iron (more than 2%), the increase of acid amount led to get more impurities in the leaching solution, especially iron. Therefore, it was necessary to undertake a study on the selection of an appropriate acid consumption to save the cost on the one hand, and to avoid the increase of impurities concentration in the solution on the other hand, which have a great influence with the process of following ion exchange purification.

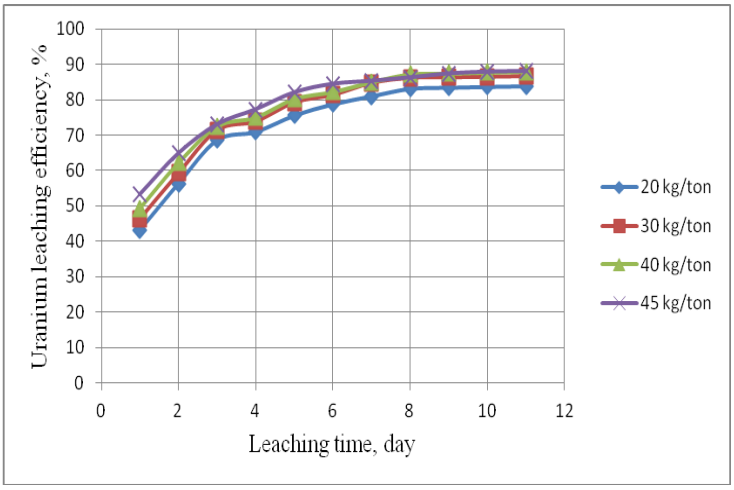

Fig. 3 Effect of acid consumption on uranium leaching efficiency

The experimental results also showed that due to the relatively low ratio between liquid and solid phases in leaching process, acid solution could not penetrate into the core of large size ore particles, which might cause an excess of acid on the surface of ore particle and no reaction occurring at the core. In the washing process, water was flushed through the ore mixtures and it could improve the osmosise of excess acid to react the ore core, which resulted in the increase of pH in solution and enhanced the uranium leaching yield. An acid consumption of 35 - 40 kg/ton was thus selected as the optimum condition for heap leaching of the low-grade uranium sandstone ore in large scale.

Effect of Irrigation Flow Rate on Uranium Recovery Efficiency

The irrigation flow rate of acid solution was varied from 10 to 50 $l/m^2.h$ in these leaching tests. The dependency of uranium leaching efficiency on the leaching time at various the irrigation flow rates is shown in Fig. 4. From these tests, it was found that the uranium recovery efficiency was increased with the increase of flow rate. However, the increase of irrigation flow rate might lead to channeling of solution. Furthermore, it was better to use a spraying solution with less acidity, as too low acidity could cause a risk of jarosite precipitation. As can be seen from Fig. 4, the uranium recovery efficiency reached 82.58% after 11 leaching days with an irrigation flow rate of 30 $l/m^2.h$. For this reason an irrigation flow rate of 20- 30$l/m^2.h$ was chosen.

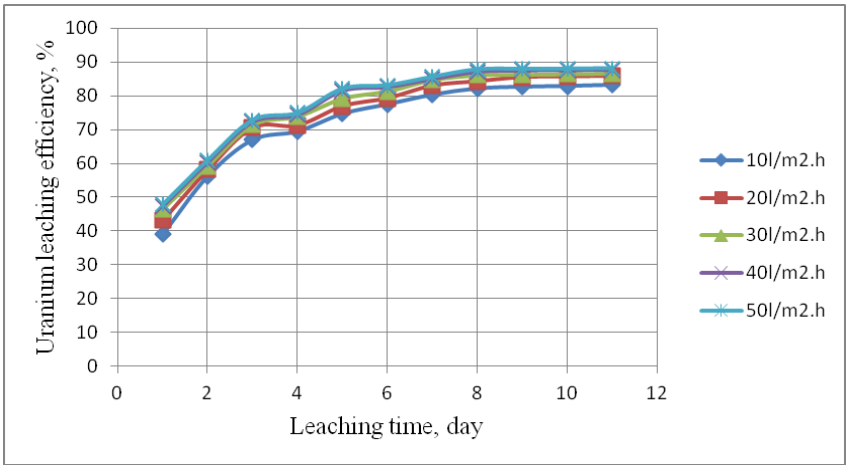

Fig. 4 Effect of irrigation flow rate on uranium recovery efficiency

Effect of The Ore Column Height on Uranium Recovery Efficiency

The tests were carried out in different columns at varying the height from 1 to 3 metres. The uranium recovery efficiency was obtained variously as a function of the leaching time as plotted in Fig.5. Experimental results showed that the increase of the column height decreased slowly the uranium recovery efficiency. It was because of the solution flowed from the top down, the upper ore particles in the column reacted with the acid solution that resulted in the decrease of acid concentration. This solution continued to contact the lower ore layers but acid concentration was further reduced to lead the overall reducing the rate of reaction and slowed down the uranium recovery.

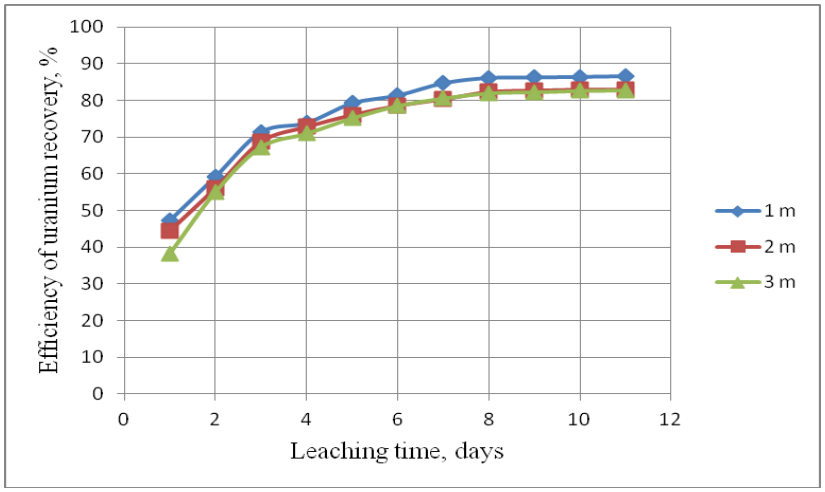

Fig. 5 Effect of the ore column height on uranium recovery efficiency

Semi-Pilot Column Tests with 500 kg of Ore

On the basis of the laboratory column tests, suitable heap leaching parameters were chosen for both semi-pilot column and pilot box tests. The processing parameters were fixed as follows: ore crushing size ≤ 1 cm, sulfuric acid concentration of irrigation solution about 50 g/L – 75g/L, spraying flow rate from 10 to 30l/m^2.h. The optimum conditions which were set up for semi-pilot column tests are given in Table 2.

Table 2. Optimum conditions established for semi-pilot column tests

Parameters	Values
H_2SO_4 acid consumption, kg/t	37.5
Oxidant, kg MnO_2/t	4
Spraying flow rate, l/m^2.h	30
H_2SO_4 concentration in spraying solution, g/L	50
Uranium yield estimated within 15 days, %	76.8

The uranium recovery efficiency reached the maximum value at 76.8% after 15 days leaching process. This value was somewhat lower than that obtained in laboratorial scale. However, it was high than at the pilot scale.

Pilot Box Study with Capacity 3000 Kg of Ore/Box

Each box test was loaded with 3000 kg of uranium sandstone ore. The acid solution was passed through the test box from above to below. The efficiency of uranium recovery was plotted against the leaching time, which was also compared with that in the semi-pilot scale column test. These curves were depicted in Fig. 6. It can be seen that in order to get a similar recovery efficiency at leaching in box, it needed a longer time (25 days) compared to the 15 days in the semi-pilot test column tests. Uranium recovery efficiency reached the maximum value at 75.2% after 25 days leaching process.

The slower rate of reaction during heap leaching in the test box seemed due to the overall kinetics of uranium leaching and/or the density of ore loading and the widespread irrigation, and other effects. However, after 15 leaching days, the difference between columns and box tests was less than 2%. This difference was most certainly due to flow hydrodynamics. In the column tests, the ore was delicately introduced with very few channels, whereas in the box channels readily formed within the first few days as the ore compacted and cracks appeared, particularly on the heap surface. In the columns, all of the ore compacted simultaneously and the flow rapidly resembled plug flow.

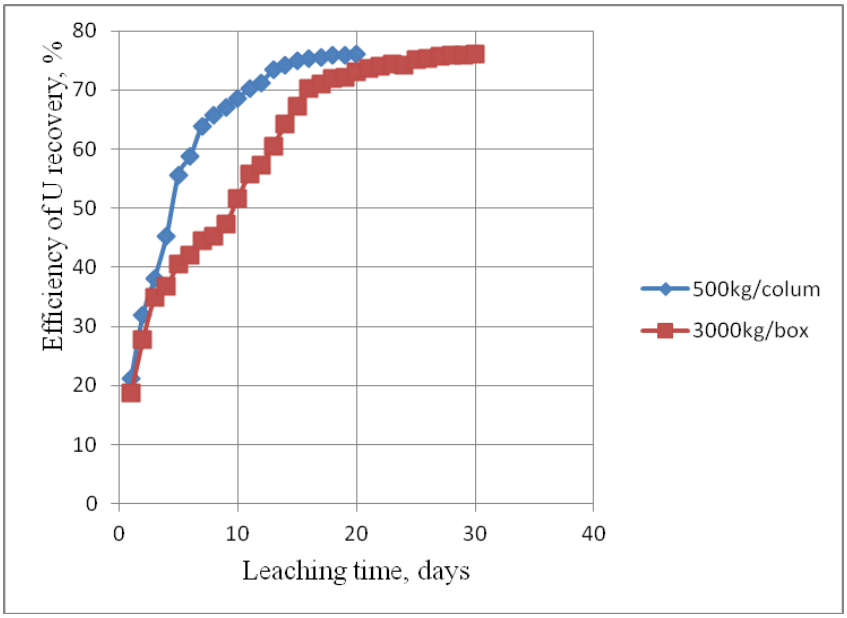

Fig. 6. Effect of the leaching time on uranium recovery efficiency

The optimum conditions established for box tests is shown in Table 3.

Table 3: Optimum conditions established for pilot box study

Parameters	Values
H_2SO_4 acid consumption, kg/t	40
Oxidant, kg MnO_2/t	4
Spray flow rate, l/m^2.h	20
Acidity of the spray solution, g/L	50
Uranium yield Estimated within 25 days, %	75.2

The components of the leach liquor after leaching for 25 days are listed in Table 4. The concentration of uranium was 1.25 g/L, and that of iron, aluminium, calcium and vanadium were 10.87; 4.64; 0.23 and 0.05 g/L, respectively. The other impurities such as molybdenum, cadmium, nickel, and arsenic were at very low level. Hence, the leaching liquor obtained from box leaching was suitable for the next process - ion exchange to produce uranium pregnant solution.

Table 4. Chemical components of leach liquor ($g \cdot L^{-1}$)

U	Fe	SO_4	Al	Mn	K	Mg	Ca	Ti	V	Sr
1.25	10.87	125	4.64	2.82	1.34	1.28	0.23	0.12	0.05	0.02

Ion Exchange Process

In order to clarify the leaching solution, the ion exchange process was applied with ion exchange resin GS300 and using column ion – exchange tests with the conditions as following:

Column size: Inside diameter = 0.2 m, and length = 1.5 m
Feed **-** solution with constituents in grams per litre as shown in Table 4.

pH of leaching solution: 1.6 – 1.8 (pH of leaching solution was adjusted by NaOH)
Feed solution temperature: 25°C.

Flow rates of adsorption - 5 BV (Bed volum)/h (retention time in resin bed = 5 min.).

After the adsorption period was completed, the residual feed solution was washed from the resin bed by passing deionized water through at the rate of about 5 BV/h until pH of effluent was about 3.5.

Elution - regeneration: uranium was eluted from the resin bed by passing eluant (mixture of 0.9 M NaCl and 0.1 M HCl) through at a rate of 2.5 BV/h (Retention time in resin bed = 10 min.). The concentration of uranium and iron of elution – solution was 8.5 g/L and 0.75 g/L respectively.

Precipitation of Yellowcake Product

The eluted solution obtained from the ion exchange process was used to precipitate yellowcake product. Although the iron was largely eliminated from the ion exchange process due to the anionite resin usage, the concentration of iron was still too high (0.75g/L) to directly precipitate because the product would not meet the standard on iron content. Therefore, it was necessary to include a neutralization stage to adjust the pH to about 3.8 in order to remove more iron before precipitating the product.

In terms of precipitation agent, MgO was selected. The precipitation conditions were as follows: pH = 7.0-7.2 and temperature 60^{o}C.

The main chemical components (U, Fe) of precipitated yellowcake product and uranium recovery efficiency at this stage are given in Table 5.

Table 5. Main chemical components (U, Fe) of yellowcake product

Temperature °C	pH	Leach liquor after precipitation		Precipitation product		U recovery %
		U, g/L	Fe, g/L	U_3O_8, %	Fe, %	
60 - 62	7.05	0.001	0.002	80.17	0.081	95.25

Flowsheet

From the results of pilot study, a flowsheet to treat the Palua - Parong low-grade uranium sandstone ores by heap leaching method was identified, as shown in Fig.7.

Some further pictures of the uranium processing pilot at Palua – Parong deposit (Quang-Nam Provice) are given in Fig.8.

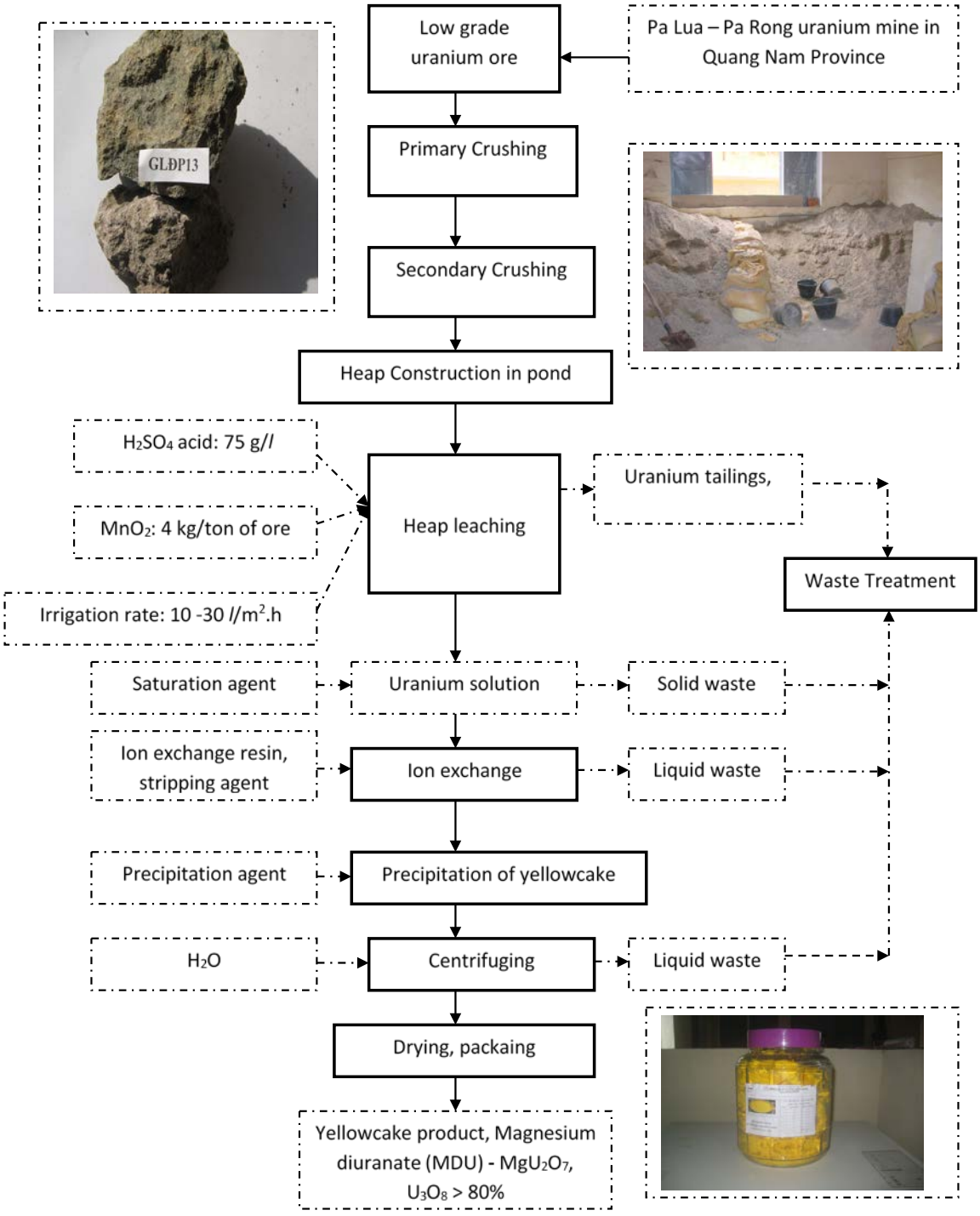

Fig. 7: Flowsheet for Vietnam low grade uranium ore processing by heap leaching method

Fig. 8. Heap leaching on pilot scale at uranium deposit in Quang Nam province

CONCLUSIONS

The heap leaching method was proven to be suitable for Palua-Parong uranium low- grade sandstone ore processing. The tests were carried out at semi-pilot and pilot scale for the treatment of uranium low-grade ore containing 0.05% U by the heap leaching method with column capacities of 500 kg ore/batch and 3000 kg ore/box. Suitable parameters of for leaching conditions were identified such as: crushing size of ore ≤ 1 cm, H_2SO_4 acid concentration of the irrigation solution 50 – 75 g/L, irrigation flow rate 10-30 l/m^2.h, oxidant powder MnO_2 4 kg/ore ton, required leaching duration for a batch about 15 days and for a box about 25 days, acid consumption around 40 kg/ore ton, leaching efficiency of uranium recovery about 75%. The uranium concentration of leach liquor after 25 days was 1.25 gU/L, and that of iron was 10 – 12 gFe/L. Treatment of leaching solution by ion-exchange with GS300 resin was conducted and was followed by precipitation to obtain high quality of yellowcake product containing over 80% U_3O_8.

ACKNOWLEDGMENTS

The authors acknowledge the financial support from the Vietnam Ministry of Science and Technology under Project coded ĐTCB04/16/VCNXH. The corresponding author would like to thank IAEA for the financial support to attend in this conference. The experimental contribution of colleagues at the Institute for Technology of Radioactive and Rare Elements (ITRRE, VINATOM) to our work is highly appreciated.

REFERENCES

1. Durupt Nicolas. Heap leaching of low grade uranium ores at Somair. Technical Meeting on Uranium Small-Scale and Special mining and Processing Technologies. Vienna. 19-22 June 2007.
2. IAEA, Significance of Mineralogy in the Development of Flowsheets for Processing Uranium Ores, Technical reports series No. 196, p. 74-82; 90-100, Vienna,1980.
3. IAEA, Manual on Laboratory Testing for Uranium Ore Processing, Austria, pages 61-85; 117-118, 1990.
4. IAEA. Recent Developments in Uranium Resources and Production with Emphasis on in situ Leach Mining. Proceedings of technical meeting organized by the IAEA in co-operation with the OECD Nuclear Energy Agency, the Bureau of Geology, and China National Nuclear Corporation held in Beijing. 18-23 September 2002. IAEA-TECDOC-1396. 6/2004.
5. Merritt R.C. The Extractive Metallurgy of Uranium. First printing. Library of Congress Catalog Card No. 71-157076. p. 209. 417 - 490. USA. 1971.

ANION EXCHANGE OF URANIUM FROM SULFURIC ACID SOLUTION: ADSORPTION AND KINETICS CHARACTERISTICS

By

Yasser M. Khawassek

Nuclear Materials Authority, Egypt

Presenter and Corresponding Author

Yasser Khawassek
yasser_khawassek@yahoo.com

ABSTRACT

The present work deals with the adsorption of uranium from sulfuric acid solution using the strong base anion exchange Lewatit Mono Plus M500 (LMP) resin. Batch shaking sorption experiments are carried out to evaluate the performance of (LMP) anion exchange resin in the uranium adsorption. The adsorption parameters including contact time, pH, initial uranium concentration and temperature have actually been optimized. The physical parameters including the adsorption kinetics, the isotherm models and the thermodynamic data have also been determined to describe the nature of the uranium adsorption by the LMP resin. The working resin has been found to agree with both the pseudo second order reaction and the Langmuir isotherm.

Keywords: Uranium, Adsorption, sulfate liquor, ion-exchange, Lewatit

INTRODUCTION

Uranium is an immensely concentrated source of energy. Solid-liquid extraction of uranium from its ores has proved to be more advantageous in view of the total insolubility of the applied solid in the aqueous phase, its low rate of physical degradation besides its high sorption capacity as well as its good flexibility and kinetic properties[1][2]. Ion exchange is a highly effective, low-cost method, efficient and easy to operate among the physicochemical treatment processes. Ion exchange methods are widely used for the hydrometallurgical recovery of uranium from sulfuric acid leached mineral ore bodies[3].

The earliest uranium separation process had been based on the development of ion exchange resins containing anion exchange functional groups. This is due to the fact that uranium in the sulfate leach liquors is generally present as anionic sulfate complex and can thus be selectively extracted leaving the other impurities in cationic species. Consequently, the most commonly used resins in uranium recovery processes were strong base anion exchange resins containing quaternary ammonium groups[4]. Based on this fact, many researches have reported the application of several anion exchange resins upon the sulfate leach liquors such as Amberlite IRA-400[5,6]. Amberlite IRA-402[7], AMn resin[8], Amberlite IRA-425[9], Dowex-IX8[10], Ambersep 920U Cl[11] for uranium recovery from its solutions.

In recent years, among various commercial resins available a number of Lewatit commercial resins such as Lewatit TP-208[12], Lewatit TP-260[13][14], Lewatit Mono plus SP-112[15], Lewatit MP-62[16], Lewatit MP-64[17], Lewatit TP-207[18], Lewatit S-100[19] and Lewatit CNP-80[20], have been used to remove heavy metals or recover uranium(VI) from waste or saline water and leach liquors.

Kinetic investigation on a certain ion exchange process may be undertaken either to ascertain the kinetic mechanism in a new system or, more generally, to confirm experimentally the existing rate theories or one may desire to know, at a certain stage of development of a new application, moreover to determine experimentally mass transfer coefficients and other kinetic parameters necessary to design an ion exchange plant[21].

From this point of view, the current paper is focused on the uptake behavior of uranium(VI) from sulfuric acid media by solid phase extraction using the strong base Lewatit Mono Plus M 500 resin (LMP). The objective of this work was to establish the parameters affecting the rate of uranium extraction from aqueous sulfuric acid solution as an indication of the performance of LMP resin. In the meantime, the optimum loading conditions were interpreted via sorption kinetic and adsorption isotherm modeling.

EXPERIMENTAL

Materials and Analytical Procedure

All reagents used were of analytical reagent grade, manufactured by Riedel-de Haen. The working Lewatit Mono Plus M 500 resin (LMP) was purchased from Lanxess E. Chemistry. The physical and chemical characteristics of strongly basic LMP are presented in Table 1. It was cleaned and regenerated with 1 M H_2SO_4 and distilled water.

Table 1: The physical and chemical characteristics of strongly basic LMP gel type anion exchange resin

Characteristics	Value	Units
Ionic form as shipped,	Cl^-	
Functional group	Quaternary amine	
Mean bead size	0.62 (+/- 0.05)	mm
Density	1.08	g/ml
Water retention	48-55	%
Total capacity (min)	1.3	Eq/l
Volume change, Cl^- --> OH^-	20	Max. vol.%
Stability at pH range	0-14	
Storability of product	2	years
Operating temperature	70	^0C
Regenerant	NaOH	
Operating pH range	0-12	

The standard uranium sulfate solution was prepared by dissolving an appropriate amount of uranyl sulfate trihydrate $UO_2SO_4.3H_2O$ from Ibilabs, Florida, USA.

The quantitative analysis of uranium was carried out by UV-spectrophotometer "single beam multi-cells-positions model SP-8001", Metretech Inc., version 1.02 using Arsenazo III indicator[22] at 655 nm[23] and confirmed by an oxidimetric titration against ammonium metavanadate using N-phenyl anthranilic acid indicator (Sigma-Aldrich)[24][25].

Equilibrium Studies

To investigate the influences affecting the adsorption process, a series of batch experiments were achieved using the standard uranium sulfate solution. These factors involved contact time, pH, initial uranium concentration and the effect of adsorbent dose (amount). From the achieved results, Langmuir and Freundlich as well as Dubinin-Radushkevich (D-R) isotherms were determined. The adsorption experiments were performed by shaking 0.1 g LMP resin with 40 ml of the uranium sulfate synthetic solution (of 300 mg/L initial uranium concentration) using a magnetic stirrer. The adsorbed amounts of uranium were calculated by the difference between its equilibrium and initial concentrations. The amount of uranium adsorbed on the solid phase q_e (mg/g) was calculated using the following relation:

$$q_e = (C_o - C_e) \times \frac{V}{m} \qquad (1)$$

where C_o and C_e are the initial and equilibrium concentrations of the uranium (mg/L), respectively, V is the volume of the aqueous phase (L), and m is the weight of the LMPR resin used (g). The adsorption percent of ions from the aqueous phase is calculated from the following relation:

$$\text{Uranium adsorption } \% = \frac{C_o - C_e}{C_o} \times 100 \qquad (2)$$

The distribution coefficient (K_d) of uranium between the aqueous bulk phase and the solid phase was calculated from the following relation:

$$K_d = \frac{C_o - C_e}{C_e} \times \frac{V}{m} \qquad (3)$$

Equilibration Calculation

All uranium speciation in this study were performed with Hydra-MEDUSA, a chemical equilibrium calculation program[26].

RESULTS AND DISCUSSION

Effect of Contact Time

The impact of the contact time was examined through a series of experiments by contacting a fixed weight of LMP resin (0.1 g) with a uranium solution (40 ml) having a concentration of 300 mg/L and pH 2 at temperature (25, 37, 42 and 58 ^{0}C).

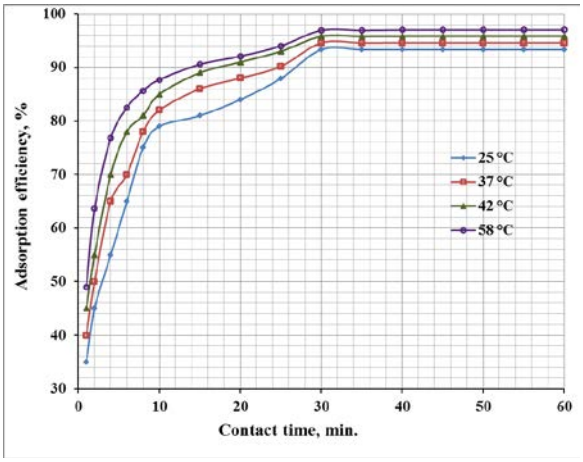

Figure 1: Effect of contact time upon the uranium adsorption efficiency on the LMP resin
(resin weight = 0.1 g, volume = 40 ml, pH = 2, U conc.= 300 mg/L)

The studied time ranged from 1 to 60 minutes. The reached results were plotted in Figure 1. It was detected that the uranium adsorption efficiency attained about 93.33% for 30 minutes contact time at temperature 25 °C while it reached to 97% at 58 °C. By increasing the contact time from 30 to 60 minutes, the uranium adsorption efficiencies remained constant. Consequently, 30 minutes contact time could be selected as the suitable time.

Effect of pH

The influence of pH on the adsorption of uranium on LMP resin from sulfate solution was explored by contacting a fixed weight of the LMP resin (0.1g) with (40 mL) uranium synthetic solution of 300 mg/L at 25 °C for 30 minutes. The examined pH ranged from 0.8 to 6. The achieved data were presented in Figure 2. From the obtained results, it could be seen that the maximum uranium adsorption was achieved at pH between 2 and 3 of 90 % adsorption efficiency. This could be due to the presence of anion complexes of uranium ($UO_2(SO_4)_2^{2-}$). Accordingly, pH 2-3 was the best range and consequently, pH2 was selected for the subsequent experiments.

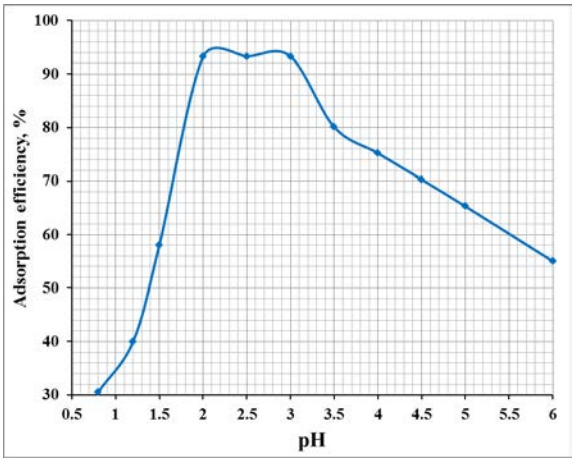

Figure 2: Effect of pH on the adsorption of uranium onto the LMP resin (U conc.= 300 mg/L, resin weight = 0.1 g, volume = 40 ml, 30 min, 25 ^{0}C)

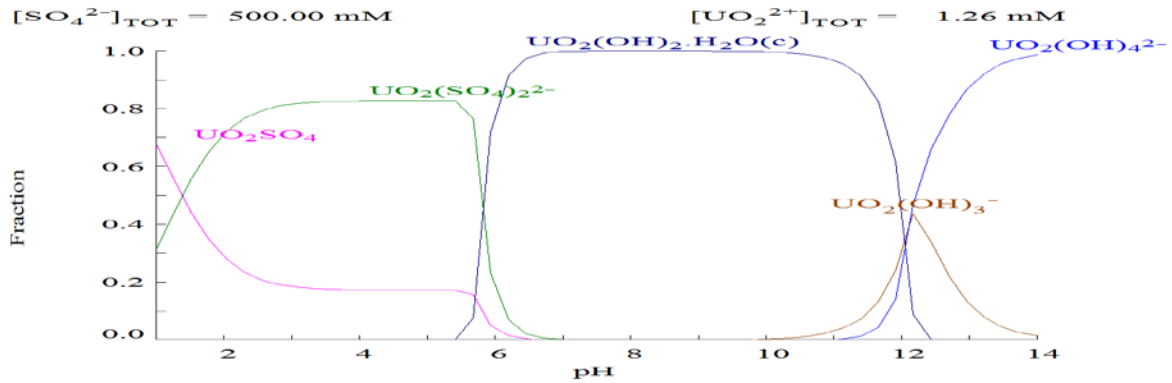

Figure 3: Expected aqueous speciation of uranium (300 mg/L) as a function of pH in 0.5 M H_2SO_4 using Medusa and Hydra program

The aqueous speciation distribution of uranium was calculated and represented in Figure 3. The results showed that the complexes of UO_2SO_4 and $UO_2(SO_4)_2^{2-}$ were the predominant species at the pH range from 0.0 – 5.5 with a mean total percent of 31 and 69% respectively at pH 0 while 18 and 82 % at pH 5.5. U-hydroxide complexes start to dominate the aqueous phase at pH near 6. The dominate complex of $UO_2(OH)_2.H_2O$ became the major species with about 100% of total concentration at pH range from 6 to 12. After pH 12, $UO_2(OH)_4^{2-}$ and $UO_2OH_3^-$ became the major species. According to the initial pH of 2-3, the following adsorption scheme is more appropriate to be considered and the possible coordination mechanism for the interaction between $UO_2(SO_4)_2^{2-}$ and the LMP resin is as followed:

$$2(R_4N^+)Cl^- + UO_2(SO_4)_2^{2-} = (R_4N^+)_2UO_2(SO_4)_2^{2-} + 2Cl^-$$

Effect of Initial Uranium Concentration

To inspect the influence of initial uranium concentration upon the adsorption efficiency onto LMP resin, a series of experiments were performed by contacting a fixed weight (0.1 g) of the studied resin with 40 ml of 300 mg/L uranium concentration and pH 2 for 30 min at room temperature (≈ 25 ºC). The studied initial uranium concentrations ranged from 50 up to 1000 mg/L. The obtained results were plotted in Figure 4. From the obtained data, the uranium adsorption efficiency decreases with increasing its initial concentration. In contrast, the adsorption capacity increased with increasing the initial uranium concentration until constant after 300 mg/L. Therefore, the experimental adsorption capacity of the adsorbent was about 112 mg uranium/g resin.

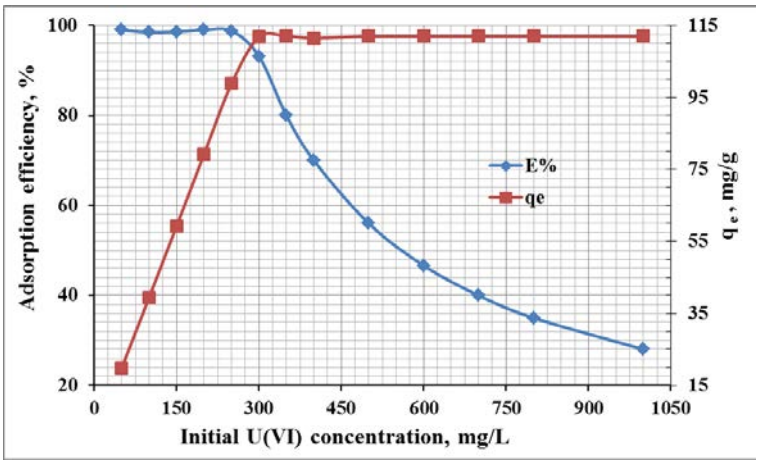

Figure 4: Effect of initial uranium concentrations on uranium adsorption efficiency and uranium uptake onto the LMP resin
(resin weight = 0.1 g, volume = 40 ml, pH=2, 30 min, 25 ^{0}C)

Adsorption Isotherm

A number of common adsorption isotherm models were considered to fit the attained isotherm data under the equilibrium adsorption of the LMP resin. Examples of these models are Langmuir, Freundlich and Dubinin–Radushkviech (D–R isotherm) isotherms.

A- Langmuir Isotherm

Langmuir model suppose that, the adsorption occurs uniformly on the active sites of the sorbent, and once a sorbate occupies a site, no further sorption can take place at this site[27-29].

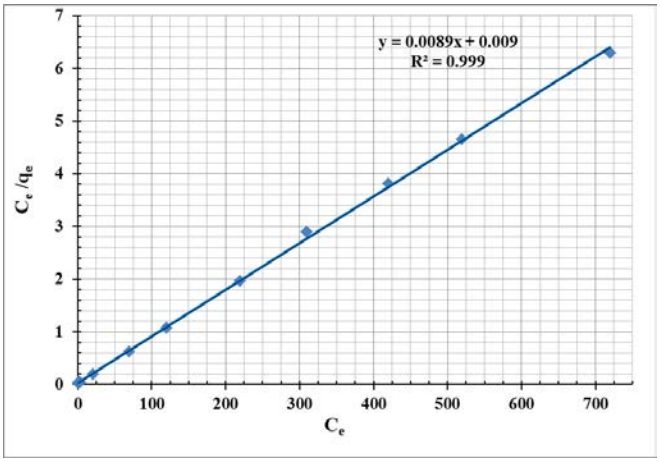

Figure 5: Langmuir isotherm plot for adsorption of uranium onto LMP resin

Thus, the Langmuir model is given by the following equation:

$$\frac{C_e}{q_e} = \frac{1}{bq_0} + \frac{C_e}{q_0} \qquad (4)$$

where: q_o and b, the Langmuir constants, are the saturated monolayer sorption capacity and the sorption equilibrium constant, respectively. A plot of C_e/q_e versus C_e would result in a straight line with a slope of $1/q_o$ and intercept of $1/bq_o$ as seen in Figure 5. The Langmuir parameters are given in Table 2.

B- Freundlich Isotherm

The Freundlich model stipulates that the ratio of solute adsorbed to the solute concentration is a function of the solution. The empirical model was shown to be consistent with exponential distribution of active centers, characteristic of heterogeneous surfaces[27-29]. The amount of solute adsorbed at equilibrium, q_e, is related to the concentration of solute in the solution, C_e, by the following:

$$q_e = K_F C_e^{1/n} \qquad (5)$$

This expression can be linearized to give:

$$\log q_e = \log K_F + \frac{1}{n}\log C_e \qquad (6)$$

where K_F and n are the Freundlich constants, which represent sorption capacity and sorption intensity, respectively. A plot of ($\log q_e$) versus ($\log C_e$) would result in a straight line with a slope of (1/n) and intercept of ($\log K_F$) as seen in Figure 6. Freundlich constants are given in Table 2.

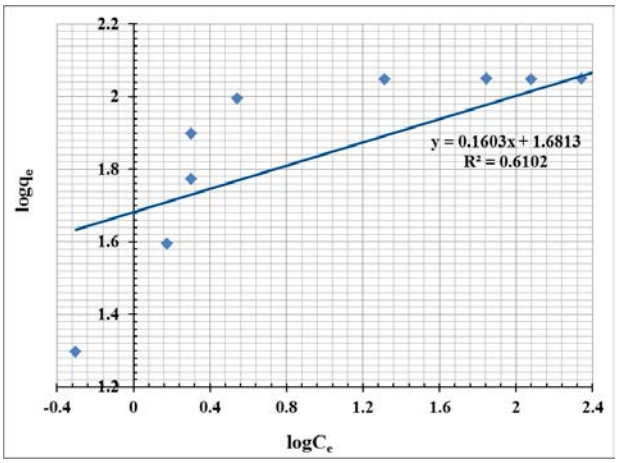

Figure 6: Freundlich isotherm plot for adsorption of uranium onto LMP resin

C- Dubinin–Radushkviech isotherm (D–R isotherm)

The Dubinin-Radushkevich (D-R) isotherm model was applied to the data in order to assume the heterogeneity of the surface energies of adsorption and the characteristic porosity of the adsorbent[29]. The linear form of the D-R isotherm is given in following equation:

$$\ln q_e = \ln q_m - \beta\varepsilon^2 \qquad (7)$$

where q_m is the maximum amount of ions that can be adsorbed onto unit weight of LMP resin, i.e. adsorption capacity (mg/kg), β the constant related to the adsorption energy (mol^2/kJ^2); and **ε** is the Polanyi potential = RT ln(1+1/C_e), where R is the gas constant (mol/KJ), and T is the absolute temperature (K). The mean free energy of adsorption is the free energy change when one mole of uranium is transferred to the surface of the LMP resin from infinity in the solution and it is calculated from:

$$E_a = \frac{1}{(2\beta)^{\frac{1}{2}}} \qquad (8)$$

The D–R plots of $\ln q_e$ versus $\boldsymbol{\varepsilon^2}$ for the sorption of uranium ions onto LMP resin are given in Figure 7. Linear regression analysis using paired of $\ln q_e$ and $\boldsymbol{\varepsilon^2}$ resulted in the derivation of q_m, β, and the correlation factor (R^2). These parameters are listed in Table 2.

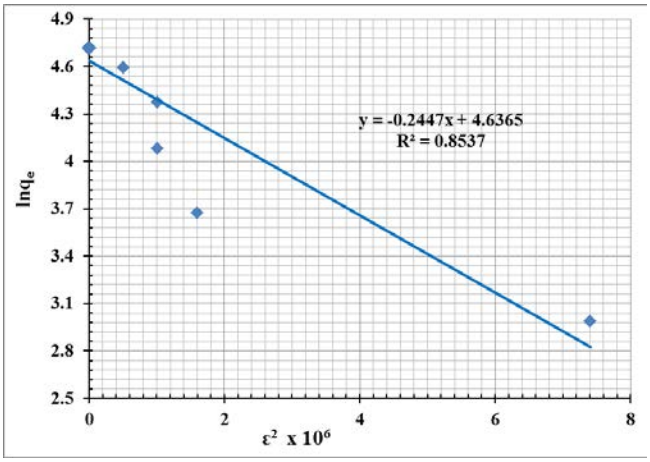

Figure 7: D–R isotherm plot for adsorption of uranium onto LMP resin

Table 2: Langmuir, Freundlich and D–R isotherms parameters for uranium adsorption onto LMP resin

Langmuir model parameters			Freundlich model parameters			D–R model parameters			
q_o (mg/g)	b (L/mg)	R^2	1/n	K_f (mg/g)	R^2	β (mol^2/kJ^2)	q_m (mg/Kg)	E_{ads} ($kJmol^{-1}$)	R^2
112.36	0.989	0.999	0. 158	48.31	0.602	0.244	103.13	0.7	0.853

Comparing the isotherms applied with the experimental results, Langmuir gave the best fit, while Dubinin-Radushkevich and Freundlich isotherms did not fit well. A comparison of the adsorption capacity of LMP resin with some other sorbents is provided in Table 3.

Table 3: The experimental capacity of LMP resin compared with the adsorption capacity of some resins and different solvent modified polymers

Type	adsorption capacity (mg/g)	Ref.
polyethyl eniminephenyl phosphonamidic acid	39.66	(30)
N-dimethyl-N,N-dibutyl malonamide functionalized polymer	18.78	(31)
succinic acid impregnated amberlite XAD-4	12.33	(32)
gel-amide	28.98	(33)
gel-benzamide	18.64	(33)
natural clinoptilolite zeolite	0.7	(34)
Ambersep 920U Cl	51.2	(11)
Lewatit TP 214	81.75	(35)
Lewatit TP 208	308.65	(35)
4-(2-Pyridylazo)resorcinol (PAR), Amberlite XAD-16	115.5	(36)
Amberlite IRA-910	64.26	(37)
Lewatit MonoPlus M 500	112.3	Present work

Effect of Adsorption Temperature

The influence adsorption temperature on the uranium adsorption efficiency by LMP resin was explored by contacting fixed portions 0.1g of LMP resin with 40 ml of uranium standard solution of 300 mg/L. The other factors were fixed at a contact time of 30 min, and solution pH of 2. Several experiments were carried out at different temperatures from 25 to 58 °C. The experimental results are presented in Figure 8 as a relation between uranium adsorption efficiency and temperature. The obtained results show that, the uranium adsorption efficiency slightly increases by increasing the temperature. The increase of uranium sorption onto LMP resin at higher temperature may be attributed to increase in the activation of the sorbent surface. As the uranium adsorption efficiency was not distinguished, there is no need to control or alter the temperature.

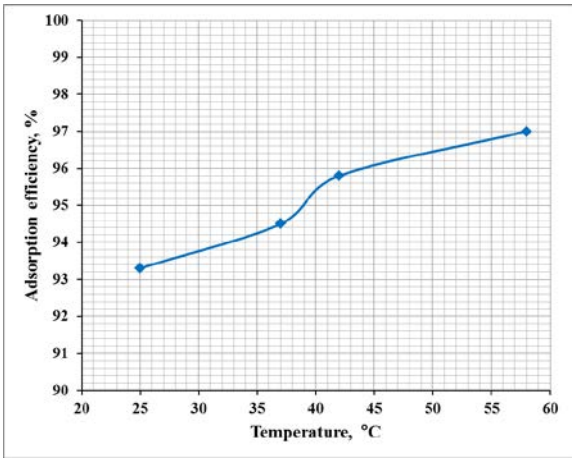

Figure 8: Effect of temperature on uranium adsorption efficiency onto LMP resin

Effect of Resin Amount

The amount of the adsorbent used in the uranium adsorption process is very critical from the economic point of view. The influence of adsorbent amount on the uptake of uranium was confirmed in Figure 9. A series of adsorption experiments was achieved using different adsorbent doses ranging from 0.25 up to 7.5 g resin/L. The experiments were done under constant initial uranium concentration of 300 mg/L at room temperature (≈ 25 ºC) for 30 min shaking time and pH of 2. From the achieved results the adsorption efficiency increases significantly with increasing adsorbent amount (adsorbent dose) from 0.25 to 2.5 g resin/L of about 9.33 up to 93.33% respectively. The increase became slight by increasing the amount from 2.5 to 3 g resin/L till the adsorption efficiency was constant. This observation is possibly due, increase in the adsorbent dose the active sites increase, consequently the associated adsorption increases. By further increasing of the LMP resin amount the active sites become more plentiful than the available uranium ions in the solution. Consequently, the adsorptive capacity of adsorbent available was not fully utilized at a higher adsorbent amount. Based on the latter, 2.5 g LMP resin/L is preferred as the usable adsorbent amount.

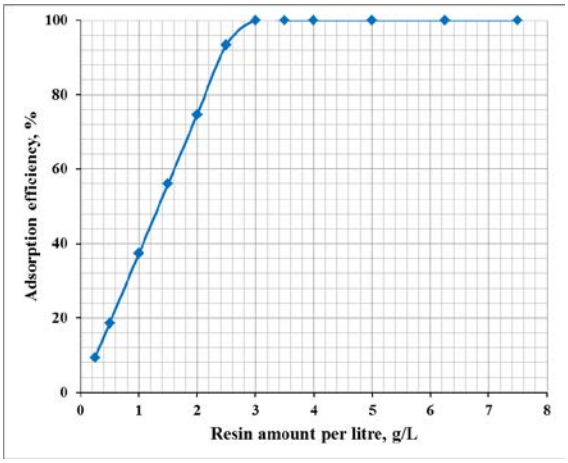

Figure 9: Effect of adsorbent dose upon uranium adsorption efficiency onto LMP resin

Adsorption Kinetics and Mechanism

The data obtained from batch experiments which were performed at different temperatures (25–58) ^{0}C were evaluated by using the simple Lagergren equation[38] to determine the rate of the sorptive interactions assuming pseudo first order kinetics:

$$\log(q_e - q_t) = \log q_e - \left(\frac{k_1}{2.303}\right)t \qquad (9)$$

where q_t and q_e are the amounts of uranium adsorbed (mg/g) at time, t (min) and equilibrium time (30 min), respectively and K_1 is the pseudo first order Lagergren adsorption rate constant (min $^{-1}$). The k_l values could be obtained by plotting log (qe – q_t) versus t for adsorption of uranium at different temperatures as shown in Figure 10. The values of the first order rate constant (k_l) and correlation

coefficient (R^2) obtained from these plots are listed in Table 4. The values of k_l indicate that the rate of the process increases with temperature.

The first order mechanism suffered from inadequacies when applied to uranium sorption on the LMP resin. One of the major discrepancies was observed when q_e values obtained from the pseudo first order plots were compared with the experimental q_e values are seen in Table 4. The experimental q_e values differed from the corresponding theoretical values. Thus, the interaction of uranium with the LMP resin does not follow the first order kinetics

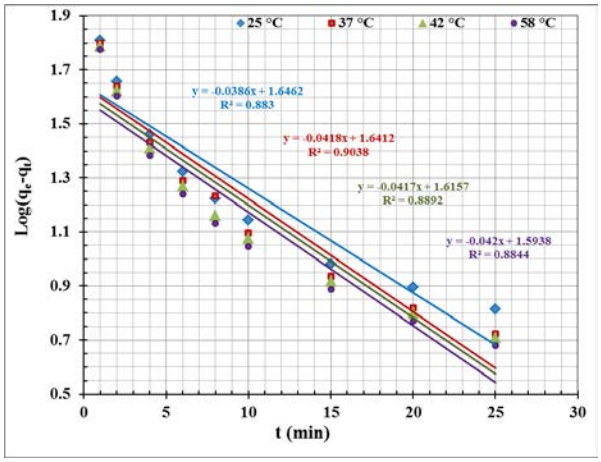

Figure 10: Lagergren plots for the adsorption of uranium
(resin amount = 0.1 g, volume = 40 ml, pH 2, U Conc. = 300 mg/L)

In order to insure the description of the kinetics, second order kinetic equation was applied. The pseudo second order kinetics can be represented by the following linear equation[39]:

$$\frac{t}{q_t} = \frac{1}{K_2 q_e^2} + \left(\frac{1}{q_e}\right) t \qquad (10)$$

where k_2 is the second order rate constant (g. mg^{-1} min^{-1}). The kinetic plots of t/q_t versus t for uranium are shown in Figure 11.

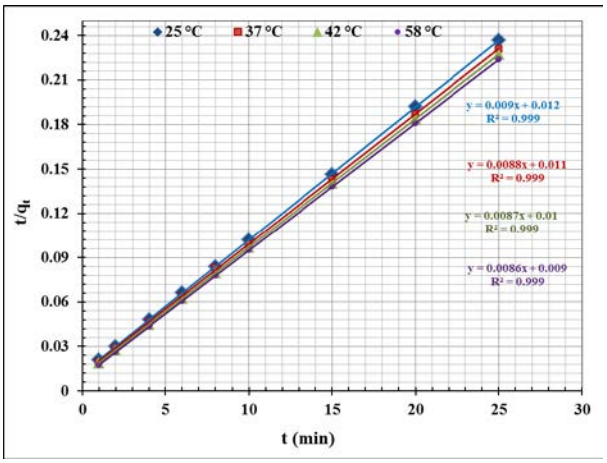

Figure 11: Pseudo second-order plots for the adsorption of uranium
(resin amount = 0.1 g, volume = 40 ml, pH 2, U Conc. = 300 mg/L)

The plots show straight lines with good linearity temperatures. The calculated correlation coefficients are closer to unity for the pseudo second order kinetic model. The calculated equilibrium adsorption capacity (q_e) is consistent with the experimental data. The k_2 values show the applicability of the above equation for the resin. Therefore the sorption reaction can be approximated more favorably by the pseudo second order sorption as the predominant mechanism.

Table 4: Data of kinetic parameters for uranium adsorption onto LMP resin

Temp, °C	Lagergreen pseudo first-order				pseudo second-order			
	K_1 (min $^{-1}$)	q_{ecal} (mg/ g)	q_{eexp} (mg/ g)	R^2	K_2 (min $^{-1}$)	qe_{cal} (mg/ g)	qe_{exp} (mg/ g)	R^2
25	0.087	44.26	112.0	0.883	6.75 x 10^{-3}	111.11	112.0	0.999
37	0.094	43.75	113.52	0.903	7.04 x 10^{-3}	113.64	113.52	0.999
42	0.094	41.21	115.0	0.889	7.57 x 10^{-3}	114.94	115.0	0.999
58	0.097	39.17	116.4	0.884	8.22 x 10^{-3}	116.28	116.4	0.999

Thermodynamic Characteristics

The thermodynamic parameters of the studied adsorption process have been determined for uranium adsorption upon Lewatit Mono Plus M 500 resin. Series of experiments were carried out at various temperatures ranging from 25 to 58 ºC. These parameters were calculated for this system using the following Van't Hoff equation:

$$\log K_d = \frac{\Delta S}{2.303R} - \frac{\Delta H}{2.303RT} \qquad (11)$$

where K_d (ml/g), ΔH (KJ/mol), ΔS (J/mol.K), T (Kelvin) and R (KJ/K.mol) are the distribution coefficient, the enthalpy, the entropy, the temperature in Kelvin and the molar gas constant respectively. The plotting of log K_d against 1/T for uranium adsorption is shown in Figure 12.

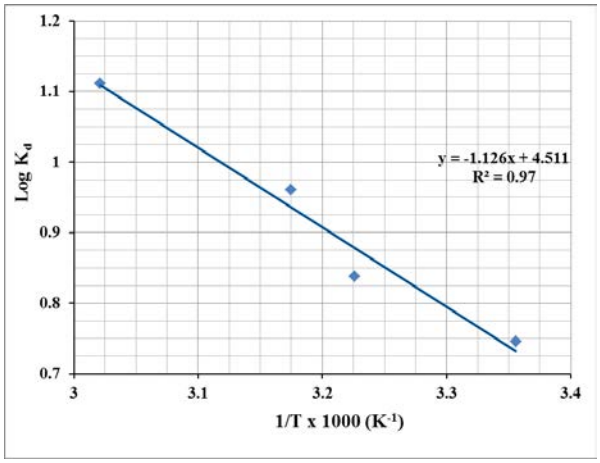

Figure 12: Plot of Ln Kd versus 1/T of uranium ions onto LMP resin

The values of ΔH and ΔS were obtained from the slope and intercept of the latter plot while the Gibbs free energy, ΔG (KJ/mol), is calculated from the following equation:

$$\Delta G = \Delta H - T\Delta S \qquad (12)$$

The calculated values of the thermodynamic parameters for U (VI) adsorption on LMP resin are given in Table 5. It was found that the enthalpy change (ΔH) and the entropy change (ΔG) were calculated to be 21.56 KJ/mol and -4.18 KJ/mol respectively. Thus, the adsorption process was found to be endothermic and spontaneous. The positive value of ΔS indicates an increase in the randomness at the solid/solution interface during the sorption of the metal ion onto the sorbent, while the negative free energy value, indicating that the process of uranium adsorption is favored at high temperatures.

Table 5: Thermodynamic data for sorption of uranium ions onto LMP resin

ΔH KJ/mol	ΔS J/mol.K	ΔG KJ/mol			
		25 ^{0}C	37 ^{0}C	42 ^{0}C	58 ^{0}C
21.56	86.37	-4.18	-5.21	-5.65	-7.03

Elution and Reusability Procedures

The elution step is the key to the implementation of the anion exchange system on the commercial scale. The uranium(VI) desorption from the loaded LMP resin has been carried out using different concentrations of 10 ml NaCl solution ranging from 0.1 to 2M in presence of 0.1M H_2SO_4 upon 1g loaded resin for 60 min contact time at room temperature. The obtained results reveal that the maximum eluting efficiency (98.5%) is achieved at 1M NaCl. Adsorption-desorption procedure was repeated several cycles to regenerate and its recycle. In this manner, it has been possible to attain a desorption efficiency exceeding 98.5% with 10 ml of 1 M NaCl solution for U(VI) desorption from 1g of the loaded LMP resin.

On the other hand, to determine the reusability of the studied resin, consecutive adsorption–desorption cycles aare achieved upon the same adsorbent dose using a fresh solution for each cycle under the optimum conditions. From the first to the 20th cycles, it is found that an almost complete uranium adsorption and desorption has been realized. Behind the latter, the adsorption efficiency of the LMP resin is decreased from 99.5 to 96% in the 26th cycle (RSD of 1.22%). However the desorption efficiency is decreased from 98.5 to 95% in 25th cycle (RSD of 0.82%). Therefore, it would be possible to reuse the working resin for about 20 cycles without any noticeable loss of the adsorption capacity indicating that the developed resin matrix has an adequately high mechanical stability in a manner to be recycled for 20 times.

FT- IR Spectroscopy and Scan Electron Microscopy

FT-IR spectroscopy and SEM were employed to demonstrate the interactions between LMP resin and U(VI) ions. The spectra of LMP resin before and after loading with U(VI) ions were presented in Figure 13. The FT-IR spectrums of the studied LMP resin and U(VI) loaded resin exhibited several peaks. The peak around 3446 cm^{-1} for strong band of the -OH stretching vibrations was observed for both situations. On the lower frequency side of this band at about 2923cm^{-1} related to the stretching vibrations of the ring C–H bands of the resin (cross-linked polystyrene). The sharp peaks were found at 2348 cm^{-1} (C=C stretching vibration), 1635 cm^{-1} (C=C skeletal vibration), 1426 cm^{-1}(C-N vibration), and 1380 cm^{-1} (O-H bending vibration). The ring C–C stretching and the scissoring of the methylene groups (bending -CH_2) appeared at 1488 and 1453cm^{-1}. After the adsorption, the intensity of some bands changed and transmittance of peaks was relatively greater in the case of LMP resin loaded with U(VI) ions compared to the LMP resin. After adsorption, the most bands were shifted from 10-15 cm^{-1}, that provided evidence of the interaction between U(VI) and the nitrogen atom of tertiary amine group in LMP resin as uranyl anion complex. A signal corresponding to the vibration of O=U=O at 925 cm^{-1}[40][41]was also observed, suggesting the uptake of U(VI) by LMP resin.

The SEM images of the LMP resin before and after uranium(VI) adsorption are shown in Figure 14 a and b, respectively. The SEM images were clearly shown the difference between the surfaces of the LMP resin. Although a good uniformity and smooth surface was observed in the conventional resin, the surface after U(VI) adsorption was observed bright spherical spots on the resin beads. As can be seen from the results, a visible change of the surface morphology in the U(VI) adsorbed resin demonstrated that the sorption of U(VI) had taken place onto the LMP resin.

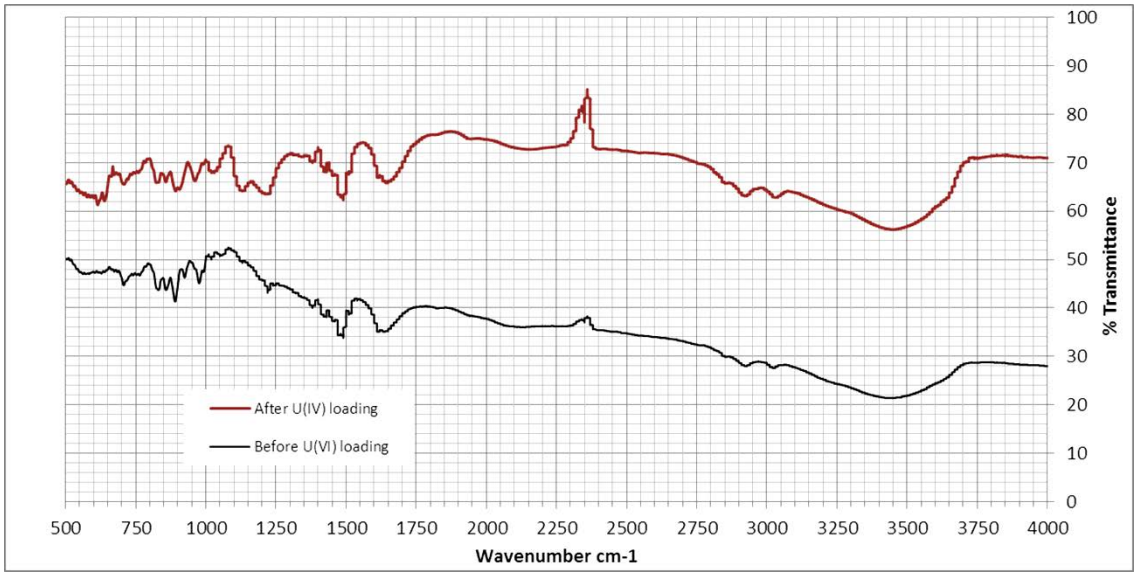

Figure 13: FT-IR spectrum of LMP resin before and after uranium adsorption

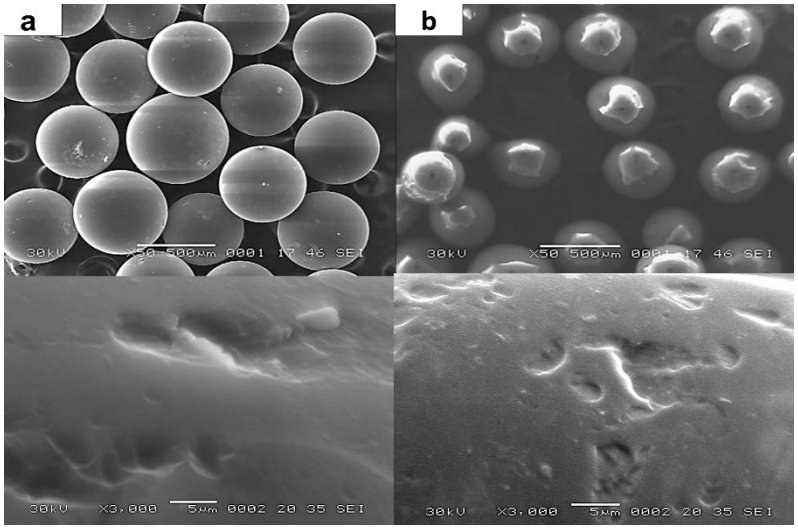

Figure 14: SEM micrographs of LMP resin (a) before and (b) after U(VI) adsorption

A Case Study: Gattar Leach Liquor

From the above giving, it is evident that the LMP resin can be used to extract uranium ions from sulfate solutions. Therefore, it was tested for this purpose on the prepared Gattar pregnant leach solution. The leaching process was completely studied previously[42] and illustrated on the technological Gattar ore material sample. The optimum leaching conditions involved were 0.5 M sulfuric acid, agitation time for 6 h, ore sample to leach acid ratio (S/L) of 1/2, ore particle size of -60 mesh and 40 ml H_2O_2/ Kg ore at 40 ^oC. The leaching efficiency was 95%. The obtained leach liquor was assayed as 150 mg/L uranium(VI) Table 6. The applied extraction experiment was carried out under the previously determined optimum conditions by mixing 50 L of the leach liquor with 66.8 g of the LMP resin (pH 2 for 30 min. contact time at room temperature). The obtained result has revealed that the uranium adsorption amount attained almost 6.6gU. Comparing this loading capacity with the theoretical capacity of the working LMP (112.3 mg U/g LMP), indicated that under the working conditions, 88 % of the theoretical capacity was realized. The decrease in the LMP capacity after contacting with the working sulfate leach liquor may be due to the competition between uranium and different ions presented in the sample (as iron). Furthermore, about 6.5 gU (98.5%) of the loaded uranium was eluted with 1M NaCl acidified with 0.1M sulfuric acid solution, and then precipitated with 20% NaOH as sodium diuranate.

Table 6: Chemical analysis of Gattar leach liquor

Metal ions	Si^{4+}	Al^{3+}	Fe^{3+}	Mg^{2+}	Ca^{2+}	Na^{+}	K^{+}	Ti^{4+}	P^{5+}	Mn^{2+}	REEs
g/L	1.33	1.3	1.82	0.02	0.06	0.12	0.05	0.02	0.01	0.01	0.45
Metal ions	Cr^{3+}	Co^{3+}	Zr^{4+}	Ni^{2+}	Cu^{2+}	Zn^{2+}	Nb^{5+}	Ba^{2+}	Pb^{2+}	Hf^{4+}	U^{6+}
mg/L	25	5	33	14	15	30	10	5	43	2	150

CONCLUSIONS

A commercial sorbent Lewatit MonoPlus M 500 (LMP) resin was tested for uranium extraction. The extraction efficiency was determined as a function of various parameters such as contact time, pH, initial uranium concentration, resin dose and temperature. Equilibrium was attained after 30 min of contact time and the practical loading capacity was 112.3 mg U(VI)/g resin. The kinetics of uranium adsorption on LMP resin followed the second order rate reaction. The equilibrium isotherm for adsorption of the investigated metal ions had been modeled successfully using the Langmuir isotherm. The thermodynamic parameters confirmed the spontaneous, randomness and endothermic nature of chemisorption. Finally, the optimum extraction conditions were applied on the prepared Gattar pregnant leach solution.

REFERENCES

1. Technical Reports Series No. 359, 1993. Uranium Extraction Technology" International Atomic Energy Agency, Vienna,

2. Donat, R., Cılgı, G.K., Aytas, S., Cetisl, H., 2009. Thermodynamics Parameters and Sorption of U (VI) on ACSD. Radioanalytical and Nuclear Chemistry 279, 271-280.

3. Merritt, R.C., 1971. The Extractive Metallurgy of Uranium, Colorado School of Mines Research Institute.

4. Streat M., Naden, D., 1987. Ion Exchange in Uranium Extraction, Critical Reports on Applied Chemistry Vol. 19, Ion Exchange and Separation Processes in Hydrometallurgy.

5. Guettaf, H., Becis, A., Ferhat, K., Hanou, K., Bouchiha, D., Yakoubi K., Ferrad, F., 2009. Concentration–Purification of Uranium from an Acid Leaching Solution. Physics Procedia 2, 765–771.

6. Khawassek, Y.M., 2014. Production of Commercial Uranium Concentrate from El-Sela Shear Zone Mineralized Ore Material, South Eastern Desert- Egypt, at Inshas Pilot Plant Unit. Nuclear Sciences Scientific Journal 3, 169 – 179.

7. Abdel Aal, M., 2014. Purification of Uranium Concentrate from Abo- Rushied Ore Material with Emphasize Upon Ion Exchange Technique, South Eastern Desert, Egypt, Faculty of science, Ain Shams University.

8. Mirjial, K., Roshani, M., 2007. Resin-in-pulp method for uranium recovery from leached pulp of low grade uranium ore. Journal of Hydrometallurgy 85(2-4), 103-107.

9. Abd El-Ghany, M.S., Mahdy, M.A., Abd El-Monem, N.M., El-Hazek, N.T., 1994. Pilot Plant Studies on the Treatment of El-Atshan Uranium Ores, Eastern Desert. Egypt. 2nd Arab Conf. Peaceful Uses of Atomic Energy, AAEA, Cairo.

10. Barnes, C. D., da Silva Neves R. A., Streat M., 1974. Anion Exchange of Uranium from Aqueous Sulphuric Acid Solutions: Diffusion Kinetics. J. appl. Chem. Biotechnol. 24, 787-801.

11. Cheira, M. F., El-Didamony, A. M., Mahmoud, K. F., Atia, B. M., 2014. Equilibrium and Kinetic Characteristics of Uranium Recovery by the Strong Base Ambersep 920U Cl Resin, IOSR-JAC, 7(5), 32-40.

12. Porsch, B., Wittgren, B., 2005. Analysis of calcium salt of carboxymethyl cellulose: size distributions of parent carboxymethyl cellulose by size-exclusion chromatography with dual light scattering and refractometric detection. Carbohydr Polym. 59(1), 27–35.

13. McKevitt, B., Dreisinger, D., 2009. A comparison of various ion exchange resins for the removal of ferric ions from copper electrowinning electrolyte solutions part I: electrolytes containing no other impurities. Hydrometallurgy 98(1–2), 116–121.

14. Alguacil F.J., 2003. A kinetic study of cadmium (II) adsorption on Lewatit TP 260 resin. J Chem Res. 3, 144–146.

15. Dizge, N., Keskinler, B., Barlas H., 2009. Sorption of Ni(II) ions from aqueous solution by Lewatit cation-exchange resin. J Hazard Mater. 167(1–3), 915–926.

16. Riegel, M., Tokmachev, M., Hoell, W.H., 2008. Kinetics of uranium sorption onto weakly basic anion exchangers. React. Funct. Polym. 68(6), 1072–1080.

17. Galàn, B., Calzada, M., Ortiz, I., 2006. Separation and concentration of Cr(VI) from ground waters by anion exchange using Lewatit MP-64: mathematical modelling at acidic pH. Solvent Extraction and Ion Exchange 24, 621–637.

18. Silva, R.M., Manso, J.P., Rodrigues, J.R., Lagoa, R.J., 2008. A comparative study of alginate beads and an ion-exchange resin for the removal of heavy metals from a metal plating effluent. J Environ Sci. Health 43(11), 1311–1317.

19. Bedoui, K., Bekri-Abbes, I., Srasra, E., 2008. Removal of cadmium (II) from aqueous solution using pure smectite and Lewatite S100: the effect of time and metal concentration. Desalination 223(1-3), 269-273.

20. Pehlivan, E., Altun, T., 2007. Ion-exchange of Pb^{2+}, Cu^{2+}, Zn^{2+}, Cd^{2+}, and Ni^{2+} ions from aqueous solution by Lewatit CNP 80. J Hazard Mater. 140(1-2), 299-307.

21. Liberti, L., Helfferich, K., 1983. Mass Transfer and Kinetics of Ion Exchange, 1st ed., Martinus Nijhoff Publishers, The Hague, Netherlands.

22. Marczenko, Z., Balcerzak, M., 2000. Separation Preconcentration and Spectrophotometry in Inorganic Analysis, Elsevier Science B.V., Amsterdam the Netherlands, p.521.

23. Rohwer, H., Rheeder, N., Hosten, E., 1997. Interactions of uranium and thorium with arsenazoIII in an aqueous medium. Anal Chim. Acta. 341(2), 263–268.

24. Davies, W., Gray, W., 1964. A rapid and specific volumetric method for the precise determination of uranium using ferrous sulfate as a reductant. Talanta 11, 1203-1211.

25. Mathew, K.J., Mason, B., Morales, M.E., Narayann, U.I., 2009. Uranium assay determination using Davies and Gray titration: An overview and implementation of GUM uncertainty evaluation. Radio analytical and Nuclear Chemistry 282, 939-944.

26. Puigdomenech I. HYDRA (hydrochemical equilibrium-constant database) and MEDUSA (make equilibrium diagrams using sophisticated algorithms) programs, Royal Institute of Technology, Sweden. https://www.kth.se/en/che/medusa/downloads-1.386254

27. Sheng, L., Zhou, L., Huang, Z., Liu, Z., Chen, Q., Huang, G., Adesina, A.A., 2016. Facile synthesis of magnetic chitosan nano-particles functionalized with N/O-containing groups for efficient adsorption of U(VI) from aqueous solution. J. Radioanal Nucl. Chem. 310, 1361-1371.

28. Li, L., Ding, D., Hu, N., Fu, P., Xin, X., Wang, Y., 2014. Adsorption of U(VI) ions from low concentration uranium solution by thermally activated sodium feldspar. J. Radioanal Nucl. Chem. 299, 681–690.

29. Manes, M., Hofer, L.J.E., 1969. Application of the Polanyi adsorption potential theory to adsorption from solution on activated carbon. The Journal of Physical Chemistry 73(3), 584–590.

30. Abderrahim, O., Didi, M.A., Villemin, D., 2009. A new sorbent for uranium extraction polyethyleniminephenylphosphonamidic acid. J. Radioanal. Nucl. Chem. 279(1), 237–244.

31. Ansari, S.A., Mohapatra, P.K., Manchanda, V.K., 2009. A novel malonamide grafted polystyrene-divinyl benzene resin for extraction pre-concentration and separation of actinides. J. Hazard Mater. 161(2-3), 1323-1329.

32. Metilda P., Sanghamitra K., Mary Gladis, J., Naidu, G.R.K., Prasada Rao, T., 2005. Amberlite XAD-4 functionalized with succinic acid for the solid phase extractive preconcentration and separation of uranium(VI). Talanta 65(1), 192–200.

33. Venkatesan, K., Sukumaran, V., Antony, M.P., Vasudeva Rao, P. R., 2004. Extraction of uranium by amine, amide and benzamide grafted covalently on silica gel. J. Radioanal Nucl. Chem. 260(3), 443–450.

34. Camacho, LM., Deng, S., Parra RR., 2010. Uranium removal from groundwater by natural clinoptilolite zeolite: effects of pH and initial feed concentration. J. Hazard Mater. 175(1–3), 393–398.

35. Ferrah, N., Abderrahim O., Didi, M.A., 2015. Comparative Study of Cd^{2+} Ions Sorption by Both Lewatit TP214 and Lewatit TP 208 Resins: Kinetic, Equilibrium and Thermodynamic Modelling. Chemistry Journal 5(1), 6-13.

36. Cheira, M.F., 2015. Synthesis of pyridylazo resorcinol – functionalized Amberlite XAD-16 and its characteristics for uranium recovery. Journal of Environmental Chemical Engineering 3, 642–652.

37. Rahmati, A., Ghaemi, A., Samadfam, M., 2012. Kinetic and thermodynamic studies of uranium (VI) adsorption using Amberlite IRA-910 resin. Ann. Nucl. Energy 39, 42–48.

38. Lagergren S., 1898. Zur theorie der sogenannten adsorption gelo ¨ster stoffe Kungliga venska Vetenskapsakademiens. Handlingar 24(4),1–39.

39. Ho Y.S., McKay, G., 1999. Pseudo-second order model for sorption processes, Process Biochem. 34,451- 465.

40. Wazne, M., Korfiatis, G.P., Meng, X.G., 2003. Carbonate effects on hexavalent uranium adsorption by iron oxyhydroxide. Environ. Sci. Technol. 37,3619-3624.

41. Abdien, H.G., Cheira, M.F., Abd-Elraheem, M.A., El-Naser, T.A., Zidan, I.H., 2016. Extraction and pre-concentration of uranium using activated carbon impregnated trioctyl phosphine oxide. Elixir International Journal Applied Chemistry 100,43462- 43469.

42. Internal Report Series, Recovery of Uranium from Gattar (II) Mineralization, 2015, Nuclear Materials Authority, Egypt.

RECOVERY OF RARE EARTH, URANIUM AND THORIUM FROM INDUSTRY RESIDUE LEACHING EXPERIMENTS

By

Janúbia C.B.S. Amaral, Carlos A. Morais, Pedro H. M. Andrade and Monique R. Salum

Centro de Desenvolvimento da Tecnologia Nuclear (CDTN), Brasil

Corresponding Authors

Janúbia C.B.S. Amaral and Carolos A. Moraia
djannamaral@gmail.com; cmorais@cdtn.br

Presenter

Janúbia C.B.S. Amaral
djannamaral@gmail.com

ABSTRACT

This paper comprises the study of the recovery of rare earth elements (REE), uranium, and thorium from an industrial residue. REE are important in many areas of materials science, and their application in industry has grown rapidly in recent years. On the other hand, thorium and uranium are elements of great interest in the nuclear area. Thus, the recovery of these elements from secondary sources is important both from the point of view of sustainability and the environmental aspects. The residue used in this work was obtained by the liming treatment of an acid mine water generated in a closed uranium mining site. The main constituents of the residue are REE (4.55%), U (0.20%), Th (0.03%), Ca (15.8%), Al (9.63%), S (6.09%), Fe (4.13%), P (0.59%), and Si (1.92%). Additionally, Mn, Zn and K are present.

The leaching experiments were carried out under mechanical agitation, with temperature and final acidity control, using hydrochloric and sulphuric acid as leaching agent. The variables investigated were solids percentage, reaction time, temperature, and the acid/sample ratio. For the conditions evaluated, the recovery of REE was more efficient when hydrochloric acid was used. The dissolution of U and Th was practically the same for both acids. However, due to technical problems, such as solid – liquid separation, purity of the liquor and the fact that HCl is more aggressive than H_2SO_4, sulphuric acid was selected as the leaching agent. Using HCl in an acid/sample ratio of approximately 600 kg t^{-1}, 10% of solids and 2 hours of mechanical agitation at room temperature, a recovery of 99 % of rare earths, 90 % of Th and 98 % of U was obtained. When sulphuric acid was used with acid/sample ratio of 700 kg t^{-1}, the recovery of the metals was 93.6 % of rare earths, 81.1 % of thorium and 96.7 % of uranium. After the optimization of the leaching parameters, a sulphuric liquor containing 0.082 gL^{-1} Th, 0.35 gL^{-1} U, 9.1 gL^{-1} REE, 16 gL^{-1} Al, 7.8 gL^{-1} Fe, 0,47 gL^{-1} Ca, 0.75 gL^{-1} Zn and 0.1 gL^{-1} Si was obtained.

Keywords: Rare earth, Thorium, Uranium, Leaching, Industry Residues, Secondary Sources

INTRODUCTION

The lanthanides group, together with yttrium and scandium are known as rare earth elements (REE). The rare earth elements have similar chemical properties and, according to their chemical properties, they are used in various fields, such as permanent magnets, electronics, superconductors, hydrogen storage, and medical and nuclear technologies. The rare earth metals have been progressively establishing themselves as industrial materials due to their particular spectroscopic and magnetic properties[1–5].

The rare earth (RE) elements are important in many areas of material science, and their application in industry has grown year after year. Thorium (Th) and uranium (U) are elements of great interest in the nuclear area. Generally, uranium and thorium are present in rare earth minerals, hence they are present in the residues generated in rare earths processing[6–9].The recovery of the aforementioned elements from secondary sources is important for both sustainability and environmental aspects. The use of rare earths from mine tailings, one of the main secondary sources of these elements, offers great opportunities to secure their supplies. The relatively low concentration of REE in the mine tailings (1000 - 1500 $kg.g^{-1}$) has made the extraction of REE from these resources a very challenging process[10]. The separation of thorium and uranium from rare earths has been researched and presented in literature. The separation of these elements from rare earths is important in order to obtain effective measures to control the radiation pollution due to thorium and uranium during the processing of rare earth and also the management of the tailings produced during the process[6][9][11].

The influence of sulphuric and hydrochloric acids on rare earth dissolution from electronic residue is mentioned in literature. Resende and Morais[12] studied the leaching of rare earth residues from scraped color TV screens using sulphuric and hydrochloric acid as the leaching agent. The results of this study indicated the technical viability of the recovery of the metals when using these acids.

This paper presents the study of recovery of rare earths, uranium and thorium from a residue that can be considered a secondary source of rare earth generated in the neutralization, with lime, of an acid water producted in a closed uranium mine site[13] belonging to Industrias Nucleares do Brazil - INB - Caldas Unit. The main constituents of the residue are Ca (15.8%), Al (9.63%), S (6.09%), RE (4.55%), U (0.20%) and Th (0.03%) in addition to Fe, Mn, Si, Zn and K. In this work, a study of the dissolution of Th, U and RE elements present in the industrial residue was carried out. Hydrochloric and sulphuric acids were used as leaching agents. The variables percentage of solids, temperature, pH and acid concentration, were investigated.

EXPERIMENTAL PROCEDURES

The leaching studies were carried out with a dry sample of the residue in batches, with temperature control. The initial temperature of the leaching reached values close to 60 ºC due to the exothermic reaction. The experiments were performed by adding the solids to the acid, thus reducing the heat and the formation of bubbles in the beaker. This stage was performed in a 400 mL beaker under mechanical agitation. Once the best condition for the leaching of the residue was established, the liquor required for precipitation and extraction experiments was produced.

The leaching experiments were carried out using sulphuric and hydrochloric acids solution (H_2SO_4 and HCl) as leaching agents. All solutions were prepared with analytical grade reagents and distilled water. The acid digestion with concentrated sulphuric acid was also investigated. In this case, the acid was added directly to the solids, and the initial temperature reached around 130ºC. As usually, the product of the acid digestion was leached with water in order to dissolve the soluble sulphates and to produce the liquor for the metals separation study. The solid-liquid separation was carried out by vacuum filtration. Once the best condition for the leaching of the residue was stabilised, the liquor required for the study of the separation of the metals was produced.

The chemical characterization of the samples was done by energy dispersive X-ray fluorescence spectrometry - EDXRF (Shimadzu - EDX 720), with inductively coupled plasma optical emission spectrometry - ICP-OES, wavelength dispersive X-ray fluorescence spectrometry – WDX (Rigaku - ZSX Primus II) and ion specific electrode potentiometry using a pH meter (Digimed - DM 22)[6][14–16].

The sample studied, supplied by the “Nuclear Industries of Brazil –INB”, was generated by the neutralization of acid mine water produced in a closed uranium mine site located in Caldas, Minas Gerais state, Brazil[13]. Table 1 shows the chemical composition of the residue. The distribution of particle size in the sample indicated an average size around 18.33 µm.

Table 1: Chemical composition of the residue

Sample	Th	U	RE	Ca	Al	P	Fe	Si	S
Residue (%)	0.03	0.20	4.55	15.87	9.63	0.52	4,13	1.92	6.09

Chemical Process

The properties and compositions of substances containing rare earths, uranium and thorium elements are quite varied. The analytical chemistry of these elements plays an important role in hydrometallurgical process for separation and attainment of its compounds in the pure form. The rare earth elements are highly electropositive and form compounds that are essentially ionic in nature. All the rare earths form M^{3+} ions, although some of them also occur in M^{+2} and M^{+4} states. However, these states are always less stable than the M^{+3} state. The occurrence of M^{+2} and M^{+4} states in certain rare earths is of considerable importance in rare earths extractive metallurgy, and is related to their electronic structures and ionization potentials[4]. Uranium has positive valences from 3 to 6 in its compounds. The hexavalent and tetravalent uranium compounds are of greater importance, and the compounds of hexavalent uranium are the most stable and form uranyl ion (UO_2^{2+}) in aqueous solutions. Thorium presents the positive valence of 4 and compounds of this element in its lower valence states are unstable in aqueous solutions. The overal reaction for rare earths, thorium and uranium during acid leaching with sufphuric acid and hydrochloric acid are expressed in Eqs. 1 – 9[1][9][17][18].

$$RE(OH)_3 + {SO_4}^{2-} + 3H^+ \rightleftarrows {RESO_4}^+ + 3H_2O \quad (1)$$

$${RESO_4}^+ + SO_4^{2-} \rightleftarrows {RE(SO_4)_2}^{-1} \quad (2)$$

$$RE(OH)_3 + 3HCl \rightleftarrows RECl_3 + 3H_2O \quad (3)$$

$$RECl_3 + Cl^- \rightleftarrows {RECl_4}^- \quad (4)$$

$$UO_2(OH)_2 + SO_4^{2-} + 2H^+ \rightleftarrows UO_2SO_4 + 2H_2O \quad (5)$$

$$UO_2SO_4 + SO_4^{2-} \rightleftarrows {UO_2(SO_4)_2}^{2-} \quad (6)$$

$$UO_2(SO_4)_2^{2-} + SO_4^{2-} \rightleftarrows UO_2(SO_4)_3^{4-} \quad (7)$$

$$Th(OH)_4 + 3{SO_4}^{2-} + 4H^+ \rightleftarrows {Th(SO_4)_3}^{2-} + 4H_2O \quad (8)$$

$${Th(SO_4)_3}^{2-} + {SO_4}^{2-} \rightleftarrows {Th(SO_4)_4}^{4-} \quad (9)$$

RESULTS AND DISCUSSION

Leaching

In this stage, the parameters investigated were leaching agent, acid/sample ratio, percentage of solids, reaction time, and temperature of leaching. The leaching experiments were carried out with hydrochloric and sulphuric acids.

Hydrochloric Acid

Influence of Percentage of Solids Without pH Adjustment

The results of the influence of percentage of solids on the dissolution of the metals without pH adjustment are presented in Figure 1. The percentage of solids ranged from 10% to 30%, using hydrochloric acid 7.5 $molL^{-1}$ as the leaching agent at room temperature (25 ± 2)ºC and 2.0 h of stirring. No pH adjustment was made during the experiment. Figure 1 shows that the recovery of the metals (RE, Th and U) decreases as the solid percentage rises due to the increase of the final pH. The acid added is not enough to neutralize the residue and dissolve the metals as the percentage of solids increases. The combination of the variables suggests a solids content between 10% and 15% as the most indicated. For 10% of solids, the Th, U and RE dissolution output was 94.3%, 99.0% and 97.4%,

respectively. For 15% of solids, the dissolution yield for Th, U and RE was 89.7%, 98.2% and 97%, respectively. Table 2 presents the pH of the solutions after the leaching experiments. It shows that the final pH could be between 1 and 2.

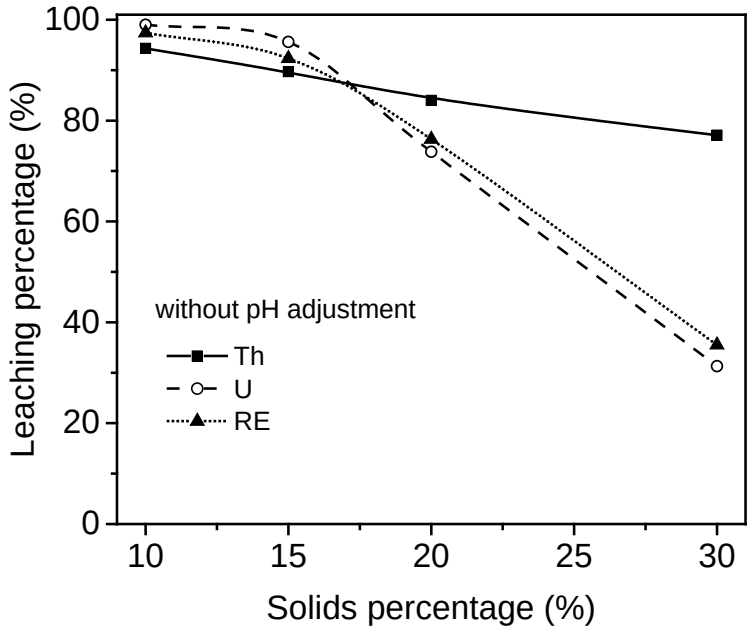

Figure 1: Influence of solid percentage in the residue leaching at 25 ºC using HCl as the leaching agent, 2.0 h stirring without pH adjustment

Table 2: pH after residue leaching with variation of the solid percentage, 2.0 h stirring without pH control

Solids percentage (%)	Final pH
10	0.9
15	2.0
20	3.5
30	4.1

Influence of the Percentage of Solids on Leaching with pH Control

The results of the influence of percentage of solids with the final pH control were presented in Figure 2. The solids percentage ranged from 10% to 25% when hydrochloric acid was used as the leaching agent. The experiments were carried out at room temperature (25 ± 2) ºC, 3.0 h of stirring and the pH was maintained at 1.0 by addition of HCl solution. Figure 2 shows a slight decrease in the metals dissolution as the percentage of solids rises. The results showed a solids content between 10% and 15% as the most indicated. For 10% of solids, the dissolution of Th, U and RE reaches values of 95.3%, 99.2% and 99.5% respectively, and for 25% of solids, a dissolution yield of 91.2% for Th, 98.5% for U and 98.0% RE was achieved.

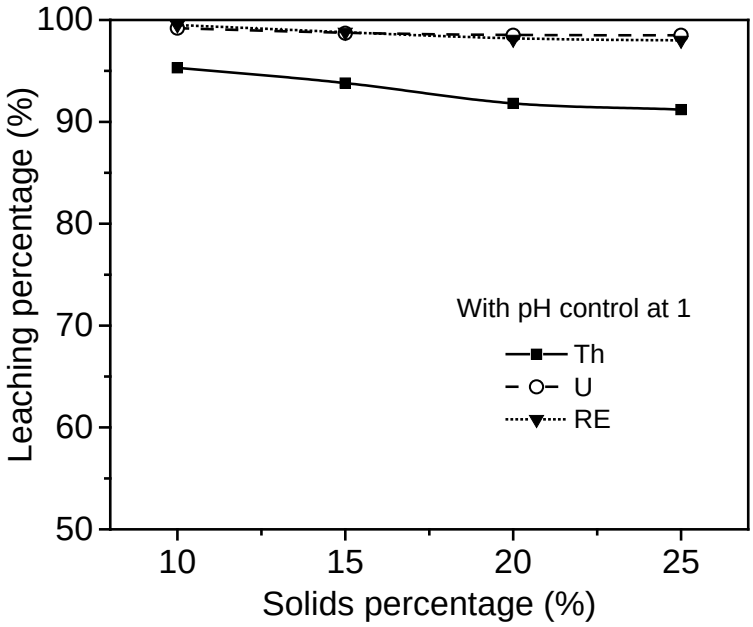

Figure 2: Influence of solids percentage in the residue leaching at 25ºC using HCl as the leaching agent, 2.0 h stirring and control pH in 1

Influence of the Acid/Sample Ratio

The influence of the acid/sample ratio on the Th, U and RE leaching was investigated in the interval between 550 and 640 kgt^{-1}, using HCl 7.5 $molL^{-1}$ as the leaching agent at 25 ^{o}C and 3 h leaching time and 10% of solids. Figure 3 shows that the efficiency of the leaching of Th improved gradually with the increase of the acid/sample ratio, reaching a maximum of 90.0% at an acid/sample ratio of 600 kgt^{-1}. For the acid/sample ratio investigated, the dissolution of U remained constant, at 98%, and a slight increase in the dissolution of Th was observed. The acid/sample ratio of 600 kgt^{-1} will be adopted in the leaching of the material with HCl.

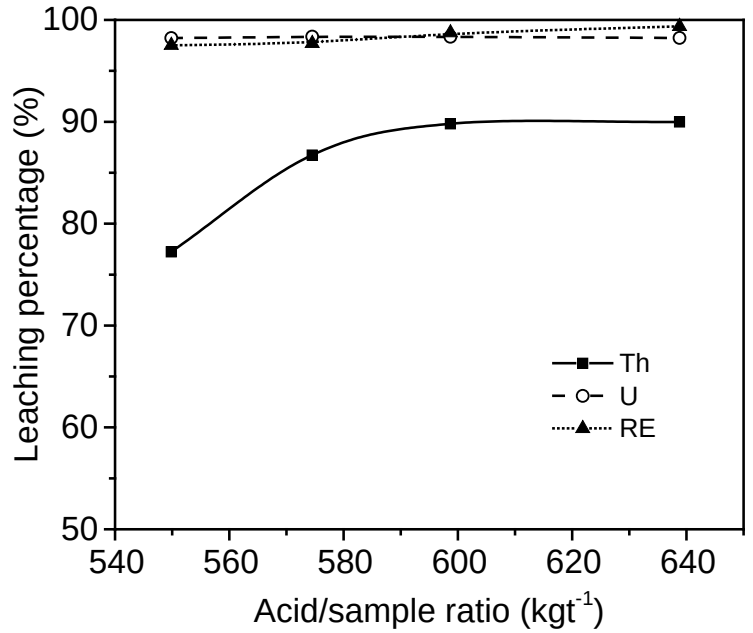

Figure 3: Influence of the acid/sample ratio on the leaching of RE, U and Th by hydrochloric acid 7.5 $molL^{-1}$, temperature 50 ºC and 4 h leaching time

It can be observed that HCl can be used as leaching agent reaching a recovery of 98% for U, 99% for REE and 90% for Th. Considering the low concentration of Th in the residue (0.03%), 90% of recovery will be considered a good result. Among the parameters of leaching investigated the final pH and the percentage of solids are important variables in the dissolution of metals, and the optimal

results were obtained when pH was controlled at 1 throughout the experiment. At pH 1 and 10% of solids, 95.3% of Th, 99.2% of U and 99.5% of RE were obtained. However, the leaching of HCl presented many problems during the filtration. This occurred due to the presence of very fine particles, considering that the residue consists of particles with diameters ranging from 0.6 µm to 85 µm.

Sulphuric Acid

Influence of the Solids Percentage Without pH Adjustment

Figure 4 presents the results of the study of the influence of the solids percentage without the adjustment of the pH when sulphuric acid was used as the leaching agent. The solids percentage ranged from 10% to 30% and sulphuric acid 2.0 moL^{-1} was used the leaching agent, at room temperature (25 + 2) ºC and 2.0 h stirring. No pH adjustment was made during the experiments. The behavior of the solubilization when H_2SO_4 was used was similar to that accomplished with HCl. Figure 4 shows that the recovery of the metals (RE, Th and U) decreases as the solids percentage rises. The combination of the variables suggests a solids content between 10% and 20% as the most indicated. For 10% of solids, the dissolution of Th, U and RE reach values of 84.1%, 97.2% and 85.6% respectively and pH 0.7, as shown in Table 3. A considerable reduction in the dissolution of Fe and Ca was observed when H_2SO_4 was used in the experiments, as compared with HCl.

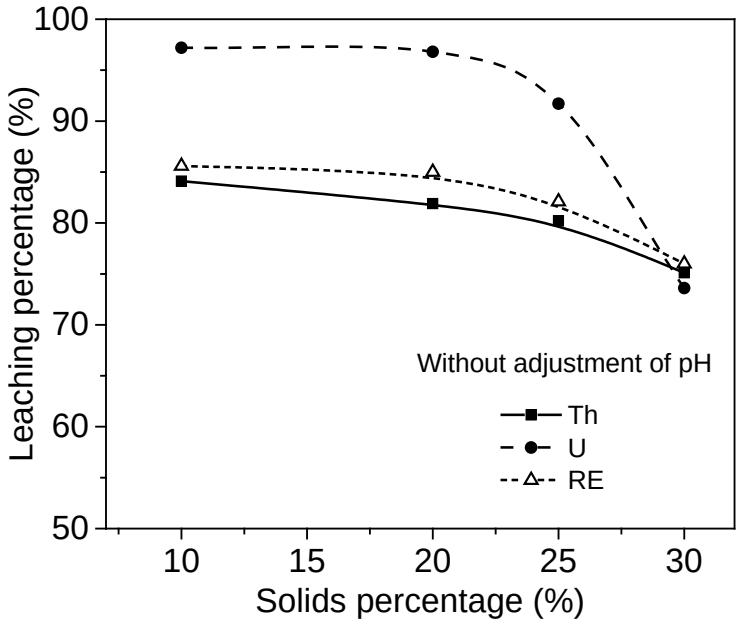

Figure 4: Influence of solids percentage in the residue leaching at 25 ºC using H_2SO_4 as leaching agent, without pH adjustment

Table 3: pH after residue leaching with variation of the solid percentage, 2.0 h stirring without pH control

Solids percentage (%)	Final pH
10	0.7
20	1.7
25	2.9
30	3.6

Influence of the Solids Percentage on Leaching with pH Control

Figure 5 shows the results of the study of the influence of the solids percentage with the initial and final pH controled to 1. The solids percentage ranged from 25% to 40% when sulphuric acid was used as the leaching agent at room temperature (25 ± 2) ºC and 2.0 h stirring. The pH was maintained at 1.0 by addition of H_2SO_4 solution. Figure 5 shows that the recovery of the metals (RE, Th and U) decreases as the solids percentage increases. The results presented a solid content of 25 % as the

most indicated. For 25 % of solids, the dissolution of RE, U and Th reaches values of 85.4%, 96.7% and 88.7% respectively.

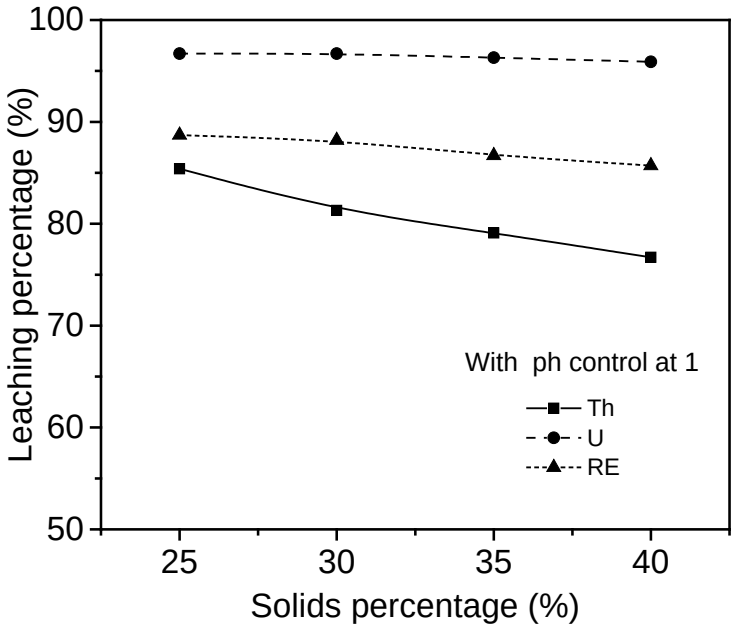

Figure 5: Influence of solids percentage on the residue leaching at 25 ºC using H_2SO_4 as the leaching agent, with pH control

Sulphuric Acid Digestion and Water Leaching

Preliminary experiments of sulphuric acid digestion indicated that 700 kgt^{-1} acid/sample and 2 hours of reaction time as enough to reach the maximum dissolution of the metals of interest by this technique. In these experiments, the acid/sample ranged from 600 kgt^{-1} to 1000 kgt^{-1} and the reaction time from 1 to 4 hours. Thus, the sulphuric acid digestion was carried out using concentrated sulphuric acid and acid/sample ratio of 700 kgt^{-1} with a static reaction for 2 hours, followed by water leaching. In this case, the acid was added directly to the solids and the initial temperature achieved around 130ºC. During the sulphuric acid digestion, some soluble sulphates are formed, like $RE_2(SO_4)_{3(s)}$, $Al_2(SO_4)_{3(s)}$,$Fe_2(SO_4)_{3(s)}$, $UO_2SO_{4(s)}$, $Th(SO_4)_{2(s)}$ among others. The simple sulphates of trivalent rare earths ($RE_2(SO_4)_3$) are soluble in water and their solubility decreases with an increase in the temperature[4][15]. Therefore, water leaching was carried out at room temperature, with 1 h of mechanical stirring in a percentage of solids of 20%. Thus, the leaching experiments were carried out at room temperature. The dissolution of RE, U and Th reaches values of 81.1%, 96.7% and 93.6% respectively. The recovery of 80% Th can be considered good, since the content of Th in the sample and consequently in the leaching residue is very low. The experimental conditions of the sulphuric acid digestion are present in Table 4.

Table 4: Experimental conditions of the acid digestion

Acid digestion	Sulphates dissolution
Concentrated H_2SO_4	Water leaching
Without temperature control – (130 – 30) ºC	Room temperature (25 ± 2) ºC
Acid/sample ratio: 700 kgt^{-1}	Percentage of solids: 20%
Time: 2 hour	Time: 1 hour

The results obtained in the acid digestion and water leaching steps indicated the technical viability of recovering RE, Th and U of the residue studied. Accordingly, the dissolution of REE, U and Th from the residue of the acid mine water neutralization can be carried out in two steps; (i) sulphuric acid digestion: acid sample ratio of 700 kgt^{-1}; reaction time of 2 hour, without temperature control (the temperature of the process ranged from 130ºC to 30ºC); (ii) water leaching: room temperature (25 ± 2ºC), 1 h of mechanical stirring and 20% of solids.

Under these conditions, a liquor containing 9.1 gL^{-1} of RE, 0.35 gL^{-1} of U and 0.082 gL^{-1} of Th and pH of 1.4 was obtained. The composition of the liquor is presented in Table 5. After the overall process, there is a reduction of approximately 30% of the initial sample. After the variables were investigated,

a flow sheet of the process to recovery RE, U and Th from the acid mine water residue neutralization was proposed. The flow sheet proposed for the recovery of RE, U and Th present in the residue is shown in Figure 6.

Table 5: Chemical composition of the sulphuric liquor

Content (gL^{-1})										pH
RE	U	Th	Al	Fe	Mn	Ca	Si	Zn	SO_4^{2-}	
9.1	0.35	0.082	16	7.8	1.9	0.47	0.10	0.75	130	1.4

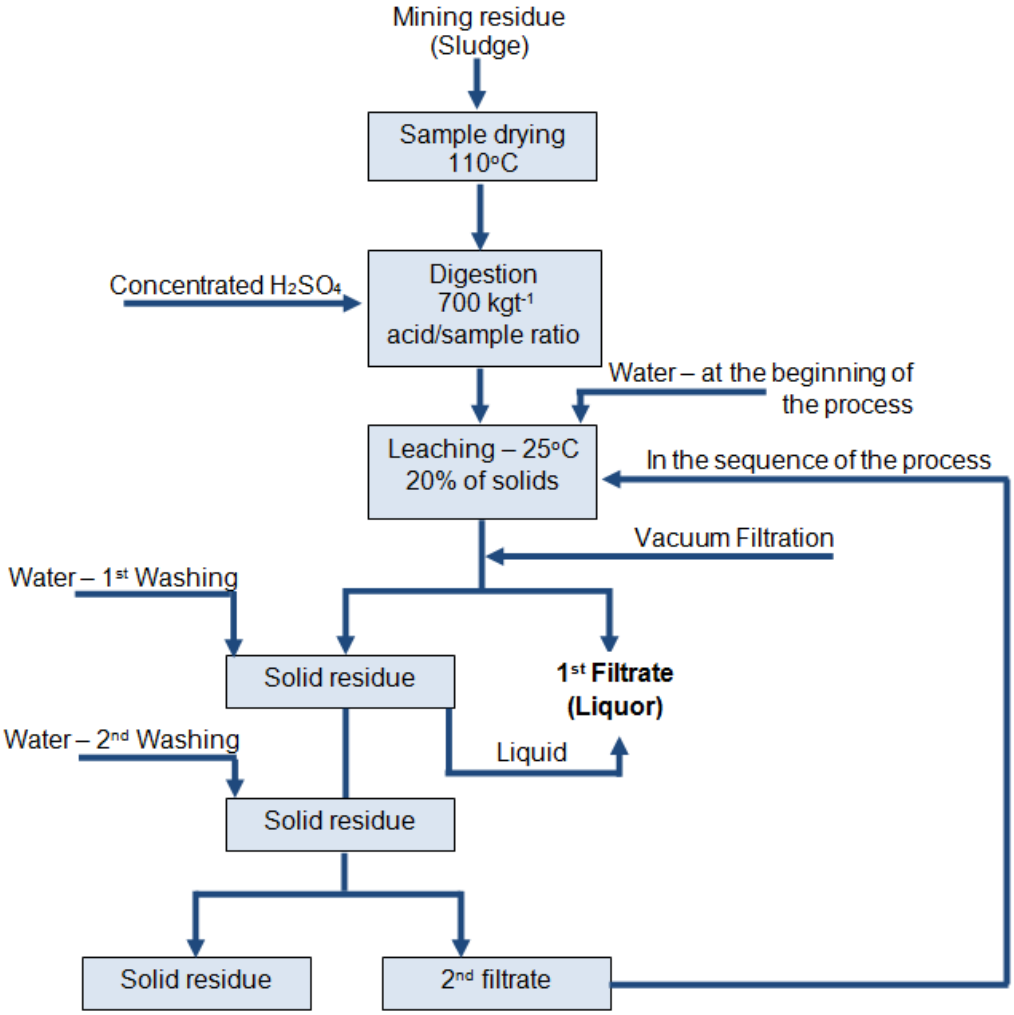

Figure 6: Simplified flow sheet the recovery of RE, U and Th from mining residue by acid cure

CONCLUSIONS

The residue presents significant amounts of rare earth elements, with low content thorium and uranium and high amount of contaminant. However, it can be considered as a secondary source of REE. The recovery of U and Th occurs naturally during the recovery of rare earth and is important for its economical and environmental aspects.

Experiments performed with the residue presented many drawbacks during execution, due mainly to very fine suspended solids. The study showed that sulphuric and hydrochloric acid can be used as the leaching agent in other to dissolve the metals REE, U and Th. For the conditions evaluated, the recovery of REE was more efficient when hydrochloric acid was used. The dissolution of U and Th was practically the same for both acids.

Using HCl in an acid/sample ratio of approximately 600 kgt^{-1}, 10% of solids and 2 hours of mechanical agitation at room temperature, a recovery of 99% of rare earths, 90% of Th and 98% of U was obtained. However, the liquor produced had a very high content of impurities, like Fe, Al and Ca, among others, and a very difficult solid liquid separation was observed.

When acid digestion was used, no problem with the separation of solid-liquid was observed and the content of the impurities in the liquor was reduced. The best condition of acid digestion was: concentrated H_2SO_4, reaction temperature, acid/sample ratio of 700 kgt^{-1}, 2 hour of static reaction and the best condition of water leaching of the digestion product was: 1 hour of mechanical stirring at room temperature (25 ± 2ºC) and 20% of solids. Under these conditions, the recovery of metals was 93.6% of RE, 81.1% of Th and 96.7% of U. As the concentration of Th in the sample is very low (0.03%), the recovery of 80% Th could be considerate as a good recovery, considering the Th that remains in the leaching residue.

ACKNOWLEDGMENTS

The authors would like to acknowledge ‘‘INB - Indústrias Nucleares do Brasil S.A.’’ for supplying the sample and the government agencies FAPEMIG, FINEP and CNPq for the financial support. Sincere thanks to CDTN technicians who were involved in this work.

REFERENCES

1. Panda, R., Kumari, A., Jha, M.K., Hait, J., Kumar, V., Rajesh Kumar, J., et al., 2014. Leaching of rare earth metals (REMs) from Korean monazite concentrate. Journal of Industrial and Engineering Chemistry. 20(4): 2035–2042.

2. Ochsenkühn-Petropulu, M., Lyberopulu, T., Ochsenkühn, K.M., Parissakis, G., 1996. Recovery of lanthanides and yttrium from red mud by selective leaching. Analytica Chimica Acta. 319(1–2): 249–254.

3. Kim, C.J., Yoon, H.S., Chung, K.W., Lee, J.Y., Kim, S.D., Shin, S.M., et al., 2014. Leaching kinetics of lanthanum in sulfuric acid from rare earth element (REE) slag. Hydrometallurgy. 146: 133–137.

4. Gupta, C.K., Krishnamurthy, N., 2005. Extractive metallurgy of rare earths. II. Data L of CC in publication (ed.) Boca Ratton, London, New York, Washington: CRC Press. 484 p.

5. Abreu, R.D., Morais, C.A., 2010. Purification of rare earth elements from monazite sulphuric acid leach liquor and the production of high-purity ceric oxide. Minerals Engineering. 26(6):536-540.

6. Amaral, J.C.B.S., Morais, C.A., 2010. Thorium and uranium extraction from rare earth elements in monazite sulfuric acid liquor through solvent extraction. Minerals Engineering. 23(6): 498–503.

7. Kanazawa, Y., Kamitani, M., 2006. Rare earth minerals and resources in the world. Journal of Alloys and Compounds. 408–412:1339–1343.

8. Souza, Junior. C. S., Ximenes, D. S., Nascimento, M., Ranuro, N.K.R.P., Cunha, O.GC., 2012. Modelagem termodinânica por extração por solventes de metais divalentes em meio sulfato usando D2EHPA. Quimica Nova. 35(2): 301–307.

9. Zhu, Z., Pranolo, Y., Cheng, C.Y., 2015. Separation of uranium and thorium from rare earths for rare earth production – A review. Minerals Engineering. 77: 185–196.

10. Peelman, S., Sun, Z.H.I., Sietsma, J., Yang, Y., 2014. Leaching of rare earth elements: past and present. Proceeding of the 1st conference on European Rare Earth Resources (ERES), 4-7 September 2014. 446–456.

11. Jha, M.K., Kumari, A., Panda, R., Rajesh Kumar, J., Yoo, K., Lee, J.Y., 2016. Review on hydrometallurgical recovery of rare earth metals. Hydrometallurgy. 165: 2–26.

12. Resende, L. V., Morais, C.A., 2010. Study of the recovery of rare earth elements from computer monitor scraps - Leaching experiments. Minerals Engineering. 23(3): 277–280.

13. Santos, E.A., Ladeira, A.C.Q., 2011. Recovery of uranium from mine waste by leaching with carbonate-based reagents. Environmental Science and Technology. 45(8): 3591–3597.

14. Abreu, R.D., Morais, C.A., 2011. Study of the fractioning of heavy rare earth elements by solvent extraction addressing the separation of terbium and dysprosium. International Nuclear Atlantic Conference - INAC 2011. Belo Horizonte - MG: ABEN, CD ROM.

15. Resende, L. V., Morais, C.A., 2015. Process development for the recovery of europium and yttrium from computer monitor screens. Minerals Engineering. 70: 217–221.

16. Busev, A.I., Tiptsova, V.G., Ivanovm, V.M., 1981. Analytical Chemistry of Rare Elements. 1st edn. Moscow: Mir Publishers; 1981. 416 p.

17. Rand, M., Fuger, J., Grenthe, I., Nech, V., Rai, D., 2008. Chemical Thermodynamics of thorium. Mompean FJ, Perrone J, Illemassè M (eds.) NEA - Nuclear Energy Agency. France: OECD Nuclear Energy Agency; 2008. 1-945.

18. Dean, J.A., 1992. Lange's Handbook of Chemistry. 15th edn. Dean JA (ed.) Materials and Manufacturing Processes. Soil Science; 1990. 687-688.

JAROGAIN PROCESS FOR RECOVERING VALUE-ADDED METALS FROM RLE ZINC RESIDUE

By

[1]Pertti Koukkari, [1]Petteri Kangas, [1]Max Nyström [2]Mari Lundström, [2]Benjamin Wilson, [3]Jussi Rastas and [3]Pekka Saikkonen

[1]IVTT, Technical Research Centre of Finland, Finland
[2]Aalto University, Finland
[3]Promeca Consulting Oy, Finland

Presenter and Corresponding Author

Pertti Koukkari
pertti.koukkari@vtt.fi

ABSTRACT

Jarosite [typically of formula $MFe_3(SO_4)_2(OH)_6$, where M represents a metal cation (Na,K, Pb/2 etc.) or ammonium is produced as leach residue in several hydrometallurgical base metal processes. Its most abundant source is zinc RLE (roast-leach-electrolysis) process. In the recent history, RLE jarosite has been usually compiled in the plant vicinity and is generally considered as problem waste.

Even though RLE zinc producers are looking for novel solutions to avoid excess formation of leach residues, the estimated rate of stockpiling is further up to 5 million tonnes/yr worldwide. While zinc ore typically is a carrier of many other metals, the content of both commercial and critical metals in such heaps is significant. Thus, e.g. gallium and indium are readily precipitated in jarosite-type compounds and are often present in considerable amounts in the jarosite heaps. The analysis of a typical jarosite stack shows content of zinc 2%, lead up to 3%, silver 150 g/t, gold 0.5 g/t, indium 100 g/t and gallium 40 g/t. Iron content is at least 15%. Such compositions are comparable with the present day commercial ores.

Major research of jarosite processing so far has been focusing on its bulk metals recovery by pyrometallurgical methods, while stabilizing the formed slag to be utilized as a construction or landfilling component. Yet, as the stack necessarily contains also poisonous constituents (As, Cd), such developments have had a limited success. Thus, interest in reprocessing jarosite to recycled value added products has also been increasing during the last few years [(1)]. A hydrometallurgical route for recovering and recycling the metal contents of jarosite has been proposed earlier [(2)]. In the present work, a hydrometallurgical flow sheet consisting of a coupled treatment of jarosite and zinc containing electric arc furnace (EAF) dust is presented [(3)].

The experimental proof-of-concept of key stages of the holistic hydrometallurgical recovery of metals present in jarosite and EAF dust (Fe, Zn, Pb) as well as value added components including Ag, In and Ga as concentrates is outlined when using industrial residues as raw materials. Economic potential and environmental benefits of the process will be discussed.

Keywords: Jarosite Processing, Acid Leach, Recovery of Metal Values, Hydrometallurgy, Holistic Process, Proof of Concept

INTRODUCTION

Presently, a main part (85 %) of the world's zinc production takes place by the Roast-Leach-Electrowinning (RLE) process [1,2]. This approach was largely adapted after the year 1970 and has been called as jarosite or goethite technology. Although the obtained yield of zinc increased from less than 90% to 97–98%, the adverse result of these new processes was their large amount of waste, appearing in the form of jarosite and goethite residues. For every tonne of zinc metal produced using the RLE process typically 0.5 tonne of such residues is generated.

The remainders of zinc manufacturing are classified as a hazardous waste due to their content of e.g. Cd, As and Pb. Traditionally jarosite has been disposed of in problem waste facilities, or stored in on-site residue areas or tailings dams. During over 40 years of operation, significant volumes of such metal containing deposits has been stockpiled both in the EU and elsewhere.

As for uses of zinc metal, nearly 50 % of the currently produced zinc is applied in prevention of corrosion, whereby a major portion will be returned with steel scrap into the electromelting-type processes of the steel industry. During this processing, zinc becomes evaporated and oxidized, and is carried away from the process with the formed dusts. The zinc oxide content of these dusts of the steel factories varies from 8 up to 40%. The estimated production of steel melting electric arc furnace (EAF) dust globally is ca. 7.5 Mt/a, from which ca 45% is recycled (within EU the EAF dust recycling rate exceeds 80 %).

The dusts are commonly processed using the Waelz process (see e.g. [3]), in which the EAF dust is fed to a rotary kiln, reduced to Zn-vapor that is then finally oxidized and recovered at baghouse filters. The recovered dust is called Waelz oxide, including well over 250 000 t/a of zinc in the EU. Trace amounts of halogens (chlorides and fluorides) remain in the Waelz kiln product and must be removed before the thus treated oxides can be fed to the electrolytic zinc process, as they will cause corrosion and fuming problems while also disturbing the electrolysis [4].

Due to environmental concerns, increasing restrictions on the construction and management of zinc residue storage facilities have emerged. Governments are strengthening environmental legislation to force companies to find commercially and environmentally viable means to develop such process flowsheets that will allow either significant reduction of residue formation or their recirculation into useful products. It would also pose a considerable advantage if the zinc containing dusts of the steel industry could be processed in a manner facilitating early removal of halogens, taking place in a close vicinity to the zinc manufacturer.

OVERVIEW OF RLE LEACHING PROCESSES

A number of optional routes for the hydrometallurgical leaching in the RLE zinc production process exist, depending on the Fe content of the raw material and on the chosen strategy for its removal. Thus, the leaching may proceed either as 1) jarosite, 2) goethite or as 3) hematite process and variations thereof. In figure 1 an overview of alternative strategies for Fe-removal are shown [5,6]. Various options to reduce the amount of Fe-containing residue have been implemented. For example, in the Netherlands the Budel plant has transformed its jarosite process to be applied using raw material with low Fe-content. However, with scarcity of such advantageous raw material, the leaching residue is concurrently being treated by plasma metallurgy [7,8].

The jarosite or goethite precipitates, however, have formed during several decades and usually stockpiled on site. In Finland only, it is estimated that there is a build-up of altogether 6 Mt of jarosite. A lumpy estimate of the global amount of jarosite deposits from zinc plants is roughly tenfold.

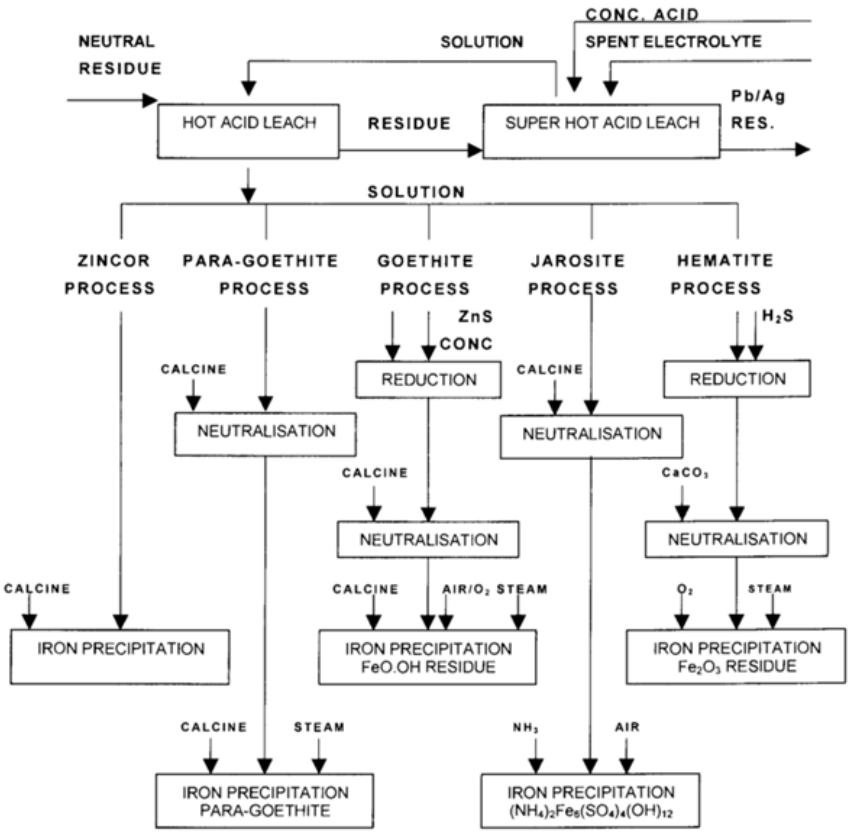

Figure 1: Basic options of Fe-removal from the RLE-zinc process [5].

While the zinc bearing ores are carriers of several co-existing metals the respective content of both commercial and critical metals in zinc processing is significant. Consequently, in many cases the zinc manufacturing processes have been updated to allow for the recovery of e.g. indium and silver as by-products. Yet, in the basic jarosite process, they have been precipitated and can be found in the existing waste deposits. The analysis of a typical jarosite stack shows contents of zinc 2 %, lead ca 3 %, silver 100-150 g/t, gold ca. 0.5 g/t, indium ca. 100 g/t and gallium up to 50 g/t. Iron content is at least 15 %. The composition thus is comparable with commercial ores concurrently in use. The pure metal content distribution of the characteristic jarosite heap is depicted in figure 2, deduced from metal values of year 2012.

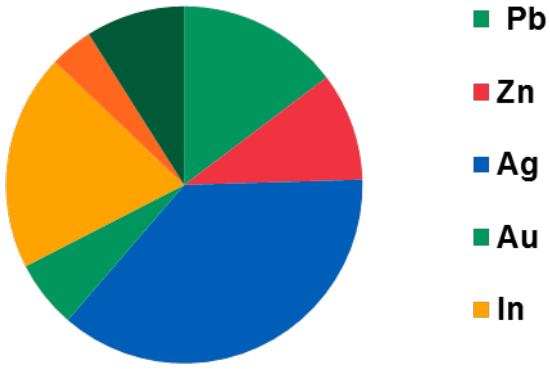

Figure 2: Typical jarosite content as pure metal values, 2012

BENEFICIATION OF JAROSITE

Strategies for Jarosite Processing

Three major lines for the treatment of jarosite waste have been proposed: stabilisation to be used as landfill or component in e.g. road construction, pyrometallurgical smelting to produce an inert slag and recover some of the metal contents and finally various hydrometallurgical techniques for more complete recovery of the valuable components within it. Due to the aforementioned harmful constituents (As, Cd) the stabilisation developments have had but limited success. The stabilisation processes do not recover the contained metal values while the cost of reagents required as part of the process can be expensive.

Pyrometallurgical treatments have been adapted e.g. in Korea and China [1,9,10] and will offer a robust solution; yet are hampered by their required investment and unavoidable high energy consumption and carbon footprint. Thus, interest in reprocessing jarosite to recycled value added products by hydrometallurgical means similar to those readily applied in the RLE process has also been increasing during the last few years [11-16]. The challenge is in proofing the viability of hydrometallurgical treatment for both in recovery of the contained metals and producing an inert material suitable for safe disposal of non-product elements.

Based on earlier studies [17-18], a novel hydrometallurgical Jarogain process, which combines recycling treatment of jarosite with recovery of zinc from the EAF dust has been developed [19]. In the Jarogain process, a holistic operation consisting of low cost and energy efficient techniques is targeted at the recovery of concentrates which will then bear the major value-added metal components, without leaving a problematic waste.

The Coupled Treatment of Jarosite and EAF Dust by Hydrometallurgical Fractionation

The hydrometallurgical fractionation process proposed by VTT and Aalto University takes advantage of jarosite being readily fine powder and directly available for wet chemical processing. In a sequential holistic operation, including controlled dissolution-precipitation steps four different concentrates will be recovered. In the first stage, the dissolution of the soluble constituents to sulfuric acid-sulfur dioxide leachate will allow for subsequent precipitation of lead and silver as sulphides together with insoluble fines, from which Pb and Ag are recovered with conventional flotation techniques. Further processing of the liquid phase will be used to fractionate In and Ga as hydroxides and then, after pH- adjustment Zn and As can again be recovered as sulphides. The process will be continued at reducing conditions to maintain Fe^{2+} in soluble form until it will be deposited in an evaporation-crystallisation stage to ferrous sulphate. The precipitate will include Mg used in the former stages as the key neutralising agent. A thermal roasting process will then be applied to recover iron as hematite and recycle sulphur dioxide. With further processing, MgO could be recovered via dissolution and with a secondary roasting stage. The originally insoluble sludge, from which Pb and Ag are removed does not contain harmful constituents and can be utilised either as a construction material or as landfill. Sulfur is recovered from the thermal treatment of sulphates and can be re-used in the Jarogain process or processed to sulphuric acid. Finally, the proposed approach may be merged with treatment of recycled zinc containing dust from steel plants. In such case, the amount of zinc and iron recovered will substantially increase, improving the process economy.

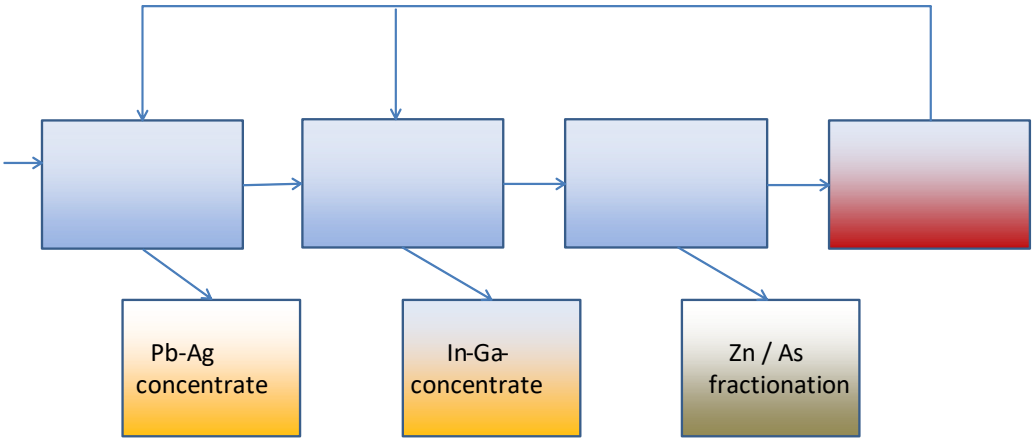

Figure 3: Recovery of metal containing concentrates from jarosite waste and zinc dust [19].

The overall process includes the following steps:

- a sulphuric acid treatment carried out on the dust to convert the oxides to sulphates. The exothermic reaction will raise the temperature of the mixture up to 250 C (or even higher), which will lead to release of halogen compounds (chlorides, fluorides) as vapour
- a sulphur dioxide (SO_2) and hot sulphuric acid dissolution step carried out on the mixture of the acid-treated dust and jarosite
- sulphidisation and flotation of the SO_2 dissolution residue,
- separation of indium and gallium (and possibly germanium) from the combined solution obtained from the SO_2 dissolution by hydroxide precipitation with optional solvent extraction/ion exchange for In/Ga/Ge fractionation
- sulphide precipitation from the solution phase obtained from the hydroxide precipitation,
- an ammonium polysulfide treatment of the sulphide precipitate, in order to separate the As_2S_3, Sb_2S_3 and SnS, which are dissolved into the NH_4 solution, from the CuS, CdS and ZnS, which remain undissolved,
- a sulphuric acid treatment of the thus obtained NH_4 solution, whereby the sulphides of arsenic, antimony and tin are precipitated,
- a step of concentrating the solution phase obtained from the sulphide precipitation, followed by a thermal treatment, where the iron, manganese, nickel, cobalt and aluminium are turned into their oxide forms, whereas magnesium remains as a sulphate, and
- finally, a washing step, where a non-soluble oxide phase (mostly containing Fe_2O_3) is obtained.

EXPERIMENTAL

Materials and Methods

The raw materials utilised in this study were jarosite and EAF-dust, obtained from respective industrial sources in the EU area. The key elementary composition of the raw materials is given in Table 1. Iron, lead and zinc are the main metalliferous elements of jarosite while it also contains exploitable fractions of silver, indium and gallium. In EAF-dust, zinc is the key element that makes this material suitable for co-processing within the Jarogain process. However, EAF-dust also includes chlorine and fluorine (Table 1.), which are unwanted species in Roast-Leach-Electrowinning (RLE) process.

Table 1: Content of key components in the raw materials.

Element	Content Jarosite	Content EAF-dust
Fe	15 %	21 %
Zn	2 %	33 %
Ag	150 g/t	-
Pb	3 %	-
In	100 g/t	-
Ga	40 g/t	-
Cl	<0.02	2 %
F	-	0.2 %

The batch experiments were conducted in glass reactors (1, 2 or 10 litres) with mechanical stirring (100-300 rpm). Oil jacket was applied for controlling the temperature (60-90°C) for the hydrometallurgical processing steps. All stages were performed in ambient pressure. The applied chemicals are sulfuric acid (96%), gaseous SO_2 and H_2S, slurries of $Mg(OH)_2$, ZnO and $CaCO_3$, solutions of NaOH, NaHS and K_2S_X, laboratory grade. The reaction times varied from 1 hour to 18 hours during the trials. Gaseous N_2 and Ar were used for preventing unwanted oxidation of the solution after each leaching / precipitation period. The basic setup of hydrometallurgical experiments is illustrated in Figure 4. The separation of solids was conducted with vacuum assisted filtration. Milli-Q water was used for washing the filter-cake. (The sulphidization and flotation of the SO_2 dissolution residue of was conducted by Geological Survey of Finland and description of this process is excluded from this paper, see e.g. [18]). Finally, the Fe rich solution was crystalized in a rotary evaporator (90 °C, decreasing pressure) and the subsequent thermal treatment was done in an electrical laboratory furnace (750 °C).

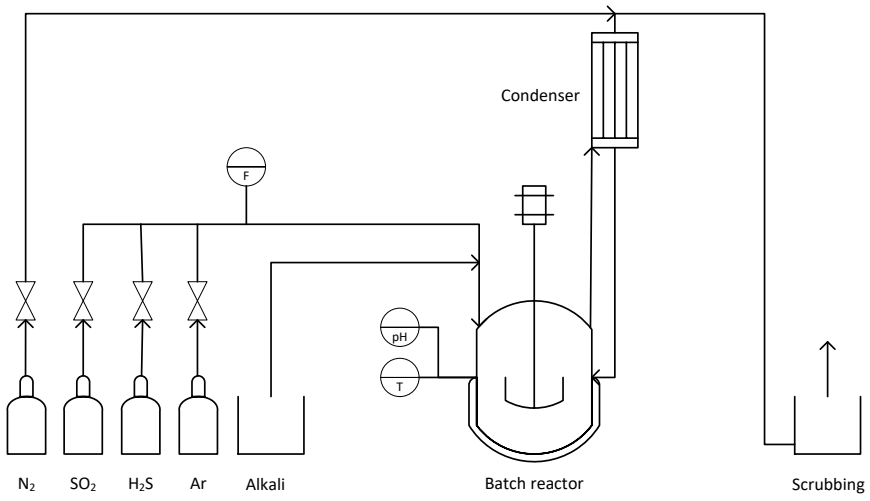

Figure 4: Experimental setup applied for hydrometallurgical process steps.

During the experiment, the temperature and pH were continuously measured. Fe^{2+} and Fe^{3+} as well as Zn^{2+} concentrations were analysed during the experiments with photometric measurement (Hach Lange). Solutions and precipitates were analysed using ICP, XRF and XRD measurements. In addition, SEM-EDS and EPMA analysis were conducted for solids after SO_2 dissolution.

Results

The treatment of the EAF dust results with nearly 90 % yield of the zinc content as sulphate while the content of halogens (both chlorine and fluorine) are reduced to low levels, Table 2. To remove halides from the dust before its dissolution will be advantageous as eventually in the zinc plant they would be unwanted due to increased corrosion, possible chlorine fuming and by fluoride caused adhesion problems in the electrolysis.

Table 2: Results from EAF dust H_2SO_4 treatment

	EAF-dust	Sulfated EAF-dust
Cl (XRF)	2,2 %	0,03 %
F (Pot. Melt)	0,197%	0,053%

Leaching of the combined dust and jarosite with sulphuric acid and SO_2 dissolution leaves a solid residue with practically all lead and silver undissolved. The conventional technology for the recovery of Pb and Ag from such leaching residue by means of sequential sulphidation and flotation should then be applied [18,20]. The present-day jarosite residues may yet contain significant amounts of elemental sulphur, which then will hamper the flotation stage. The option is to remove sulphur from the leaching residue e.g. by thermal treatment (roasting to SO_2) before the recovery of the Ag-Pb concentrate. In Table 3 the yields of the various Jarogain batch treatments are given based on the batch experiments and respective yields.The percentage is based on the ratio of recovered metal compared to metal content in the raw materials as Pb-concentrate before flotation, Zn-concentrate before polysulfide treatment and Fe-concentrate before thermal treatment.

Table 3: Estimates of Jarogain process performance.

	Pb-concentrate	In,Ga,Ge-concentrate	Zn-concentrate	Fe-concentrate
	[%]	[%]	[%]	[%]
Pb	90 %			
Au	90 %			
Ag	90 %			
In	0 %	80 %		
Ga	50 %	45 %		
Ge	0 %	67 %		
Zn	10 %	5 %	86 %	
Fe	5 %	5 %	1 %	85 %

Small amounts of copper, antimony and tin appear co-existing with the Ag-Pb concentrate. Then, indium and gallium are collected separately as hydroxide precipitate. The tentative results show enrichment of In as 30-fold; Ga 20-fold and Ge as 4-fold. Yet, yield of Ga remained poor and its recovery was split between the three indicated batches (Pb-fraction, In-precipitate and Zn-fraction). However, with the given content of Ga in the raw material its contribution in the overall process is minor. The same applies to Ge, yet additional measures are being taken to improve the yield of these two critical metals. Zinc is successfully recovered in the sulphide precipitation step, the target being to achieve such Zn-concentrate that could directly be used in the RLE process. However, blocking As from this concentrate must be further improved. As for Fe, the leaching process was found satisfactory (without fouling with goethite kind precipitates), nevertheless the end part of the process including ferrosulphate precipitation and its thermal treatment must be optimized to prevent ferrous sulphate leaks in the waste water.

ENVIRONMENTAL AND ECONOMIC POTENTIAL OF JAROSITE PROCESSING

The concerns regarding environmental issues and the increasing incentive of using deposits formerly considered as waste as potential raw material sources appear as strong drivers to re-use zinc residues. The existing stockpiles are often viewed as an existing liability instead of looking for a permanent solution for their utilisation. However, the limits in land availability and potentially increasing cost of waste deposition have become additional arguments in favour of the development of environmentally benign processes, which do not leave harmful residues while generating valuable products.

Ostensibly, the utilisation of jarosite contents will seem economically interesting, provided that the metal values depicted e.g. in Figure 2 could be recovered with reasonable yields. Even though the prices of metal products and concentrates are prone to large cyclic variations depending on the world economy, all the potential product metals are either those with established commodity markets (Zn, Pb, Fe) or those of increasing interest in many high-tech areas. In particular, silver and indium are known as indispensable for e.g. novel solar energy techniques and touch screen electronics. Gallium belongs to the fourteen metal and mineral products which are listed according to their critical availability within the EU region.

The economic feasibility of the Jarogain concept was estimated based on the operational and capital expenses. The experimental work was for assessing raw-material and chemical consumptions of Jarogain process. Utilities, waste and energy estimates were obtained from process simulation based on tools such as HSC-Sim and ChemSheet. Investment estimate was calculated based on the main process units for each process steps. Here the experience within the experimental studies was applied for process conditions and related material selections.

The economic assessment was based on the discounted cash flow analysis (DCF). Here 30-year lifetime was considered for the plant with 9% discount rate. Calculations were done on EBITDA basis (Earnings Before Interest, Taxes, Depreciation and Amortization). The aim of this analysis was to find the break-even price or levelized cost of production (LCOP) compared to pure metal prices. Here the estimate of break-even price of concentrates is 92% of pure metal prices. In figure 5, the distribution of the cost per tonne of material processed is shown. The chemical costs are most significant cost factor followed by the capital costs.

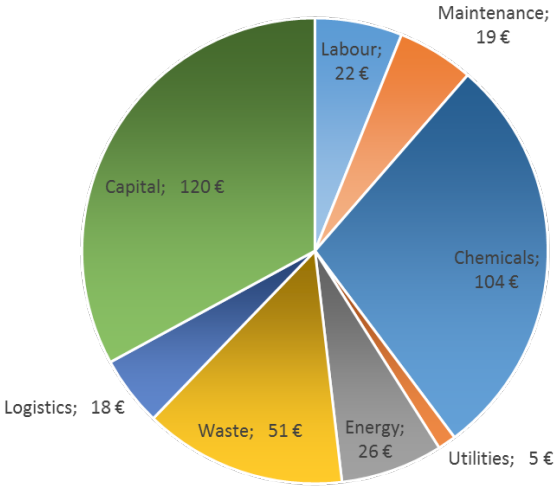

Figure 5: Cost distribution of the Jarogain process

Due to the complexity of the process, the economy with concurrent raw material prices is somewhat challenging. However, with the long-time trend of increasing demand of zinc (e.g. by the extensive car manufacturing in developing countries) as well as that of all the EU critical metals, including indium and gallium, the utilisation of unconventional secondary raw materials as their sources will become better remunerating. Trends towards increasing stockpile cost will equally encourage the beneficiation of jarosite wastes. Jarogain technology will then open a possibility for hydro-metallurgists to develop a viable route for treatment of zinc producing residues in a sustainable manner.

In figure 6, the Net Present Value (NPV) of the Jarogain process vs. the expected price of the concentrates is shown, using the assumed processing volume of 400 000/yr jarosite in a 350 M€ (2016) plant. Break-even price is 92% of concentrates. Applied discount rate is 9% and life-time of the plant is 30 years. If the prices of produced concentrates would be 75% of pure metal values, the payback time of investment would be approximately 28 years.

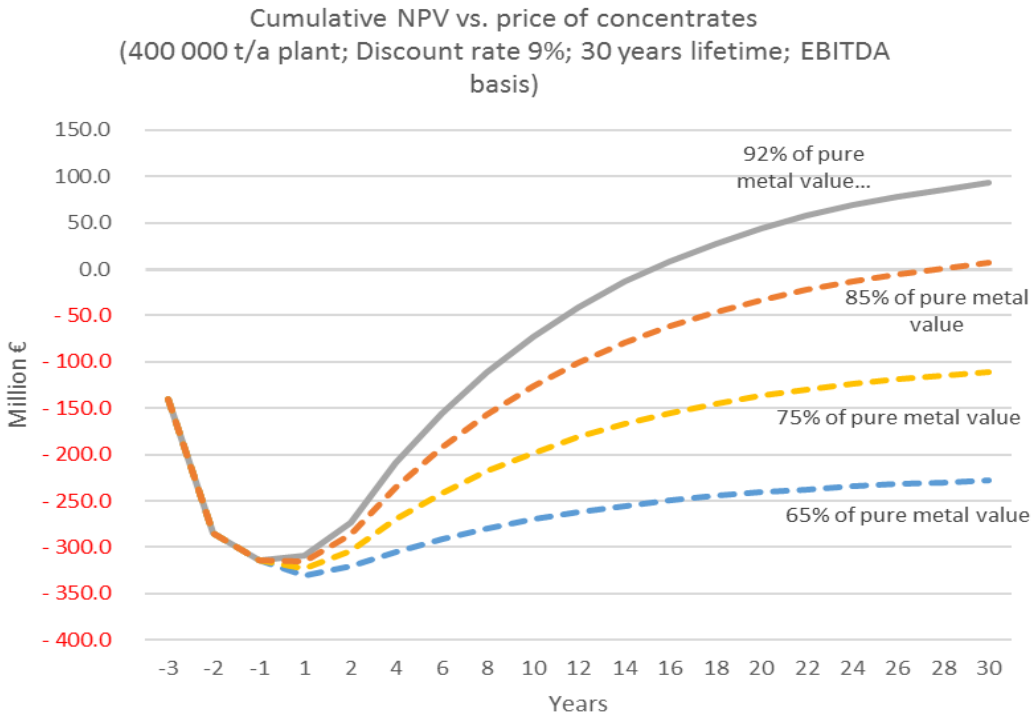

Figure 6: Cumulative NPV of Jarogain process vs. the price of the concentrates.

A schematic Sankey diagram of metal value earnings, using the yield results from the batch experiments, is further shown in Figure 7. Value of products from the process are given as €/t of processed raw material (80% jarosite; 20% sulphated EAF dust). Here, too the values are estimated for the Pb-concentrate before flotation, Zn-concentrate before polysulfide treatment and Fe-concentrate before thermal treatment. The value of metals concentrates is assumed as 92% of respective market value of metals (USGS, 2016). Inferring from the graph, the economy of the process should be based on the recovery of commercial metals, including that of Ag-Pb concentrate. Zinc with its relatively good recycling yield is straightforward to be recycled in the RLE process. With low content of chromium, Fe could be recycled as e.g. a haematite concentrate, which could be a component of blast furnace feed, replacing the fraction of recycled scrap iron. Indium, with reasonable content and recovery rate and with its present day demand in the high tech market could offer an important contribution. The economic contribution of Ga and Ge is of less importance, however, the Jarogain process provides an opening for their utilization as value-added future products, worthy of further study. Estimated annual production volumes (as metals) from a plant processing 400 000 - 450 000 tonnes of jarosite annually are further listed in Table 3.

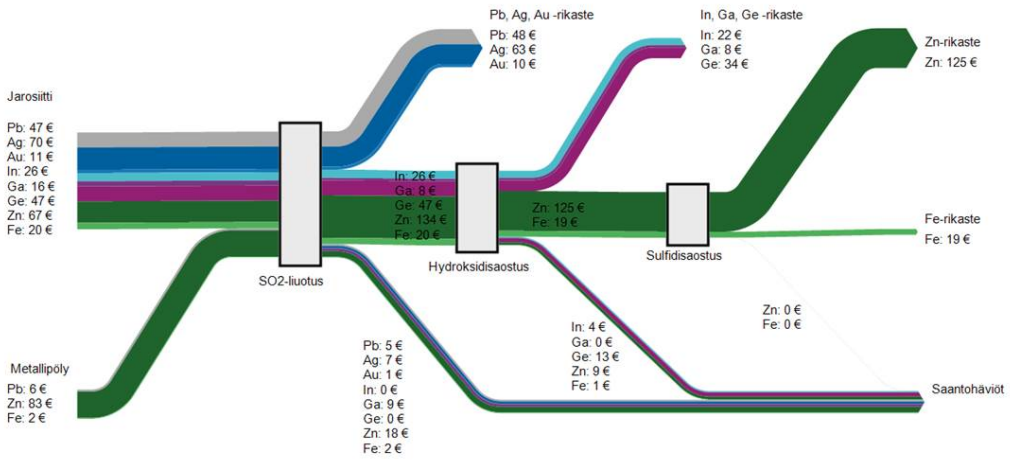

Figure 7: Value of products from the process.

Table 4: Annual volumes of a holistic jarosite recovering plant

Component	Content in jarosite	Annual production
Zn	2 %	27000 t
Fe	15 %	80000 t
Pb	3 %	11000 t
Ag	150 ppm	49000 kg
Au	0.5 ppm	120 kg
In	100 ppm	23000 kg
Ga	40 ppm	9000 kg
Ge	60 ppm	15000 kg

CONCLUSION

The hydrometallurgical processing route of jarosite waste ('Jarogain') is one of the first of its kind with holistic methodology to recover both bulk metals (Zn, Pb, Fe) and value-added and critical metals as concentrates while recycling jarosite to useful products. It provides an alternative to the proposed pyrometallurgical routes, which, though robust in technology may be less attractive in the long-term due to their more complex implementation to RLE zinc production and their required carbon footprint, which is potentially larger than that required in a hydrometallurgical process.

The research performed so far has shown the proof-of-concept of the hydrometallurgical Jarogain approach, which combines treatment of electric arc furnace dust and leaching residues from zinc manufacturing. Further study is needed for coupling the batch processes to a continuous operation with optimized yields and with sustainable means for entrapment of the potentially harmful trace compounds.

REFERENCES

1. Creedy, S., Glinin, A., Matusewics, R., Hughes, S. & Reuter, M. 2013. Outotec Ausmelt Technology for Treating Zinc Residues. World Metall. - ERZMETALL 66(4), 230–235.

2. Goodwin, F.E. 2012. Zinc and Zinc Alloys, in: Kirk-Othmer Encycl. Chem. Technol., Hoboken, NJ, USA.doi:10.1002/0471238961.2609140307151504.a01.pub3

3. Lausch, H. & Lommert, H. 1999. Method for processing metalliferous sludge, EP 0709472 B1, 1999

4. Befasa n.d. The SDHL-Waelz Process. . http://www.befesa-steel.com/web/en/nuestra_tecnologia/detalle/The-SDHL-Waelz-Process/

5. Claassen, J.O. 2002. Characterisation and optimisation of the Zincor iron removal process, University of Pretoria.

6. Fugleberg, S. 2014. Improving the competitiveness of the electrolytic zinc process by chemical reaction engineering approach reaction engineering approach, Åbo Akademi University.

7. Bergfald 2014. Nyrstar Hoyanger - Environmental impact of a new raw material, Oslo, Norway. http://www.miljodirektoratet.no/Global/dokumenter/horinger/horing2013-86-1_mra.pdf

8. Kemperman, D. & Steeneken, S. n.d. Modifications Budel Leach Circuit after closure of Century Mine, in: Int. Miner. Process. Congr.,

9. Hughes, S., Reuter, M.A., Baxter, R., Kaye, A., Hughes, S., Reuter, M.A., et al. 2008. Ausmelt Technology for Lead and Zinc Processing, in: Lead Zinc 2008,

10. Outotec 2016. Successful Zinc Residue Smelter Project for Xingan. http://www.outotec.com/en/Search-material/Customer-newsletter-Smelting-News/Smelting-Newsletter-Issue-1-April-2016/Successful-residue-smelter-project-for-XingAn/

11. UNEP 2013. Metal Recycling: Opportunities, Limits, Infrastructure.doi:978-92-807-3267-2

12. Ju, S., Zhang, Y., Zhang, Y., Xue, P. & Wang, Y. 2011. Clean hydrometallurgical route to recover zinc, silver, lead, copper, cadmium and iron from hazardous jarosite residues produced during zinc hydrometallurgy. J. Hazard. Mater. 192(2), 554–8. doi:10.1016/j.jhazmat.2011.05.049

13. Ju, S., Zhang, L., Peng, J., Shi, Z., Guo, S., Liu, B., et al. 2013. Thermodynamics of leaching roasted jarosite residue from zinc hydrometallurgy in NH4Cl system. Trans. Nonferrous Met. Soc. China 23(4), 1179–1183. doi:10.1016/S1003-6326(13)62581-9

14. Han, H., Sun, W., Hu, Y., Jia, B. & Tang, H. 2014. Anglesite and silver recovery from jarosite residues through roasting and sulfidization-flotation in zinc hydrometallurgy. J. Hazard. Mater. 278, 49–54. doi:10.1016/j.jhazmat.2014.05.091

15. Elgersma, F. 1992. Integrated Hydrothermal Jarosite Treatment, TU Delft.

16. Swain, M., Sahu, K.K. & Roy, B.N. 2016. Recycling of Jarosite For Recovery of Valuable Metals and its Utilisation. Int. J. Sci. Tech. Res. Eng. 1(4), 36–46.

17. Rastas, J., Saikkonen, P. & Honkala, R. 1982. Process for the treatment of a raw material which contains oxide and ferrite of zinc, copper and cadmium, US 4355005 A, 1982

18. Rastas, J., Järvinen, A., Hintikka, V. & Leppinen, J. 1989. Recovery of lead, silver and gold in the zinc process and possibility of non-waste technology in zinc production, in: VTT Symp. - Non-Waste Technol., Vol. 2,

19. Rastas, J., Saikkonen, P., Hintikka, V. & Koukkari, P. 2016. Processing of Industrial Metal-containing waste materials, Finnish Patent Application FI20165972, 2016

20. Korhonen, T. 2017. Alustavat sulfidointi- ja vaahdotuskokeet. GTK Internal Report (in Finnish).

SEPARATION OF THORIUM, URANIUM AND RARE EARTH ELEMENTS FROM SULPHURIC LIQUOR

By

Carlos A. Morais and Janúbia C. B. S. Amaral

Centro de Desenvolvimento da Tecnologia Nuclear (CDTN), Brasil

Presenter and Corresponding Author

Carlos A. Morais
cmorais@cdtn.br

ABSTRACT

This paper describes the study of separation of thorium and uranium from rare earths elements and some contaminants present in sulphuric liquor through a solvent extraction technique. The liquor was generated by dissolution of an industrial residue obtained by the neutralization of the acid water generated in an old uranium mine in Caldas, State of Minas Gerais – Brazil. The solvent extraction process was adopted in order to separate Th and U from the rare earth elements and the other metals present in the liquor. The influence of the type and concentration of the extractant, acidity of the liquor, aqueous/organic volumetric ratio and type and concentration of the stripping solution were investigated. The experiments were carried out using a liquor containing 0.38 gL^{-1} of U, 0.082 gL^{-1} of Th, 9.1 gL^{-1} of REE, 16 gL^{-1} of Al, 7.8 gL^{-1} of Fe, 0.47 gL^{-1} of Ca, 1.9 gL^{-1} of Mn, 0.10 gL^{-1} of Si, 0.75 gL^{-1} of Zn, 131 gL^{-1} of SO_4^{2-} among other impurities. Uranium and thorium can be extracted separately or simultaneously, using amines as extractants. For the simultaneous extraction, the separation of Th and U can be done from the stripped solution, where the metals are in higher concentration. The results showed that 97.1% of uranium and 94.4% of thorium were extracted with a Primene®JM-T and Alamine®336 mixture. Separation factors of 142 for Th/RE and 292 for U/RE were achieved. In the case of the extraction of thorium and uranium separately, the separation factor for Th/U was 151. The separation factor for Fe/REE was 10.3 for Primene®JM-T 0.05 $molL^{-1}$ and 7.7 for Primene®JM-T 0.2 and 0.3 $molL^{-1}$. The extraction of the other metals present in the liquor was less than 0.2%.

Keywords: Uranium extraction, Thorium extraction, Rare earth sulphuric liquor, Separation of thorium and uranium.

INTRODUCTION

Mining is characterized as an economic activity that operates in a certain region with the objective of extracting minerals from the earth's crust. This activity includes a series of operations ranging from research to large-scale ore exploration and subsequent, recovery of the area affected by mining. One of the main problems of the mining industry is related to the production and proper management of its tailings. These residues resulting from the extraction and treatment processes of ores can represent serious risks of pollution to the environment. In light of the worldwide tendency to transform these residues, with an added economic value, into raw materials, it is important to develop techniques to recover these materials and make them available for consumption[1].

The Brazilian region of “Poços de Caldas” is considered a very promising area for deposits of rare earth elements. In this region is located a unit of the “Industrias Nucleares do Brasil” – INB, the Mineral Treatment Unit - MTU/Caldas-INB. Currently, the MTU/Caldas is deactivated and has an old uranium mine inactive since 1995. During the its operation, between 1982 and 1995, this mine generated residues that have been sources of acid drainage, with a pH between 2.5 and 3.0 containing various metals, such as uranium, thorium, rare earth elements, aluminium, iron, zinc, manganese, silica and others. The acid water treatment is done with the addition of lime and generates a slurry containing most of the metals present in the acid drainage water. In this process, contaminants are precipitated in a solid phase composed of calcium diuranate and metal hydroxides, in a matrix of calcium sulphate[1][2].

The technological development of the last decades in sectors of electronics industry has increasingly relied upon a supply of highly purified rare earth oxides. Rare earths compounds are also used in X-ray screens, high-intensity mercury vapour lamps, neutron scintillators, charged-particle detectors and optical memory systems[3][4]. The presence of uranium and thorium in the mining industry residue causes considerable concern due to their radioactivity. Appropriate methods to separate them from rare earths have been developed. The separation of U and Th from RE is important in order to avoid environmental pollution and the contamination of rare earth products and to make proper management of Th and U favourable[5][6]. According to Zhu, Pranolo and Cheng[7] if uranium can be economically recovered as a by-product it can be sold as nuclear fuel, as for thorium, it could be used in nuclear industry in the future.

This work focuses on the extraction and separation of Th and U from rare earth elements (REE), Fe and other metals present in the solution generated in the leaching of the residue produced by the acid water mine neutralization with lime by using primary and tertiary amines. The results obtained provided the basis to establish the conditions applied to the processing of the solution generated.

EXPERIMENTAL

Reagents and Solutions

The sulphuric liquor was prepared through the leaching of an industrial residue supplied by “Indústrias Nucleares do Brasil” – INB. The residue was generated by neutralization of acid mine water produced in a closed uranium mine site located in Caldas, MG-Brazil[2]. The residue was dissolved in sulphuric acid with the acidity adjusted for the conditions of the experiments. The residue containing rare earths was dissolved in a volume of concentrated H_2SO_4 under stirring. Afterwards, water was added in order to solubilized the sulphates metals[7]. Table 1 presents the composition of the liquors generated by dissolution of the residue.

Table 1: Chemical composition of the sulphuric liquor

Content (gL^{-1})										pH*
REE	U	Th	Al	Fe	Mn	Ca	Si	Zn	SO_4^{2-}	
9.1	0.38	0.082	16	7.8	1.9	0.47	0.10	0.75	131	1.7 – 1.4

*The pH of the liquor, initially at 1.7, stabilised at pH 1.4 after some days

The efficiency of the solvent extraction of metals from sulphuric liquors was investigated with the use of two different extractants; PRIMENE®JM-T (P.JMT) and ALAMINE®336 (A.336), at room temperature (25 ± 2)ºC. The organic solutions were prepared by dilution of the extractants in dodecane and with addition of 5% of tridecanol used as a modifier[8]. The extractants solutions were

prepared separately and pre-treated with a sulphuric acid solution in the same concentration, with an aqueous/organic phase ratio of 1 before the mixture or the extraction experiments.

The extraction experiments were carried out in 150 mL beakers with mechanical stirring. After contact between the phases, the mixture was transferred to a separation funnel, and the aqueous and organic phases were separated, collected and analysed. The process control was performed by determination of the metals in the aqueous phase, using Dispersive X-ray Fluorescence Spectrometry - EDXRF (Shimadzu - EDX 720), with Inductively Coupled Plasma - Atomic Emission Spectrometry ICP-OES, Wavelength Dispersive X-ray fluorescence spectrometerery – WDX (Rigaku - ZSX Primus II) and ion-specific electrode potentiometric using a pH meter (Digimed - DM 22)[8–11]. When necessary the contents of metals were also determined in the organic phase.

RESULTS

Extraction

Influence of Primene®JM-T and Alamine®336 Mixture Concentration

The aim of these experiments was to evaluate the selective extraction of uranium and thorium from the sulphuric liquor containing REE and some impurities at high levels. Primene JM-T (P.JMT) preferably extracts thorium whereas Alamine 336 (A.336) preferably extracts uranium[8]. The concentration of P.JMT was varied from 0.025 to 0.1, while the concentration of A.336 was varied from 0.05 to 0.2 molL^{-1}. The difference in concentration of the extractants is explained by the thorium concentration in the liquor, which is much lower than the concentration of uranium. The organic solution was pre-treated with a sulphuric acid solution to promote protonation of the amines. The experiments were carried out using the liquor and a volumetric ratio between the aqueous and organic phases equal to 1. The results are presented in Figure 1.

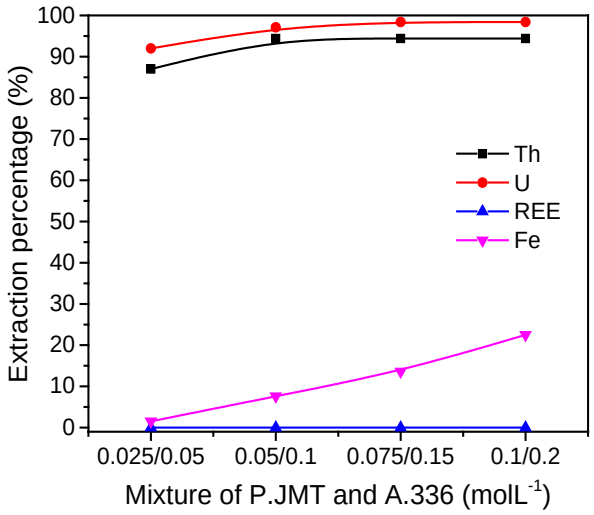

Figure 1: Influence of Primene JM-T and Alamine 336 concentration in the extraction percentage of Th, U, RE and Fe

It can be observed in Figure 1 that when the concentration of the extractants is increased the extraction of Fe increases. The REE were not extracted in the experimental conditions, and U and Th extraction had a slight increase from 0.025/0.05 to 0.05/0.10 molL^{-1} of P.JMT/A.336 maintaining at nearly 95% for higher concentrations. Since the Fe extraction increases with the increasing concentration of the extractans, 0.05/0.10 molL^{-1} were selected for the extraction of U and Th. For this condition, the separation factor was 145 for Th/RE, 292 for U/RE, 203 for Th/Fe and 410 for U/Fe. The extraction of the other metals present in the liquor was less than 0.2%.

Influence of Primene JM-T and Alamine 336 Concentrations Separately

The extraction of the metals by P.JMT and A.336 separately was evaluated in the concentration interval of 0.05 to 0.20 molL^{-1}. The results of REE, U, Th and Fe extraction with P.JMT are shown in Figure 2(a) while the results with A.336 are shown in Figure 2(b). When P.JMT was used, Th

extraction remained constant, at 94.2% throughout the range of concentrations investigated. The extraction of the other metals increased as the extractant concentration increased. U increased from 6.6% to 28.8%; the REE varied from 0.89% to 4.8% and Fe from 8.4% to 27.9%, as observed in Figure 2a. When 0.05 molL^{-1} of P.JMT was used, separation factors of 142 for Th/RE and 176 for Th/Fe were obtained.

The experiments carried out with A.336 indicated a high extraction of U and low extraction of the other metals. In the concentrations of A.336 investigated, the extraction of U remained constant at 99% while the extraction of REE remained around 0.8%, the extraction of Fe stayed at about 2%, and the extraction of Th was not observed, as shown in Figure 2b.

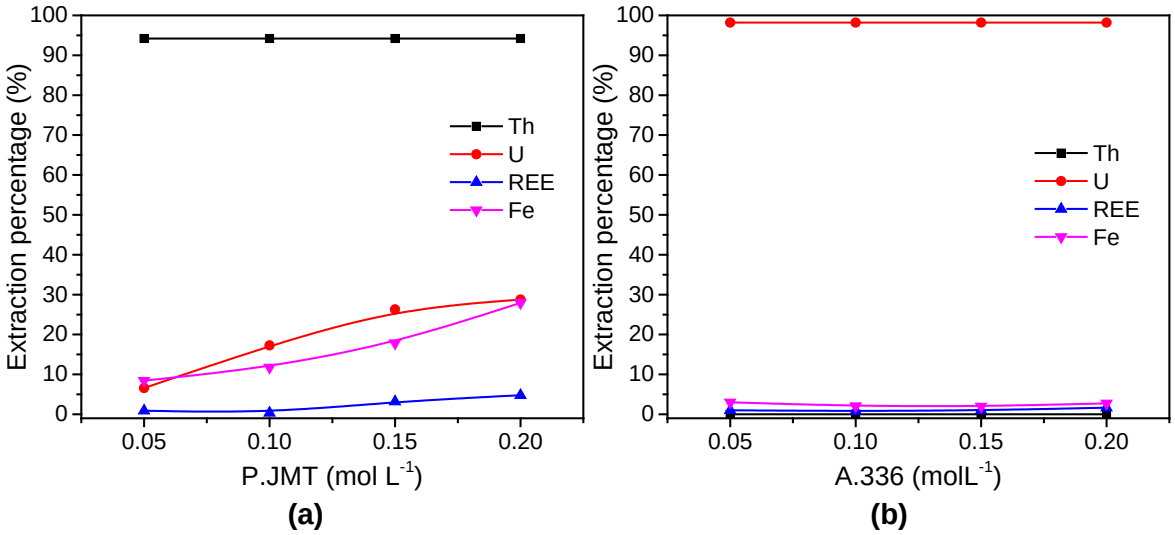

Figure 2: Influence of Primene JM-T (a) and Alamine 336 (b) concentration

Influence of pH

An important variable affecting the extraction of the metals is the acidity of the liquor. This was investigated in the interval between pH 0.5 and pH 1.7. Acidities higher than the initial liquor (pH 1.7) were obtained through the addition of sulphuric acid solution. The influence of the acidity on the extraction of RE, U, Th and Fe was investigated with the mixture of the extractants and with each extractant separately. The influence of the sulphuric liquor pH on the extraction of the metals with the mixture of extractants was carried out using an organic phase containing 0.05 molL^{-1} of P.JMT and 0.1 molL^{-1} of A.336. The results of these experiments are presented in Figure 3. One can see that the extraction of U and Th was not influenced by the liquor acidity in the interval investigated, remaining around 99% for U and 94% for Th. It is also shown in Figure 3 that the extraction of Fe increases with the increase of the liquor pH and the extraction of REE remains around 0.5%. The separation factor (SF) of FE/REE at pH 1.4 (stabilised pH) was 7.7.

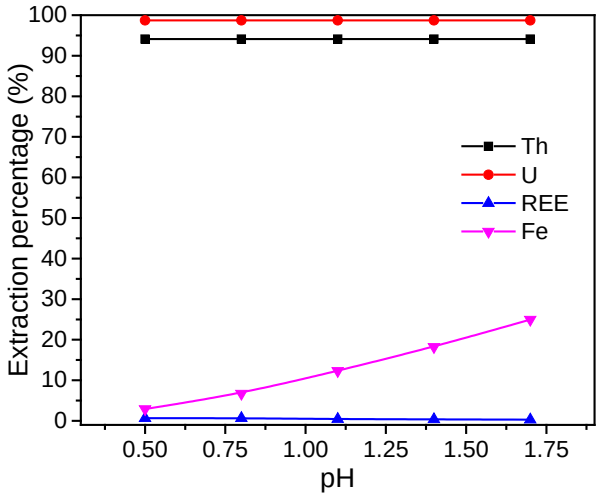

Figure 3: Influence of pH in the RE, U, Th and Fe extraction. Organic phase: mixture of 0.05 molL^{-1} of Primene JM-T and 0.1 molL^{-1} of Alamine 336

Despite the high separation factor of Fe/REE observed, the extraction of Fe with the mixture of P.JMT and A.336 at the low concentration investigated (0.05 molL^{-1} of P.JMT and 0.1 molL^{-1} of A.336) is not viable due to the high concentration of Fe in the liquor. Thus the study of the influence of the pH on the extraction of metals with the isolated extractants was investigated using a high concentration of the extractants with the objective of evaluating the extraction of Fe and REE. These experiments were carried out with 0.3 molL^{-1} for both P.JMT and A.336. The results are shown in Figures 4a and 4b.

Figure 4a shows the results obtained when P.JMT was used as extractant. As expected, 100% of Th was extracted in the whole pH interval investigated. The extraction of U remained between 70 and 60%. A slight increase in the extraction of Fe with the increase of the pH of the liquor, from 5 to 10%, was observed. The extraction of REE remains around 0.5% with the increase of the liquor pH. Experiments carried out with A.336 indicated the high selectivity of these extractant for U. No significant influence of the acidity of the liquor on the extraction of the metals in the interval investigated was observed (Figure 4b). We can observe a very slight extraction of Th and Fe and no extraction of REE.

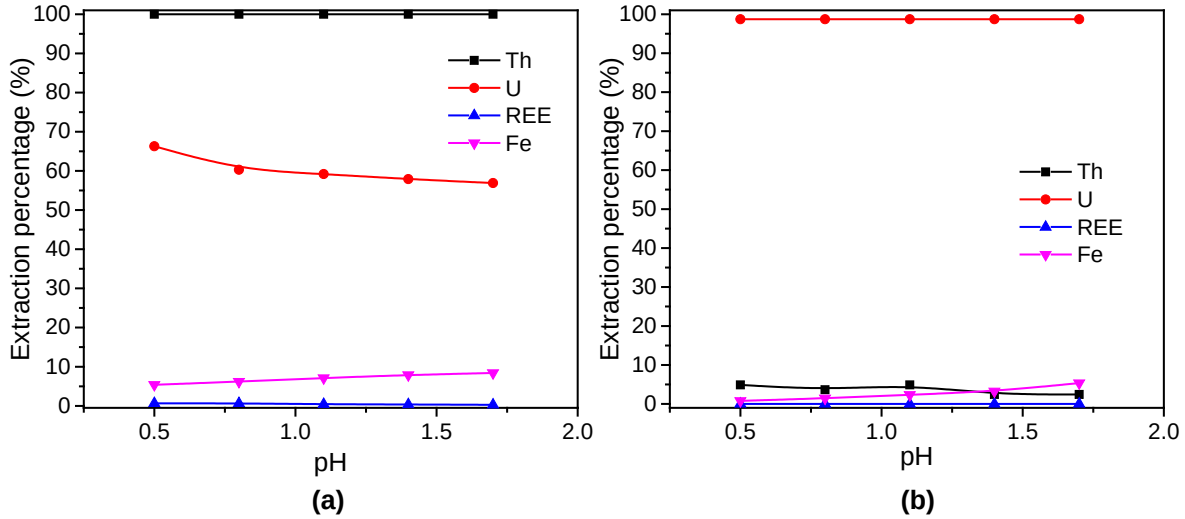

Figure 4: Influence of pH in the RE, U, Th and Fe extraction. Organic phase: 0.3 molL^{-1} of P.JMT (a) and 0.3 molL^{-1} of A.336 (b)

Extraction Isotherms of Uranium and Thorium

The uranium and thorium extraction isotherms (equilibrium curves) were constructed and McCabe–Thiele Diagrams were drawn to estimate the theoretical number of stages and the volumetric feed ratio of the liquor and solvent to be used in the mixer-settler continuous experiments. The results obtained for the solvent extraction parameters indicated that due to the low content of U and Th in the liquor, it is better to extract the metals simultaneously, since the separation of them can easily be done in the stripped solution. The concentration of the metals in the stripped solution will be much higher than in the liquor, which reduces the costs of separation. In this case U can be extracted with Alamine 336, maintaining the Th in the rafinate.

The extraction isotherms were drawn according to the successive contact technique to deplete the liquor and load the organic, using aqueous and organic volumetric ratio of 1/5 and an extractant mixture containing 0.05 molL^{-1} of P.JMT and 0.1 molL^{-1} of A.336. The U extraction isotherm with the McCabe–Thiele diagram is shown in Figure 5a. During the construction of the Th isotherm, it was observed that during the organic loading experiments, the extracted Th began to return to the aqueous phase according Figure 5b. The stripping of the Th by the liquor itself occurs after the third successive contact of the organic with the aqueous phase.

The McCabe-Thiele diagram obtained for uranium, indicated that 3 extraction stages are needed to extract all U present in the liquor. A loaded organic with 4.3 gL^{-1} of U at an A/O ratio of 11 can be obtained. The thorium extraction isotherm indicated a Th stripping by the sulphuric liquor itself, indicating that the simultaneous extraction of U and Th must be done in few stages. The ideal number of stages for the extraction of U and Th will be defined through continuous experiments.

The cause of the return of thorium to the aqueous phase should be investigated. In another work conducted by the same authors, using similar conditions, an organic loading of 5.3 gL-1 was obtained, although when using two extraction stages, the stripping of Th during the construction of the isotherm extraction was not observed[8].

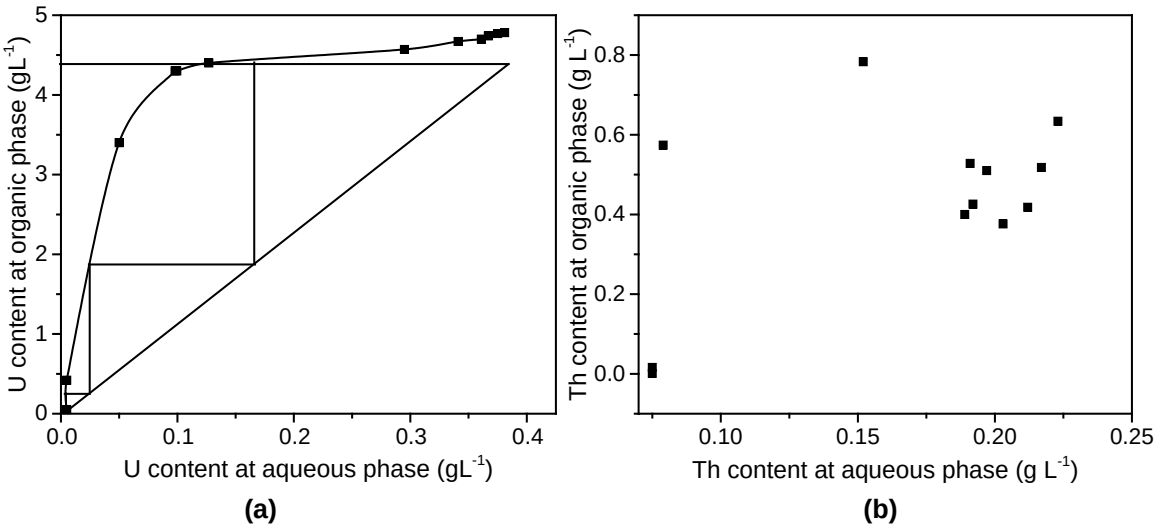

Figure 5: Extraction Isotherm of U (a) and Th (b). Organic phase: P.JMT/A.336 0.05/0.1 molL^{-1}; A/O = 5/1

Stripping

Stripping of thorium and uranium from the loaded solvent can be performed using mineral acid solutions or some complexing agent solutions. According to Amaral and Morais[8], thorium and uranium could be effectively stripped from loaded P.JMT/A.336 mixture by using hydrochloric acid (HCl), sodium chloride (NaCl) and sodium carbonate (Na_2CO_3). The stripping percentage of Th and U was similar for all reagents, therefore no separation of the metals was observed during stripping. In this work HCl and NaCl were used as stripping agent. The acidity of the NaCl solution was adjusted to pH 1.2 by addition of H_2SO_4 solution.

Influence of HCl Concentration on Stripping of Metals U and Th

The loaded organic (mixture P.JMT/A.336) used in the stripping experiments was obtained in 3 contacts of the solvent and the liquor using a volumetric organic/aqueous ratio of 5. The concentration of U and Th in the loaded organic phase was 4.4 gL^{-1} and 1.1 gL^{-1}, respectively. The influence of the concentration of the hydrochloric acid solution on the stripping of U and Th was investigated in the interval from 0.25 to 2.0 molL^{-1}. The results of this experiments are presented in Figure 6. The metal stripping percentage increases until 1.0 molL^{-1} HCl reaching 99% stripping for both metals and remaining constant for higher concentrations of HCl.

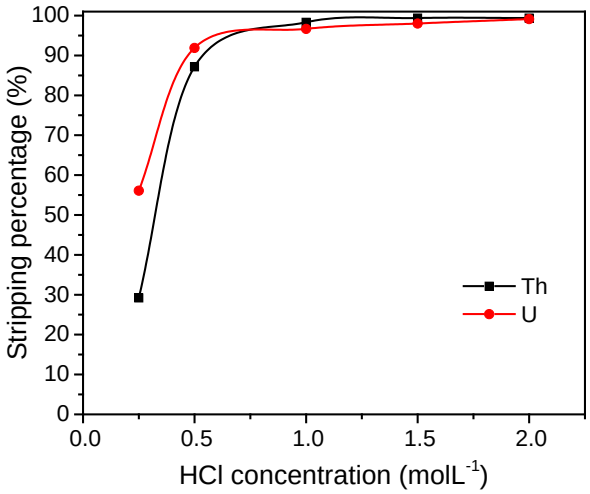

Figure 6 – Influence of HCl concentration on stripping of U and Th from the loaded solvent

Influence of NaCl Concentration on Stripping of Metals U and Th

The effect of sodium chloride concentration on the stripping of U and Th was investigated with NaCl solutions at pH of 1.2 adjusted with sulphuric acid. The influence of the concentration of NaCl solution was investigated in the interval from 0.5 and 2.0 molL^{-1} (Fig. 7). Figure 7 shows that the stripping percentage increased from 72.3% to 98.6% for U and from 46.5% to 99.4% for Th with the increase of NaCl concentration from 0.5 to 1.5 molL^{-1}, remaining constant until 2.0 molL^{-1} NaCl.

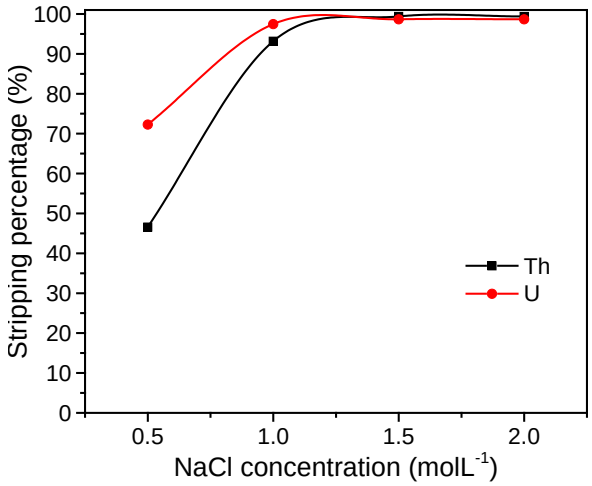

Figure 7 – Influence of NaCl concentration at pH=1.2 on stripping of U and Th from the loaded organic

Stripping Isotherm of Uranium and Thorium

In order to construct the McCabe-Thiele diagram for the stripping of uranium and thorium from the loaded organic (mixture of P.JMT/A.336), the stripping isotherm was obtained by the successive contacts technique. The organic phase was composed of the mixture of 0.05 molL^{-1} P.JMT and 0.1 molL^{-1} A.336. The loaded organic phase was prepared by extraction of U and Th from sulphuric solution at an A/O ratio of 5/1. A sodium chloride solution of 1.7 molL^{-1} and initial pH 1.2 was employed as the stripping solution. The concentration of U and Th in the loaded organic phase was 4.4 gL^{-1} and 1.1 gL^{-1}, respectively. As shown in Figure 8a, the McCabe-Thiele diagram drawn for the stripping of U, 4 counter-current stages are required for the complete stripping of uranium from the loaded organic phase at an O/A ratio of 8. For this condition a stripped solution containing 35 gL^{-1} of U can be obtained. The Th stripping isotherm and the McCabe-Thiele diagram are presented in Figure 8b. The McCabe-Thiele diagram for Th stripping with NaCl solution indicated also 4 stripping stages for the complete stripping of Th at an O/A phase ratio of 9/1. According to the stripping isotherms, a stripped solution containing around 35 gL^{-1} of U and 7 gL^{-1} of Th can be obtained.

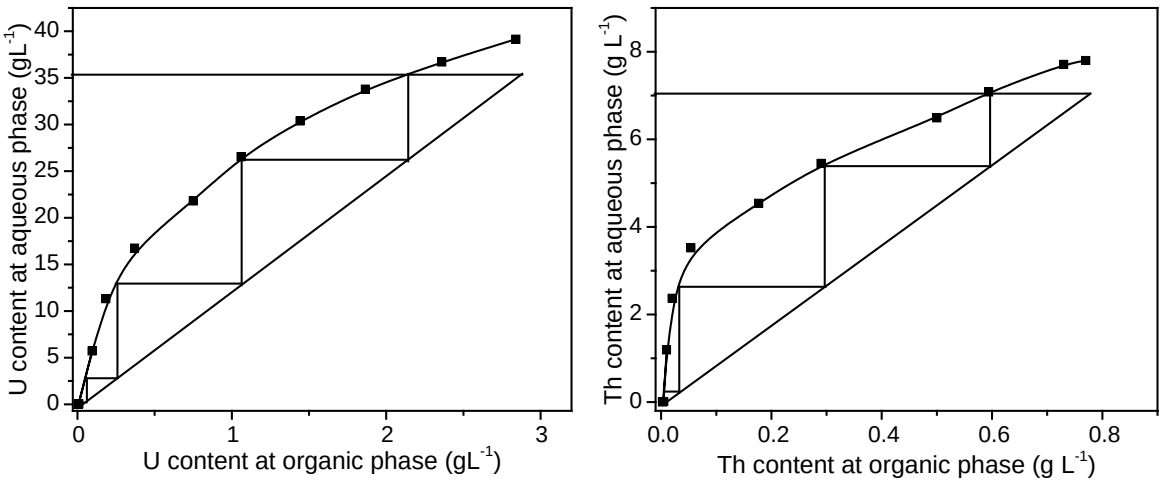

(a) **(b)**

Figure 8 – Stripping Isotherm of U (a) and Th (b). Org. phase: P.JMT/A.336 (0.05/0.1molL^{-1}) containing 4.4 gL^{-1} U and 1.1 gL^{-1} Th; O/A = 1; Aqueous phase: 1.7 molL^{-1} NaCl at pH = 1.2

CONCLUSIONS

U and Th ions are preferentially extracted over REE, Fe and the other metals present in the liquor by Primene®JM-T and Alamine®336 mixture from a sulphuric acid solution in the interval of acidity investigated (pH 0.5 to 1.7). Separation factors of about 145 for Th/RE, 203 for Th/Fe, 292 for U/RE and 410 for U/Fe were obtained using a mixture of 0.05 $molL^{-1}$ of Primene®JM-T and 0.1 $molL^{-1}$ of Alamine 336®. For this condition, 94.4% of Th and 97.1% of uranium were extracted in one extraction contact. Uranium and thorium can be extracted simultaneously in three stages using an aqueous and organic volumetric ratio of 11.

Stripping is proposed for the simultaneous removal of U and Th from the loaded organic phase by using 1.7 $molL^{-1}$ NaCl solution at pH 1.2 adjusted with H_2SO_4 solution. The McCabe-Thiele diagrams of Th and U show that in this process, four stripping steps would be required to simultaneously remove these metals. Using four stripping stages and a phase ratio (O/A) of 8, a stripping solution containing around 35 gL^{-1} U and 7 gL^{-1} of Th can be obtained.

ACKNOWLEDGMENTS

The authors would like to acknowledge ‘‘INB - Indústrias Nucleares do Brasil S.A.’’ for supplying the sample and the government agencies FAPEMIG, FINEP and CNPq for the financial support. Sincere thanks to CDTN technicians who were involved in this work, especially Luiz C. da Silva and Liliane P. Tavares

REFERENCES

1. Santos, E.A., Ladeira, A.C.Q., 2011. Recovery of uranium from mine waste by leaching with carbonate-based reagents. Environmental Science Technology. 45(8):3591–7.

2. Lima, P., Fukuma, H.T., Nakamatsu, S., Campos, M.G.N., Ramos, E.C.T., et al., 2016 Contaminants Recovery from Acid Mine Drainage. Material Science Forum. 869, August 2016:1023–1027.

3. Haxel, G.B., Hedrick, J.B., Orris, G.J., 2002. Rare Earth Elements — Critical Resources for High Technology. United States Geological Survey Fact Sheet. 87:4.

4. Morais, C.A., Ciminelli, V.S.T., 1998. Recovery of europium from a rare earth chloride solution. Hydrometallurgy. 49:167–77.

5. Soldenhoff, K., 2013. Challenge in rare earth processing. In: ALTA 2013 Uranium-REE Conference. May 25-June. Perth, Western Australia.

6. Zhu, Z., Pranolo, Y., Cheng, C.Y., 2015. Separation of uranium and thorium from rare earths for rare earth production – A review. Minerals Engineering. 77, 185–96.

7. Morais, C., Amaral, J.C.B.S., Salum, M., 2016. Acid Leaching of Rare Earth , Thorium and Uranium from Mining Industry Residues. In: Hydroprocess 2016 8Th International Seminar on Process Hydrometallurgy. Santiago, Chile: GECAMIN Digital Publications; p. 366–75.

8. Amaral, J.C.B.S., Morais, C.A., 2010. Thorium and uranium extraction from rare earth elements in monazite sulfuric acid liquor through solvent extraction. Minerals Engineering. 23(6), 498–503.

9. Abreu, R.D., Morais, C.A., 2010. Purification of rare earth elements from monazite sulphuric acid leach liquor and the production of high-purity ceric oxide. Minerals Engineering. 23(6), 536–40.

10. Resende, L. V., Morais, C.A., 2010. Study of the recovery of rare earth elements from computer monitor scraps - Leaching experiments. Minerals Engineering. 23(3), 277–80.

11. Morais, C.A., Ciminelli, V.S.T., 2004. Process development for the recovery of high-grade lanthanum by solvent extraction. Hydrometallurgy. 73(3–4), 237–44.

Uranium-REE Proceedings

Lithium Processing Forum

APPLICATIONS OF ADVANCED ANALYTICAL AND MASS SPECTROMETRY TECHNIQUES TO THE CHARACTERISATION OF LITHIUM BEARING ORES

By

Mark G. Aylmore[1], Kelly Merigot[1], William D.A. Rickard[1,4], David W. Saxey[1,2,4], Denis Fougerouse[2,3,4], Steven M. Reddy[2,3,4], Zakaria Quadir[1], Noreen Evans[1,2,3], Bradley McDonald[1,3], Brent I.A. McInnes[1, 2], Enej Catovic[5], Peter Spitalny[5]

[1]John de Laeter Centre, Faculty of Science & Engineering, Curtin University (Australia)
[2]The Institute for Geoscience Research, Curtin University (Australia)
[3]Department of Applied Geology, Curtin University (Australia)
[4]Geoscience Atom Probe, Advanced Resource Characterisation Facility, Curtin University (Australia)
[5]Lithium Australia (Australia)

Corresponding Author
Mark Aylmore
mark.aylmore@curtin.edu.au

Presenter
William Rickard
W.Rickard@curtin.edu.au

ABSTRACT

Lithium has become a critical material for many modern technologies, most particularly in rechargeable batteries for portable electronic devices. The ability to extract lithium from ores economically is essential to creating a sustainable lithium production. However, a comprehensive understanding of the deportment of lithium and associated minerals in some ore bodies is limited. Lithium is a light element which makes it very difficult to analyse using conventional x-ray based methods and therefore requires special analytical techniques to quantify the abundance and distribution in minerals. In addition, the deportment of other elements (e.g., Rb, Cs, B, Be, Fe, Al, Mn, F) associated with minerals within pegmatite deposits also need to be considered in process development.

This presentation demonstrates the capabilities of the integrated use of the John de Laeter Centre's state-of-the-art analytical techniques to characterise lithium-bearing pegmatite ores. The mineralogy, mineral associations and liberation characteristics of both ore-bearing and gangue minerals in spodumene and lithium bearing micaceous pegmatites were characterised using a Tescan integrated mineral analyser. The distribution of lithium and other elements within the minerals were defined in a suite of ores using a combination of Laser-ablation ICP-MS, field emission scanning electron microscopy techniques with ESBD and ToF-SIMS capabilities, as well as Atom Probe Microscopy for 3D atomic imaging to identify lithium zonation within mineral matrices.

Keywords: Lithium, Li-bearing ores, automated mineralogy, LCT pegmatite, ToF-SIMS, TIMA, Atom Probe microscopy

Background

Importance of Lithium (Li)

- Lithium has become a critical material for many modern technologies, most particularly in rechargeable batteries for portable electronic devices.

One major source of lithium

- High grade lithium-caesium-tantalum (LCT) pegmatite deposits
  - Spodumene (6.0–7.5% Li_2O),
  - Petalite (3.5–4.5% Li_2O)
  - Li-bearing micas (polylithionite, trilithionite, lepidolite, zinnwaldite, 2.0-7.7% Li_2O)
    - Source of Rb and Cs.
  - Contain Ta, Nb, Sn & rare earths

Processing of LCT pegmatites

- Physical beneficiation required to liberate and concentrate the Li-bearing minerals from gangue minerals.
- Mineralogy of the ore dictates the selection of the treatment route and what improvements can be made to a process

- **Detailed understanding of LCT mineralogy provides opportunities for significant process improvements**

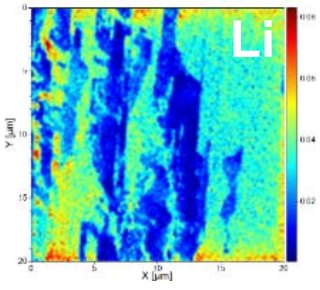

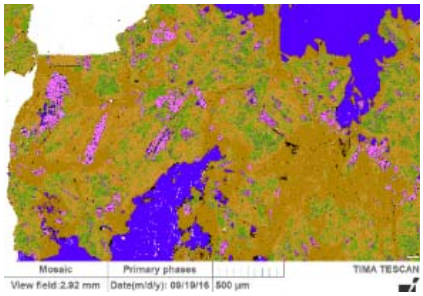

Challenges associated with Lithium mineral analyses

- Conventional chemical analysis does not provide contextual information (i.e. lithium deportment and the minerals associated with lithium).
- X-ray based methods (XRF, SEM-EDS) generally not possible due to the low energy Li x-rays.
- Difficult to distinguish some lithium mineral assemblages optically
  - Lithian muscovite vs "lepidolite“ - distinctive colour caused by Mn & not Li content.

New and emerging analysis workflows are overcoming these issues

The John de Laeter Centre

Tescan integrated mineral analyser (TIMA)

Resonetics S-155-LR 193nm excimer laser ablation system coupled to an Agilent 7700x quadrupole ICPMS.

Tescan MIRA FE-SEM with EBSD/EDS system

Bruker x-ray diffractometers

FEI Talos F200X transmission electron microscope

Tescan LYRA FIB-SEM with ToF-SIMS

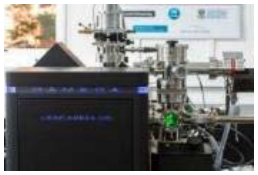

Cameca LEAP 4000X HR atom probe microscope

Sample preparation approach

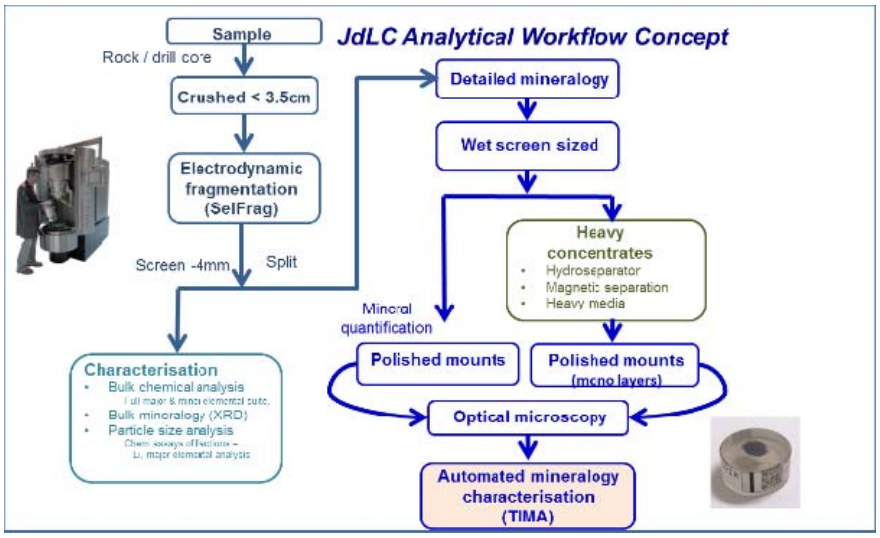

Electrodynamic fragmentation process preserves the original crystal morphology and shape, crystal structure and physical and textural features that are often sacrificed during grinding and milling.

Analytical approach

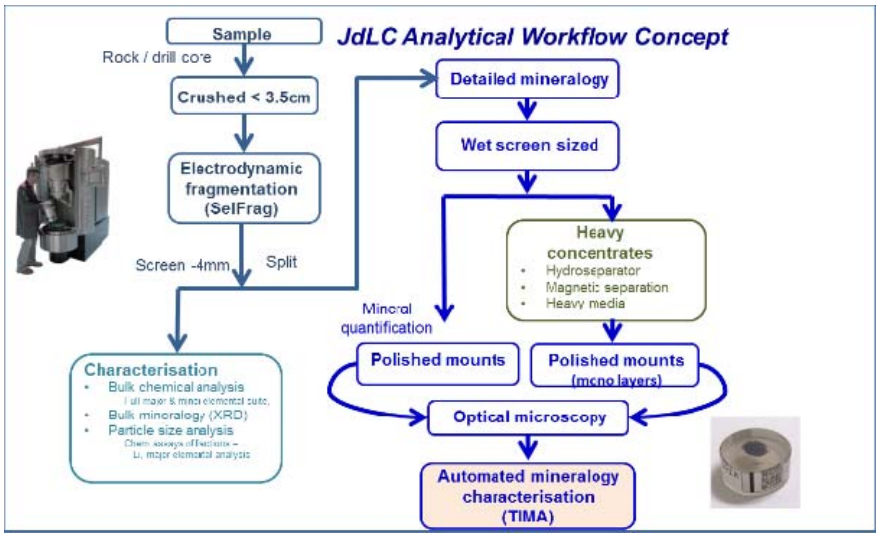

X-ray powder diffraction

- X-ray powder diffraction studies can be used to model and quantify micas
  - Micas exists as different polytypes and can be related to Li content
    - Li content increases → ($2M_1$ → $2M_2$ → 1M or 3T)

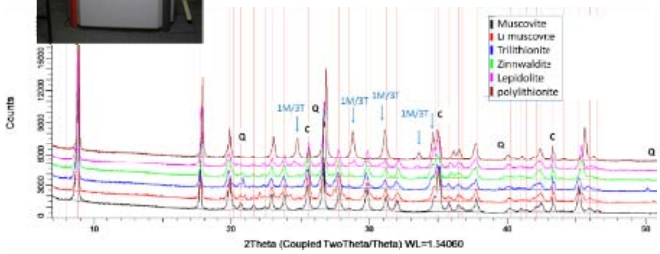

Quantitative phase analysis using the Rietveld method

Mineral specimen	Muscovite/ Li-Muscovite $2M_1$ (C2/c) (wt%)	Zinnwaldite $2M_1$ (Cc) (wt%)	Trilithionite $2M_2$ (C2/c) (wt%)	Polylithionite 1M (C2) (wt%)	Albite (wt%)	Quartz (wt%)
Muscovite	93					7
Li muscovite	84				12	4
Trilithionite	84		11			6
Zinnwaldite	46	54				
Lepidolite	55		17	28		
Polylithionite	7			93		

Tescan Integrated Mineral Analyser

Automated mineralogy characterisation (TIMA)

Qtz-feldspar micaceous ore

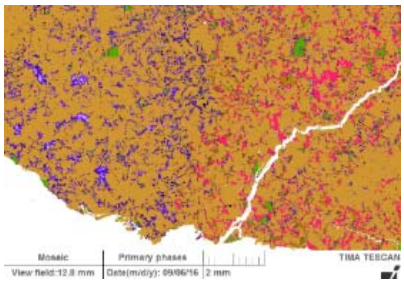

Spodumene ore

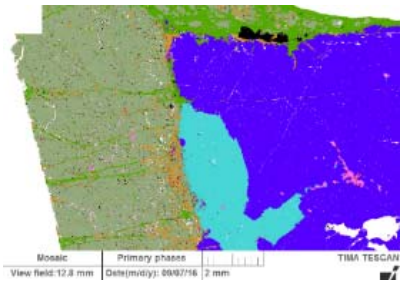

High resolution mapping & Point Spectroscopy modes

- Mineral composition mapping
- Mineral abundance
- Mineral associations
- Liberation characteristics

Lepidolite rich ore

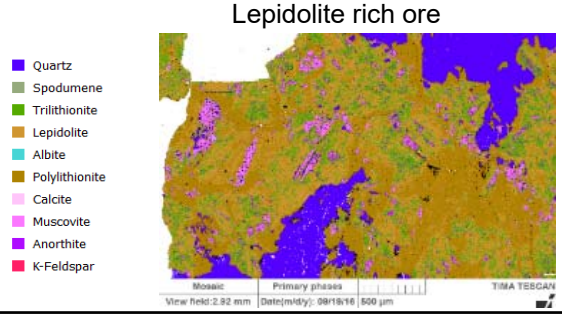

- Fast
- Large area
- Automated
- Quantitative

- Cannot distinguish polymorphs or detect Li
- Results enhanced with combination with other analyses

Identification of mica compositions

- Identify different micas based on their composition (e.g. Al:Si ratio & F content).
- Can't detect Li on EDS

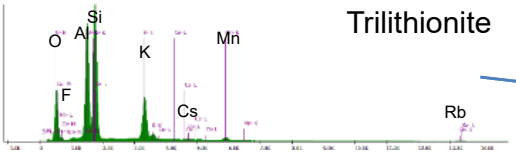

Trilithionite

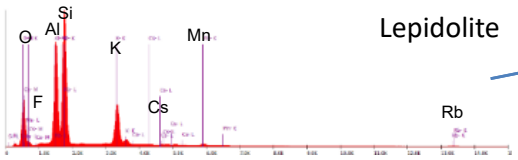

Lepidolite

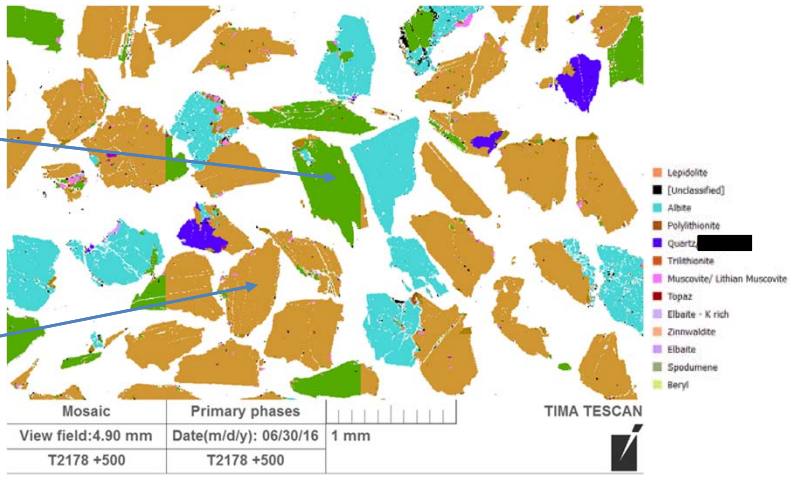

Modal analyses and mineral distributions

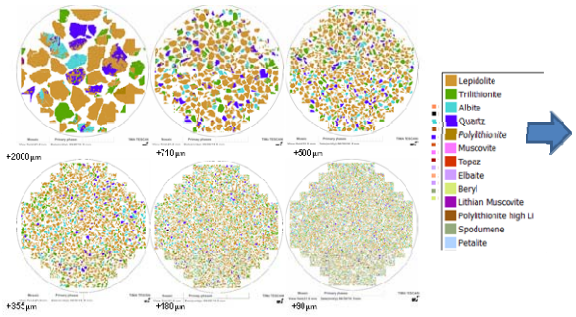

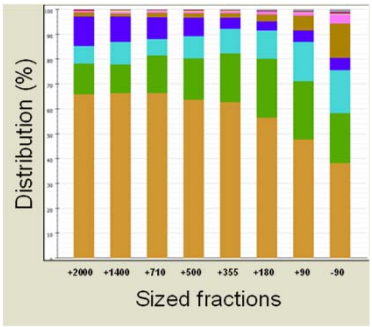

Process metallurgical information

- Li deportment
- Liberation characteristics
- Particle/phase size

Minerals / Mass [%]	
Lepidolite	59.3
Trilithionite	17.4
Albite	10.3
Quartz	7.4
Polylithionite	3.5
Muscovite	1.0
Topaz	0.2
Elbaite	0.2
Beryl	0.2
The rest	**0.5**
Total	**99.9**

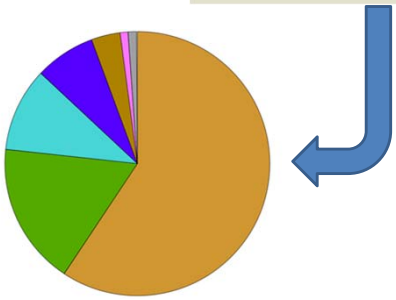

Laser ablation system coupled with ICP-MS

Laser ablation ICPMS

↓

Quantification of Li-bearing minerals & associated minerals

↓

Grain elemental distribution
- Major elements Li Al, Si, Na, K, Cs, Rb, F, Mn

Laser spot size 25 - 75 µm

Quantify and determine trends in Li-bearing minerals (e.g. micas)

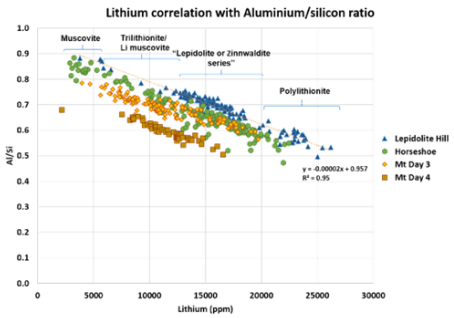

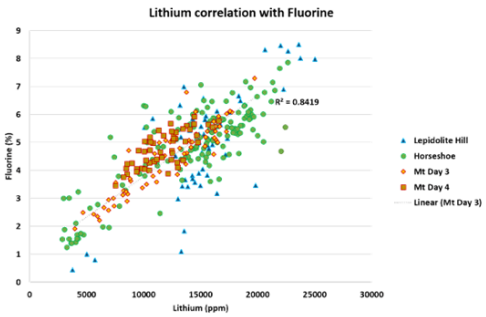

Establish compositional trends;

- Lepidolite (trilithionite → polylithionite series) - Al/Si ratio inversely proportional to the Li content.
- F content in micas is linearly correlated with Li

Tescan LYRA FIB-SEM with insitu ToF-SIMS

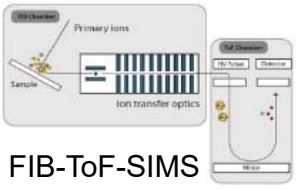

FIB-ToF-SIMS

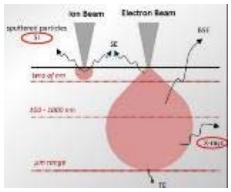

Mass spectrometry inside a SEM

High spatial resolution SIMS
Lateral resolution <50 nm
Depth resolution <20 nm
Light element analysis
Isotopic analysis

- Used to map lithium and other elements with high spatial resolution.

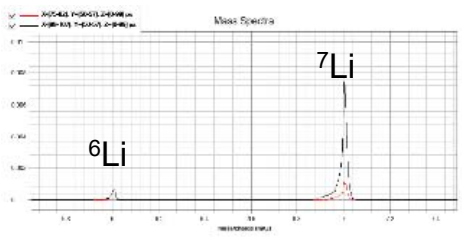

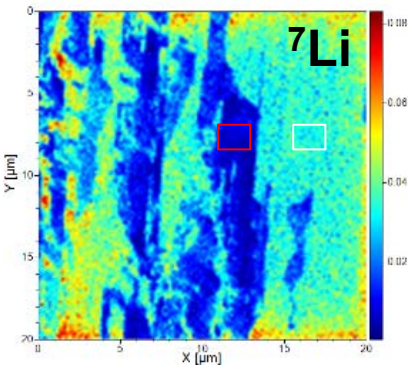

Lithium variation in a mica over 20 x 20 µm

12

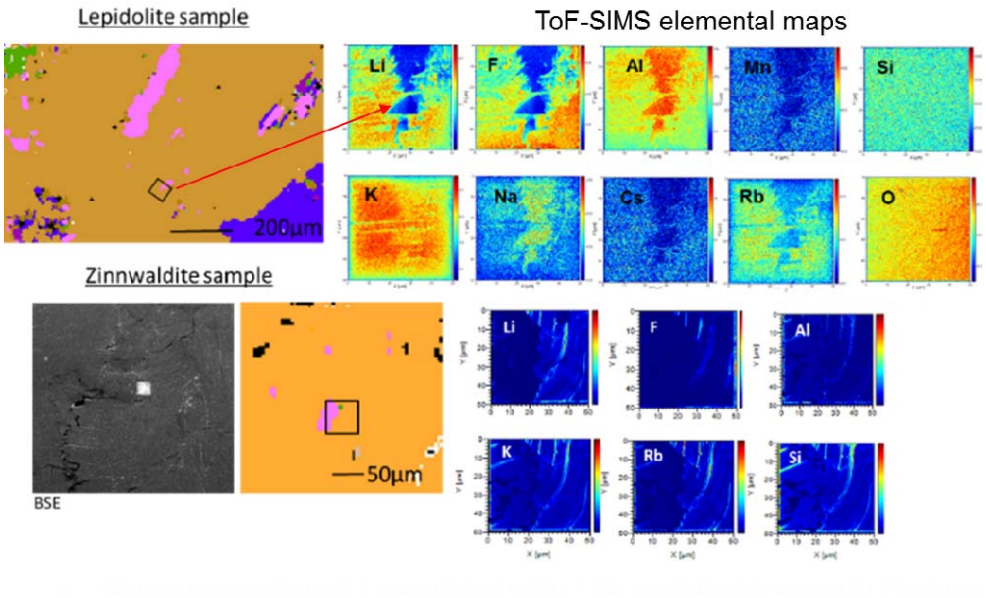

- Strong correlation of Li associated with F, Cs and Rb rich zones in Li micas.
- Li-poor zones correlate with high Na and Al zones -associated with the muscovite

13

Electron backscatter diffraction (EBSD)

Mineral map of micaceous grain

- Identification of discrete grains and orientation
- Can be used to describe the difference in crystallinity and orientation between phases

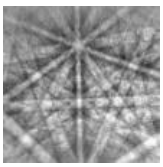

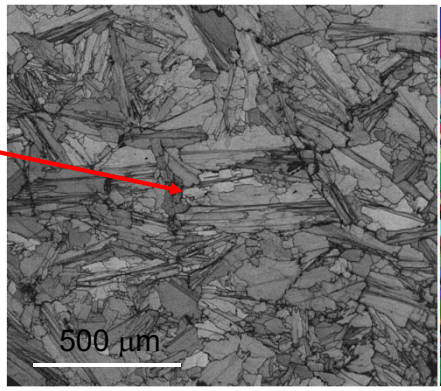

Band contrast map

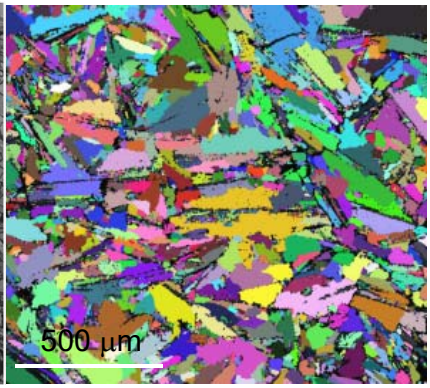

EBSD orientation map showing micas in different orientations (different colors)

Atom Probe Microscopy

- Using crystallography data obtained from EBSD, an area can be selected and lifted for analysis at the atomic level of discrete grains at certain orientations.

a axis

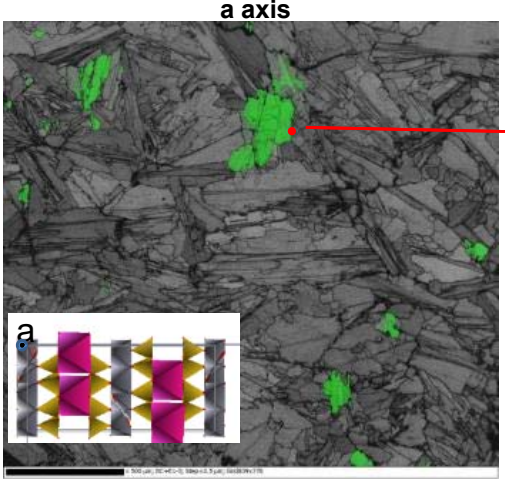

Sample preparation for Atom probe

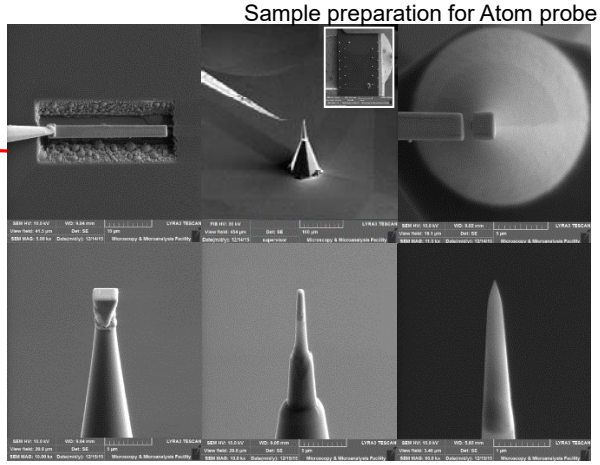

Sharp long needle-like tips are produced using a FIB-SEM and transferred to the atom probe for analysis.

15

Atom Probe Microscopy

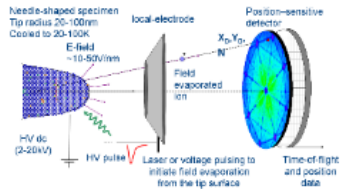

- Lithium distribution at the atomic level in mica
- Reveals variations in chemistry across fine domains.
- Technique can be used for determining the deportment of metal contents in both feed and process residues.

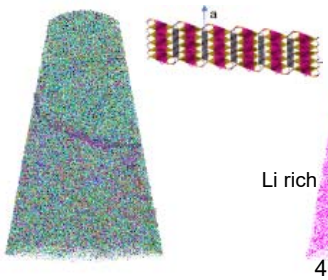

Reconstructed tip

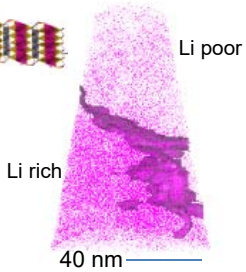

Li distribution in tip

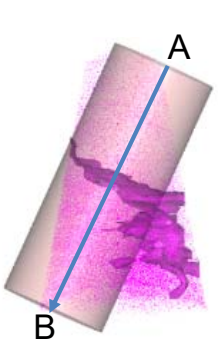

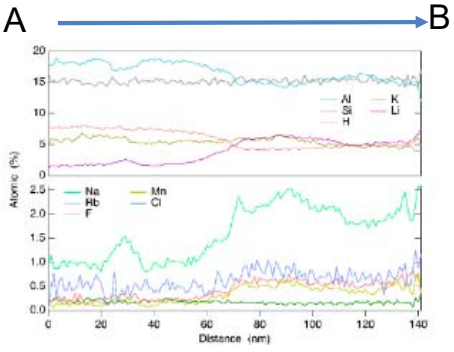

Cross-section of the tip can be evaluated to determine elemental trends

16

Conclusions

- A combination of advanced analytical and mass spectrometry techniques available allows for the comprehensive analysis of lithium in ore and metallurgical samples.

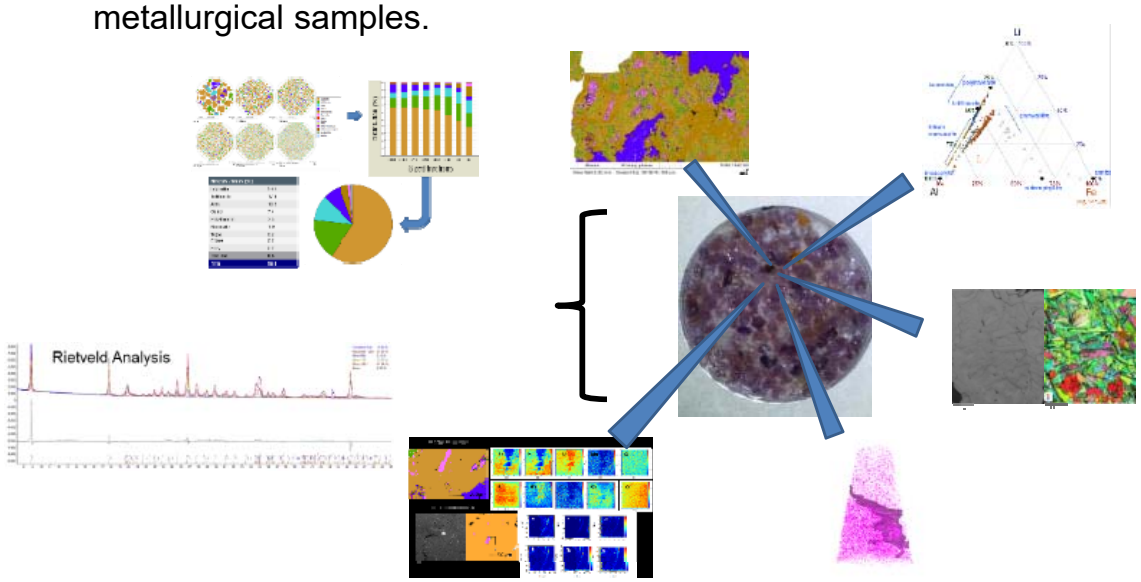

References

Aylmore, M. G. Merigot, K., Rickard, W., Evans, N., McDonald, B., Catovic, E., Spitalny, P. (2017) Assessment of a lithium ore to determine its amenability to processing for the extraction of lithium, Proceedings of EMC 2017, 20pp.

Aylmore, M. G. Merigot, K., Quadir, Z., Rickard, W., Evans, N., McDonald, B., Catovic, E., Spitalny, P. (2017) Applications of advanced analytical and mass spectrometry techniques to the characterisation of micaceous lithium-bearing ores, Minerals Engineering (submitted).

Aylmore, M. G. Merigot, K., Rickard, W., Evans, N., McDonald, B., Catovic, E., Spitalny, P. Assessment of a spodumene ore to determine its amenability to processing for the extraction of lithium, Minerals Engineering (to be submitted).

Aylmore, M. G. Merigot, K., Claridge, T., Catovic, E., Spitalny, P. A comparison of electrodynamic fragmentation to cone crushing of some lithium bearing pegmatites to liberate Li bearing minerals, Minerals Engineering (to be submitted).

ONLINE LITHIUM ANALYSIS IN SPODUMENE CONCENTRATION

By

Lauri Koresaar and Juha Timperi

Outotec, Finland

Presenter and Corresponding Author

Lauri Koresaar
Lauri.koresaar@outotec.com

ABSTRACT

The requirement for lithium has grown recently due to the increased demand in battery applications. Due to the increasing demand for lithium, hard rock sources have become an economical source for lithium production. Compared to brine sources, the hard rock lithium production utilises the same beneficiation methods as traditional minerals beneficiation. Effective process control can be regarded as one of the fastest paying investments for a minerals processing plant. Process optimisation in flotation circuits requires constant feedback of the process state. Spodumene ($LiAl(SiO_3)_2$ laboratory analysis can be very time consuming and the results do not represent the true process state due to the delay. Standard X-Ray analysers, used in base metals processing, fail to measure the weak X-Rays from lithium. Good results from online lithium measurement have been achieved using an analyser based on Laser-Induced Breakdown Spectroscopy (LIBS). LIBS uses a high energy laser to generate plasma in the sample surface, the light emitted from the plasma is then analysed using Optical Emission Spectroscopy (OES). Promising results have been obtained for simultaneous measurement of Li, Al, Fe, Si, K, Ca and Mg for a spodumene concentrator. The online measurement results are planned for controlling magnetic separation and flotation performance.

Keywords: Spodumene Concentration, Process Control, Online Analysis, Laser-Induced Breakdown Spectroscopy

INTRODUCTION

Lithium is the third element by atomic number (Z), and is the lightest and least dense solid element. As other alkali metals, lithium has a single valence electron, and is highly reactive. Lithium is also a good conductor of heat and electricity. As a result of the application of lithium as an anode in batteries, the demand of lithium has increased since the end of the 20th century. Of all battery metals (Co, Li, Mn, Ni and P), lithium has the highest charge-to-weight ratio, thus it is least likely to be substituted (Goonan 2012). The high charge-to-weight ratio is especially important in electric vehicle applications. Other important applications for lithium include ceramics and glass, lubrication greases, and pharmaceuticals and polymers.

Traditionally brine sources have been the major source of lithium due to their low processing cost. With the increasing demand of lithium and the increase in lithium price, pegmatite mineral sources of lithium have become a feasible option for lithium production (U.S. Geological survey 2015). Lithium bearing minerals which are exploited include, spodumene ($LiAl(SiO_3)_2$), jarosite $LiNaSiB_3O_7(OH)$, lepidolite $K(Li,Al,Rb)_3(Al,Si)_4O_{10}(F,OH)_2$ or other lithium bearing minerals. Spodumene is the most abundant mineral of these, and may contain up to 1-3% of lithium oxide (Talens Peiro et al. 2013). Froth flotation using fatty acid collectors is the most commonly used method to separate spodumene from associated silicate minerals. In some cases it has been feasible to use gravity separation as the spodumene concentration method. Other beneficiation methods include wet magnetic separation and optical sorting (Luong et al 2013).

MATERIALS AND METHODS

Spodumene Processing and Analysis

At one example hard rock lithium concentrator (site X), the tailings of the primary concentrate contain valuable amount of lithium, averaging 0.5 % Li. A simplified block diagram of the process is presented in Figure 1. The tolerated Fe_2O_3 content in the final concentrate varies according the intended use, from 0.1 % in ceramic grades to 3 % in chemical grades. The iron oxide is reduced in the beginning of the process using SLon® vertically pulsating high gradient magnetic separators. The vertical carousel of the separator allows strongly magnetic and coarse particles to be removed without having to pass through the full depth of the matrix volume (Elder & Sherrell 2011).

The non-magnetic product of the magnetic separation reports to flotation. The flotation circuit consists of a rougher, scavenger and cleaner spodumene circuits. The scavenger tailings produce an albite concentrate. The cleaner concentrate reports to apatite flotation followed by mica flotation. In the apatite and mica flotation, the overflow is considered as the tailings, and the underflow is treated as the concentrate. The tailings of the apatite and mica flotation produce a low grade spodumene concentrate. The final concentrate reports to dry magnetic separation, which produces chemical and high grade spodumene concentrates.

Manual samples are taken from all major feed, concentrate and tailings points of the process flowsheet. The samples are analysed in a site laboratory for Li, Al, Ca, Fe, K, Mg, and Si. The sample preparation of LiO_2 in the laboratory can be time consuming, as the silicate minerals in the ore generally require either digestion in four acids, perchloric, nitric, hydrofluoric and hydrochloric. If the digestion using acids is not complete enough, a peroxide fusion may be required, where the sample is fused with sodium peroxide and the melt is dissolved in hydrochloric acid. The sample is then analysed using ICP–OES or AAS methods. The delay between taking the sample and obtaining the analysis result can vary from 4 hours up to 24 hours.

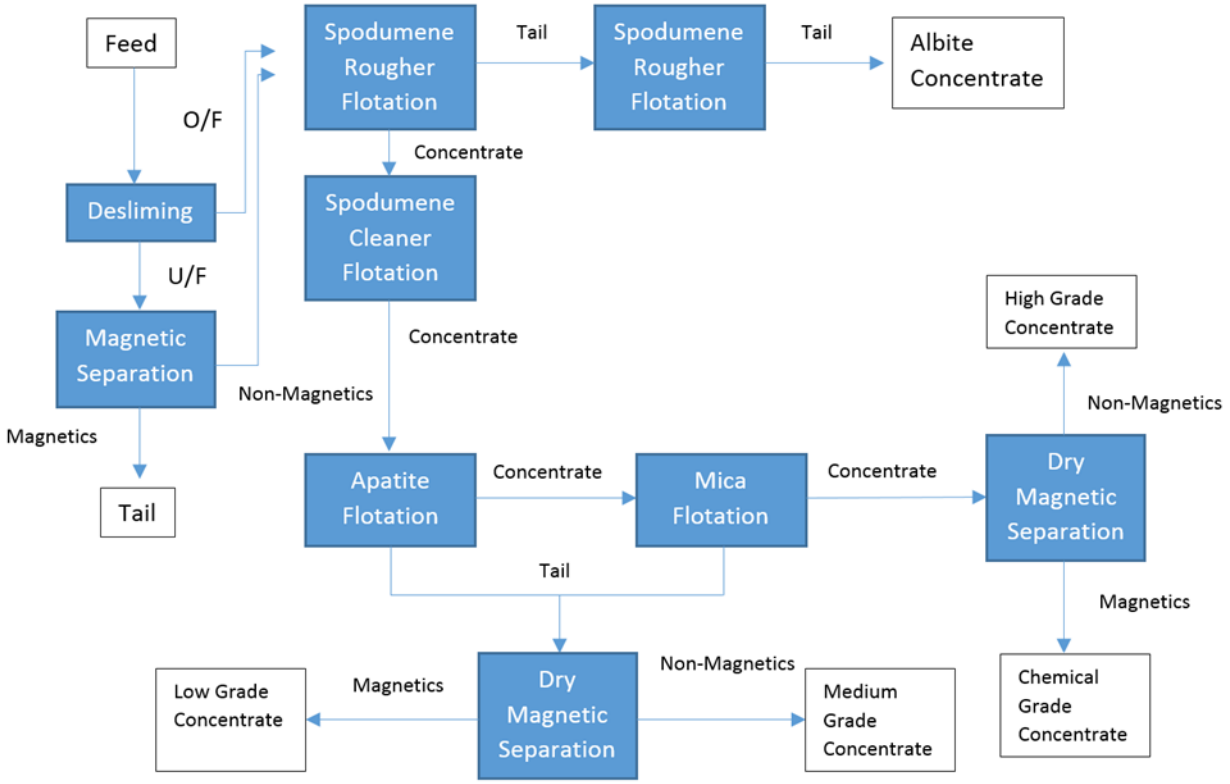

Figure 1. Block diagram of spodumene concentrator plant (site X).

In the spodumene flowsheet at site X, sulphuric acid is used as a pH controller, fatty acid is used as collector and alcohol ethoxylate is used as an emulsifier. For the average feed grade, the planned fatty acid consumption is 1.4 kg/t. Without real time information of the feed grade, tailings grade and concentrate grade, the chemicals are usually added in excess to maximise recovery. The benefit of an on-line instrument would be the potential optimisation of reagent consumption.

Laser-Induced Breakdown Spectroscopy

Laser-Induced Breakdown Spectroscopy (LIBS) (Cremers and Radziemski, 2006) is a variant of optical emission spectroscopy (OES). OES methods e.g. ICP-OES are routinely used in laboratories to determine elemental concentrations of samples. The basic principles of any OES are:

1. Atomization of the sample to produce free atomic species
2. Excitation of the atoms
3. Detection of the emitted light
4. Calibration of the measured intensity to concentration
5. Determination of concentrations

A high energy laser (10 – 1000 mJ) is used to vaporize part of the sample and to form a cloud of plasma. The atoms in the plasma are excited to higher energy levels. In the beginning of the plasma the temperature is extremely hot and the emission spectrum is dominated by continuum emission, as local thermodynamic equilibrium does not exist. As the plasma cools down, the atoms return to lower energy states by emitting photons at characteristic wavelengths, as illustrated in Figure 2. First a laser pulse is directed towards the sample, and a small volume of the sample is ablated. High luminous plasma and a shockwave are formed and the ablated material is dissociated into excited ionic and atomic species. As the plasma cools down the excited species return to lower energy states emitting photons at characteristic wavelengths.

The light emitted by the plasma is measured using an Echelle spectrometer equipped with CCD camera. Intensity measured at a wavelength characteristic for the analysed element is proportional to the concentration of the element in the plasma. As the amount of sample vaporized by one laser pulse is small, several hundreds of pulses are averaged in one spectrum. Generally 300 – 1500 laser

pulses are measured per sample. The frequency of the laser is 5 Hz, making the total measurement time per sample 1 – 5 minutes.

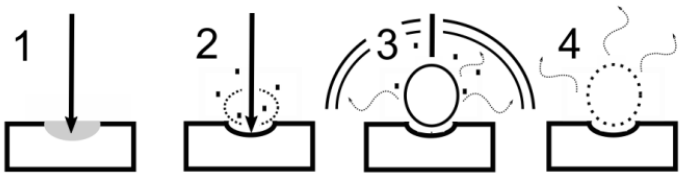

Figure 2. High energy laser pulse is directed to the sample, which absorbs the energy of the laser pulse and generates a plasma.

Alkali metals have a relatively high emission signal in OES analysis, allowing a good signal to noise ratio of the emission lines. This is partially due to the low ionization energies of the alkali metals. An example Li emission line at 670.8 nm of spodumene feed, tailings and concentrate is presented in Figure 3. The lithium line is a result of an electron transition from $1S^2 2P^1$ to $1S^2 2S^1$ configuration. The Full Width at Half Maximum (FWHM) resolution of the Li line is ~0.09 nm.

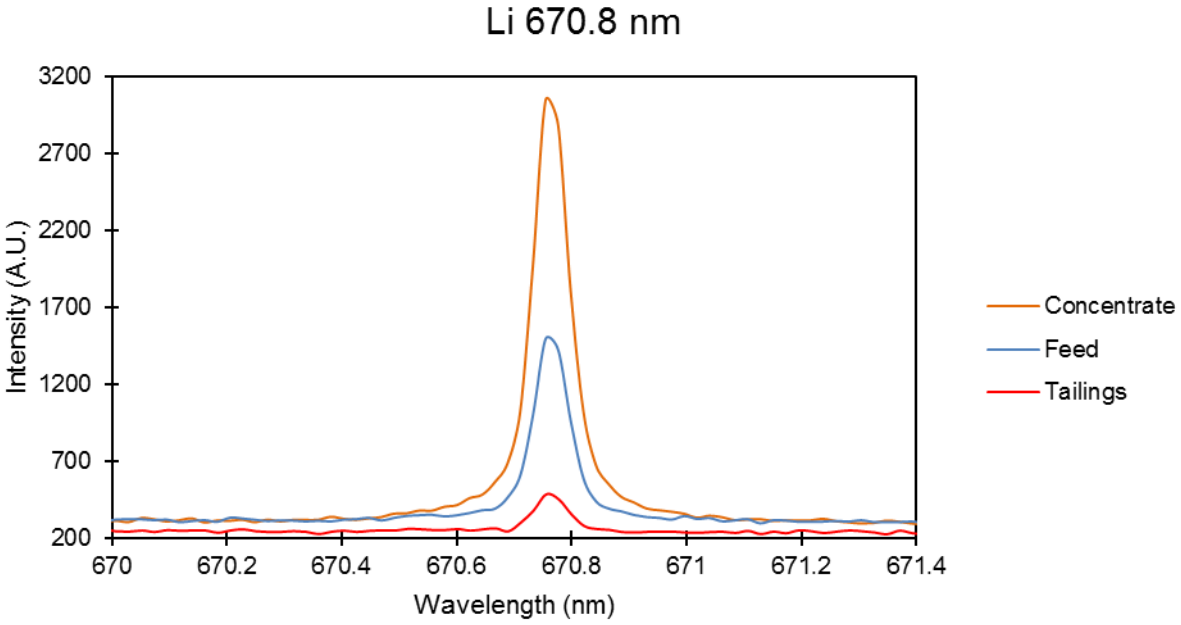

Figure 3. Characteristic Li emission at 670.8 nm. The X-axis represents the wavelength and the Y-axis represents the measured intensity. The red, blue and green lines represent tailings, feed and concentrate samples, respectively.

A primary sampler is used to take 100-300 L min^{-1} sample to a multiplexer which can be fed up to 12 sample lines at once. Primary sample can be taken continuously or on-demand. The multiplexer takes a secondary sample of ~25 L min^{-1} from one sample line at a time and feeds this to the analyser for measurement. The sample is introduced to the measurement as slurry. A schematic layout of the analyser is presented in Figure 4.

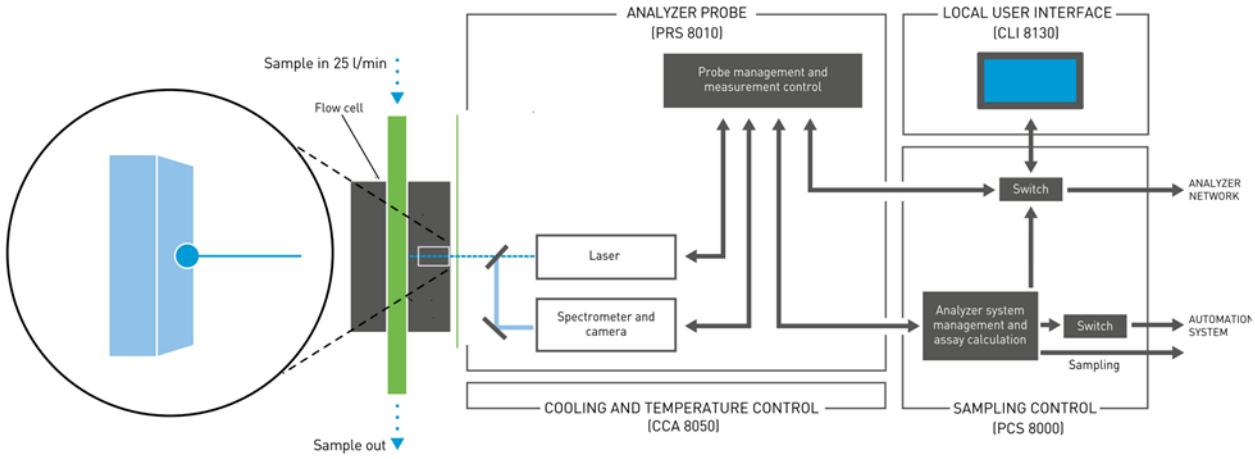

Figure 4. Schematic layout of the analyser. A small portion of the sample is heated into hot plasma in the flow cell by a short laser pulse. The spectrum emitted by the excited atoms and ions in the cooling incandescent plasma is measured after a short delay. The concentration of elements in the sample are calculated from averaged spectra using calibration equations based on laboratory assays of samples.

The analyser had been previously installed on a sulphide gold concentrator plant. Several validation samples were collected from the analyser on July 2016, where the analyser result was compared with the laboratory results (Koresaar et. al 2017). As most of the gold in the plant is carried by sulphides, the analysers main priority has been analysis of sulphur. On-line trend of sulphur during a 90 h test run is presented in Figure 5.

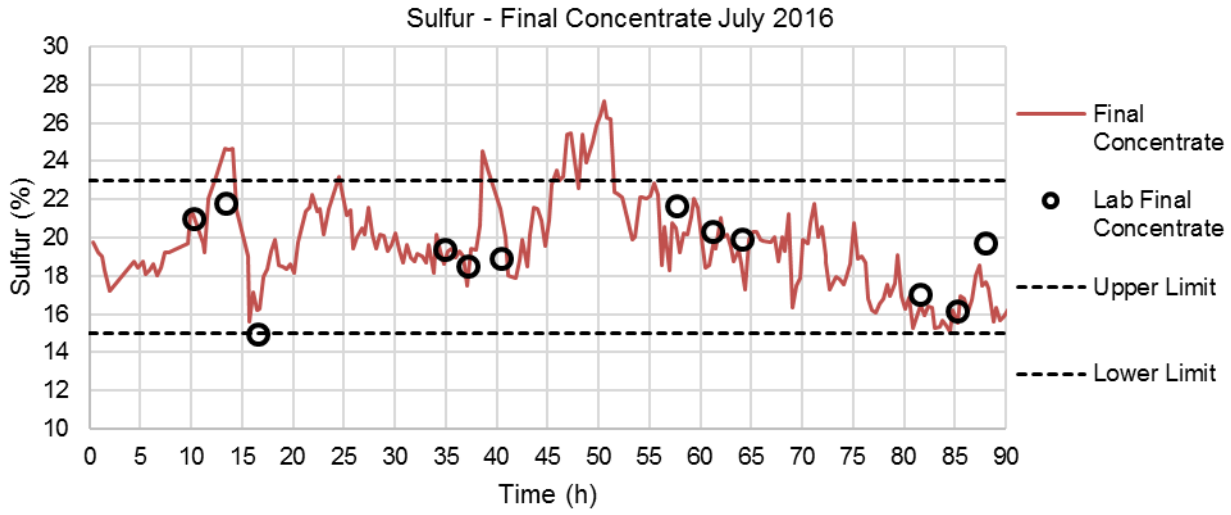

Figure 9 – Analyzer produced trend of sulfur during 90 hours and the validation laboratory values. The dashed lines represent process control limits.

Experimental

Total of 16 dry samples from a spodumene concentrator pilot plant were received. The mass of the samples was ~2 kg per sample. The particle size of the samples was analysed using Outotec's PSI500i laser diffraction particle size analyser. The average Dv(50) and Dv(80) of the samples were 157 +/- 28 and 273 +/- 62 µm, respectively. 50g aliquot of the samples was sent to a third party laboratory for analysis, where they were analysed by sodium peroxide fusion, followed by ICP-OES analysis. The samples were assayed for Al, Ca, Fe, K, Li, Mg and Si. As sodium hydroxide fusion was used, the samples could not be analysed for Na content. The laboratory assays of the samples are presented in table 1.

The samples were mixed with 6 L followed by 7.5 L of water to produce slurry at ~20 - 25 % solids content, so that each sample was measured in two different solids content. The samples were

circulated to the sample cell at 25 L min^{-1} using a closed slurry loop, equipped with an agitator. The samples were analysed using a spectrometer which wavelength range from 230 to 950 nm. The samples were analysed using a 5 Hz laser pulse frequency. The energy of each laser pulse was 120 +/- 1 mJ. 150 laser pulses averaged 3 times were used for each measurement, making the total measurement time 90 seconds per measurement. Each sample was measured three consecutive times. The measured spectra were analysed for Al, Ca, Fe, K, Li, Mg and Si using elemental lines at 396, 422, 404, 770, 671, 280 and 288 nm, respectively, a good signal for Na was also observed at 589 nm.

Table 1. Sample assays.

Sample	Al (%)	Ca (%)	Fe (%)	K (%)	Li (%)	Mg (%)	Si (%)
1	8.21	3.66	5.39	1.63	0.44	1.87	27.70
2	7.72	0.66	0.90	1.55	0.52	0.19	29.80
3	8.08	0.65	0.93	1.56	0.48	0.18	29.30
4	13.00	2.43	0.87	1.05	2.46	0.08	26.60
5	7.81	0.31	0.41	1.59	0.56	0.03	27.20
6	13.10	2.47	0.84	1.04	2.48	0.08	26.90
7	7.82	0.30	0.40	1.58	0.56	0.03	28.90
8	13.00	2.54	0.84	1.02	2.50	0.07	26.50
9	6.39	0.10	0.27	1.53	0.04	0.00	23.60
10	6.43	0.09	0.27	1.56	0.04	0.00	27.00
11	10.46	1.64	0.87	1.28	1.55	0.13	28.09
12	9.57	1.27	0.55	1.28	1.23	0.04	25.00
13	7.01	0.36	0.56	1.54	0.27	0.09	26.47
14	10.85	1.65	0.88	1.27	1.58	0.12	27.98
15	9.27	1.10	0.51	1.34	1.08	0.03	26.96
16	7.05	0.30	0.52	1.56	0.20	0.07	27.86

RESULTS

The results of the feasibility test were evaluated using the Root-Mean-Square Error (RMSE) with n-2 degrees of freedom and the coefficient of determination, R^2. Elements with a gap between the grade distributions were separated to a high and low grade analysis. In normal analyser operation each sample line is usually calibrated separately. The analyser predicted values plotted versus the laboratory assays of Li in low and high grades are presented in Figure 6. The results from all measured assays are provided in Table 2.

The Fe and Mg samples contained one sample with significantly higher grade (sample 1) than the rest of the samples. This one high grade sample was removed from the analysis of Fe and Mg due to its excessively high influence on the analysis model. The Fe model is presented in Figure 7. Samples 9 and 12 were not used in the Si analysis as they had significantly lower Si content than the rest of the samples.

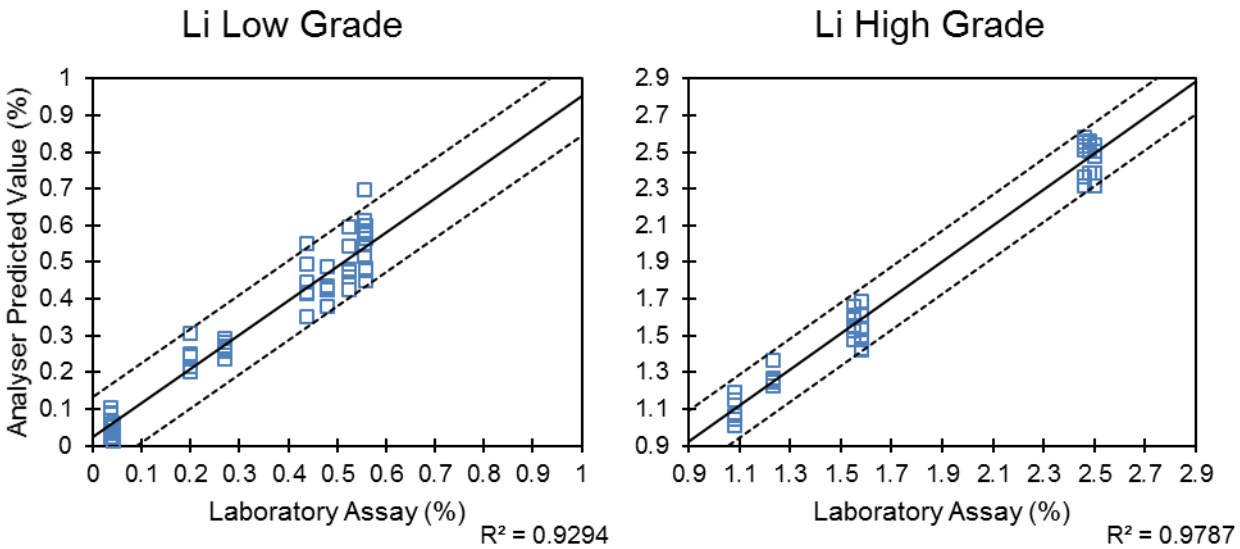

Figure 6. Li calibrations in low and high grades. The Y-axis represents the analyser predicted value and the X-axis represents the laboratory assay. The broken lines represent the 2σ confidence intervals.

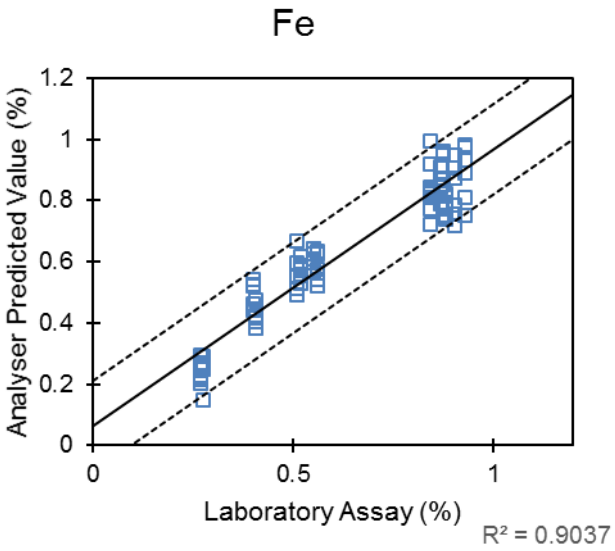

Figure 7. Fe calibration model. The Y-axis represents the analyser predicted value and the X-axis represents the laboratory assay. The broken lines represent the 2σ confidence intervals.

Based on the test on the samples from a spodumene concentrator pilot plant, the results from the LIBS analyser are good enough to be utilised in process control. The Outotec Courier 8® LIBS analyser will be installed to the spodumene concentrator. The main purpose of the analyser is to monitor the Li grades and recovery, the secondary target is to monitor the Fe removal from the material.

Table 2. Calibration results.

Assay	n	Min (%)	Max (%)	Average (%)	R^2	RMSE (%)
Li Low Grade	54	0.04	0.56	0.35	0.93	0.05
Li High Grade	42	1.08	2.50	1.84	0.98	0.09
Al	96	6.39	13.10	9.11	0.95	0.52
Ca Low Grade	48	0.09	0.66	0.35	0.85	0.08
Ca High Grade	48	1.10	3.66	2.10	0.92	0.23
Fe	90	0.27	0.93	0.64	0.90	0.07
K	96	1.02	1.63	1.40	0.87	0.08
Mg	90	0.00	0.19	0.08	0.78	0.03
Si	84	26.47	29.80	27.66	0.62	0.64

CONCLUSIONS

Traditionally, Li online analysis has been out of reach with previous methods. A new LIBS based analyser has now proven successful on the analysis of low atomic number elements. The LIBS analyser has successfully been able to measure Li from slurry samples obtained from a spodumene concentrator pilot plant.

The analyser will be installed in the concentrator during construction, to provide online information of Li content for process control. The operational results from the use of LIBS process control of Li at this concentrator will be watched with great interest, given obvious economic benefits.

REFERENCES

1. Cremers, D.A., & Radziemski, L.J., 2006. Handbook of laser-induced breakdown spectroscopy. *Cambridge University 25.*

2. Elder, J. & Sherrell, I., 2011, Dry versus wet magnetic separation: horses for courses. *In Proceedings: Heavy Minerals Conference* (5-6 October, Perth, WA, Australia).

3. Goonan, T.G., 2012, Lithium use in batteries: U.S. Geological Survey Circular 1371, http://pubs.usgs.gov/circ/1371/

4. Koresaar, L., Timperi, J., Balbin, T., & Astakhov, V., 2017, Online elemental analysis of slurry using laser-induced breakdown spectroscopy. *In Proceedings: 49th Annual Canadian Mineral Processors Operators Conference* (January 17-19, Ottawa, Ontario, Canada).

5. Luong, V.T., Kang, D.J., An, J.W., Kim, M.J. & Tran, T., 2013, Factors affecting the extraction of lithium from lepidolite. *Hydrometallurgy 134-135*, pp. 54-61.

6. Talens Peiro, L., Villalba Mendez, G., & Ayres, R., 2013, Lithium: Sources, Production, Uses and Recovery Outlook. *JOM 65*, pp. 986-996.

7. U.S. Geological Survey, 2015, Mineral commodity summaries 2015: U.S. Geological Survey, pp 94-95 http://dx.doi.org/10.3133/70140094

SPECIALIZED IMPELLERS FOR HYDROMETALLURGICAL PROCESSING APPLICATIONS WITH FOCUS ON LITHIUM

By

Wolfgang Keller and Jochen Jung

EKATO RMT, Germany

Presenter and Corresponding Author

Jochen Jung
jochen.jung@ekato.com

ABSTRACT

Hydrometallurgical processing of Lithium, rare earths and uranium has gained in importance as the production must keep up with growing world-wide demand and the increased requirement for product qualities. Although significant improvements have been made for non-ferrous and precious metals processing, adapted or new agitator solutions had to be provided for these applications.

For processing of battery grade lithium carbonate, to name an example, the crystallization and gassed units are crucial for the overall plant performance. Unlike precipitation steps, crystal morphology and particle size distribution in crystallizers must be precisely controlled. This paper will present the newly developed EKATO Torusjet, which is an improved draft tube impeller with a significantly higher efficiency compared to standard solutions. For the same motor power it achieves higher pumping rates, a better degree of slurry homogeneity and an improved surface renewal, which finally leads to a more uniform crystal growth. Due to the optimized blade geometry the local and overall shear rates are decreased minimizing crystal breakage and decreasing abrasion issues.

For gassed applications, especially if a very high degree of gas utilization must be achieved, EKATO has successfully applied the self-inducing gassing turbine EKATO Gasjet. This paper will present different examples from minerals processing, e.g. for the carbonization/ de-carbonization step at a lithium carbonate processing plant in which carbon dioxide gas can be used in a closed loop system.

Key words: crystallization, self-inducing gassing impeller, gas utilization, agitator, draft tube

INTRODUCTION

Agitators are fundamental in hydrometallurgical processes for the recovery of precious and base metals and for the production of pure industrial minerals. Technological milestones in recent years have been the development of process and abrasion improved mixing equipment for world-scale autoclave applications, such as POX, PAL and HPAL. For atmospheric gassed leach tanks, the EKATO Combijet technology has set new standards for economy of large scale hydrometallurgical plants for processing of precious and base metals.

A further field for the application of agitators in minerals processing is the extraction of salts or metallic compounds by crystallization. Examples are aluminum hydroxide, potassium nitrate, potassium chloride, nickel and cobalt sulfates, precipitated calcium carbonate only to name a few. One important and demanding process step herein is the controlled crystal formation during production in order to achieve defined, predominantly large crystals with uniform size and morphology. For such applications EKATO has developed a very efficient draft tube technology that is used in continuously operated crystallizers for mass production of potash fertilizers and ammonium sulfate, amongst others.

Another example, where such technology is being operated successfully is the crystallization of lithium carbonate. The main driver of the growing demand for lithium compounds is the battery market. Moreover, purity requirements for the battery grade lithium carbonate are higher compared to those of standard product. Therefore new process routes had to be established, such as the carbonation - decomposition method, which includes a gassing and a degassing process step with carbon dioxide. For gassed applications, as mentioned above, for which complete gas utilization is required, EKATO has successfully applied the self-inducing gassing turbine EKATO Gasjet. The proof of feasibility was part of an engineering study that EKATO carried out for a new lithium carbonate plant. The results show, that it is possible to recirculate a high percentage of carbon dioxide in a closed-loop system and that only a small amount of gas must be replaced by fresh carbon dioxide.

BASICS OF LITHIUM CARBONATE PROCESSING

The two main sources for lithium extraction are brines from salt lakes and ore deposits[1]. The largest exploitable brine deposits can be found in South America, in the USA and China. Large ore deposits mainly exist in Australia and Northern America (USA and Canada), China and Africa (e.g. Zimbabwe), as described by Bertau et. al[1].

Natural brine deposits are solutions containing a mixture of different salts. The lithium compounds, such as lithium chloride, can occur in concentrations from as low as 200 ppm up to 2 g of lithium per liter, as noted by Habashi[2].

A general flowsheet for the processing of brine from the Salar de Atacama in Chile is presented by Garret[3]. Brine of low concentration is pumped in solar ponds, where a large part of the water evaporates over time. The solution becomes more concentrated. During this step accompanying salts such as sodium chloride, potash and part of the magnesium chloride precipitate. However, not lithium chloride as it is more soluble compared to the aforementioned salts. In a next step further purification is carried out in stirred tanks by adding quicklime and soda ash in order to precipitate magnesium carbonate, magnesium hydroxide, calcium sulfate and lime stone.

When lithium is recovered from ore sources, roasting and acidic leaching are the state-of-art methods prior to the process steps that are described in the following:

Crystallization/ Precipitation of Lithium Carbonate:

$$LiCl\ (aq.) + \tfrac{1}{2}\ Na_2CO_3\ (aq.) \rightarrow \tfrac{1}{2}\ Li_2CO_3\ (s) + NaCl\ (aq.) \qquad \text{(equation 1)}$$

Lithium carbonate is precipitated by adding sodium carbonate to the solution, as shown by the chemical reaction equation 1. Lithium carbonate is the least soluble alkali metal carbonate which is the physical basis of this process step. E.g. at 20°C 17.6 g of sodium carbonate is soluble in 100 g solution, whereas only 1.31 g of lithium carbonate is soluble in 100 g solution, as noted by Habashi[2].

However, the purity of the lithium carbonate in suspension is not sufficiently high to meet the quality requirements of battery grade material.

Gassing and Degassing Steps for Lithium Carbonate Purification:

The carbonation - decomposition method is an established way to synthesize lithium carbonate of very high purity, which is used as starting chemical for the lithium-ion battery production.

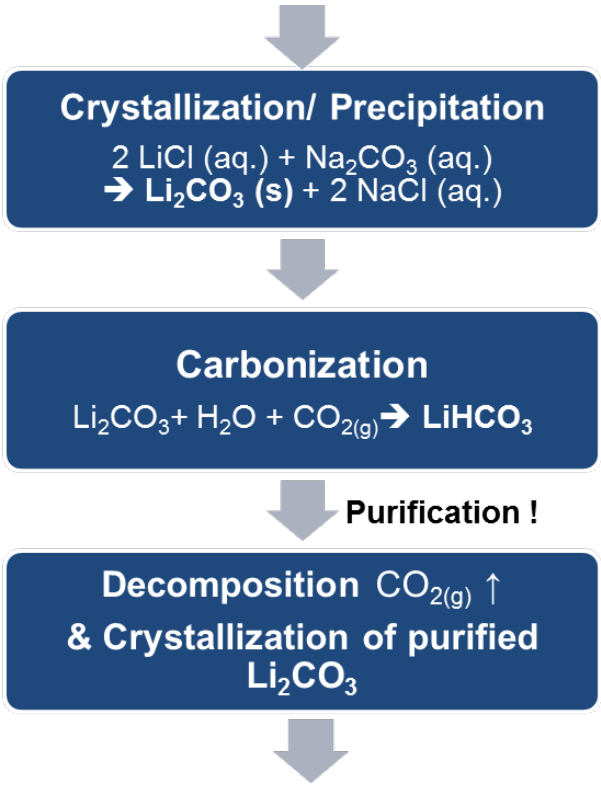

Figure 1: General simplified flow diagram

In the carbonization step pure carbon dioxide is added to the lithium carbonate slurry in order to obtain highly soluble lithium bicarbonate.

$$Li_2CO_3\ (s) + CO_2\ (g) + H_2O \leftrightarrow 2\ LiHCO_3\ (aq.) \qquad \text{(equation 2)}$$

The chemical reaction (equation 2) is typically carried out at temperatures of 10 – 20°C as carbon dioxide is more soluble in aqueous solutions at lower temperatures. Part of the impurities precipitate. The dissolved impurities can be separated by means of suitable purifying methods, such as ion exchange or solvent extraction, as described by Wen-tao Yi et. al. in[4].

After the purification step the solution is heated up to higher temperatures of 70 – 90 °C. Due to the lower solubility most of the carbon dioxide is again released and pure lithium carbonate forms and crystallizes. Solubility data for carbon dioxide in aqueous solutions can be found in text books, as e.g. in Air Liquide's 1x1 der Gase[5]. Finally the carbon dioxide gas that has been released in the decomposition unit can be recirculated to the upstream carbonization reactors to produce lithium bicarbonate for purification.

For a plant with an annual production rate of e.g. 20.000 tons of Lithium carbonate, a minimum of 12.000 tons of carbon dioxide is required which is the theoretical stoichiometric amount for the carbonization reaction. This amount of carbon dioxides equals approximately 3.3 million liters of diesel fuel if it were generated by combustion. These impressive figures underline the importance for an efficient recirculation and management of carbon dioxide in such purification plants.

The design of industrial scale crystallizers is a complex task, as the crystallization process is always integrated into the entire process. Consequently, crystallizers have to fulfill strict process requirements in order to provide a consistently high product quality especially for continuously operated mass production. Challenges in designing a suitable crystallization process are to develop an optimum setup comprising vessel, agitator, impellers, baffles as well as feed and discharge positions, in addition to the knowledge of the optimal physical and chemical conditions. For more details please refer to handbooks such as Crystallization[6]. A typical mixing task that is found in any

crystallization process is blending which minimizes the concentration or temperature differences over the total product volume inside of the vessel. Solids suspension is another important mixing task. One task is to lift large crystals off the bottom to keep them in suspension and secondly to achieve a homogeneous suspension of the smaller crystal size fraction for maintaining a constant crystal growth rate.

Draft tube agitators are also used for the crystallization of lithium carbonate by addition of sodium carbonate. In this process the mixing of the sodium carbonate and the fresh lithium chloride solution must happen immediately to prevent concentration differences that would lead to uncontrolled precipitation, increasing the risk of inclusions of impurities during the crystal formation process.

The acceleration and precise control of heat exchange between the vessel content and the cooling media is a very important task for cooling crystallization processes, such as for the production of Glauber's salt, potash and magnesium recovery.

Heating is required e.g. for the recrystallization of purified lithium carbonate from a clean lithium bicarbonate solution. The decomposition reaction of lithium bicarbonate is typically carried out at temperatures of 70 – 90 °C. Please refer to chemical reaction equation 3 below.

$$2\ LiHCO_3\ (aq.) \rightarrow Li_2CO_3\ (s) + CO_2\ (g) \uparrow + H_2O \qquad \text{(equation 3)}$$

Although the solubility of carbon dioxide falls with increasing temperature, the process is kinetically limited by the physical mass transfer as described by Wen-tao Yi et. al. in[4]. However, the formation of larger gas bubbles of carbon dioxide gas can be significantly accelerated by intensive agitation which is required in order to obtain sufficiently high degassing rates.

CONSIDERATIONS FOR TEST WORK

New processing plants, e.g. for lithium carbonate purification, must be planned very carefully. Typically, hydrometallurgical test work programs are carried out in order to determine the ore chemistry, the required processing and leaching steps for recovery, the most favorable reaction conditions to obtain high yields and last but not least to know the consumption of chemicals under different processing conditions. On the other hand, it must be possible to scale-up the results from such campaigns and the process equipment then needs to be selected accordingly.

An example is a lithium carbonate purification plant where EKATO has been involved in at an early project stage for a process concept study. A detailed engineering study was then conducted for the proof of the feasibility, in order to optimize the agitator design and to select and correctly scale-up the agitator equipment. Generally speaking, important aspects are:

- Measurement of gas transfer rate of carbon dioxide for the carbonization step
- Evaluation of overall reaction time by measuring the change of pH and conductivity over the time of the lithium carbonate/ bicarbonate solution
- Measurement of the degassing rate of carbon dioxide for the decomposition step
- Detailed analysis of chemical composition of the crystallized lithium carbonate
- Measurement of crystal size distribution and crystal morphology

DESIGN CRITERIA FOR CRYSTALLIZERS

As discussed above, the main mixing tasks can differ very much, especially when comparing batch and continuous crystallization processes. Batch crystallization is frequently applied for recrystallization of specialty chemicals or intermediates in typically small vessel sizes. Often precipitation or cooling crystallization is applied. Since batch crystallizers are mainly used in multipurpose plants, the mixing system has to flexible. In continuous crystallizers, as discussed in this paper, supersaturation is usually generated by vacuum or evaporation. Compared to the batch crystallizers, these are used to produce dedicated products in medium to large vessels and are typically designed for high throughput of substances such as sodium chloride, ammonium sulfate or sugars and derivatives. The mixing tasks differ compared to batch operation. In the majority of cases

the crystallizer is not only operated with the objective to provide a high product purity and yield but also to achieve a specific particle size or particle size distribution. With such a constant product quality subsequent process steps as e.g. solid-liquid separation and drying can be smoothly operated as well. For this purpose, the generation of a homogeneous suspension during design and scale-up of crystallizers is most critical. At the same time, too high local energy input has to be avoided as crystals can be destroyed and production of fines has to be prevented. In addition to this, stationary conditions and constant product quality are also positively influenced by a well-considered positioning of feed and discharge points.

Draft tube arrangements are ideally suited for continuous bulk crystallization as for example DTB (Draft Tube Baffled) crystallizers as shown in figure 3. More details can be found in EKATO.THE BOOK[7] and as presented by Himmelsbach et. al. in[8].

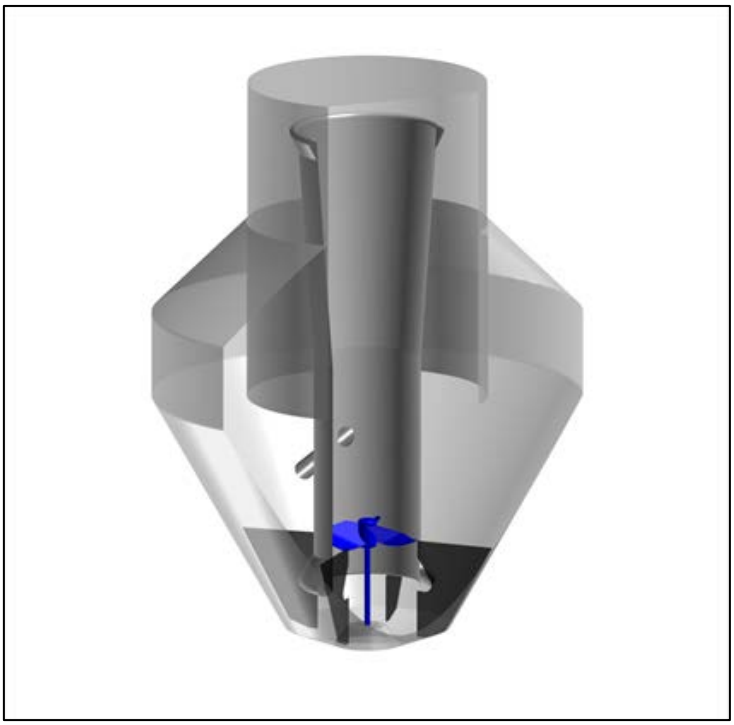

Figure 2: Continuous crystallizer equipped with a draft tube

The power input of this equipment can be effectively converted into a high suspension performance in order to enable a controlled nucleation process and growth rate. The impeller is installed as a bottom or top entry design in the draft tube and acts as a recirculation pump. Typically the saturated solution is added on the suction or pressure side of the impeller. The internal recirculation or pumping rate in the vessel is adjusted to prevent a local oversaturation in the evaporation zone. This could lead to a spontaneous, uncontrolled nucleation and therefore to an undesired broad particle size distribution. During a continuous crystallization process, new particles are continuously being produced through secondary nucleation, which then continue to grow. This results in a cross-section of all grain size classes. Therefore the correct positioning of the different discharge locations is very important in order to discharge coarse crystals and fines separately. In addition, crystal breakage and formation of further crystal nucleus must be avoided.

By using an optimally efficient axial pump module which consists of a draft tube impeller and baffles, high pumping rates and suspension performance with low shear can be achieved at the same time. The more efficient this kind of module works and the more gently it handles the crystals, the less overall fluctuation can be found in the product and it is therefore easier to achieve an efficient and at the same time robust mode of operation.

The following points are decisive for the design of an efficient axial pump module in draft tube crystallizers:

- An impeller that provides a gentle handling of the crystals
- Suitable baffles and guide vanes that are adjusted to the blade shape
- Largest possible impeller diameter ratio to the draft tube
- Optimum distance between the impeller and guide vanes
- Optimum distance between draft tube and vessel bottom
- A flow-conform shape of the draft tube inlets and outlets
- Flow-conform shape of the vessel bottom

To reach the correct pumping rate it is absolutely mandatory to take the presence of solids into account, especially when bigger particle sizes are crystallized.

A solids concentration of only 5 wt. % already easily increases the power requirement to achieve a fixed pumping rate by 60 %! For slurries with 25 wt. % solids, a factor of 5 to 6 has to be considered! Therefore it is very important to have corresponding models including available empirical data to accurately design the entire system with the agitator.

Figure 3: The EKATO Torusjet impeller (patent pending PCT/EP2016/077327)

The EKATO Torusjet impeller, shown in figure 3, has been specially designed for the use in draft tube operated crystallizers. In order to transform the power input efficiently into a suspension performance, an axial and homogeneous flow direction is required that covers the entire cross-section of the draft tube. The shape of the impeller blades of the Torusjet has been specifically adapted to the flow behavior emerging from the draft tube geometry. The hydrodynamic shape of the blades produce a very directed axial flow profile which lowers internal pressure losses and therefore minimizes the shaft power requirements for a given flow rate. In addition, the static baffles that have been designed based on the impeller geometry are responsible for an efficient flow near the draft tube on the way inwards and outwards.

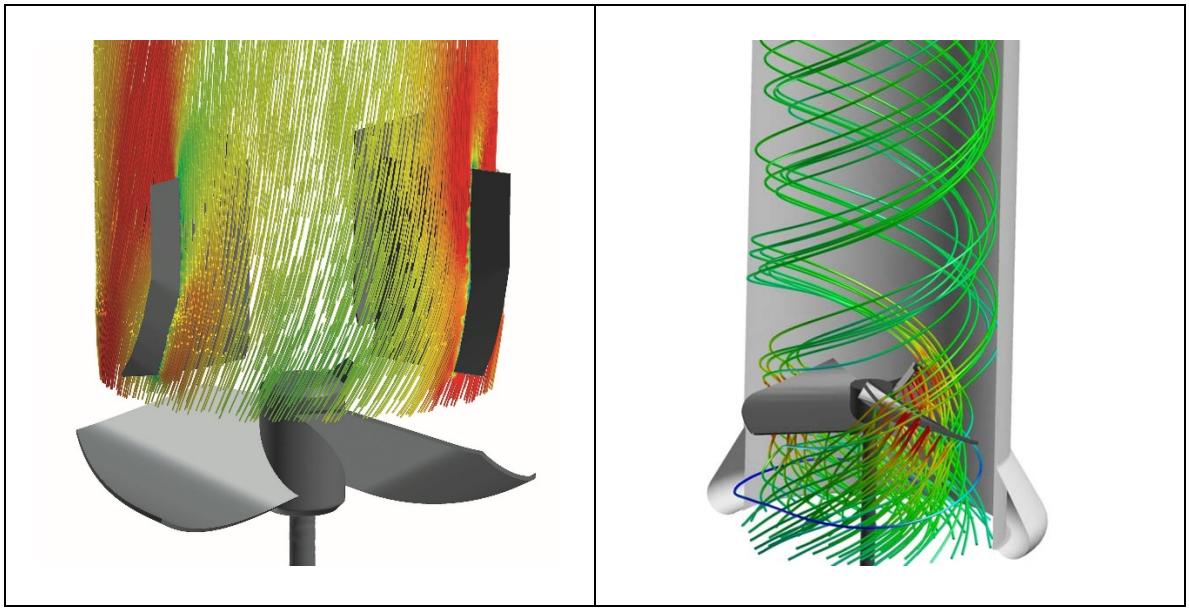

Figure 4: Flow lines in a draft tube – Left: The EKATO Torusjet and flow directing vanes/ right: Standard draft tube solution without baffles.

Figure 4 shows the results of two CFD simulations. The figure on the right-hand side shows a flow field with strong vortices for a standard draft tube solution with incorrect baffling. This results in higher shear rates and lower pumping rates, compared to the EKATO Torusjet solution shown in figure 4 on the left-hand side. As one result, the Torusjet impeller will provide a more controlled particle formation and allows the production of larger crystals with a narrower particle size distribution. Moreover, the engineered impeller profile creates very little shear, minimizing crystal break and abrasion issues.

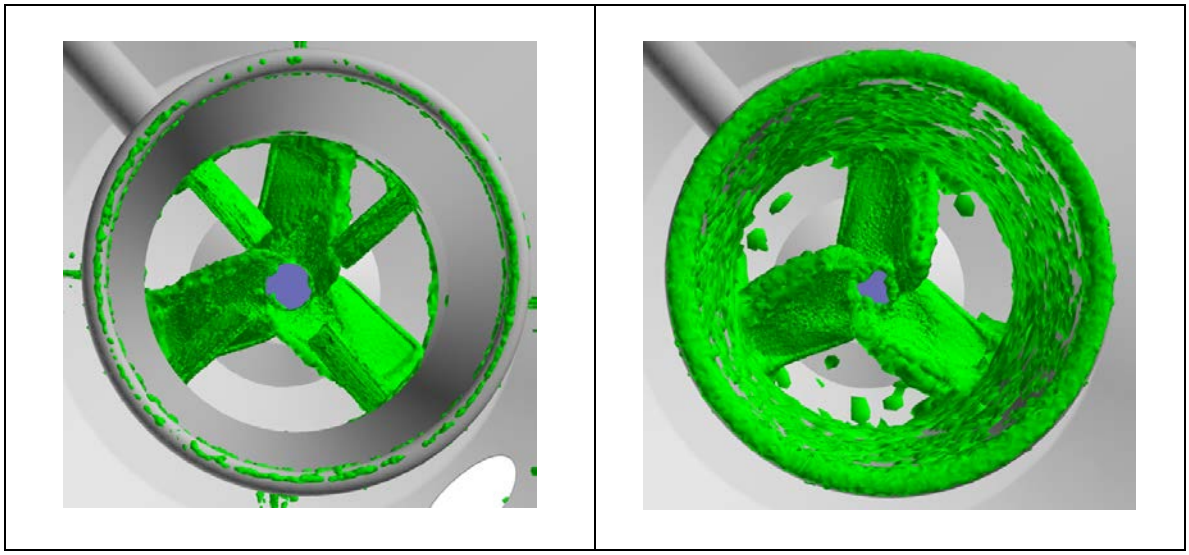

Figure 5: Iso-surfaces showing the shear rate at the draft tube impeller with (left) and without (right) baffles

Figure 5 shows the impeller from the top. The green surfaces are so-called iso-surfaces of same shear rate. The area of highest shear is naturally found on the impeller blades and/or also in the area of the baffles. However, the extent of the highest shear in this area is strongly reduced with the same pumping rate by using the EKATO Torusjet and streamlined baffles. In consequence, the crystallizer with streamlined baffles can provide a gentle circulation that enables a more robust process resulting in the creation of larger crystallized substances, see figure on the left. In contrary an incorrect setup is less efficient and additionally leads to higher local shear at the inner draft tube walls which will cause attrition and crystal breakage, as shown by the CFD results on the right.

The greater efficiency that can be achieved with the shaped blades and guide vanes permits a reduction of the tip speed at the same time. The circulation rate can be maintained with a lower power

input of 70 % compared to baffled standard solutions which leads to a lower mechanical stress of the draft tube impeller as well as the crystallized product itself.

Table 1: Comparison of the performance of different draft tube solutions

	Standard impellers	EKATO EDTC	EKATO Torusjet
motor power required to achieve the same pumping rate	100 %	78 %	70 %
pumping rate achieved with the same motor power	100 %	128 %	143 %

In table 1 the performance of the EKATO Torusjet impeller is compared to standard impeller types and the former EKATO EDTC all for baffled conditions.

To bring the figures above in to a practical context: With the EKATO EDTC it already was possible to design a draft tube system with one motor size lower compared to a system with standard impellers. The EKATO Torusjet now makes it possible to use up to two motor sizes less, e.g. P = 110 kW with EKATO Torusjet or P = 160 kW to achieve the same pumping rate with a conventional system.

On the other hand, for the same motor power the EKATO Torusjet achieves a 1.43 times higher pumping rate compared to a conventional draft tube impeller which means a 1.43 faster surface removal, higher evaporation rates, more homogenous mixing and finally a better crystallization performance.

As a matter of course all before discussed characteristics and advantages of the EKATO Torusjet are very important during the design phase for lithium carbonate crystallizers as well.

EKATO GASJET (CARBONIZATION STEP)

The use of technically pure gases is only economical, if a high gas utilization rate can be achieved. Therefore it is important to recycle unreacted gas from the head space and to bring it back into the solution. An advantageous solution for this task represents the EKATO Gasjet, which is a self-aspiring gas turbine, as shown in Figure 6.

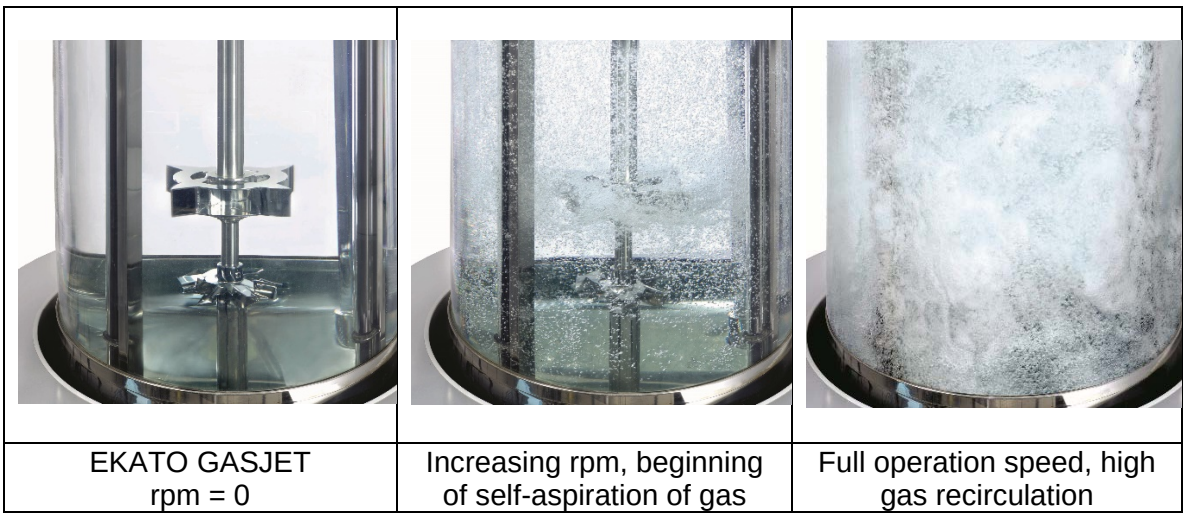

EKATO GASJET rpm = 0	Increasing rpm, beginning of self-aspiration of gas	Full operation speed, high gas recirculation

Figure 6: EKATO GASJET in operation

The basic principle of the EKATO GASJET is that it creates a low pressure zone around the turbine tips which allows sucking gas directly from the head space through a hollow shaft. The gas flows downwards through the openings of the EKATO GASJET turbine and is injected directly into the slurry. Therefore no additional equipment such as compressors is required for gas recirculation. Fig.7 shows a typical reactor exemplarily.

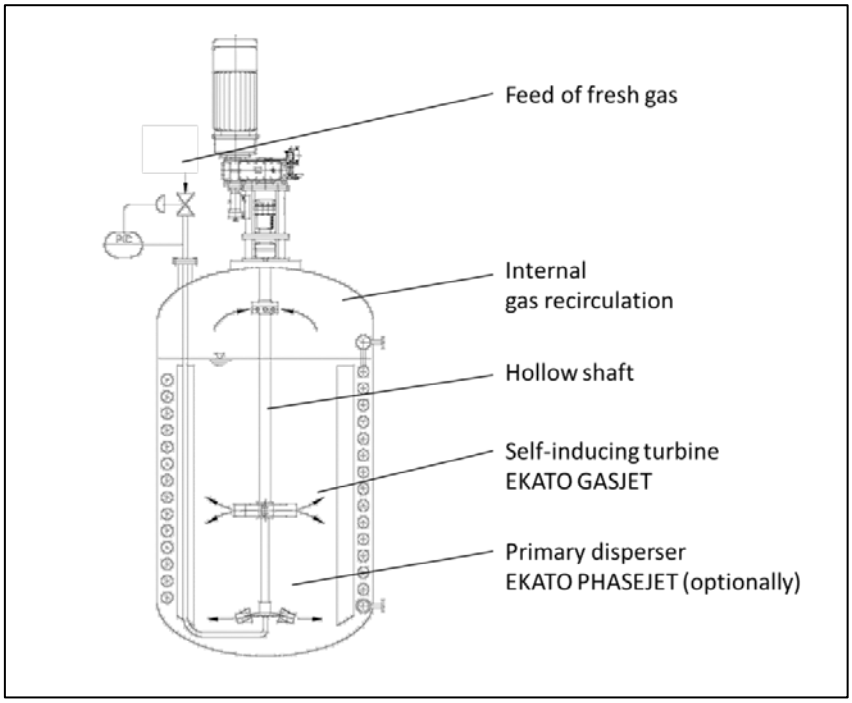

Figure 7: EKATO GASJET – exemplary

Furthermore the agitator disperses the gas into very fine gas bubbles and thus creates an extremely large gas-liquid interface area. Fast reactions are not limited by the mass transfer and productivity is increased. EKATO Gasjet and EKATO Combined Gassing are now used worldwide in more than 500 gas-liquid reactors mainly in the chemical industry. A comprehensive overview is given in EKATO.THE BOOK[7].

In minerals processing this concept was successfully applied for nickel oxidation autoclaves and lithium carbonate processing. It is also worthwhile to mention, that such technology could also be beneficial for the production of precipitated calcium carbonate, reduction reactions with hydrogen, e.g. nickel recovery, or for the leaching of scandium and rare earth ores by using pure sulfur dioxide gas for recovery.

CONCLUSIONS

The production of purified lithium carbonate is a good example of how production equipment and technology have to keep up with changing tasks and rising complexity. One possible way for the processing of battery grade lithium carbonate is the carbonization - decomposition method, where especially crystallization, carbonization and the decomposition units become crucial for the overall plant performance.

In this case, the crystal morphology and particle size distribution of lithium carbonate needs to be precisely controlled, unlike when using simple precipitation tanks as was done in the past. Controlling the crystallization process is only possible with improved draft tube agitator systems, such as the EKATO Torusjet which achieves instantaneous mixing of the reactants in order to control the crystal growth and avoid inclusions of impurities.

This type of lithium carbonate plant is only economically operated, if the carbon dioxide is recirculated which leads to a complete reaction/utilization of the gas. As an example, a plant processing 20.000 tons/ year of Lithium carbonate only requires a minimum of 12.000 tons/ year of carbon dioxide to meet the stoichiometric demands. However, self-aspiring gassing turbines such as the optimized EKATO Gasjet can recirculate unreacted gas from the head space, in order to achieve very high gas

utilization rates and completely reuse the carbon dioxide coming from the down-stream decomposition units. At the same time the high local power input at the impeller blades provides a very high degree of gas dispersion and accelerates the gas-liquid mass transfer which otherwise is limiting the carbonization reaction.

A similar challenge occurs during the decomposition step which is physically limited by the mass transfer of degassing. Therefore the agitators must provide very high local power inputs to promote the progression of carbon dioxide which was found in good agreement with the results of Wen-tao Yi et. al. in[4]. These kinds of solutions are known from POX autoclaves, where high local power inputs are common and for which EKATO has developed an abrasion reduced flat blade disc turbine, the EKATO EPOX-R.

The degassing then triggers the crystallization. An optimal control of crystallization is achieved by selecting optimized draft tube agitators, such as the EKATO Torusjet. It is characterized by a very high efficiency, compared to standard solutions. Given the same motor power, it achieves higher pumping rates, a better degree of slurry homogeneity and surface renewal for degassing and the release of carbon dioxide. This finally leads to a more uniform crystal growth and a higher extraction of lithium carbonate. Due to the optimized blade geometry the local and overall shear rates are decreased, minimizing crystal breakage and reducing abrasion issues. Coarse crystals of pure lithium carbonate are the result.

EKATO has supplied successfully operating agitator equipment for different lithium processing plants, where the carbonization - decomposition method has been implemented.

REFERENCES

1. Martin Bertau, Wolfgang Voigt, Anke Schneider, Gunther Martin, Lithium Recovery from Challenging Deposits: Zinnwaldite and Magnesium-rich Salt Lake Brines, WILEY-VCH Verlag, Chem.Ing.Tech. 2017, 89, No.1-2, 64-81.

2. Fathi Habashi, Textbook of Hydrometallurgy, Laval University, Quebec City, Canada, ISBN 2-980-3247-7-9.

3. Donald E. Garrett, Handbook of Lithium and Natural Calcium Chloride, Their Deposits, Processing, Uses and Properties, Elsevier University Press, 2004, ISBN 978-0-12-276152-2.

4. Wen-tao Yia, Chun-yan Yana , Pei-hua Mab, Crystallization kinetics of Li2CO3 from LiHCO3 solutions – Journal of Crystal Growth 312 (2010) 2345–2350.

5. 1x1 der Gase, Air Liquide Deutschland GmbH, 3rd edition 2007.

6. Crystallization: Basic Concepts and Industrial Applications, Wiley VCH Verlag (2013).

7. EKATO. THE BOOK 3rd edition, ISBN 978-3-00-038660-2.

8. Dr. Bernd Nienhaus, Nicole Rohn, Wolfgang Keller, Werner Himmelsbach, Kontinuierlich Kristallisieren, CIT Plus 1-2, 2013.

REVIEW OF LITHIUM PRE-CONCENTRATION, EXTRACTION, SEPARATION AND OR PURIFICATION USING DOW WATER AND PROCESS SOLUTIONS TECHNOLOGIES

By

Jaco Bester, Daryl Gisch and Valeria Burlakova

Dow Water & Process Solutions, Netherlands

Presenter and Corresponding Author

Jaco Bester
JBester@dow.com

ABSTRACT

A review of Dow Water and Process Solutions technologies capability for:

1. the pre-treatment and concentration of Lithium brines using FILMTEC™ - nano filtration and reverse osmosis membranes

2. the extraction, separation and or purification of Lithium solutions using DOWEX™ / AMBERSEP™ - ion exchange resins.

Keywords: Lithium, Reverse Osmosis, Nano Filtration, Ion Exchange Resin

Overview

- Introduction/Background
- Brines pre-treatment and concentration
- Primary lithium extraction
- Metals removal
- Boron removal
- Chlorides removal
- Organics removal
- Summary

Dow Water & Process Solutions - products within the mining process value chain

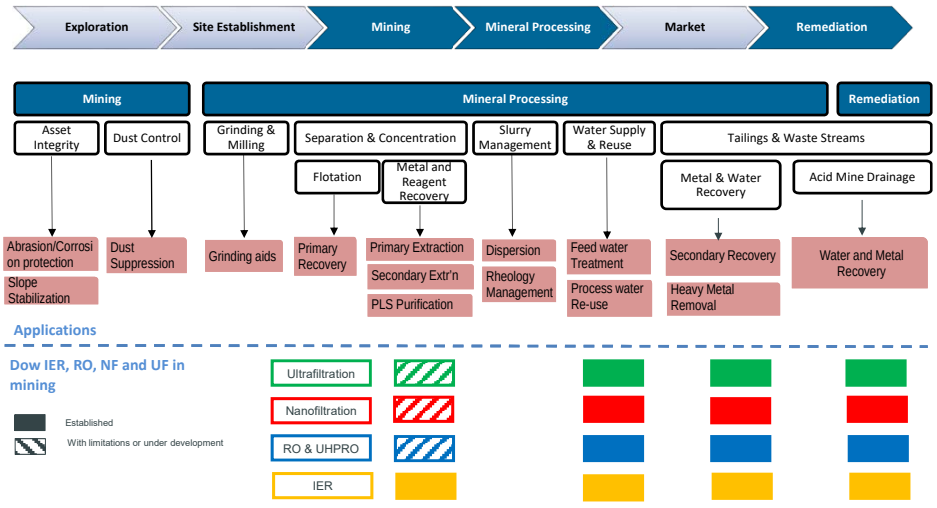

Introduction / Background

Increased demand for battery grade Lithium

Increase in Lithium price

Electrical Vehicle market growth projections (exponential surge)

Battery composition for EV's and Grid storage requires Li, Co, Ni, Mn

Carbondioxide emission reduction protocols

Li Products

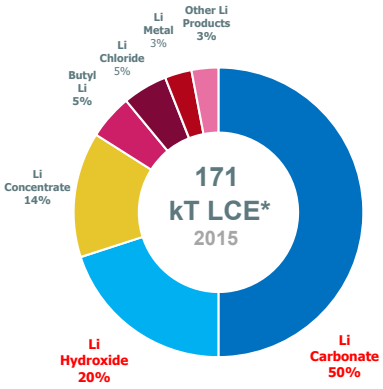

LCE - Lithium Carbonate Equivalent – key metrics in Li industry
EV - Electric Vehicle
Source: Deutsche Bank Lithium 101 report, 9 May 2016

Li Carbonate & Li Hydroxide Grades

Applications

	Purity		Segment Share 2015
Industrial grade	‹ 99.0%	Glass, Air, Ceramics, Casting, Al, Polymers etc	61%
Technical grade	99,0%		
Battery grade	99.5%	Traditional batteries	25%
EV* grade	≥ 99.9%	EVs	14%

✓ Battery application (incl EVs) – highest quality needed and biggest growth expected

Batteries Demand Growth

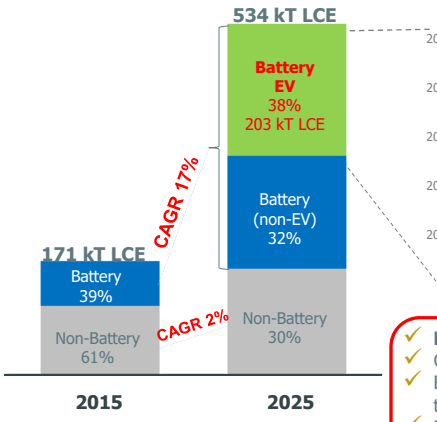

Source: Deutsche Bank Lithium 101 report, 9 May 2016
Source: Global Lithium Market 2016-2020 - Technavio 2016

EV Is A Key Application

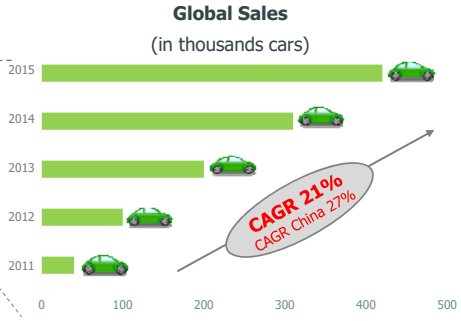

- ✓ **EV market requires highest lithium products purity**
- ✓ China is the largest market
- ✓ EV's heavily subsidized in many countries eg. Norway, the Netherlands & Germany
- ✓ Environmental impact
- ✓ Fuel economy regulations
- ✓ Government subsidies

Lithium sources/resources

Two key Lithium sources

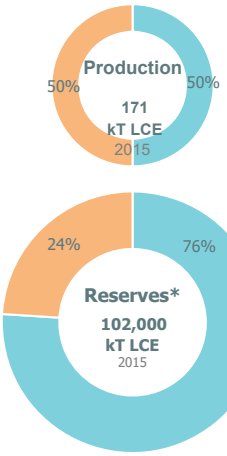

Dominating Regions By Production

(LAR, Australia, China)

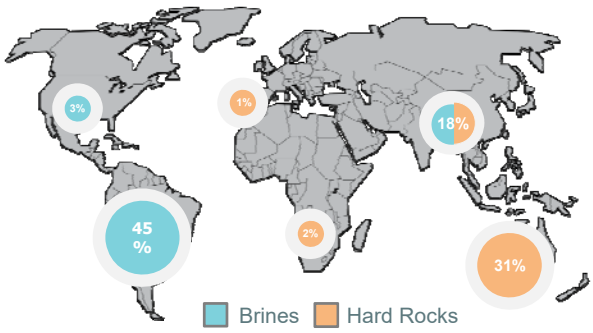

- ✓ **Li brine deposits** - accumulations of saline groundwater that are enriched in dissolved lithium, typically carrying 200–1,400 ppm of lithium (0.06-0.15% Li)
- ✓ **Hard-rock deposits** - pegmatites containing high-grade petalite and spodumene with 1-7% Li_2O concentration

Reserves – identified mineral resources
Source: Deutsche Bank Lithium 101 report, 9 May 2016
Source: Global Lithium Market 2016-2020 - Technavio 2016
Source: U.S. Geological Survey, Mineral Commodity Summaries, January 2016

Alternate/Secondary sources

Geo-thermal / waste brines

Battery / electronics waste recycle

What about other metals associated with battery industry ?

(increased demand for supply of Co, Ni, Cu, Graphite)

But first it is important to define the composition of feed upon which primary extraction is to be carried out and/or the composition of the partially processed Li containing liquors.

Brines pre-treatment / concentration
RO & NF fundamentals

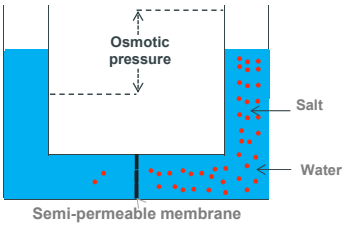

Performance:
Permeate flux and salt retention are the main parameters that determine the performance of an RO & NF.

Factors that are influencing **RO & NF performance:**

- Pressure
- Temperature
- Recovery
- Salt concentration of the feed water

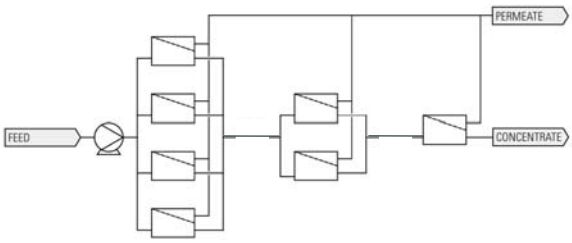

Christmas tree or feed and bleed, it depends from case to case

Brines pre-treatment / concentration

Nanofiltration

- Rejects > 99% of divalent salts, monovalent salts or acids pass
- Selectively concentrate & recover metals
- Less scaling potential
- High permeability → Low feed pressure

Reverse Osmosis

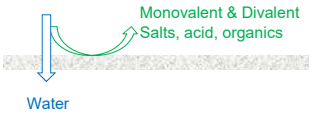

- Rejects monovalent and divalent salts, organics and acids > 99%, only water passes
- High permeate quality
- Medium to long term stability at pH<2

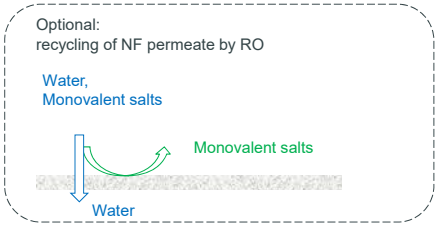

Dow RO & NF Membrane products and applications for mining

Products	Features	Applications in mining
FILMTEC™ NF345HP-370 Element	• Long term stability pH2 – pH11 • Selective rejection (monovalent/divalent)	• Purification / reduction of process and AMD waste water • Bi-carbonate Recovery • Heavy metal rejection • Enhances downstream precipitation • Sulfate removal from brines
DOW FILMTEC™ FORTILIFE™ Product Series	• RO & NF Membrane Series for Treating Challenging Wastewaters	• Concentration of mine waste water like AMD or run off and process water (> pH2) • Water reuse and metal or reagent recovery
DOW™ Specialty Membranes XUS1808 Ultra-High Pressure RO Element Series	• 120 bar operating pressure	• Concentrating any kind of waste water (> pH2) • Reduces downstream unit operation size by 20-50% • Concentration of Li brines. Eg. max achievable concentration for LiCl = 85g/L

Extraction / Purification
Ion Exchange Resin fundamentals

Polymeric insoluble solids containing functional groups capable of undergoing reversible exchange reactions with mobile ions from solution.

Mechanisms :

- By Ion Exchange of metallic ions M^{n+}
- Absorption of metal complex from solution $[MX_4]^{2-}$
- Complex between ligand and metal (chelation)

The challenge – Li monovalent ion, lowest selectivity

$Li^+ < H^+ < Na^+ < NH_4^+ < K^+ < Ag^+ < Mg^{2+} < Zn^{2+} < Co^{2+} < Cu^{2+}$

Primary Lithium extraction

Dow has >30 ion exchange related patents on Li extraction / recovery.

For example;

US4347327A - An anion exchange resin, containing Al(OH)3 suspended therein, is reacted with aq. LiOH to form microcrystalline LiOH.2Al(OH)3 which is then reacted with a halogen acid or halide salt to form microcrystalline LiX.2Al(OH)3. The resin, after having a portion of the LiX eluted by using an aqueous wash, is used to recover Li+ values from aqueous brines.

US9146823B2 - Method for separation of monovalent metals from multivalent metals using sulfonic functionalized resin media (elution chromatography using SAC) The monovalent metal is lithium. The multivalent metal is magnesium. The concentrated solution comprises sodium, or potassium. The functionalized resin media is in sodium form.

Primary Lithium extraction

In latter concentration steps once the feed is in the >85-90% Li
to reach higher concentrations a chromatographic pulse process using
DOWEX™ Retardion 11A8 Ion Exchange Resin or
DOWEX MONOSPHERE™ 99Na/310 Chromatography Resin
may be employed to further enrich to 95-99% purity levels.
We continue to develop new proprietary material.

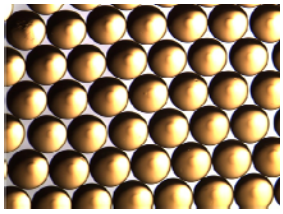

Metals removal

During the latter stages of Li solutions purification we have various
chelating type resins to remove divalent contaminants,
like Ca, Mg, Fe, Al etc.

AMBERSEP™ IRC747 UPS Resin

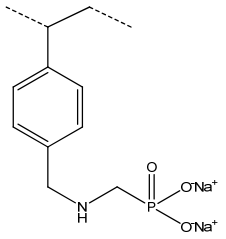

AMBERSEP™ IRC748 UPS Resin

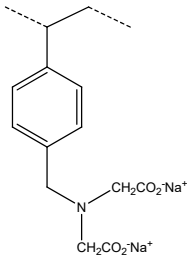

Boron removal

Boron removal from MgCl2 brines
Boron removal from LiHCO3 (Harrison & Blanchett 2011)
eg. for the production of pure LiCl

Boric acid / Borate removal from slightly acidic to alkaline pH
Low salinity to highly concentrated brines
Operating capacity depends on brine concentration and specific flow rate

AMBERSEP™ IRA743 Resin (N-Methyl glucamine)

Chlorides removal

DOWEX™ Retardion 11A8 (Amphoteric Ion Exchange Resin)
Chloride removal from LiOH (not disimilar to NaOH purification)

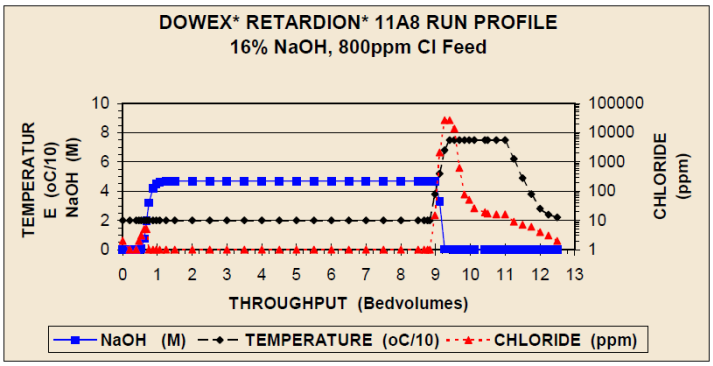

Organics removal

DOWEX OPTIPORE™ / XAD™ Adsorbents

- Crosslinked polymer adsorbents with high surface area
- Effective for hydrocarbon removal from both aqueous and vapor streams
- Removal of kerosenes from aqueous phase – SX circuits
- Thermally/Chemically regenerable

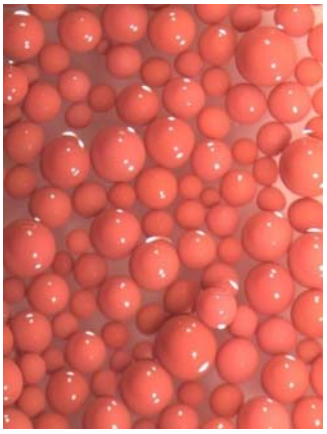

Summary

- Dow Water & Process Solutions has a long track record and experience with Lithium extraction technology.
- FILMTEC™ NF and RO established technology in treatment of highly saline solutions.
- AMBERSEP™ Ion Exchange Resin applications in brine treatment and metals extraction, separation and purification

ACKNOWLEDGEMENTS

With gratitude to the team / co-authors for their contributions;

www.dowwaterandprocess.com

www.dow.com/en-us/oil-gas-mining/mining-solutions

Disclaimer

NOTICE: No freedom from infringement of any patent owned by Dow or others is to be inferred. Because use conditions and applicable laws may differ from one location to another and may change with time, Customer is responsible for determining whether products and the information in this document are appropriate for Customer's use and for ensuring that Customer's workplace and disposal practices are in compliance with applicable laws and other government enactments. The product shown in this literature may not be available for sale and/or available in all geographies where Dow is represented. The claims made may not have been approved for use in all countries. Dow assumes no obligation or liability for the information in this document. References to "Dow" or the "Company" mean the Dow legal entity selling the products to Customer unless otherwise expressly noted. NO WARRANTIES ARE GIVEN; ALL IMPLIED WARRANTIES OF MERCHANTABILITY OR FITNESS FOR A PARTICULAR PURPOSE ARE EXPRESSLY EXCLUDED

NOTICE: The data provided in this slide presentation was collected during April 2017, and is included to illustrate approximate trends in the industry. The data provided in this slide presentation is given in good faith for informational purposes only. Dow assumes no obligation or liability for the industry data presented herein. NO WARRANTIES ARE GIVEN; ALL IMPLIED WARRANTIES OF MERCHANTABILITY OR FITNESS FOR A PARTICULAR PURPOSE ARE EXPRESSLY EXCLUDED.

THE CASE FOR SECONDARY LITHIUM MINERAL PROJECTS

By

Grant Harman

Lithium Consultants Australasia, Australia

Presenter and Corresponding Author

Grant Harman
grant.harman@lithiumconsultants.com

ABSTRACT

In this paper secondary lithium mineral deposits are considered to be those hosting predominantly non-spodumene minerals. These include lithium bearing micas, sedimentary deposits such as clays and jadarite. In general, these resources have a lower grade of lithium and the amount of ore that needs to be processed is significantly more than for a corresponding spodumene producer. A common perception is that this will result in a higher operating cost as a result of higher energy and reagent costs and therefore, as long as there are additional spodumene resources, there is little chance of a secondary lithium mineral resource being developed.

This paper discusses the challenges facing the companies producing lithium from brines as well as from spodumene. The question is asked if the new spodumene concentrates should be regarded as identical to the Talison SC6.0 concentrate, which currently is the industry standard. A comparison of the cash cost to produce lithium carbonate is made between four spodumene concentrate supply cases with significant variation in outcomes. Using the same basis, a comparison is then also made with the proposed production of lithium carbonate from a Zinnwaldite concentrate from European Metals Holding's Cinovec project. While the attractive economics of this project are in part attributable to project specific factors, such as its by-product credits and geographic location, they support the case for consideration of secondary lithium mineral projects for development to supply lithium to fill the growing demand for lithium chemicals.

Keywords: Lithium recovery, lithium extraction, spodumene, zinnwaldite, lepidolite, hectorite, clays, lithium micas, mica, operating cost, project development

DISCLAIMER

This paper has been prepared by Lithium Consultants Australasia Ltd (LCA). This paper contains forecasts and forward looking information. Such forecasts, projections and information are not a guarantee of future performance, involve unknown risks and uncertainties. Actual results and developments will almost certainly differ materially from those expressed or implied. LCA has not audited or investigated the accuracy or completeness of the information, statements and opinions contained in this presentation. Accordingly, to the maximum extent permitted by applicable laws, LCA makes no representation and can give no assurance, guarantee or warranty, express or implied, as to, and takes no responsibility and assumes no liability for, the authenticity, validity, accuracy, suitability or completeness of, or any errors in or omission, from any information, statement or opinion contained in this presentation.

Throughout this paper all figures are quoted in US$ dollars unless otherwise stated.

INTRODUCTION

The demand for lithium is unprecedented in 2017 and the current annual growth shows no signs of abating in the foreseeable future with the critical mass being close to being achieved in the solar Photovoltaic Cell (PV) market and its close association with lithium batteries for storage. It is projected that the global battery consumption will increase 5x over the next 10 years, placing pressure on the lithium ore miners, converters and battery manufacturers to supply the market.

It is reflective to consider that the Greenbushes Mine (now owned by Talison Pty Ltd) only commenced mining of lithium minerals in 1983 and commissioned a 30,000tpa lithium mineral concentrator two years later in 1984-1985. Production capacity was increased to 750,000 tpa after completion of the new concentrator plant in 2013. (Golden Dragon Capital, 2017). Talison is reported to currently supply approximately 40% of worlds lithium, and has recently announced its intentions to double the current production rate.

In addition, there are a number of new spodumene projects either being constructed or awaiting financial approval that could see a significant number of new suppliers of spodumene concentrate joining the market.

There has also been increasing interest in secondary lithium mineral deposits and a handful of these projects are currently in the feasibility stage of evaluation. One of these projects is the Cinovec project which is discussed in more detail in this paper to answer the question as to whether there is a place for such projects in the future supply of lithium.

WHAT ARE SECONDARY LITHIUM MINERALS?

Historically the source of lithium from mineral origins has been dominated by spodumene, supplied almost exclusively from the Talison mine located in Greenbushes, Western Australia. In this paper all non-spodumene lithium minerals are defined as secondary lithium minerals. These include the hectorite and polylithionite clays, the zinnwaldite and lepidolite lithium micas and jadarite.

There are some 127 known lithium containing minerals of which 9 are deemed to be of commercial interest and are listed in Table 1. The lithium minerals have vastly different compositions, with spodumene and petalite being comprised of lithium, silicon, oxygen and aluminium, whereas the secondary minerals contain additional elements, such as boron, potassium, sodium, iron and fluoride. This results in the concentration of lithium in the secondary minerals being lower than in spodumene.

Table 1: Common Lithium Containing Minerals and their Properties

Mineral		Chemical Composition	Measured Li_2O%
Spodumene	Australia	$Li_2OAl_2O_3(SiO_2)_4$	8.0
Petalite	Zimbabwe	$Li_2OAl_2O_3(SiO_2)_8$	4. 5
Zinnwaldite	Czech Republic	$KLiFeAl(AlSi_3)O(F,OH)$	2.19 - 3.72
Lepidolite	Zimbabwe	$K(Li,Al)_3(Si,Al)_4O_{10}(F,OH)_2$	7.7
Hectorite	Mexico,USA	$Na_{0.3}(Mg,Li)_3Si_4O_{10}(OH)_2$	1.17
Jadarite	Serbia	$LiNaSiB_3O_7(OH)$	7.3
Amblygonite	Canada	$LiAlPO_4(F,OH)$	10.1
Eucryptite	Zimbabwe	$Li_2OAl_2O_3(SiO_2)_2$	11.8
Zabuyelite	China	Li_2CO_3	40.4

WHAT ARE THE SUPPLY OPTIONS FOR LITHIUM?

Figure 1 shows a well know global cost curve which compares the operating costs between the current producers of lithium chemicals from brine and hard rock. This version of the comparison was published by the Deutsche Bank in May 2016 and shows the costs have increased in over the last years. SQM is generally thought to be the lowest cost producer at a cost of around $2,600/ t LCE and Albemarle marginally higher at around $ 3,000/ t LCE.

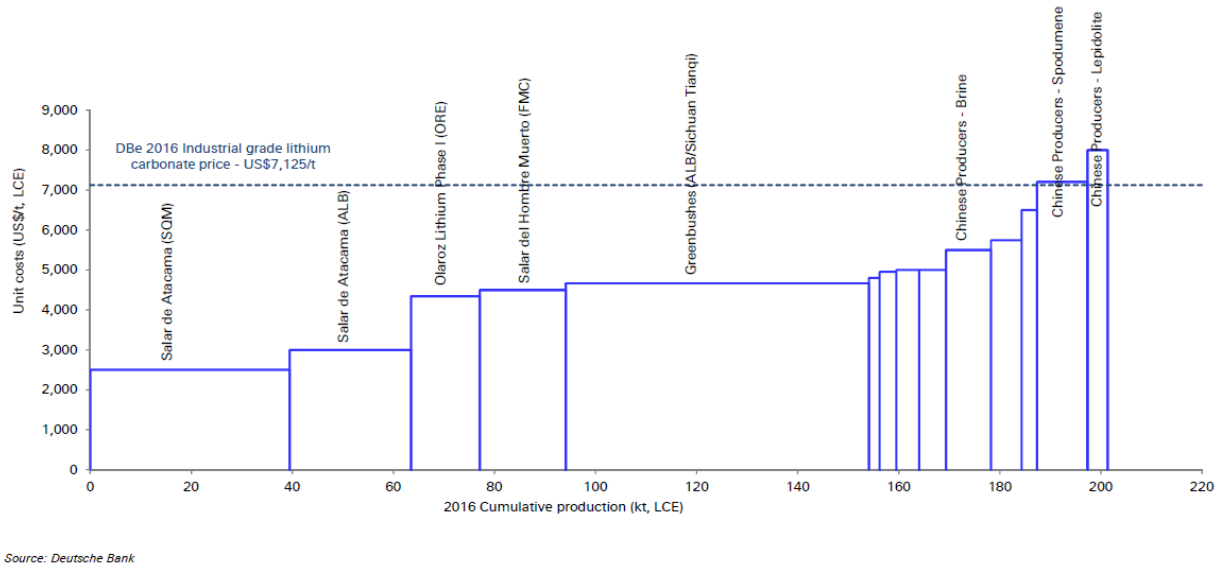

Source: Deutsche Bank

Figure 1: Global Cost Curve for Lithium Carbonate Supply

Brines

Olaroz Phase 1 is shown with a cost of production of around $4,300/t LCE. Orocobre recently published figures based on production of 12,000 t lithium carbonate which would suggest that the actual cost is closer to $3,600/ t lithium carbonate.

While SQM and Albemarle have both continued to produce at the lowest cost from the Atacama, newcomers have costs considerably higher and the commonly held belief that hard rock would never be able to compete with brine producers, is clearly no longer true.

There appear to be a growing list of challenges for the current and potential new producers of lithium from brine. These include:

1. Most brines were formed as a result of volcanic activity and are therefore located close to volcanos and are on fault lines prone to earthquakes.

2. The grade of the lithium in the Atacama brine in the South continues to fall and is thought to now be around 1,400 ppm.

3. Albemarle has recently negotiated a new license with Fosco with a royalty of up to 40% on sales, which is a significant shift in government expectations.

4. The higher pump rate, although small compared with the current SQM pump rate, is raising real concerns that it is not sustainable in the Atacama.

5. The Chilean Government is reported to be preventing any new projects that require evaporation of water.

6. New projects have more challenging chemistry compared with the brine from the South end of the Atacama.

7. Potential sovereign risk and Government restrictions in some South America countries.

8. Adverse weather conditions affecting production.

As a consequence of the challenges listed above, it is not surprising that a number of observers have stated the bulk of additional lithium production will need to be sourced from hard rock resources.

Hard Rock

The predominant source currently is spodumene will a little petalite, and lepidolite reported to being supplied in China, Brazil and Europe. Further the bulk of the spodumene historically has been supplied by Talison's Greenbushes mine in Western Australia. In the following section different spodumene concentrates are compared to better understand the challenges that spodumene concentrate producers face.

ARE ALL SPODUMENE CONCENTRATES THE SAME?

The simple answer is that they are not. There are significant differences between the ores types, the ore texture and variability within the ore body. That means a concentrate will vary over time even if mined from the same ore body.

Concentrate Composition

Although a 6% Li_2O spodumene concentrate contains roughly 85% spodumene it also contains a number of other minerals such as mica as shown in Table 2. In the case of spodumene this mica is generally muscovite but it could also contain biotite or lepidolite. Small quantities of these lithium micas (lepidolite) do not change the fact that the predominant mineral is spodumene.

Table 2: Comparison between Typical Spodumene Concentrates

Minerals Present	Spodumene A	Spodumene B
Spodumene	77.2	77
Quartz	11.3	2
Albite	3.8	5
K-feldspar	3.1	1
Muscovite (Mica)	0.8	8
Phosphates	0.2	1
Iron Minerals	3.6	
Amphibolite		6

Ore Texture

The ore texture is a key element in developing the beneficiation flowsheet for a given resource. (MinAssist, 2017). This is specifically pertinent for DSO (Direct Shipped Ores) sourced from the Pilbara, which in reality is neither a concentrate nor a particularly high grade ore.
The texture of an ore includes:

- grain size distribution,
- grindability of the ore,
- degree of liberation of the target mineral,
- phase specific surface area of the target mineral,
- the amount of fines generated, and
- the number of coarse composite particles.

For example, an ore such as that studied in the preliminary studies for Tawana, with a lower grade of 0.9 – 1.4 % Li_2O, requires only minimal crushing and dense media separation to produce a 6.7% Li_2O concentrate. The Talison ore with a high lithium feed grade of around 2.65% Li_2O, requires a more complex processing plant to produce 6% Li_2O.

Lithia Content

The industry standard for chemical grade spodumene concentrate is Talison SC6.0, which has a Li_2O (Lithia) content of 6%. Most of the Spodumene-to-chemical conversion plants were designed or modified to accept the Talison SC6.0 feed.

If the grade is lower than 6% Li_2O then more mass needs to be processed in order to produce the same amount of the lithium chemical. In reality the mass flow through a chemical plant is fixed and a decrease in the concentrate grade would result in less lithium chemical being produced and less revenue being earned.

Non-Spodumene Content (Impurities)

The pure spodumene mineral, with the chemical composition $Li_2OAl_2O_3(SiO_2)_4$, contains 8.03 wt% Li_2O. This implies that the SC6.0 is 75% pure spodumene and that the balance of the concentrate is made up of gangue minerals such as quartz, mica, feldspar and amblygonite. Two potential issues with higher impurity levels are (i) that the impurities will produce a lower melting temperature eutectic mixture in the calciner and (ii) that these impurities can be leached from the concentrate making the purification of the leach solution more difficult.

The main issue for converters is the behaviour of the ore in the calciner. In the calciner α-spodumene is converted to β-spodumene at around 1,080°C and there are typically a number of impurities that will melt below the calcination temperature, as shown in the Table 3.

Table 3: Melting Point of Some Minerals Found in Spodumene Concentrates

Mineral	Melting Temperature [°C]
Amphibole	800
Micas	700-1,000
Albite	1,100
K-Feldspar	1,250
Spodumene	1,420
Quartz	1,670

Spodumene Conversion Temperature [1,080 °C]

The minerals present in the concentrate that melt at lower temperatures (above the red line) will likely melt and contribute to clinker formation. If the amount of the low temperature melting minerals is small, then the amount of clinker formed will be around 2%, which is not a problem. If the amount of these minerals present is higher, then the amount of clinker formed is higher and the extraction of lithium from clinker, even after grinding, is likely to be lower than 75%.

Iron content is normally a critical impurity and Kings Mountain plant used to add chlorine gas to the calciner to convert the iron to iron chloride which was volatized to prevent the formation of excess clinker and glassing. Some of the current producers also face the challenge of increasing iron content.

Size Distribution

The spodumene concentrate is produced differently in every plant and depends on the ore texture as discussed above.

If the concentrate is produced using only HMS (Heavy Media Separation), the particle size is relatively coarse i.e. in the region 3 mm to 0.5 mm, while if the concentrate is recovered by flotation, then the particle size will be considerably finer, in the region of 0.6 mm to 0.075mm.

The particle size of the feed affects the performance of the calciner in two ways namely, (i) dusting and (ii) the rate of heating up the ore.

The finer the feed particle size is, the more will be blown out (elutriated) from the calciner. In general, the dust blown out of the calciner is not converted to β-spodumene and there may be limits as to how much of the dust can be recovered and successfully returned to the calciner. Dust may have to be dumped or the calciner gas firing rate decreased, to reduce the gas velocity in the calciner, which will impact on the conversion of the ore and capacity of the calciner.

The second impact is the time it takes to heat up the ore. The larger the particle size, the longer it takes to heat up and conversely, small particles heat up much faster. If the calciner has been designed for smaller particles, then changing to a coarser feed will require more heat input which will result in higher temperatures in the calciner leading to clinker formation.

In summary, each spodumene concentrate is different and changing concentrate source and supplier may have an impact on the existing facility, such as reduced production and operational issues that would require modifications to the plant.

THE CASH COST OF PRODUCING LITHIUM CARBONATE FROM SPODUMENE

In Table 4 the costs of producing lithium carbonate based on concentrate sourced from different sources are compared. It needs to be stressed that there is limited transparency in the lithium market and most of the data used in the cost model has been obtained from a combination of information published in the public domain and from people in the lithium industry.

Four cases have been considered based on supply of spodumene from Australia.

CASE 1: Galaxy Concentrate is transported to a conversion plant in China located on the Eastern side of China. Furthermore, the spodumene concentrate is supplied through a third party that charges a fee and VAT is payable on ore imported into China.

CASE 2: In this case Tianqi and Albemarle source the concentrate from their Talison mine and send it to China for conversion, such as the toll treating currently being done by Albemarle. No profit has been allowed for the toll treating in this case.

CASE 3: Similar case to CASE 2 except that the concentrate is sourced from the Pilbara, Western Australia and the beneficiation cost of the ore is higher due to the low ore grade which is offset by the tantalum credits.

CASE 4: In this case a combination of existing tailings or mined ore with a grade around 1.5% Li_2O is shipped to China. It is assumed that the ore can be beneficiated to 5 – 6% Li_2O and that the overall lithium recovery would be 70%.

Table 4: Comparison Four Spodumene Concentrate Supply options on the Estimated Total Cost of LCE Production

		Chinese Converter using Galaxy Con	Tianqi/ Albemarle using Talison Con	Chinese Converter using Pilbara Con	Chinese converter using Pilbara DSO
Cost SPOD FOB	USD/t SPOD	$905	$200	$171	$120
Transport to Asia	USD/t SPOD	$50	$50	$36	$36
Inland transport	USD/t SPOD	$40	$40	$40	$40
Li Grade	wt% Li_2O	6	6	6	1.5
VAT 17% CIF	USD/t SPOD	$162.35	$42.50	$35.19	$26.52
Mitsubishi margin 15%	USD/t SPOD	$143.25	$0	$0	$0
Total cost	USD/t SPOD	$1,301	$333	$282	$223
Lithium content	kg Li_2O/ t SPOD	60	60	60	15
Lithium recovery in LCP	%	88	88	88	70
Lithium recovered in LCP	kg Li_2O/ t SPOD	52.8	52.8	52.8	10.5
	kg Li_2CO_3/t SPOD	130.24	130.24	130.24	25.9
Conversion cost	USD/t Li_2CO_3	$3,000	$3,000	$3,000	$3,000
	USD/ t SPOD	$391	$391	$391	$78
TOTAL cost	USD/ t SPOD	$1,691	$723	$673	$300
	USD/t Li_2CO_3	$12,986	$5,553	$5,167	$11,592

Assumptions:

1. Galaxy, Mount Cattlin mine, Western Australia spodumene cost is US$905/t (FOB Esperance) for 6% Li_2O delivered in Q1 2017. (Commsec Online Trading Website, 2017).

2. Transportation for concentrates from the South-West of Western Australia is assumed from Bunbury or Esperance ports to a port in China. The additional transport cost is for truck or barge cost to the Chinese converter plant.

3. Transportation from the Pilbara based on Pilbara Minerals ASX announcement (Pilgangoora DFS Confirms World-Class Australain Lithium Project, 2016).

4. VAT is an import tax on the spodumene entering China. There is also a cost if lithium chemicals are sold internationally. It is assumed in this model that consumption by Chinese converted chemicals is within China.

5. It is assumed that Mitsubishi, purchasing agent, would charge a fee for the procurement of the spodumene. Nominally this has been set at 15%.

6. The Talison concentrate price is based on the Namaska value of USD 200/ t FOB Greenbushes, Western Australia (How to Profit from the Booming Lithium Markets, 2016).

7. The conversion cost for the spodumene using the sulphation route is based on Orocobre Ltd ASX announcement (Investor Update, 2016).

8. The sales price for DSO (direct shipped ore) is not known. A value of $150/t was stated in a local West Australian newspaper but thought to be too high. The model above tends to support the view that a price around $120/t is plausible.

9. There is no profit added for the supply of the concentrate nor for the sale of the lithium carbonate product.

10. Spodumene concentrate production costs include tantalum by-product credits and deduction of royalties.

The takeaways are:

- The growing lithium industry will become increasingly reliant on minerals containing lithium for the supply of lithium chemicals.
- The days of lithium carbonate at US$ 6,000/ t LCE are gone and even prices above US$8,000/ t LCE could be possible in the longer term.
- In the short to medium term selling prices will be high in China until they find cheaper sources of supply.

SECONDARY LITHIUM MINERAL PROJECTS

There are only a handful of secondary lithium projects that are currently known to be actively progressed beyond Scoping Study level. These are:

Project	Company	Minerals
Sonoro	Bacanora Minerals	Hectorite clay
Nevada Lithium Project	Lithium America	Hectorite clay
Cinovec	European Metals Holdings	Zinnwaldite
Jadar	Rio Tinto	Jadarite

In this paper the Cinovec project will be discussed in detail and an overview provided of the clays projects in Nevada, USA and Sonora, Mexico.

WHAT IS ZINNWALDITE?

The mineral got its name from the locality Zinnwald, Erzgebirge, Saksen (nowadays known as Cínovec in the Czech Republic). Zinnwaldite is a phyllosilicate with properties similar to that of biotite, while it resembles lepidolite in its chemical aspects with high Si/Al ratio, high Li content and replacement of OH by F.

Zinnwaldite can be considered to be part of a solid solution series of the ferrous lithium micas. The main criteria being:

- If the Li occupies fewer than 0.25 octahedral sites the mineral is termed a siderophyllites;
- If the Li occupies between 0.25 and 0.75 sites the mineral is termed a protolithionites;
- If the Li occupies between 0.75 and 1.25 sites are defined as zinnwaldites; and
- If the Li occupies more than 1.25 sites are considered lepidolites.

The series is characterized by the progressive replacement by Li^{+l} by Fe^{+2}, with an average replacement ratio of 2.0 Li^{+1} for 1.5 Fe^{+2}. Siderophyllites and protolithionites can contain significant amounts of

Fe^{+3}, zinnwaldites have some Fe^{+2}, while Fe^{+2} is low in all the lepidolites.

Zinnwaldites are commonly found in pegmatites rich in rare elements, especially lithium, where they are associated with other lithium bearing minerals such as lepidolite and spodumene.

The iron content of the zinnwaldite results in the para-magnetic behavior of the ore which is the reason that Cinovec ore can be magnetically separated so effectively.

Figure 2 shows the mica books which characterize this mineral.

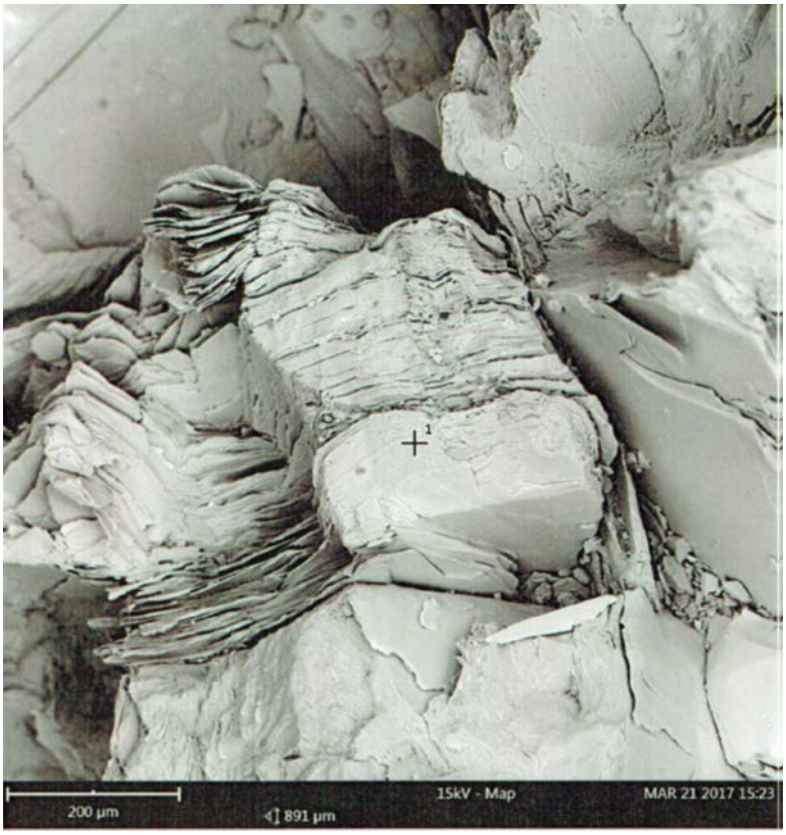

Figure 2: SEM pictogram showing typical mica books

The composition below shows the main elements present in Cinovec zinnwaldite excluding the lithium and fluoride. The photograph shows typical zinnwaldite rocks which have characteristic mica plates. In general, the darker grey the rock the higher is the amount of zinnwaldite present (and lithium). The rocks can also have a green colour due to the zinnwaldite.

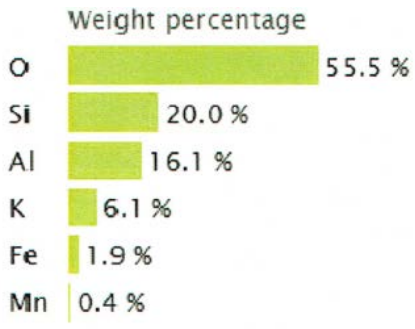

THE OPPORTUNITY FOR ZINNWALDITE

The Cinovec project is located 100km North West from Prague, Czech Republic on the border with Germany and is part of the Cinovec-Zinnwald mining district that has been mined since the 14th century. Modern underground mining ceased in 1972 in the central part of the Cinovec district. As the high-grade tin ore was running out, the Czech State Company initiated an extensive underground exploration program that reported significant blind tin-tungsten-lithium mineralization associated with greisenization and silicification. All operations at the mine ceased with the demise of the centralized economy in 1990.

The main minerals of economic interest are cassiterite, wolframite, scheelite, zinnwaldite, topaz and fluorite. The project is estimated to contain a resource of up to 656.5Mt of ore @ 0.43% Li_20 (or 7.0 Mt LCE) and including 262,600 tonnes of Sn.

Proposed Flowsheet

The proposed high level flowsheet, shown in Figure 4, consists of mining, comminution, beneficiation and the lithium chemicals plants.

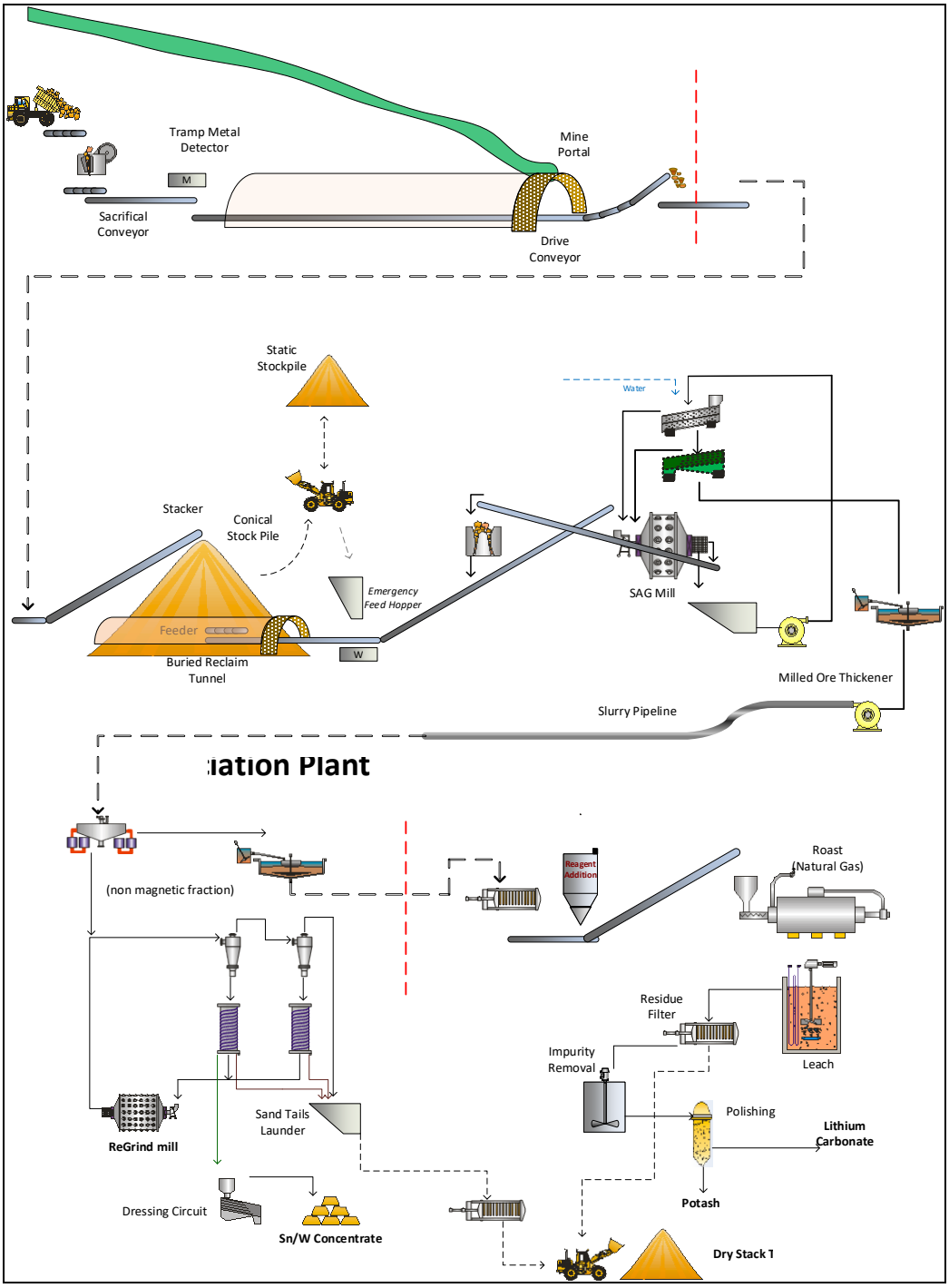

Figure 4: Proposed Flowsheet for the Cinovec Project, Czech Republic.

The ore from underground is crushed prior to being conveyed to a stockpile upstream of the comminution plant.

The Comminution Plant is a simple design with a single SAG mill in closed circuit with screens to produced milled ore suitable for the beneficiation plant.

The Beneficiation Plant has magnetic separators in which the paramagnetic zinnwaldite is separated for the non-magnetic fraction which is transferred to the tin recovery circuit. The lithium bearing mica, is concentrated to an average grade of 1.28 % Li from a ROM grade of 0.31 % Li. The concentrate is roughly 20% of the mass flow of the ROM and contains roughly 90% of the lithium in the feed.

The LCP (Lithium Chemical Plant) receives the concentrate from the Beneficiation plant and in the first step the ore is roasted with recycled sodium sulphate and lime to produce soluble lithium sulphate which is extracted in the leach. The Leach liquor is purified and battery grade lithium carbonate is produced.

SOME THOUGHTS ON LITHIUM BEARING CLAYS

In 1975 Chevron USA undertook an exploration program for uranium in the sediments of the McDermitt Caldera in Nevada, USA. At the same time lithium-bearing clays of the McDermitt caldera were identified by the U.S. Geological Survey and they alerted Chevron to the presence of anomalous concentrations of lithium, which resulted in Chevron adding lithium to its assays and ultimately in Chevron producing a resource estimate with a 0.25% Li cut-off in 1985.

The Unites States Bureau of Mines (USBM) conducted extensive research into technologies to recover lithium from these clays. The extraction techniques investigated which showed the most promise were selective chlorination and limestone-gypsum roasting. The lithium recoveries achieved by the USBM were 70% for selective chlorination and 80- 85% for the limestone-gypsum roast. They concluded that although the process of extracting lithium from hectorite clay was not economical, that the technology exists for lithium recovery from McDermitt clays. (L. Crocker)

Chevron ran beneficiation studies that concluded that dry grinding followed by separation of the fines coupled with upgrading of the coarse material gives the best overall upgrading. They managed to beneficiate the ROM ore with a Li head grade of 0.34% to a final concentrate with a grade of 0.37% by rejecting 35% of the feed. The beneficiated ore was then acid pugged and cured following by water leaching. The best results showed that 85% of the lithium could be extracted with an acid usage of around 1,000 pounds of acid per ton of ore.

Both Chevron and USBM achieved similar results which showed that lithium recovery was proportional to the amount of acid consumed. (Lithium America Corp, June 2016)

The current Lithium Americas Corp flowsheet appears to consist of size reduction, thermally treating the ore by calcining the ore mixed with anhydrite and dolomite followed by leaching.

The initial capital cost estimate for the Western Lithium Project was $247,935 (case 2 with a mining Rate of 4,200tpd) and the estimated corresponding operating cost was $3,472/ t LCE. (WESTERN LITHIUM USA CORPORATION, 2014). The operating cost sits in between the brines and the spodumene producers in figure 1 and on this basis the project should be attractive to investors. It was reported that the project did not manage to get financial backing based on these figures.

There are a number of challenges to exploration companies developing clay projects. These are:

1. The lithium grade of the clays is low and the impact on the increased mass of material to produce the same amount of lithium carbonate is shown pictorially in the two Sankey diagrams below. A typical grade is in the region of 0.3 wt% Lithium (0.6 wt% Li_2O).

2. The lithium, while contained in lithium minerals such hectorite, fordite and polylithionite, is present throughout the clay. This means that there is limited ability to beneficiate the ore other than to remove larger chunks/ rocks of quartz.

3. While the clay is reactive and lithium can be extracted from the clay at low temperature, the acid usage is typically around 1 ton Sulphuric acid: 1 ton of ore. Not only is a significant amount of neutalisation required, there is also typically significant amounts of other elements that are co-extracted. The main element extracted with the lithium is magnesium which increases reagent cost as well as causes problems in the solid and liquid separation of the magnesium hydroxide formed.

4. The projects do not have sufficient metal by-products to materially off-set the operating cost.

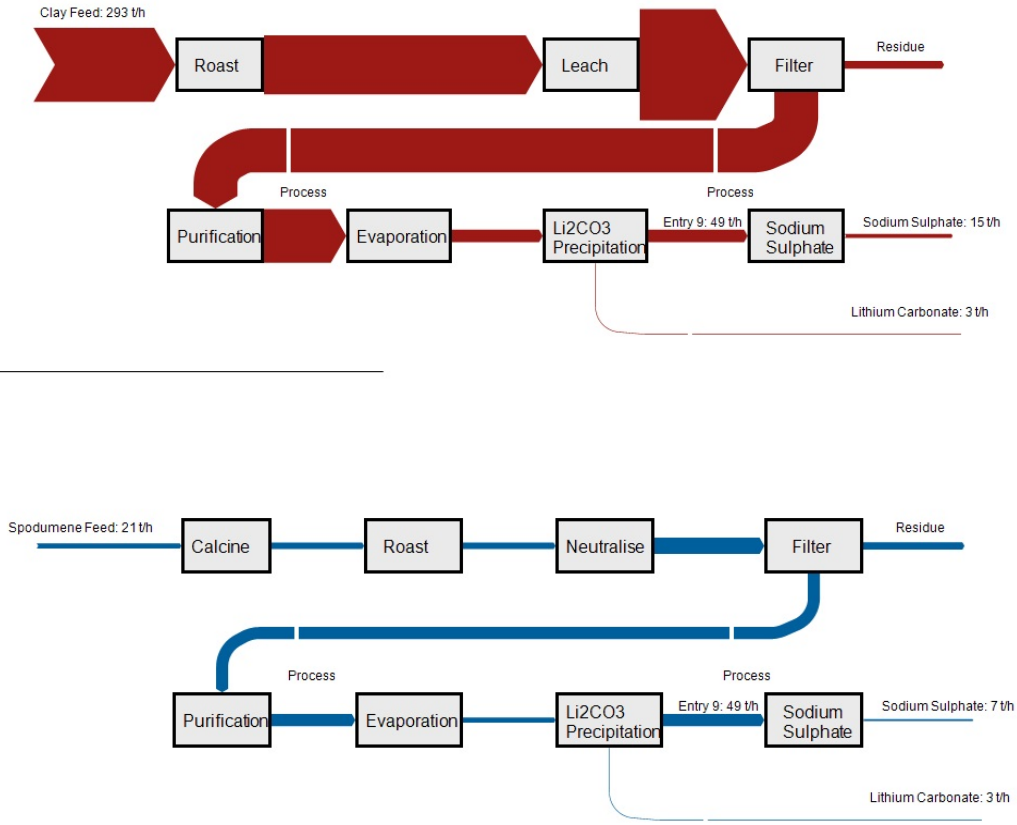

Figure 3: Comparison of Mass Flows through a typical Spodumene and Clay lithium Extraction Plant

THE CASH COST OF PRODUCING LITHIUM CARBONATE FROM SECONDARY LITHIUM SOURCES

Table 5 compares the operating cost of the Cinovec Project with that of the spodumene examples in CASE 2 and CASE 3 in Table 4, using the same model. Based on the assumptions stated below, there is $2,000/ t LCE difference between the cost of lithium carbonate produced by a Chinese converter and the proposed Cinovec plant with the benefit that in the Cinovec case the lithium carbonate would be produced in the heart of Europe.

Table 5: Comparison on the Estimated Cost of Produced Lithium Carbonate from Zinnwaldite versus Spodumene Ores

		Cinovec	Tianqi/ Albemarle using Talison Con	Chinese Converter using Pilbara Con
Cost Concentrate (FOB) net Sn, W & Ta credits and royalties	USD/t Con	$91	$200	$171
Transport to Asia	USD/t Con	$0	$50	$36
Inland transport	USD/t Con	$0	$40	$40
Li Grade	wt% Li_2O	2.7	6	6
VAT 17% CIF	USD/t Con	$0.00	$42.50	$35.19
Total cost	USD/t Con	$91	$333	$282
Lithium content	kg Li_2O/ t Con	27.0	60	60
Lithium recovery in LCP	-	0.85	0.88	0.88
Lithium recovered in LCP	kg Li_2O/ t Con	22.95	52.8	52.8
	kg Li_2CO_3/t Con	56.61	130.24	130.24
Conversion cost	USD/t Li_2CO_3	$2,274	$3,000	$3,000
	USD/ t Con	$129	$391	$391
Potash Credit	USD/t Li_2CO_3	$324	0	0
Conversion cost net of credits	USD/t Li_2CO_3	$1,950	$3,000	$3,000
	USD/ t Con	$110	$391	$391
TOTAL cost	USD/ t Con	$201	$723	$673
	USD/t Li_2CO_3	$3,555	$5,553	$5,167

Assumptions:

1. The cost of zinnwaldite concentrate production includes the average life of mine tin and tungsten credits and royalties. The mining cost assumed is USD 30/t for underground mining compared with USD 3/t for open pit mining.

2. The overall lithium extraction is estimated to be 85% for Zinnwaldite which is lower than spodumene which commercially was able to achieve 88%.

3. Zinnwaldite conversion cost based on prefeasibility study operating costs.

Reasons Supporting a Competitive Operating Cost for Zinnwaldite

There are a number of factors that drive the cost of Li production from the Cinovec project down:

1. The beneficiation plant flowsheet is simple, requiring only high intensity magnetic separation and single stage milling (SAG mill). This is significantly simpler than a Talison of Pilbara Minerals flowsheet.

2. Superior beneficiation recovery of 90% of the lithium into 21% of the mass.

3. 60% recovery of Sn and recovery of W. Genuine by-product credits as Cinovec was previously a tin mine but current grades are not high enough to support a mine producing only tin.

4. Recycling sodium sulphate to the roast results in a significant reduction in reagent requirements for the whole plant.

5. Reusing the sodium sulphate so that the sodium reports to the residue and there is not the problem that spodumene producers have in having to sell or dispose of a significant mass of soluble sodium sulphate, with a limited market.

6. Zinnwaldite needs a single stage of roasting at 850°C. Spodumene typically needs calcination at around 1,100°C, cooling, milling followed by roasting at 250°C.

7. The plant produces a commercial amount of potassium sulphate which can be considered a genuine by-product.

8. The lithium carbonate product is available in central Europe for European customers and transport cost are low.

CONCLUSION

The paper initially poses the questions as to whether all spodumene concentrates are the same and concludes that they vary considerably. These differences can impact on the ability of existing conversion plants if the feed concentrate is changed. It is also expected that the processing costs of these new concentrates will differ from that for Talison SC6.0. Further, even if the supplier of the spodumene concentrate is not changed, rising levels of impurities, especially iron, will increase the conversion cost and pose serious operational challenges.

The production costs of all producers have risen greatly over the last couple of years and with the strong demand for lithium chemicals expected, there will be opportunity for a number of companies to enter the lithium market.

The Cinovec project was used as an example of a secondary lithium mineral, Zinnwaldite. This project has a number of advantages over spodumene producers, such as the simple beneficiation plant and tin/ tungsten by-products, which offset the higher mining cost. In this paper the cost of producing battery grade lithium carbonate from the traditional spodumene ore was compared with the cost of producing battery grade lithium carbonate from secondary lithium ores, and specifically from zinnwaldite.

Based on the recent feasibility study completed on the European Metal Holdings Cinvovec project, the operating cost estimate suggest that the cost to produce battery grade lithium carbonate from Zinnwaldite is competitive with a Chinese converter using Talison SC6.0 concentrate. The estimated cost is considerably lower than cost for Chinese converters using either Galaxy concentrate or Direct shipped ore from the Pilbara.

REFERENCES

1. (2016, April). Retrieved from Orocobre: https://www.orocobre.com.au/PDF/ASX19Apr16_Investor_Relations_Presentation.pdf

2. (2016, Feb/ Mar). Retrieved from Nemaska Lithium.

3. (2017, February 8). Retrieved from Commsec Online Trading Website: https://research.commsec.com.au/LoadPDF?docKey=B64ENCeyJkayI6IjE0MTAtMDE4MTI3MzUtMTQwMjA2U1REQ0c3U08yU1ZSTk8yNjVRM0siLCJmaWQiOm51bGwsImR0IjpudWxsfQ==

4. Chagnes A., S. J. (2015). Lithium Process Chemistry. Netherlands: Elsevier.

5. Golden Dragon Capital. (2017, February 7). Retrieved from http://www.goldendragoncapital.com/greenbushes-lithium-mine/

6. L. Crocker, R. L. (n.d.). Lithium and its recovery from low-grade Nevada Clays. US Burea of Mines.

7. Lithium America Corp. (June 2016). Independent Technical Report for the Lithium Nevada Property, Nevada, USA. SRK Consulting.

8. MinAssist. (2017, April 8). Retrieved from http://www.minassist.com.au/site/downloads/The-Influence-of-Rock-Texture-on-Processing.pdf

9. Pilbara Minerals. (2016, September 20). Retrieved from http://www.pilbaraminerals.com.au/sites/pilbaraminerals.com.au/files/sharelink/43b9hfcnxw18g6.pdf

10. WESTERN LITHIUM USA CORPORATION. (2014). Updated NI 43-101 Technical Report Kings Valley Property Humboldt County, Nevada. Tetra Tech.

A BROAD LOOK AT LITHIUM EXTRACTION

By

Mike Dry

Arithmetek Inc., Canada

Presenter and Corresponding Author

Mike Dry
mike.dry@arithmetek.com

ABSTRACT

This paper examines a number of published processes for the production of lithium carbonate or hydroxide from ore and brine. The circuits are described and the capital and operating costs for each, as published by the developers, are summarized and compared.

The economics associated with the production of lithium carbonate and lithium hydroxide via established technology are discussed in the context of the manufacture of lithium-ion batteries.

Keywords: Lithium, extraction, spodumene, brine, capex, opex.

INTRODUCTION

The rise of electric vehicles and the environmentally driven desire for energy production from non-fossil sources has given rise to a need for significantly better battery technology than was the norm until recently. The lithium-ion battery is currently the clear leader, and this has caused a substantial rise in the projected future demand for lithium and thus the projected price for the lithium compounds that go into the manufacture of lithium-ion batteries. Figure 1 is from a report [(1)] recently published by Deutsche Bank. It predicts a doubling of lithium supply between 2017 and 2025, the bulk of the increase coming from "possible greenfield projects", i.e. projects not yet committed. Figure 2, from the same Deutsche Bank report, shows a projection in which the overall demand for lithium more than doubles between 2017 and 2025, with the increase over that period dominated by e-bikes and electric vehicles. Energy storage becomes noticeable towards 2025.

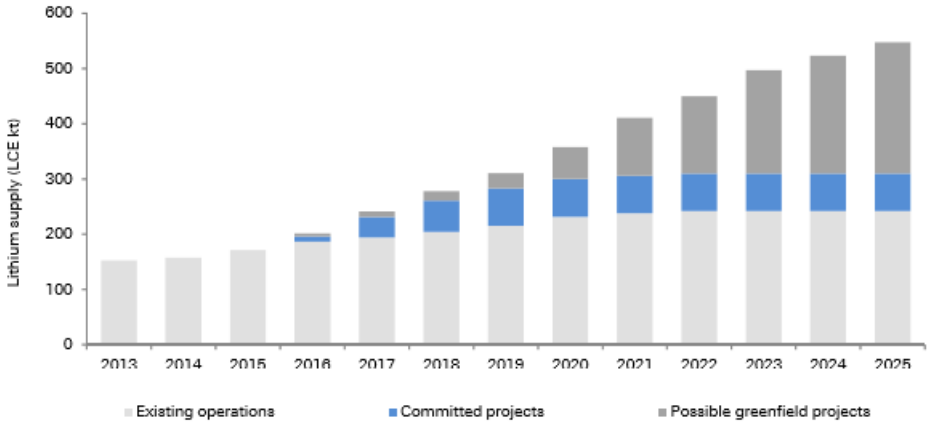

Figure 1 – Lithium supply projection (source: Deutsche Bank)

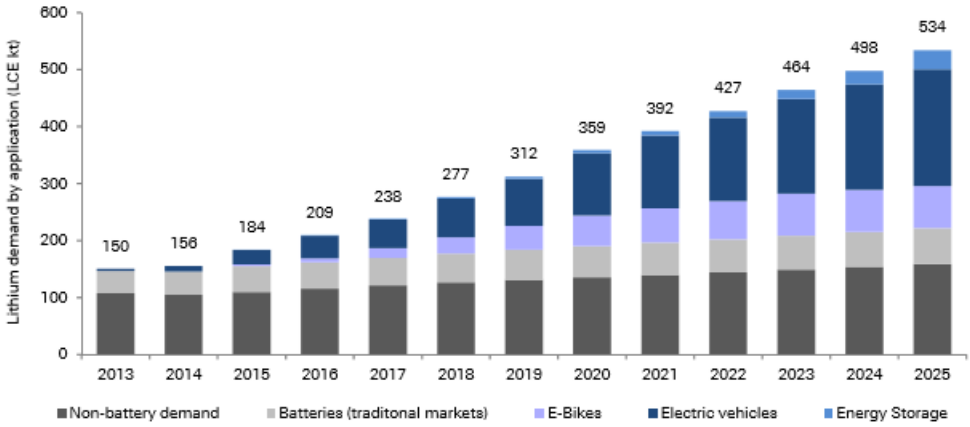

Figure 2 – Lithium demand forecast (source: Deutsche Bank)

What this means is that the need for lithium is real and increasing substantially. According to the Deutsche Bank report, (Figure 1), existing operations will not expand their output significantly, so the increase is going to have to come from new operations. While it is difficult to believe that the existing producers will not increase their output in view of a doubling in market demand, it is easy to believe that such a doubling presents opportunities for new operations.

This paper presents a broad-brush look at technology for the production of lithium that has advanced to at least the preliminary economic evaluation stage and for which the appropriate information has been published.

While there is a non-battery market for lithium that, according to Deutsche Bank's projection, will remain essentially steady over the next decade, the expansion in overall demand for lithium will be dominated by the need for lithium-ion batteries. For this exercise, the market was assumed to be the producers of lithium-ion batteries. Two lithium compounds that go into the manufacture of lithium-ion batteries are lithium carbonate and lithium hydroxide, for which reason these are the two products considered in this paper.

SOURCES AND PRODUCTS

The two main sources from which lithium is extracted are hard-rock deposits, the most common lithium mineral being spodumene ($LiAlSi_2O_6$), and lithium-bearing brines. The lithium brines occur as geothermal brines, salar brines and oilfield brines. Geothermal brines come from areas of the earth's crust that are hot enough for the brine to be used for the generation of electricity. Where the geothermal brine contains sufficient lithium, it can be extracted before the brine is re-injected into the geothermal system. Salar brines come from saline aquifers that are not hot and oilfield brines are associated with the extraction of oil and gas. Table 1 shows examples of the analyses of geothermal, salar and oilfield brines [7]. The main differences between these analyses are that the geothermal and oilfield brines contain substantially more silicon non-monovalent ions than the salar brines and the salar brines are higher in lithium. Current lithium operations are based on ore or on salar brines.

Table 1 - Examples of brine analyses, parts per million

Assay	Geothermal brine	Salar brine	Oilfield brine
Fe	1200 - 3700	-	35 -41
Mn	1000 - 2000	-	25 - 30
Zn	800 - 700	-	-
Mg	700 - 5700	-	2900 - 3500
Ca	22600 – 39000	300 - 530	29100 - 34500
Na	50000 - 70000	65000 - 910000	54900 - 67000
K	13000 - 34200	18500 - 31300	2400 - 5900
Li	100 - 400	1500 - 2420	146 - 386
Cl	142000 – 209000	159000 - 189500	144500 - 171700
SO_4	42 - 50	8000 - 19000	375 - 450
B	400 - 500	400 - 685	123 - 366
Si	40	-	90

Table 2 shows a mineral suite representing a spodumene ore and a concentrate produced from this ore, based on a report on the Whabouchi lithium project, published by Nemaska Lithium Inc [3]. The concentrate is extracted from milled ore using processes such as flotation, magnetic separation and dense-medium separation.

Table 2 – Spodumene ore and concentrate

Mineral	Ore	Conct.
SiO_2	33.4	10.8
$LiAlSi_2O_6$	20.8	74.4
$NaAlSi_3O_8$	29.3	9.5
$KAlSi_3O_8$	11.5	3.7
$Ca_2Mg_4FeSi_7AlO_{22}(OH)_2$	1.0	0.3
$KAl_3Si_3O_{10}(OH)_2$	4.0	1.3

Lithium carbonate and lithium hydroxide are sold as technical and battery grade products, the grade of interest to this exercise being the battery grade. Table 3 shows a specification for battery grade lithium carbonate [4]. Table 4 is a specification for battery grade lithium hydroxide monohydrate [5].

Table 3 – Battery grade lithium carbonate specification

Li_2CO_3	>99.9%	Na	<20 ppm	Mn	<5 ppm
Si	<40 ppm	Cl	<20 ppm	Al	<2 ppm
SO_4	<30 ppm	Mg	<10 ppm	Cu	<2 ppm
Ca	<25 ppm	Pb	<5 ppm	Fe	<2 ppm

Table 4 – Battery grade lithium hydroxide monohydrate specification, mass %

$LiOH•H_2O$	>99.3	CO_2	<0.30
Na	<0.005	Ca	<0.002
K	<0.005	Fe	<0.0007
Cl^-	<0.003	Insol (HCl)	<0.005
SO_4^{2-}	<0.01	Insol (H_2O)	<0.005

TECHNOLOGY – ORE

Producing lithium compounds from hard-rock deposits entails mining and mineral beneficiation to produce a lithium concentrate, typically a spodumene concentrate, that is then processed further. Figure 3 is a block diagram of the spodumene concentration process as practiced at Companhia Brazileira de Litio (CBL) in Brazil [6]. Figure 4 is a block diagram of the process used by CBL to produce lithium carbonate from the spodumene concentrate [6].

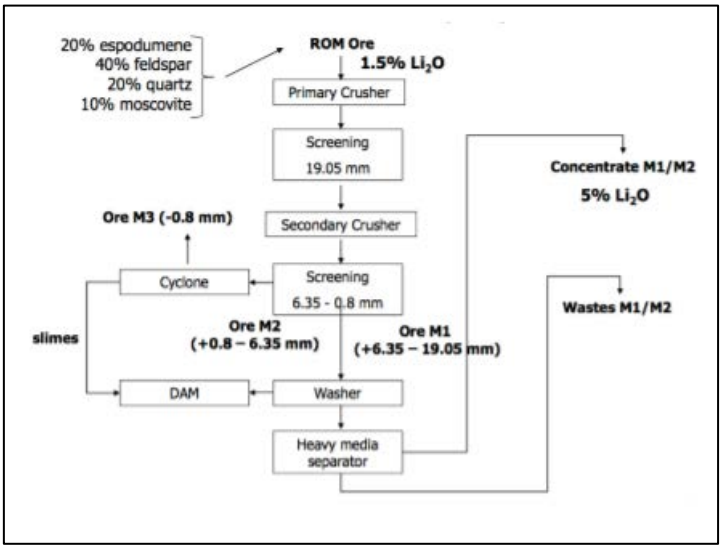

Figure 3 – Spodumene concentration

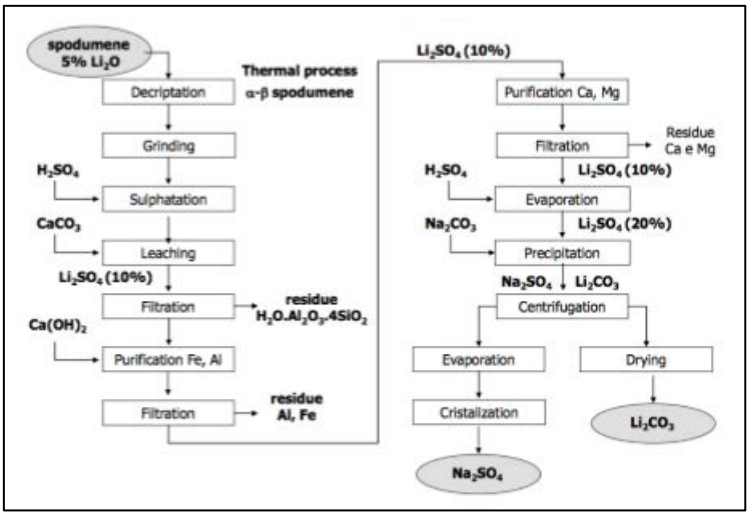

Figure 4 – Spodumene processing

In general, the mineral processing sequence is comminution, screening and physical separation. Dense medium separation, flotation and magnetic separation are used, in combinations depending on the particular ore, to separate the different minerals. Processing of the concentrate entails a step called decrepitation, in which the concentrate is heated to over 1000°C to convert the spodumene from the stable alpha to the less stable beta form. The converted concentrate is baked

with sulphuric acid to convert the beta-spodumene into lithium sulphate and aluminium silicate, then leached with water to dissolve the lithium sulphate. The resulting solution is purified by pH adjustment and hydroxide and/or carbonate precipitation of impurities such as base metals, magnesium and calcium, as well as by ion exchange. Lithium carbonate is produced from the purified solution by adding sodium carbonate. Lithium hydroxide is produced from the purified solution via electrolysis in cation-selective membrane cells similar to chlor-alkali cells, followed by concentration of the catholyte and crystallization of lithium hydroxide monohydrate. A process has also been developed in which the beta-spodumene is converted to lithium carbonate and sodium aluminium silicate, from which the lithium carbonate is extracted and recovered.

TECHNOLOGY - BRINE

The established technology for extracting lithium from brines entails solar evaporation of the brine in a sequence of ponds to concentrate the brine to a lithium level at which the precipitation of lithium carbonate is feasible, precipitation of magnesium hydroxide and calcium sulphate, precipitation of calcium carbonate and magnesium carbonate, removal of the precipitates and finally precipitation of lithium carbonate from the remaining solution. Figure 5 shows such a circuit [7].

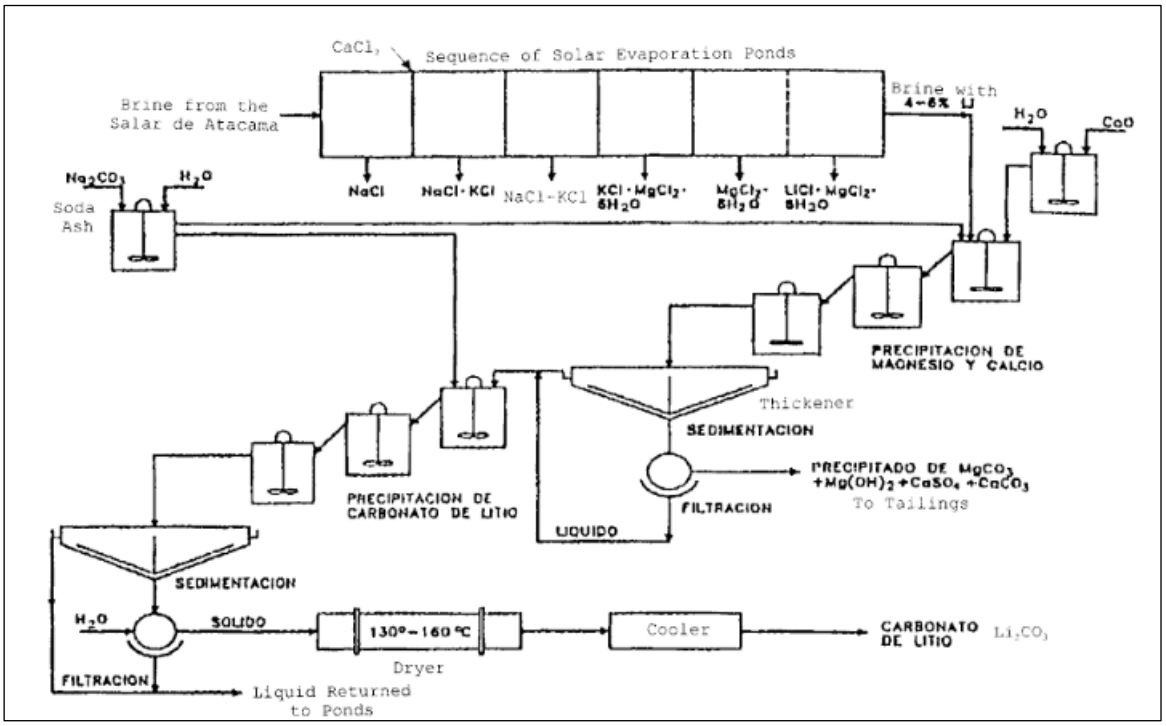

Figure 5 – Production of lithium carbonate from Salar de Atacama brine

As the solar evaporation proceeds and depending on the composition of the starting brine, various salts are crystallized. The following sequence [7] is an example:

- Halite (NaCl);
- Halite and sylvite (KCl) as a mixture of NaCl and KCl called sylvinite;
- Halite, sylvite and potassium lithium sulphate ($KLiSO_4$);
- Halite, kainite ($KCl•MgSO_4•2¾H_2O$) and lithium sulphate ($Li_2SO•H_2O$);
- Halite, carnallite ($KCl•MgCl_2•6H_2O$) and lithium sulphate;
- Bischoffite ($MgCl_2•6H_2O$);
- Bischoffite and lithium carnallite ($LiCl•MgCl_2•7H_2O$).

In some operations lime is added to precipitate magnesium hydroxide and calcium sulphate, which prevents the subsequent formation of magnesium- and sulphate-bearing salts, thus keeping lithium in the liquid phase and maximizing its recovery to the fully concentrated brine.

PUBLISHED PROJECTS

Published information on five projects was used for this exercise, three spodumene-based and two based on salar brine. Two of the spodumene-based projects produce lithium hydroxide and lithium carbonate, respectively, via decrepitation, acid-baking and water leaching. The third produces lithium carbonate via decrepitation and a sodium carbonate leach.

Nemaska Lithium Project

A recent NI 43-101 report [3] published by Nemaska Lithium Inc. describes a circuit developed to produce mainly lithium hydroxide and some lithium carbonate from the Whabouchi lithium deposit in Quebec, Canada. The project entails mining the ore, producing a spodumene concentrate and processing the concentrate via hydrometallurgy. The beneficiation entails crushing, dense media separation, grinding, flotation and magnetic separation.

In the hydrometallurgy circuit, the concentrate is first heated to 1050°C to convert the spodumene from the stable alpha phase to the reactive beta phase. The beta spodumene is cooled, mixed with sulphuric acid in a pug mill and baked at 230-280°C to convert the spodumene to lithium sulphate and aluminium silicate. The solids from the acid bake are leached with water, dissolving the lithium sulphate. The leached slurry is filtered, the filter cake is washed with water and the washed solids are discarded. The filtrate is treated with hydrated lime to precipitate iron and aluminium as hydroxides, the hydroxide slurry is thickened and filtered and the filter cake is discarded. The pH of the solution is raised further to precipitate more dissolved metals (presumably base metals such as ferrous iron, zinc, etc.) and the slurry is passed through candle filters that capture micron-sized solids. That filtrate is purified further by the addition of more reagents and again by ion exchange. (The NI 43-101 report does not detail this part of the process, but there is enough other information in the literature to demystify it.) The purified solution of lithium sulphate is then electrolyzed in electrolysis cells containing cation exchange membranes. Water is split into molecular hydrogen and hydroxyl ions at the cathodes, and the lithium ions migrate through the membranes, forming a solution of lithium hydroxide on the cathode side. Water is split into molecular oxygen and hydrogen ions at the anodes, the hydrogen ions replacing the lithium ions that leave the anolyte, generating sulphuric acid in the anolyte. The anolyte leaving the electrolysis cells is concentrated by evaporation and returned to the pug mill, thereby recycling the sulphuric acid. The catholyte from the electrolysis cells is concentrated by evaporation and crude lithium hydroxide monohydrate is crystallized. The crude crystals are recovered on a centrifuge, re-dissolved in water and re-precipitated in the same way as the crude lithium hydroxide, producing purified lithium hydroxide monohydrate that is dried and packaged for sale. The mother liquor from the second evaporation and crystallization sequence is recycled to the feed to the first evaporation-crystallization sequence. The mother liquor from the first evaporation-crystallization sequence is contacted with carbon dioxide to produce lithium carbonate that is recovered by filtration, dried and packaged for sale.

Quebec Lithium Project

An older NI 43-101 technical report [14] prepared for Canada Lithium Corp. in 2012 outlines a circuit for producing lithium carbonate from spodumene ore. In this study, mined ore is crushed in two stages, with photometric sorting between the two crushing stages separating the white spodumene ore from grey/black waste granitic material, rejecting a substantial fraction of the waste rock. The crushed spodumene ore is milled in a rod- and ball-mill combination and de-slimed in high pressure cyclones with an intermediate attrition scrubber. De-slimed ore is sent to flotation which recovers a spodumene concentrate. The concentrate is roasted at 1025°C in a decrepitation kiln to convert the spodumene from the alpha to the beta form. The transformed spodumene is cooled and then baked with sulphuric acid to form lithium sulphate. The acid-baked material is leached with water to dissolve the lithium sulphate and other sulphates formed in the acid bake. The resulting slurry is neutralized with lime to about pH 6 to precipitate iron and aluminium, then filtered and washed with water. The washed filter cake is discarded and the wash filtrate is recycled. The filtrate is treated with sodium hydroxide and sodium carbonate, raising its pH to about 10 and precipitating manganese and calcium. The precipitate is filtered off, washed with water and discarded. The filtrate is further purified by ion exchange to extract residual calcium and magnesium. The resulting solution is heated to 95°C and mixed with a solution of sodium carbonate to precipitate lithium carbonate that is recovered by thickening and filtration, washing and drying to produce battery grade lithium carbonate. The solution remaining after the precipitation of lithium carbonate contains sodium sulphate that has to be recovered or otherwise disposed of. The NI 43-101 report mentions making and selling anhydrous sodium sulphate.

Rose Tantalum-Lithium Project

An NI 43-101 report prepared for Critical Elements Corporation [23] on the Rose Tantalum-Lithium Project in James Bay, Quebec, Canada, outlines a mine and a concentrator producing spodumene and tantalum oxide concentrates. The ore is mined, crushed and milled and a concentrate is produced in a rougher/scavenger/cleaner flotation circuit. The flotation concentrate is passed through a series of wet high intensity magnetic separators, separating it into a magnetic concentrate of tantalum oxide and a non-magnetic spodumene concentrate. The spodumene concentrate is heated to 1038°C for 40 minutes to convert the alpha-spodumene to beta-spodumene, then leached for one hour with a saturated solution of sodium carbonate at 215°C and 310 psi, converting the spodumene to solid lithium carbonate and a stable hydrated mineral known as analcite or analcime (sodium aluminium silicate). The converted slurry is then cooled and contacted with gaseous carbon dioxide at 150 psi, reacting the solid carbonate to dissolved bicarbonate, thus dissolving the lithium carbonate as lithium bicarbonate. The resulting slurry is filtered under pressure, the filter cake is washed with water and the washed solids leave the lithium circuit. The filtrate is then depressurized and heated, releasing gaseous carbon dioxide and precipitating lithium carbonate that is recovered by thickening and filtration, dried and processed for onward shipment. The remaining solution is treated with sodium hydroxide, converting the sodium bicarbonate back to sodium carbonate, and recycled to the leach step. The carbon dioxide released in the precipitation of the lithium carbonate product is recompressed and recycled, with a make-up of fresh carbon dioxide. The NI 43-101 report states that over 90 percent of the carbon dioxide is recycled.

Cauchari-Olaroz

Western Lithium USA Corp. owns the Cauchari-Olaroz Project [16,17]. Brine from the wells is pre-concentrated in solar evaporation ponds in which Glauber's salt (sodium sulphate decahydrate) is precipitated and removed. The pre-concentrated brine is dosed with lime to precipitate magnesium hydroxide that is filtered off and disposed of and the filtrate is further concentrated in more solar evaporation ponds in which potassium chloride, potassium sulphate and borate salts are precipitated, removed and sent to a KCl recovery plant. The concentrated solution is acidified to a pH of 3 to 4 with hydrochloric acid and passed through a solvent extraction sequence in which the remaining boron is extracted. The loaded organic phase is stripped with sodium hydroxide at pH 10-11 and recycled. The boron-loaded strip liquor is sent to disposal and the boron-depleted raffinate is treated with sodium hydroxide and sodium carbonate to precipitate residual magnesium and calcium as magnesium hydroxide and calcium carbonate that are removed. Sodium carbonate, as a 30% Na_2CO_3 solution, is added to the purified brine to precipitate lithium carbonate that is filtered off, washed with water, dried and packaged for sale. The remaining solution is recycled to the evaporation pond system to recover the dissolved lithium.

Sal de Vida

In the Sal de Vida project in Argentina [8], brine from the wellfield is dosed with slaked lime to precipitate magnesium hydroxide, gypsum and borate. The precipitate is settled out and discarded, and the remaining brine is concentrated by solar evaporation, first crystallizing sodium chloride that is removed for disposal, then crystallizing sylvinite (NaCl/KCl) that is recovered and separated into sodium chloride that goes to disposal and potassium chloride that is sold as potash. Most of the residual boron in the brine from the solar evaporation sequence is removed by solvent extraction. The raffinate is treated with sodium carbonate to precipitate calcium and magnesium carbonate that is removed by thickening, and the remaining solution is further purified by ion exchange. The purified brine is then dosed with sodium carbonate to precipitate lithium carbonate that is settled out and recovered, re-slurried with water and re-dissolved with carbon dioxide as lithium bicarbonate, then re-precipitated as battery-grade lithium carbonate [18].

New processes for Brine

Processes that do not concentrate the brine by solar evaporation have been proposed. Instead, they remove only the salts that would interfere, then selectively extract lithium from the dilute brine. The resulting barren brine is then returned to the source. The advantages claimed for this approach are substantially less in-process time for lithium because the lengthy solar evaporation sequence is eliminated, and a significantly smaller environmental footprint [9,11] because large areas for solar evaporation and for salt impoundment are not needed, and also because the ground water of the brine source is not depleted. One of these new technologies has, as its enabling step, selective solvent extraction of lithium from a sodium/potassium chloride brine [10,22], stripping the lithium from

the loaded organic phase with acid. Another technology selectively extracts lithium chloride from the brine into a lithium aluminate solid matrix [11], then strips it from the loaded matrix using water. At the time of writing, published information on these new processes was not available, excluding them from this exercise.

CAPITAL AND OPERATING COSTS

The published capital costs for the projects examined in this exercise were adjusted to 2016 US dollars via the Chemical Engineering Plant Cost Index (CEPCI) [15]. The published operating costs were adjusted to 2016 US dollars via inflation data taken from the US Inflation Calculator [24]. The various projects were designed for annual productions of 20-30 kt/y LCE (lithium carbonate equivalent). For comparative purposes in this exercise, the various capital costs were converted to 2016 US$ per annual ton of LCE ($/t-y LCE), without differentiating between tonnes and tons because that distinction is not clear in all the published reports.

Nemaska

The capital costs in Table 5 are those published by Nemaska Lithium in 2016, converted to US dollars at 0.8 USD/CAD. The Whabouchi project was designed to produce 27645 tonnes per year of lithium hydroxide monohydrate and 3267 tonnes per year of lithium carbonate, making the total production 27.6 kt/y LCE. Table 6 lists the operating costs published by Nemaska Lithium, converted from Canadian to US dollars at 0.8 USD/CAD and expressed as $/t LCE.

Table 5 – Capital cost summary, Nemaska Lithium

Mine and concentrator	US$ million	$/(t/y) LCE
Direct costs	120	4353
Mine development	3	110
Rehabilitation	3	107
Indirect costs	48	1733
Contingencies	17	629
Sub-total for mine site	191	6932
Processing plant	US$	$/(t/y) LCE
Total direct costs	184	6671
Total indirect costs	36	1321
Contingencies	28	1000
Sub-total for processing plant	248	8992
Total project	439	15924

Table 6 – Operating costs, Nemaska Lithium

Cost	US$/t LCE
Mine	439
Concentrator	684
Concentrate transport	314
Hydrometallurgical plant	1046
Total operating cost	2482

Quebec Lithium

The Quebec Lithium project was designed to produce 20 kt/y of lithium carbonate. Table 7 lists the published operating costs, converted into US$/t LCE in 2016 currency and Table 8 lists the capital costs published for this project, adjusted to 2016 US dollars.

Table 7 – Operating costs, Quebec Lithium

Cost	US$/t LCE
Mining	1079
Processing	2160
Administration	126
Total operating cost	3366

Table 8 – Capital costs, Quebec Lithium project

Item	US$ million	$/(t/y) LCE
Mining	10	521
Crushing, flotation	41	2030
Hydrometallurgy	82	4110
Photometric sorting	5	232
TMF, infrastructure, other	16	785
Pre-strip	2	93
Total direct costs	155	7770
EPCM, owners costs	25	1268
Contingency	11	539
Total indirect costs	36	1806
Total capital cost	192	9577

Rose Ta-Li

Table 9 lists the capital costs published for the Rose Ta-Li project, converted to 2016 US dollars. This circuit was designed to produce two products, lithium carbonate and tantalum oxide concentrate. Although the production of the tantalum oxide concentrate (109 t/y) was much lower than that of lithium carbonate (27kt/y), the selling price assumed tor the tantalum concentrate was $260/kg, making the revenue from the tantalum concentrate about 28 percent of the total operating cost. Table 10 lists the operating costs presented in the technical report on the Rose Ta-Li project, adjusted to 2016 US dollars.

Table 9 – Capital costs, Rose Ta-Li project

	US$	$/(t/y) LCE
Mine development	82	3050
Process plant	98	3611
Power & infrastructure	23	838
Indirect costs	40	1494
Closure costs	14	503
Contingency	26	947
Total capital cost	282	10442

Table 10 – Operating costs, Rose Ta-Li project, $/t LCE

Mining	1453
Spodumene concentrator	976
Lithium carbonate plant	1224
G & A	466
Total operating cost	4119
Revenue from tantalum concentrate	1139
Operating cost after Ta credit	2980

Cauchari-Olaroz

The capital cost published for the Cauchari-Olaroz project, adjusted to 2016 US dollars in Table 11, is based on an operating capacity of 20 kt/y of lithium carbonate. The feed being a brine that is pumped from the wells, the equivalent of the mine is the well field, and the mining cost is the cost of pumping the brine from the wells to the evaporation ponds and maintaining the pumping system, which is included in the published operating costs listed in Table 12.

Table 11 – Capital cost estimate, Cauchari-Olaroz

	US$ million	$/(t/y) LCE
Brine extraction wells	16	795
Evaporation ponds	104	5216
Lithium carbonate plant	67	3350
Infrastructure and general	24	1216
Indirect costs	15	749
Contingencies	23	1133
Total capital cost	249	12459

Table 12 – Operating costs, Cauchari-Olaroz, $/t LCE

Reagents	1226
Salt removal and transport	126
Energy	201
Manpower	143
Services	48
Maintenance	109
Transport	65
G & A	59
Total operating cost	1978

Sal de Vida

The capital costs published for the Sal de Vida project, adjusted to 2016 US dollars, are summarised in Table 13. The design production is 25 kt/y LCE. The published operating costs, adjusted to 2016 US dollars, after by-product credit for the sale of KCl, are listed in Table 14.

Table 13 – Capital cost estimate, Sal de Vida

	2016	$/(t/y) LCE
General	7	267
Brine Extraction & evaporation ponds	109	4377
Lithium Carbonate Plant	59	2360
Potash Plant	25	993
Power Plant & Onsite Infrastructure	54	2147
Other	10	386
Total Direct Costs	263	10527
EPCM	34	1360
Owners Costs & Spares	12	497
Freight	11	435
Total Indirect Costs	57	2292
Contingency	32	1280
Total Capital Investment	353	14102

Table 14 – Operating costs, Sal de Vida, $/t LCE

Reagents	954
Salt removal and transport	454
Energy	159
Manpower	341
Services, maintenance, G&A	363
Total operating cost	2249

DISCUSSION

Production

Table 15 is a summary of the capital and operating costs calculated in the various studies done on the projects discussed in this exercise, converted to 2016 US dollars. Interestingly, even though the spodumene projects include hard-rock mines and concentrators in addition to the hydrometallurgical circuits, the capital costs of the brine projects examined fall between those of the spodumene projects, as do the calculated operating costs.

Table 15 – Capital and operating cost summary

Project	Source	Main Li product	Capex $/(t/y) LCE	Opex $/t LCE
Nemaska Lithium	Spodumene ore	Hydroxide	15924	2482
Quebec Lithium	Spodumene ore	Carbonate	9577	3366
Rose Ta-Li	Spodumene ore	Carbonate	10442	2980
Cauchari-Olaroz	Salar brine	Carbonate	12459	1978
Sal de Vida	Salar brine	Carbonate	14102	2249

According to the Deutsche Bank projection shown in Figure 2, over the next decade or so the demand for lithium carbonate and lithium hydroxide will rise by almost 300 kt/y LCE. At something like 20 kt/y LCE per operation and if the existing producers do not ramp up appreciably, that would require ten to fifteen new lithium operations. Figure 6 shows a Deutsche Bank forecast [(1)] for the prices of spodumene concentrate, lithium carbonate and lithium hydroxide, the left vertical axis being for lithium carbonate and hydroxide, the right vertical axis for spodumene.

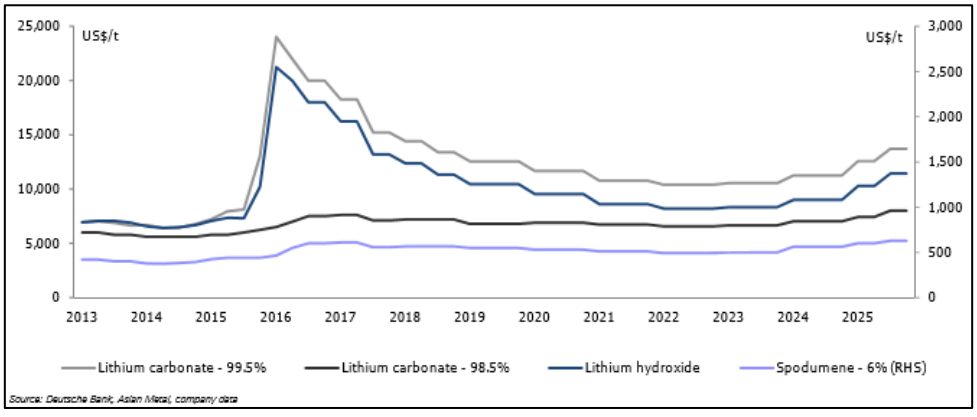

Figure 6 – Lithium price forecast

If these projections are accurate, a slightly conservative long term average of US$10/kg LCE would not seem unreasonable. Assuming that and the capital and operating costs listed in Table 15, simple cash flow calculations yield the curves for internal rate of return versus project life shown in Figure 7.

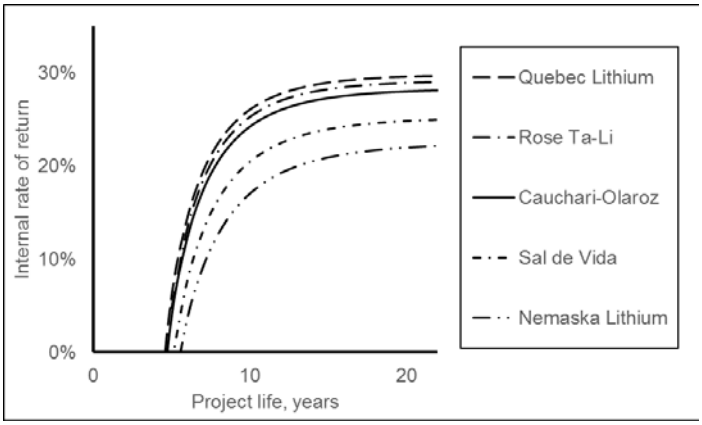

Figure 7 – IRR curves

These calculations are based on a design production of 20 kt/y LCE, capital expenditure in two equal portions in the first two years, 25 percent of design production in the third year, 50% in the fourth year, 75 percent in the fifth year and 100% thereafter. Corporate tax was assumed to be 30%, based on the before-tax profit.

From these curves, it would seem that all five of the projects examined would be profitable, all with a 20-year internal rate of return between about 25 and 30 percent.

Li-ion Batteries

While a long-term price of $10/kg for lithium carbonate might well be a tempting assumption from the viewpoint of the lithium producer, it is worth examining this from the perspective of the other side, i.e. the lithium battery manufacturers who would be buying the lithium carbonate or hydroxide. Lithium-ion batteries use various mixed oxides of lithium and other metals as the active cathode material [19]. Table 16 lists some of the cathode materials used and their practical storage capacities per unit of the cathode material.

Table 16 – Li-ion cathode materials

Active material	Practical capacity, Ah/kg
$LiCoO_2$	140
$LiNiO_2$	120
$LiMn_2O_4$	120
$LiNi_{⅓}Mn_{⅓}Co_{⅓}O_2$	200
$LiFePO_4$	160

Table 17 gives a breakdown by mass of the constituents of a 100 amp-hour high-energy lithium-ion battery designed for use in electric vehicles [19]. The current (April 2017) price of cobalt is about $55/kg ($25/lb, close to it's long-term average), that of nickel is close to $10/kg ($4.5/lb, somewhat below its long-term average of about $7.3/lb) and that of manganese is just under $2/kg (its long-term average is $0.84/kg). Assuming the active cathode material in Table 17 to be $LiCoO_2$, $10/kg for lithium carbonate and the long-term average prices for cobalt, nickel and manganese ($55/kg, $16/kg and $1/kg, respectively), and extrapolating to the other active cathode materials gives the numbers listed in Table 18. According to a brief internet survey, pure iron powder and high-purity phosphoric acid sell for approximately $1/kg. Figure 8 shows a cost breakdown for the manufacture of lithium-ion batteries and Figure 9 is a breakdown of the materials cost component, both based on data from 2000 [26] and assuming that the active material is $LiNi_{⅓}Mn_{⅓}Co_{⅓}O_2$.

Table 17 – Composition, 100 Ah high-energy cell

Component	Mass, kg
Cathode material	1.41
Separator	0.06
Electrolyte	0.62
Graphite	0.56
Can and vent	0.29
Binder	0.16
Copper	0.15
Aluminium	0.06
Carbon	0.04
Other	0.07

Table 18 – Rough cathode material costs for a 100 Ah Li-ion battery, $/kWh

Input	$LiCoO_2$	$LiNiO_2$	$LiNi⅓Mn⅓Co⅓O_2$	$LiFePO_4$
Li_3CO_3	51	64	29	28
Co	445	-	83	-
Ni	-	161	24	-
Mn	-	-	1	-
Fe	-	-	-	4
H_3PO_4	-	-	-	7
Total	496	225	137	40

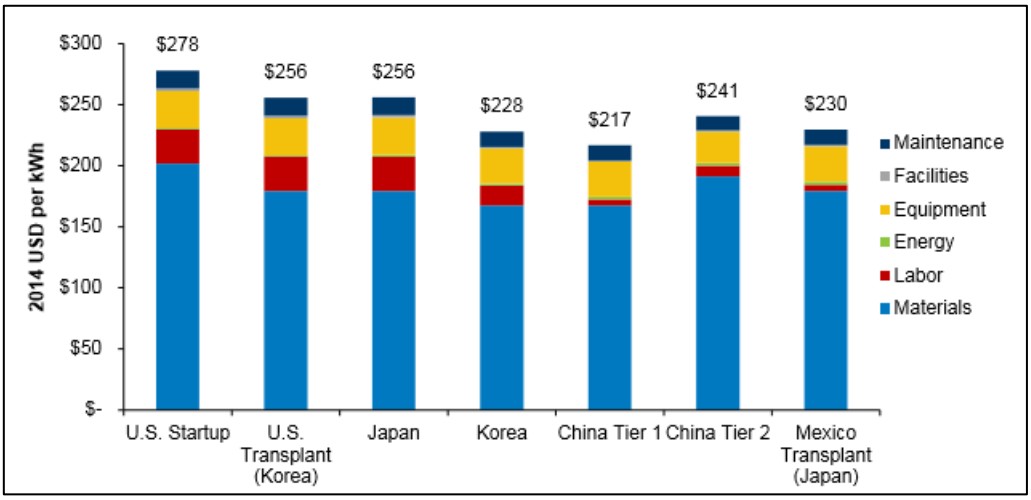

Figure 8 – Cost breakdown for Li-ion battery manufacture

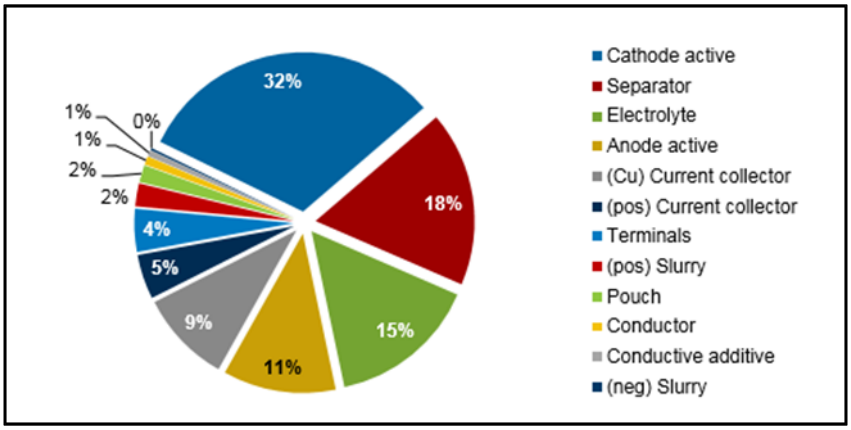

Figure 9 – Material cost breakdown for Li-ion battery manufacture

According to Figure 8, the material cost was about $200/kWh in 2014. According to Figure 9, the cost of that particular active cathode material is about a third of the total materials cost, or about $70/kWh, which is about half of the value of $137/kWh in Table 18.

A projected total battery cost for 2020 is $270-300/kWh [20] and the ultimate cost goal set by USABC (Unites States Advanced Battery Consortium) is about $210/kWh [19] in 2016 currency. If the cost of all but the active cathode material remains roughly as at present in terms of $/kWh, the cost of the active cathode material will need to drop by about $90/kWh to meet the ultimate cost goal. If $LiFePO_4$ can become the active material of choice, that goal might be achieved. If that happens, then the cost of lithium carbonate (or hydroxide) will become a major part of the raw material cost for making the active cathode material, in which case desire for further battery cost reductions could cause downward pressure on the price of lithium carbonate and lithium hydroxide.

It would seem prudent, therefore, for the producers of lithium carbonate and lithium hydroxide to keep the selling price as low as remains commensurate with acceptable lithium project economics. If the various assumptions used in this exercise are reasonable, though, $10/kg LCE could be a sustainable price for lithium carbonate or hydroxide.

CONCLUSIONS

From the results found in this exercise, it would appear to be an exciting time for lithium. With the demand set to double or more over the next decade due to the increasing demand for lithium-ion batteries, marketing product of the right quality should not be a challenge of any note for new lithium operations. New operations using established technology should, absenting any major unforeseen events and assuming good engineering, enter the market smoothly. For the foreseeable future, the lithium market will not only have room for many, it will also need many new lithium operations.

Even though the future presently looks rosy for new lithium carbonate or lithium hydroxide projects, the manufacturers of lithium-ion batteries are striving for lower manufacturing costs, of which materials costs are a significant portion. For the lithium-ion battery industry to become a large, stable market, the market price of lithium carbonate and lithium hydroxide needs to be such that the lithium-ion battery industry can meets its targets; therefore, the price of lithium carbonate cannot remain unfettered in the long term.

REFERENCES

1. Hocking, M., Kan, J., Young, P., Terry, C. and Begleiter, D. Deutsche Bank, Markets Research. Lithium 101, 9 May 2016. https://www.slideshare.net/Tehama/welcome-to-the-lithium-ion-age-lithium-101-deutsche-bank-may-9-2016

2. http://www.albemarle-lithium.com/pdf/402202.pdf

3. Nemaska Lithium Inc. Feasibility study update on the Whabouchi lithium deposit and hydromet plant. NI 43-101 Technical Report, April 2016. http://www.nemaskalithium.com/assets/documents/docs/2015-024%20Nemaska%20NI%2043-101%20May%2019%202016%20Final-SEDAR.pdf

4. China Lithium Products Technology Co., Ltd. Lithium Carbonate 99.50% Battery Grade 1 http://lithium-chemical.com/product/?32_320.html

5. Targray product data sheet. Lithium hydroxide http://targray.com/medialibrary_old/documents/pds-lithium-hydroxide.pdf

6. Borges, P. H. R., Santos, F. A., Milikic, N., Benieny, F. J. Jr. and Barsante, C.A. Lithium aluminosilicate residue as raw material in the production of sustainable concrete masonry units: a Brazilian case. https://www.researchgate.net/publication/304574387_Lithium_Aluminosilicate_Residue_as_Raw_Material_in_the_Production_of_Sustainable_Concrete_Masonry_Units_A_Brazilian_Case

7. Garrett, D.E. Handbook of lithium and natural calcium chloride. Their deposits, processing, uses and properties. Elsevier Academic Press, 2004. ISBN 0-12-276152-9.

8. Galaxy Resources Limited, media release, 12 April 2013. Sal de Vida definitive feasibility study supports low cost, long life lithium and potash operation. http://stream1.newswire.ca/media/2013/04/11/20130411_C4655_DOC_EN_25468.pdf

9. http://www.pureenergyminerals.com/technology-overview/ Accessed 2017-04-04.

10. Lipp, J. LiSX™ A new technology for lithium recovery. Hydrometallurgy 2014 – Volume II, Canadian Institute of Mining, Metallurgy and Petroleum, ISBN 978-1-926872-23-0.

11. Simbol Materials. Sustainable extraction of valuable elements, 2013. https://www.aiche.org/sites/default/files/docs/conferences/event/b.1_burba_suschem.pdf, accessed 2017-04-04.

12. Tenova Bateman Technologies. LiSX™ - Lithium solvent extraction. Client brochure.

13. www.canadianforex.ca/forex-tools/historical-rate-tools/historical-exchange-rates. May 2016 data.

14. Canada Lithium Corp. Feasibility Study update NI 43-101 Technical Report, Quebec Lithium project, October 12, 2012.

15. Chemical Engineering www.chemengonline.com, April 2016.

16. Western Lithium USA Corp. Cauchari-Olaroz Project www.westernlithium.com/wp-content/uploads/2015/01/WLC_Presentation_January_2016.pdf

17. Lithium Americas. NI 43-101 Technical Report. Feasibility Study, Reserve Estimation and Lithium Carbonate and Potash Production at the Cauchari-Olaroz Salars, Jujuy Province, Argentina. July 11, 2012.

18. Amouzegar et al. Process for the purification of lithium carbonate. US Patent 6 048 507, April 11, 2000.

19. Gaines, L. and Cuenca, R. Costs of lithium-ion batteries for vehicles. Argonne National Laboratory report ANL/ESD-42, May 2000.

20. Oswal, M., Paul, J. and Zhao, R. A comparative study of lithium-ion batteries. University of Southern California, may 2010.

21. Julien, C. M., Mauger, A., Zaghib, K. and Groult, H. Comparative issues of cathode materials for Li-ion batteries. Inorganics 2014, 2, 132-154.

22. Pranolo, Y., Zhu, Z. and Cheng, C. Y. Separation of lithium from sodium in chloride solutions using SSX systems with LIX 54 and Cyanex 923. Hydrometallurgy 154 (2015) 33-39.

23. Critical Elements Corporation. Technical report and preliminary economic assessment of the Rose Tantalum-Lithium Project. NI43-101 report prepared by Genivar Inc., December 10, 2011.

24. http://www.usinflationcalculator.com/inflation/historical-inflation-rates/

25. Enirgi Group announces positive results of definitive feasibility study for Salar del Rincon Lithium Project. July7, 2106. http://www.marketwired.com/printer_friendly?id=2140673

26. Anderson, D. L. An evaluation of current and future costs for lithium-ion batteries for use in electrified vehicle powertrains. Nicholas School of the Environment, Duke University, May 2009.

27. Chung, D., Elgqvist, E. and Santhanagalopalan, S. Automotive Lithium-Ion Cell Manufacturing: Regional Cost Structures and Supply Chain Considerations. CEMAC Technical Report, April 2016. http://www.nrel.gov/docs/fy16osti/66086.pdf

LITHIUM EXTRACTION FROM COMPLEX SILICATES

By

Damian Connelly

Mineral Engineering Technical Services Pty Ltd (METS), Australia

Presenter and Corresponding Author

Damian Connelly
Damian.Connelly@metsengineering.com

ABSTRACT

The demand for high purity battery grade lithium carbonate is expected to grow significantly in the near term. The lithium-ion battery sector is one of the fastest growing and largest consumers of lithium. Lithium-ion batteries have superior energy density, are more efficient and environmentally friendly than traditional acid batteries and the cost is falling based on innovation and technical development.

Lithium ores of major economic importance are spodumene ($Li_2O.Al_2O_3.4SiO_2$), lepidolite ($3LiF.K_2.2Al_2O_3).7SiO_2$), ambylgonoite ($Li.Al.F.PO_4$), petalite ($LiAlSi_4O_{10}$,), zinnwaldite (KLiFeAl(AlSi3)O10(OH,F)2) and brines (Li.Na.PO4). Spodumene because of its abundance is the most important source of lithium.

The metallurgy of lithium ores is very ore specific depending on lithology and the lithium silicate minerals are generally refractory. Physical concentration using dense media or flotation is common followed by hydrometallurgical process routes. The hydrometallurgical difficulties specifically managing impurities is ore specific and often means that some lithium ores are not economic. At the same time some lithium ores contain valuable by products which can enhance the project economics if saleable products can be produced.

Keywords: Pegmatite, spodumene, lepidolite, beneficiation, dense media separation, flotation, magnetic separation, micas, liberation, calcination, leaching, purification, lithium hydroxide, lithium carbonate, alpha spodumene, beta spodumene, battery grade lithium carbonate.

Introduction

- Lithium production increasing to meet increasing demand
  - In particular the need to produce battery grade lithium salts
- Brines are still the dominant source of the worlds lithium
- Spodumene processing is well developed for producing battery grade lithium 99.99% lithium.
- New processes are being developed to exploit other "hard-rock" lithium sources and clay resources that have previously been ignored

Lithium Production

- Lithium demand increasing across all uses
- Demand for lithium use in batteries is particularly strong
  - Electric Vehicles, renewable storage, electronic devices, etc.
  - The need for battery grade lithium carbonate (≥99.5 wt%) is expected to grow

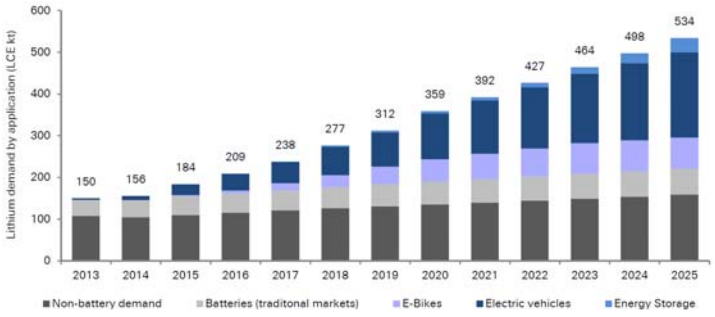

Source: Deutsche Bank

Lithium Production

- The use of lithium is expected to change significantly

2015 Lithium Demand

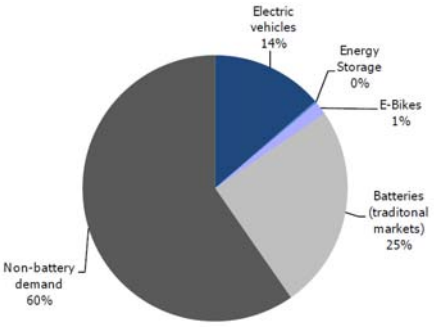

2025 Lithium Demand

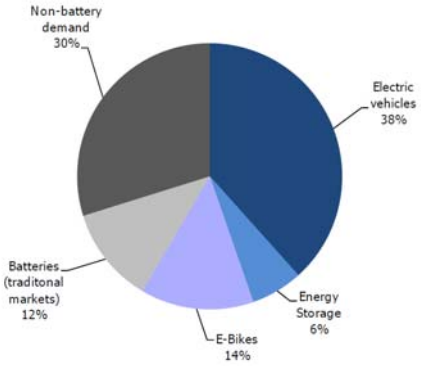

Source: Deutsche Bank

Lithium Production

- Today lithium is produced from brines or “hard-rock” deposits, clay is yet to see commercial viability
- Brines (66%)
  - Continental
  - Geothermal
  - Oil-field
- Pegmatite or “hard-rock” deposits (26%)
  - Spodumene ($Li_2O.Al_2O_3.4SiO_2$)
  - Lepidolite ($3LiF.K_2.2Al_2O_3).7SiO_2$)
  - Amblygonite ($Li.Al.F.PO_4$)
  - Petalite ($LiAlSi_4O_{10}$)
  - Zinnwaldite ($KLiFeAl(AlSi_3)O_{10}(OH,F)_2$

Source: University of Pittsburgh

  - ➢ Of these, spodumene is the most significant hard-rock deposit
  - ➢ Lithium silicate minerals are generally refractory
- Li-containing sedimentary deposits (8%)
  - Clay deposits
  - Lacustrine evaporites

Lithium Deposits Common

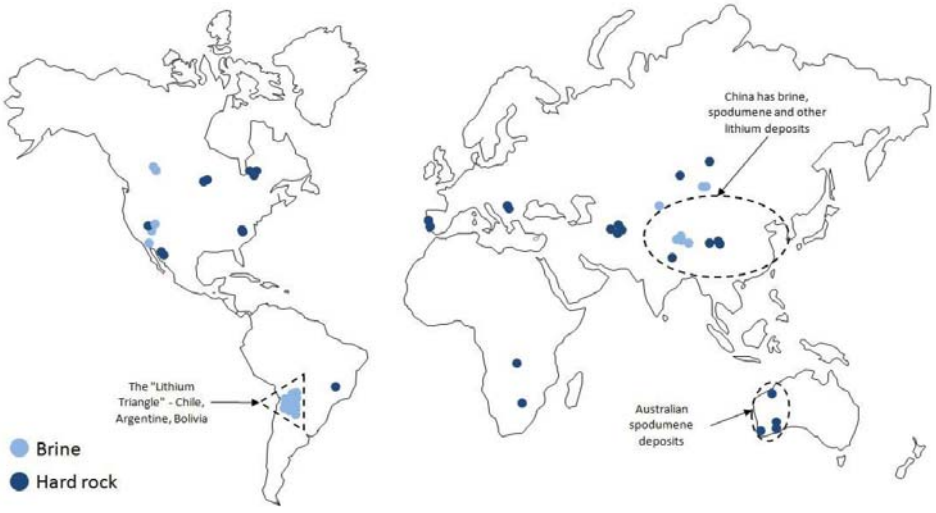

Source: Deutsche Bank

Lithium Brines

- More economical than hard-rock processing
- Typical concentrations range from 200 to 1,500 ppm
- Utilises solar evaporation
  - Occurs over 18-24 months to get a final concentration of ~6%
- Lithium recovery is low, ≤ 50%
- Generally lithium produced from brines is below battery-grade quality with most going towards chemical application markets
- Impurity removal is the biggest technical challenge

Source: Mining.com website (2013)

Recovery of Lithium From Complex Silicates

- Recovery of lithium is an ore specific process dependent on lithology
  - Many impurities are carried through the processes and removal is complicated
- Theoretical lithium content of the main lithium bearing minerals is 3% to 5.53% but most mineral deposits have 0.2% to 2% Li.
- Beneficiation byDense Media Seperation (DMS) and flotation
- Lithium is extracted by two main chemical processes
  - Acidic; and
  - Alkaline
  - It can also be extracted through chlorination
- Produce either Li_2CO_3 or LiOH
- Almost all commercial processes have been developed for spodumene
  - New developments are required to make these processes more competitive with lithium brines
  - Lepidico and Lithium Australia Technology are testing processes that demonstrate the feasibility of extraction from Li Micas
  - Only significant petalite production is from Bikita, Zimbabwe

Hard Rock Challenges

Beneficiation

- Selective separation of gangue materials by DMS or flotation
- Contamination by other micas is an issue (elutriation/magnetic separation)
- Slimes interfere with flotation and consume expensive reagents
  - Requires desliming

Impurities

- A large complication associated with this process is impurity content of the ores
  - Many similar elements are present in the ores e.g. Fe, Al, Mg, Ca, Mn
  - The chlorides and sulphates of all these metals are soluble in water
- These elements are leached alongside the lithium and the resultant solution requires purification steps

Recovery of Lithium From Sulphate Route

- Comminution
  - Pegmatite is a hard, abrasive rock making the process energy intensive and accounts for up to 50% of the processing cost
- Flotation
- Calcination
  - At 1050-1100°C to force a phase change from α-spodumene or petalite to β-spodumene
  - β-spodumene has ~20% more volume and is much more amenable to acidic and alkaline leaching
- Roasting
  - 200-250°C
  - Roasting with H_2SO_4 gives a high yield of lithium and has favourable energy consumption
  - HCl less common due to higher difficulty in impurity removal
  - Lime is used to produce lithium hydroxide directly

Jiangsu Flowsheet-Spodumene

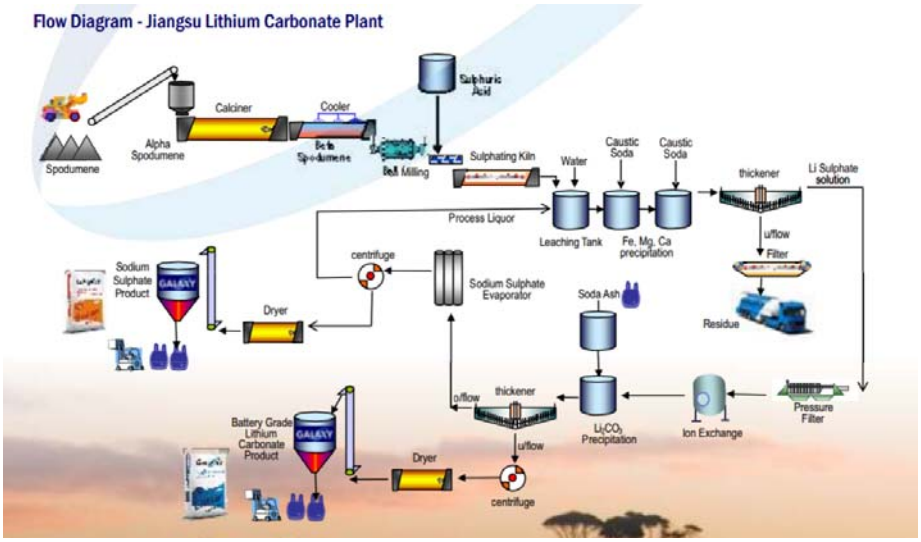

Recovery of Lithium From Sulphate Route

Source: researchgate.com

- Leaching
  - In water
- Impurity Removal
  - Achieved by precipitation and ion exchange processes
  - Typically add NaOH which neutralises the acid and precipitates
- Refining
  - Addition of bicarbonate precipitates Li_2CO_3

ANZAPLAN

- Pilot plant running slightly altered beneficiation process for spodumene
- Features selective fragmentation following by optical sorting of minerals
  - Suited to coarser grained lithium bearing pegmatites
  - Ore is broken along crystal boundaries
- Advantageous in that it produces two new products, quartz and low iron feldspar
  - Conventional methods produce a tough to market mix of the two

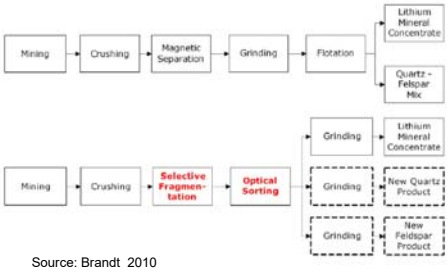

Source: Brandt 2010

Electrolysis Processes Lithium Solutions

- Emerging Processes from Nemaska Lithium and a joint venture between Neometals (70%) and Mineral Resources (30%)
  - Nemaska Process and Eli Process respectively
- Both take a spodumene feed and utilise electrolysis for Li_2CO_3 production
  - Process viability limited to regions with low electricity prices
  - Main difference in the electrolysis step is the solution (LiCl vs Li_2SO_4)
- Direct product is $LiOH•H_2O$
  - Tesla using LiOH as their lithium source for their gigafactory
  - Carbonation produces Li_2CO_3
  - Typically an extra process step is required to attain LiOH from Li_2CO_3 making it advantageous to directly produce LiOH

ELi Process

- **Calcine:** Between 1050-1100°C to convert α-spodumene to β-spodumene
- **Leaching:** 20% HCl at 108°C for ~8 hours
- **Impurity Removal:**
  - Pyrohydrolysis
  - Precipitation
  - Precipitation 2
  - Concentration
  - Fractional Crystallisation
  - Ion exchange
- **Membrane Electrolysis:** 35-40% w/w LiCl solution at 90°C in a membrane cell where chlorine and hydrogen gas are produced. Lithium migrates across the membrane enriching a LiOH solution (4%->6%)
- **Production:** The LiOH solution undergoes either evaporation processes to give crystalline LiOH or it goes to carbonation with CO_2 to produce Li_2CO_3 depending on which product you want to produce.

ELi Process

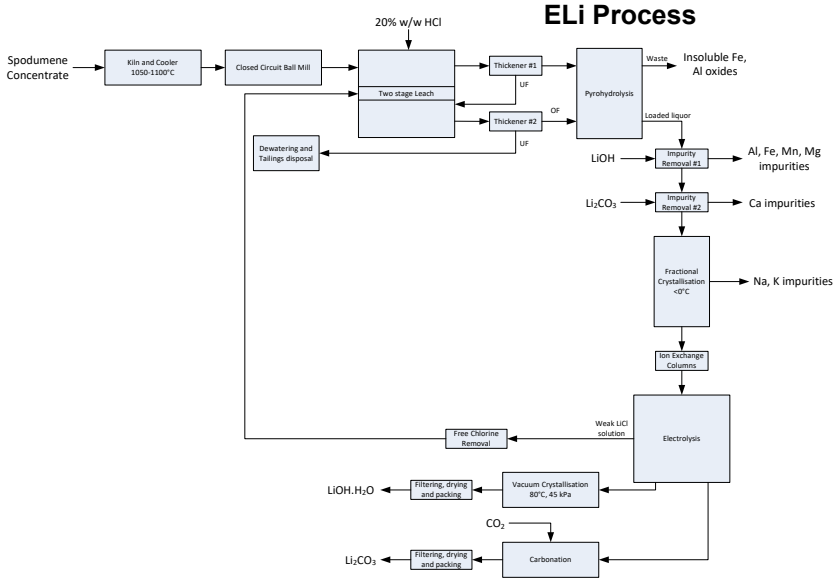

ELi Process

Impurity Removal

- **Pyrohydrolysis**
  - At 300°C to convert Al and Fe chlorides into insoluble oxides/hydroxides. Excess HCl is also recovered here. Probably through condensation and absorption
  - Solid liquid separation
- **Precipitation**
  - Removal of Mn, Mg and remaining Fe and Al precipitated by raising the pH to 9 with LiOH
  - Solid liquid separation
- **Precipitation 2**
  - Removal of Ca using Na_2CO_3 or Li_2CO_3
  - Solid liquid separation
- **Concentration**
  - Likely through vacuum evaporation
- **Fractional Crystallisation**
  - Cooled down to <0°C to crystallise Na, K
- **Ion exchange columns**
  - Remove any residual Ca, Mg and other multivalent cations down to below 10 ppm

ELi Process

Membrane Electrolysis

- LiCl fed at 90°C
- Process produces H_2 and Cl_2 gas which are combined to produce HCl for the leaching step
- Lithium migrates across a membrane as the concentration of lithium increases in the LiCl brine. The lithium from the LiCl solution migrates into a weak solution of LiOH and increases it from 4 to 6%
- The weak LiCl ("depleted brine") is recycled to the leach step
- The weak LiOH (4%) is from the crystallisation stages

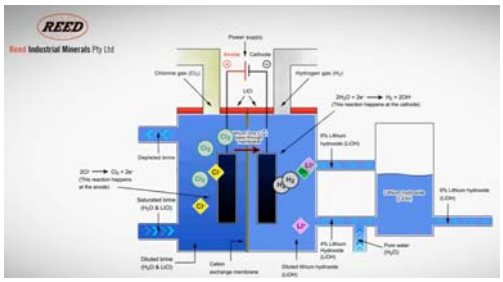

Source: Neometals

Nemaska Process

- **Calcine:** At approximately 1050°C
- **Acid Roast:** Traditional Sulphation roast @ 250°C, 98% sulphuric acid roasting step.
- **Water Leach:** Produce an impure Li_2SO_4 solution
- **Impurity Removal:**
  - Primary Impurity Removal
  - Secondary Impurity Removal
  - Tertiary Impurity Removal
  - Quaternary Impurity Removal
  - Ion exchange
- **Membrane Electrolysis:** With lithium sulphate solution
- **Crystallisation:** To produce $LiOH \cdot H_2O$ or carbonation to produce Li_2CO_3
- Pilot Plant had a Li recovery of 95.8%

Nemaska Process

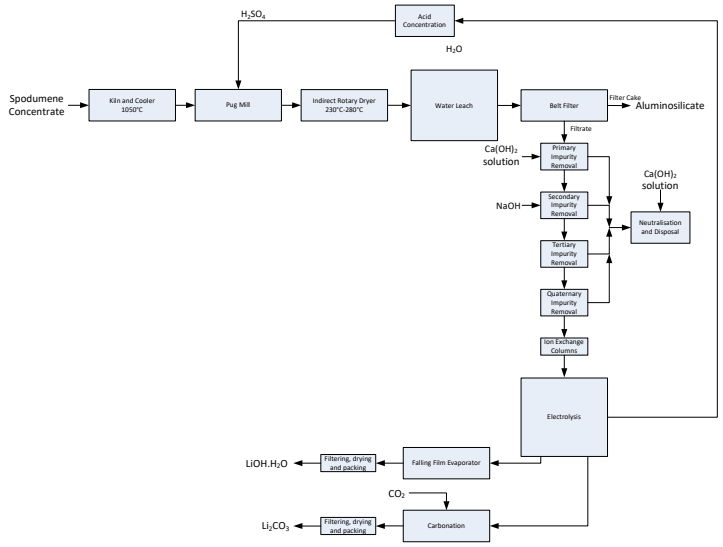

Nemaska Process

Membrane Electrolysis

- Similar to ELi process however sulphuric acid is produced instead of H_2 and Cl_2
  - H_2SO_4 is concentrated and recycled
- Li_2SO_4 electrolyte is recirculated until lithium content drops to ~2.1-2.7 g/L Li
- Spent electrolyte recirculated to leach
- LiOH recycled from crystallisation process

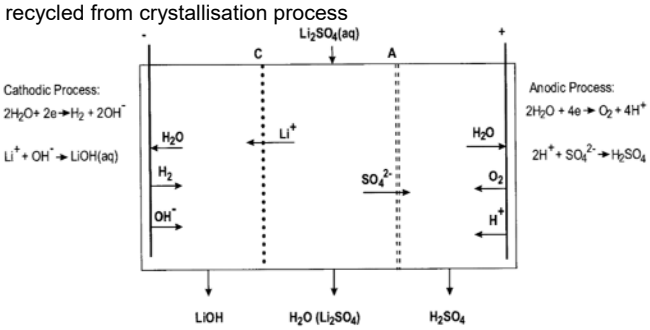

Nemaska Process

- Nemaska Lithium Phase 1 plant under construction
  - Electrolysis cell has been operated for 400 hours
  - Operated before commissioning the purification systems prior to membrane electrolysis
  - Commissioning is now complete and tests and a solution is being processed

Source: Nemaska Lithium

Lepidolite Treatment

- Commonly studied
  - Flotation is difficult
  - Wide spread distribution of ore
  - Contains the rare earth metals rubidium (Rb) and caesium (Cs)
- Extraction processes comprised of 2 stages, sulphation and water leaching, much like spodumene processing
  - Benefits from not requiring a thermal treatment step

Sulphation

- Sulphuric acid method uses highly concentrated H_2SO_4
- Lime method uses limestone
  - Requires a large amount of energy

Water Leaching

- To achieve Li extraction of over 90% by water leaching defluorination is required
  - Typically conducted at temperatures of 860°C or higher

Zinnwaldite

- Is regarded as a variety of lepidolite with high iron content
  - High iron content compared to lepidolite has meant zinnwaldite has gone largely ignored
- Zinnwaldite concentrate lithium content is below that of other lithium bearing concentrates
  - 3 wt% Li_2O vs 3.3-4.1 wt% Li_2O in lepidolite and 4.1-7.1 wt% Li_2O in spodumene
- Often contains increased Rb and Cs content

L-Max Process

- **Fine Milling:** Increasing leach rates of the mica
- **Acid Leach:** leaching with H_2SO_4
- **Impurity Removal:**
  - Alum crystallisation
  - Fluoride Removal
  - Low pH precipitation
  - High pH precipitation
  - Calcium removal
- **Lithium Recovery:** precipitation of Li_2CO_3
- Currently undergoing pre-feasibility study for a Phase 1 L-Max Plant for Pioneer Resources targeting production for 2019
  - Bench scale test produced 99.7% Li_2CO_3
  - 93% of Cs extracted
  - Total lithium recovery of ~90%

L-Max Process

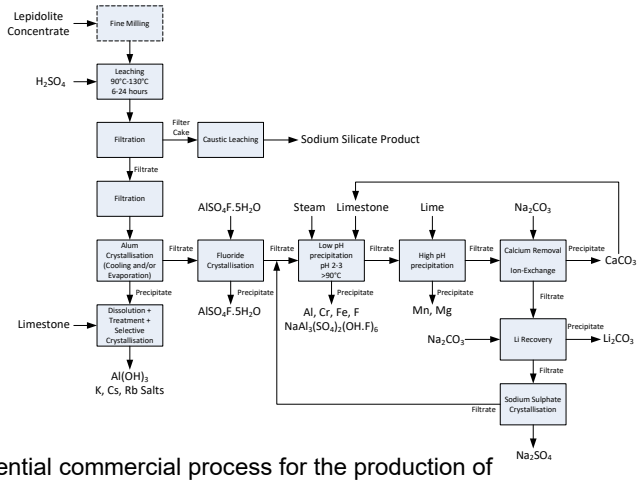

- Potential commercial process for the production of lithium from lithium bearing mica found in pegmatites
  - Lepidolite, amblygonite, zinnwaldite

SiLeach Process

- Lithium Australia Technology
- Halogen based process
- Designed to recover lithium and other metals from any silicate including spodumene, lithium micas, petalite, amphiboles, pyroxenes, tourmalines etc.
- Pure hydrometallurgical process
  - No roasting of spodumene,
  - Uses sulphuric acid leach
  - Lower CAPEX and OPEX

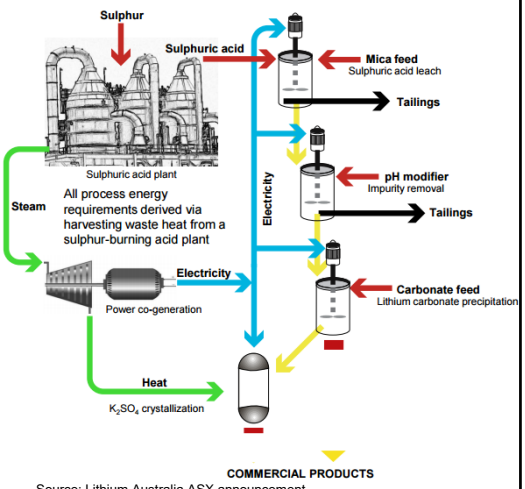

Source: Lithium Australia ASX announcement

SiLeach Process

- Pilot Plant
  - Fed continuously
  - Approximately 650 kg of lepidolite ore produced 6 kg/hr of Li_2CO_3 concentrate with a purity of 99%
  - Extraction of lithium in the leach circuit exceeded 95%
- Key feature of the process is skipping the traditional roasting step, which has very high energy costs.
- Large scale pilot plant for Port Headland in planning stages
- Working with Alix Resources to implement technology in Mexico on lithium-bearing hectorite and polylithionite clays

Source: Lithium Australia ASX announcement

SiLeach Process

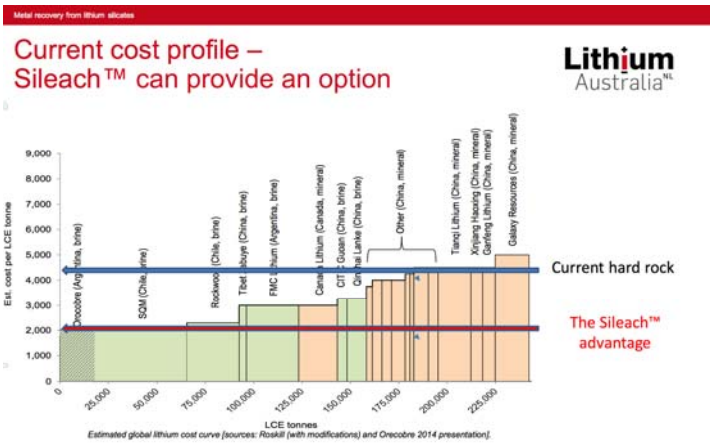

Source: Lithium Australia

Outotec Process

- Alkaline Pressure Leaching Process

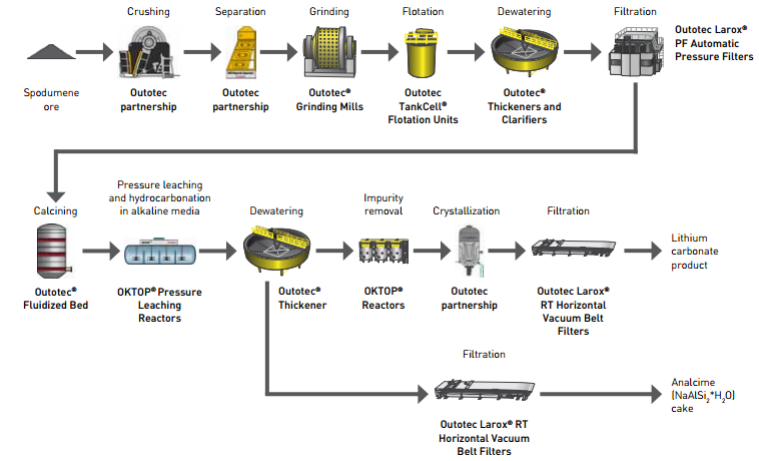

Source: Outotec

Outotec Process

- Patent applies to the processing of the concentrate
- Calcining is done and is necessary (spodumene concentrate)
- Leached in a series of autoclaves
  - High pressure steam with Na_2CO_3
  - 160-250°C
  - Produces Li_2CO_3 solution
- Leachate Carbonation
  - Counter current
  - Atmospheric pressure
  - 5°C-40°C
- Impurity Removal
  - Ion exchange: removal of trivalent and divalent cations, especially Ca, Mg, Al, Fe
- Lithium Carbonate Precipitation
  - Purified solution is heated
  - Decomposed bicarbonate precipitates Li_2CO_3

European Metals Holdings

- Completed pre-feasibility study regarding processing zinnwaldite
- Beneficiation plant utilised magnetic separation over flotation to produce lithium concentrate
- Lithium carbonate plant uses sodium sulphate roast
  - Mica concentrate/sodium sulphate/lime mixture
- Water leach to dissolve lithium potassium sulphate
  - Impurities leach into solution also
- Precipitation and adsorption stages to remove impurities
- Salt recycled back to the roaster
- Precipitation of lithium carbonate by addition of sodium carbonate to leach solution
- Purification stages to produce battery grade lithium carbonate

European Metals Holdings

- Potassium sulphate by-product
- Tested the L-Max process, although achieved higher recoveries, lower impurities and estimated lower OPEX with sodium sulphate roast

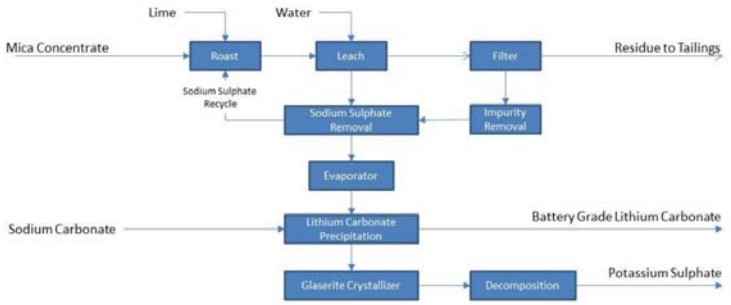

Source: European Metals Holdings

Lepidolite Project

- Flotation is the first stage to produce a concentrate
- For spodumene lithium concentrate roast alpha to beta followed by acid bake (sulphuric) followed by leaching and purification well established
- For lepidolite Testwork using sulphuric acid creates problems with impurity removal and waste stream issues
- Testwork showed sodium sulphate and lime roast for lepidolite is a selective process and relatively low reagent costs and.
- For lepidolite deflourinating roast followed by an alkaline sulphate pressure leach results very encouraging

OPEX Comparison Lepidolite

Process	LIT Aust	Gypsum Lime Roast	Sodium Sulphate Roast	Alkaline Pressure Leach	WL Clay Process	Sodium Chloride Roast
* $/tonne	2,600	2,700	1,700	1191	2,700	2,700
Ranking			2	1		

- Desktop studies and published resources
- Based on bench scale testwork
- Factored to suit specific project

CAPEX Comparison Lepidolite

Process	LIT Aus	Gypsum Lime Roast	Sodium Sulphate Roast	Alkaline Pressure Leach	WL Clay Roast
* CAPEX $M	180	140	100	112	135
Ranking			1	2	

- Desktop studies and published resources
- Based on bench scale testwork
- Factored to suit specific project

Other Considerations Lepidolite

- No commercial plants for lepidolite
- Results based on studies and bench scale test results
- No “new technology” . All unit operations are proven technology
- Carbon footprint comparison should be undertaken
- Piloting of best option is mandatory

Conclusions

- Producing battery grade lithium carbonate is still difficult from brine
- Lithium extraction from silicates, other than spodumene, is still a developing area
- Lithium extraction from spodumene still not the dominant source of lithium carbonate as brines are much cheaper to operate
- Impurity removal adds to the cost of production and technical difficulties of producing 99.99% lithium hydroxide or carbonate.
- New processes are emerging to extract lithium economically from the less common lithium ores
  - Sileach, L-Max etc.

Conclusions (Cont.)

- Spodumene flowsheets well established
- Lithium extraction from lepidolite is indicating alternative flowsheets are more applicable
- Lithium extraction from lepidolite indicates interesting OPEX and CAPEX conclusions. By-product credits can skew comparisons.
- Piloting will be mandatory
- Other considerations will impact on the final process flowsheet selection

Acknowledgements

- Thanks to ALTA 2017 for the opportunity
- Thanks to companies for permission to publish
- Thanks also to all colleagues, laboratory staff and other consultants for their help and contribution
- Thanks to vendors for the photos

References

- Alix Resources. *Electra Project*. Available at: http://www.alixresources.com/?page=projects&name=Electra-Project [Accessed 05/04/17]
- Anzaplan. *Conversion of Spodumene to Lithium Chemicals.* 2017
- Anzaplan. *Recovery of Lithium from Mica*, 2017
- Bauer R.J, Wietelmann U. Lithium and Lithium Compounds - Available at: https://www.researchgate.net/229749201_fig3_Figure-2-Flow-sheet-for-lithium-carbonate-production-from-spodumene [Accessed 7 Apr, 2017]
- Deutsche Bank. *Deutsche Bank Market Research: Lithium 101*. 2016
- European Metals Holdings. *Preliminary Feasibility Study Confirms Cinovec as Potentially Low Cost Lithium Carbonate Producer*. 2017. Available at: https://www.europeanmet.com/wp-content/uploads/2017/03/2017019_-_EMH_Completion_of_PFS-2.pdf [Accesses 20/04/17]
- Felix Brandt, Reiner Haus, New concepts for lithium minerals processing, Minerals Engineering, Volume 23, Issue 8, July 2010, Pages 659-661, ISSN 0892-6875, http://dx.doi.org/10.1016/j.mineng.2010.03.021. (http://www.sciencedirect.com/science/article/pii/S0892687510000920)
- Gunther Martin, Carsten Pätzold, Martin Bertau, Integrated process for lithium recovery from zinnwaldite, International Journal of Mineral Processing, Volume 160, 10 March 2017, Pages 8-15, ISSN 0301-7516, http://doi.org/10.1016/j.minpro.2017.01.005. (http://www.sciencedirect.com/science/article/pii/S0301751617300054)
- J. Jandová, P. Dvořák, Hong N. Vu, Processing of zinnwaldite waste to obtain Li2CO3, Hydrometallurgy, Volume 103, Issues 1–4, June 2010, Pages 12-18, ISSN 0304-386X, http://dx.doi.org/10.1016/j.hydromet.2010.02.010. (http://www.sciencedirect.com/science/article/pii/S0304386X10000484)
- Lepidico. 2016. *L-Max ® Technology*. Available at: http://www.lepidico.com/the-technology/lmax/ [Accessed 04/04/17]
- Lithium Australia. 2016. ASX ANNOUNCEMENT. Available at: https://lithium-au.com/wp-content/uploads/2016/11/0292017-ANSTO-Pilot-Results-Run-1A.pdf [Accessed 05/04/2017]
- SEDAR- Western Lithium, King Valley PFS.

References

- Lithium Australia. 2016. SiLeach – Processing Overview – Lithium Australia. Lithium Australia Youtube Video. Available at: https://www.youtube.com/watch?v=t6fjsCyrYiA [Accessed 04/04/17]
- Nemaska Lithium Incorporated. 2016. *Feasibility Study Update on the Whabouchi Lithium Deposit and Hydromet Plant (revised)*. Available at: http://www.nemaskalithium.com/assets/documents/docs/2015-024%20Nemaska%20NI%2043-101%20June%208%202016%20Final-SEDAR.pdf [Accessed 30/11/16]
- Neometals. 2014. *Electrolysis of LiCl to produce LiOH.* Neometals - Youtube video. Available at: https://www.youtube.com/watch?v=aDv-aZ9GBeU [Accessed 24/11/16]
- O. Sitando, P.L. Crouse, Processing of a Zimbabwean petalite to obtain lithium carbonate, International Journal of Mineral Processing, Volumes 102–103, 25 January 2012, Pages 45-50, ISSN 0301-7516, http://dx.doi.org/10.1016/j.minpro.2011.09.014. (http://www.sciencedirect.com/science/article/pii/S0301751611001402)
- Orocobre Limited, *Lithium Market* [ONLINE] Available at: https://www.orocobre.com.au/Lithium_Market.htm [Accessed 04 April 2017]
- Pioneer Resources . *L-Max Process Generates High Specification Battery Grade Lithium Carbonate Using Pioneer Dome Lepidolite.* 2017
- Pratima Meshram, B.D. Pandey, T.R. Mankhand, Extraction of lithium from primary and secondary sources by pre-treatment, leaching and separation: A comprehensive review, Hydrometallurgy, Volume 150, December 2014, Pages 192-208, ISSN 0304-386X, http://dx.doi.org/10.1016/j.hydromet.2014.10.012. (http://www.sciencedirect.com/science/article/pii/S0304386X14002278)
- University of Pittsburgh. *Pegmatitic Textures* [ONLINE] Available at: http://www.pitt.edu/~cejones/GeoImages/2IgneousRocks/IgneousTextures/5Pegmatitic.html [Accessed 04 April 2017]
- Sharma, Yatendra. 2014. *Processing of Lithium containing material*. Reed Advanced Materials. Patent Number: WO 2014026217 A1. Available at: https://www.google.com/patents/WO2014026217A1?cl=en [Accessed 24/11/16]
- Sharma, Yatendra. 2014. *Production of Lithium Hydroxide.* Reed Advanced Materials. Patent Number: WO 2016070217 A1. Available at: http://www.google.com/patents/WO2016070217A1?cl=en [Accessed 24/11/16]

- ACKNOWLEDGEMENTS

This document is a dynamic record of the knowledge and experience of personnel at Mineral Engineering Technical Services. As such it has been built upon over the years and is a collaborative effort by all those involved. We are thankful for the material supplied by and referenced from various equipment manufacturers, vendors, industry research and project partners.

LITHIUM PROCESS FLOWSHEETS - CHALLENGES AND OPPORTUNITIES

By

Chris Griffith

ANSTO Minerals, Australia

Presenter and Corresponding Author

Chris Griffith
cgz@ansto.gov.au

ABSTRACT

Over the last 4 years, ANSTO Minerals has undertaken a significant amount of work on the processing of lithium deposits to produce saleable lithium chemical concentrates. This work has encompassed everything from bench top process development through to continuous piloting (1-2 kg/h solid feed and 5-10 L/h liquor feed), and demonstration plant design and operation (2 m3/h brine feed).

Our execution of these programs has provided an excellent opportunity to compare and contrast the processing of brine and hard rock lithium deposits. It has become clear from this work that the processing of Li resources using conventional process flowsheets poses a number of challenges depending on the grade, mineralogy (for hard rock), impurity suite and location of the deposit. These challenges have in turn highlighted a number of opportunities for improvement, which we have examined for our clients.

Table I displays a brief summary of the main advantages, challenges and opportunities for conventional processing flowsheets for brine and hard rock deposits.

In the presentation we will provide an overview of the conventional process flowsheets for brine and hard rock deposits, plus several alternative process flowsheets, which are currently being developed for both types of projects.

Table I Brine and Hard Rock Process Flowsheets: Advantages, Challenges and Opportunities

Brine Processing		
Advantages	**Challenges**	**Opportunities**
Abundant resources	Resource estimation	Raw brine processing
By-product production	Resource utilisation	Integrated / efficient process
'Simple' processing	Remote location logistics	Li selective concentration step
↓Energy requirement	Time to production (>1 y)	
Proven production	Production losses	
	↑Mg:Li ratio	
Hard Rock Processing		
Advantages	**Challenges**	**Opportunities**
Abundant primary resources	Comminution	↓Temp. processes
Abundant secondary resources	Comparatively ↓grade	Spodumene hyromet. process
Resource estimation	↑Temp. - ↑Energy	Integrated / efficient processes
Supply diversity	Broad impurity suite	Li selective concentration step
Ready beneficiation		
By-product production		
Proven production		

Keywords: Lithium, Processing

Outline

- About ANSTO Minerals
- **Conventional** Lithium Process Flowsheets – Brines & Hardrock
- **Challenges/Opportunities** – Brines
- **Challenges/Opportunities** – Hardrock
- Summary
- Questions

About ANSTO Minerals

- Primarily contract research for listed and private companies
- Dedicated research team – **KEY** differentiator from service laboratories
- Extensive experience with U, RE, Zr, Nb, Ti, Li and other critical metals
- Process modelling and scoping engineering studies
- Control/Management of radioactivity in hydro- and pyro- flowsheets
- Pilot and demonstration plant operation

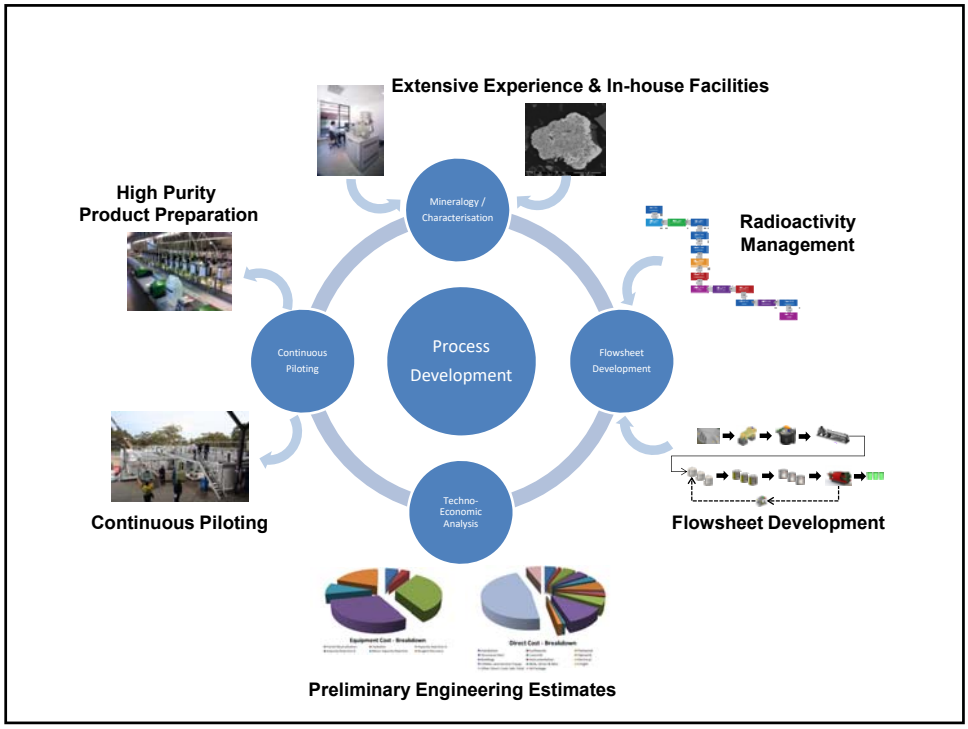

Lithium Brine Processing

Conventional Flowsheets

Lithium Brines

- Lithium-bearing brines
  - Endorheic salt lakes
  - Geothermal brines
  - Oil field brines
- Salt lake brines constitute a significant proportion of Li resources
- Commercial 'brine' operations only process salt lake brines
- Characteristics:
  - Evaporation >> Precipitation
  - Li-host rock – weatherable volcanic rocks
  - Geothermal energy source

Brine Deposits

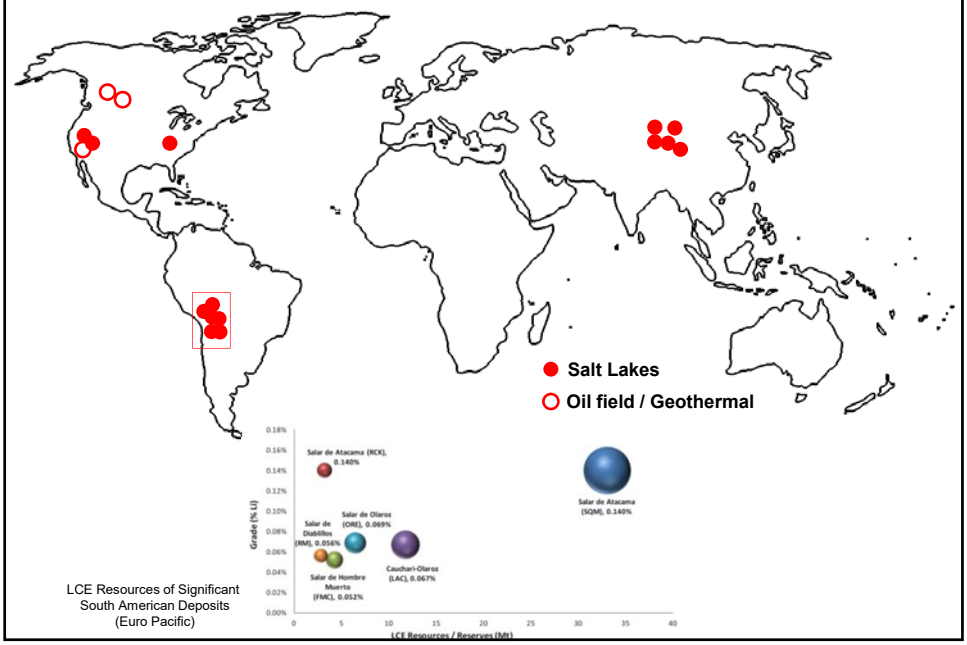

LCE Resources of Significant South American Deposits (Euro Pacific)

Brine - Compositions

- Characterised by elevated NaCl
- Varying K, Mg and S(SO_4)
- Gypsum saturated
- B content – ulexite ($NaCaB_5O_9.8H_2O$) relationship

Source	Salar de Atacama (Chile)*	Salar de Uyuni (Bolivia)#	Clayton Valley (USA)**
Element/Species	(~g/L)		
pH	Typically 6 to 7		
B	0.44	0.8	0.07
Ca	0.45	0.3	0.45
Cl	230	50	77
K	38	11	4.2
Li	1.6	0.4	0.16
Mg	11.8	8	0.19
Na	111	70	49.6
S	5.8		1.2

Brine – Extraction

- Hydrogeology is key
- Brine deposits are fluids hosted in porous stratified structures
- Intermixing occurs naturally + after extraction commences

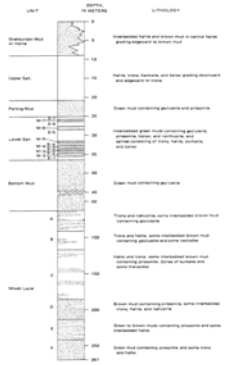

Searles Lake – stratigraphic section
(taken from Smith, 1979)

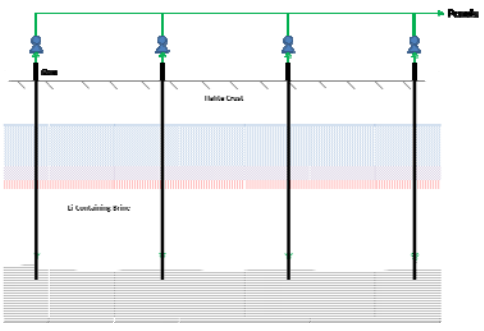

Brine – Solar Evaporation

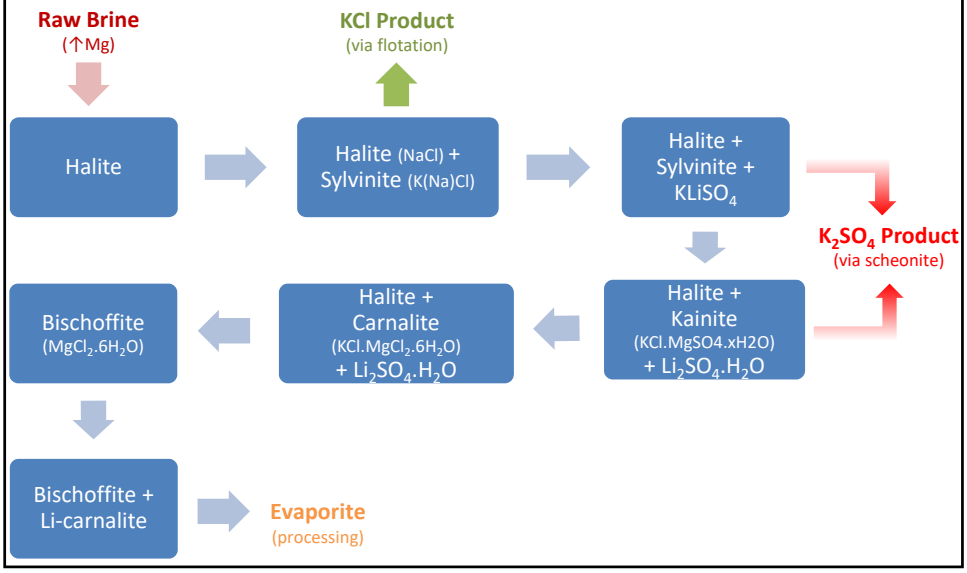

Conventional Processing

Brines

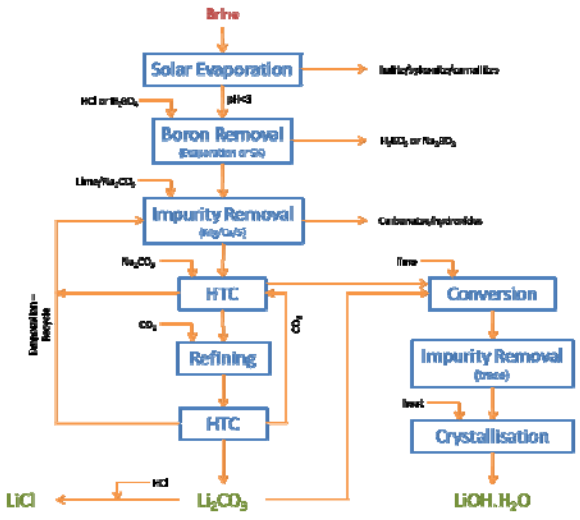

- Simplistic flowsheet
- Major Li products
- Common approaches:
  - » Impurity Removal
  - » Refining of LC
  - » Conversion to LH
  - » Recycle of Li

FMC ALBEMARLE SQM Chemetall

Conventional Processing
Salar del Hombre Muerto

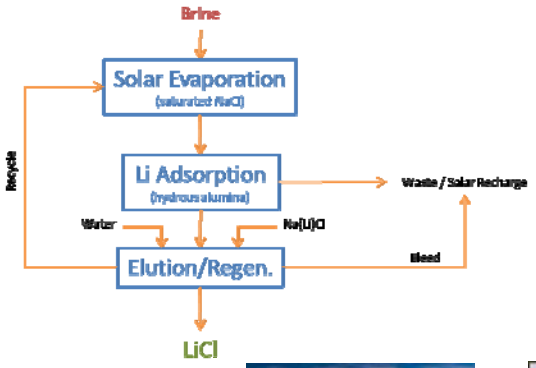

- FMC, commercial op.
- 1997 start-up
- LiCl product
- 'Novel' adsorbent use
- Logistics challenges

FMC

Conventional Processing
Brines - Challenges / Opportunities

Advantages	Challenges	Opportunties
Abundant resources	Resource estimation	**Raw brine processing**
By-product production	Resource utilisation	**Integrated/efficient processes**
'Simple' processing	Remote location logistics	**Li selective conc. step**
↓Energy requirement	Time to production (>1 y)	**'Direct' LH production**
Proven production	Production losses	
	↑Mg:Li ratio	

» Alternative processing technologies – near-term…

Alternative Processing

Brines

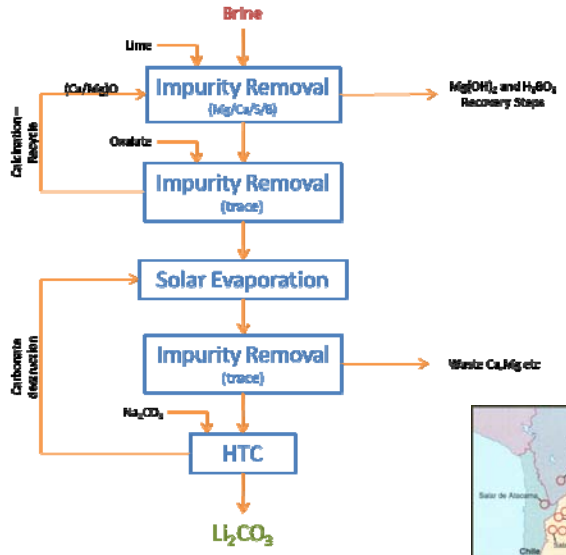

- Salar de Uyuni brine
- Scoping (lab) study
- ↑Mg+B circumvented
- Solar evap. required
- Mg and B by-products
- Opex unclear

Tran et al, Hydromet. (2012)

Alternative Processing

Brines

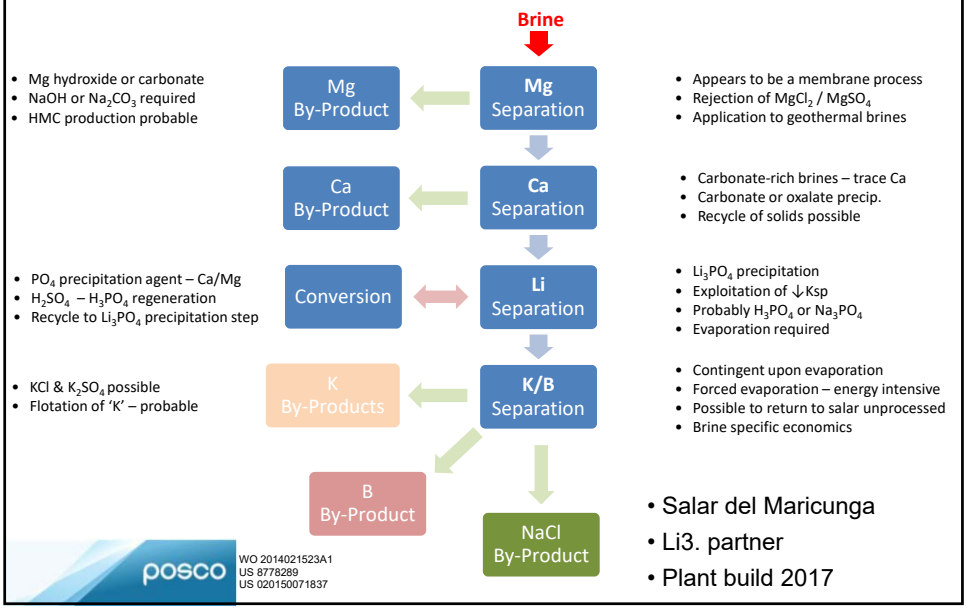

- Mg hydroxide or carbonate
- NaOH or Na_2CO_3 required
- HMC production probable

- Appears to be a membrane process
- Rejection of $MgCl_2$ / $MgSO_4$
- Application to geothermal brines

- Carbonate-rich brines – trace Ca
- Carbonate or oxalate precip.
- Recycle of solids possible

- PO_4 precipitation agent – Ca/Mg
- H_2SO_4 – H_3PO_4 regeneration
- Recycle to Li_3PO_4 precipitation step

- Li_3PO_4 precipitation
- Exploitation of ↓Ksp
- Probably H_3PO_4 or Na_3PO_4
- Evaporation required

- KCl & K_2SO_4 possible
- Flotation of 'K' – probable

- Contingent upon evaporation
- Forced evaporation – energy intensive
- Possible to return to salar unprocessed
- Brine specific economics

- Salar del Maricunga
- Li3. partner
- Plant build 2017

Alternative Processing
Brines

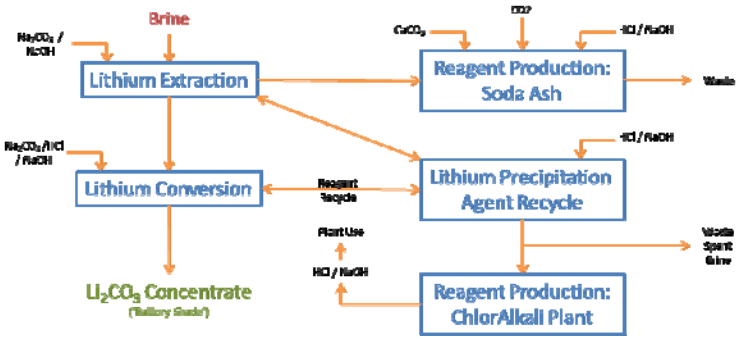

- Salar de Rincon, Argentina
- Enirgi Ltd 100%
- DFS issued 2016
- Demonstration plant 2017

Alternative Processing
Brines

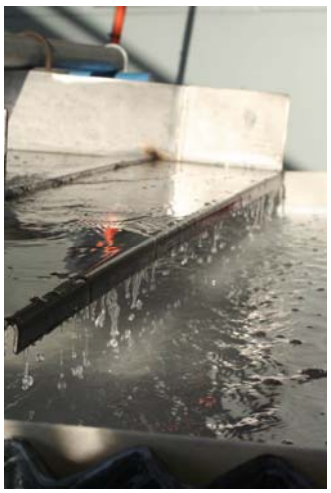

- Modular demo plant built at ANSTO
- 1 month operation, 2015

Alternative Processing

Brines

- Mg&Ca-Cl/SO_4 salt rejection
- NF – feasible, some scaling
- pH adjustment – trace Mg/Ca

- M^{2+} removal required for Li SX
- pH re-adjustment required
- Li_2SO_4 product stream
- [Li] possibly >10g/L
- Organic losses – critical

- Electrolysis – LiOH and H_2SO_4
- Neometals – Cl-based
- [Li] ~20g/L (~33g/L sat.)
- H_2SO_4 balance unclear

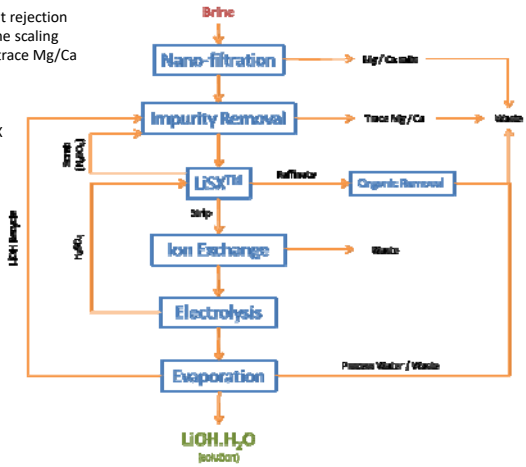

- Waste to aquifer
- Organic removal – key
- Trace elements – key

- IX for divalents
- Others – unspecified

tenova BATEMAN TECHNOLOGIES

- Pure Energy, Clayton Valley South
- PEA in 2017

Lithium Hardrock Processing

Conventional Flowsheets

Hardrock Deposits

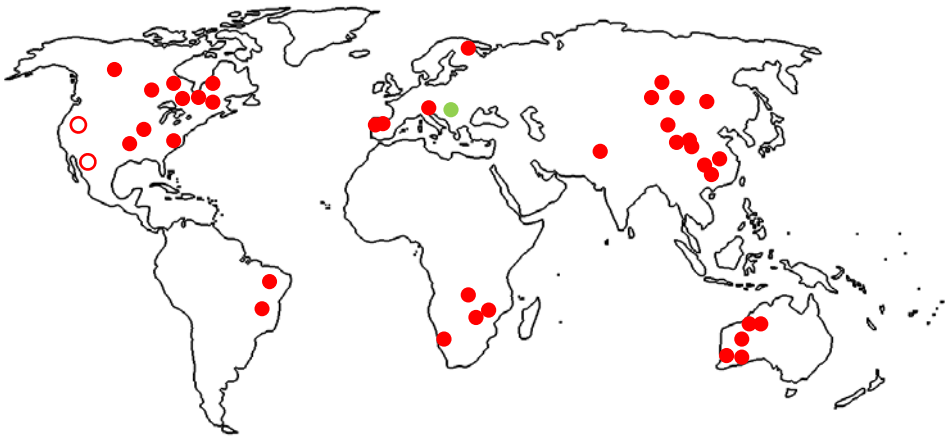

Compilation of various sources including:
Euro Pacific (2013), BRGM (2015)

Hardrock Lithium

- Multitude of lithium-bearing minerals
  - >130 identified / reviewed*
  - dominated by silicates & phosphates
- Deliberate limitation to minerals of economic importance
- Classic resource defn (vs challenges with brines)

Mineral	Formula	Li_2O	Li
		(~%)	(~wt%)
Spodumene	$LiAl(SiO_3)_2$	8	3.7
Lepidolite	$K(Li,Al)_3(Si,Al)_4O_{10}(F,OH)_2$	7.7	3.6
Jadarite	$LiNaSiB_3O_7(OH)$	7.3	3.4
Zinnwaldite	$Li_2K_2Fe_2Al_4Si_7O_{24}$	3.4	1.6
Petalite	$LiAl(Si_2O_5)_2$	4.5	2.1
Hectorite	$Na_{0.3}(Mg,Li)_3Si_4O_{10}(OH)_2$	1.2	0.6

*Anstett (1990), USGS (2002) Kesler (2012), BRGM (2015)

Conventional Processing

Spodumene

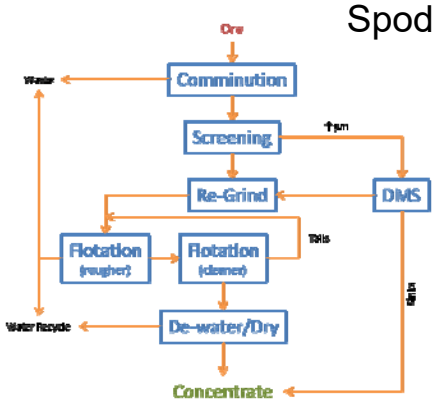

- Crushing / screening / grinding
- Collector – fatty acid
- Flot rougher grade – ≥2wt% Li
- Flot cleaner grade – >>3wt% Li
- S-Q and S-M(L) associations
- Deposit specifics

*Redeker (1979), Andrews (1993), Mendez (2004)

Conventional Processing

Spodumene

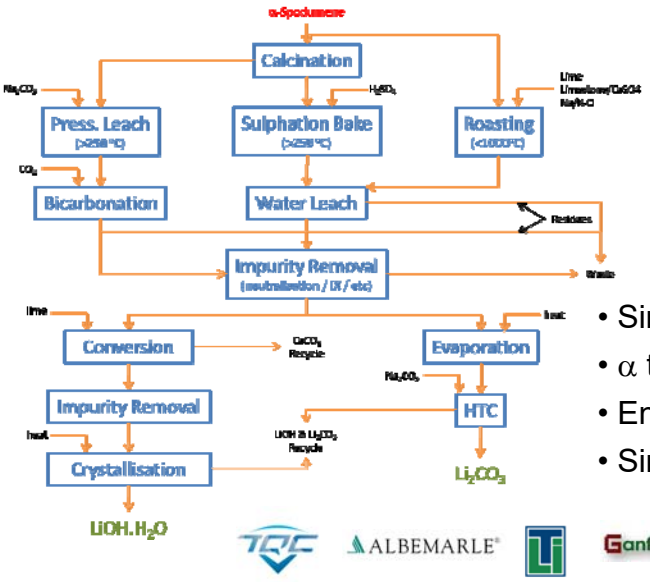

- Simplified flowsheet/s
- α to β essential
- Energy intensive
- Simple back-end/s

Conventional Processing

Clays (hectorite)

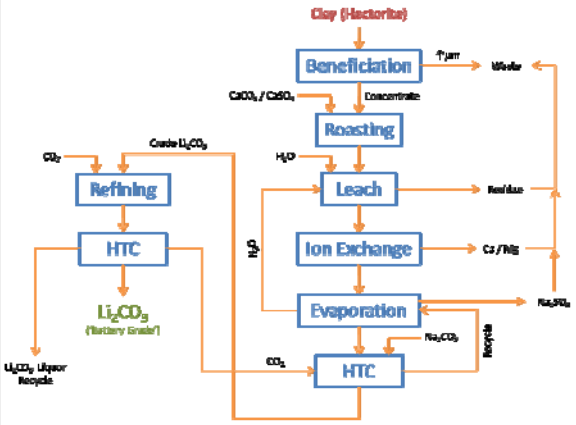

- Simplistic flowsheet
- Beneficiation essential
- Dependent on roasting:
  - » ↑% Li extraction
  - » Al&Mg rejection key
  - » Recycle of Li
  - » Refining of LC required
- Bacanora Minerals & Lithium Nevada (L/Am.)

*modified from LA NI43-101 06/06/16 and BM PFS 16/04/16)

Conventional (?) Processing

Lepidolite

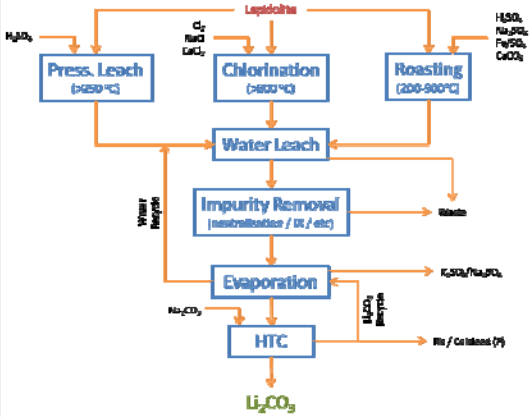

- V.limited processing data
- Simplified flowsheet/s
- Wide variety of reagents
  - » Reflective of feedstock(?)
  - » Secondary resource utilisation
- Energy intensive
- Impurity challenges
  - » F, K, Rb and Cs

Conventional Processing
Hardrock - Challenges / Opportunities

Advantages	Challenges	Opportunties
Abundant 1º resources	Comminution	↓Temp. processes
Abundant 2º resources	Comparatively ↓grade	Spodumene hydromet. process
Resource estimation	↑Temp. - ↑Energy	Integrated/efficient processes
Supply diversity	Broad impurity suite	Li selective concentration step
Ready beneficiation		'Direct' LH production
By-product production		
Proven production		

» Alternative processing technologies – near-term…

Alternative Processing
Spodumene

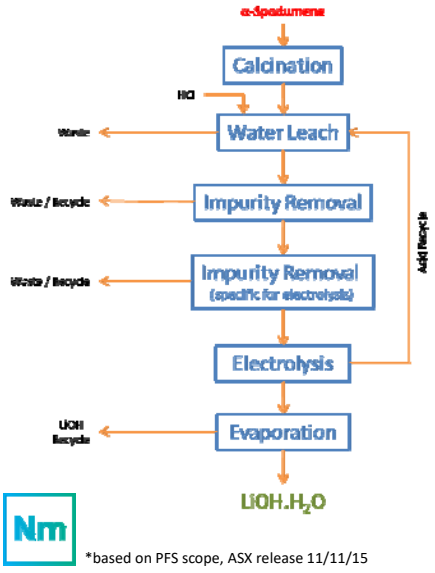

*based on PFS scope, ASX release 11/11/15

- Simplified flowsheet
- Calcination still required
- Energy intensive but..
- Simplified back-end
- 'Direct' LH prodⁿ

Alternative Processing

Spodumene

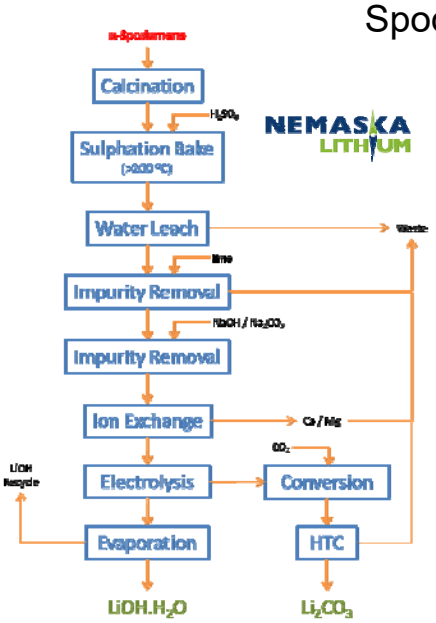

- Simplified flowsheet
- Calcination still required
- Energy intensive but…
- Simplified back-end
- 'Direct' LH prod^{n}
- 'Indirect' LC prod^{n}

*modified from NI43-101 FS revised 08/06/16

Alternative Processing

Lepidolite

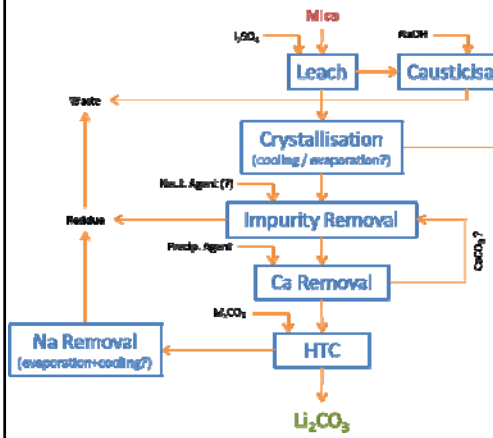

*modified from www.lepidico.com.au

Lepidico

- Simplified flowsheet (public)
- Not applicable to spodumene
- Continuous piloting
- Indicated by-products:
  - » Na_2SiO_3
  - » SOP
- Avoids roast / calcination
- Impurity challenges
  - » Na, K, Rb and Cs, and others

Alternative Processing

Lepidolite

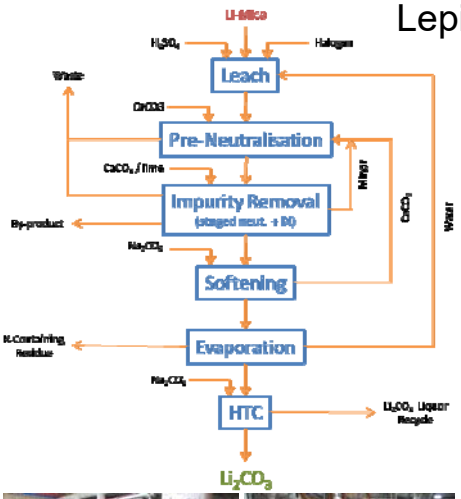

- Simplified flowsheet
- Applicable to all micas and spodumene (with 'tweek')
- Continuous piloting
- Indicated by-products:
  - » SOP
- Avoids roast / calcination
- LC to LH conversion

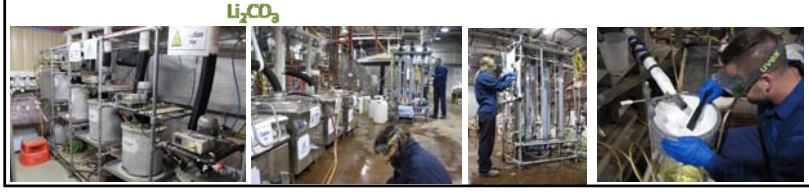

Lithium Australia NL

Alternative Processing

Jadarite

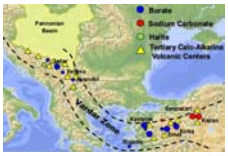

RioTinto

- $LiNaSiB_3O_7(OH)$ – kryptonite
- V.Limited process details
- Specific only to Jadar deposit
- Piloting at Bundoora
- Beneficiation - undefined
- Indicated products:
  - » H_3BO_3
  - » Li_2CO_3
- B – SX or xtal step (like brine)
- Impurity challenges (like hardrock)

Summary

- Conventional flowsheets for brines and hardrock have pros/cons
- Brines – key opportunities
  - » Raw brine processing
  - » Integrated/efficient processes
  - » Li selective concentration step
  - » 'Direct' LH production
- Hardrock – key opportunities
  - » ↓Temperature processes
  - » Spodumene hydromet process
  - » Integrated/efficient processes
  - » Li selective concentration step
  - » 'Direct' LH production
- Several new process flowsheets for brine and hardrock projects tick these 'boxes', but there is significant scope for further development

HYDROMETALLURGICAL PROCESSES FOR THE RECOVERYOF LITHIUM FROM SILICATES

by

Adrian Griffin

Lithium Australia, Australia

Presenter and corresponding author

Adrian Griffin
adrian.griffin@lithium-au.com

ABSTRACT

Lithium Australia NL has been developing a number of hydrometallurgical process flowsheets for the recovery of lithium from silicates. The most advanced of these, the halogen-based SiLeach™ process, was developed specifically for the digestion of spodumene, a refractory lithium pyroxene previously able to be processed only by roasting, followed by sulphation bake and water leach. The SiLeach™ process, which relies on the reaction of halogens with silicon-oxygen bonds, is widely applicable to the dissolution of all categories of silicate minerals and has found practical application in the processing of lithium micas. SiLeach™ is currently being commercialised, utilising pilot facilities established at ANSTO Minerals (a division of the Australian Nuclear Science and Technology Organisation).

With SiLeach™, the halogens can be added to the process slurry in a number of ways. However, the preferred method is via the addition of ground fluorine minerals (which may include the lithium micas themselves) to the process slurry prior to the addition of sulphuric acid. Due to the kinetics of competing reactions, this sequence allows the momentary generation of fluoride in solution – and its almost instantaneous reaction with the silicates – without any accumulation of hydrogen fluoride (‘HF’) in the slurry. Process plant operations can be accomplished without the hazards often considered a risk with fluorine-based processes.

The SiLeach™ process is capable of recovering a wide range of by-products, as all metals in the target silicate are dissolved. The low energy requirements of the process, as well as by-product credits, enhance the economics, which may result in lithium production costs using SiLeach™ to be among the lowest currently experienced.

SiLeach™ has the potential to provide access to a wide range of plant feed previously not considered viable. Such feed includes low-grade spodumene concentrates and micas as primary feed sources. Furthermore, vast quantities of lithium minerals currently discharged as tailings from non-lithium mining operations create very attractive targets for the application of this type of technology. Utilisation of these materials as lithium sources will greatly enhance the sustainability of the lithium industry.

Keywords: SiLeach™, lithium, spodumene, mica, halogen, fluorine, hydrometallurgy

INTRODUCTION

There are two historic sources of lithium: hard rock and brine occurrences. Each presently accounts for about half of global lithium demand (USGS, 2017). Lithium-bearing 'clays' are also a promising source, with a number currently under investigation for future production (Ausenco, 2016).

Regardless of type, all commercially significant lithium sources have a common provenance – they result from magmas that have accumulated a high concentration of volatile elements. Those volatile elements, including lithium, reach the near-surface, exploitable accumulations by:

- emplacement of pegmatites;
- development of greisens;
- degassing of aqueous components, or
- generation of hydrothermal fluids.

Very specific tectonic conditions are required to provide an environment in which volatile components and lithium accumulate. It is the chemistry of the last stages of volatile magma emplacement that provide many of the keys to dissolution of silicate minerals under commercial conditions. Indeed, due to the unique circumstances encountered in these intrusions, which invariably solidify at shallow crustal levels or generate violent explosive volcanic events, natural fluxes and solvents accumulate in abundance.

High quantities of water in these melts depress the liquidus and high pressures (relative to atmospheric) prevent the water separating as a single phase – such conditions are beyond the critical point of water. Other accumulated fluxing elements further **depress** the solidus, in particular lithium ('Li'), boron and phosphorus. As the magmas rise and pressures reduce in these melts, the distinction between magmatic and hydrothermal fluid blurs.

These final fluid phases are of great interest, since their behaviour demonstrates the possibility of recreating similar conditions within commercial processing systems that can reverse the natural sequence and take minerals back into solution. The SiLeach™ process has achieved this reversal; as such, it can be considered a digestion process rather than a simple leach.

THE PYROMETALLURGICAL/HYDROMETALLURGICAL TRANSITION

In terms of extractive metallurgy, the definitions of 'pyro' and 'hydro' are quite distinct, but within the bowels of the earth the processes cross – there is no distinct boundary: the extreme pressures can generate a process continuum. However, other factors are also at work. The fluxing characteristic of many of the 'incompatibles' results in hydrous melts of specific chemistry with very low melting points. At the extreme, the water-saturated melts approach the operating conditions that can be achieved in mineral processing autoclaves. That being the case, the phase chemistry of these late-stage magmatic products offer some keys as to how the processes may be reversed, exploiting the ability of metals to return to an aqueous phase.

Late-stage magmas, and magmatic fluids accumulate incompatible elements – those that don't readily fit into the lattice of the common rock-forming minerals. Some are too big to fit conveniently into most silicates and get a 'free ride' into the late-stage fluids, particularly as temperatures and pressures drop below the critical point of water, which decompresses to form an aggressive solvent that harbours the incompatible elements.

Other elements, such as fluorine, generate such a depression of the solidus that they become a self-fulfilling component – one that remains in a molten state (morphing into the late-stage aqueous fluids) because they act as fluxing agents and their ever-increasing concentration creates an ever-reducing solidus temperature. As fractional crystallization in the magma chamber advances, the fluid phase composition trends towards a complex eutectic point, while the remaining magma has a relatively low viscosity. High-level intrusives solidifying within a few kilometres of the earth's surface may transgress the critical point of water, explosively propelling the remaining low-viscosity fluids into brittle fractures of the surrounding country rock. This is how pegmatites are formed.

So, it is the behaviour of water and the fluxing agents that provides the key to reversing the process in a synthetic, controlled environment, resulting in the dissolution of silicate minerals at low temperatures and pressures.

VULNERABILITY OF SILICATES TO HYDROTHERMAL PROCESSES

Examination of naturally occurring, low-temperature magmatic processes may provide empirical evidence as to which minerals are best suited to attack by hydrometallurgical processes, as well as the conditions in which that attack may be effectively controlled.

TAKING NATURE ONE STEP FURTHER

The dissolution of ore minerals in sulphuric acid systems is commonplace. Sulphides are oxidised at atmospheric or low-pressure conditions, to a large extent mimicking weathering processes. Taking these natural processes and exaggerating the corrosion conditions in a synthetic system may amplify the kinetics – and this amplification may be great enough to render the process of metal extraction a commercial reality within an acceptable residence time.

High-pressure acid leach processes employed in nickel extraction reduce the dissolution and deportment of the chemical components from millions of years to hours or even minutes. The natural secrets of these chemical processes remain preserved in the lateritic profile for the astute student to observe.

The dissolution of silicates may be considered a reversal of the crystallization processes preserved in the geological record as pegmatites and greisens. To artificially reverse such processes, water must be introduced into the system and other volatiles/fluxes added to the mineral slurry. The halogens, principally fluorine ('F') and chlorine ('Cl'), play an important role in the natural systems. Indeed, at elevated temperatures and pressures, Cl may well be a significant factor in transporting other elemental species. At lower temperatures and pressures, the dominant reactive halogen is F, as recorded in the composition of mineral species – mica in particular – as crystallization proceeds.

Increased concentrations of F in late-stage pegmatite fluids often result in fluorite ('CaF_2') overgrowths on earlier F-bearing phases such as topaz or tourmaline, which both crystallize earlier than CaF_2 and contain significantly less F than CaF_2. This attests to the rising concentration of this important halogen in the final stages of pegmatite crystallization. In many cases, the miarolitic cavities within which the CaF_2 crystalizes are silent witnesses to the relatively low-pressure conditions under which the pregnant F liquors may carry soluble components. Jacobson (2013) summarised many of these occurrences as follows.

> *The anorogenic … granites formed from the melting of lower crustal rocks during crustal thinning are due to tension, not compression related to continental collisions or subduction. The miarolitic, vuggy character of these granites is due to the upper part of the magma rising to a shallow emplacement in the crust. This shallower, lower pressure environment allowed water to exsolve from the magma as the pressure decreased and to form bubble-like pegmatite cavities. Almost any NYF [niobium yttrium fluorine] granite with miarolitic pegmatites may contain attractive fluorite crystals.*

Although the miarolitic pegmatite of the NYF association is a very specific example, it does serve to demonstrate that aqueous F solutions are the medium for mass transfer in natural systems with temperatures as low as 200 degrees Centigrade and pressures of 200-250 megapascals (London *et al*, 2012).

Without resorting to the pressures found in geological systems, the activity of F can be harnessed to break the silicon-oxygen ('Si=O') bond (Kuang *et al*, 2012), the very building block of silicate minerals. Moderate concentrations of F are required in solution, as is elevated temperature. Lithium Australia NL ('Lithium Australia') has been developing its 100 per cent owned SiLeach™ process to achieve that goal.

CONVENTIONAL PROCESSING

Spodumene has long been the only commercially processed hard-rock lithium mineral. Conventional processing relies on a phase conversion from low-temperature α-spodumene to the higher-temperature polymorph β-spodumene to enhance leach performance in sulphuric acid. While this process – which effectively rejects the gangue elements, leaving lithium as the principal revenue source – is energy intensive, its selectivity is an advantage, since it results in simple processing steps following the initial phase conversion. That said, lack of significant by-product credits is a commercial disadvantage with conventional processing of spodumene.

The cost of producing lithium carbonate('Li_2CO_3') from a spodumene concentrate of 7 per cent lithium oxide a ('Li_2O') is about US$4,500 per tonne ('t') (Roskill, 2016). It follows that the cost of producing Li_2O using similar processes but with lithium mica at half the grade should be twice as much. Deutsche Bank (2016) has confirmed the veracity of this assumption, indicating that the operating costs of Chinese producers using a lithium mica feed approach US$8000/t (see Figure 1 – far right-hand bar).

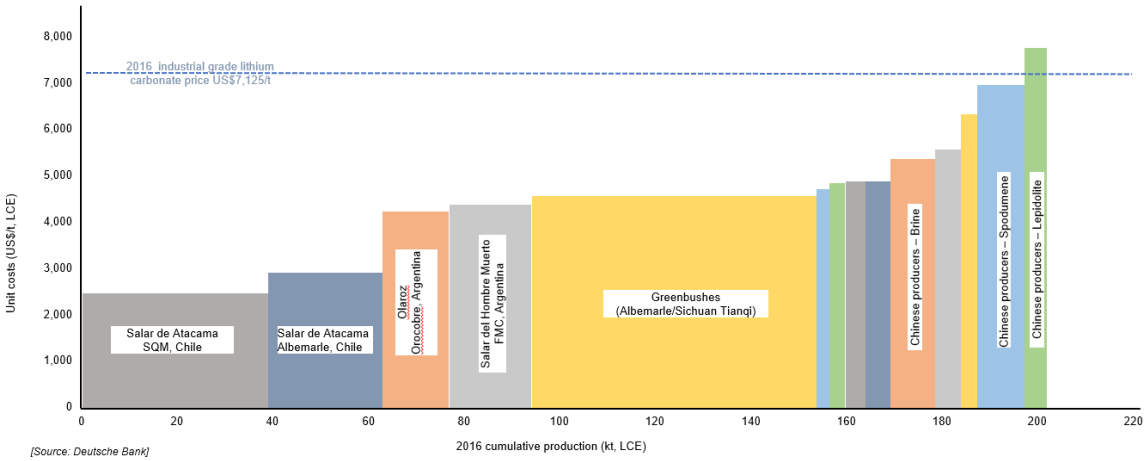

Figure 1. Li_2O cost curve, after Deutsche Bank (2016). If conventional processing technology is used, the lowest-cost production is from brines, followed by spodumene (and petalite) and, lastly, lithium micas.

DEVELOPMENT OF THE SILEACH™ PROCESS

Having studied the paragenesis of pegmatites and greisens, Lithium Australia made the following observations.

- Many hard-rock lithium occurrences demonstrate crystallization of lithium minerals from magmatic phases with high levels of water and fluorine.
- Many of the late-stage, relatively low temperature and pressure minerals contain F as a major constituent of the crystal lattice.
- Li and F increase in the magma towards the eutectic, which arises from partial crystallization of fertile magmas.

A critical component in the genesis of lithium ore minerals is F chemistry and, if high temperatures and high pressures are to be avoided during the extraction of lithium from lithium minerals, that chemistry remains critical in the re-dissolution processes.

SiLeach™ is a broad-spectrum, halogen-based digestion process developed to recover metals from silicates without the requirement to roast. In fact, SiLeach™ is a reversal of the last stages of fertile magma crystallization. Lithium recovery is the principal aim of SiLeach™, although it may be commercially applied to other alkali metals. Aluminium ('Al') and silicon ('Si') are also available for the production of valuable by-products.

LITHIUM MINERAL ACTIVITY SERIES

Lithium Australia studied a number of both lithium and non-lithium minerals to determine digestion characteristics under comparable conditions using sulphuric acid at elevated temperature (see Figure 2).

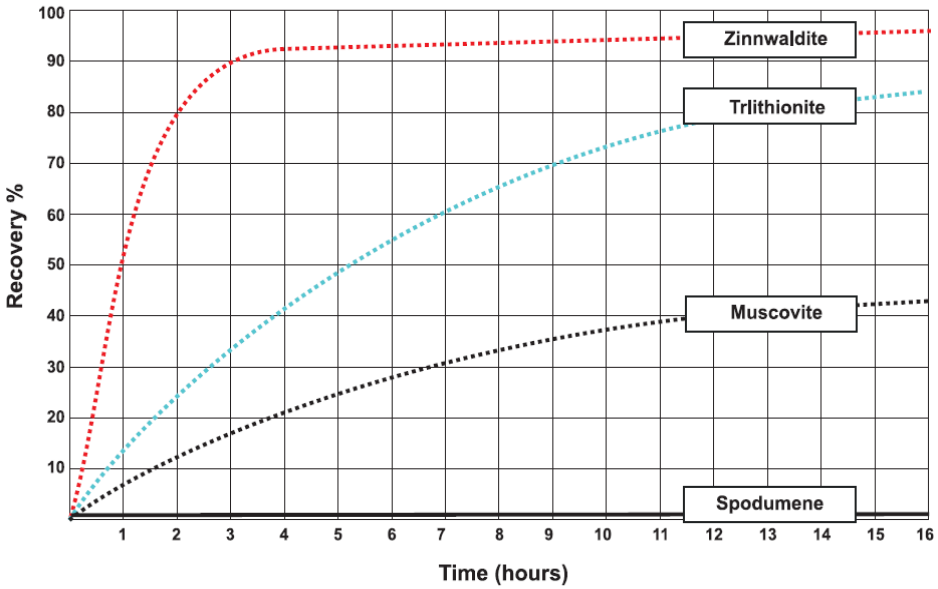

Figure 2. Digestion curves for a number of lithium silicates in sulphuric acid at 90 degrees Centigrade. The micas show a range of reaction kinetics, whereas spodumene, a lithium pyroxene, is unreactive.

The fundamental difference between the reactivity of these mineral species is the F activity generated by dissolution of the minerals themselves in sulphuric acid. Zinnwaldite typically contains around 7 per cent F, trilithionite (lepidolite) 4 to 5 per cent F and muscovite around 1 per cent F. Spodumene contains no F in the mineral lattice. Alterations in the contained F within the mica have a profound influence on the reaction rates of micas in sulphuric acid, and changing the amount of F available to react with the silicates can modify the reaction curves to such an extent that it is possible to create conditions for the kinetically slower species to approach the reaction rate of zinnwaldite.

MICA REACTIONS

A mica's reactivity depends on its structure and the way in which that structure presents active lattice sites, or exposed chemical bonds, to the lixiviant. Reactions that liberate metals from phyllosilicates include:

- ion exchange;
- protonation of anions, or
- destruction/replacement of Si=O or other tetrahedrally coordinated oxygen bonds.

The mica group can be divided into dioctahedral and trioctahedral structures. The latter have more reactive sites per lattice unit that the dioctahedral micas and hence greater ion exchange capacity and greater reactivity in acids. How hydroxyl dipoles (OH^-) are oriented also influences mineral reactivity.

In strong sulphuric acid solutions, ion exchange reaction mechanisms are less important than the protonation of anions, OH^- and F^- in particular. These are only exposed on surfaces perpendicular to the minerals' perfect cleavage. Indeed, when viewed perpendicular to the C-axis, micas expose only outward-facing oxygen atoms, being the base of silica tetrahedra. The exposed atoms, and the connecting Si=O bonds, are inert to sulphuric acid and consequently the reaction kinetics are controlled largely by the surfaces exposed perpendicular to the cleavage planes.

As the aspect ratio of exposed surfaces in micas (C:A or C:B crystallographic axes) is very large, and as the large surface area is dominated by oxygen at the termination of Si=O bonds, most of the

exposed surfaces are unreactive. The abundance of the reactive OH- bonds is low, due to their exposure only on the relatively small surface areas exposed perpendicular to the cleavage. This results in long reaction times in sulphuric acid, as few reactive species, OH^- and F^-, are exposed to the attack of hydrogen ions ('H^+'). The reaction of the acid on the mica is generally slow but, as it progresses, it releases F^- from the lattice, which is then available to attach to the Si=O bonds that form the framework of the mica (see Figure 3).

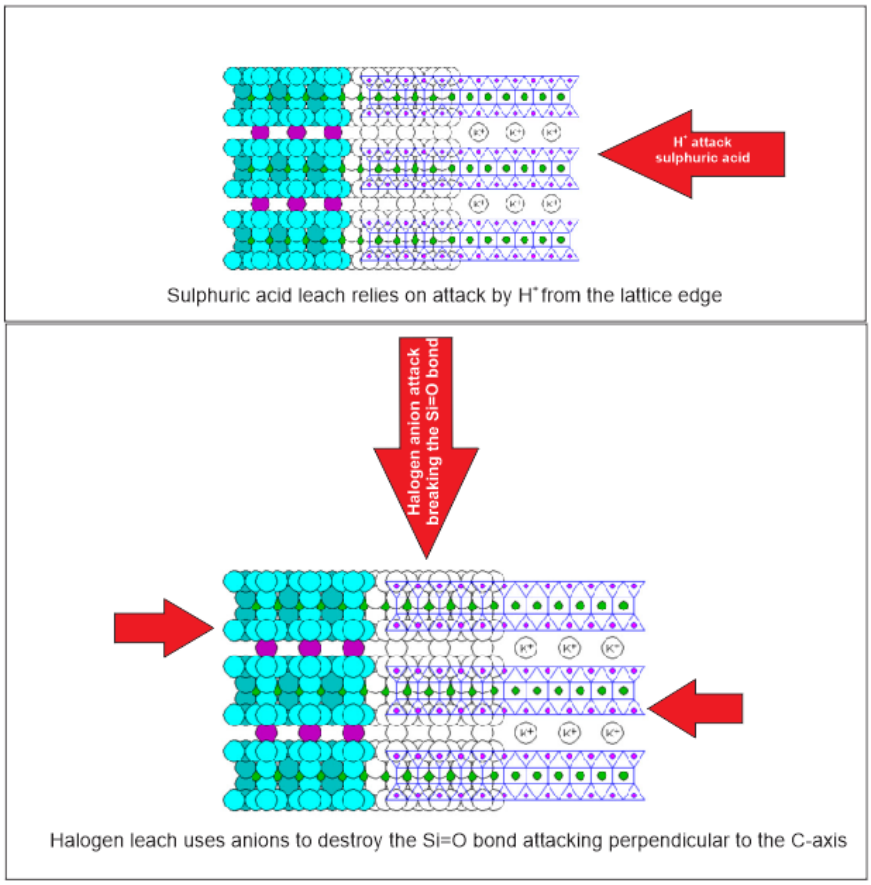

Figure 3. Hydrogen ions attack micas only on the very limited exposed area perpendicular to cleavage, whereas fluoride ions can attack the vast surface area exposed on cleavage planes, significantly improving reaction kinetics.

Thus, the rate of attack of F^- on Si=O bonds, and hence the rate of digestion of a mica in sulphuric acid, is determined by the amount of F^- the mica can release into solution.

If the amount of F^- in solution is increased by the addition from a source not derived from the mica, then the reaction kinetics can be changed. For example, the stoichiometric addition of F^- to lepidolite, resulting in the same concentrations that would be expected from zinnwaldite, will create a digestion rate for lepidolite that is similar to that of zinnwaldite in sulphuric acid.

Taken to the extreme, spodumene, a Li pyroxene, can also be made to react at a similar rate, and it is the control of these reaction rates that forms the basis of the SiLeach™ process (see Figure 4).

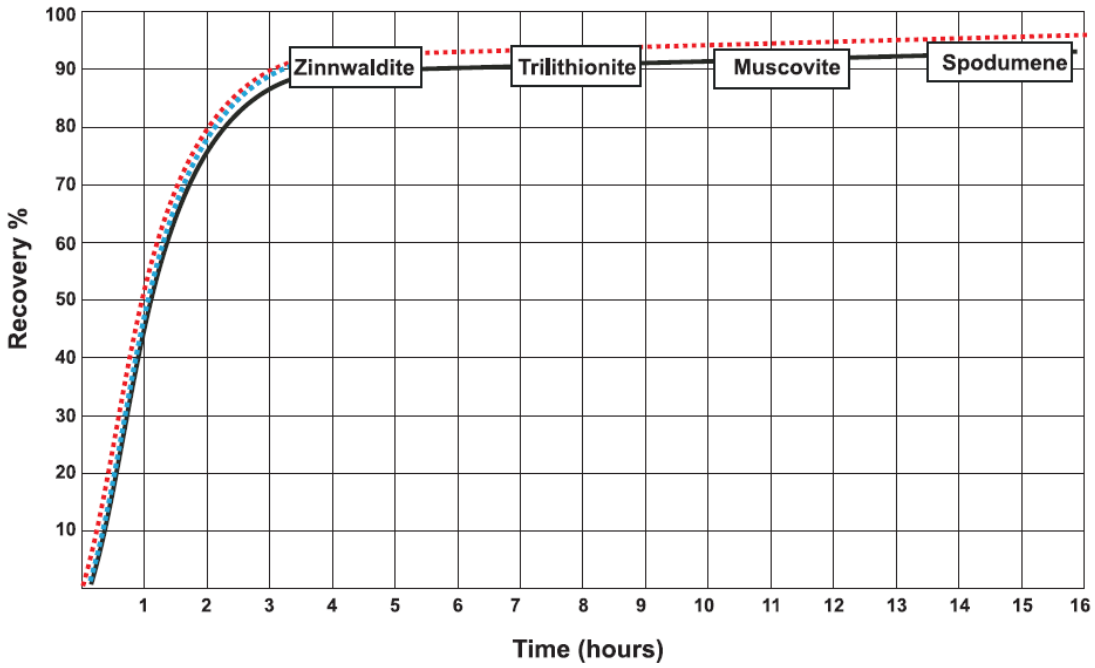

Figure 4. Addition of F to sulphuric acid can result in most silicate materials, including spodumene, having similar dissolution curves.

BENEFITS OF SILEACH™

SiLeach™ is a non-selective, halogen-based digestion system. By facilitating the destruction of Si=O bonds, it allows access to cations in the silicate lattice that release all metals into solution. Thus, there is the opportunity to recover metals other than lithium from minerals digested using the SiLeach™ process. In the case of the lithium micas, the framework of the lattice provides abundant Si and Al, whereas the octahedral sites harbour abundant Group 1 metals, among them potassium, Li, rubidium and caesium. To a lesser extent, sodium, manganese and iron may also be present in the lattice. The potential for abundant by-product credits, together with the elimination of the requirement to roast, are key elements of the SiLeach™ processing strategy.

While process flowsheet specifics vary with mineral species, the flowsheet for micas is a good example of the steps involved in the process (see Figure 5).

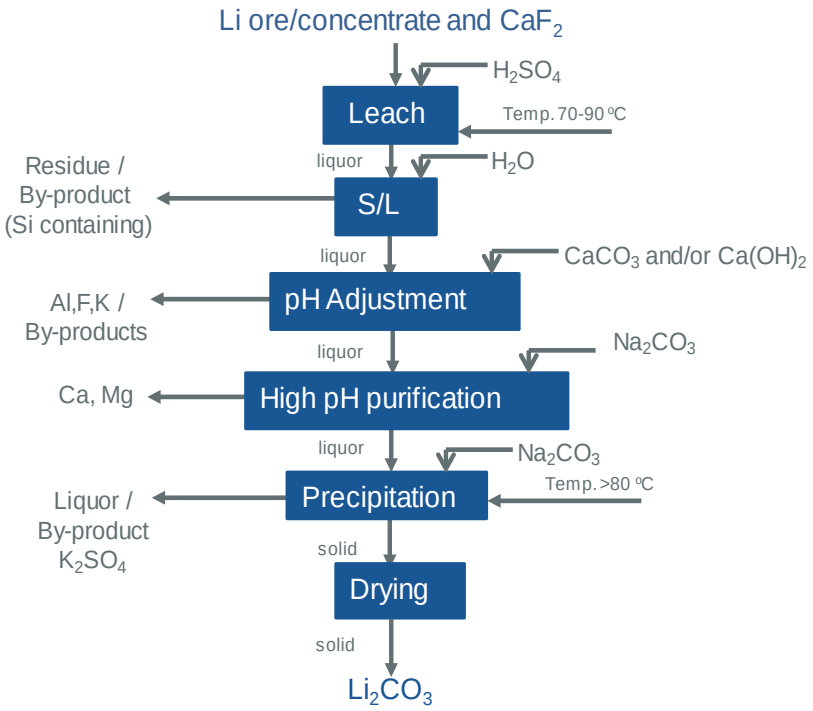

Figure 5. SiLeach™ flowsheet for lithium mica plant feed

ALTERNATIVES TO SILEACH™

Clearly, conventional processing is an alternative to SiLeach™ but the energy cost is high and revenue is restricted largely to Li. In the case of micas, the release of fluorine, in the form of HF vapour, is a safety issue. Moreover, materials of construction and corrosion of the equipment are of practical concern.

Hydrometallurgical alternatives to SiLeach™ are few, and leaching in sulphuric acid alone is kinetically restrictive on all but the most reactive Li minerals.

Elevating temperature and pressure – the domain of platinum producers and lateritic nickel operations – is an alternative. The application of pressurised reaction vessels certainly presents another dimension to the processing of Li silicates, allowing the options of both acid and caustic systems. Lithium Australia, in association with ANSTO Minerals (a division of the Australian Nuclear Science and Technology Organisation) has been developing the LieNA™ process – a moderate temperature caustic leach that requires pressure containment. LieNA™, which is capable of digesting all the common Li minerals (including spodumene), allows for project-specific process optimisation, facilitating capitalization on unique factors such as local logistics, reagent costs and energy casts.

CONCLUSIONS

While the reactivity of most Li minerals in sulphuric acid is kinetically limited, the kinetics can be improved by adding fluorine to the processing system in a way that minimises the production of volatile F species – HF in particular – that would otherwise present an occupational health and safety risk. The operational perfection of F-assisted leaching is the essence of Lithium Australia's 100 per cent owned SiLeach™ process.

Raising temperatures, and elevating pressures beyond atmospheric, provides the flexibility to digest Li silicates in either acidic or caustic environments. Caustic digestion is the foundation of the LieNA™ process, currently under development by Lithium Australia.

ACKNOWLEDGEMENTS

The author wishes to acknowledge the contributions of Lithium Australia, its staff and consultants; in particular, work undertaken at ANSTO Minerals and Murdoch University and partially funded by two Innovation Connections Grants under the Entrepreneurs' Programme of the Department of Industry, Innovation and Science, plus a grant provided by the Minerals Research Institute of Western Australia.

Pioneers of hydrometallurgical work such as Arthur J Moxham (1925) laid the foundations of much modern sulphuric acid process development and have been an inspiration to all. Enej Catovic led Lithium Australia team's research, while Andrew Skalski, also at lithium Australia, has begun the task of transforming that research into a commercial reality.

Also instrumental in development of these processes have been Lithium Australia's shareholders, not only as owners of the Company but as its financiers, and their support is also gratefully acknowledged.

REFERENCES

1. Ausenco: Technical Report on the Prefeasibility Study for the Sonora Lithium Project, Mexico (prepared for Baconora Minerals Ltd). *April 2016. 186 p.*

2. Deutsche Bank Market Research: Lithium 101. *May 2016. 177 p.*

3. Jacobson, M.I.: Fluorite in granitic pegmatites. *Rocks and Minerals, 2013, Vol. 88 (2).*

4. Kuang, G., Chen Z., Guo, H. & Li, M.: Lithium extraction method for α-spodumene by fluorine chemical method. *Advanced Material Research. 2012, Vol. 524-527, pp 2011-16.*

5. London, D., Morgan, G.B., Paul, K.A. & Guttery, B.M.: Internal evolution of miarolitic granite pegmatites at the Little Three Mine, California, USA. *Can Mineral, Aug 2012, Vol 50 (4), pp 1025-54.*

6. Moxham, A.J.: US Patent 1,538,837 Manufacture of aluminium sulphate, May 19, 1922.

7. Roskill: Lithium. Global Industry, Markets and Outlook to 2025. *2016, 13 Ed., 386 p.*

8. U.S. Geological Survey (USGS): Mineral commodity summaries 2017. *U.S. Geological Survey 2017, 202 p.*

Uranium-REE Proceedings

Not Presented

Included in proceedings but not presented

QUANTITATIVE ANALYSIS OF URANIUM AND THORIUM CONTAINING MATERIALS USING INDUSTRIAL ON-LINE XRF ANALYZER

By

Elena Hasikova, Alexander Sokolov and Vitaly Titov

Baltic Scientific Instruments, Latvia

Corresponding Author

Elena Hasikova
e.hasikova@bsi.lv

ABSTRACT

Precise and accurate determination of uranium (U) and thorium (Th) in mineral materials in real time is essential for many industrial processes. Laboratory and pilot tests show the possibility to provide acceptable measurement accuracy at high representativeness and speed of analytical feedback using the online X-ray fluorescence analysis. Results are demonstrated for continuous measurement of U and Th at wide ranges of concentrations (from 100 ppm up to several %) in various materials: rutile and zircon heavy mineral sands; phosphate rock and fertilizers; limestone rocks as unconventional U and Th resources; monazite concentrate as U and Th associated resources; U ore residues after heap-leaching, and other similar materials.

Keywords: uranium and thorium, mining, mineral materials, online XRF analysis, industrial conveyor analyzer, pilot test, analytical parameters of measurement.

INTRODUCTION

Currently economically viable U ores contain 0.05-0.07 % uranium oxide (U_3O_8). 1000 metric tons of U ore that contains < 0.1 % U_3O_8 has to be withdrawn from the depth of the earth (or dissolved with in-situ-leaching process) to produce each 1 ton of U_3O_8, without considering the enormous amount of dead rock from the open pits or shuffles[1].

Small amounts of Th are present in all rocks (for example, granite) and soils. Soils usually contain 5-12 parts per million (ppm) of thorium. Thorium is concentrated mainly in monazite - a mixed phosphate of rare earth elements (mainly - cerium) and thorium: it may contain up to 12% ThO_2. It is the rare earth elements (REE) minerals that are the source of thorium production. Thorium itself is usually not mined; it is extracted as a by-product in the extraction of REE and uranium [2,3]. Nevertheless, Th as a nuclear fuel is clean and safe and offers significant advantages over uranium. The technology for several types of thorium reactors is proven but still must be developed on a commercial scale. In the case of commercialization of thorium nuclear reactor Th raw material will be in demand [4].

With all this, mining and processing companies producing uranium, thorium and rare earth elements will require prompt and reliable methods and instrumentation for U and Th quantitative analysis. In most mining and mineral processing operations, the ore or other material flow is transported with the help of conveyor belts between various stages of processing. The quality and grade of the flow is typically tested by periodically selecting several samples from material on the conveyor and the sample bags are sent to a laboratory for analysis. The laboratory results are usually available several hours later for the process operators, which is too late for making any adjustments. Also, the method of taking discrete point samples from the ore flow results in sampling errors, since one cannot be sure about the material flow being homogenous from hour to hour and minute to minute.

In present paper we demonstrate results of laboratory studies and small-scale industrial tests of on-line XRF analysis for concentration measurements of U and Th on conveyor belt in real time mode. Thus, the analysis data is immediately available for the process operators to make necessary adjustments for the next processing steps. Application of on-line XRF analysis doesn't require sampling preparation and allows making the measurement process fully automated.

ON-LINE ANALYZER DESCRIPTION

All results have been obtained using on-line XRF analyzer CON-X [5], equipped with analytical software for calculation of elements concentration. It is generally known that results of online analysis are influenced by the changes in external industrial parameters: temperature and humidity of the material and production environment, changes in grain size of material, variation of flow height on the conveyor etc. Online XRF analyzer CON-X is designed and fabricated accounting for the actual situation at the industrial conveyors. Changes in the distance between the moving flow and the analyzer and humidity variation are compensated by special software mathematical algorithms. Analyzer was mounted directly above the conveyor belt to measure and analyze crushed U- and Th-bearing materials (uranium ore, residues after heap leaching, heavy mineral sands etc). A photo of industrial on-line XRF Analyzer CON-X is shown in Fig.1.

Fig.1.On-line XRF analyzer CON-X02 on the industrial conveyor

Uranium can be found as one of the components in phosphate ores in the amount of 50-200 ppm[6]. The world U resources in phosphate rock are estimated as $9x10^6$ metric tons [7]. In production, U is left in fertilizers as a radioactive contaminant. Figure 2 below shows spectra of Moroccan phosphate rock and phosphate fertilizers produced form the rock (mono-calcium=MCP and mono-ammonium=MAP phosphates). U lines are identified in all these materials even in 5-10 minute measurements.

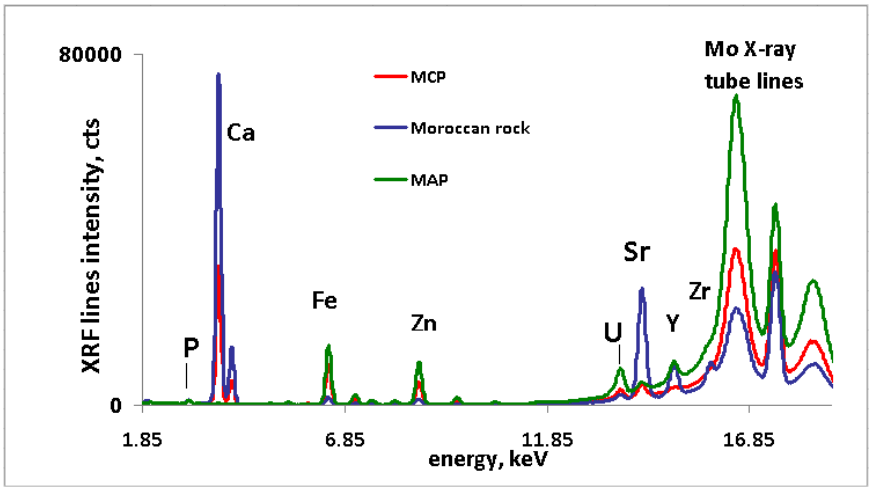

Fig.2. Spectra of phosphate rock and MCP and MAP fertilizers. Parameters of measurement: X-ray tube voltage - 39 kV, current – 100 μA, 100 μm thick Mo filter of primary radiation, measurement time 600 seconds, distance between sample and detector 50 mm.

Detection limit (DL) of U in phosphate rock was quantitatively estimated in line with the procedure 40CFR part 136 of EPA as 30 ppm U in the range of concentrations 50-300 ppm. Estimated accuracy of U determination was ≤ 10 ppm (2σ). This level of quantification allows the analyzer to facilitate sorting of raw phosphate rock or monitoring of uranium level in commercial fertilizers.

URANIUM ORE RESIDUES AFTER HEAP-LEACHING

The residues of U ore after the process of heap leaching are materials of complex composition: they can contain a wide variety of components in different amounts. On-line measurement of U in ore residues was carried out on a pilot conveyor at Areva Mines. The study showed that U may be determined in the matrices containing a number of interfering elements (rubidium, molybdenum and zircon) with accuracy ≤ 10% (2σ) at a measurement time of 600s.The level of U remaining in ore residue after heap leaching is critical for process quality.100 ppm U is indicated as the upper critical level in order for the residues to be discharged to the dumps.

Test samples of leached residues from different deposits were provided for study. Samples contained from 60 to 500 ppm U. Examples of XRF spectra measured for U-ore residues from different deposits are shown in Figure 3. One can see that about 15 elements can be measured from the same spectra. Detection limit (DL) is estimated at 30-50 ppm U in 5-10 minute measurements depending on interfering element.

Dedicated software BSIKit based on the Method of Fundamental Parameters was successfully used to solve the problem of the overlapping lines Rb Ka and U La and to calculate U concentrations in the solid residues after U extraction with accuracy ≤ 10%.

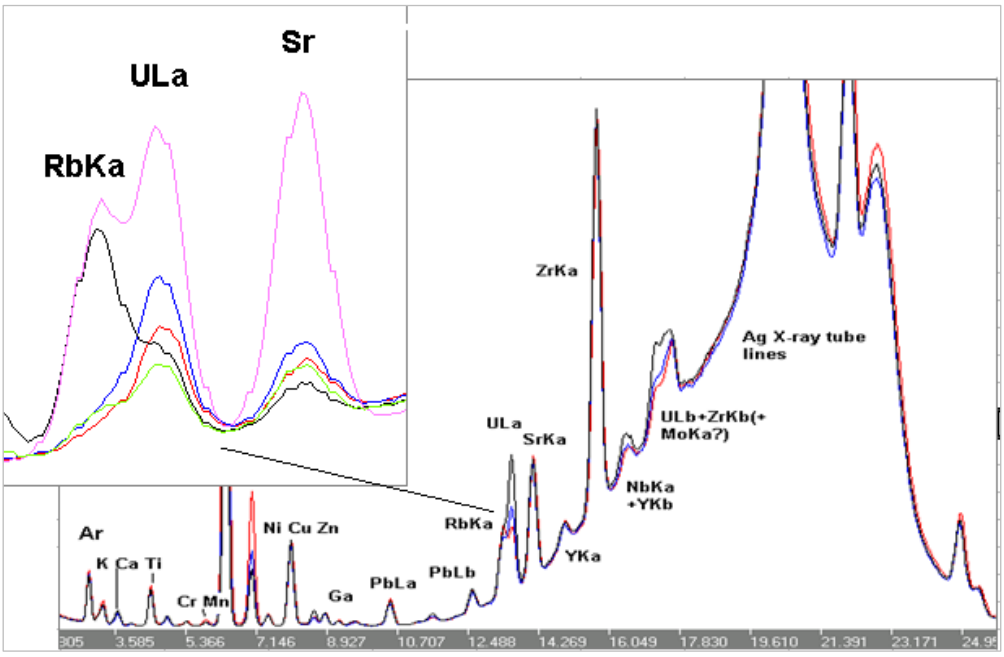

Fig.3. XRF spectra of U ore residues after heap-leaching process. Parameters of measurement: Ag X-ray tube voltage - 36 kV, current – 500 μA, 100 μm thick Ag filter of primary radiation, measurement time 600 seconds, distance between sample and detector 50 mm.

Calibration curves measured with Ag X-ray tube and a set of calibration samples are demonstrated on Figure 4. Intensities of U La and U Lb are plotted vs. uranium concentrations. Linearity in the range of uranium content from 30 to 220 ppm is high, correlation coefficient R^2 is close to 1. U La and Lb lines grow proportionally with U concentrations.

The CON-X conveyor analyzer can be a useful tool for controlling changes in the residual content of U (Th) in uranium wastes, providing the operator with operational information on the efficiency and quality of heap leaching technology. Real-time measurements can give a quick response about the

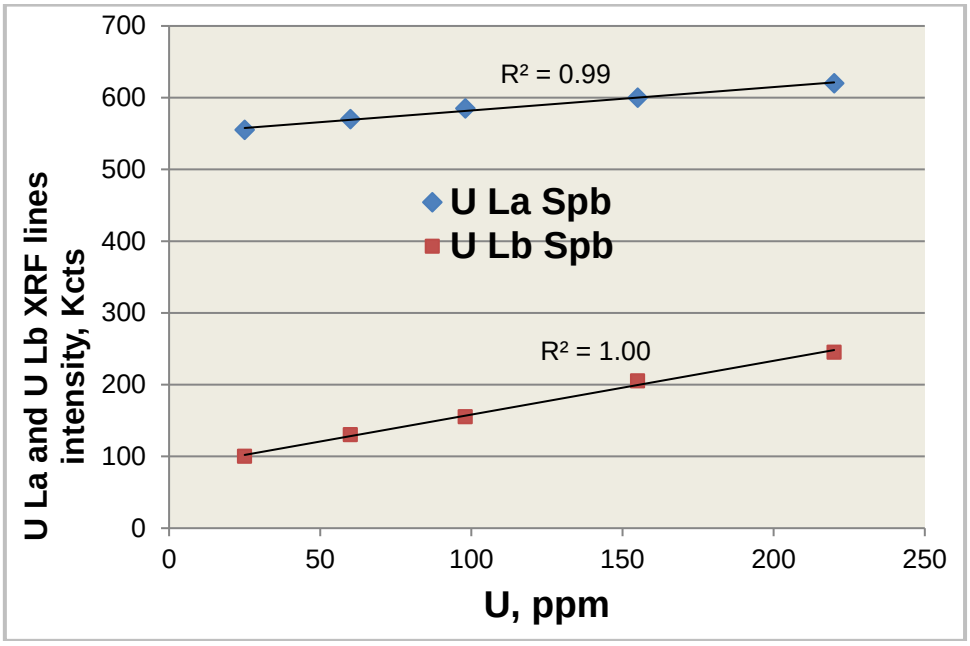

Fig.4: Calibration curves: U La and U Lb lines intensity (Ag X-ray tube) are plotted vs. uranium concentrations

undesirable increase of U (Th) in the residues. It can also be a very useful tool for assessing the environmental impact by measuring the concentration of radioactive and rare earth elements sent to the dumps[8].

Figure 6 demonstrates a screen-shot of U concentration trend that was obtained during small-scale testing of analyzer CON-X at Areva Mines pilot conveyor. It is obvious from the Figure 6 that the analyzer confidently distinguishes between different concentration levels. So it can serve as modern tool that enables to measure or monitor uranium traces in process residual materials.

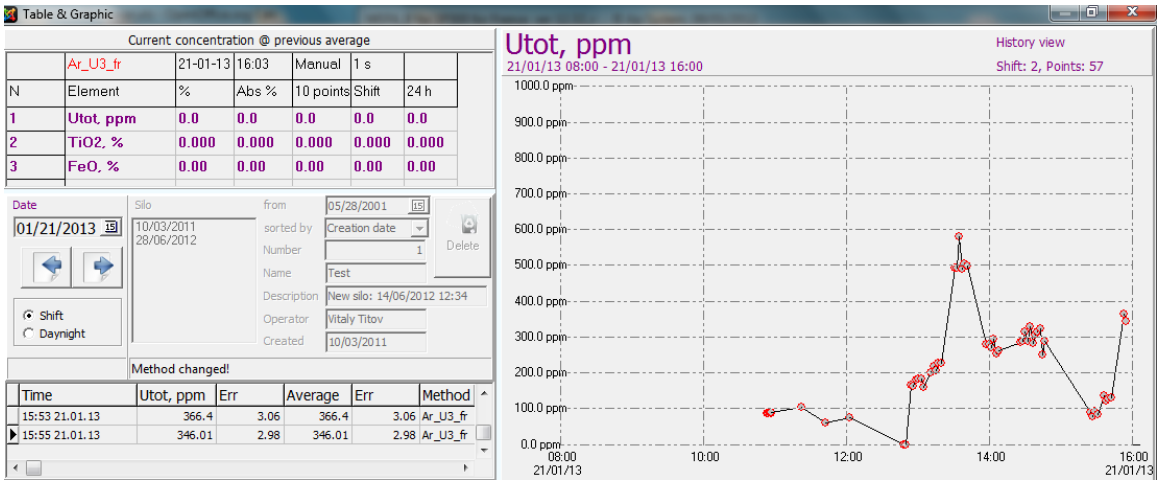

Fig.6. Trend of U concentrations measured on pilot conveyor during small-scale test at Areva Mines site

URANIUM AND THORIUM IN RUTILE AND ZIRCON HEAVY MINERAL SANDS

The applicability test of CON-X02 analyzer was carried out at Richard Bay Minerals (RMB) heavy mineral sand separation plant on an industrial conveyor. The target of analyzer application at the RMB separation plant was to measure Zr and Ti content in the material flow. Besides these major components, heavy mineral sands contain numerous minor and trace elements. The presence of natural radionuclides from thorium and uranium series in beach sands is a well recognized fact. U and Th are concentrated in zircon and rutile fractions after separation of silica. This may cause an environmental and safety problems.

The commercial specifications of rutile and zircon concentrates specify the maximum total uranium and thorium content not exceeding 450 ppm [9]. The materials of the IAEA [XXX_IAEA Tech Report 419, p 84] indicate that the content of uranium and thorium in South African mineral rutile and zircon can range from 10 to 500 ppm, but in concentrates it can increase to 800 ppm [10].

During the industrial test we managed to confirm the capability of the analyzer to monitor the level of U and Th traces thus providing the operator with the real-time information about the unwanted growth of dangerous elements in material flow.

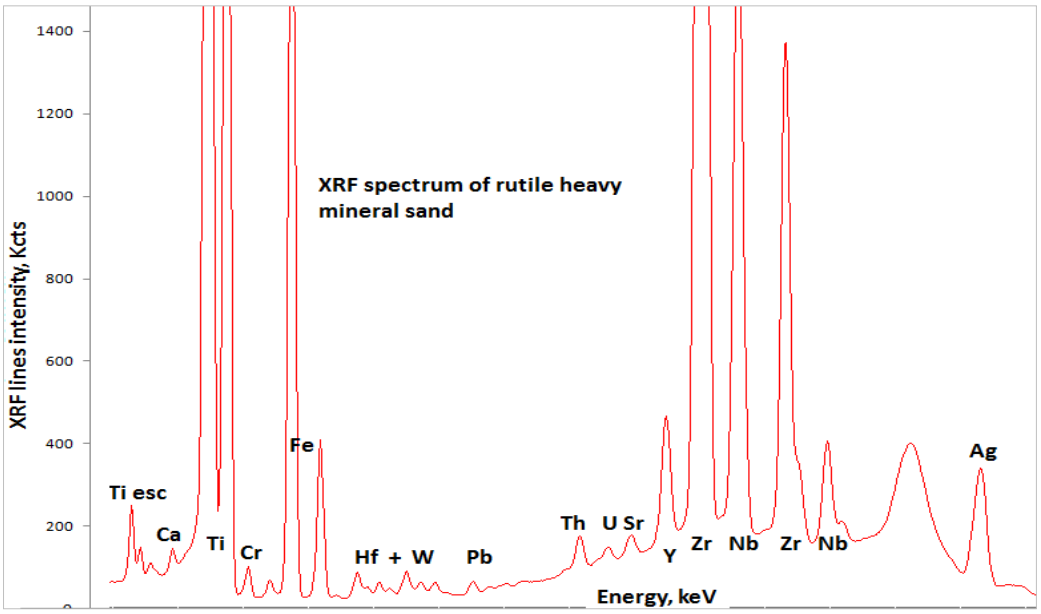

Fig.7: Spectrum of rutile heavy mineral sand after separation from silica. Parameters of measurement: Ag X-ray tube voltage – 39 kV, current – 100 μA, 50 μm thick Rh filter of primary radiation, measurement time 600 seconds, distance between sample and detector 50 mm. Ag line is an instrumental XRF line of Ag X-ray tube.

Rutile Sand

Spectrum of the mixed rutile and zircon mineral sand after separation from silica is shown below in Figure 7. Besides Ti and Zr, up to 10-12 minor and trace components can also be detected and measured from the same spectrum. After measurement during 10 minutes U and Th XRF lines are clearly visible in the rutile sample mostly consisting of TiO_2. Depending on time of measurement and type of interfering elements, DL of U and Th in rutile mineral sand is 25-50 ppm; statistical precision is estimated as ≤ 15% relative.

Zircon Sand

Elevated Th concentration in zircon sand is generally known: from 10 to 600 ppm Th can be found in South African heavy mineral sands. XRF spectra of this material containing traces of ThO_2 are shown on Figure 8. In 10 minute measurements, Th and U lines are clearly visible in target concentration range.

Before industrial testing, the analyzer was calibrated at our application laboratory with zircon sand samples provided from mining site. Samples of zircon sand with unknown Th concentrations were spiked with known amounts of Th-containing material. Linear dependence between Th La line intensity and Th concentration is shown on Figure 9. Linear correlation of intensity vs. concentration is sufficiently high ($R^2 = 0.98$).

A screen shot of the measuring program window demonstrates the trend of Th concentration that was obtained in the laboratory study of the samples of zircon sand containing different amount of Th (Figure 10). Th DL is estimated at 25-50 ppm in 10 minute measurements depending on the type of material and interfering elements. Statistical precision is estimated at 25 ppm.

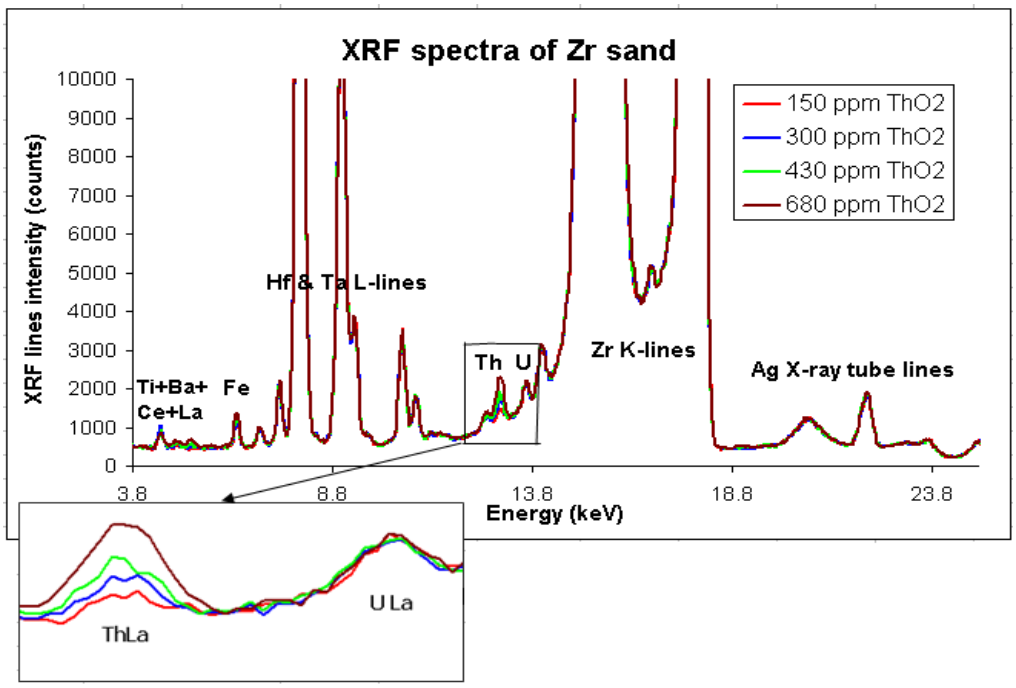

Fig.8: Spectra of zircon heavy mineral sand spiked with increasing Th concentrations. Parameters of measurement: Ag X-ray tube voltage – 36 kV, current – 100 µA, 60 µm thick Ag filter of primary radiation, measurement time 600 seconds, distance between sample and detector 50 mm.

Industrial test of the CON-X analyzer for real-scale time measurement of zircon sand on the conveyor was conducted at the heavy mineral sand separation plant. The analyzer was installed above the conveyor after separation of silica. Along with positive results for Ti and Zr (target major elements), the test has shown reliable correlation of Th and U on-line measurements with plant laboratory results. Difference between the results of on-line measurement and laboratory was within 20 % relative.

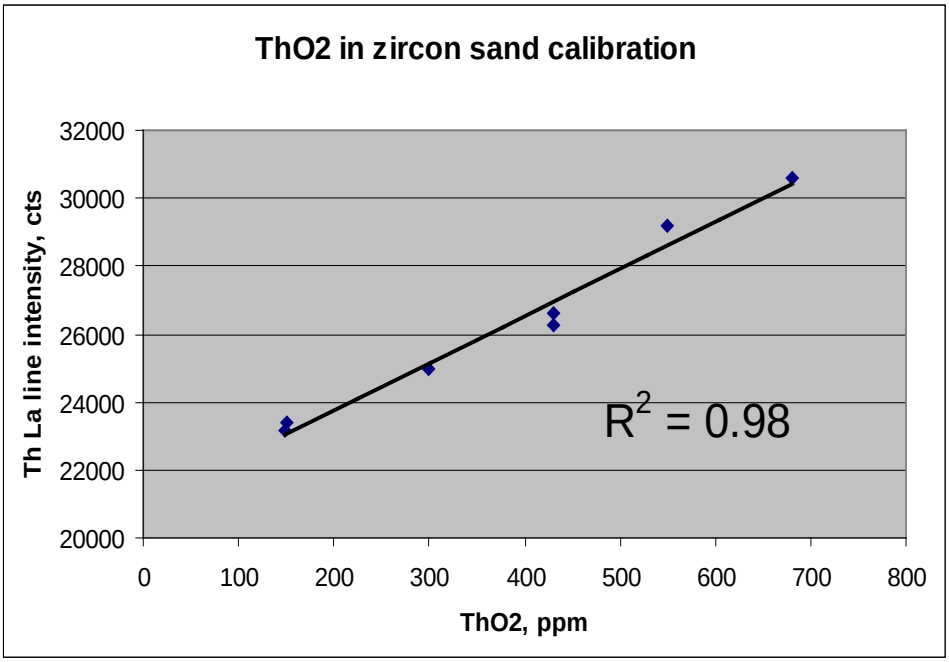

Fig.9: Calibration curve: Th La line intensity (Ag X-ray tube) are plotted vs. thorium concentrations

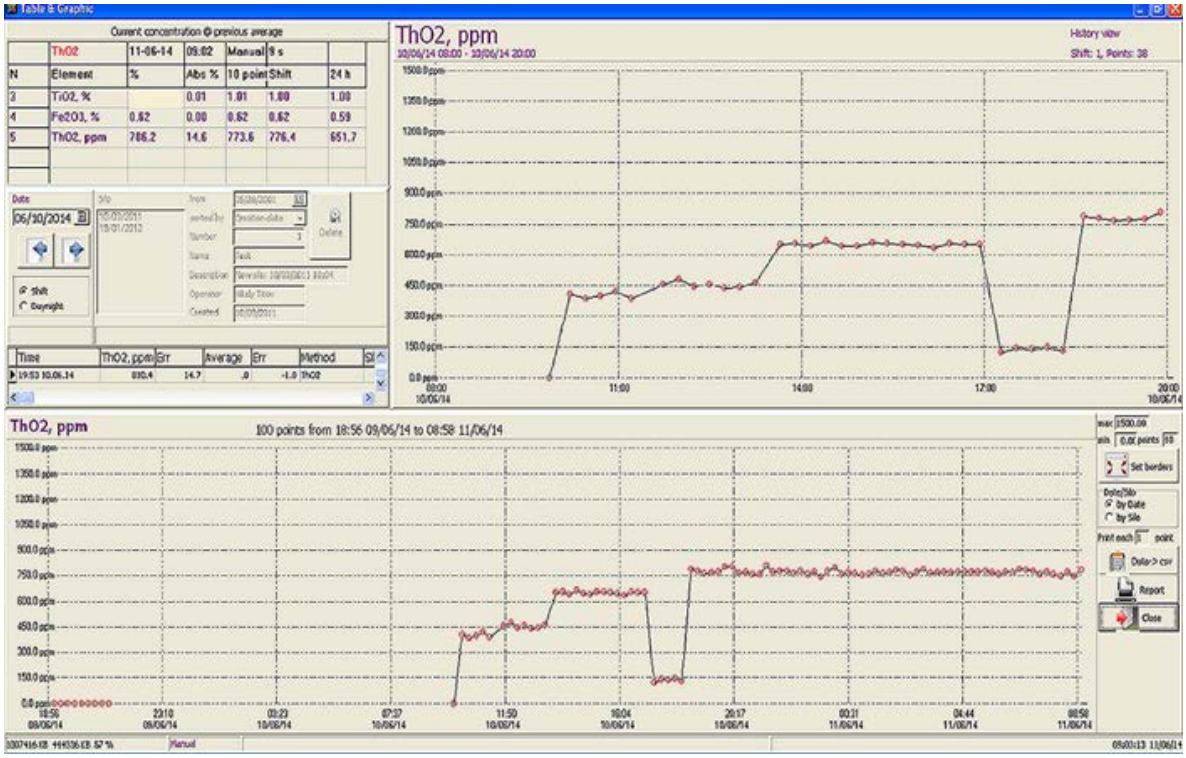

Fig.10. Trend of Th concentrations measured continuously with static sample holder during laboratory test

The plot in Fig. 11 shows the trend of U and Th concentrations measured in real-scale. Results were obtained during the industrial test on the zircon sand conveyor at RBM site.

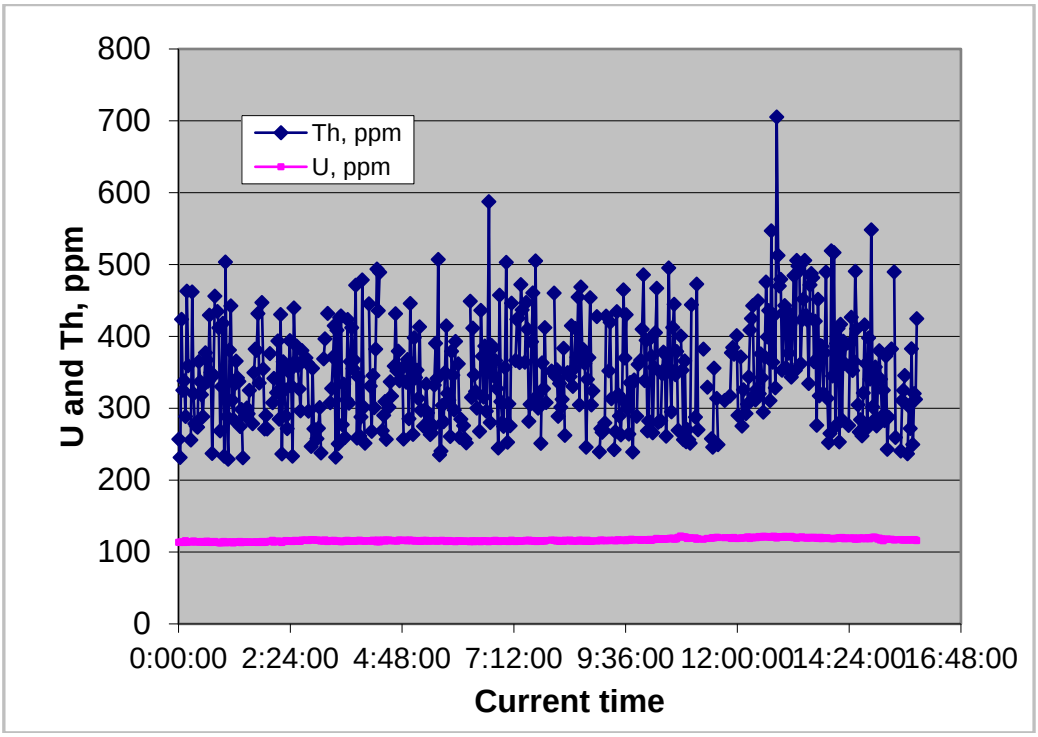

Fig.11. Trend of U and Th concentrations measured on moving conveyor with zircon sand during industrial test

Th TRACES IN OTHER Th-BEARING MINERALS

Precise and accurate determination of Th and U at trace levels in geochemical materials (granite, calcite, ankerite and others) is essential for many geochemical and geophysical studies [11].

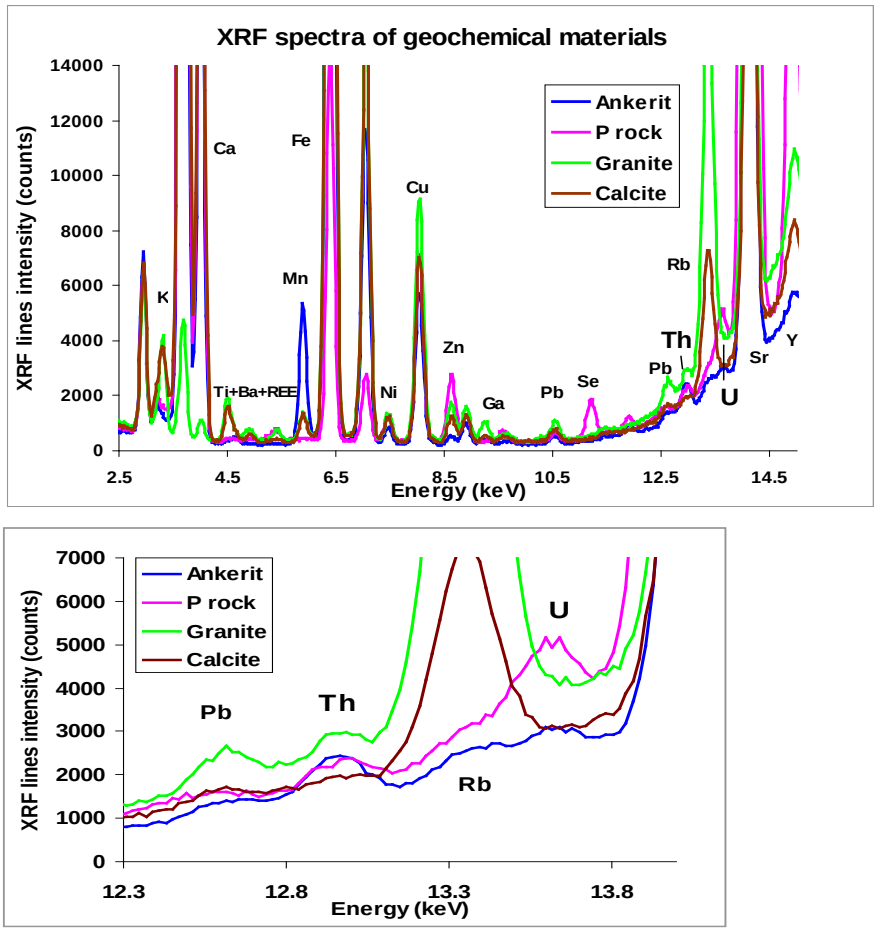

Fig.12 and 13. Overview (12) and zoom into low intensity lines (13) of XRF spectra of geological samples indicated in the legend. Parameters of measurement: Ag X-ray tube voltage – 36 kV, current – 100 µA, 60 µm Ag filter of primary radiation, measurement time 600 seconds, distance between sample and detector 50 mm.

Although XRF only provides data with the precision comparable to dilution mass spectroscopy and neutron activation analysis at Th and U concentrations > 10 ppm, it has the advantage of determining many other useful elements in the same run. Spectra of various geochemical materials measured with CON-X analyzer are shown on Fig.12 and 13.

ANALYSIS OF U AND Th AS MINOR AND MAJOR COMPONENTS OF MONAZITE ORE

Currently economically viable U ores contain 0.05-0.07 % of uranium oxide (U_3O_8)[2]. This means that even before beneficiation uranium ores normally contain a higher amount of U than in the cases described above (trace amount ~ 100 ppm). In these applications measurement of U concentration becomes more rapid, accurate and reliable. For example, the average U concentration in monazite ore is ~ 0.2% whereas Th content is as high as 4-7%.XRF spectrum of monazite ore is shown on Fig.14.

In this application X-ray tube voltage was increased to 45 kV to enhance excitation of K-lines of rare-earth elements (La, Ce, Pr, Nd etc.). The high resolution provided by the SDD detector enables uranium Lα line to be clearly seen alongside the significantly more intense Th lines. Their partial overlap does not essentially influence the accuracy and precision of analysis due to the well developed algorithm of spectral deconvolution in the software. Despite strong neighboring Th lines, high-quality analytical parameters are achieved. Uranium MDL cal culated from spectral data is

approximately 30 ppm and precision is approximately 25 ppm (at 2σ level).Thorium DL estimated from the spectrum of monazite concentrate is on the level of 20 ppm and accuracy is less than 1% relative.

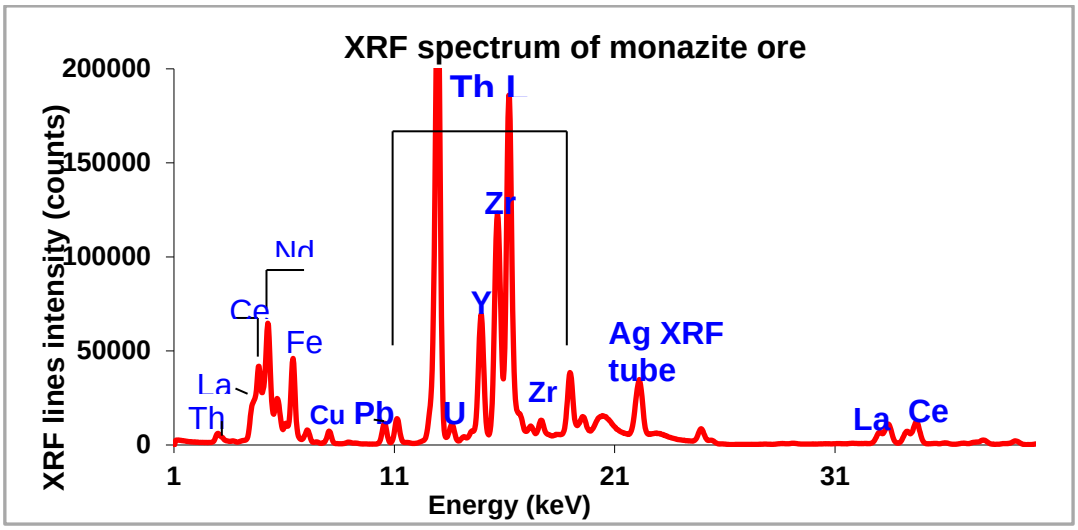

Fig.14. Spectrum of monazite ore. Parameters of measurement: Ag X-ray tube voltage 45 kV, current 100 μA, 100 μm Ag filter, time of measurement 600 s.

ANALYSIS OF URANIUM AS A MAJOR ELEMENT

Measurement of U content in rich uranium ores is also possible. At high U concentrations two ways of measurements can be used: direct uranium determination from its XRF spectral lines intensity (Fig.15*)* or on the basis of the intensities of the main admixture elements. The combination of both methods can be implemented in the software providing high accuracy which is typically less than 1% relative for high U contents.

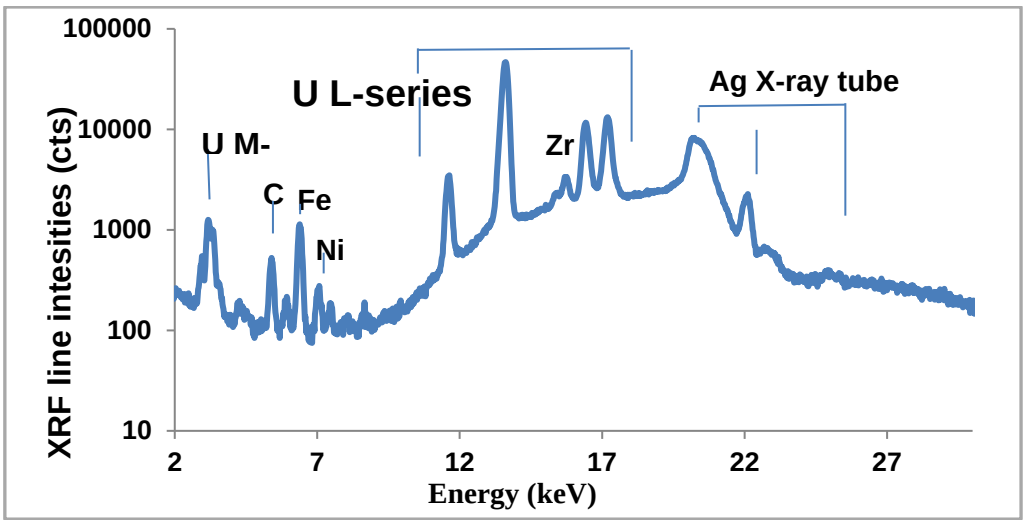

Fig.15.Spectrum of U_3O_8 on the Teflon substrate. Parameters of measurement: Ag X-ray tube voltage 39 kV, current 100 μA, measurement time 600 s, distance between sample and detector 50 mm

CONCLUSION

Results of the present paper show that on-line XRF analysis is really applicable for measurement of U and Th content in different types of mineral materials on conveyor belt. The CON-X on-line analyzer is able to measure U and Th content in real time even if these elements are only moderately concentrated compared to the average crust composition. Results obtained with phosphate rock and fertilizers (50-200 ppm U), rutile and zircon sands (50-350 ppm U and 100-600 ppm Th), carbonate minerals, U ore residues after heap-leaching (≤100 ppm U), monazite concentrate (0.2% U3O8 and 5-7% ThO2) demonstrate acceptable measurement accuracy at high representativeness and speed of analytical feedback. These results show that the industrial conveyor analyzer CON-X can be effectively used for analytical control of mining and processing streams of U- and Th-containing materials. For this application, on-line XRF analysis doesn't require samples preparation and allows the measurement process to be fully automated.

REFERENCES

1. D.Reily, N.Ensslin, H.Smith, S.Kreiner. Passive Nondestructive Assay of Nuclear Materials. Los Alamos National Laboratory, US NRC, 1991.

2. IAEA. Role of Thorium to Supplement Fuel Cycle of Future Nuclear Energy Systems. IAEA Nuclear Energy Series Publications No. NF-N-2.4, Vienna, 2012.

3. F.Bartel, H.Tulsidas.Thorium. Occurrences, geological deposits and resources, IAEA International Symposium on Uranium Raw Materials for Nuclear Energy URAM 2014, Vienna, 23-27 June 2014 (URAM2014 proceedings).

4. Investing in the future of thorium. Special report, Energy and Capital 2013:11.

5. http://www.bsi/lv/online_xrf_conveyor_analyzer_con_x_eng.html

6. Ashraf Khater. Uranium and Heavy metals in phosphate fertilizers.

   DOI: 10.1007/978-3-540-87746-2_26.

7. Ceyhan, M. (Ed.). World Distribution of Uranium Deposits (UDEPO) with Uranium Deposits Classification. IAEA-TECDOC-1629, Division of Nuclear Fuel Cycle (2009).

8. Nuclear Energy Agency. Managing of Health and Environmental Impacts of Uranium Mining. OECD 2014. NEA No. 7062.

9. World Nuclear Association. Mineral Sands, Naturally Occurring Radioactive Materials, Appendix 1 (2013).http://www.world-nuclear.org/info/inf30a.html

10. G.E. Williams, J.D. Steenkamp. Heavy mineral processing at Richard Bay Minerals. Southern African Pyrometallurgy, 2006. Ed. By R.T. Jones.

11. R.J. Hart, D.L. Reid, J.S. Stuckless, H.J. Welke. Comparison of three techniques for the determination of uranium and thorium in rocks. Chemical Geology, 29(1980) 345 – 350.

Included in proceedings but not presented

ALUMINUM OXIDE GRAFTED KAOLINITE FOR EFFICIENT URANIUM REMOVAL FROM AQUEOUS SOLUTION

By

Hussein A. E. M.

Nuclear Materials Authority, Egypt

Corresponding Author

Hussein A. E. M.
Ah_mady@yahoo.com

ABSTRACT

Due to extensive diversity of nuclear applications, efficient adsorbents are highly required for radioactive liquid waste treatment. In this investigation, costless and simple approach for removing uranium from liquid waste by aluminum oxide grafted kaolinite (AOGK) was stated. The influences of contact time, solution pH, initial uranium concentration, adsorption temperature, adsorbent amount (dose) on the adsorption of uranium (VI) ions from radioactive liquid waste were investigated. The theoretical capacity of AOGK adsorbent is about 95 mg/g AOGK. The optimum adsorption conditions were recommended. About 95% of the loaded Uranium (VI) on AOGK adsorbent has been eluted by ascorbic acid as an efficient eluent.

Keywords: uranium, removal, aqueous solution, grafted kaolinite

INTRODUCTION

Through uranium mining, milling, processing, enriching and in nuclear fuel amenities a large amount of wastes polluted by uranium will be formed. Where the concentrations of uranium can be increases to beyond 50 mg/l[1-3]. So it is very important –from the environmental point of view- to develop refinement methods. In this concern, the current investigation deals with uranium removal from aqueous liquid waste.

Frequent methods have been applied for uranium removal from wastewaters and radioactive wastes. Chemical precipitation, ion exchange, liquid membrane, solvent extraction and adsorption are the most commonly used methods[4-8]**.** One of the effective methods to deal with the treatment of a radio-contaminated aqueous liquid wastes is adsorption[9-11]. Three types of adsorbents are mostly applied for the removal of radio-cations: natural and modified clay minerals[9-12], synthetic selective adsorbents [13-15] and bio-sorbents[16-18]. Compared with the last two types of adsorbents, natural and modified clay minerals have its advantages, such as huge extents, easy obtainability, low price, high stability, etc. Thus, many researches have been conducted on the elimination of radionuclides by using various types of clay materials[10,12, 19-24].

In this study, we assessed the feasibility of kaolinite clay as a support for aluminum oxide in treating radioactive wastewater and developed a novel modification process for kaolinite clay. Consequently, the adsorption performance of the aluminum oxide grafted kaolinite clay (AOGK) in removing uranium(VI) through batch adsorption experiments was investigated. The possible reason for the different adsorption behaviors is also explored along with some surface characterization techniques. In addition, much effort has been assumed to determine the adsorption mechanism of uranium(VI) on the AOGK, which is especially important for its further performance improvement and practical application, through adsorption isotherm, and desorption studies. For de-sorption (or elution) of the loaded uranium (on the prepared AOGK), many eluents were tested.

EXPERIMENTAL

Materials and Analytical Procedure

The liquid waste experimental sample used in this study was provided by the **Uranium Purification Unit, Nuclear Material Authority, Egypt**. Its average chemical composition is shown in Table 1.

Table 1: Chemical composition of the studied raffinate waste sample

Constituent	
Fe_2O_3	0.60 g/l
HNO_3	1M
U	100 mg/l
Ca^{2+}	1.9 g/l

A uranium stock standard solution assaying 1000 mg/L was prepared by dissolving 0.1782 g of uranyl acetate [$UO_2(CH_3COO)_2.2H_2O$] from ***BDH Chemicals Ltd. Poole, England*** in 100 ml distilled water.

Uranium was analyzed in the different working aqueous phases using the ArsenazoIII spectrophotometric method[25]**.** Absorbance of the formed uranium ArsenazoIII complex was measured at 650 nm against proper standard solutions using a ***Perkin-Elmer, USA*** UV/VIS spectrophotometer. On the other hand, SO_4^{2-} and Fe^{3+} were determined spectro-photometrically using the methods described by Marczenko[25]. The initial pH of the working solution was adjusted by addition of a buffer solution.

Commercial kaolinite clay sample was obtained from **Al Amier Ceramic Co. Cairo;** with the chemical composition listed in Table 2. The provided clay sample was crushed, ground and sieved to the used grain size of 0.09 mm (200 mesh size).

Table 2: Chemical composition of the working kaolinite sample

Constituent	Wt., %	Constituent	Wt., %
SiO_2	52.65	Na_2O	0.19
Al_2O_3	28.31	TiO_2	1.54
Fe_2O_3	4.71	Loss of ignition	11.27
CaO	0.31		
MgO	0.18		

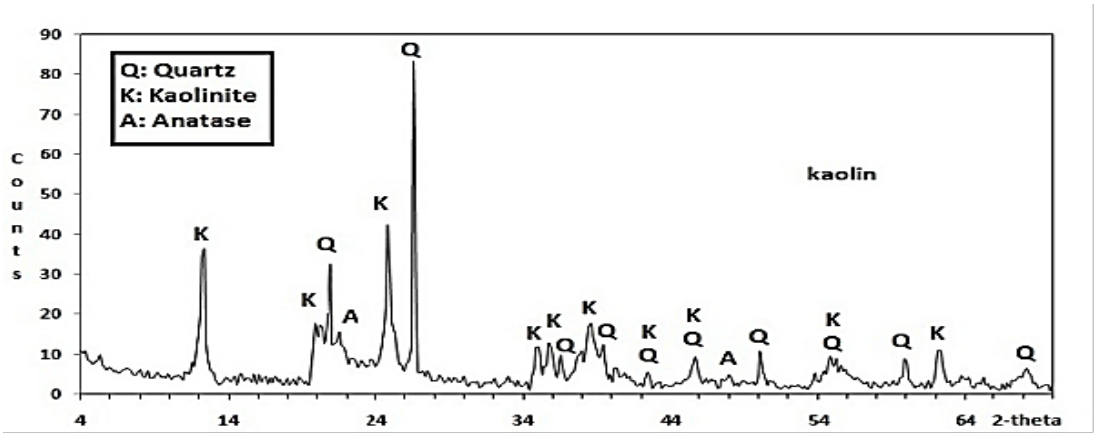

Figure 1: XRD Pattern of the natural kaolinite sample.

Preparation of the Aluminum Oxide Grafted Kaolinite Clay (AOGK)

Modified kaolinite was prepared as described by **Dahu Ding**[26], where the working kaolinite sample was powdered and sieved (200 mesh size). The grafting process of the working kaolinite clay sample involved mostly three steps. Firstly, 10 g of the dried clay was added to 100 mL of 0.5 M $AlCl_3$ solution and mixed carefully for about 10 min. Then, 100 mL of 1 M NaOH solution was added into the mixture gradually. The resultant mixture was left to react for 1 h under energetic stirring at 70 °C. The resulting kaolinite clay was repeatedly washed (to be nearly neutral), centrifuged and finally dried at 105 °C. Finally, the dried clay was ground into powder form and heated in air at 600 °C for 1 h in a muffle furnace.

Equilibrium Studies Factors

To monitor the influences affecting the adsorption process, a series of batch experiments were undertaken using the standard uranium synthetic solution. These factors involved contact time, initial uranium concentration, pH and the effect of adsorbent dose (amount). From the attained results, Langmuir and Freundlich isotherms were determined. The adsorption experiments were performed by shaking 0.01 g sample portions of the AOGK sample with 15 ml of the uranium synthetic solution (of 100 mg/L initial uranium concentration) using a magnetic stirrer. The adsorbed amounts of uranium were calculated by the difference between its equilibrium and initial concentrations. The amount of uranium retained in the solid phase qe (mg/g) was calculated using the following relation:

$$q_e = (C_o - C_e) \times \frac{V}{m} \qquad (1)$$

Where C_o and C_e are the initial and equilibrium concentrations of the uranium (mg/L), respectively, V is the volume of the aqueous phase (L), and m is the weight of the AOGK used (g). The removal percent of ions from the aqueous phase is calculated from the following relation:

$$\text{Uranium adsorption } \% = \frac{C_o - C_e}{C_o} \times 100 \qquad (2)$$

The distribution coefficient (K_d) of uranium between the aqueous bulk phase and the solid phase was calculated from the following relation:

$$K_d = \frac{C_o - C_e}{C_o} \times \frac{V}{m} \qquad (3)$$

For eluting (de-sorption) the loaded uranium from the AOGK, firstly the loaded AOGK washed with a diluted nitric acid solution having the same molarity of the working liquor. Afterwards, the following eluents were tested, namely ascorbic acid, citric acid, H_2O, HCl, HCl and NaCl acidified by H_2SO_4.

Equilibration calculation

All uranium speciations in this study were performed with Hydra-MEDUSA, a chemical equilibrium calculation program[27].

RESULTS AND DISCUSSION

Results of Uranium Adsorption

Effect of Contact Time

The effect of the contact time was examined by performing a sires of experiments by contacting a fixed weight (0.01 g) of AOGK with a uranium solution (15 ml) having a concentration of 100 mg/l at room temperature and pH 4 and AOGK/solution volume phase ratio of 0.66 g AOGK /l. The studied time intervals ranged from 1 up to 180 minutes. The attained results were plotted in Fig. 2. It is observed that the uranium adsorption efficiency attained about 55% in the second experiment with 15 minutes contact time. By increasing the contact time to 60 minutes, significant increase of uranium adsorption efficiency was achieved (be about 84 %). Slight increase in uranium adsorption efficiency (89 %) was observed at the experiment with 90 min. contact time. Beyond 90 min. contact time, a clear plateau was observed. Therefore, 90 min. could be selected as the suitable contact time.

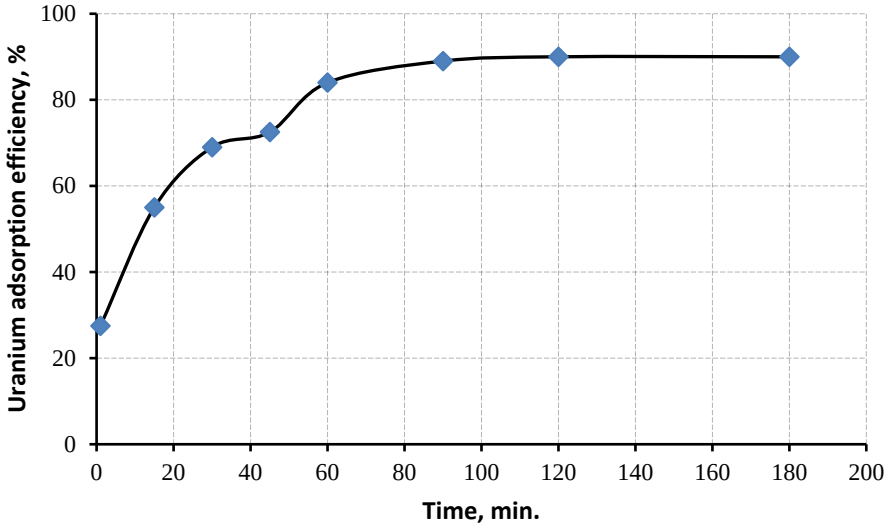

Figure 2: Effect of contact time upon uranium adsorption efficiency on the prepared AOGK sample

Effect of pH

The influence of solution pH on uranium adsorption on AOGK was explored by contacting a fixed weight of the prepared AOGK (0.01g) with fixed volume (15 ml) from the prepared standard uranium solution of (100 ppm) at 25°C for 90 min. and AOGK/solution volume phase ratio of 0.66 g AOGK /l. The examined pH values ranged from 0.6 to 8.2. The attained data are shown in Fig. 3. From this figure it is noticeable that uranium adsorption efficiency increases gradually with increasing pH values till pH 4 (of about 85%). Beyond pH 6, uranium adsorption efficiency slightly deceases (to about 80%) in the last experiment at pH 8.2. Thus, we can recommend the use of solution pH having pH values ranged from 4 to 8.

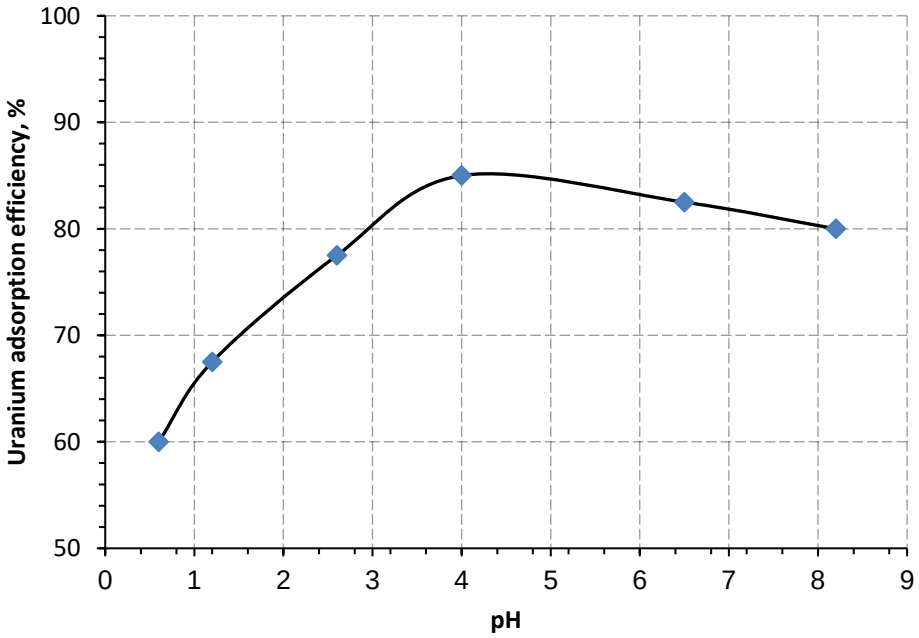

Figure 3: Effect of solution pH on uranium adsorption onto the prepared AOGK.

It is important to indicate that uranium adsorption is strongly dependent on the solution pH. At low value pH (≤ 4), the number of H_3O^+ ions exceeds that of the UO_2^{2+} several times and the surface is most likely covered with H_3O^+ ions, reducing the number of binding sites for the adsorption of UO_2^{2+}. On the other hand, at high pH values more H_3O^+ ions leave the clay mineral surface making the sites available to the cation exchange with the UO_2^{2+} ions and hydrolysis precipitation starts due to the formation of complexes in aqueous solution, i.e. $UO_2(OH)^+$, $(UO_2)_2(OH)_2^{2+}$, $(UO_2)_3(OH)_5^{3+}$, $(UO_2)(OH)_2$, which increase uranium (VI) adsorption[28-32].

Aqueous speciation distribution of uranium was calculated and represented in Fig. 4. The results showed that the complexes of $UO_2(NO_3)^+$ and UO_2^{2+} were the predominant species at the pH range from 0.0 - 3 with mean total percent of 15% and 85% respectively. U-hydroxide complexes start to dominate the aqueous phase at pH near 3 of $(UO_2)_2(OH)_2^{2+}$ and $(UO_2)_2OH^{3+}$. At pH 4, the $UO_2(OH)_2.H_2O_{(C)}$ became the major species with about 100% of total concentration at pH range from 4.5 to 12, while at pH 12, $UO_2(OH)_4^{2-}$ became the major species within a total percent of about 100% of the total concentration.

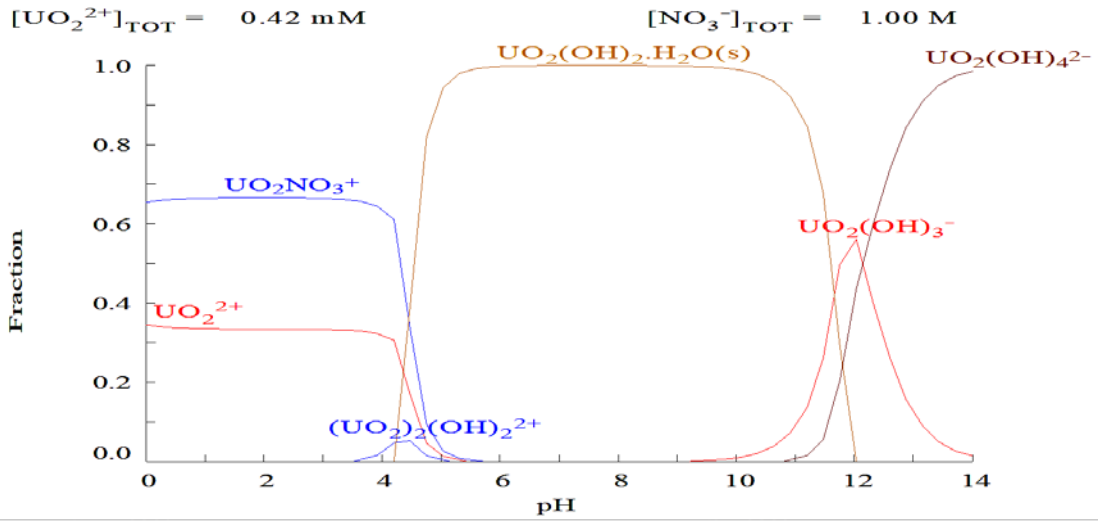

Figure 4: Expected aqueous speciation of U (VI) as a function of pH by Hydra-MEDUSA, equilibrium calculation program

Effect of Initial Uranium Concentration

In order to examine the effect of initial uranium concentration upon the adsorption efficiency onto AOGK, a series of experiments was performed by contacting a fixed weight (0.01 g) for 90 min. at room temperature (≈ 25 ºC) and pH 4 and AOGK/solution volume phase ratio of 0.66 g AOGK /l. The studied initial uranium concentrations ranged from 100 up to 600 mg/l. The obtained results were plotted in Fig. 5. From the obtained data, the uranium adsorption efficiency decreases significantly with increasing its initial concentration. Therefore the uranium solution of 100 mg/l concentration could be chosen as the preferred concentration. Another result could be determined from Fig. 5, which is the experimental capacity of the adsorbent was determined by (about 100 mg uranium/g AOGK).

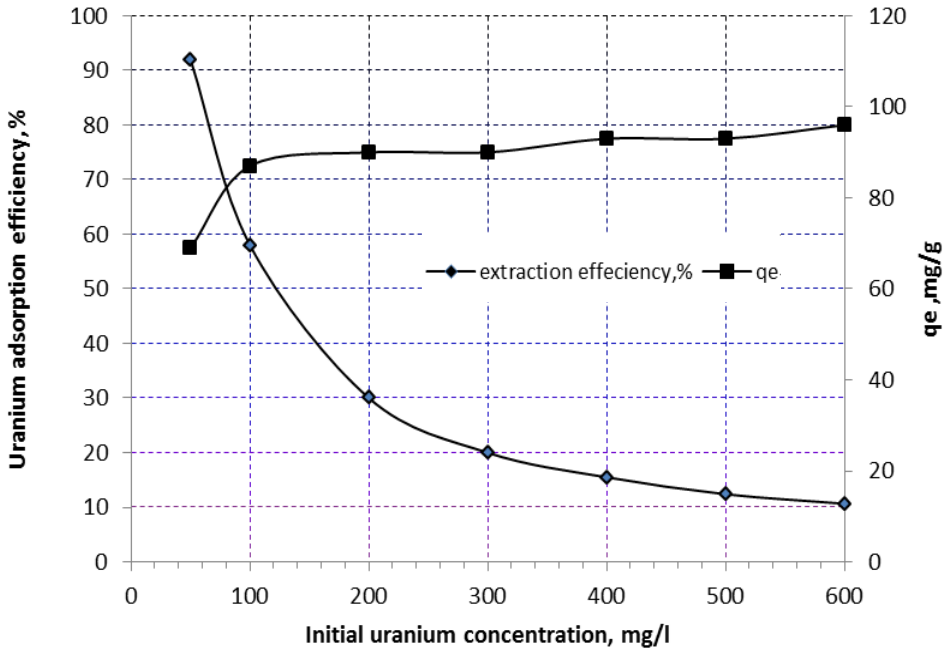

Figure 5: Effect of initial uranium concentrations on uranium adsorption efficiency onto the prepared AOGK

Adsorption Isotherm

A number of common adsorption isotherm models were considered to fit the attained isotherm data under the equilibrium adsorption of the AOGK. Examples of these models are Langmuir, Freundlich and Dubinin–Radushkviech (D–R isotherm) isotherms.

A- Langmuir Isotherm

Langmuir model supposes that, the adsorption occurs uniformly on the active sites of the sorbent, and once a sorbate occupies a site, no further sorption can take place at this site. Thus, the Langmuir model is given by the following equation [33-39]**.**

$$C_e/q_e = 1/bQ_o + C_e/Q_o \qquad (4)$$

Where: Q_o and b, the Langmuir constants, are the saturated monolayer sorption capacity and the sorption equilibrium constant, respectively. A plot of C_e/q_e versus C_e would result in a straight line with a slope of $(1/Q_o)$ and intercept of $1/bQ_o$ as seen in Fig. (6). The Langmuir parameters given in Table 3 can be used to predict the affinity between the sorbate and sorbent using the dimensionless separation factor R_L[33-39]**.**

$$R_L = 1/ (1 + bC_o) \qquad (5)$$

The R_L value indicates the type of isotherm to be irreversible ($R_L = 0$), favorable ($0<R_L<1$), linear ($R_L= 1$) and unfavorable ($R_L>1$). The values of R_L for adsorption of uranium (VI) onto AOGK are shown in Fig. (7), which indicate that adsorption of uranium(VI) is more favorable at higher initial uranium(VI) concentrations than at lower concentrations.

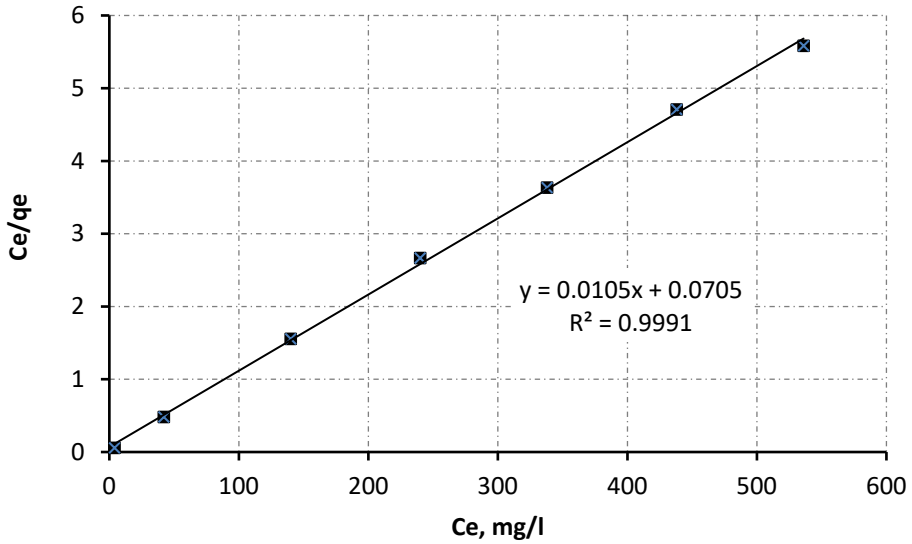

Figure 6: Langmuir isotherm plots for adsorption of uranium onto AOGK

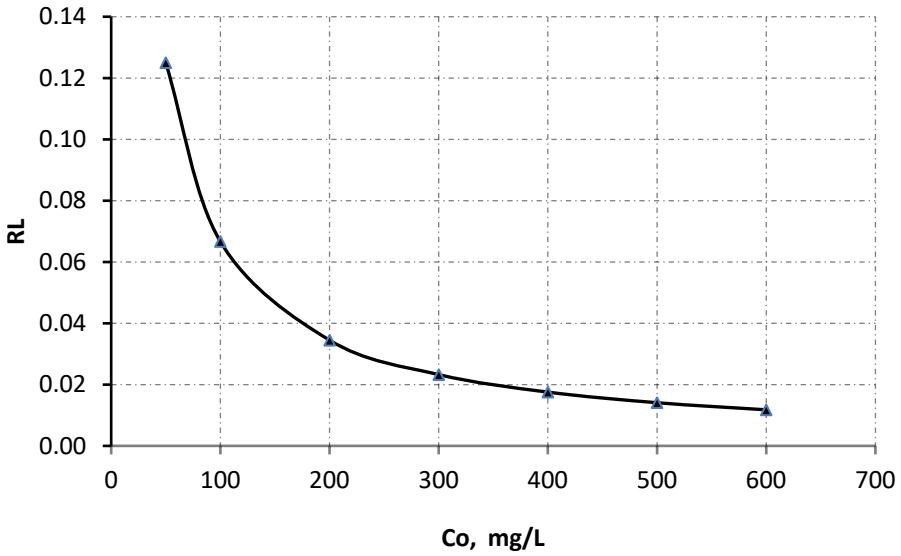

Figure 7: Separation factor R_L of uranium (VI) adsorbed onto AOGK

B- Freundlich Isotherm

The Freundlich model stipulates that the ratio of solute adsorbed to the solute concentration is a function of the solution. The empirical model was shown to be consistent with exponential distribution of active centers, characteristic of heterogeneous surfaces. The amount of solute adsorbed at equilibrium, q_e, is related to the concentration of solute in the solution, C_e, following [33-39].

$$q_e = K_F C_e^{1/n} \qquad (6)$$

This expression can be linearized to give

$$\log q_e = \log K_F + (1/n) \log Ce \qquad (7)$$

Where K_F and n are the Freundlich constants which represent sorption capacity and sorption intensity respectively. A plot of ($\log q_e$) versus ($\log C_e$) would result in a straight line with a slope of (1/n) and intercept of ($\log K_F$) as seen in Figure 8. Freundlich constants are given in Table 3.

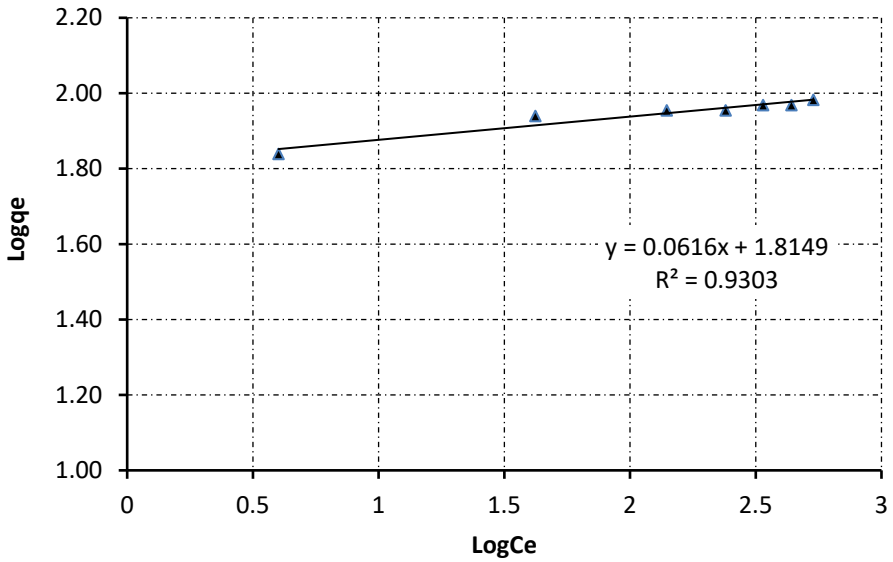

Figure 7: Freundlich isotherm plots for adsorption of uranium onto AOGK.

C- Dubinin–Radushkviech isotherm (D–R isotherm)

The Dubinin-Radushkevich (D-R) isotherm model was applied to the data in order to assume the heterogeneity of the surface energies of adsorption and the characteristic porosity of the adsorbent[39]. The linear form of the D-R isotherm is given the following equation:

$$\ln q_e = \ln q_m - \beta\, \varepsilon^2 \qquad (8)$$

Where q_m is the maximum amount of ions that can be sorbed onto unit weight AOGK, i.e. sorption capacity (mg/kg), β the constant related to the sorption energy (mol^2/kJ^2); and **ε** is the polanyi potential = RT ln(1+1/Ce), where R is the gas constant (mol/KJ), and T is the absolute temperature (K). The mean free energy of sorption is the free energy change when one mole of uranium is transferred to the surface of the prepared AOGK from infinity in the solution and it is calculated from the following equation:

$$\mathbf{Ea = 1/ (- 2}^{\beta}\mathbf{)½} \qquad (9)$$

The D–R plots of $\ln q_e$ versus ε^2 for the sorption of uranium ions onto AOGK are given in Fig. 9. Linear regression analysis using paired of $\ln q_e$ and ε^2 resulted in the derivation of q_m, β, and the correlation factor (R^2). These parameters are listed in table 3.

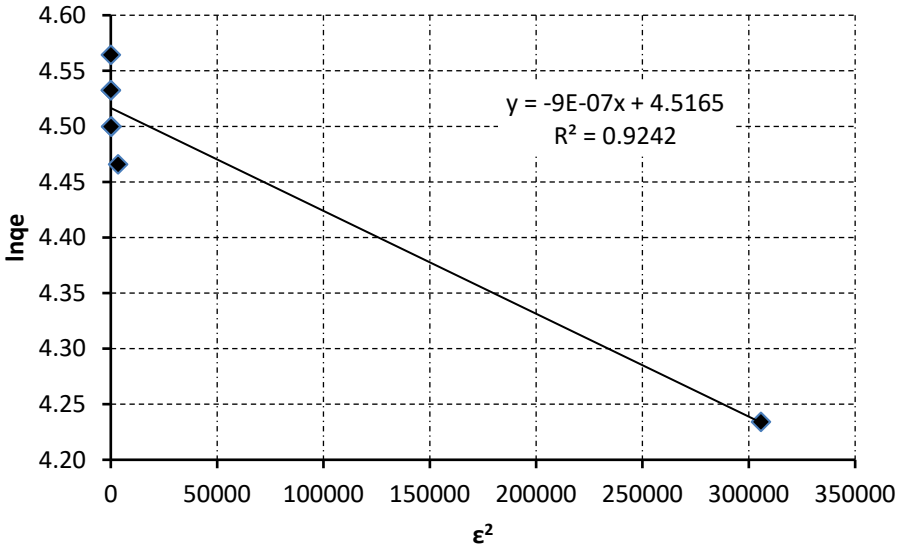

Figure 9: D–R isotherm plot for adsorption of uranium onto AOGK

Table 3: Langmuir, Freundlich and D–R isotherm parameters for uranium adsorption onto AOGK

Langmuir model parameters			Freundlich model parameters			D–R model parameters			
Q_o (mg/g)	b (L/mg)	R^2	1/n	K_f (mg/g)	R^2	β (mol^2/kJ^2)	Q_m (mg/Kg)	E_{ads} ($kJmol^{-1}$)	R^2
95.23	0.14	0.99	0.06	65.29	0.93	9×10^{-7}	91.51	1	0.92

Comparing the isotherms applied with the experimental data, the Langmuir gave the best fit, followed by Dubinin-Radushkevich while the Freundlich isotherm gave the worst fit.

Effect of Adsorption Temperature

The effect of adsorption temperature on the uranium adsorption efficiency by AOGK was investigated by contacting fixed portions of prepared AOGK with 15 ml of uranium standard solution of 100 ppm. The other factors were fixed at contact time of 90 min., solution pH of 4 and AOGK/solution ratio of 0.66 g AOGK/l. Several experiments were carried out at different temperature from 25 to 60 °C. The experimental results are presented in Fig. 10 as a relationship between uranium adsorption efficiency and temperature.

The obtained results showed that, the uranium adsorption efficiency was not affected by the increase in temperature (from 25 to 60 °C). Accordingly, the room temperature signifies the favored temperature.

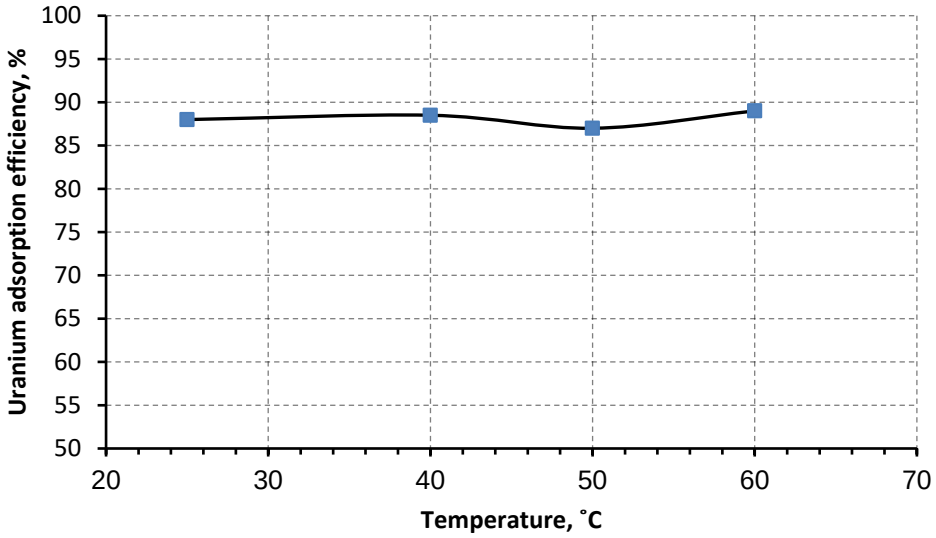

Figure 10: Effect of temperature on uranium adsorption efficiency onto AOGK

Effect of Adsorbent Amount

As is familiar, the amount of the adsorbent used in the uranium adsorption process is very critical for the financial point of view. The influence of adsorbent amount on the uptake of uranium was confirmed in Figure 11. A series of adsorption experiments was performed using different adsorbent doses ranging from 0.25 up to 2.66 g AOGK /l. The later experiments were performed under constant initial uranium concentration of 100 mg/l at room temperature (≈ 25 ºC) for 90 min shaking time and pH of 4. From the obtained results the adsorption efficiency decreases with increasing adsorbent amount (adsorbent dose). This observation could be explained as follows, increasing the adsorbent dose may (probably) cause aggregation of the latter. Consequently, the available adsorptive capacity of adsorbent was not fully utilized at a higher adsorbent amount (dose) in comparison to lower adsorbent amount where the available adsorption sites may decrease[40-42].

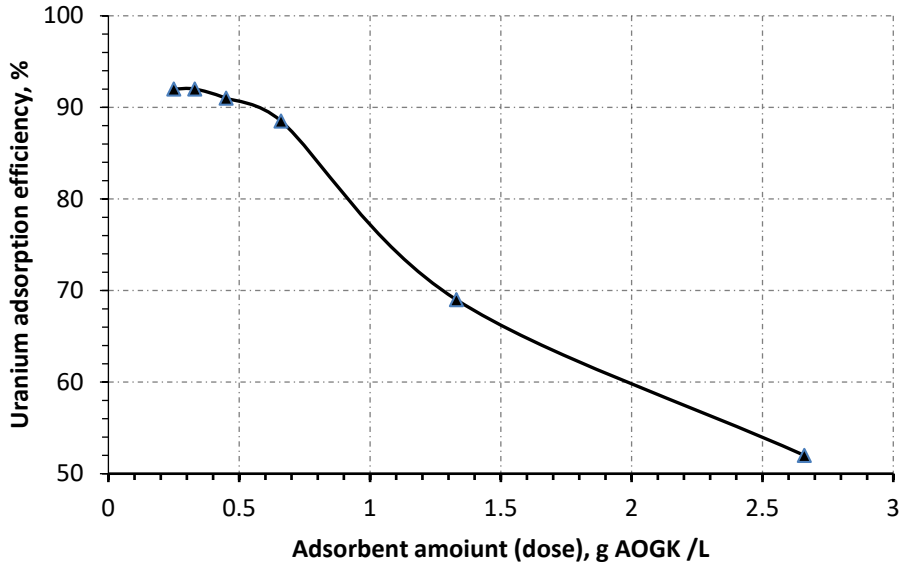

Figure 11: Effect of adsorbent dose upon uranium adsorption efficiency onto AOGK

Uranium De-sorption

De-sorption (elution) of uranium from the loaded AOGK was studied using solutions of citric acid, ascorbic acid, HCl, and NaCl acidified with H_2SO_4 as eluent reagents. The results for de-sorption efficiency are plotted in Fig. 12. From the obtained data, it is clearly evident that; about 95% from the loaded uranium can be eluted by 0.1M ascorbic acid.

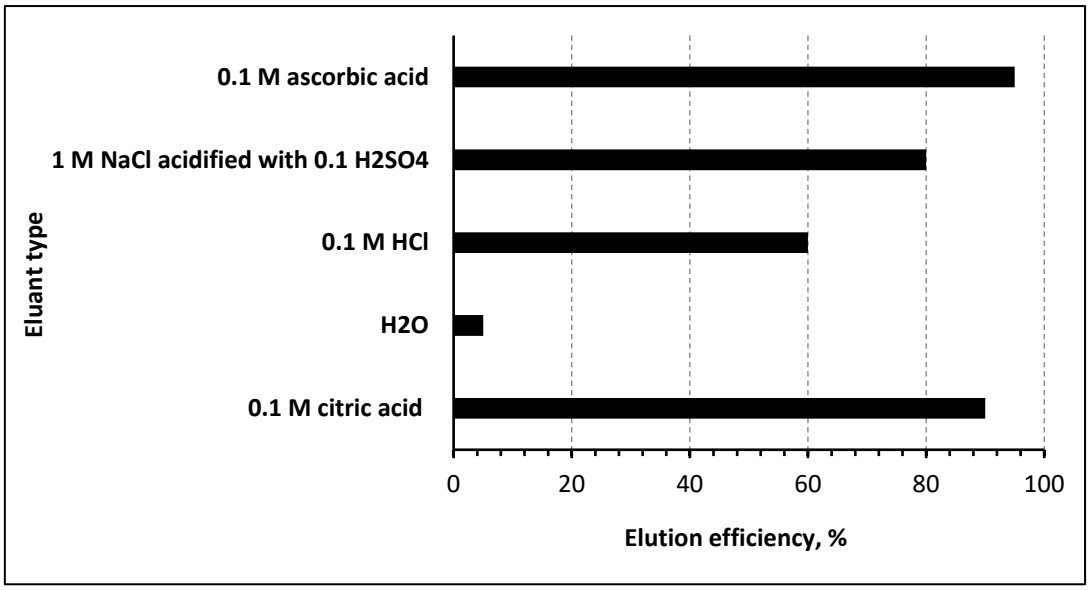

Figure 12: Elution yields using different eluent reagents, ascorbic acid, NaCl acidified with 0.1M H_2SO_4, 0.1 M HCl. H_2O and citric acid

FT-IR

The FT-IR patterns for AOGK before (A) and after (B) adsorption are presented in Fig. 13. As shown in Fig. 13A, the O–H stretching vibration transpired at 3,775.72 and 3,515.93 cm^{-1}. This may be credited to the silanol (Si–OH) group and water molecules (H–O–H) on the surface, respectively. The band at 1,598.99 cm^{-1} for the bending of Al–O–H and the stretching occurred in the band at 1081.1 cm^{-1}[43]. The bands for Al–O–Si stretching and bending vibrations were at 818.9 and 460.1 cm^{-1}, respectively.

As shown in Fig.13B, after adsorption of uranium(VI), the bands of most groups had changed in their amplitudes and locations. The O–H stretching vibration bands had shifted from 3,515.9 to 3,485.62. In the meantime, the adsorption intensity had decreased greatly after adsorption for uranium(VI), and this indicated that the –OH group played an important role in the creation of the U bond. From Fig.13B, it can be seen that a new peak appeared at 1384.5 cm^{-1}. This may be the characteristic peak of the uranyl ions adsorbed onto AOGK[44].

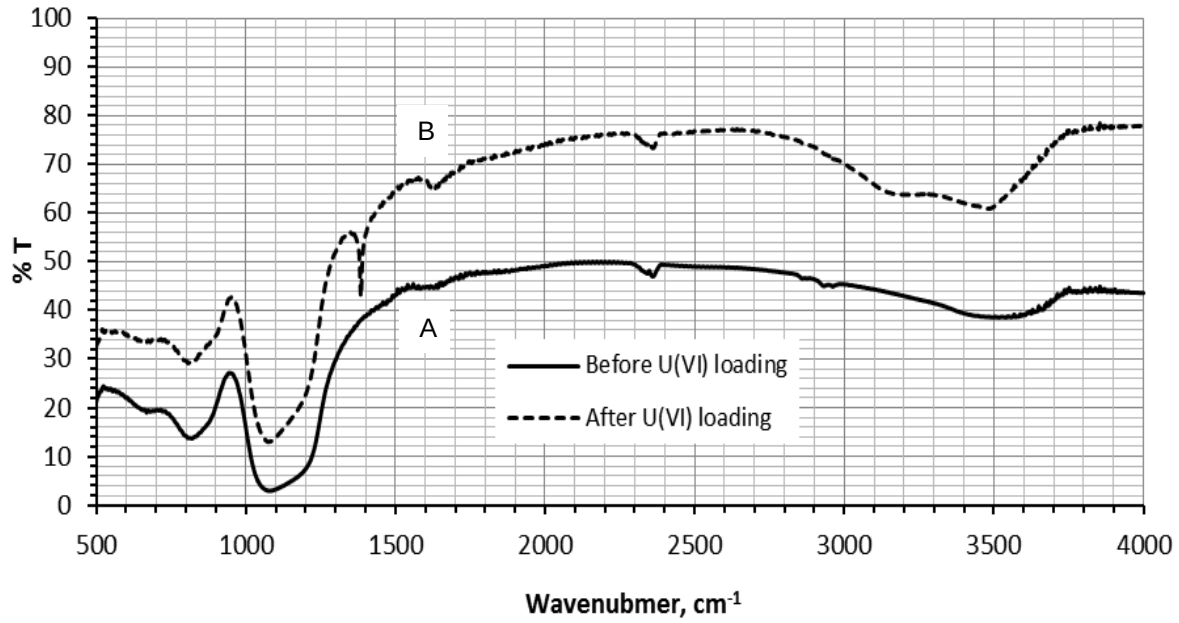

Figure 13: The FT-IR patterns for AOGK before (A) and after (B) adsorption

SEM

The SEM images of the AOGK before and after adsorption for uranium(VI) ions are presented in Fig. 14. As shown in Fig. 14A, the surface of AOGK before adsorption was smooth, neat and uniform. However, after adsorption its surface became lumpy and covered with some materials containing uranium, as shown in Fig. 14B. It can also be observed that there were some cleavages and small openings after adsorption. The latter observations may be due to the rehydration of AOGK in the aqueous solution which resulted in the improvement of the d-spacing[45].

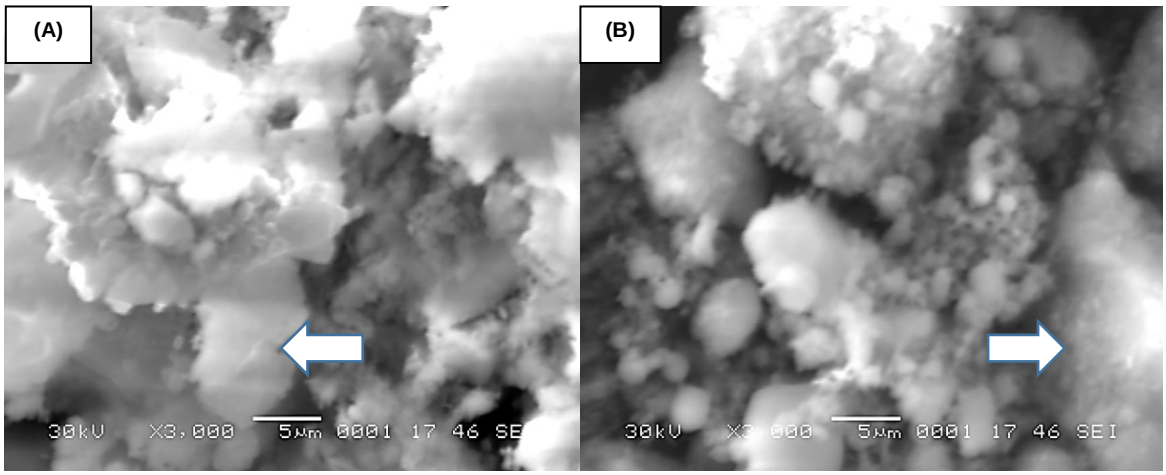

Figure 14: SEM images for AOGK before (A) and after (B) adsorption for U(VI) ions

Re-usability of the AOGK

The reliability of the attained data on successive usage was confirmed by equilibrating 0.5 g of AOGK sample with uranium solution of 400 mg/L under the improved experimental conditions. The de-sorption was carried out and the uranium concentration in each case was assessed. The results attained on successive usage of the same AOGK sample showed reproducible results with relevant standard

deviation (R.S.D.) values about 3.89% after eight adsorption-desorption cycles. The obtained data reflects good reusability of AOGK.

Choice of the Optimum Adsorption Conditions

From the obtained results of the relevant factors affecting uranium adsorption onto the prepared AOGK, careful selection of the optimum values of these results would depend primarily on economic considerations. In the light of the studied factors, it would seem economic to select the following conditions for uranium removal by the prepared AOGK as summarized table (4).

Table (4): Preferred conditions of uranium adsorption onto AOGK.

Parameters	Optimum conditions
pH	4
Contact Time	90 min
Initial uranium Conc.	100 mg/l
Adsorbent mass (dose)	0.25 g/l
Temperature	25ºC
Capacity	**95.23 mg/g**
De-sorption	By using 0.1M ascorbic acid
Reusability	Up to eight cycles with R.S.D. of -3.89%

Case study (Uranium removal from the raffinate solution)

- *Uranium adsorption*

As previously stated, the prepared adsorbent has a suitable uranium adsorption capacity (about 95 mg U/g AOGK). In the present work, the study of uranium removal from **Nuclear Material Authority, Egypt**, liquid raffinate solution was carried out. A batch experiment was performed by contacting 0.1g AOGK with 200 ml of raffinate for 90 min. by calculating the loaded uranium content from its analysis in the effluent samples exposed that only 5.93 mg U/g AOGK. Comparing this loading capacity with the obtained theoretical capacity of the prepared AOGK (about 95 mg U/g AOGK), designates that under the working conditions, 62.3% of the theoretical capacity was realized. The decrease in the AOGK capacity after contacting with the raffinate sample may be due to the competition between uranium and different ions in the studied nuclear waste sample (specially iron).

- *Uranium elution*

Using the 0.1M ascorbic acid as an eluent was found effective in uranium elution from the loaded AOGK adsorbent bed. Calculation of the eluted uranium amounts revealed that this elution solution gave about 96 % uranium elution efficiency (5.64 mg U were eluted).

CONCLUSIONS

The results of this study indicate that kaolinite clay could be converted into an efficient adsorbent material for uranium removal from aqueous solution by aluminum oxide grafting. The maximum adsorption capacity of the modified kaolinite clay for uranium is greater than 95 mg/g, much higher than the unspoiled kaolinite clay probably due to the increase in negative surface charge. High pH value is preferred for uranium adsorption on the modified kaolinite clay because of increased negative surface charge. Adsorption isotherms indicate that the uranium adsorption onto the modified kaolinite clay is a monolayer. Resulting test on the uranium ion removal from raffinate solution using modified kaolinite could serve as potential applicability of this adsorbent in industrial wastewater treatment.

ACKNOWLEDGEMENT

The author would like to express his sincere thanks to ***Prof. Dr. E. M. Hussein*** for deeply useful scientific discussions during the preparation of this paper.

REFERENCES

1. Bargar, J.R., Reitmeyer, R., Davis, J.A., 1999. Spectroscopic confirmation of uranium(VI)–carbonatoadsorption complexes on hematite. Geochimica et Cosmochimica Acta 33, 2481–2484.

2. Bargar, J.R., Reitmeyer, R., Lenhart, J.J., Davis, J.A., 2000. Characterization of uranium(VI)–carbonato complexes on hematite: EXAFS and electrophoretic mobility measurements. Geochimica et Cosmochimica Acta 64, 2737–2749.

3. Yusan, S., Akyil, S., 2008. Sorption of uranium (VI) from aqueous solutions by akaganeite. J. Hazard.y Mater. 160, 388–395.

4. Ganesh, R., Robinson, K.G., Chu, L.L., Kucsmas, D., Reed, G.D., 1999. Reductive precipitation of uranium by *Desulfovibrio*, *desulfuricans*: evaluation of cocontaminant effects and selective removal. Water Res. 33, 3447–3458.

5. Kryvoruchko, A.P., Yurlova, L.Y., Atamanenko, I.D., Kornilovich, B.Y., 2004. Ultrafiltration removal of U(VI) from contaminated water. Desalination 162, 229–236.

6. Mellah, A., Chegrouche, S., Barkat, M., 2006. The removal of uranium (VI) from aqueous solutions onto activated carbon: kinetic and thermodynamic investigations. J. Colloid Interface Sci. 296, 434–441.

7. Sodayea, H., Nisanb, S., Poletikoc, C., Prabhakara, S., Tewaria, P.K., 2009. Extraction of uranium from the concentrated brine rejected by integrated nuclear desalination plants. Desalination 235, 9–32.

8. Donia, A.M., Atia, A.A., Moussa, M.M., Sherif, A.M., Magied, M.O., 2009. Removal of uranium (VI) from aqueous solutions using glycidyl methacrylate chelating resins. Hydrometallurgy 95, 183–189.

9. Van Loon, L. R.; Glaus, M. A. Environ. Sci. Technol. 2008, 42 (5), 1600−1604.

10. Karamanis, D.; Assimakopoulos, P. A. Water Res. 2007, 41 (9), 1897−1906.

11. M. M. Zareh, A. Aldaher, A. E. M. Hussein, M. G. Mahfouz, M. Soliman, 2013, Uranium adsorption from a liquid waste using thermally and chemically modified bentonite. J. Radio-analytical and Nucl. Chem. Feb. 2013, V. 295, Issue 2, pp 1153-1159.

12. Bouzidi, A.; Souahi, F.; Hanini, S. *J. Hazard. Mater.* 2010, *184* (1−3), 640−646.

13. Avramenko, V.; Bratskaya, S.; Zheleznov, V.; Sheveleva, I.; Voitenko, O.; Sergienko, V. *J. Hazard. Mater.* 2011, *186* (2−3), 1343−1350.

14. Lin, Y.; Fryxell, G. E.; Wu, H.; Engelhard, M. *Environ. Sci. Technol.* 2001, *35* (19), 3962−3966.

15. Sangvanich, T.; Sukwarotwat, V.; Wiacek, R. J.; Grudzien, R. M.; Fryxell, G. E.; Addleman, R. S.; Timchalk, C.; Yantasee, W. *J. Hazard. Mater.* 2010, *182* (1−3), 225−231.

16. Parab, H.; Sudersanan, M. *Water Res.* 2010, *44* (3), 854−860.

17. Ding, D.; Zhao, Y.; Yang, S.; Shi, W.; Zhang, Z.; Lei, Z.; Yang, Y. *Water Res.* 2013, *47* (7), 2563−2571.

18. Morsy A. M. A. and Hussein A. E. M., 2011. Adsorption of uranium from crude phosphoric acid using activated carbon. J Radioanal Nucl Chem, 288;341–346.

19. Melkior, T.; Yahiaoui, S.; Motellier, S.; Thoby, D.; Tevissen, E. *Appl. Clay Sci.* 2005, *29* (3−4), 172−186.

20. Vejsada, J.; Jelínek, E.; Řanda, Z.; Hradil, D.; Prikryl, R. *Appl. Radiat. Isot.* 2005, *62* (1), 91−96.

21. Miah, M. Y.; Volchek, K.; Kuang, W.; Tezel, F. H. *J. Hazard. Mater.* 2010, *183* (1−3), 712−717.

22. Osmanlioglu, A. E. *J. Hazard. Mater.* 2006, *137* (1), 332−335.

23. Tsai, S.-C.; Wang, T.-H.; Li, M.-H.; Wei, Y.-Y.; Teng, S.-P. *J. Hazard. Mater.* 2009, *161* (2−3), 854−861.

24. Volchek, K.; Miah, M. Y.; Kuang, W.; DeMaleki, Z.; Tezel, F. H. *J. Hazard. Mater.* 2011, *194* (0), 331−337.

25. Marczenko Z., "Spectrophotometric determination of elements",1976 Ellis Horwood Ltd., Coll House, Westergate, chichester, Sussex, England, Book.

26. Dahu Ding, Zhongfang Lei, Yingnan Yang, Chuanping Feng, and Zhenya Zhang., 2013 “Nickel Oxide Grafted Andic Soil for Efficient Cesium Removal from Aqueous Solution: Adsorption Behavior and Mechanisms” ACS Appl. Mater. Interfaces, 5, 10151 −10158.

27. Chen, Y., Wu, F., Lin, Y.X., Deng, N.S., Bazhin, N., Glebov, E., 2007. Photodegradation of glyphosate in the ferrioxalate system. J. Hazard. Mater. 148, 360–365.
28. Arami. M., N.Y. Limaee, Mahmoodi. N.M., Tabrizi. N.S., 2005 “Removal of dyes from colored textile wastewater by orange peel adsorbent” equilibrium and kinetic studies, J. Colloid Interface Sci. 288 371–376.

29. Misaelides P., Godelitsas A., Filippidis A., Charistos D., Anousis C., 1995 “Thorium and uranium uptake by natural zeolitic materials” The Science of the Total Environment 173/174, 237-246.

30. Xie Shuibo, Zhang Chun, Zhou Xinghuo, Yang Jing, Zhang Xiaojian, Wang Jingsong, 2009 “Removal of uranium (VI) from aqueous solution by adsorption of hematite” Journal of Environmental Radioactivity 100,162–166.

31. Fangli Fan, Huajie Ding, Jing Bai, Xiaolei Wu, Fuan Lei, Wei Tian, Yang Wang and Zhi Qin., 2011” Sorption of uranium(VI) from aqueous solution onto magnesium silicate hollow spheres” J Radioanal Nucl Chem, 289;367-375.

32. Parab, H., Joshi, S., Shenoy, N., Verma, R., Lali, A., Sudersanan, M., 2005. Uranium removal from aqueous solution by coir pith: equilibrium and kinetic studies Bioresour. Technol. 96, 1241–1248

33. Lin ShengLimin ZhouEmail authorZhiwei HuangZhirong LiuQuanshui ChenGuolin HuangAdesoji A. Adesina., 2016 ”Facile synthesis of magnetic chitosan nano-particles functionalized with N/O-containing groups for efficient adsorption of U(VI) from aqueous solution”. Radioanal Nucl Chem. 310: 1361.

34. Chegrouche. S., Mellah. A., Telmoune. S., Water Res. 31 (1997) 1733–1737.

35. Mellah. A., Chegrouche. S., Water Res. 31 (1997) 621–629.

36. Bhatnagar. A., Jain. A.K., J. Colloid Interface Sci. 28 (1) (2005) 49–55.

37. Ho. Y.S., McKay. G., Water Res. 33 (1999) 578–584.

38. Le Li, Dexin Ding, Nan Hu, Pingkun Fu, Xin Xin, Yongdong Wang, 2014 “Adsorption of U(VI) ions from low concentration uranium solution by thermally activated sodium feldspar” J Radioanal Nucl Chem. 299:681–690.

39. Manes, M. Hofer, B.J.E. 1969"Application of the Polanyi adsorption potential theory to adsorption from solution on activated carbon". The Journal of Physical Chemistry, 73 (3), pp 584–590.

40. M. R. Ajimal, A. K. Rao, J. Ahmed and R. Ahmad, Journal of Environmental Science and Engineering, 2006, 48(3), pp 221- 224.

41. Garg V. K, Gupta R., Yadav A. B., and R. Kumar, Bioresource Technology, 2003, 89, pp 121-124.

42. G. Ndongo Kounou, J. Ndi Nsami, D. P. Belibi Belibi, D. Kouotou, G. M. Tagne, D. D., Dina Joh and J. Ketcha Mbadcam., 2015 “Adsorption of Zinc(II) ions from aqueous solution onto Kaolinite and Metakaolinite” Der Pharma Chemica, 7(3):51-58.

43. Zhu WB, Liu ZJ, Lei C, Dong YH., 2011 “Sorption of uranium(VI) on Na-attapulgite as a function of contact time, solid content, pH, ionic strength, temperature and humic acid”. J Radioanal Nucl Chem 289:781–788.
44. Liu M, Dong F, Yan X, Zeng W, Hou L, Pang X., 2010 ”Biosorption of uranium by saccharomyces cerevisiae and surface interactions under culture conditions”. Bioresour Technol 101:8573–8580.

45. Mukhopadhyay B, Walther JV., 2001 “Acid-base chemistry of albite surfaces in aqueous solutions at standard temperature and pressure”. Chem Geol 174:415–443.

Included in proceedings but not presented

STUDY ON REES LEACHED IN PHOSPHATE CONCENTRATE WITH PHOSPHORIC ACID

By

Jiang Xunxiong, Feng Lingyong, Wang Shengdong, Fan Yanqing, Jiang Wei, Liu Wei, Zhang Denggao, LiDa, and Zhao Feng

Beijing General Research Institute of Mining & Metallurgy (BGRIMM), China

Corresponding Author

Feng LinYong
FLY2712@sina.com

ABSTRACT

A new hydrometallurgical leaching process, which dissolves REES with phosphoric acid, was proposed and investigated. It studied the effects of H_3PO_4 concentration, temperature, reaction time, and liquid-solid ratio on REES leached. The results showed that an extraction of about 90% was achieved under the leaching conditions: 25% H_3PO_4, 65°C, liquid-solid ratio 10, and reaction time of 8 hours. SEM and XRD analysis indicated that no new reaction solid product was formed on the surface of leaching residue particles. The dissolution kinetics of REES with phosphoric acid solution was found to fit the shrinking core model. The kinetic study indicated that REES leached was controlled by the interfacial chemical reaction in the whole leach process. The apparent activation energy was 46.6 kJ/mol and a semi-empirical rate equation was obtained to describe the process.

Keywords: Phosphate, phosphoric acid, REES, leaching

INTRODUCTION

It is well known that certain deposits of the mineral apatite, specifically fluorapatite ($3Ca_3(PO_4)_2.CaF_2$), contain significant amounts of the rare earth metals (typically 0.1%-1.0%, calculated as RE_2O_3). One such deposit occurs at ZhiJin, China and supplies the feed material to a wet-process phosphoric acid plant in the same locality[1-2]. The ZhiJin phosphorite ores-deposits rich in REEES occur in the early Cambrian Meishucun stage and belong to the Yangzi stratum section[3]. The phosphate belongs to an isomorphic series of carbonate fluorapatite, occurs in the form of the crypto-crystalline, non-crystalline and collophane, and is substituted by living-clastic sediment, clastic-cryptocrystalline and non-crystalline. The companion mineral contain dolomite, calcite, quartz, clay mineral, sphalerite, anatase and pyrites.[4-5]

In the WPA process, the apatite concentrate are dissolved with a mixture of sulphuric acid and phosphoric acid, at the same time, half of REES in apatite go into the phosphogypsum ($CaSO_4•2H_2O$) formed in this reaction. The remainder of REES are dissolved in the crude dilute phosphoric acid (25% P_2O_5)[6], and finally precipitated in the form of sludge during preparation of commercial grade phosphoric acid (54% P_2O_5). Many literatures report the recovery of REES from apatite or phosphogypsum with the conventional sulfuric acid or nitric acid route[7-12]. Although the conventional leaching methods are successful for recovery of REES, there are some problem, such as emission releasing toxic gas, high temperature, long reaction time and bad technical economy[13].

For simplifying the technology process and improving the recovery rate of REES and P_2O_5, the paper studied recovering REES and it`s kinetics that by leaching with phosphate acid from ZhiJin phosphate concentrate. Factors effecting the leaching rate were studied, such as reaction temperature, acid concentration, reaction time, liquid to solid ratio and kinetic model[14-17].

EXPERIMENTAL

Materials

The phosphate ore concentrate (-200 mesh accounts for 64%) used in the present study is from ZhiJin, China. The ground concentrate is analyzed by chemical method and characterized by X-ray powder diffraction (XRD). The composition is given in Table 1 and the XRD pattern is shown in Fig. 1. The chemical analysis shows that the sample contains P_2O_5 31.9%，TRE_2O_3 0.17%, CaO 50.5%，SiO_2 5.2%，FeO 1.0%, MgO 1.4% and Al_2O_3 0.3%. X-ray diffraction (XRD) pattern shows that collophane ($Ca_4F(PO_4)_3$) (77.9%), dolomite($CaMg(CO_3)_2$) (6.5%), calcite ($CaCO_3$) (8.8%), quartz (SiO_2) (3.9%) are the major components. More than 92.5% of the REES is distributed in the cellophane phase in the form of isomorphism and its distribution is show in Table 1. The reagent H_3PO_4 is of analytical reagent grade. Deionized water is also used.

Table 1: Distribution of different REES (wt.%)

La_2O_3	CeO_2	Pr_2O_3	Nd_2O_3	Sm_2O_3	Eu_2O_3	Gd_2O_3	Tb_2O_3
21.4	11.6	3.4	14.3	2.8	0.7	3.0	0.5
Dy_2O_3	Ho_2O_3	Er_2O_3	Tm_2O_3	Yb_2O_3	Lu_2O_3	Y_2O_3	ΣRE_2O_3
3.1	0.6	1.8	0.3	1.2	0.2	34.9	100

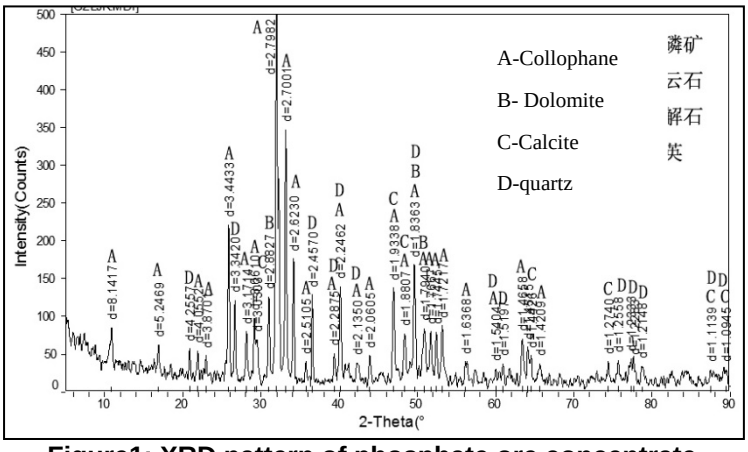

Figure1: XRD pattern of phosphate ore concentrate

Procedure

Tests are carried out in a 1000 mL pyrex reaction flask. The flask, equipped with an agitator and a thermometer, was heated using a thermostatically controlled water bath. In each experiment, the flask with 600 mL leaching solution (a certain proportion of phosphoric acid and deionized water) is heated to the required temperature before phosphate ore concentrate is added, at the same time, the slurry is well-agitated. The reaction is stopped by placing the reactor in an ice bath at the end of each reaction. The slurry is then filtered and then the residue is analysed for REES and P_2O_5 after washing and drying. According to assay, the recovery of REES and P_2O_5 is calculated.

Analyses

The concentration of REES is determined by High Resolution Inductively Coupled Plasma-Mass Spectrometry (ICP-MS, Agilent 8800). The concentrations of P_2O_5 is determined by atomic emission spectrometer (ICP-AES, SPECTRO GENESIS).

RESULTS AND DISCUSSION

Effect of Reaction Time

Fig. 2 presents the results obtained from leaching tests under different reaction times at 65°C, 25% phosphoric acid (P_2O_5 w/w) and liquid to solid ratio 10(V/W). It is obvious that the reaction time has a significant effect on the dissolution of REES. As reaction time increases, the percentage of leaching REES rapidly increases. After 8 h, the reaction is ended. The ratio of P_2O_5 leached is up to 97.6% after 2 hours and 98.8% after 7 hours. Therefore, the suitable leaching time is 8 h.

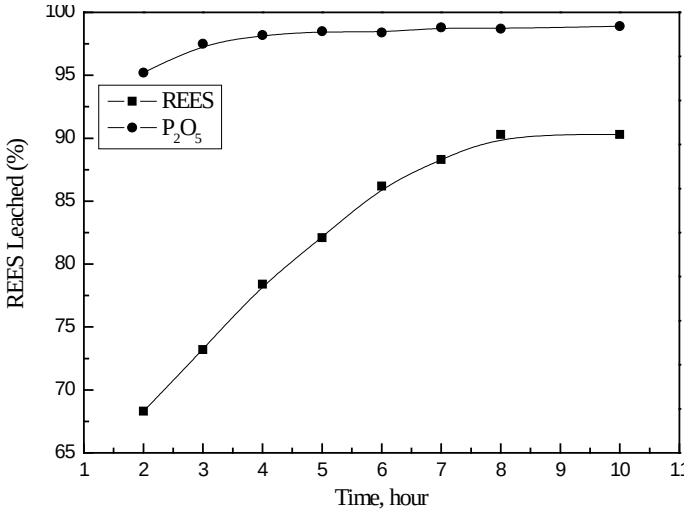

Figure2: Effect of leaching time

Effect of Acid Concentration

A plot of the percentage of leached REES against time is presented in Fig. 3 under the reaction condition of temperature 65°C, liquid to solid ratio 10:1 and reaction time 8 h. The results indicate that the dissolution of REES is strongly dependent on the increase in the concentration of phosphoric acid. When the phosphoric acid concentration increases from 17.0% to 25.0%, the ratio of REES leached also increases from 56.8% to 90.4%, and then remains almost constant when the acid concentration is more than 25%. The ratio of P_2O_5 leached follows the similar rule. Because the wet phosphoric acid concentration is less than 28% in ZhiJin industrial production, the suitable acid concentration is 25% P_2O_5 (w/w).

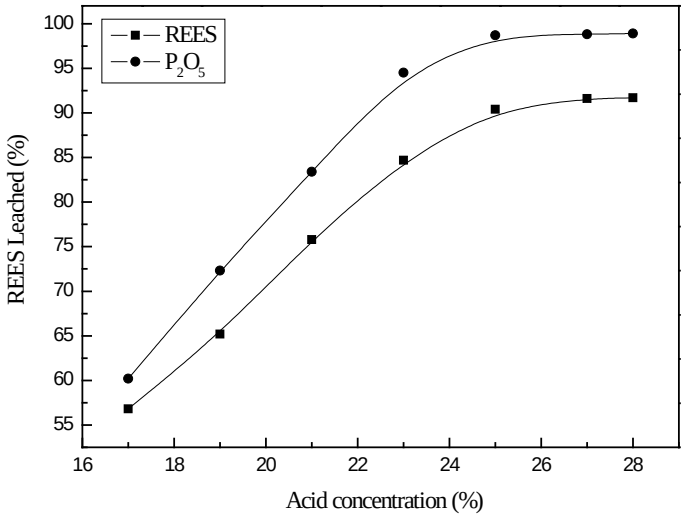

Figure3: Effect of phosphoric acid concentration

Effect of Temperature

A plot of the percentage of leached REES against temperature is presented in Fig. 4 under the reaction condition of acid concentration 25%, liquid to solid ratio 10:1 and reaction time 8 h. The results indicate that the ratio of REES leached increases from 50.2% to 90.4% as the temperature increases from 46 to 65°C and then remains almost constant. The leaching ratio of P_2O_5 increases from 59.8% to 98.7% with increasing temperature and then remained stable. The higher temperatures improve the reaction rate but there is no other benefit in extraction of REES above 70°C. The most suitable temperature is 65°C.

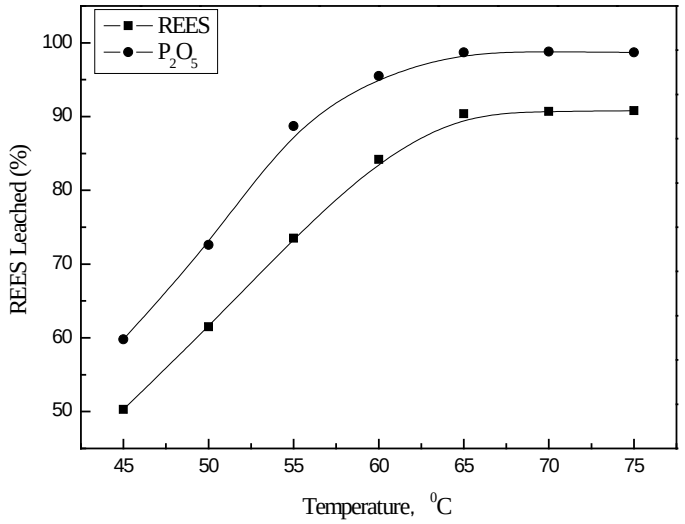

Figure4: Effect of leaching temperature

Effect of Liquid/Solid Ratio

A plot of the percentage of leached REES against liquid to solid ratio is presented in Fig. 5 under the reaction condition of acid concentration 25%, temperature 65°C and reaction time 8 h. The results indicate that higher liquid/solid ratio shows an appreciable increase in leaching of the REES. At the liquid to solid ratio of 4 and 5, the ratios of REES leached only are up to 30.5% and 51.2% respectively, while when the liquid/solid ratio increased to 10, the ratio of REES leached can reach 90.4%. The ratio of P_2O_5 leached followed the similar rule. For high liquid/solid ratio, there is more free phosphoric acid in solution and benefit to form the soluble $Ca(H_2PO_4)_2$. The suitable liquid to solid ratio is 10.

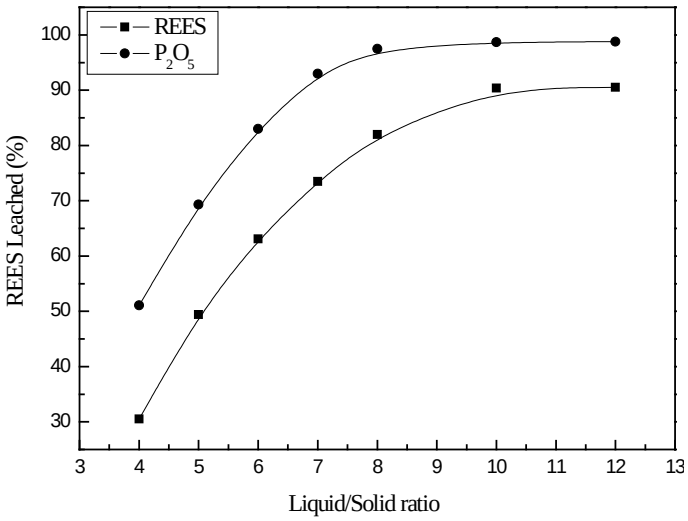

Figure5: Effect of liquid-to-solid ratio

Final Optimum Experiment

According to the test result of different effect factors, it can be concluded that it is feasible to recovery of REES in phosphate concentrate by phosphoric acid.

At the optimization condition acid concentration 25%, temperature 65°C. Liquid/solid ratio 10 and reaction time 8h, the ratios of P_2O_5 and REES are 98.7% and 90.4% respectively. Characterized by XRD, it showed that the collophane shape has disappeared and the quartz, dolomite and fluoride calcium are the main composition (Fig. 6).

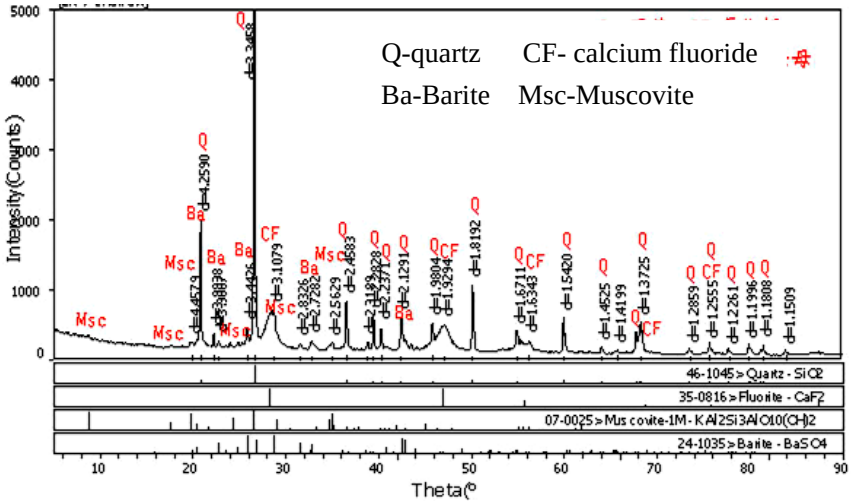

Figure6: XRD pattern of residue

KINETICS ANALYSIS

In heterogeneous solid-liquid reactions, the soluble reactants diffuse across the interface and/or through the porous solid layer. Afterwards, chemical reactions occur. The reaction rate is controlled either by the diffusion of reactant through the solution boundary layer, or through a solid product layer, or by the rate of the chemical reaction at the surface of the core of unreacted particles.

The shrinking core model considers that the leaching process is controlled by fluid film diffusion or chemical reaction. The simplified equations of the shrinking core model when either diffusion or the surface chemical reactions are the slowest step can be expressed as follows, respectively:

$$1-\frac{2}{3}a-(1-a)^{\frac{2}{3}}=k_d t \qquad \text{(Eq.1)}$$

$$1-(1-a)^{\frac{1}{3}}=k_r t \qquad \text{(Eq.2)}$$

where α=fraction reacted; k=kinetic constant; t=reaction time; k_d and k_r=rate constants, which are calculated from Eqs. (1) and (2), respectively.

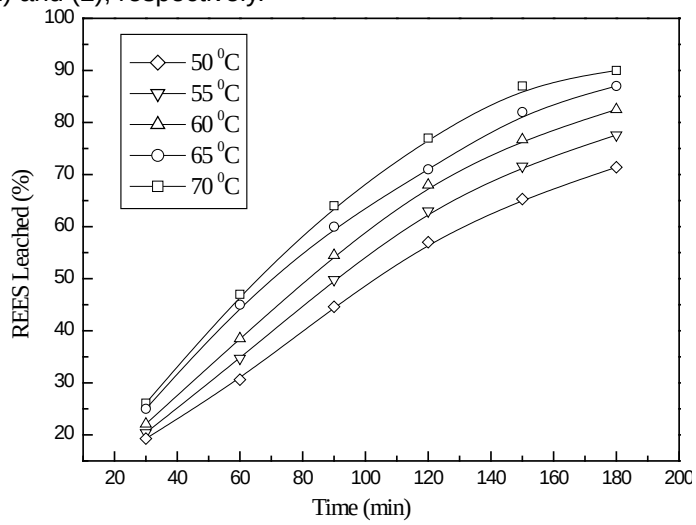

Figure7: Conversion of REES at various reaction temperatures

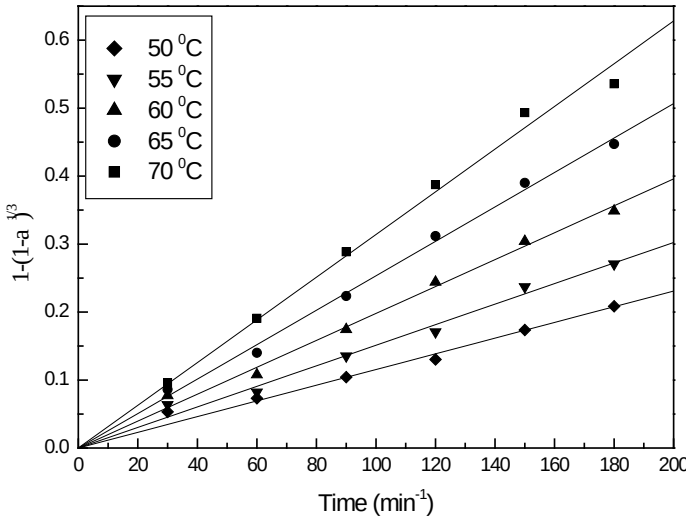

Figure8: Relationship between $(1-(1-\alpha)^{1/3})$ and time

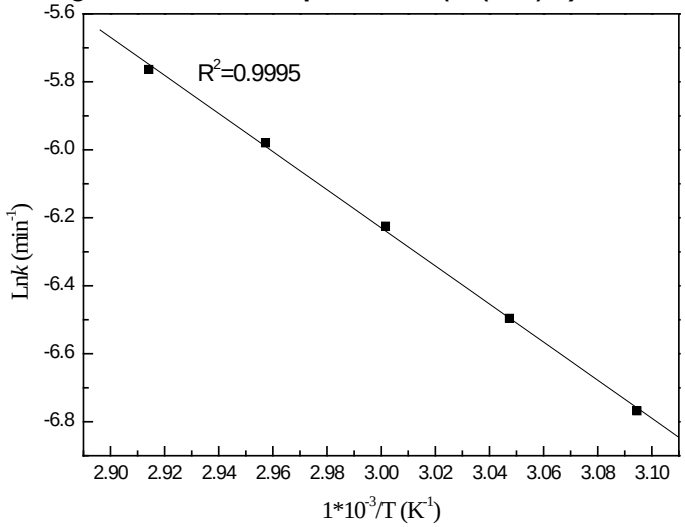

Figure9: Relationship between k_r and 1/T

Table 2：The Rate constants and correlation coefficient values of the kinetics model

Leaching temperature(℃)	Chemical reaction and outer diffusion controlled model		Inner diffusion controlled model	
	Rate constants(min^{-1}) k_r	Correlation coefficient(R^2)	Rate constants(min^{-1}) k_d	Correlation coefficient(R^2)
50	0.00115	0.9938	0.00017	0.9692
55	0.00151	0.9915	0.00028	0.9730
60	0.00198	0.9955	0.00045	0.9857
65	0.00253	0.9975	0.00069	0.9895
70	0.00314	0.9954	0.00097	0.9930

The rate constants values, k_d and k_r calculated from Eqs. (1) and (2), for each temperature are given in Table2. These results indicate that the dissolution rate of REES is controlled by surface chemical reactions. The conversion of REES at various reaction temperatures is presented in the Fig. 7. The application of the surface chemical reaction kinetic model $(1-(1-\alpha)^{1/3})$ using a specific size range of particles and the acid concentration under known percent solids for different temperatures is shown in Fig. 8. Using the Arrhenius equation, $k_r = k_0\, e^{-Ea/RT}$, a plot of ln k_r versus 1/T is a straight line with a slope of $-E_a/RT$ and an intercept of ln k_0 (Fig.9). Using the Arrhenius equation, the following values were calculated:

$$E_a = 46.6 \text{ kJ/mol and } k_0 = 3.93 \times 10^4 \text{ min}^{-1}$$

After the evaluation of activation energy and pre exponential factor, the kinetics model for the leaching process (Eq. (3)) can be expressed as:

$$1-(1-\alpha)^{1/3} = 3.93 \times 10^4 e^{-46.6/RT} t \quad (3)$$

This value of activation energy clearly suggests chemical reaction control for the process[18-19] as this value is consistent with the values obtained in other fluid–solid reaction systems[20-21]. In most of the studies, including the dissolution of REES with acid[22], it has been concluded that the overall rate of dissolution is controlled by chemical reactions.

CONCLUSIONS

Phosphoric acid is used to leach the REES in phosphate concentration from sedimentary Mountain of phosphate deposit in China which contained about 32% P_2O_5. The optimum leaching condition is determined to be as follows: H_3PO_4 concentration 25% P_2O_5, 65°C, liquid-to-solid ratio 10, and reaction time 8 hour. Under the most suitable conditions, the leaching ratios of REES and P_2O_5 are up to 90.4% and 98.7% respectively.

The dissolution kinetics of the REES with phosphoric acid solution are found to fit the shrinking core model for a chemical reaction controlled process. XRD analysis shows that no new reaction solid product was formed on the leaching residue particle surface. The apparent activation energy is found to be 46.6 kJ/mol and consistent with a chemically controlled reaction.

ACKNOWLEDGMENTS

The authors gratefully acknowledge the financial support from the National Nature Science Foundation of China (No. 51374037).

REFERENCES

1. Lounamaa, N., Mattila, T., Judin, V.P. and Sund, H.E., 1980. Recovery of rare earths from phosphorus rock by solvent extraction. In: Proc. 2rid. Int. Congr. Phosphorus Compounds, Institut Mondial du Phosphate, Paris, pp. 759-768.

2. Habashi, F., 1985. The recovery of the lanthanides from phosphate rock. J. Chem. Tech. Biotechnol., 35A, 5-14.

3. Zhang Jie, Shun Chuanmin, Guofeng, 2006. Separation and Enrichment of Rare Earth Elements in Phosphorite in Xinhua , Zhijin, Guizhou. J. JOURNAL OF RARE EARTHS. 24, 413-414

4. Zhang J, Chen D L. 2000. Scanning electron microscope study of the ore-bearing REE in Xinhua Phosphorite, Zhijin Guizhou. J. Journal of Mineralogy and Petrology. 3, 59-62.

5. 5.Zheng S F, Wang Y G. 1984. The petrology of meishucun age phosphorites in Yangzi Province, Guizhou . Guiyang: The People's Publishing House of Guizhou (in Chin.) , pp. 135.

6. Long Zhiqi, Wang Liangshi, Huang Xiaowei, 2008. Study on the rare earth distribution control during wet process of phosphoric acid production, J. Journal of the Chinese Rare Earth Society. 3, 307-312.

7. J.S. Preston et al. 1996, The recovery of rare earth oxides from a phosphoric acid by-product. Part 1: Leaching of rare earth values and recovery of a mixed rare earth oxide by solvent extraction. J. Hydrometallurgy. 41,1-19.

8. Lonescu, E., Tomescu, E. and Rachita, R., 1980. Contributions h la recuperation des lanthanides des phosphates naturels. In: Proc. 2nd. Int. Congr. Phosphorus Compounds, Institut Mondial du Phosphate, Paris, pp. 745-758.

9. Rusin, N.F., Deyneka, G.F., Andrianov, A.M., 1980. Extraction of sum rare-earth metals from phosphogypsum. In: D.P. Borris and P.W. Boody (Editors), Proc. Int. Symp. on Phosphogypsum, (Florida Institute of Phosphate Research, 2, pp. 407-423.

10. Kijkowska, R., 1983. Recovering rare-earth elements from Kola apatite and Moroccan phosphate rock.J. Phosphorus Potassium. 127, 24-26.

11. Milanova, M., Minkova, N., Todorovsky, D., 1991. Purification of rare earth oxide mixtures from a concentrate obtained during the processing of apatite.J. Hydrometallurgy. 26, 369-378.

12. Zielinski, S., Szczepanik, A., Buca, M. and Kunecki, M., 1993. Recovery of lanthanides from Kola apatite in phosphoric acid manufacture. J. Chem. Tech. Biotechnol., 56: 355-360.

13. A.T. Kandil, M.M. Aly, E.M. Moussa. 2010. Column leaching of lanthanides from Abu Tartur phosphate ore with kinetic study. J. JOURNAL OF RARE EARTHS. 28, 576.

14. Lokshin E P, Vershkova Yu A, Vershkov A V, 2002. Efficiency of sulfuric acid leaching of lanthanides in relation to quality of phosphosemihydrate obtained from khibiny apatite concentrate. J. Russian Journal of Applied Chemistry. 75, 1572.

15. Chi R, Zhang X, Zhu G,. 2004. Recovery of rare earth from bastnasite by ammonium chloride roasting with fluorine deactivation. J. Minerals Eng. 17,1037.

16. Zhu G, Chi R, Xu Y. 2000. Separation and recovery of RE and Mn from MN rare earth mud. J. Miner. Process (in Chin.). 59,163.

17. Chi R, Wang D. B, 1996. Eneficiation of Rare Earth Ore and Extraction Technology. Beijing Science Press: Beijing (in Chin.). 196.

18. Habashi, F., 1999. Kinetics of metallurgical processes. Second edn., Metallurgie Extractive Quebec, Quebec, Canada.

19. Abdel-Aal, E.A., 2000. Kinetics of sulphuric acid leaching of low grade zinc silicate ore. J. Hydrometallurgy. 55, 247-254.

20. Ngoc, N.V., Shamsuddin, M., Prasad, P.M., 1990. Oxidative leaching of an off-grade/ complex copper concentrate in chloride lixiviants. Metall. Trans. 21B, 611-620.

21. Demir, F., Donmez, B., Colak, S., 2003. Leaching kinetics of magnesite in citric acid solutions. J. Chem. Eng. Jpn. 36, 683-688.

22. WANG Sheng-dong, JIANG Kai-xi, JIANG Xun-xiong, 2011. Kinetic study on leaching of RE in phosphorite. J. Nonferrous Metals (Extractive Metallurgy) (in Chin.). J. 9, 24-27.